DEVELOPMENT OF CARBON-CARBON AND CARBON-HETEROATOM BOND-FORMING REACTIONS *VIA* GOLD AND GOLD/SILVER CO-OPERATIVE CATALYSIS

A THESIS
SUBMITTED TO AcSIR FOR THE AWARD OF
DEGREE OF

DOCTOR OF PHILOSOPHY

IN CHEMISTRY

BY

PRADIP N. BAGLE

AcSIR ENROLLMENT NO. 10CC13A26002

UNDER THE GUIDANCE OF

Dr. NITIN T. PATIL

DIVISION OF ORGANIC CHEMISTRY
CSIR-NATIONAL CHEMICAL LABORATORY
PUNE - 411 008, INDIA

MAY – 2018

सीएसआईआर - राष्ट्रीय रासायनिक प्रयोगशाला
(वैज्ञानिक तथा औद्योगिक अनुसंधान परिषद)
डॉ. होमी भाभा मार्ग, पुणे - 411 008. भारत
CSIR - NATIONAL CHEMICAL LABORATORY
(Council of Scientific & Industrial Research)
Dr. Homi Bhabha Road, Pune - 411 008, India

CERTIFICATE

This is to certify that the work incorporated in this Ph.D. thesis entitled "***Development of Carbon-Carbon and Carbon-Heteroatom Bond-forming Reactions via Gold and Gold/Silver Co-operative Catalysis***" submitted by **Mr. Pradip N. Bagle** to Academy of Scientific and Innovative Research (AcSIR) in fulfillment of the requirements for the award of the Degree of Doctor of Philosophy, embodies original research work under our supervision. We further certify that this work has not been submitted to any other University or Institution in part or full for the award of any degree or diploma. Research material obtained from other sources has been duly acknowledged in the thesis. Any text, illustration, table etc., used in the thesis from other sources, have been duly cited and acknowledged.

Bagle PN.

Mr. Pradip N. Bagle
(Student)

Dr.Nitin T. Patil
(Supervisor)

Communication Channels

NCL Level DID : 2590
NCL Board No. : +91-20-2590 2000
EPABX : +91-20-2589 3300
: +91-20-2589 3400

FAX
Director's Office : +91-20-2590 2601
COA's Office : +91-20-2590 2660
COS&P's Office : +91-20-2590 2664

WEBSITE
www.ncl-india.org

CANDIDATE'S DECLARATION

I hereby declare that the original research work embodied in this thesis entitled, ***"Development of Carbon-Carbon and Carbon-Heteroatom Bond-forming Reactions via Gold and Gold/Silver Co-operative Catalysis"*** submitted to Academy of Scientific and Innovative Research for the award of degree of Doctor of Philosophy (Ph.D.) is the outcome of experimental investigations carried out by me under the supervision of **Dr. Nitin T. Patil**, Division of Organic Chemistry, CSIR–National Chemical Laboratory, Pune. I affirm that the work incorporated is original and has not been submitted to any other academy, university or institute for the award of any degree.

May 2018

Place: CSIR-National Chemical Laboratory, Pune - 411 008

Bagle P. N.

Mr. Pradip N. Bagle
(Research student)

ACKNOWLEDGMENTS

First of all, I would like to express my special gratitude to my research supervisor **Dr. Nitin T. Patil** for his constant support and excellent guidance for my research studies. I sincerely acknowledge the freedom rendered by him in the laboratory for the independent thinking, planning, and execution of the research. He taught me everything he knows and always encourages me to think creatively and be prepared to learn new things. I am grateful to him for all the ways in which he has prepared me to move forward in my career and life. I truly feel lucky to have been able to be a part of NTP group.

I express my sincere thanks to my DAC members Dr. Benudhar Punji, Dr. Samir H. Chikkali, and Dr. Chepuri V. Ramana for their continued support, guidance, and suggestions. I am grateful to Prof. Dr. Ashwini K. Nangia (Director, NCL), Prof. Vinod K. Singh (Director, IISER Bhopal), Dr.Vijayamohanan K. Pillai and Prof. Dr. Sourav Pal (Former Directors, NCL), Dr. S. P.Chavan, Head, Division of Organic Chemistry, Dr. Pradeep Kumar, and Dr. R. A. Joshi (Former HoDs, Division of Organic Chemistry) for providing me an opportunity to work at prestigious institute and for providing all the research amenities necessary to carry out this work. I would like to extend my thanks to Dr. P. R. Rajamohanan, Dinesh, Pramod, for their timely help with NMR spectra recording, Mrs. Shantakumari for HRMS facility. I express my heartiest gratitude towards Dr. Rajesh Gonnade, Samir Shaikh and Shridhar for their help in X-Ray crystallographic analysis. Dr. Kumar Vanka, Dr. Manoj Mane for their support in DFT calculations. My sincere thanks to Dr. S. B. Mhaske, Dr. D. S. Reddy, Dr. Shashidhar and all other scientists of CSIR-NCL for their constant motivation and support. I am highly obliged to my teachers and mentors, who have been a tremendous source of inspiration. The people who helped me to achieve my goals and shape my career: Prof. M.S. Wadia, Prof. Dilip D. Dhavale, Dr. S. S. Terdale, Dr. T. Thopte, Dr. D. R. Thube and others.

It is my pleasure to thank all my lab mates and friends *Dr. Valmik, Dr. Rahul, Dr. Vivek, Dr. Suleman, Dr. Rajendra, Dr. Avinash, Dr. Aslam, Amol, Popat, Shom, Manjur, Indra, Ravindra, Chetan, Akash, Vivek, Mahesh, Sagar, Vaibhav, Smital, Kajal, Nayana, Sudheesh, Diego, Shreya, Prathyusha, Ragini, Mahendra, Dr. Brijesh, Manisha, Dnyaneshwar, Pankaj,* for devoting their precious time and made many valuable suggestions, which indeed helped me during this research work. I thank to my special friends with whom I enjoyed their friendship and their

support, *viz.* Amol Kalwaghe, Vikas Bhagwat, Gorakh Jachak, Milind Ahire, Dinesh Kalbhore, Srishti Sharma, Rani Nandkhile and many other from CSIR-NCL and IISER Bhopal. The assistance rendered by administration and CIF staff IISER Bhopal is gratefully acknowledged. I wish to say thanks to Mr. Chaturkar, Mr. Sadaphule, Mr. Mindhe, Vishal, Prashant, Saurav, Virendra, Maruti, Manoj and all supportive staff whose names not mentioned here, but have always been ready to understand my problem and helped me in all possible manners. Financial assistance from the Council of Scientific & Industrial Research (CSIR), New Delhi in the form of fellowship is gratefully acknowledged.

Completion of doctoral degree would not have been possible without my family and friends supporting me along the way. My father Nandkumar, mother Lata have always been excited about my education, even when they didn't know what exactly I was doing. I am forever grateful to my brother Gaurav and Rahul for their love and of course an ever-lasting support. I extend heartiest thanks to my dear uncles, aunts, relatives and all my well-wishers whose continuous encouragement and support have been a source of inspiration in completion of this task. Finally, this thesis is a tribute to the unconditional blessings of "Aai", "Papa" and remark of my patience and hard work.

Pradip N. Bagle

This PhD thesis is dedicated to my Mother & Father, who instilled in me the virtues of perseverance and commitment and relentlessly encouraged me to strive for excellence.

Content

List of Abbreviations I

General Remarks IV

Synopsis V

Chapter 1: Gold-catalysed Carbon-Carbon and Carbon-Heteroatom Bond-Forming Reactions - An Overview

1.1 Introduction 2

1.2 Lewis Acidity of Gold-Relativistic Effects 2

1.3 Gold Catalysed C-C and C-X Bond Forming Cascades 3

1.3.1 Gold Catalysed Cascade Cyclisation Reactions 4

1.3.2 Reactions of Gold Carbenoid 11

1.3.3 Oxidative Gold Catalysed Reactions 16

1.3.4 Reactions Under Gold/Photoredox Catalysis 19

1.3.5 Gold/Chiral Brønsted Acid Catalysed Reactions 21

1.4 Conclusion 23

1.5 Reference 23

Chapter 2: Utilization of Gold(I)/Chiral Brønsted Acid Binary Catalytic System in Combinatorial Chemistry

2.1 Introduction 26

2.2 Hypothesis 36

2.3 Results and Discussion 37

2.4 Conclusion 45

2.5 Experimental Procedures 46

2.5.1 Procedure for Preparation of Scaffold Building Agents (SBAs) 46

2.5.2 Procedure for Preparation of Alkynols 46

2.5.3 General Procedure for Enantioselective Combinatorial Synthesis 46

2.6. Characterization Data, HPLC Chromatograms and NMR Spectra of Final Products 48

2.7 References 93

Chapter 3: Au(I)/Ag(I) Co-operative Catalysis: Interception of Ag-Bound Carbocations with α-Gold(I) Enals in the Imino-Alkyne Cyclizations with N-Allenamides

3.1 Introduction 98
3.2 Present Work 103
3.3 Results and Discussion 104
3.3.1 Optimization Studies 104
3.3.2 Scope of the Reaction 106
3.4 Plausible Reaction Mechanism 108
3.5 Computational Studies 108
3.6 Modification of Products 112
3.6 Conclusion 113
3.7 Experimental Procedures 113
3.8 Characterization Data of Selected Compounds 116
3.9 ORTEP Diagram 125
3.10 2D NMR Experiments 126
2D NMR Experiments for **1s** 126
2D NMR Experiments for **3k** 129
2D NMR Experiments for **3y** 132
3.11 NMR Spectra of Selected Compounds 135
3.12 References 163

Chapter 4: Design and Development of a Strategy for Accessing 3-Alkylchromones via Gold(I)-Catalysed Carbene Transfer Reactions

4.1 Introduction 167
4.2 Literature Reports on Direct C(sp^2)-H Insertion 167
4.3 Present Work 173
4.4 Results and Discussion 174

4.4.1 Optimization Studies 174
4.4.2 Scope of the Reaction 176
4.5 Mechanistic Studies 178
4.6 Modification of Product 180
4.7 Conclusion 181
4.8 Experimental Procedures 181
4.9 Characterization Data of Selected Compounds 184
4.10 ORTEP Diagram: 192
4.11 NMR Spectra of Selected Compounds: 193
4.12 References 225

LIST OF ABBREVIATIONS

Å	Angstrom
MS	Molecular sieve
Ar	Aryl
B*H	Chiral Brønsted acid
br.s.	Broad signal
^{t}Bu	*tertiary*-Butyl
cat	Catalyst
$CDCl_3$	Deuterated chloroform
S	Singlet
d	Doublet
t	Triplet
m	Multiplet
DCE	1, 2-Dichloroethane
DCM	Dichloromethane
ACN	Acetonitrile
DMF	Dimethylformamide
THF	Tetrahydrofuran
DMSO-d_6	Deuterated dimethyl sulphoxide
d.r.	Diastereomeric ratio
ee	Enantiomeric excess
e.g.	Exempli gratia
eq.	Equation
equiv.	Equivalent
ESI	Electrospray ionization
g	Gram
h	Hour

HRMS	High resolution mass spectrometry
MHz	Megahertz
IPA	Isopropyl alcohol
^{i}Pr	Isopropyl
Me	Methyl
Cbz	Carboxy benzyl
Ts	Tosyl
Ms	Mesylate
EDA	Ethyl diazo acetate
PPh_3	Triphenyl phosphene
Tf	Triflate
bpy	bipyridine
TIPSEBX	1-[(Triisopropylsilyl) ethynyl]-1,2-benziodoxol-3(1H)-one
JohnPhos	2-(Biphenyl) di-*tert*-butylphosphine
XPhos	2-Dicyclohexylphosphino-2′,4′,6′-triisopropylbiphenyl
BrettPhos	2-(Dicyclohexylphosphino)3,6-dimethoxy-2′,4′,6′-triisopropyl-1,1′-biphenyl
MHz	Megahertz
mL	Millilitre
mM	Millimolar
mp	Melting point
MS	Molecular sieves
NMR	Nuclear magnetic resonance
Ph	Phenyl
ppm	Parts per million
R*f*	Retention factor
rt	Room temperature
temp	Temperature

TLC	Thin layer chromatography
TMS	Trimethylsilyl
t*R*	Retention time

GENERALREMARKS

All reagents, starting materials, and solvents were obtained from commercial suppliers and used as such without further purification. Solvents were dried using standard protocols. Unless otherwise specified, all reactions were carried out in oven dried vials or reaction vessels with magnetic stirring under argon atmosphere. Dried solvents and liquid reagents were transferred by oven-dried syringes or hypodermic syringe cooled to ambient temperature in a desiccators. All experiments were monitored by analytical thin layerchromatography (TLC). TLC was performed on pre-coated silica gel plates. After elution, plate was visualized under UV illumination at 254 nm for UV active materials. Further visualization was achieved by staining $KMnO_4$ and charring on a hot plate. Combined organic layers after extraction were dried over anhydrous sodium sulfate. Solvents were removed in vacuo and heated with a water bath up to 40 °C. Silica gel finer than 60-120 or 100-200 mesh was used for flash column chromatography. Columns were packed as slurry of silica gel in hexane or petroleum ether and equilibrated with the appropriate solvent mixture prior to use. The compounds were loaded neat or as a concentrated solution using the appropriate solvent system. The elution was assisted by applying pressure with an air pump.

Synopsis

	Synopsis of the Thesis to be submitted to the Academy of Scientific and Innovative Research for Award of the Degree of Doctor of Philosophy in Chemical Science
Name of the Candidate	**Pradip Nandkumar Bagle**
AcSIREnrolment No. & Date	**10CC13A26002; August 2013**
Faculty	**Chemical Sciences**
CSIR Lab affiliated with	**Division of Organic Chemistry, CSIR-NCL, Pune**
Title of the Thesis	**Development of Carbon-Carbon and Carbon-Heteroatom Bond-forming Reactions *via* Gold and Gold/Silver Co-operative Catalysis**
Research Supervisor	**Dr. Nitin T. Patil**

Key words: *Gold Catalysis, Brønsted Acid Catalysis, Cooperative Catalysis, Alkynes, Carbenes, Cascade Reactions*

Recently, the field of gold catalysis has witnessed significant developments. The exploration of new reaction modes involving Carbon-Carbon (C-C) and Carbon-Heteroatom (C-X) and bond-forming reactions in this arena has emerged as important topic of research. In majority of these transformations, the π-acidity of gold complexes triggers the activation of C-C multiple bonds such as alkenes, allenes and alkynes thereby favoring the addition of nucleophiles. In recent years, cooperative catalytic reactions wherein two catalysts (one is gold) work simultaneously to form products which cannot be obtained by the use of a single catalyst alone, have attracted considerable attention. Very recently, researchers showed that gold catalysts can generate gold-carbenes, from diazo-compounds, to mediate carbene-transfer reactions. The present thesis is focused on the C-C and C-X bond-forming process through π-acid catalysis, cooperative catalysis and carbene transfer reactions; all are catalyzed by gold complexes. The work embodied in this thesis has been divided into four chapters as described below.

Chapter 1: Gold-catalyzed Carbon-Carbon and Carbon-Heteroatom Bond-Forming Reactions - An Overview

A great number of novel transformations have appeared during the last decade based on the gold-catalyzed activation of alkynes. A historical retrospect on the progress in this area

reveals the following trends: gold catalysis, oxidative gold catalysis, organo/gold catalysis and gold/photoredox catalysis. All these reactions represents a potentially expedient and atom-economical approach to useful synthetic building blocks via C-C and C-X bond formation. In this chapter, a brief overview of the field and its impact on the development of C-C and C-X bond forming reactions is described.

Chapter 2: Utilization of Gold(I)/Chiral Brønsted Acid Binary Catalytic System in Combinatorial Chemistry

The field of asymmetric catalysis has grown rapidly, influencing almost all disciplines of science, especially healthcare. However, there is no single optimal catalyst available which works over the broad range of substrates. This is due to the fact that the enantiodetermining transition state is highly sensitive to the steric and electronic nature of substituents present in the substrates. Clearly, this kind of transition state could easily be perturbed by the additional molecules present in the reaction mixture, causing poor enantioinduction.

Scheme 1.

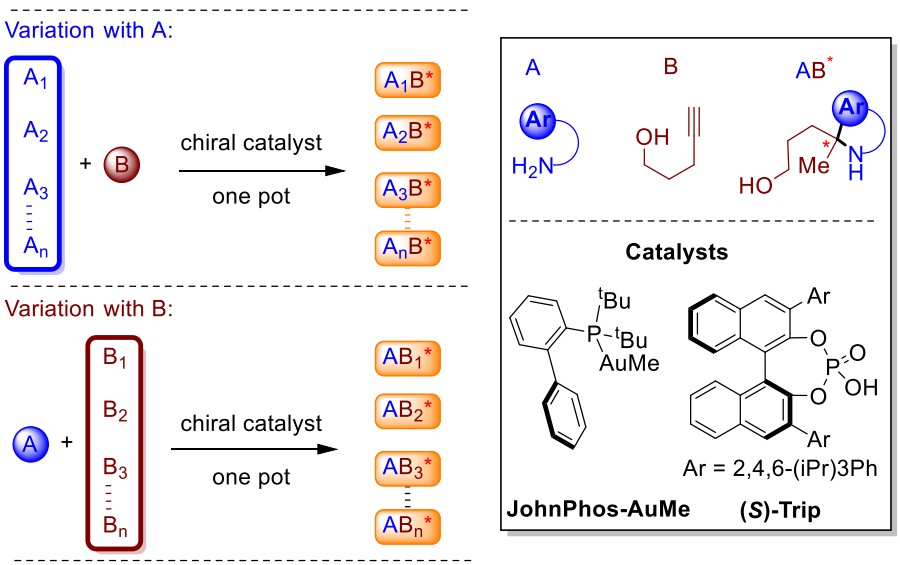

In this chapter, a unique example dealing with the synthesis of various enantioenriched molecules from multiple starting materials in one pot is described. The reaction of aminoaromatics A with alkynols B_1, B_2, B_3…B_n with a AuI/chiral Brønsted acid catalyst afforded AB_1*, AB_2*, AB_3*…AB_n*; while, the reaction of alkynols B with aminoaromatics A_1, A_2, A_3…A_n under the same reaction conditions gave A_1B*, A_2B*, A_3B*…A_nB* (Scheme 1). The work described herein has shown that with appropriate choice of catalysts and substrates,

multiple starting materials can be reacted to form multiple products in a single operation without affecting the yields and ee values. The present approach would find application in combinatorial chemistry in which a mixture of compounds are screened for biological activities.

Chapter 3: Au(I)/Ag(I) Co-operative Catalysis: Interception of Ag-Bound Carbocations with α-Gold(I) Enals in the Imino-Alkyne Cyclizations with N-Allenamides

The development of multiple-catalyst systems for organic transformations that allow for rapid construction of highly functionalized molecules represents a new frontier in organic synthesis. Individual activation of two different reacting partners by two different metal catalysts can lead to reactivities and selectivities that offer products which are otherwise difficult to obtain by using a single catalyst alone. Despite the potential advantages, reports on the co-operative catalysis involving π-acid catalysts with other metals are scarce.

In this chapter, the successful attempt on the realization of cooperative catalyst system for accessing multiply functionalized indolizines is described. For instance, a co-operative Au(I)/Ag(I) catalyst system has been developed to utilize *N*-allenamides as nucleophilic enal equivalents for the interceptive capturing of incipient carbocations generated through π-acid-triggered imino-alkyne cyclization (Scheme 2). The salient features include the in situ generation of silver-bound carbocations (from iminoalkynes), α-gold(I) enals (from N-allenamides) and union of these two species to form indolizines with the regeneration of Au and Ag catalysts.

Scheme 2.

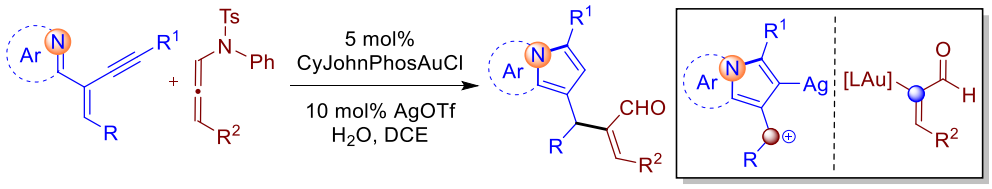

Chapter 4: Design and Development of a Strategy for Accessing 3-Alkylchromones *via* Gold(I)-Catalyzed Carbene Transfer Reactions

Chromones are a group of naturally occurring compounds that are ubiquitous in nature, especially in plants. Traditionally, chromone moieties are synthesized from *o*-hydroxy-acetophenones by the tandem cyclization process by the Baker–Venkataraman, Claisen– Schmidt or Vilsmeier–Haack reactions. Generally, these approaches lead to 3-functionalized chromones

but often utilize harsh reaction conditions. An alternative method to synthesize 3-substituted chromones involves the electrophile triggered cyclization reaction of *o*-hydroxyarylenaminones (Scheme 3a). However, traditionally, these reactions are limited to electrophiles such as halogens, acyl, SMe and alkynyl groups.

Considering the recent renaissance of gold catalysis in carbene transfer reactions, it was envisaged that *o*-hydroxyarylenaminones would undergo alkylation with diazo-compounds followed by subsequent intramolecular cyclization to produce 3-alkyl chromones (Scheme 3b). A detailed account on the realization of such process including scope and limitations is described in this chapter. The mechanism of the reaction was established by carefully conducted experimental studies. The functionality embedded in the scaffold enables their facile elaboration into more diverse structures by a variety of structural manipulations.

Scheme 3.

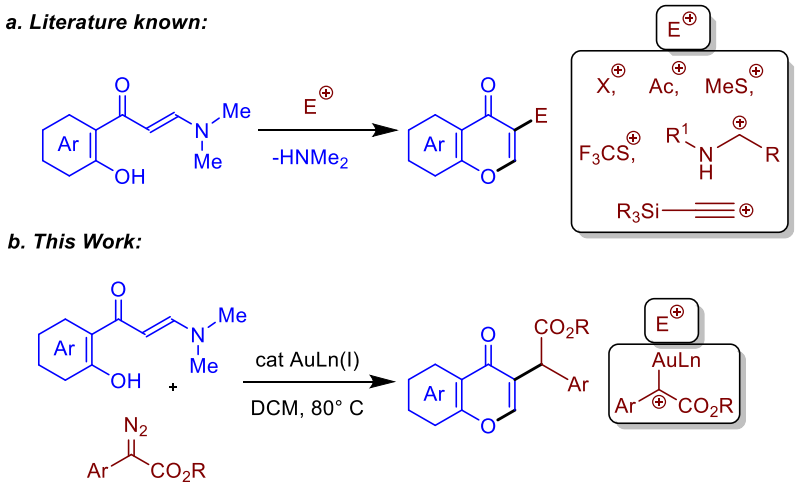

<u>Noteworthy Findings:</u>

- Elegantly utilized the concept of merging gold catalyst with chiral Brønsted acid catalyst in combinatorial chemistry
- Demonstrated an unique example of Au(I)/Ag(I) co-operative catalysis
- Development of a strategy for accessing 3-alkylchromones via gold(I)-catalyzed carbene transfer reactions

List of Publications:

1. Robustness screen in enantioselective catalysis enabled generation of enantioenriched heterocyclic scaffolds in one pot; **P. N. Bagle**, V. S. Shinde, N. T. Patil,* *Chem. Eur. J.* **2015**, *21*, 3580.

2. Au(I)/Ag(I) co-operative catalysis: interception of Ag-bound carbocations with a-gold(I) enals in the imino-alkyne cyclizations with N-allenamides; **P. N. Bagle**, M. V. Mane, K. Vanka, D. R. Shinde, S. R. Shaikh, R. G. Gonade, N. T. Patil,* *Chem. Commun.*, **2016**, *52*, 14462.

3. Design and Development of a Strategy for Accessing 3-Alkylchromones *via* Gold(I)-Catalyzed Carbene Transfer Reactions; **P. N. Bagle**, N. T. Patil,* *Manuscript under preparation.*

4. Catalytic Enantioselective 1,3-Alkyl Shift in *O*-alkylarylethers: Efficient Synthesis of Optically Active 3,3'-Diaryloxindoles; Amol B. Gade, **Pradip N. Bagle**, Popat S. Shinde, Vipin Bhardwaj, Subhrashis Banerjee, Ajit Chande, Nitin T. Patil* *Angew. Chem. Int. Ed.* **2008**, *57*, 5735.

Chapter 1: Gold-catalysed Carbon-Carbon and Carbon-Heteroatom Bond-Forming Reactions - An Overview

Table of Contents

1.1 Introduction 2

1.2 Lewis Acidity of Gold-Relativistic Effects 2

1.3 Gold Catalysed C-C and C-X Bond Forming Cascades 3

1.3.1 Gold Catalysed Cascade Cyclisation Reactions 3

1.3.2 Reactions of Gold Carbenoid 10

1.3.3 Oxidative Gold Catalysed Reactions 16

1.3.4 Reactions Under Gold/Photoredox Catalysis 18

1.3.5 Gold/Chiral Brønsted Acid Catalysed Reactions 20

1.4 Conclusion 22

1.5 Reference 22

1.1 Introduction

During the last decade, a number of novel transformations appeared on gold-catalysed activation of alkynes. The superior activity of gold complexes over other transition metals may be due to the maximum relativistic effects (vide infra) exhibited by them. Using gold has become a trend now for all kind of scientific research and still on the way of its progress for e.g., gold catalysis, oxidative gold catalysis, organo/gold catalysis and gold/photoredox catalysis. These reactions represent a highly profitable and reasonable approach to all the useful synthetic building blocks *via* C-C and C-X bond formation. In this chapter, a brief overview of this field and its significant impact on the development of C-C and C-X bond forming reactions has been described.

1.2 Lewis Acidity of Gold-Relativistic Effects

Before considering its specific properties, some of their most important and ground level characteristics are its electronic configuration i.e., [Xe] $4f^{14}\ 5d^{10}\ 6s^{1}\ 6p^{0}$ and its oxidation states which range from −1 to +5, but Au(I) and Au(III) complexes have their strong supremacy in chemistry. The cationic gold complexes are found to be exceptionallydominant and surpassing Lewis acids and afford a very high affinity for π bonds of allenes, alkenes and alkynes. The relativistic effects are believed to be the reason for the reactivity of gold catalysts and typical catalytic properties. The extreme strong relativistic contractions of the 6*s* and 6*p* orbitals (LUMO) make the electrons come closer to the nucleus. It is this contraction that helps in understanding the increase in the ionization energy of Au when differentiated in terms of other group 11 elements, Cu and Ag, or Pt (group 10) (Figure 1.1), this factor is accounted for the greater Lewis acidity of Au(I) cationic complexes and the strong electro negativity of gold (2.4 for Au, compared to Ag 1.9) can also be correlated. It concludes that relativistic effects can help in understanding the expansion of *d* and *f* orbitals, about electrons occupying the outer orbitals of *5d* and *4f* orbitals (HOMO) that they are better shielded by the electrons in the contracted *s* and *p* orbitals. Thus, there will be a weaker nuclear attraction for *5d* and *4f* orbitals, which gives the soft Lewis acidic nature of gold(I) species as an outcome which react preferentially with "soft" species (such as π-systems) and being less oxophilic. Therefore, these relative effects are noteworthyin explaining the reactivity and the respective reactive pathways of the gold.

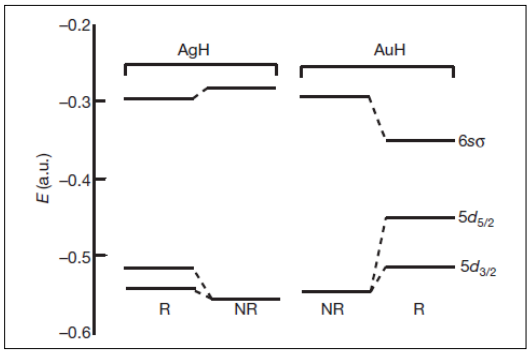

Figure 1.1: Therelativistic (R) and non-relativistic (NR) orbital energies of [AgH] and [AuH] molecules.

1.3 Gold Catalysed C-C and C-X Bond Forming Cascades

This part covers most representative examples which show the diversity of the gold catalysed transformations involving C-C and C-X bond forming cascades. While it is beyond the scope of this chapter to comprehensively describe the literature, only selected reactions in which gold participates in the transformations involving C-C and C-X bond forming cascades, which are published after the 2004, are discussed.This categorization has been done on the basis of types of reactions and mechanism involved therein.

1.3.1 Gold Catalysed Cascade Cyclisation Reactions

The simultaneous addition of carbon and heteroatom (X = O, N, C) across C-C multiple bonds represents one of the most fundamental reactions in gold catalysis, which features diverse functional group tolerance and the easy formation of carbon-carbon (C-C) and carbon-heteroatom (C-X) bonds.[1] Furthermore, the rapid growing area of cascade reactions has allowed chemists to assemble diverse complex molecular frameworks more conveniently. This section covers the transformation that occurs through activation of C-C multiple bonds *via* gold catalysis.

Schmalz and co-workers reported gold catalysed cyclisation and ring expansion reaction of 1-(1-alkynyl) cyclopropyl ketones **1** to generate 2,3,5-trisubstituted furans **2** in moderate to good yields (Scheme 1.3.1.1).[2]Keto alkynes rearranges under gold catalysis to afford

carbocations which can subsequently trapped by the indoles to obtain fused furan derivatives in moderate to good yield.

Scheme 1.3.1.1 Gold catalysed reaction for the synthesis of tri-substituted furans

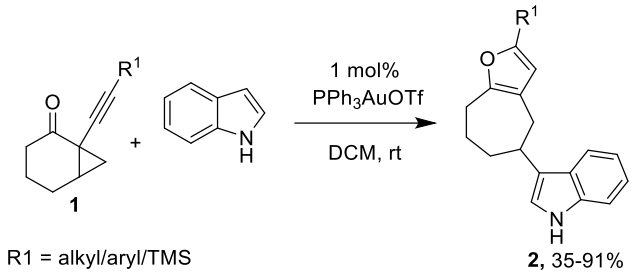

In next year 2007, Kirsch developed an method to access various analogues of furanons**4***via*Au(III) catalysed reaction of 2-alkynyl-2-hydroxy ketones **3** (Scheme 1.3.1.2).[3] This reaction typically involves 5-*endo dig* cyclisation followed by alkyl/aryl migration process.

Scheme 1.3.1.2 Gold catalysed reaction for the synthesis of furanones

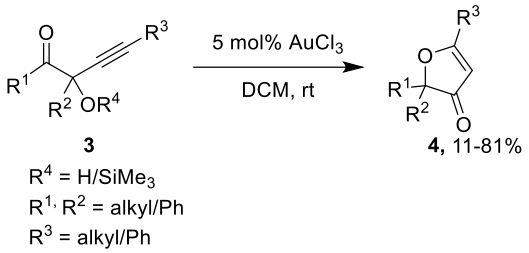

Another fascinating example of gold catalysed rearrangement of alkynylcyclopropane ketones **5** was developed by Zhang and co-workers to obtain tricyclic indene-fused pyran**6** in moderate to good yields (Scheme 1.3.1.3).[4]

Scheme 1.3.1.3 Gold catalysed reaction for the synthesis ofindene-fused pyrans

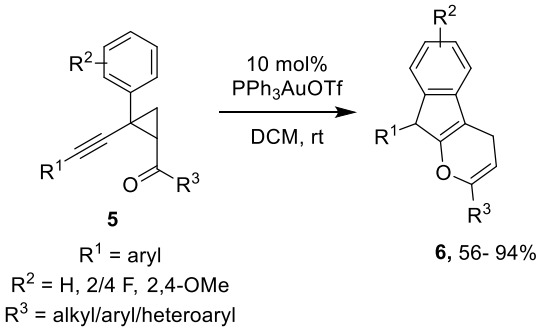

Nakamura and co-workers have demonstrated that 2,3-disubstituted benzothiophenes**8** can be synthesized from 2-alkynyl thiophenol ethers **7** by migration of the substituent from the

heteroatom to the C(3)-position (Scheme 1.3.1.4).[5] The mechanism is believed to proceed through gold(I) activation of the alkyne, attack by the sulfide, migration of the sulfur substituent, and finally re-aromatization by loss of the gold catalyst.

Scheme 1.3.1.4 Gold catalysed reaction forthe synthesis ofdisubstitutedbenzothiophenes

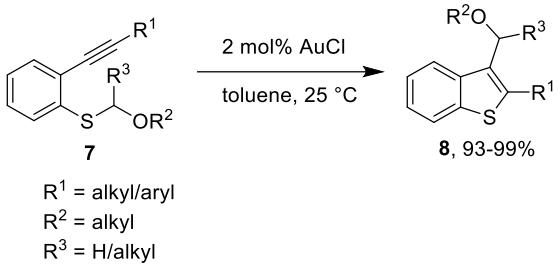

Acetylenic acids **10** were utilisedfor the synthesis of pyridooxazinones**11**.Cascade reaction between amino alcohols **9** andacetylenic acids **10** under gold(I) catalysis generated range of fused heterocycles**11** (Scheme 1.3.1.5).[6]The reaction is believed to proceed by the ring opening of the initially generated furanone by the attack of the amino moiety followed by ring closure to the *N*-acetyliminium intermediates. These *N*-acetyliminium intermediates were then trapped by the pendent hydroxyl group to obtain pyridooxazinones**11**.

Scheme 1.3.1.5 Gold catalysed reaction forthe synthesis ofpyrrolo/pyridooxazinones

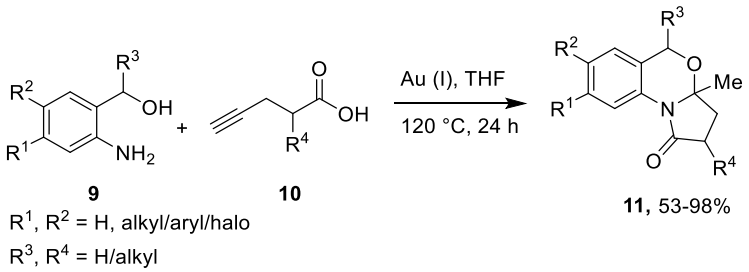

Dixon and co-workers developed a one-pot Au(I)-catalysed*N*-acyl iminium ion cyclisation cascades leading to the efficient synthesis of complex multi-ring heterocyclic compounds **14** (Scheme 1.3.1.6).[6]Alkynoic acids **12** react with aminopyrroles**13** to form tricyclic pyrrole derivatives **14** through keto amide intermediates. This isolable keto amide intermediates further treated under gold catalysis to form desired products, which proves the intermediacy of the reaction.

Scheme 1.3.1.6 Gold catalysed reaction for the synthesis of tricyclic pyrrole derivatives

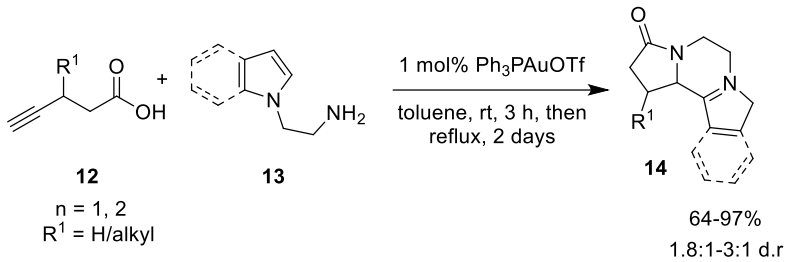

In the year of 2011, Manoharan and coworkers published an Au(III)-catalysed sequential heterocyclisation/Nazarovcyclisations of dienynes**15** to accessfused bicyclic furan derivatives **16** (Scheme 1.3.1.7).[7]

Scheme 1.3.1.7 Gold catalysed reaction for the synthesis ofbicyclic furan derivatives

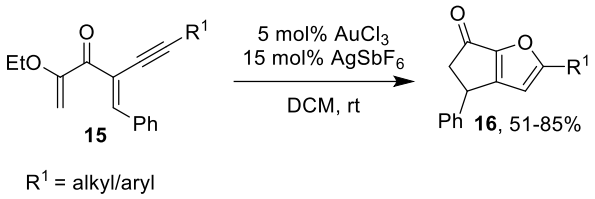

Zhang and co-workers developed catalyst dependent reaction of enynes to access highly functionalized dihydrobenzofurans and dihydroisobenzofurans (Scheme 1.3.1.8).[8]Cyclic enyne systems **17** on treatment with IPrAuSbF$_6$ afforded 3,4-fused furans**18**, whereas 2,3-fused furan **19** were obtained when AgMsOH was used instead of AgSbF$_6$. Divergence in product selectivity was noticed by the author depending upon the anion of the silver salts used.

Scheme 1.3.1.8 Gold catalysed reaction for the synthesis ofdihydrobenzofurans and dihydroisobenzofurans

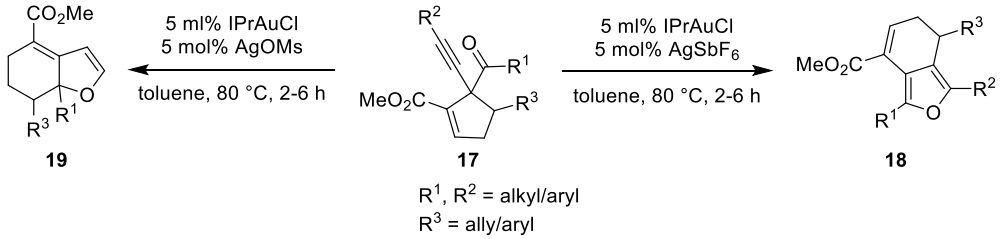

Kozmin and co-workers efficiently developed an Au(III)-catalysed double cyclisation of simple 1,5-enynes tethered oxygen nucleophiles **20**. Oxa-bicyclic alkenes containing bridged,

fused, and spirocyclic architectures **21**were obtained under mild reaction conditions (Scheme **1.3.1.9**).[9]

Scheme 1.3.1.9 Gold catalysed reaction for the synthesis ofoxa-bicyclic alkenes

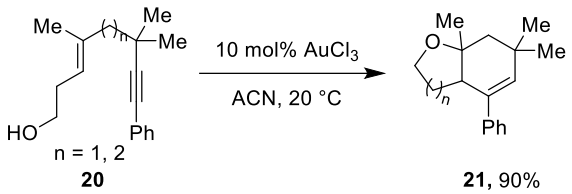

Li and co-workers, in 2006, described efficient alkynylation/cyclisation strategy to obtain 1-alkynyl-1H-isochromenes **23** by reacting terminal alkynes and *ortho*-alkynylaryl aldehydes **22** using gold catalysis (Scheme 1.3.1.10).[10]In the proposed mechanism, addition of the gold-acetylide on aldehydes tookplace prior to the 6-*endo-dig* cyclisationfor generation of corresponding isochromenes**23**.

Scheme 1.3.1.10 Gold catalysed reaction for synthesis ofalkynylisochromenes

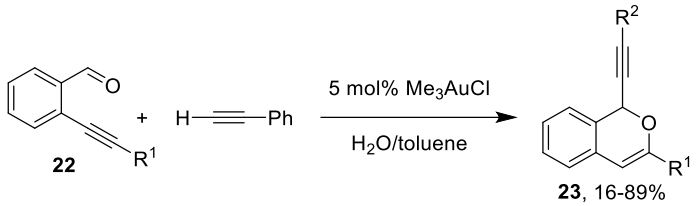

In 2011, Liu group developed a gold-catalysed cyclisation of (*o*-alkynyl)phenylaziridines**24** with electron rich arenes**25** to generate highly functionalized benzo-azepines**26** with trans stereo-selectivity (Scheme 1.3.1.11).[11]Reaction likely to proceed *via*regioselective 6-*endo-dig* cyclisation to form aziridinium ion intermediate and then nucleophilic attack of arnes to furnish tetrahydroisoquinoline**26**.

Scheme 1.3.1.11 Gold catalysed reaction for the synthesis ofarylisochromenes

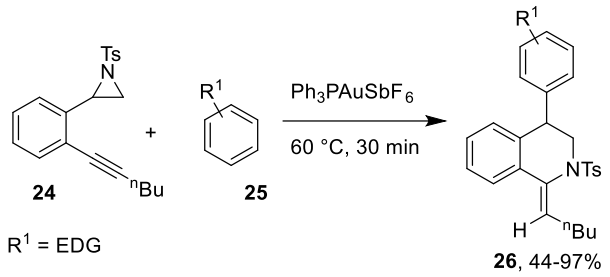

Since the general mode of reaction by gold catalysis is activation of a multiple bond, attack by a nucleophile and removal of the gold moiety by protodeauration. However, the proton involved in the final step may be replaced by other electrophiles. A more specific case is the introduction of a silylethynyl substituent in the 3-position of indoles**28** when synthesized from *ortho*-alkynylanilines**27** (Scheme 1.3.1.12).[12]The methodology is very robust and insensitive towards moisture or oxygen.

Scheme 1.3.1.12 Gold catalysed reaction for the synthesis ofalkynylindoles

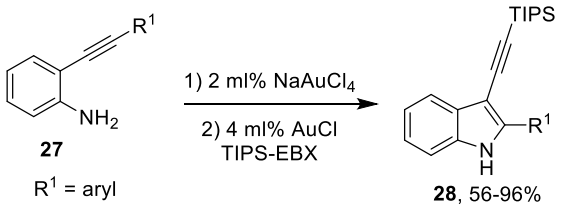

Zhang and coworkers developed an fascinating example for generation and use of an all-carbon 1,4-dipole **31**which they have employed in a formal [4+2]-dipolar cycloaddition with indoles for the synthesis of carbazole-fused furan systems **30** (Scheme 1.3.1.13).[13] Alternatively, simple aldehydes and ketones can be used as the reaction partner to obtain bicyclic compounds.

Scheme 1.3.1.13 Gold catalysed reaction for the synthesis ofcarbazole-fused furans

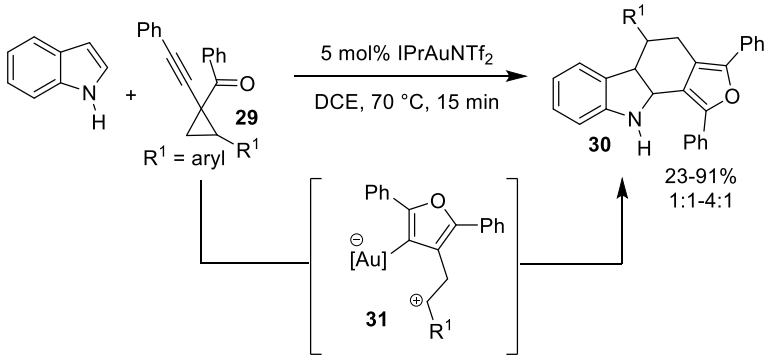

In the year of 2010, our group developed facile strategy to assemble fused isoquinolines**34***via* gold catalysis (Scheme 1.3.1.14).[14] The reaction makes use of two coupling partners such as *o*-alkynylbenzaldehydes**32** and aromatic amines **33** having tethered nucleophiles. These two starting materials reactedwith each other to generate aminal intermediatewhich subsequently underwent 6-*endo-dig* cyclisation under gold catalysis to produce fused isoquinolines.

Scheme 1.3.1.14 Gold catalysed reaction for the synthesis ofcarbazole-fused furans

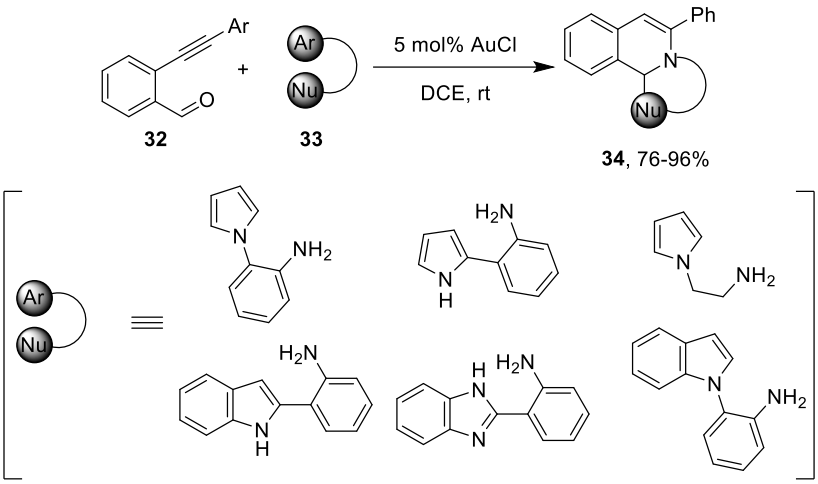

In 2012, we demonstrated Au(I)-catalysed unprecedented rearrangement reaction between 2-amino-benzaldehydes **35** and propargyl amines to obtain 3-amino quinolines**36** (Scheme 1.3.1.15).[15] This methodology enabled the rapid synthesis of useful synthetic building blocks that can be advanced to functionalized quinolines.

Scheme 1.3.1.15 Gold catalysed reaction for the synthesis of 3-amino quinolines

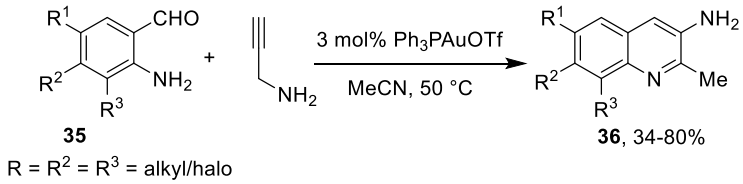

Later, our group developed Au(I)-catalysedhydroamination/hydroarylation of terminal alkynes **37**(Scheme 1.3.1.16).[16] Treatment of terminal alkynes **37** with amino-aromatics **38** in the presence of 5 mol% of $Ph_3PAuNTf_2$ to give the range of heterocyclic compounds such as multisubstitutedpyrrolo-quinoxalines, indolo-quinolines, indolo-quinoxalines, tetrahydro-quinazolinones, and benzo-imidazo-quinazolines.

Scheme 1.3.1.16 Gold catalysed reaction for the hydroamination-hydroarylation of alkynes

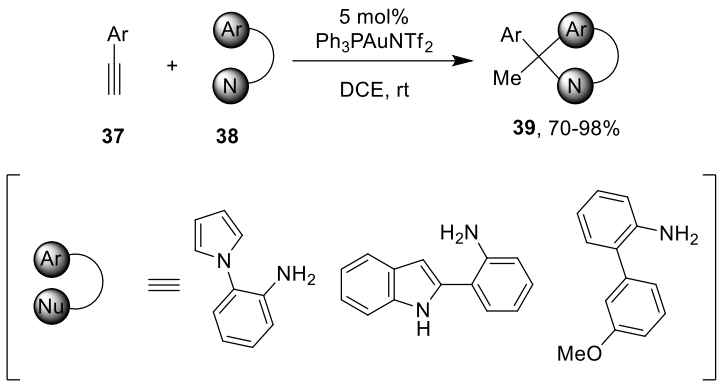

Another example of Au(I) catalysed reaction was developed by our group to produce nitrogen containing heterocycles**41** (Scheme 1.3.1.15).[17] For instance, diverse array of indolizidines and quinolizidineswere obtained*via* a gold(I)-catalysedhydroaminaloxylation and Petasis-Ferrier rearrangement from easily available aminoalkynes**40**. Developed method was further extended for the formal synthesis of (±)-antofine.

Scheme 1.3.1.17 Gold catalysed reaction for the synthesis of indolizidines and quinolizidines

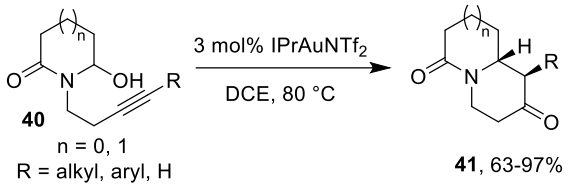

1.3.2 Reactions of Gold Carbenoid

A) Gold carbenoid*via* alkyne activations

Generally, these classes of reactions are characterized by their common α-oxo gold carbenoid intermediates formed either through oxygen transfer from an external oxidant which is not incorporated into the final products. A range of new reactions have evolved from the use of tethered sulfoxide,amine *N*-oxide or nitrone moieties to oxidise a gold-activated alkyne to an α-oxogoldcarbenoid intermediates.

Shin andco-workers described a gold-catalysed generation of azomethineylide, featuring an internal redox reaction between a tethered nitrone and an alkyne substrate **42** (Scheme 1.3.2.1).[18] In this case, the initial 7-*endo-dig* attack of the *O*-atom of the nitrone on the alkyne

tookplace and subsequent *N-O* cleavage led to α-oxo Au-carbenoid**44**. Subsequent addition of the imine to this carbenoid led to **45** from which the catalyst is regenerated to provide **43**. The azomethineylide underwent an efficient intramolecular cycloaddition reaction cascade in highly diastereoselective manner.

Scheme 1.3.2.1 Gold catalysed reaction for the synthesis of bridged polycyclic compound

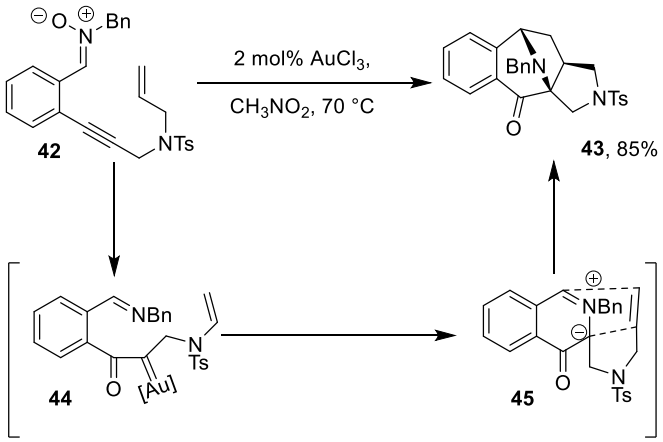

Wang and co-workers successfully showed thatthioketals**46** under gold catalysisled to a bifurcated products, yielding the dithioether**47**[19]or bis-thio-substituted allene**48**[20]depending on the number of bridging carbons in the thioketal**46** (Scheme 1.3.2.2). Both reactions were presumed to proceed *via* a gold-carbene intermediate, though **48** might be formed by a simple 1,3-shift.

Scheme 1.3.2.2 Gold catalysed reaction for the synthesis ofdisubstitutedbenzothiophenes

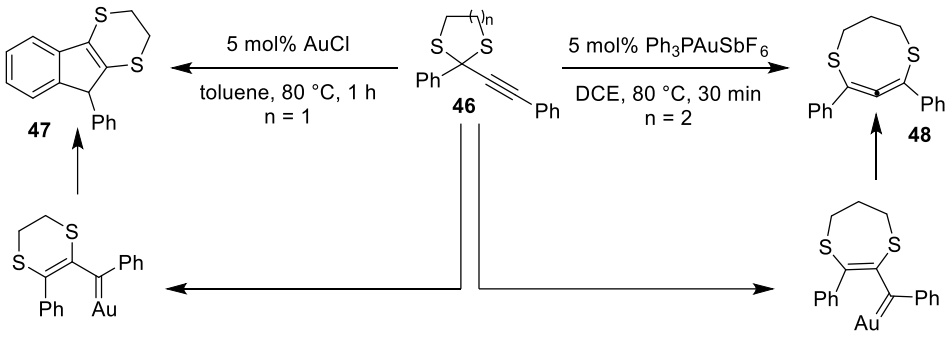

In 2009, Toste and co-workers demonstrated gold-catalysed synthesis of diazabicycles**50** from electron-rich propargylic esters and azomethine imines **49** (Scheme 1.3.2.3).[21] Mechanistically, propargylic esters underwent gold catalysed rearrangement to form

carbenoidintermediates which after formal dipolar cycloadditions with azomethine imines gave range of heterocycles in moderate to good yields.

Scheme 1.3.2.3 Gold catalysed reaction for the synthesis ofdiazabicycles

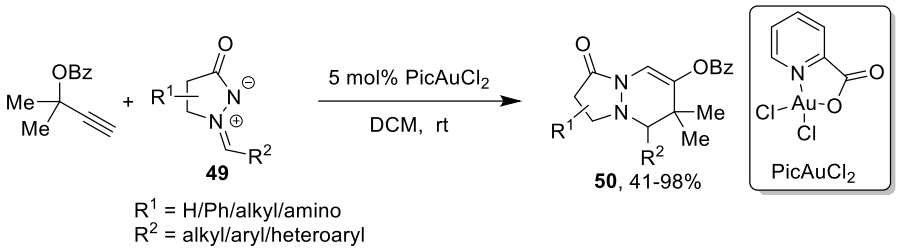

Zhang and Gagosz research groups independently described gold catalysed reactions of azido alkynes**51** to accessindoles and indolin-3-ones.This gold catalysed reaction provide a strategy to access indole derivatives otherwise difficult to prepare by conventional means(Scheme 1.3.2.4).[22,23] In this transformation, azido alkynes **51** underwent intramolecular cyclisation followed by liberation of N_2 molecule to form gold carbenoid intermediateswhich were trapped by the nucleophiles. Furthermore, Gagosz and co-workers showed that by using allylic alcohols a gold-catalysed Claisen rearrangement follows the cyclisation giving rise to indolin-3-ones **53**.[22]

Scheme 1.3.2.4 Gold catalysed reaction for the synthesis of 3-substituted indoles

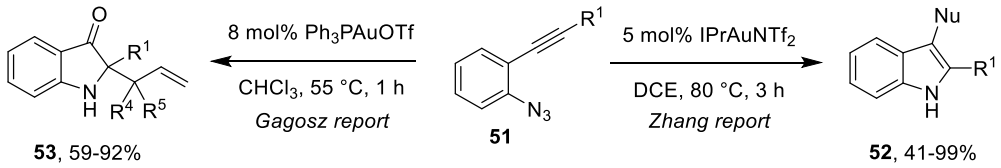

Echavarrenand coworkers developed a protocol for the synthesis of oxygen containing heterocycles**56** by reaction between enynes**54** and aldehydes **55** (Scheme 1.3.2.5).[24] Mechanistically, starting material **54** underwentenyne cyclisation to produce gold carbenoid intermediates**57** which further reacted with aldehydes**55** to produce variusbicyclic heterocycles.

Scheme 1.3.2.5 Gold catalysed reaction for the synthesis of oxygen containing heterocycles

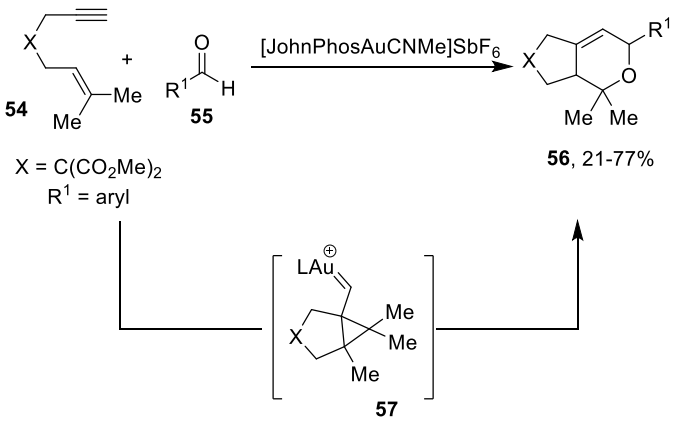

Iwasawa, in 2006, successfully utilised the imino alkynes **58** for the construction of valuable indole derivatives under Au(III) catalysis. Thus, the fused indole derivatives **59** were obtained through the formal [3+2] dipolar cycloaddition between intermediate azomethine ylides **60** and the electron-rich *tert*-butyl vinyl ethers (Scheme 1.3.2.6).[25]Mechanistically, gold carbenoids**60** obtained from imino alkynes **58** under gold catalysis underwent cycloaddition reaction with *tert*-butyl vinyl ethers to obtain range of fused indole derivatives.

Scheme 1.3.2.6 Gold catalysed reaction for the synthesis offused indoles.

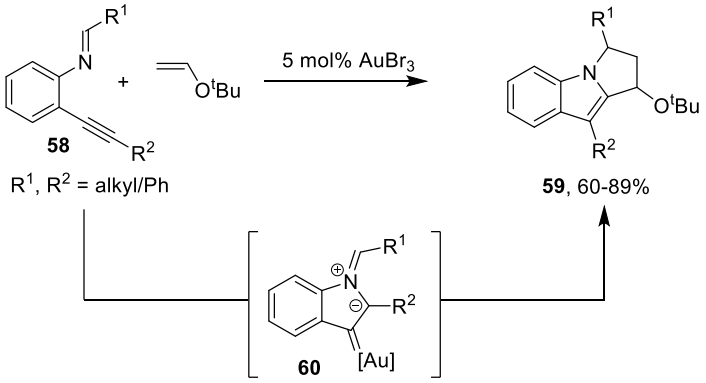

<u>B) Gold carbenoid*via* decomposition of diazo ester</u>:

Metal carbenes, generated by the site-specific metal-promoted decomposition of a reactive diazofunctionality, are employed extensively across an array of useful transformations. Conventionally, rhodium[26] and copper[27] catalysts were known to catalyse carbene transfer reactions from diazo compounds effectively. In recent years, there is resurgence of gold catalysts in carbene transfer reactions.[28] The reactivity observed in gold catalysis is unique and can

provide selectivity of the reaction otherwise not possible by Rh/Cu catalysts. This sub-section covers selected examples which includegold catalysed transformations involving C-C and C-X bond forming cascades to obtain various heterocycles*via*decopmpostion of diazo compounds under gold catalysis.

In 2013, Lopez and co-workers utilized alkenyldiazoacetates**61** to form vinyl gold carbenoids which underwent formal [3+2] cycloaddition reaction with nitriles to produce functionalized pyrroles**62** withcomplete regioselectivity (Scheme 1.3.2.7).[29] The authors assumed that the initial reaction of the alkenyldiazo compound **61** with the gold complex would generate an allyl gold cation**63**. Next, the regioselective*N*-nucleophilic addition of the nitrile to the γ-position would generate species **64** which would produce intermediate **65** by cyclisation. Final tautomerizationresults into formation of pyrrole derivatives **62**.

Scheme 1.3.2.7 Synthesis ofpyrrole derivatives *via* gold carbene transfer reactions

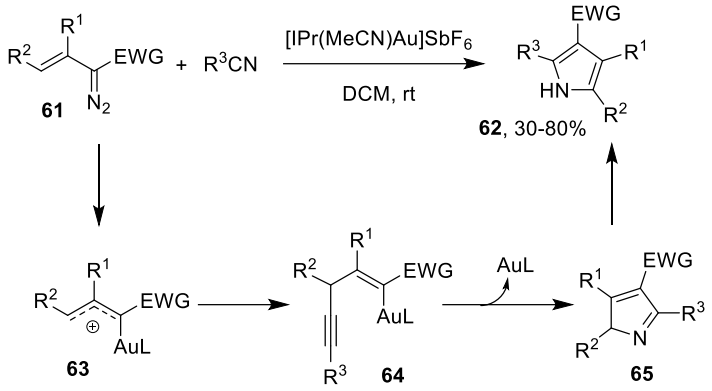

In 2011, Liu and co-workers reported a gold-catalysed formal [3+3]-cycloaddition reaction of nitrosobenzenes**66** with alkenyldiazoacetates**61** with the use of JohnphosAuNTf$_2$ to obtain quinoline*N*-oxides **67** in good isolated yields (Scheme 1.3.2.8).[30]

Scheme 1.3.2.8 Synthesis ofquinoline N-oxides *via* gold carbene transfer reactions

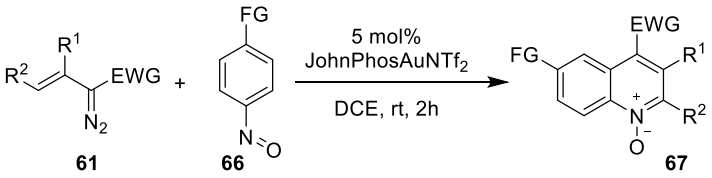

A gold catalysed tandem reaction including [4+2] cycloaddition was reported by Lee and coworkers (Scheme 1.3.2.9).[31] The 1,2-shift of the alkyl group on gold carbene species **71** from

diazo compound **68***via* Wolff rearrangement led α-oxoketene**72** which reacted with vinyl ether **69***via* [4+2] cycloaddition and subsequent elimination to give multi-substituted 4-pyrones **70**.

Scheme 1.3.2.9 Synthesis ofsubstituted 4-pyrones *via* gold carbene transfer reactions

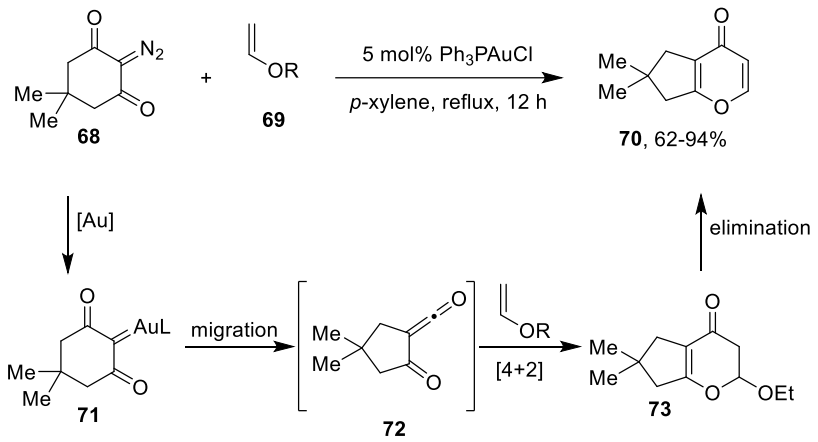

In 2015, a novel Au(I)-catalysed multi-component cycloaddition of EDA, nitrosobenzenes and alkenyldiazoacetates was developed by Liu and co-workers (Scheme 1.3.2.9).[32] In this reaction, $IPrAuSbF_6$ selectively decomposes EDA **74** over alkenyldiazoacetates**75**. A subsequent reaction of the gold carbene **77** with nitrosobenzenesgenerates the nitrone species **78**. The concerted [3+2] cycloaddition of **78** with **75** as depicted in **79** afforded the diazo-containing isoxazolidines**76**. The diazo product **76** can be further converted to valuable products under gold-catalysis.

Scheme 1.3.2.10 Synthesis ofdiazo-containing isoxazolidines*via* gold carbene transfer reactions

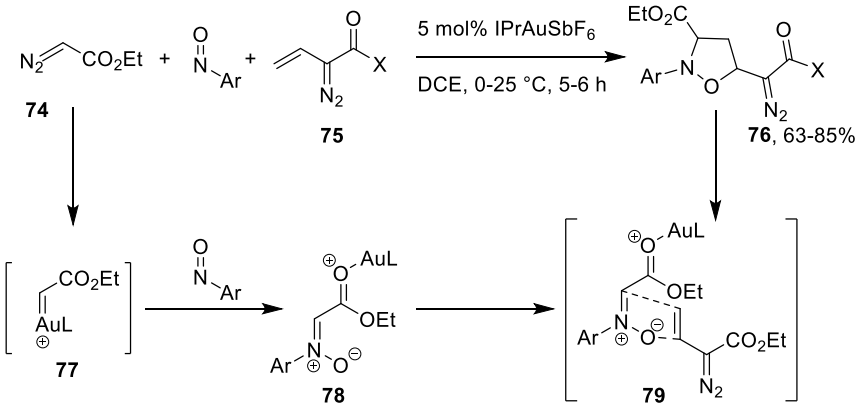

1.3.3 Oxidative Gold Catalysed Reactions

Another approach in the field of gold catalysis features external oxidant-powered Au(I)/Au(III) catalysis, where the metal oxidation state changes during the catalytic cycle.[33]A general mechanism for such processes is shown in Scheme 1.3.3.1. Gold does have two oxidation states, Au(I) and Au(III), that could potentially underwent redox cycles similar to Pd(II) and Pd(IV) catalysis.Hence, with external oxidants, gold centre of the intermediates generated in homogenious gold catalysis can be oxidized from Au(I) to Au(III). This higher valent gold species subsequently can undergo reduction to deliver oxidized products. This section covers selected examples which includeoxidative gold catalysed transformations involving C-C and C-X bond forming sequence to obtain various heterocycles using oxidative gold catalysed reaction.

Figure 1.3.3.1. Plausible reaction mechanism of Au(I)/Au(III) catalysis

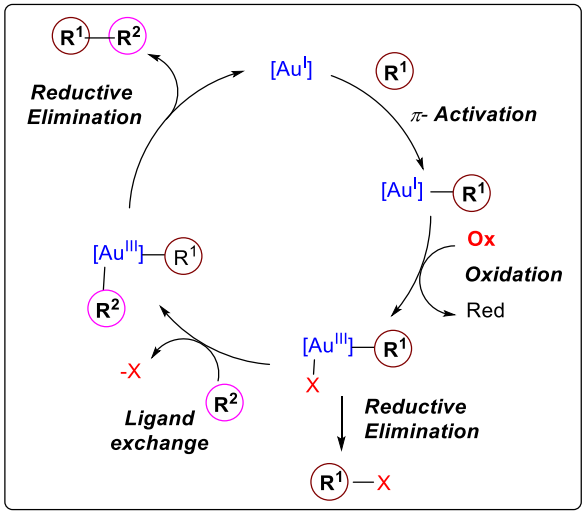

In 2009, Zhang and co-workers reported the first examples of Au(I)/Au(III) catalysis by using Selectfluor as an oxidant (Scheme 1.3.3.1).[34] Coupling of propargylic acetates**80**, boronic acids**81** in the presence of Ph_3PAuCl and Selectfluor (2.0 equiv) resulted into formation of aryl coupled enones**82** with excellent regioselectivity.

Scheme 1.3.3.1 Synthesis ofaryl coupled enones*via* gold oxidative gold catalysed reactions

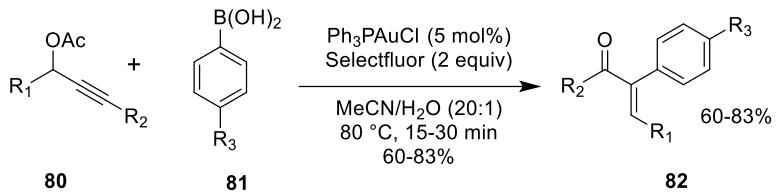

Zhang and co-workers, in the year of 2009, disclosed the carbohetero-functionalization of alkenes using oxidative gold catalysis (Scheme 1.3.3.2).[35] Mechanistically, combination of boronic acid, selectfluor and Au(I) catalyst would generate the Au(III) intermediatethat would further activates the alkenes. Finally reductive elimination would occur to produce *N*-, *O*-containing heterocycles**84**.

Scheme 1.3.3.2 Synthesis of*N*-, *O*- containing heterocycles*via* gold oxidative gold catalysed reactions

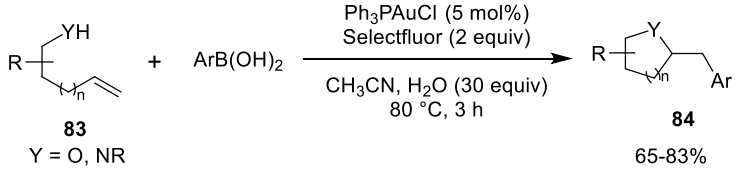

In the same year, carbohetero functionalization strategy was disclosed by Toste and co-workers in 2009. They reported a gold-catalysed aminoarylation reaction of alkenes **85** and arylboronic acids. The reaction was proposed to proceed through a redox cycle involving the initial oxidation of Au(I) into Au(III) with Selectfluor (Scheme 1.3.3.3).[36]

Scheme 1.3.3.3 Synthesis of*N*-containing heterocycles*via* gold oxidative gold catalysed reactions

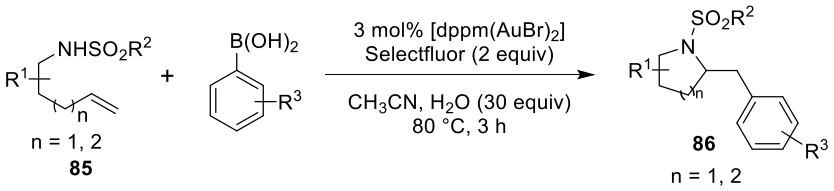

Gouverneur and coworkers reported an oxidative cross-coupling between *in-situ* generated alkenyl gold and an aromatic C–H bond.[37] In this reaction, gold(I) intermediate underwent oxidation in presence of Selectfluor to give the Au(III) intermediate which further underwentFriedel-Crafts type reaction at the Au(III) centerto obtain the tricyclic butenolides.

Scheme 1.3.3.4 Synthesis ofenones*via* oxidative gold catalysed reactions

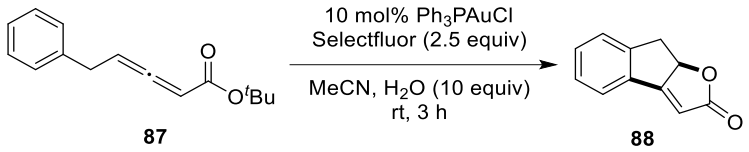

1.3.4 ReactionsUnder Gold/Photoredox Catalysis

Although oxidative gold catalysis has received a great attention over the past years, these reactions have remained fairly restricted in scope due to problems associated with homo-dimerisation or conventional hydrofunctionalisation of starting materials. In addition, oxidative gold catalysis required to use stoichiometric oxidants which also make this process eco-unfriendly.

Recently research revealed that gold complexes with two-electron redox processes could access Au(III) intermediates, which may show similar reactivity like other transition metal complexes[38] to access cross coupled products.In 2013, Glorius and coworkers discovered a new concept involving mergedgold/photoredoxcatalysed coupling reactions utilizing aryl radicals that work as both the oxidant as well as the coupling partner in general redox-neutral transformations without the use of an external oxidant. Mechanistically, the oxidation of the Au(I) complexes is believed to proceed *via* stepwise two single electron transfer processes as shown in the Scheme 1.3.4.1

Scheme 1.3.4.1 Mode of oxidation of gold(I) species under photocatalytic conditions

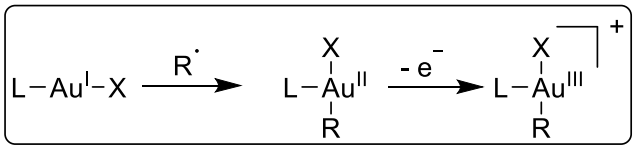

This section covers recent advantages of reactions under merged gold/photoredoxcatalysis and it has been organized with a focus on reactions which involves gold/photoredoxcatalysed transformations involving C-C and C-X bond forming sequence to construct various heterocycles.In 2013, Glorius and coworkers elegantly demonstrated an protocol to access variety of arylated heterocyclic compoundsusing merged gold and photoredox catalytic system (Scheme 1.3.4.2).[39] In this process, alkenes **88** and aryl diazonium salts

89underwent intramolecular oxy- and amino-arylation to obtain a range of *O*-, *N*- containing heterocyclic compounds.

Scheme 1.3.4.2 Synthesis of arylatedheterocycles*via*gold/photoredox catalysis

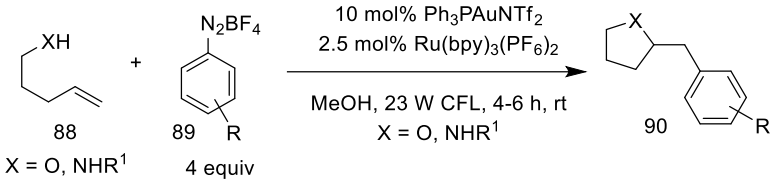

In 2016, Ollivier, Fensterbank and coworkers reported the synthesis of 2,3-disubstituted benzofurans**93** under gold and photoredoxcatalyst system (Scheme 1.3.4.3).[40] Intramolecular oxyarylation of alkynes with aryldiazonium salts occur *via* Au(I)/Au(III) catalysis which essentially the action of merging gold and photoredox catalyst. This mild arylative cyclisation of *o*-alkynyl phenols **91**with aryldiazonium salts **92** provided good to excellent yields of heterocyclic scaffolds.

Scheme 1.3.4.3 Synthesis of 2,3-disubstituted benzofurans*via*gold/photoredox catalysis

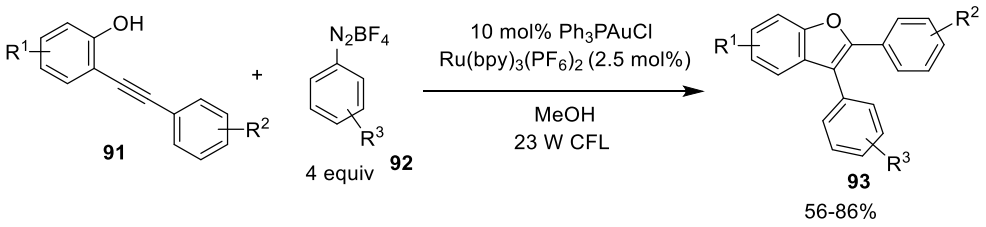

In 2016, Shin's group reported an excellent example of gold and photoredox catalysis to obtain *α*-arylated enones (Scheme 1.3.4.4).[41]Propargyl alcohols **94** after Meyer-Schuster rearrangement would generates an *α*-gold enones **97**, which further reacted with aryldiazonium salts under gold/photoredox catalyst system to give the cross coupled products.

Scheme 1.3.4.4 Synthesis of aryl enones*via*gold/photoredox catalysis

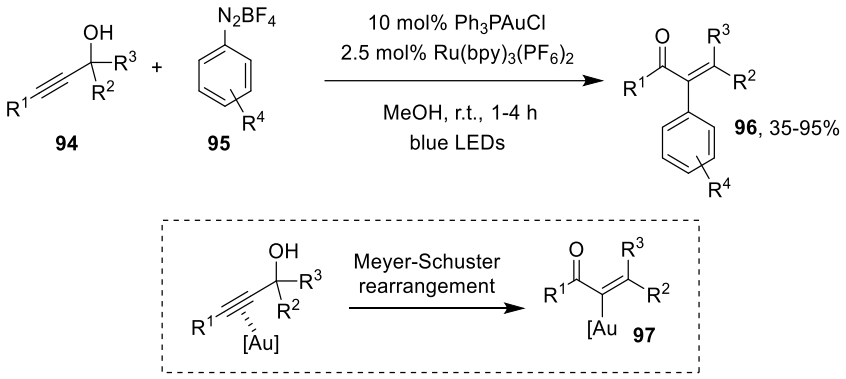

1.3.5 Gold/Chiral BrønstedAcidCatalysed Reactions

This section covers selected examples which includegold/chiral Brønsted acid catalysed transformations involving C-C and C-X bond forming cascade to obtain various heterocycles. Gong's research group reported synthesis of enantioenriched silyl containing polycyclic compounds by utilisation of gold and Brønsted acid (Scheme 13.5.1).[42] The reaction proceeded through gold-catalysed intramolecular hydrosilylation of enynylsilanol**98** to generate an active silyloxydiene intermediate **101** which would then involved in chiral Brønsted acid catalysed asymmetric Diels-Alder reaction with an electron deficient olefin **99** to afford polycyclic compounds **10**. Further isomerisation of **102** led into formation of enantioenriched polycyclic compounds **100**.

Scheme 1.3.5.1 Synthesis of enantiopure polycyclic compounds*via*gold/Brønsted acidcatalysis

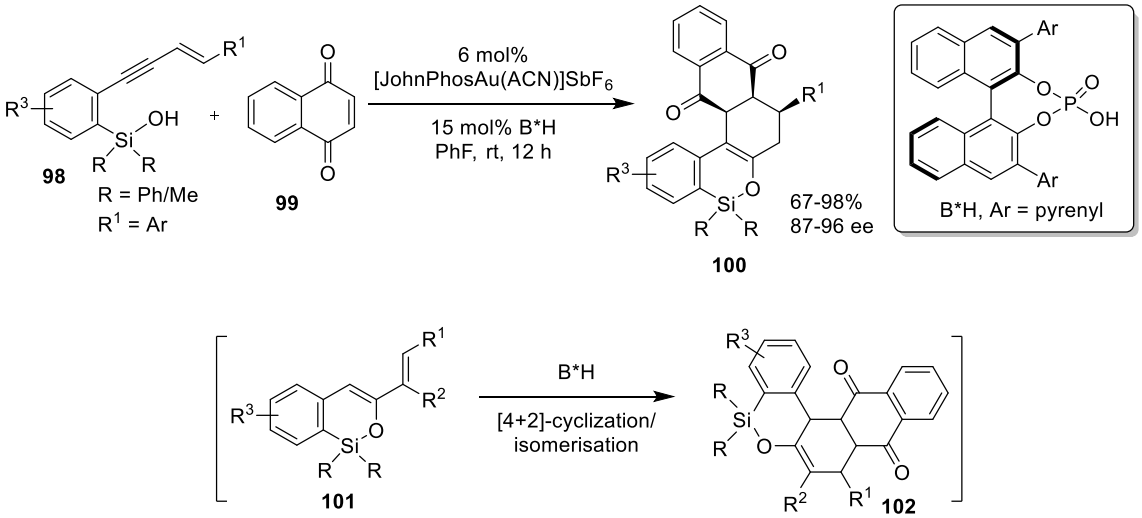

In 2013, Gong and co-workers reported the synthesis of enantiopure aromatic spiroacetals **105***via* gold(I)/Brønsted acid catalysed multi-component reaction between salicylaldehydes **103**, anilines and alkynols **104** (Scheme 1.3.5.2).[43] Exocyclic enol ether **106** andsalicylaldehydimines **107** underwentchiral Brønsted acid catalysedMannich-type reaction followed by acetalisation to access optically pure spiroacetals **105** through the oxonium intermediates**108**. However, generation of enol ether **106** andsalicylaldehydimines **107** was produced under gold andBrønsted acid catalysis respectively.

Scheme 1.3.5.2 Synthesis of enantiopurespiroacetals*via*gold/Brønsted acid catalysis

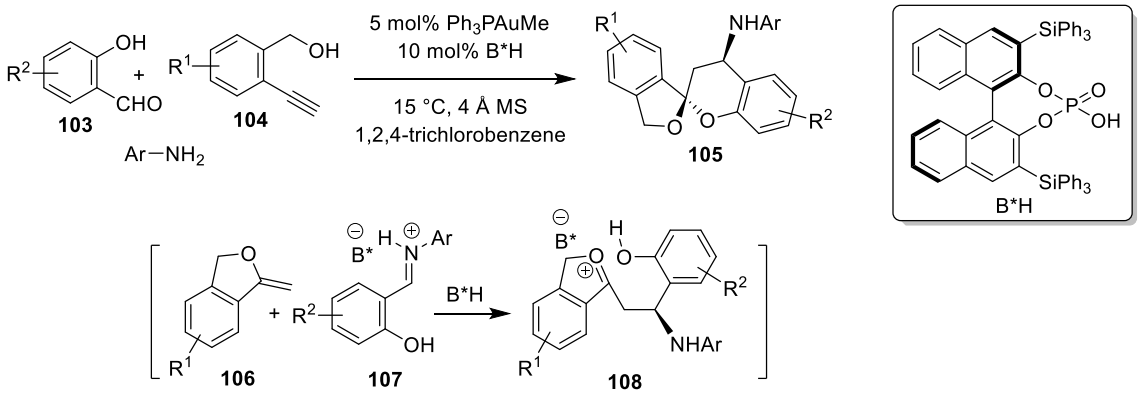

Fañanas, Rodríguez and co-workers reported gold/chiral Brønsted acid catalysed diastereo- and enantioselective synthesis of hexahydrofuro-quinolines **109** (Scheme 1.3.5.3).[44]The starting materials *viz.*alkynol, aldehyde, and aryl amine would underwent cascade reaction sequence of hydroalkoxylation/condensation/Povarov reaction to produce optically pure hexahydrofuro-quinolines **109**. The first step hydroalkoxylation would triggered by the gold catalyst whereas condensation and Povarov reaction was catalysed by the the chiral Brønsted acid.

Scheme 1.3.5.3 Synthesis of enantiopurespiroacetals*via*gold/Brønsted acid catalysis

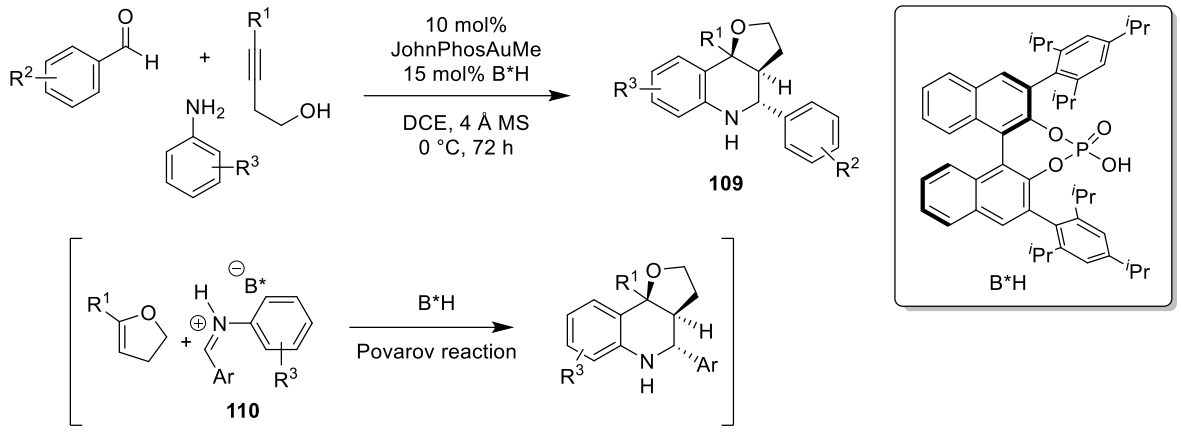

1.4 Conclusion

This chapter showshow gold catalysis in C-C and C-X cascade bond forming reactions is evolved from last decade. From this overview, it was clear that the field of gold catalysis is diverse, powerful and evolved significantly. The new families of reactions for the formation of C-C and C-X bond exhibits entirely new reactivity patterns which was previously unknown in the field of organometallic catalysis.

1.5 Reference

(1) (a)Patil N. T.; Kavthe, R. D.; ShindeV. S. *Tetrahedron***2012**, *68*, 8079.(b) Huang, H.; Zhou Y.; Liu H. *Beilstein J. Org. Chem.* **2011**,*7*, 897. (c) Hashmi, A. S. K.; Bührle, M. *Aldrichim. Acta***2010**, *43*, 27. (d) Vilhelmsen, M. H.; Hashmi, A. S. K. Gold-Catalyzed and Gold-Mediated Synthesis of Heterocycles. In PATAI's Chemistry of Functional Groups; John Wiley & Sons, Ltd: Chichester, U.K., **2009**.

(2) Zhang, J.; Schmalz, H.-G.*Angew.Chem., Int. Ed.* **2006**, *45*, 6704.

(3) Crone, B.; Kirsch, S. F. *J. Org. Chem.***2007**,*72*, 5435.

(4) X.-M. Zhang, Y.-Q.Tu, Y.-J.Jiang, Y.-Q.Zhang, C.-A.Fan and F.-M. Zhang, *Chem. Commun.***2009**, 4726.

(5) Nakamura, I.; Sato, T.; Yamamoto, Y. *Angew.Chem. Int. Ed.***2006**,*45*, 4473.

(6) Yang, T.; Campbell, L.; Dixon, D. J. *J. Am. Chem. Soc.***2007**, *129*, 12070.

(7) Krafft, M. E.; D. Vidhani, V. J.; Cran W.; Manoharan, M. *Chem. Commun.***2011**,*47*, 6707.

(8) Li, W.; Li, Y.; Zhou, G.; Wu X.; Zhang, J. *Chem.-Eur. J*. **2012**, *18*, 15113.

(9) Zhang, L.;Kozmin, S. A. *J. Am. Chem. Soc.***2005**, *127*, 6962.

(10) Yao, X.; Li, C.-J.*Org. Lett.***2006**, *8*, 1953.

(11) Zhang, Z.; Shi, M. *Chem.-Eur. J*. **2010**, *16*, 7725.

(12) Brand, J. P.;Chevalley, C.;Waser, J. *Beilstein J. Org. Chem.***2011**, *7*, 565.

(13) Zhang, G.; Huang, X.; Li, G.; Zhang, L. *J. Am. Chem. Soc.***2008**,*130*, 1814.

(14) Patil, N. T.; Mutyala, A. K.; Lakshmi, P. G. V. V; Raju, P. V. K.; Sridhar, B. *Eur. J. Org. Chem*. **2010**, 1999.

(15) Patil, N. T.; Raut, V. S.; Shinde, V. S.; Gayatri, G.; Sastry, G. N. *Chem. Eur. J.***2012**, *18*, 5530.

(16) Patil, N. T.; Lakshmi, P. G. V. V.; Singh, V. *Eur. J. Org. Chem.***2010**, 24, 4719

(17) Gade, A. B.;Patil, N. T. *Org. Lett.***2016**, *18*, 1844.

(18) Yeon, H.-S.; Lee, J.-E.; Shin, S. *Angew.Chem. Int. Ed.* **2008**, *47*, 7040.

(19) L. Peng, X. Zhang, S. Zhang and J. Wang, *J. Org. Chem.***2007**,*72*, 1192.

(20) Zhao, X.; Zhong, Z.; Peng, L.; Zhang W.; Wang, J. *Chem. Commun.***2009**, 2535.

(21) Shapiro, N. D.; Shi, Y.;Toste, F. D. *J. Am. Chem. Soc.***2009**,*131*, 11654.

(22) Wetzel, A.; Gagosz, F. *Angew.Chem. Int. Ed*.**2011**, *50*, 7354.

(23) Lu, B.;Luo, Y.; Liu, L.; Ye, L.; Wang, Y.; Zhang, L. *Angew. Chem. Int. Ed*.**2011**, *50*, 8358.

(24) Escribano-Cuesta, A.;López-Carrilo,V.; Janssen, D.; Echavarren, A. M. *Chem.-Eur. J*. **2009**, *15*, 5646.

(25) Kusama, H.; Miyashita, Y.; Takaya, J.;Iwasawa, N. *Org. Lett.***2006**, *8*, 289.

(26) For review, see: Davies, H. M. L.; Mortona, D. *Chem. Soc. Rev.***2011**, *40*, 1857.

(27) For review, see: (a) Zhu, S.-F.; Zhou, Q.-L.; *Acc. Chem. Res.***2012**, *45*, 1365. (b) Zhao, X.; Zhang, Y.; Wang, J. *Chem. Commun.***2012**, *48*, 10162.

(28) (a) Liu, L.; Zhang, J. *Chem. Soc. Rev*.**2016**, *45*, 506. (b) Fructos, M. R.; Díaz-Requejo, M. M.; Peréz, P. J. *Chem. Commun*. **2016**, *52*, 7326. (c) Fructos, M. R.; Belderrain, T. R.;

de Frémont, P.; Scott, N. M.; Nolan, S. P.; Díaz-Requejo, M. M.; Pérez, P. J. *Angew. Chem*. **2005**, *117*, 5418.

(29) Lonzi, G.; Lopez, L. A. *Adv. Synth.Catal*.**2013**, *355*, 1948.

(30) Pagar, V. V.;Jadhav A. M.; Liu, R.-S.*J. Am. Chem. Soc.***2011**, *133*, 20728.

(31) Neupane, P.; Xia, L.; Lee, Y. R. *Adv. Synth.Catal*.**2014**, *356*, 2566.

(32) Pagar,V. V.; Liu, R.-S.*Angew.Chem. Int. Ed*. **2015**, *54*, 4923.

(33) (a) Qiu, D.; Zheng, Z.; Mo, F.; Xiao, Q.; Tian, Y.; Zhang, Y.; Wang, J. *Org. Lett.* **2011**, *13*, 4988.(b) Brenzovich, Jr., W. E.; Brazeau, J.-F.; Toste, F. D. *Org. Lett.* **2010**, *12*, 4728.(c) Peng, Y.; Cui, L.; Zhang, G.; Zhang, L. *J. Am. Chem. Soc.* **2009**, *131*, 5062.(d) Kar, A.; Mangu, N.; Kaiser, H. M.; Beller, M.; Tse, M. K. *Chem. Commun*. **2008**, 386.

(34) Zhang, G.; Peng, Y.; Cui, L.; Zhang, L. *Angew.Chem. Int. Ed.* **2009**, *48*, 3112.

(35) Zhang, G.; Cui, L.; Wang, Y.; Zhang, L. *J. Am. Chem. Soc*. **2010**, *132*, 1474.

(36) Brenzovich, W. E.; Benitez, D.; Lackner, A. D.; Shunatona, H. P.; Tkatchouk, E.; Goddard III, W. A.; Toste, F. D. *Angew. Chem. Int. Ed*. **2010**, *49*, 5519.

(37) Hopkinson, M.; Tessier, A.; Salisbury, A.; Giuffredi, G.; Combettes, L.; Gee, A.; Gouverneur, V. *Chem. -Eur. J*.**2010**, *16*, 4739.

(38) Selected reviews: (a) Hopkinson M. N.; Gee A. D.; Gouverneur V. *Chem. - Eur. J.* **2011**, *17*, 8248. (b) Wegner H. A.; Auzias M. *Angew. Chem. Int. Ed.* **2011**, *50*, 8236.

(39) Sahoo, B.; Hopkinson, M. N.; Glorius, F. *J. Am. Chem. Soc.* **2013**, *135*, 5505.

(40) Xia, Z.; Khaled, O.; Mouriès-Mansuy, V.; Ollivier, C.; Fensterbank, L. *J. Org. Chem.* **2016**, *81*, 7182.

(41) Um, J.; Yun, H.; Shin, S. *Org. Lett.***2016**, *18*, 484.

(42) Han, Z.-Y.; Chen, D.-F.; Wang, Y.-Y.; Guo, R.; Wang, P.-S.; Wang, C.; Gong, L.-Z. *J. Am. Chem. Soc.*,**2012**, *134*, 6532.

(43) Wu, H.; He, Y.-P.; Gong, L.-Z.*Org. Lett.*,**2013**, *15*, 460.

(44) Calleja, J.; Alvarez, R.;Gónzalez-Pérez, A. B.; de Lera, A. R.; Alvarez, R.;Fañanas, F. J.; Rodríguez, F.;*Chem. Sci.*, **2014**, *5*,996.

Chapter 2: Utilization of Gold(I)/Chiral Brønsted Acid Binary Catalytic System in Combinatorial Chemistry

Table of Contents

2.1 Introduction 26

2.2 Hypothesis 36

2.3 Results and Discussion 37

2.4 Conclusion 45

2.5 Experimental Procedures 46

2.5.1 Procedure for Preparation of Scaffold Building Agents (SBAs) 46

2.5.2 Procedure for Preparation of Alkynols 46

2.5.3 General Procedure for Enantioselective Combinatorial Synthesis 46

2.6. Characterization Data, HPLC Chromatograms and NMR Spectra of Final Products 48

2.7 References 93

2.1 Introduction

Although transition metal catalysis and organo-catalysis hold their individual importance in modern organic chemistry, merging transition metal catalysts and organocatalysts for developing new reactions serve as a powerful tool in organic synthesis. The reactivity observed in such metal/organo dual catalysis is unique and can provide selectivity of the reaction otherwise not possible by use of either of the catalytic systems alone. This organo/metal combined catalysis has gained great attention for their potential use in synthesising highly complex molecules because of several advantages as mention bellow.

(1) It can create or improve the enantioselectivity where stereochemical control was previously absent or challenging

(2) It provides more options towards making the product chiral such as using a single chiral catalyst or both catalysts chiral

(3) If a metal catalyst and an organo-catalyst are able to triger the reactions individually, an asymmetric relay catalytic reaction can be developed with either or both chiral catalysts controlling the stereochemistry

In addition to these remarkable advantages, merging organo- and transition metal catalysis has its limitation, since it suffers from some perceived challenges. Unlike the biological processes, where nature takes advantage of enzyme architecture to facilitate a multiple reaction manifold, it is very difficult to exploit on such process in a flask. The challenge in capitalizing in such reactions is to find suitable catalyst combinations and therefore the main requirements are that either catalyst should not interact with each other and therefore retain individual identities. The key to overcome this challenge is the judicious selection of appropriate catalyst combinations which are compatible with each other and reaction conditions.

Merging Gold- and Brønsted Acid Catalysis:

As discussed in the chapter 1, homogenious gold catalysis[1] has tremendous growth in accessing highly challenging molecular structures based on its alkynophilicity as a carbophilic Lewis acid. This intrinsic π-activation property of gold catalysis has shown remarkable progress in gold catalysed transformations involving C-C and C-X bond forming cascades. In addition, gold complexes are air- and moisture-tolerant, this special feature of gold catalyst makes its co-operation viable with chiral organocatalyst which would enhance its potential towards asymmetric catalysis.

Traditionally, transition-metal catalysed enantioselective transformations rely on chiral ligands tightly bound to the metal in order to induce chirality. The development of enantioselective transformation using gold(I)-catalysis; however, is challenging because gold complexes posseses linear geometries (which makes the chiral ligand distant from substrate),[2] rendering transfer of chiral information difficult (Figure 2.1.1 A). To circumvent this problem, a clever solution was proposed by Toste's group[3] based on the principle of ion-pairing.[4] This alternative approach takes advantage of the fact that gold(I) catalysts are positively charged. Therefore, the use of a negative charged chiral counter-ion would be in proximity to the substrate and would possibly be more efficient in inducing enantioselective transformations (Figure 2.1.1 B).

Figure 2.1.1: Unique geometry of Au(I)-complexes (A) and possible intervention of a chiral counter-ion (B)

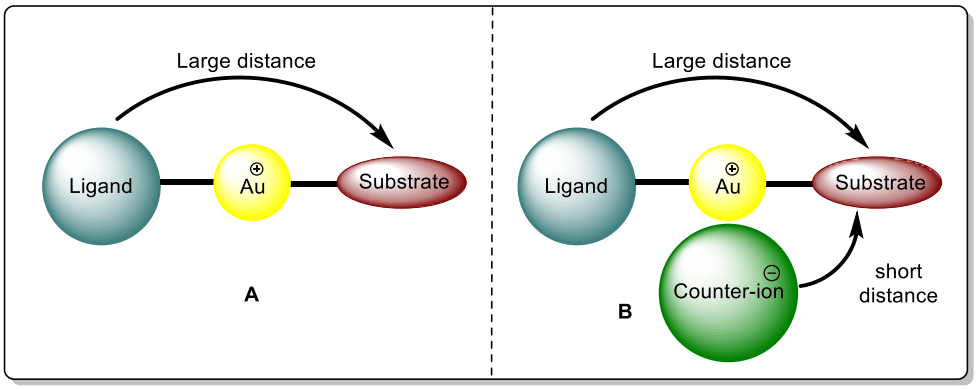

Merging gold/Brønsted acid catalysis has shown to catalyse variety of enantioselective transformations involving C-C multiple bonds with unparalleled mildness and selectivity. There are many reports that describe this chemistry which also has been documented in the form of reviews, the few distinct examples of an enantioselective processes that utilizes achiral Au-complexes and chiral binol phosphoric acids as catalysts are discussed below.

In 2007, Toste and coworkers reported intramolecular hydroalkoxylation of allenol to produce tetrahydropyran derivative by utilizing chiral gold phosphate (LnAuB), prepared from LnAuCl and silver phosphate AgB (Scheme 2.1.1, eq. 1).[5] The silver phosphate was conveniently prepared by reaction of chiral Brønsted acids and Ag_2O. In this case, hydro-alkoxylation of allenol was catalysed by the gold phosphate. Polarity of the solvent was proved to be an crucial to obtain the products with good enantioselectivity. More-polar solvents, such as nitromethane or acetone, gave significantly lower enantiomeric excess values (Scheme 2.1.1, eq.

1). However, the less-polar benzene proved to be the optimal medium, providing the desired product in an exceptional 97% ee. Similar strategy was employed for the hydrocarboxylation reaction of allene tethered carboxylic acid to obtain enantio-pure lactone (Scheme 2.1.1, eq. 2). A strong matched–mismatched pairing effect between ligands and counter-ions was observed. The mismatched combination (*R*)-L-$(AuCl)_2$/Ag(*R*)-TRIP provided a nearly racemic product; on the other hand a combination of (*S*)-L-$(AuCl)_2$/Ag(*R*)-TRIP gave lactone with 82% ee. This revealed that both the chiral ligand and chiral counter-ion was obligatory to obtain the products with good enantioselectivities (up to 97% ee). On the other hand, use of a single chiral ligand on gold center gives the product with poor enantioslectivities. The concept was further extended for the hydro-amination of allene tethered sulfonamides to afford the cyclic-sulfonamides in good yields with high level of ee's (Scheme 2.1.1, eq. 3).

Scheme 2.1.1: Chiral Au-phosphate catalysed enantioselective hydroalkoxylations hydrocarboxylations and hydroaminations

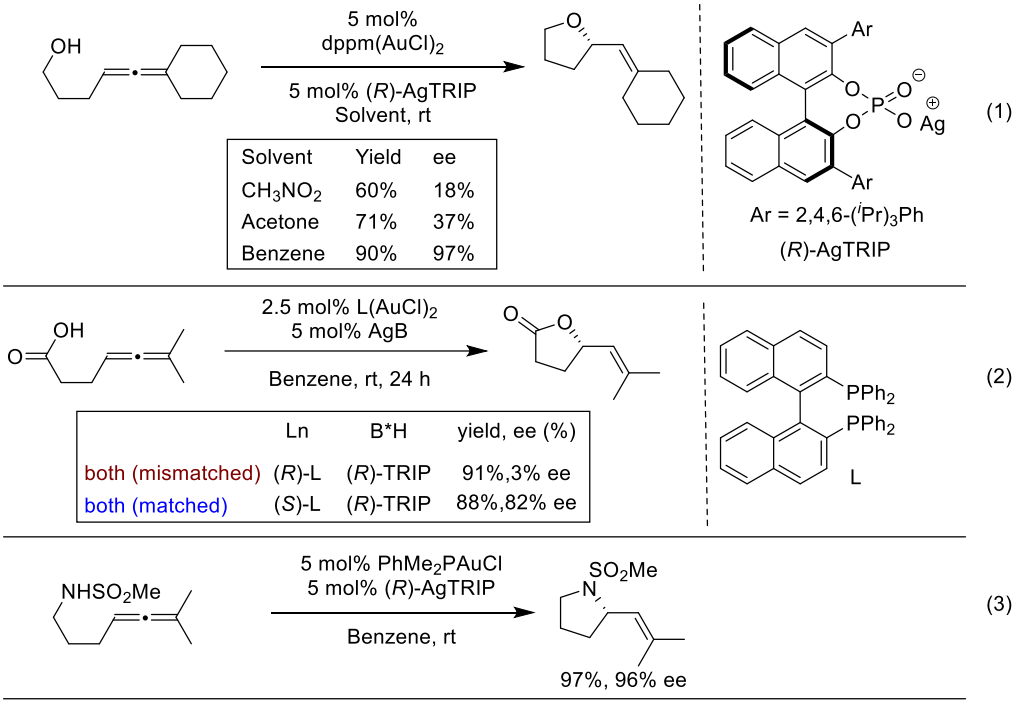

Following this report by Toste and coworkers in the field of merging Au(I) and chiral Brønsted acid catalysis, several research groups has successfully implemented this concept to access variety of enantiopure heterocyclic scaffolds.

In early 2009, Gong and coworkers reported gold (I)/chiral Brønsted acid catalysed synthesis of tetrahydroquinolines *via* consecutive hydroamination/enantioselective transfer hydrogenation between *ortho*-aminoalkyne and Hantzsch ester (Scheme 2.1.2).[6] In this reaction, 1,4-dihydroquinoline generated through hydroamination of *ortho*-aminoalkyne underwent isomerisation to form 3,4 dihydroquinoline. This 3,4 dihydroquinoline after reaction with Hantzsch ester further converted into tetrahydroquinolines by enantioselective transfer hydrogenation. In reaction sequence, hydroamination reaction was triggered by the gold phosphate, while enantioselective transfer hydrogenation process was catalysed by the chiral Brønsted acid. Controlled studies revealed that enantioselectivity of the products was completely governed by the chiral Brønsted acid.

Scheme 2.1.2: Gold/chiral Brønsted acid catalysed synthesis of optically pure fused 1,2-dihydroisoquinolines

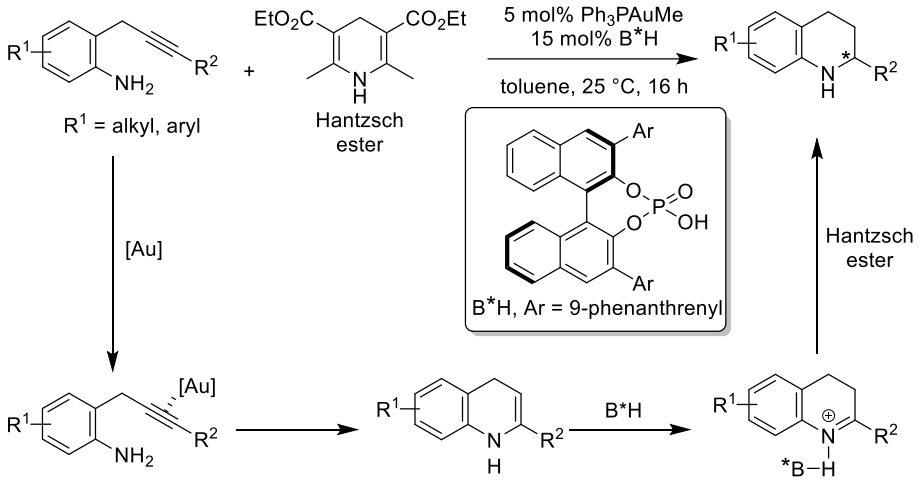

Che and coworkers utilised analogous strategy to access enantiopure secondary amines employing consecutive hydroamination/transfer hydrogenation cascade. They reported gold (I)/chiral Brønsted acid catalysed synthesis of secondary amines from terminal alkynes and aromatic amines *via* inter-molecular hydroamination followed by enantioselective transfer hydrogenation in good to excellent yields and ee's (Scheme 2.1.3).[7] The reaction proceeded through gold phosphate catalysed inter-molecular hydroamination to generate the iminium salt that subsequently underwent enantioselective transfer hydrogenation to afford secondary amines in good yields and ee's.

Both these report by Gong and Che showed that active catalytic species in the reaction was chiral gold phosphate (generated in situ *via* reaction of the catalyst LnAuMe and chiral

Brønsted acid) and the excess chiral Brønsted acid. Hence, the possibility of formation of residual achiral Brønsted acid (such as TfOH in the case of LnAuOTf), which could be the culprit for background reactions, does not exist. The reports by Gong and Che has led good foundation for preparation of chiral gold phosphate in one-pot in contrary to Toste's procedure[5] wherein two step process was required.

Scheme 2.1.3: Gold/chiral Brønsted acid catalysed intramolecular hydroamination /hydrogenation cascades

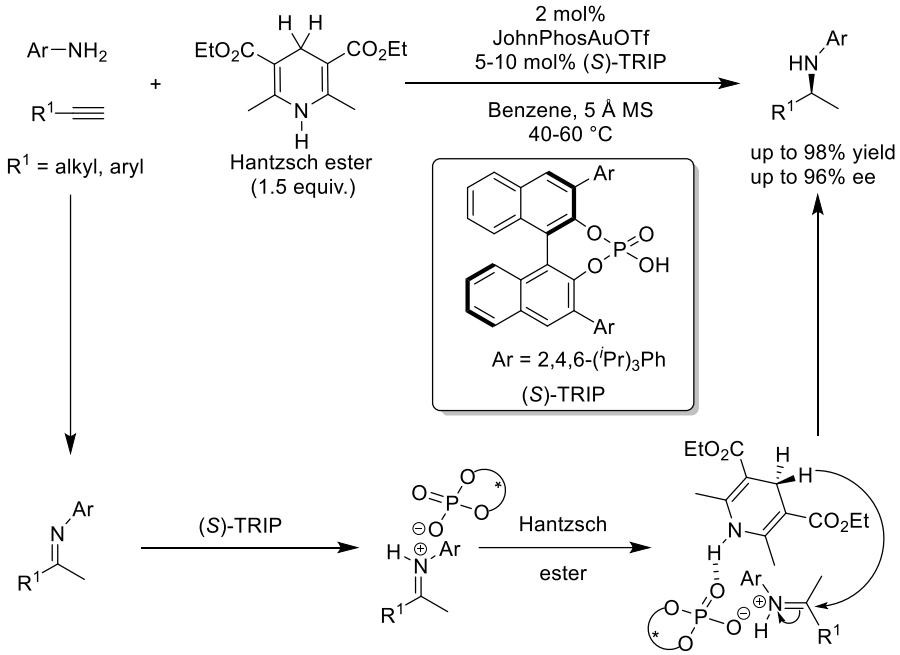

In the same year, Dixon *et al*. reported Au(I)/chiral Brønsted acid-catalysed synthesis of enantiopure polycyclic indole derivatives *via* reaction between tryptamine and alkynoic acids tethered with carboxylic group (Scheme 2.1.4).[8] Mechanistically, alkynes tethered with carboxylic group underwent Au(I)-catalysed 5-*endo-dig* cyclization to form five membered enol lactones which subsequently reacted with amine moiety of tryptamine to form isolable keto-amide intermediate. This keto-amide transformed into *N*-acyliminium intermediate which was further attacked by the appended indole moity (Pictect-Spengler type reaction) under the chiral environment of Brønsted acid to provide the enantiopure tetracyclic heterocyclic compounds in good yields and ee's.

Scheme 2.1.4: Gold/chiral Brønsted acid catalysed iminium cascades

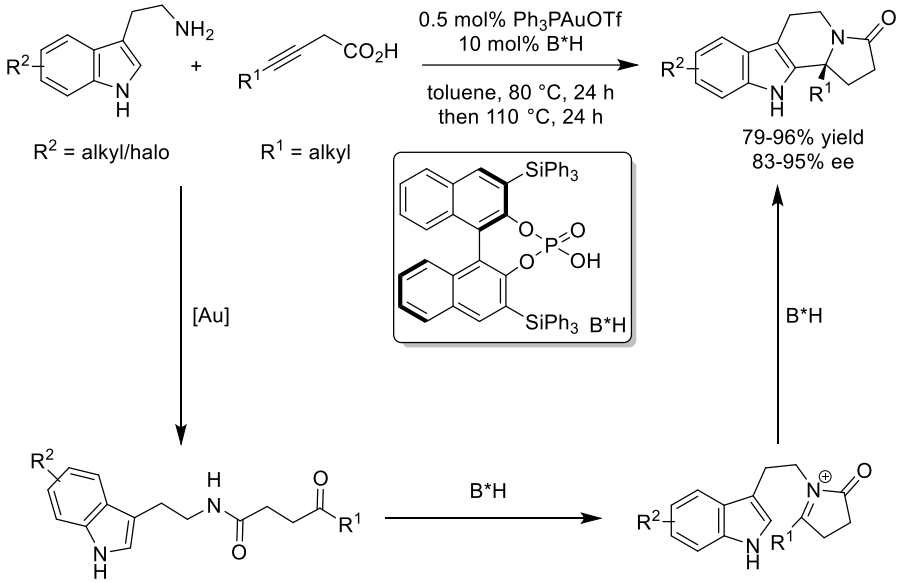

In 2010, Gong and co-workers utilised Au(I) and chiral Brønsted acid catalysed consecutive sequence of [4+2] cyclization/hydroamination/reduction to access optically pure julolidine derivatives (Scheme 2.1.5). The sequence was started with generation of iminium intermediates by condensation of aldehydes and *ortho*-propargylic anilines under the effect of Brønsted acid. This electron deficient iminium intermediates underwent Brønsted acid-catalysed [4+2] Povarov type reaction with the enamine to generate enantiopure amino-alkyne which subsequently underwent intramolecular hydromination catalysed by a gold phosphate. The stable julolidine derivatives were isolated after reduction with AcOH/NaBH(OAc)$_3$.

Scheme 2.1.5: Gold/chiral Brønsted acid catalysed cascade reaction for the synthesis of julodiline derivatives

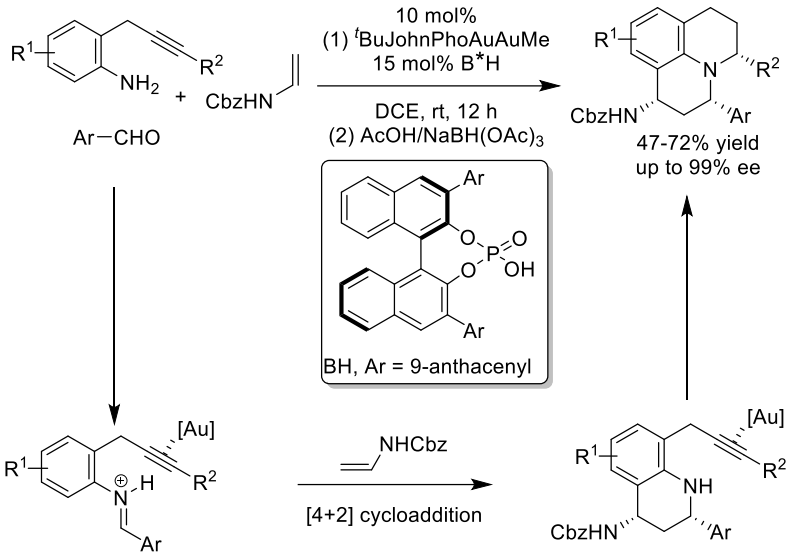

Another example of Au(I)/Brønsted acid binary catalysis demonstrated by Gong's group that allows synthesis of structurally challenging compounds that contained vicinal quaternary centres (Scheme 2.1.6). They disclosed the utility of the Au(I)/chiral Brønsted acid catalyst system for the synthesis of conformationally restricted amino acid precursors bearing vicinal quaternary stereogenic centers by the reaction of alkynols with azalactone (Scheme 2.1.6).[9] The reaction proceeded through Au-catalysed intramolecular hydroalkoxylation to obtain cyclic enol ether which after protonation by the Brønsted acid catalyst gave corresponding oxonium ion. This oxonium ion was trapped by the azalactone under chiral environment of Brønsted acid to furnish product.

Scheme 2.1.6: Gold/chiral Brønsted acid catalysed cascade reaction for the creation of vicinal quaternary centers

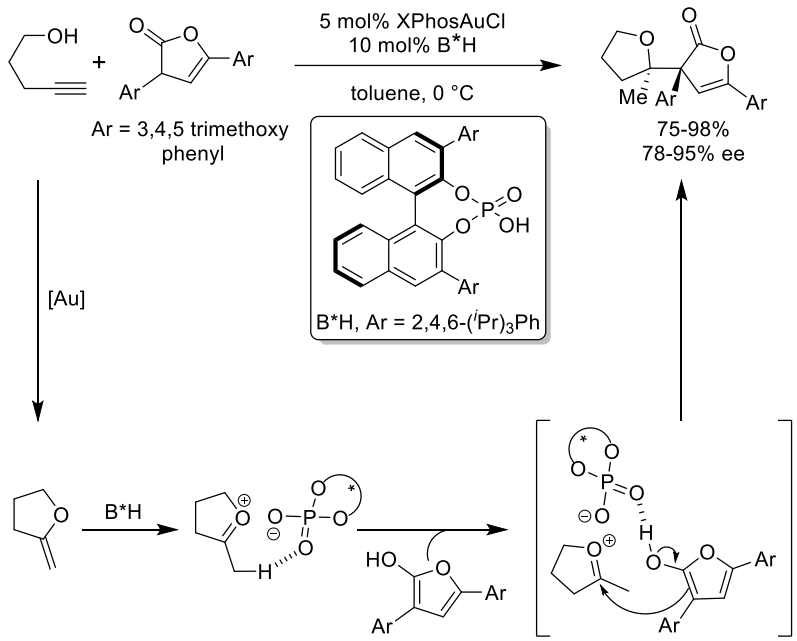

In this context our group developed an example of Au(I)/Brønsted acid binary catalysis to access Enantiopure 1,2-dihydroisoquinolines (Scheme 2.1.7).[10] 2-aminobenzamides and 2-alkynyl benzaldehydes reacted under gold/chiral Brønsted Acid to afford 1,2-dihydroisoquinolines with excellent enantioselectivities. Mechanisticaly, these two starting materials underwent chiral Brønsted acid[11] catalysed condensation reaction to obtain chiral aminals, which after 6-*endo dig* cyclization with appended alkyne afforded optically pure fused 1,2-dihydroisoquinolines.

Scheme 2.1.7: Gold/chiral Brønsted acid catalysed synthesis of optically pure fused 1,2 dihydroisoquinolines

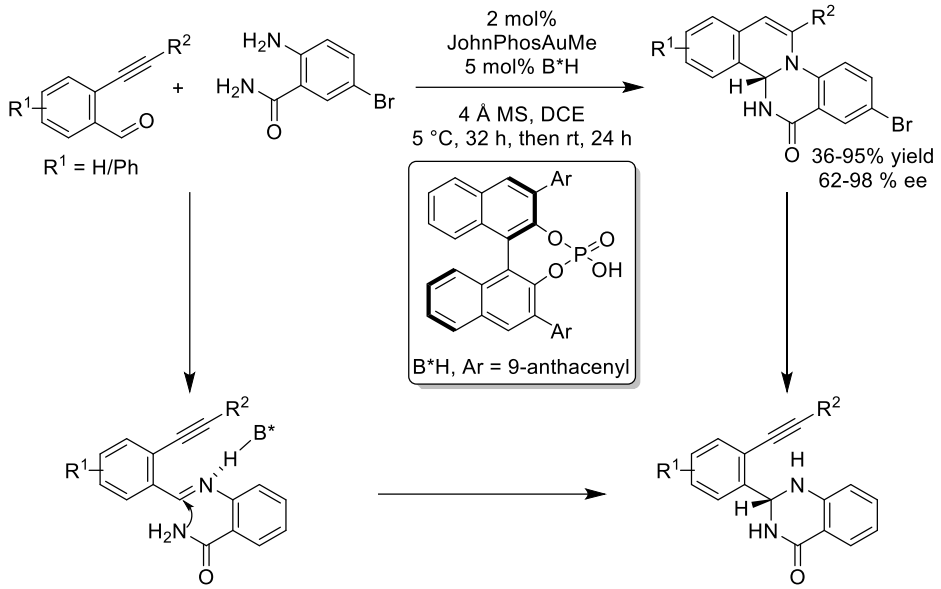

In continuation, we developed an ternary catalytic system consisting of Au(I), *p*-anisidine and chiral Brønsted acid which enabled a stereo-controlled synthesis of 2-substituted tetrahydroquinolines (Scheme 2.1.8).[12] Mechanistically, reaction between 2-amino benzaldehydes and terminal alkynes under the effect of gold and *p*-anisidine afforded quinoline. This quinoline was reduced with Hantzsch ester under chiral Brønsted acid catalysis to obtain enantiopure 2-substituted tetrahydroquinolines. To know the role of each catalyst the authors performed several controlled experiments, which shows that all three catalysts *p*-anisidine, Brønsted acid, gold phosphate (generated *in situ* from Au-catalyst and B*H) were necessary to obtain 2-substituted quinolines while enantioselective transfer hydrogenation was solely monitored by the chiral Brønsted acid to afford 2-substituted tetrahydroquinolines.

Scheme 2.1.8: Gold(I)/*p*-anisidine/chiral Brønsted acid ternary catalysts system for synthesis of 2-substituted tetrahydroquinolines

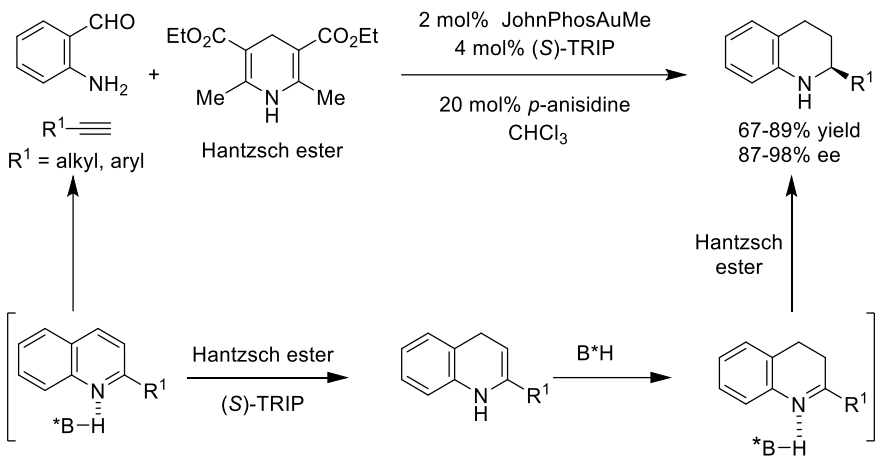

In 2015, our research group developed highly enantioselective hydroamination-hydroarylation cyclization cascade for the synthesis of enantiopure pyrrolo embedded heterocyclic scaffolds under the catalysis of Au(I)/Brønsted acid (Scheme 2.1.9).[13] Hydroamination of alkynes with amino-aromatics would occur by the Au(I) catalyst to form imine intermediates which would undergo intra-molecular attack by the tethered aromatics under the effect of chiral Brønsted acid to produce an optically pure pyrrole-based aromatic amines. The control experiments had been performed carefully which led us to conclude that the –OH group in alkyne was essential for the reaction to provide good yields and ee's. The method was very general and worked well over a range of three pyrrole-based amino-aromatics and therefore may open various unprecedented opportunities.

Scheme 2.1.9: Gold(I)/chiral Brønsted acid catalysed hydroamination-hydroarylation

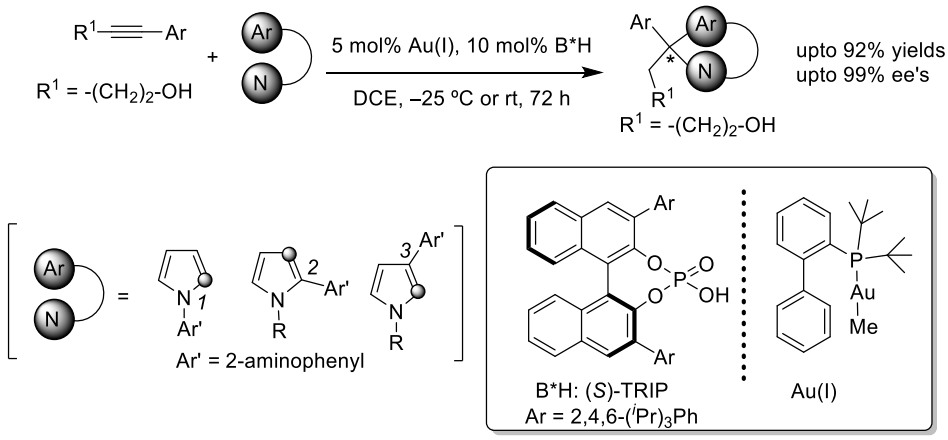

Based on these reports, it was decided to explore these gold/chiral Brønsted acid catalysed methods in the combinatorial chemistry genre to access library of multiply fused-heterocyclic scaffolds with high optical purity in one-pot. Out of these aforementioned gold/chiral Brønsted acid catalysed approaches, hydroamination-hydroarylation reaction developed by our group (scheme 2.1.3) was found to be robust which worked for the range of pyrrol-based amino aromatics.

Table no. 2.1.1: Robustness screen for enantioselective hydroamination-hydroarylation of alkynes

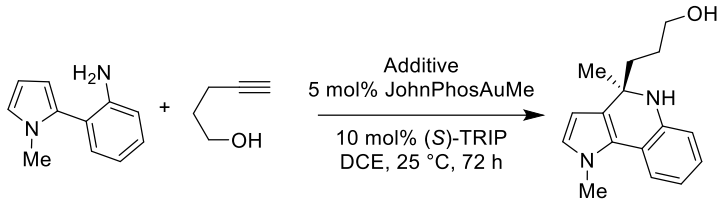

Entry	Additive	Yields/ee's	Additive remaining (%)
1	-	83/98.5	-
2	Benzyl amine	78/93.3	>95
3	Aniline	76/95.3	>95
4	Phenol	81/91.1	100
5	Benzyl alcohol	71/96.5	100

Our preliminary results on the robustness screen [4] of the hydroamination-hydroarylation reaction between amino aromatics (SBAs) and alkynols under the catalysis of (R_3P)-Au-Me[14]/(*S*)-TRIP[15] binary catalysis system[16] revealed that the outcome of the reaction was not dependent on the external aromatic amines and alkynols (Table no. 2.1.1). These observations encouraged us to develop gold/chiral Brønsted acid catalysed enantioselective combinatorial approach for rapid generation of optically pure heterocyclic scaffolds in one-pot.

2.2 Hypothesis

The field of asymmetric catalysis has grown rapidly making impacts almost in all disciplines of science, especially in healthcare. However, there is no single optimal catalyst

available which work over the broad range of substrates. This is due to the fact that the enantio-determining transition state is highly sensitive to steric and electronic nature of substituents present in the substrates. Obviously, such a kind of transition state could easily be perturbed by the additional molecules present in the reaction mixture, causing poor enantio-induction. Consequently, the robustness screen which is relatively easier to adopt in the synthesis of racemic compounds[17] is difficult to extend for enantioselective versions.[18] This may be the reason why the use of enantioselective catalysis has not yet been reported in combinatorial chemistry.

It was envisioned that the alkynols **B** would react with various scaffold building agents (SBAs) $\mathbf{A_1}$, $\mathbf{A_2}$, $\mathbf{A_3}$...$\mathbf{A_n}$ under Au(I)/chiral Brønsted acid binary catalyst system[19] to give $\mathbf{A_1B^*}$, $\mathbf{A_2B^*}$, $\mathbf{A_3B^*}$...$\mathbf{A_nB^*}$ (Fig 2.2.1). Similarly, SBAs **A** would react with various alkynols $\mathbf{B_1}$, $\mathbf{B_2}$, $\mathbf{B_3}$...$\mathbf{B_n}$ under the same reaction condition to produce $\mathbf{AB_1^*}$, $\mathbf{AB_2^*}$, $\mathbf{AB_3^*}$...$\mathbf{AB_n^*}$. The successful realization of the proposed hypothesis was supposed to be dependent on the tolerance to chemical functionalities present in the various substrates. Although, the development of enantioselective catalysis in the past two decades has been remarkably rapid, no such approach has been reported in the literature.

Scheme 2.2.1: Gold/chiral Brønsted acid catalysed enantioselective combinatorial approach – A concept

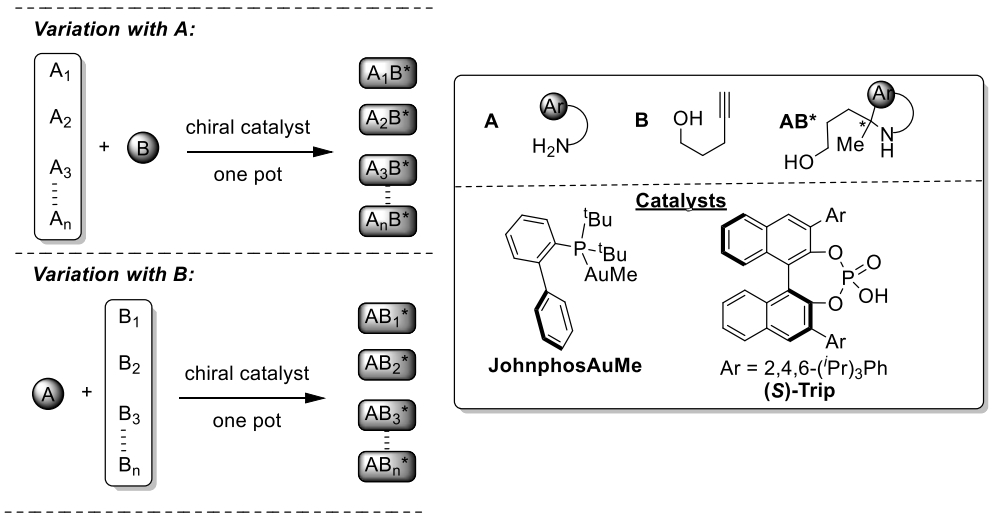

2.3 Results and Discussion

Unless otherwise specified, all reactions were carried out in oven dried vials or reaction vessels with magnetic stir bar under argon atmosphere. Dried solvents and liquid reagents were

transferred by oven-dried syringes cooled to ambient temperature in a desiccator. All experiments were monitored by analytical thin layer chromatography (TLC). TLC was performed on pre-coated silica gel plates. After elution, plate was visualized under UV illumination at 254 nm for UV active materials. Further visualization was achieved by staining with $KMnO_4$ and charring on a hot plate. Solvents were removed *in vacuo* and heated in a water bath at 35 °C. Silica gel finer than 200 mesh was used for flash column chromatography. Columns were packed as slurry of silica gel in hexane and equilibrated with the appropriate solvent mixture prior to use. The compounds were loaded neat or concentrated solution using the appropriate solvent system. The elution was assisted by applying pressure with an air pump. Melting points are uncorrected and recorded using digital Buchi Melting Point Apparatus B-540. The ^{1}H NMR spectra and ^{13}C NMR spectra were recorded on Bruker AV, 200/400/500, JEOL 400 MHz spectrometers in appropriate solvents using TMS as an internal standard or the solvent signals as secondary standards and the chemical shifts are shown in δ scales. Multiplicities of ^{1}H NMR signals are designated as s (singlet), brs. (broad singlet), d (doublet), dd (doublet of doublet), ddd (doublet of doublet of doublet), t (triplet), m (multiplet) etc. HRMS (ESI) data were recorded on a Thermo Scientific Q-Exactive, Accela 1250 pump. Optical rotation was measured with a JASCO P 2000 digital polarimeter at room temperature using 50 mm cell of 1 mL capacity. HPLC analysis was performed on Agilent 1290 Infinity LC. The gold catalyst Johnphos-AuMe were prepared following literature known procedures. All racemic compounds were synthesized using Johnphos-AuCl (5 mol%), AgOTf (5 mol%) in DCE (Reaction time = 24 h).

Scope of the Reaction

With the optimized condition (10 mol% (*S*)TRIP, DCE, rt, 72 h) developed for hydroamination/hydroarylation protocol,[12] We began our initial studies by reacting SBA with various alkynols. At first, pyrrol-2-yl aniline SBA **1a** was reacted with 4-pentyn-1-ol (**2a**) and 4-phenylbut-3-yn-1-ol (**2b**) in presence of 5 mol% Johnphos-AuMe in combination with 10 mol% (*S*)-TRIP under standard conditions.[14] Pleasingly, a corresponding mixture of products pyrrolo quinoxalines **3aa** and **3ab** was obtained in 80 and 52% yields with 86.2 and 86.9% enantiomeric excess (ee) respectively (Table 2.3.1.1, entry 1). When 2-aminophenyl pyrrole SBA **1b** was reacted with a mixture of 4-pentyne-1-ol (**2a**) and alkynol **2c**, a mixture of dihydropyrolo

quinolines **3ba** (83.5% ee) and **3bc** (82.3% ee) was obtained in 72 and 65% yields, respectively (entry 2). Similarly, dihydropyrolo quinolines **3be** and **3bf** were obtained in 56 and 73% yields in good ee's by employing **1b** and **2e/2f** as starting materials (entry 3). As shown in entry 4, dihydropyrolo quinolines **3ca** (70%) and **3cb** (60%) were produced in excellent ee's when 3-(2-aminophenyl)pyrrole SBA **1c** reacted with a mixture of **2a** and **2b.**

Table 2.3.1.1: Variation of SBAs/alkynols – three components in one-pot

Entry no.	SBA	Alkynols	Products
1[a,d]	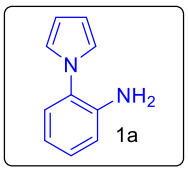	**2a** 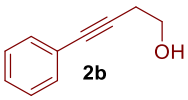 **2b**	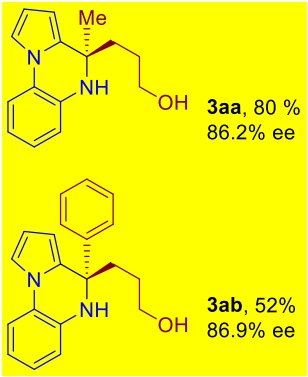 **3aa**, 80 % 86.2% ee **3ab**, 52% 86.9% ee
2[a,c,d]	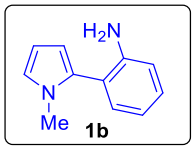	**2a** 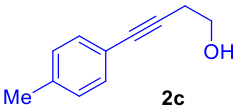 **2c**	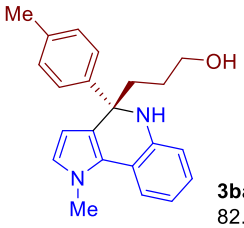 **3ba**, 65% 82.3% ee 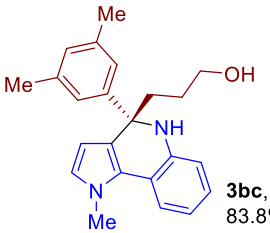 **3bc**, 56% 83.8% ee

3[a,c,d]	**1b**	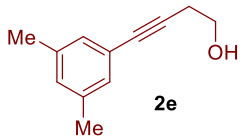 **2e** 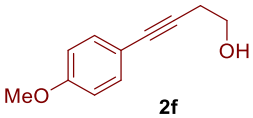 **2f**	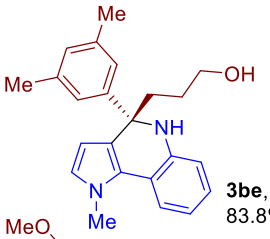 **3be**, 56% 83.8% ee 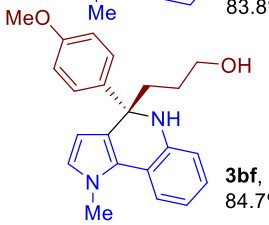 **3bf**, 73% 84.7% ee
4[a,d]	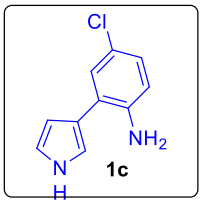 **1c**	**2a** 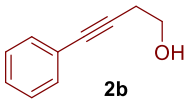 **2b**	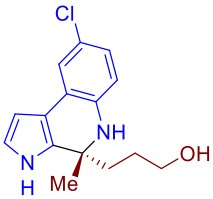 **3ca**, 70% 84.0% ee 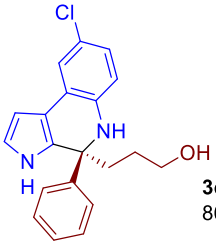 **3cb**, 60% 86.5% ee
5[b,e]	**2a**	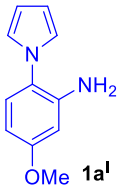 **1a^{I}** 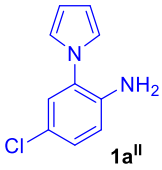 **1a^{II}**	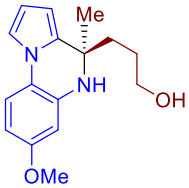 **3a^{I}a**, 87% 92.9% ee 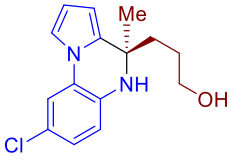 **3a^{II}a**, 52% 81.0% ee

6[b,e]	**2a**	**1a^{I}** 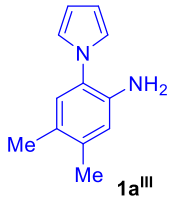 **1a^{III}**	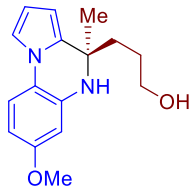 **3a^{I}a**, 64% 92.5% ee 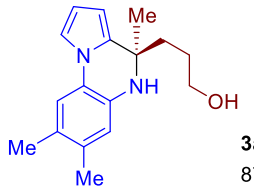 **3a^{III}a**, 73% 87.2% ee
7[b,c,e]	**2a**	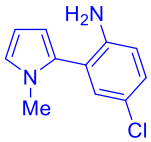 **1b^{I}** 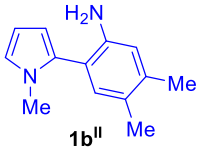 **1b^{II}**	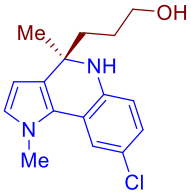 **3b^{I}a**, 63% 81.0% ee 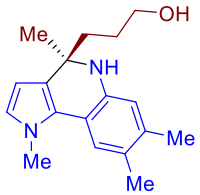 **3b^{II}a**, 72% 84.5% ee
8[b,e]	**2a**	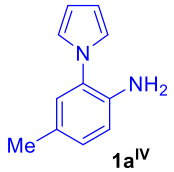 **1a^{IV}** 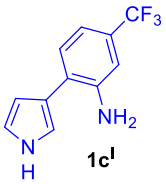 **1c^{I}**	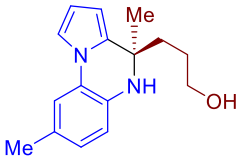 **3a^{IV}a**, 73% 86.1% ee 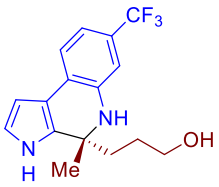 **3c^{I}a**, 76% 91.0% ee

Reaction conditions: 5 mol% Johnphos-AuMe, 10 mol% (S)-TRIP, DCE (0.075 M), -25 °C, 3 d. [a]0.30 mmol 1, 0.30 mmol 2 (1:1 mole ratio). [b]0.30 mmol 1 (1:1 mole ratio). 0.30 mmol 2. [c]Reaction was performed at rt. All were isolated yields and ee's were determined by HPLC analysis on a chiral stationary phase. [d]Yield was based on alkynol. [e]Yield was based on SBAs.

Next, the scope was evaluated by varying SBAs keeping alkynol as a stationary. Gratifyingly, when alkynol **2a** was treated with the mixture of 2-aminophenyl pyrrole SBAs **1a^{I}** and **1a^{II}** (entry 5) and a mixture of **1a^{I}** and **1a^{III}** (entry 6), pyrrolo quinoxalines **3a^{I}a**/**3a^{II}a** and **3a^{I}a**/**3a^{III}a** in varying amounts of yields (ee's = 81.0 → 92.9%) were obtained. Similarly, a mixture of pyrrol-2-yl anilines SBAs **1b^{I}** and **1b^{II}** reacted with alkynol **2a** to afford **3b^{I}a** (63%) and **3b^{II}a** (72%) with 81.0 and 84.5% ee's, respectively (entry 7). Further, as expected, a mixture of SBAs **1a^{IV}** and **1c^{I}** on treatment with alkynol **2a** gave pyrrolo quinoxaline **3a^{IV}a** and dihydropyrolo quinoline **3c^{I}a** in 73 and 76% yields with excellent ee's (entry 8).

Next, the substrate scope of the present enantioselective approach was further evaluated by keeping one of the reactant stationary and varying three other reactants (2.3.1.2). For instance, a mixture of alkynols **2a**, **2c** and **2d** were allowed to react with 2-aminophenyl pyrrole SBA **1b** in the presence of 10 mol% Johnphos-AuMe in combination with 20 mol% (*S*)-TRIP for slighly extended period of time (4d). Various optically active aza-heterocyclic scaffolds **3ba**, **3bc** and **3bd** were obtained in good yields and excellent ee's (entry 1). Similarly, alkynol **2a** on reaction with SBAs **1a^{I}**, **1b^{II}** and **1c^{I}** gave pyrrollo quinoxalines **3a^{I}a** (90%, 91.1% ee), dihydropyrolo quinoline **3b^{II}a** (78%, 91.2% ee) and dihydropyrolo quinoline **3c^{I}a** (78%, 90.0% ee) (entry 2).

To explore further the potential of this newly developed approach, various alkynols such as **2a**, **2b**, **2e** and **2f** reacted with 2-aminophenyl pyrrole SBA **1a** (2.3.1.2, entry 1). As anticipated, a number of heterocyclic scaffolds such as pyrrolo quinoxalines **3aa**, **3ab** **3ae** and **3af** were obtained in moderate to good yields and ee's (73.3 → 90.1%). However, the reaction took five days to obtain the products in meaningful yields. Simillarly, the reaction of four SBAs **1a^{II}**, **1b^{I}**, **1b^{II}** and **1c** with alkynol **2a** afforded the mixture of enantioenriched heterocyclic scaffolds **3a^{II}a**, **3b^{I}a**, **3b^{II}a** and **3ca** (entry 2) in moderate to high yields and fairly good enantiomeric excess.

Table 2.3.1.2: Variation of SBAs/alkynols – four components in one-pot

Entry no.	SBAs	Alkynol	Products

1[a,c]	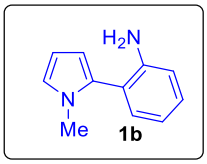 **1b**	**2a** 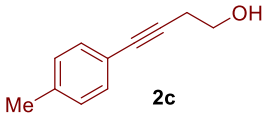 **2c** 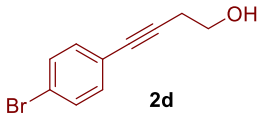 **2d**	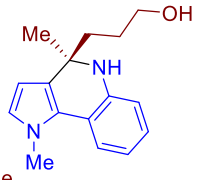 **3ba**[e] 88.0% ee 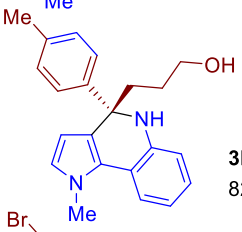 **3bc**[e] 82.6% ee 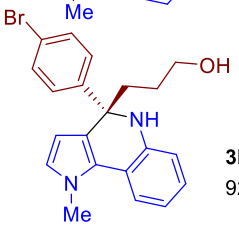 **3bd**[e] 92.4% ee
2[b,d,f]	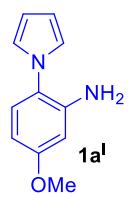 **1a**[I] 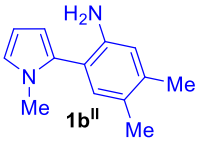 **1b**[II] 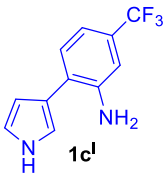 **1c**[I]	**2a**	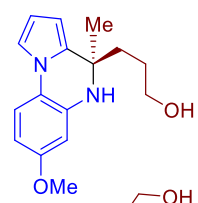 **3a**[I]**a**, 90% 91.1% ee 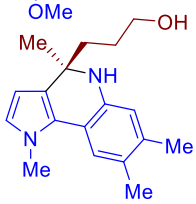 **3b**[II]**a**, 78% 91.2% ee 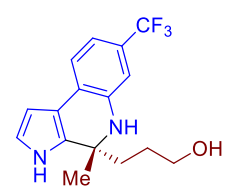 **3c**[I]**a**, 78% 90.0% ee

<u>Reaction conditions</u>: 5 mol% Johnphos-AuMe, 10 mol% (*S*)-TRIP, DCE (0.075 M), rt, 4 d. [a]0.45 mmol 1, 0.45 mmol 2 (1:1:1 mole ratio). [b]0.45 mmol 1 (1:1:1 mole ratio), 0.45 mmol 2. [c]10 mol% Johnphos-AuMe, 20 mol% (*S*)-TRIP was used. [d]Reactions was performed at 0 °C. [e]Inseparable mixture, combined yield of 59% based on alkynols. All were isolated yields and ee's were determined by HPLC analysis on a chiral stationary phase. [f]Yield was based on SBAs.

Table 2.3.1.3: Variation of SBAs/alkynols – five components in one-pot

Entry no.	SBAs	Alkynols	Products
1[a,e]	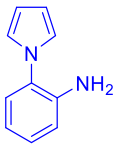 **1a**	**2a** 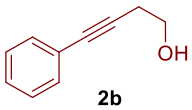 **2b** 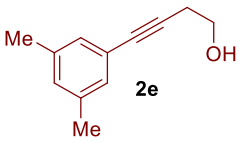 **2e** 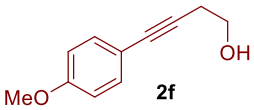 **2f**	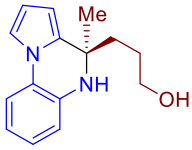 **3aa**[d] 84.0% ee 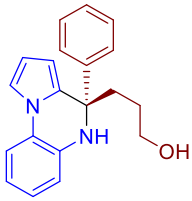 **3ab**, 37% 73.3% ee 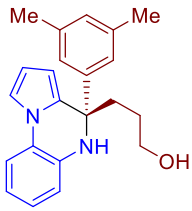 **3ae**, 55% 85.3% ee 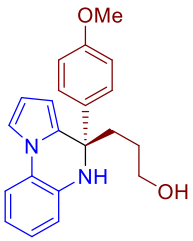 **3af**[d] 90.1% ee

2[b,c,f]	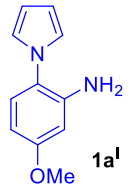 **1a^{I}** 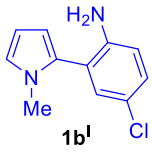 **1b^{I}** 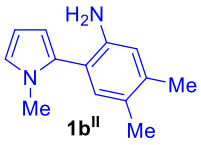 **1b^{II}** 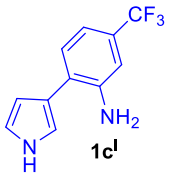 **1c^{I}**	**2a**	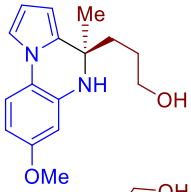 **3a^{I}a**, 72% 91.7% ee 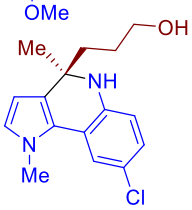 **3b^{I}a**, 63% 83.3% ee 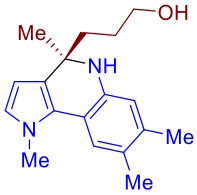 **3b^{II}a**, 83% 90.5% ee 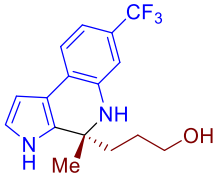 **3c^{I}a**, 75% 83.9% ee

2.4 Conclusion

The catalytic enantioselective combinatorial approach has been developed for the rapid generation of libraries of optically pure aza-heterocyclic scaffolds in a single operation. The substrate scope was turned out to be fairly broad and in all the cases products were formed in high yields and excellent enantiomeric ratios. A number of alkyne based substrates[20] and SBAs[9b] can be envisioned and therefore the approach disclosed herein should be applicable to a generation of vast number of enantiopure combinatorial libraries. In addition, the emergence of Au(I)/chiral Brønsted acid merged catalyst system for new reaction discoveries[21] would certainly provide an impetus to this area of research. With the appropriate design of substrates and catalysts many more such techniques can be envisioned which help realizing enantioselective combinatorial processes of much higher magnitude, than presented here. The concept reported herein provides a good basis for further extensions and explorations.

2.5 Experimental Procedures

2.5.1 Procedure for Preparation of Scaffold Building Agents (SBAs)

The scaffold building agents were synthesized by the procedure similar to that reported by our group.[12]

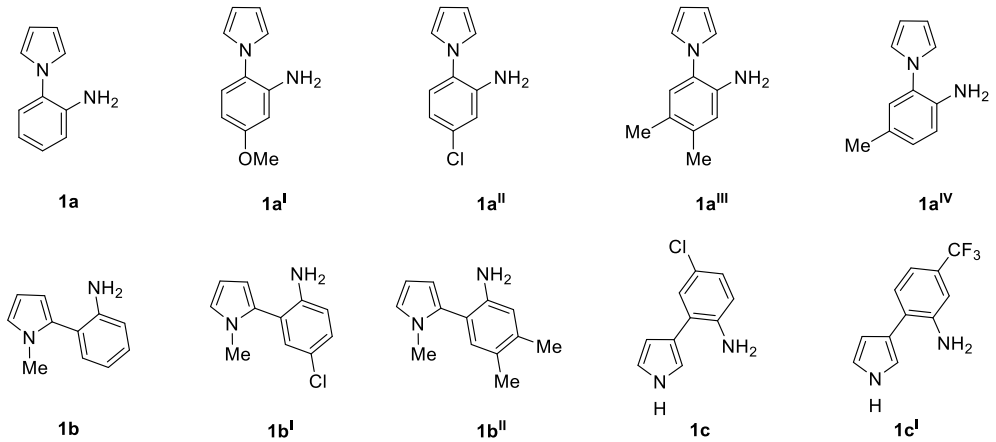

2.5.2 Procedure for Preparation of Alkynols

The alkynol **2a** was purchased from commercial sources and used as received; whereas, alkynols **2b**, **2c**, **2d**, **2e** and **2f** were prepared according to literature known procedures.[22]

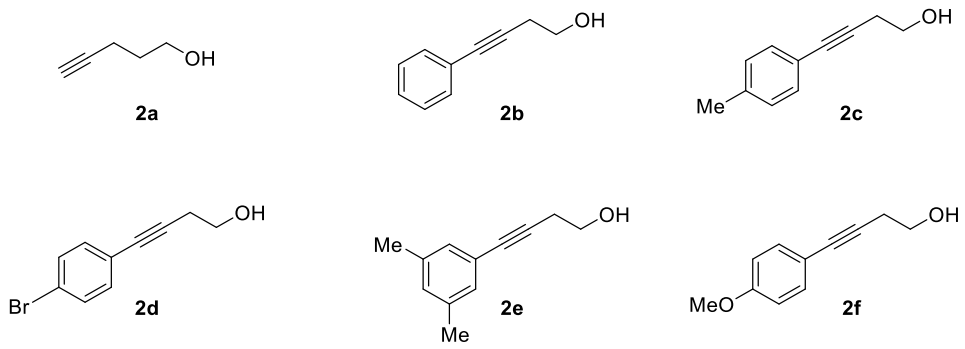

2.5.3 General Procedure for Enantioselective Combinatorial Synthesis

Variation with amino aromatics:

To a flame-dried screw-capped vial equipped with magnetic stir bar, were added (*S*)-TRIP (10 mol%) and Johnphos-AuMe (5 mol%) in DCE (0.031 molar for each 0.15 mmol of amino aromatics **1**) at room temperature and the reaction mixture was stirred for 30 min. To this

reaction mixture alkynol **2** (0.30 mmol) was introduced followed by various amino-aromatics (0.15 mmol each) under argon atmosphere. The reaction vial was fitted with a cap, evacuated and back filled with argon and stirred at a specified temperature for 72 h. The reaction mixture was diluted with ethyl acetate and filtered through plug of silica gel. The filtrate was concentrated and the residue thus obtained was purified by silica gel column chromatography using pet ether/EtOAc as an eluent to afford analytically pure final products.

Variation with alkynols:

To a flame-dried screw-capped vial equipped with magnetic stir bar, were added (*S*)-TRIP (10 mol%) and JohnphosAuMe (5 mol%), in DCE (0.031 molar for each 0.15 mmol of alkynols **2**) at room temperature and the reaction mixture was stirred for 30 min. To this reaction mixture various alkynols (0.15 mmol each) was introduced followed by amino-aromatic (0.15 mmol) under argon atmosphere. The reaction vial was fitted with a cap, evacuated and back filled with argon and stirred at a specified temperature for 72 h. The reaction mixture was diluted with ethyl acetate and filtered through plug of silica gel. The filtrate was concentrated and the residue thus obtained was purified by silica gel column chromatography using pet ether/EtOAc as an eluent to afford analytically pure final compounds.

2.6. Characterization Data, HPLC Chromatograms and NMR Spectra of Final Products

Table 1: Variation of SBAs/Alkynols – three components in one-pot

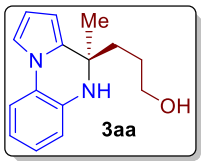

Entry 1, **(3aa):** White solid, 80% yield; mp = 142-144 R_f = 0.30 (pet ether/EtOAc = 60/40); **HPLC analysis:** 86.2% ee, t_R = 12.37 min (minor), t_R = 13.51 min (major). (Chiralpak IA, *n*-hexane/*i*PrOH (90:10), flow rate = 1.0 mL/min, λ = 254 nm); **^{1}H NMR (500 MHz, $CDCl_3$) δ** = 7.37 - 7.21 (d, J = 8.0 Hz, 1 H), 7.15 - 7.05 (m, 1 H), 6.97 - 6.84 (t, J = 7.7 Hz, 1 H), 6.79 - 6.63 (m, 1 H), 6.29 - 6.16 (m, 1 H), 5.98 - 5.83 (m, 1 H), 3.53 - 3.33 (t, J = 6.2 Hz, 2 H), 1.84 - 1.70 (m, 2 H), 1.62 - 1.43 (m, 2 H), 1.46 (s, 3 H); **^{13}C NMR (125 MHz, $CDCl_3$) δ**= 145.4, 142.3, 135.5, 128.6, 126.0, 125.2, 124.7, 123.6,120.1, 117.3, 116.3, 113.9, 103.6, 63.0, 60.7, 38.6, 37.0, 28.0, 20.6.; **HRMS** (ESI)**:** calcd for $C_{15}H_{19}N_{2O}$ $[M+H]^+$ 243.1497, found 243.1507.

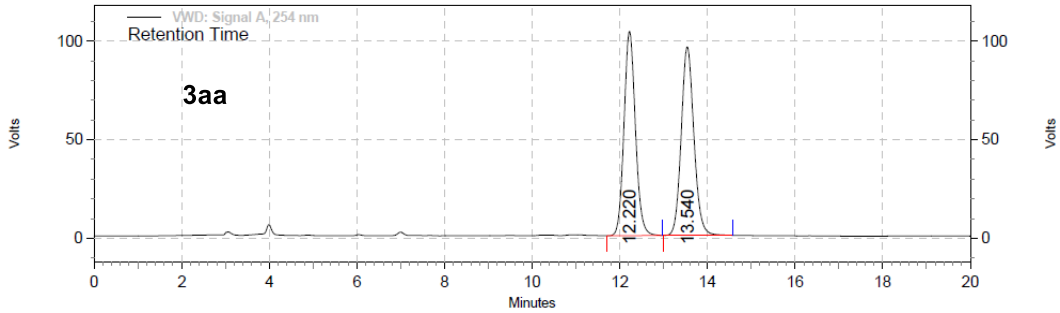

VWD: Signal A, 254 nm
Results

Pk #	Retention Time	Area	Area %
1	12.220	31490560	49.34
2	13.540	32329829	50.66
Totals		63820389	100.00

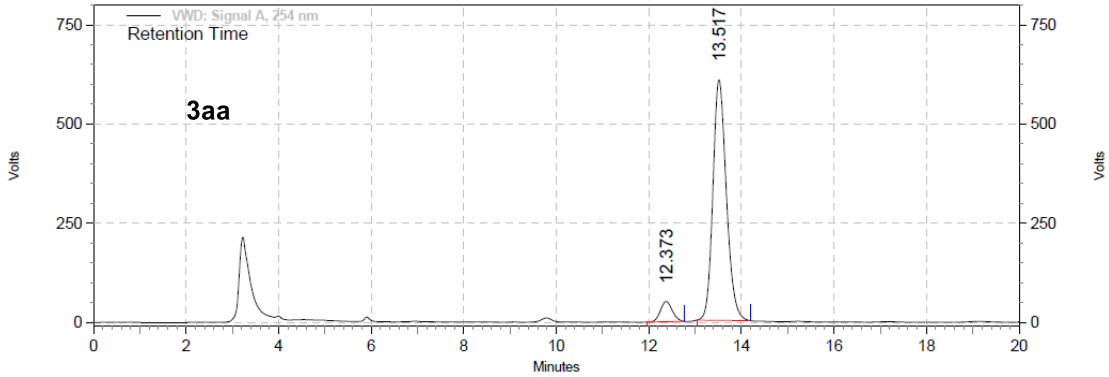

VWD: Signal A, 254 nm
Results

Pk #	Retention Time	Area	Area %
1	12.373	15234081	6.89
2	13.517	205810424	93.11
Totals		221044505	100.00

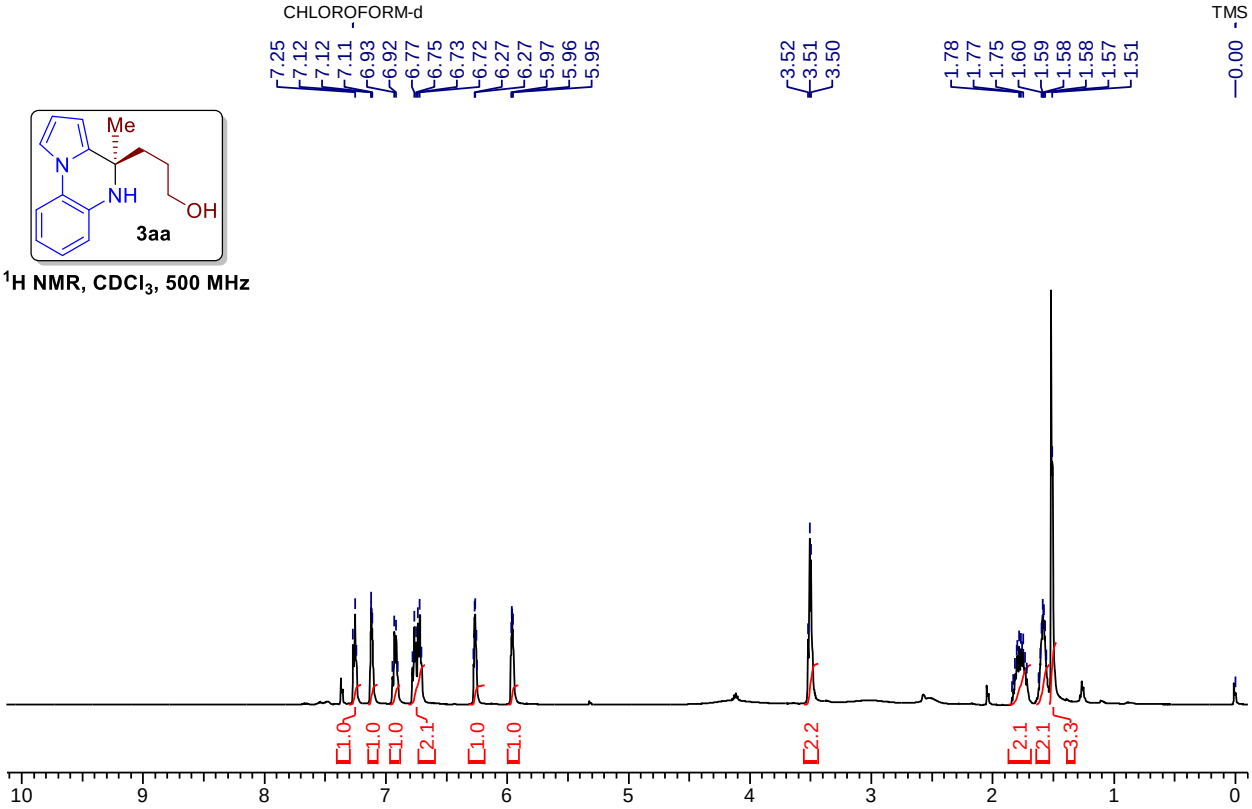

^{1}H NMR, $CDCl_3$, 500 MHz

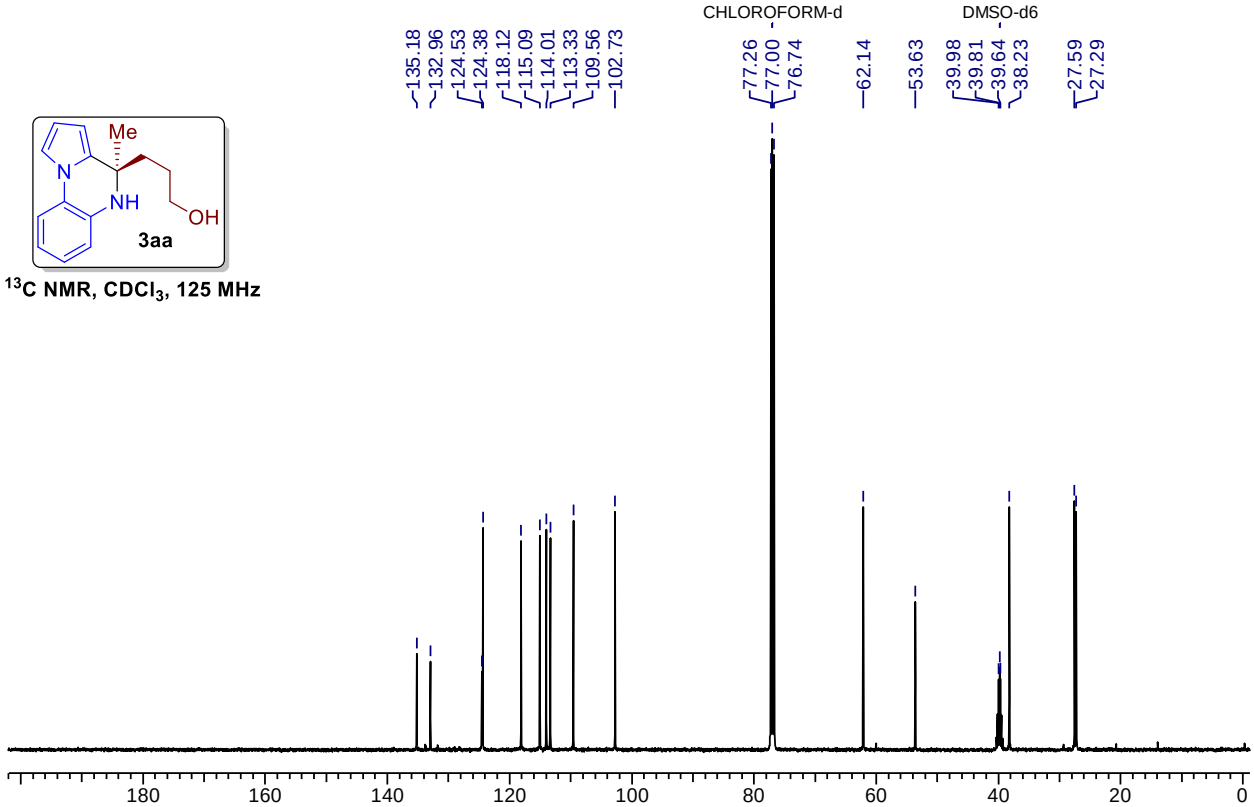

^{13}C NMR, $CDCl_3$, 125 MHz

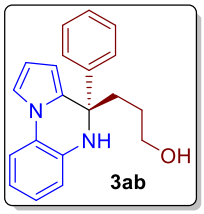

Entry 1, **(3ab):** White solid, 37% yield; mp = 95-97; $\boldsymbol{R_f}$ = 0.35 (pet ether/EtOAc = 60/40); **HPLC analysis:** 86.9% ee, t_R = 15.06 min (minor), t_R = 18.67 min (major). (Chiralpak IA, *n*-hexane/*i*PrOH (90:10), flow rate 1.0 mL/min, λ = 254 nm); **^{1}H NMR (400 MHz, $CDCl_3$) δ** = 7.34 - 7.27 (m, 2 H), 7.27 - 7.19 (m, 3 H), 7.18 - 7.10 (m, 2 H), 6.98 - 6.89 (m, 1 H), 6.84 - 6.71 (m, 2 H), 6.32 (t, *J* = 3.2 Hz, 1 H), 6.08 (dd, *J* = 1.4, 3.7 Hz, 1 H), 3.69 - 3.60 (m, 2 H), 2.39 - 2.28 (m, 1 H), 2.24 - 2.12 (m, 1 H), 1.73 (qd, *J* = 6.5, 8.9 Hz, 2 H); **^{13}C NMR (100 MHz, $CDCl_3$) δ** = 145.4, 135.1, 131.5, 128.2, 126.8, 126.0, 125.3, 124.7, 119.0, 115.6, 114.6, 114.2, 109.9, 105.0, 62.9, 60.0, 37.9, 27.6; **HRMS (ESI)** calcd for $C_{20}H_{20}N_2O$ $[M+H]^+$ 305.1648, found 305.1646.

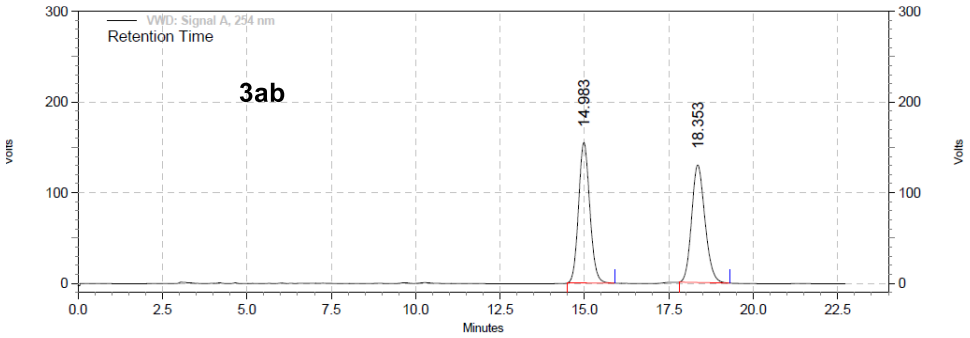

VWD: Signal A, 254 nm
Results

Pk #	Retention Time	Area	Area %
1	14.983	60013883	50.14
2	18.353	59688080	49.86
Totals		119701963	100.00

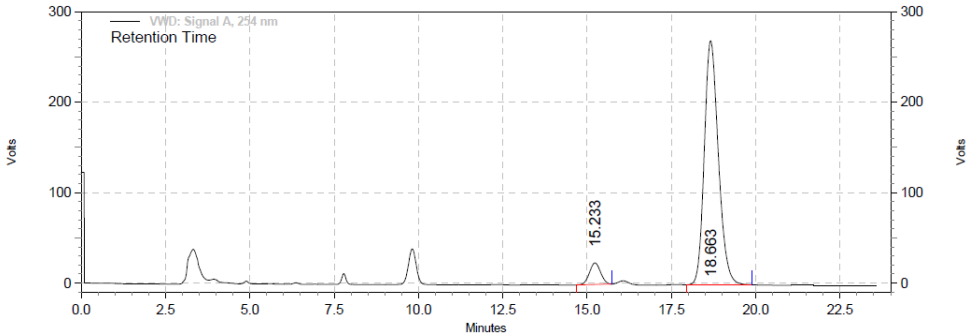

VWD: Signal A, 254 nm
Results

Pk #	Retention Time	Area	Area %
1	15.233	9193806	6.55
2	18.663	131175151	93.45
Totals		140368957	100.00

^{1}H NMR, $CDCl_3$, 400 MHz

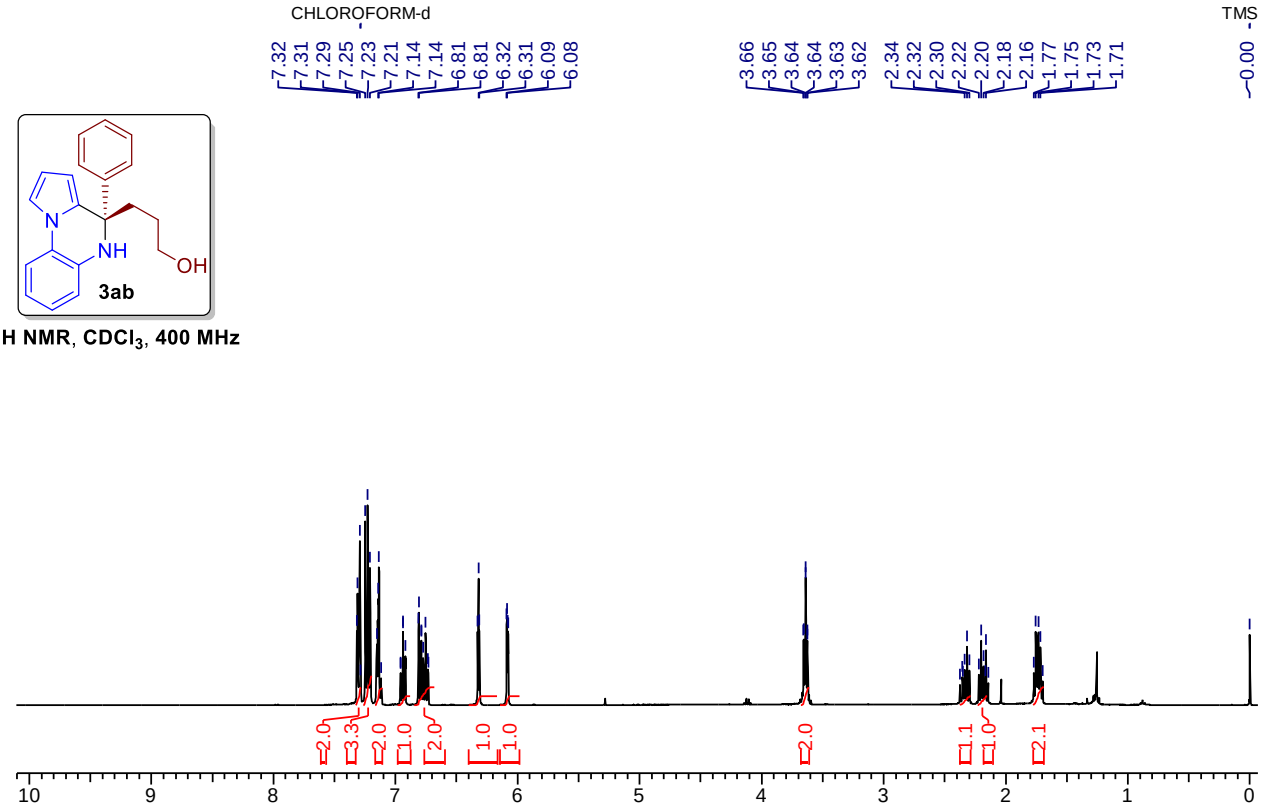

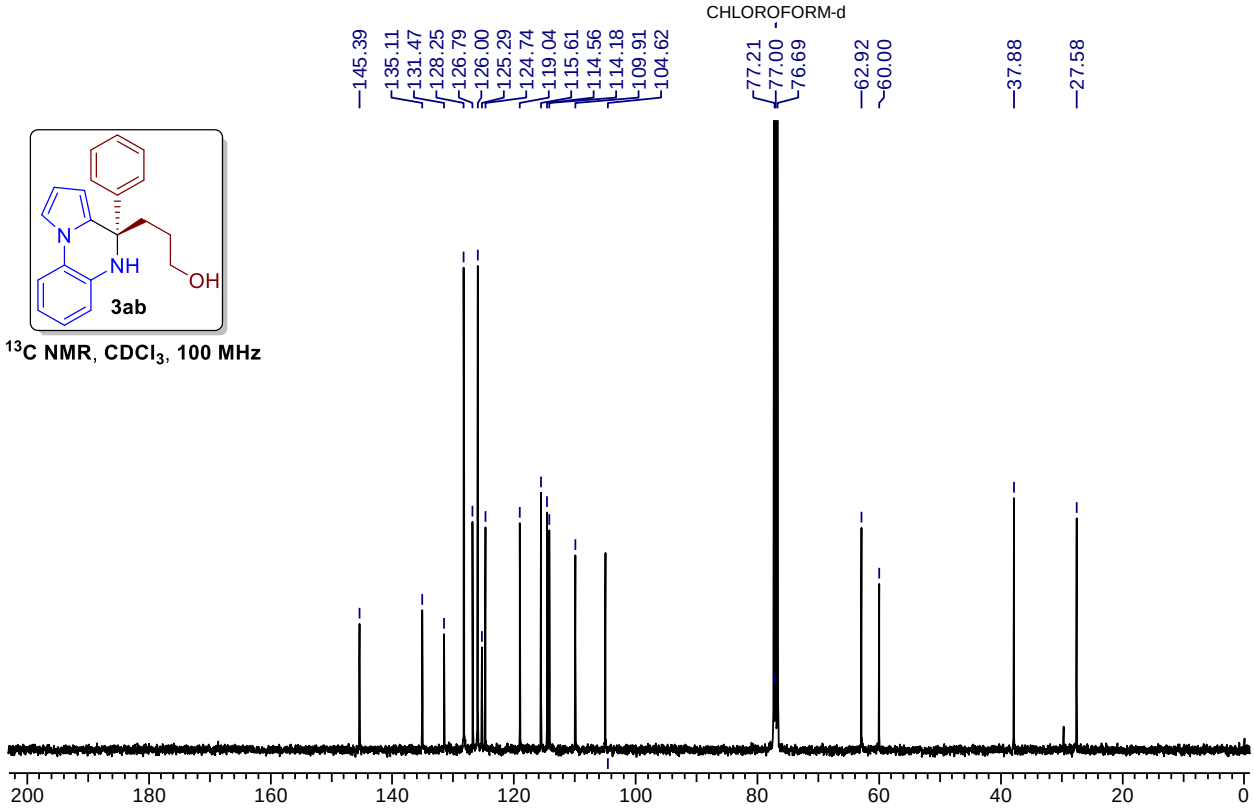

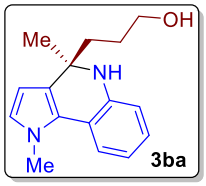

Entry 2, **(3ba):** White solid, 72 % yield; mp = 142-144°C $\boldsymbol{R_f}$ = 0.30 (pet ether/EtOAc = 60/40); **HPLC analysis:** 83.5% ee, t_R = 9.97 min (minor), t_R = 10.90 min (major). (Chiralpak IB, *n*-hexane/*i*PrOH (75:25), flow rate 1.0 mL/min, λ = 254 nm); **^{1}H NMR (400 MHz, CDCl$_3$) δ** = 7.44 - 7.36 (m, 1 H), 6.96 - 6.86 (m, 1 H), 6.74 - 6.62 (m, 1 H), 6.62 - 6.56 (m, 1 H), 6.54 (d, *J* = 2.7 Hz, 1 H), 5.92 (d, *J* = 2.7 Hz, 1 H), 3.89 (s, 3 H), 3.57 (t, *J* = 6.3 Hz, 2 H), 1.83 - 1.76 (m, 1 H), 1.70 - 1.66 (m, 1 H), 1.61 - 1.53 (m, 2 H), 1.47 (s, 3 H); **^{13}C NMR (100 MHz, CDCl$_3$) δ** = 142.6, 126.1, 124.8, 124.6, 120.1, 117.5, 116.6, 114.1, 102.7, 63.3, 55.5, 40.1, 37.2, 29.9, 28.; **HRMS (ESI)** calcd for $C_{16}H_{21}N_2O$ $[M+H]^+$ 257.1648, found 257.1643.

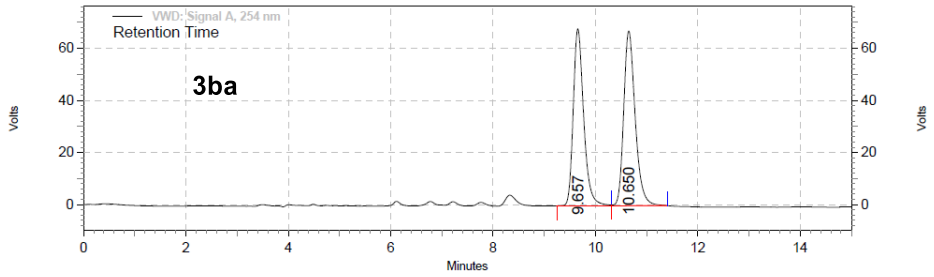

VWD: Signal A, 254 nm
Results

Pk #	Retention Time	Area	Area %
1	9.657	16171512	48.02
2	10.650	17506533	51.98
Totals		33678045	100.00

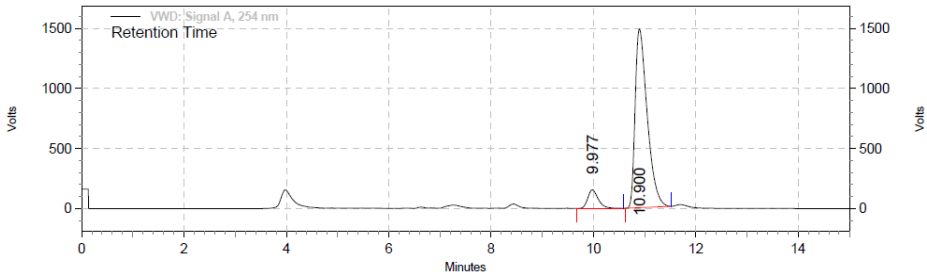

VWD: Signal A, 254 nm
Results

Pk #	Retention Time	Area	Area %
1	9.977	36706690	8.24
2	10.900	408518694	91.76
Totals		445225384	100.00

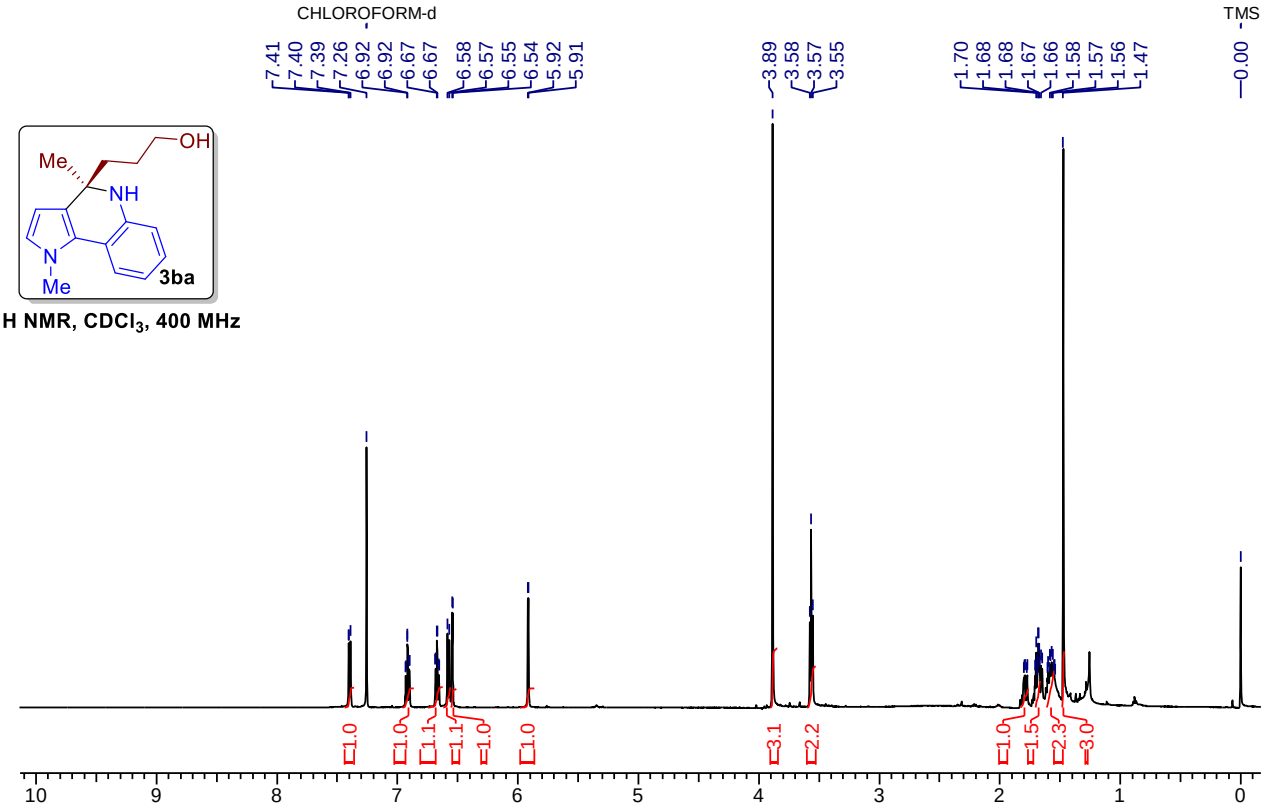

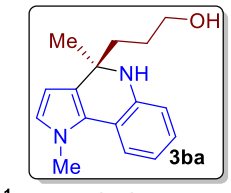

^{1}H NMR, $CDCl_3$, 400 MHz

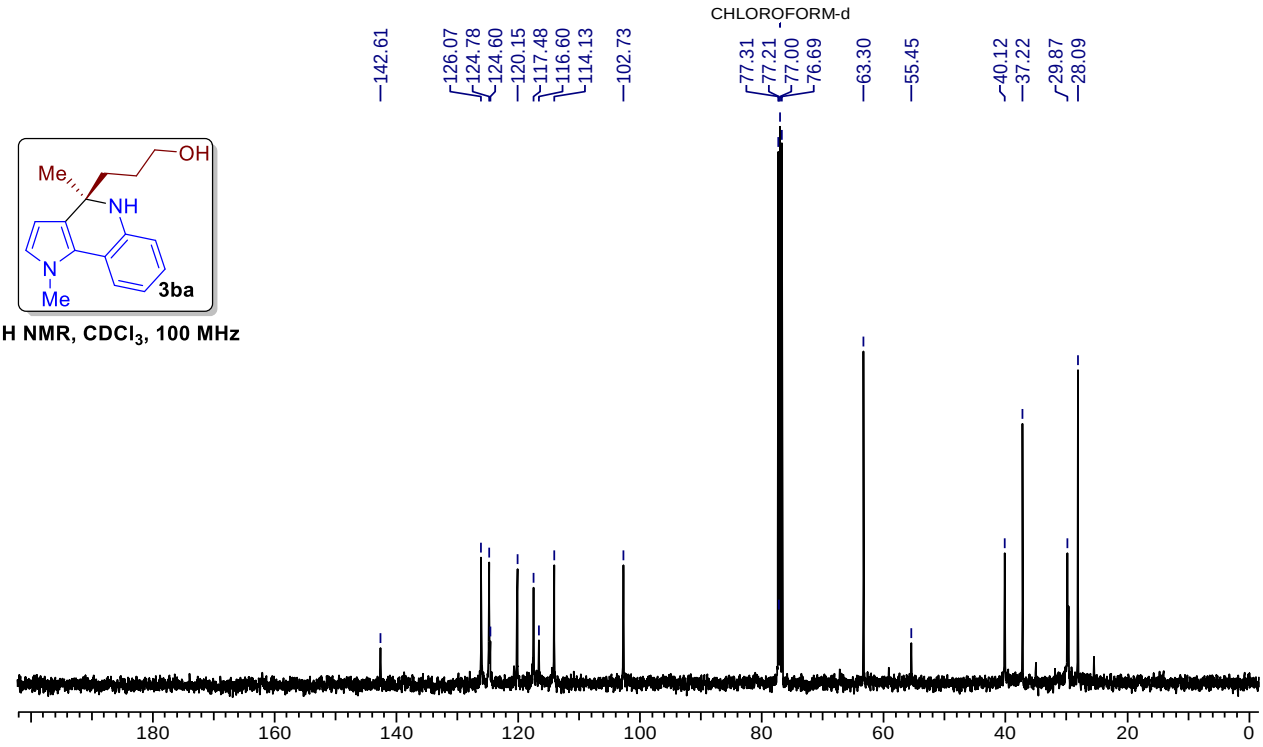

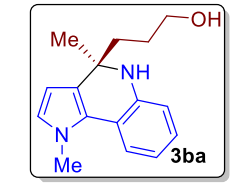

^{1}H NMR, $CDCl_3$, 100 MHz

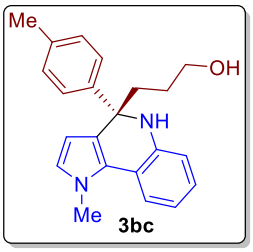

Entry 2, (3bc): White solid, 45% yield; mp = 151-153°C R_f = 0.37 (pet ether/EtOAc = 60/40); **HPLC analysis:** 82.3% ee, t_R = 19.58 min (minor), t_R = 15.77 min (major). (Chiralpak IB, *n*-hexane/*i*PrOH (75:25), flow rate 1.0 mL/min, λ = 254 nm); **^{1}H NMR (400 MHz, $CDCl_3$) δ** = 7.45 - 7.38 (m, 1 H), 7.38 - 7.31 (m, 2 H), 7.08 (d, *J* = 8.3 Hz, 2 H), 7.02 - 6.93 (m, 1 H), 6.76 - 6.62 (m, 2 H), 6.57 (d, *J* = 2.7 Hz, 1 H), 5.98 (d, *J* = 2.9 Hz, 1 H), 3.87 (s, 3 H), 3.65 (t, *J* = 6.4 Hz, 2 H), 2.34 (td, *J* = 5.5, 8.6 Hz, 1 H), 2.29 (s, 3 H), 2.16 - 2.08 (m, 1 H), 1.83 - 1.67 (m, 2 H); **^{13}C NMR (100 MHz, $CDCl_3$) δ** = 145.4, 142.3, 135.5, 128.6, 126.0, 125.2, 124.7, 123.6, 120.1, 117.3, 116.3, 113.9, 103.6, 63.0, 60.7, 38.6, 37.0, 28.0, 20.6; **HRMS (ESI)** calcd for $C_{22}H_{25}N_2O$ $[M+H]^+$ 333.1961, found 333.1954.

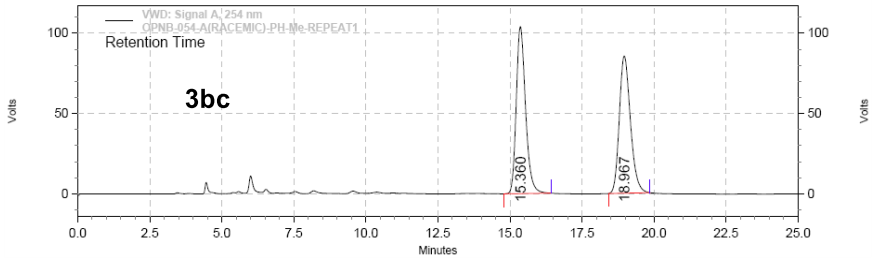

VWD: Signal A, 254 nm
Results

Pk #	Retention Time	Area	Area %
1	15.360	39132462	50.44
2	18.967	38447058	49.56
Totals		77579520	100.00

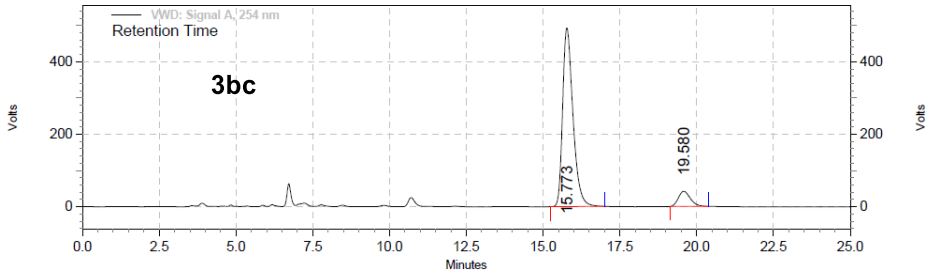

VWD: Signal A, 254 nm
Results

Pk #	Retention Time	Area	Area %
1	15.773	193733083	91.14
2	19.580	18837824	8.86
Totals		212570907	100.00

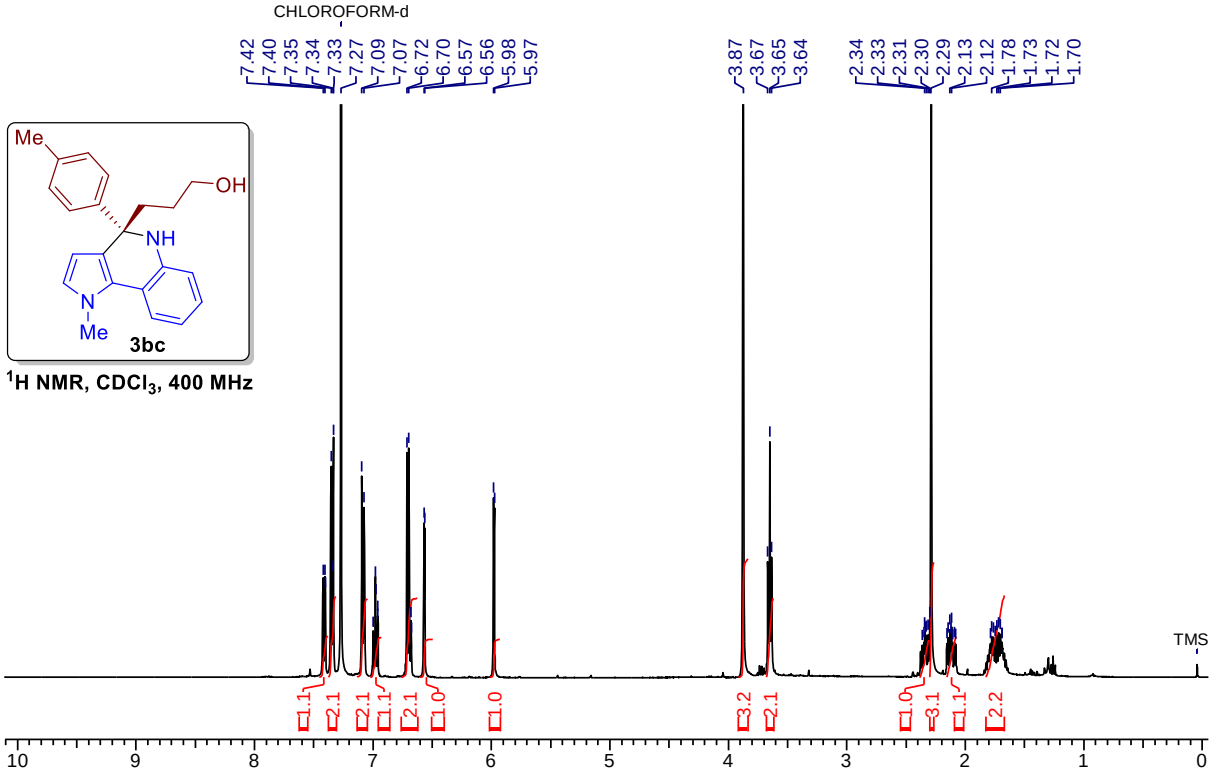

^{1}H NMR, $CDCl_3$, 400 MHz

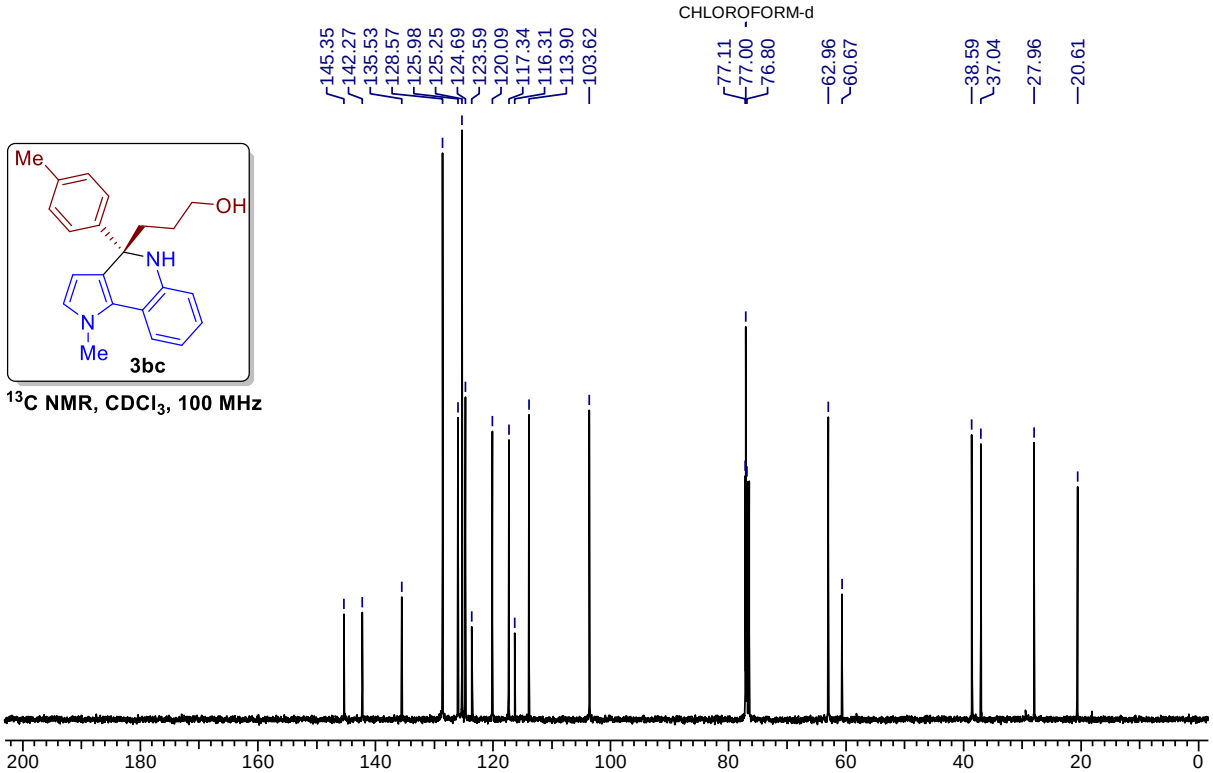

^{13}C NMR, $CDCl_3$, 100 MHz

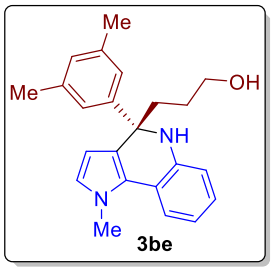

Entry 3, **(3be):** Thick liquid, 24% yield, R_f = 0.42 (pet ether/EtOAc = 60/40); **HPLC analysis:** 83.8% ee, t_R = 4.69 min (minor), t_R = 5.18 min (major). (Chiralpak IB, *n*-hexane/*i*PrOH (70:30), flow rate 1.0 mL/min, λ = 254 nm); **^{1}H NMR (400 MHz, $CDCl_3$) δ** = 7.43 (d, *J* = 7.6 Hz, 1 H), 7.07 (s, 2 H), 6.97 (t, *J* = 7.6 Hz, 1 H), 6.80 (s, 1 H), 6.73 - 6.65 (m, 2 H), 6.59 - 6.48 (m, 1 H), 5.99 - 5.89 (m, 1 H), 3.89 (s, 3 H), 3.65 (t, *J* = 6.6 Hz, 2 H), 2.35 - 2.30 (m, 1 H), 2.27 (s, 6 H), 2.11 - 2.04 (m, 1 H), 1.81 - 1.73 (m, 1 H), 1.70 - 1.64 (m, 1 H); **^{13}C NMR (100 MHz, $CDCl_3$) δ** = 146.8, 140.2, 137.4, 128.3, 126.2, 125.1, 124.7, 123.7, 123.2, 120.4, 119.3, 117.7, 115.7, 104.4, 63.0, 62.0, 38.9, 37.2, 28.0, 21.5; **HRMS (ESI)** calcd for $C_{23}H_{27}N_2O$ $[M+H]^+$ 347.2118, found 347.2113.

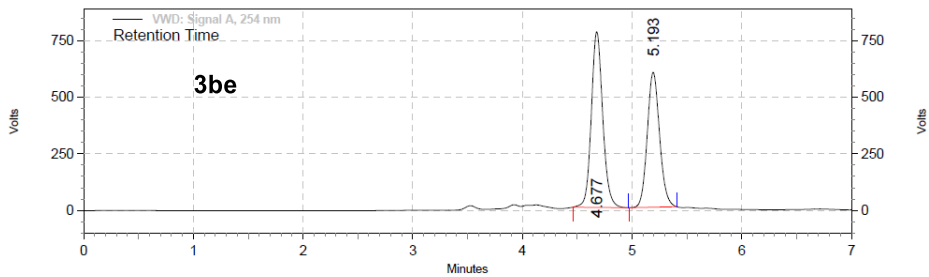

VWD: Signal A, 254 nm
Results

Pk #	Retention Time	Area	Area %
1	4.677	94259236	54.71
2	5.193	77995880	45.27

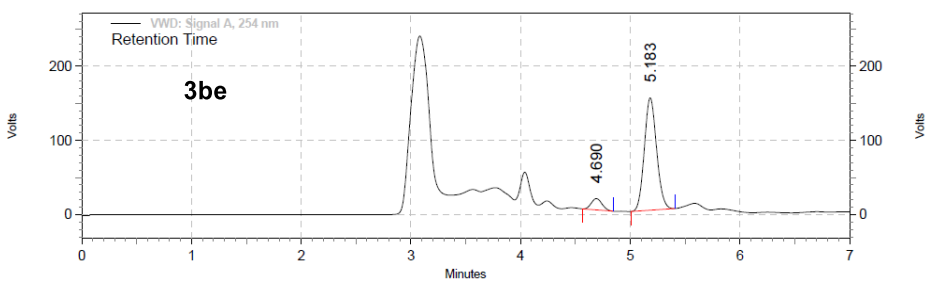

VWD: Signal A, 254 nm
Results

Pk #	Retention Time	Area	Area %
1	4.690	1737857	8.09
2	5.183	19744529	91.91

Totals		21482386	100.00

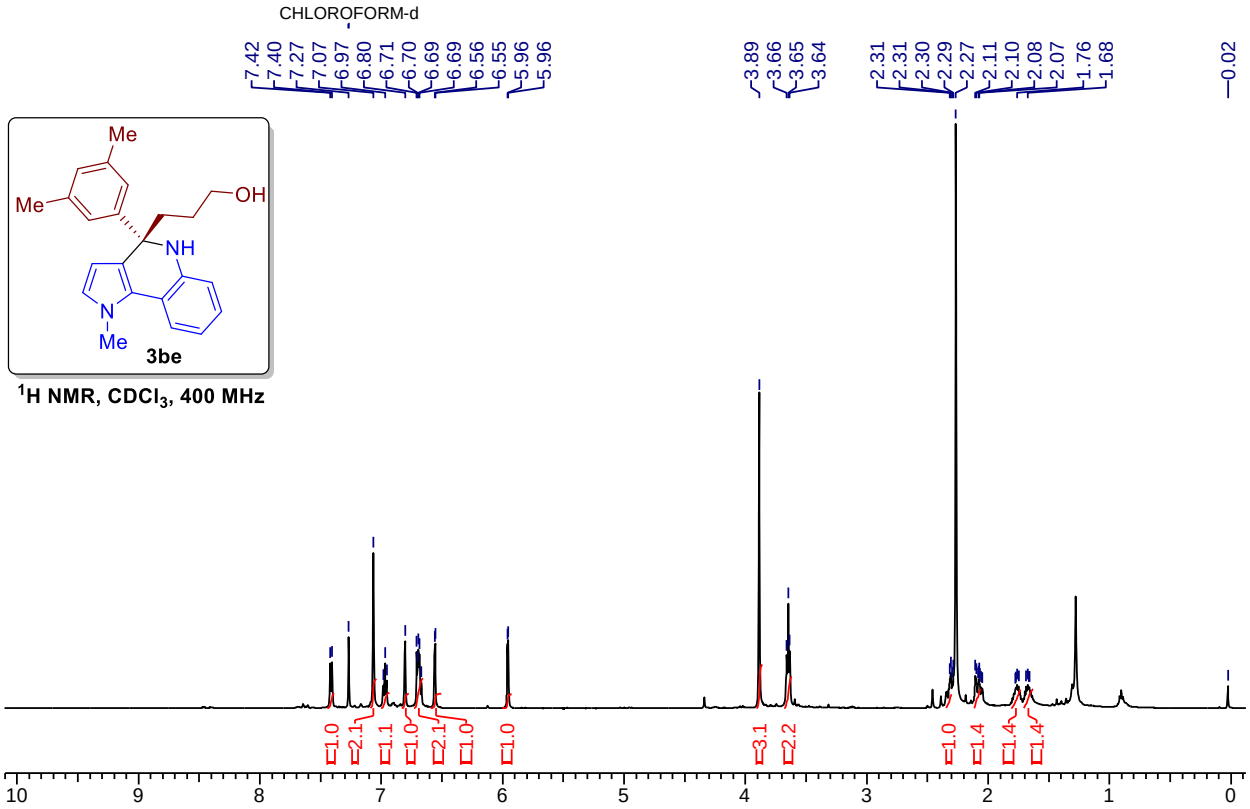

^{1}H NMR, $CDCl_3$, 400 MHz

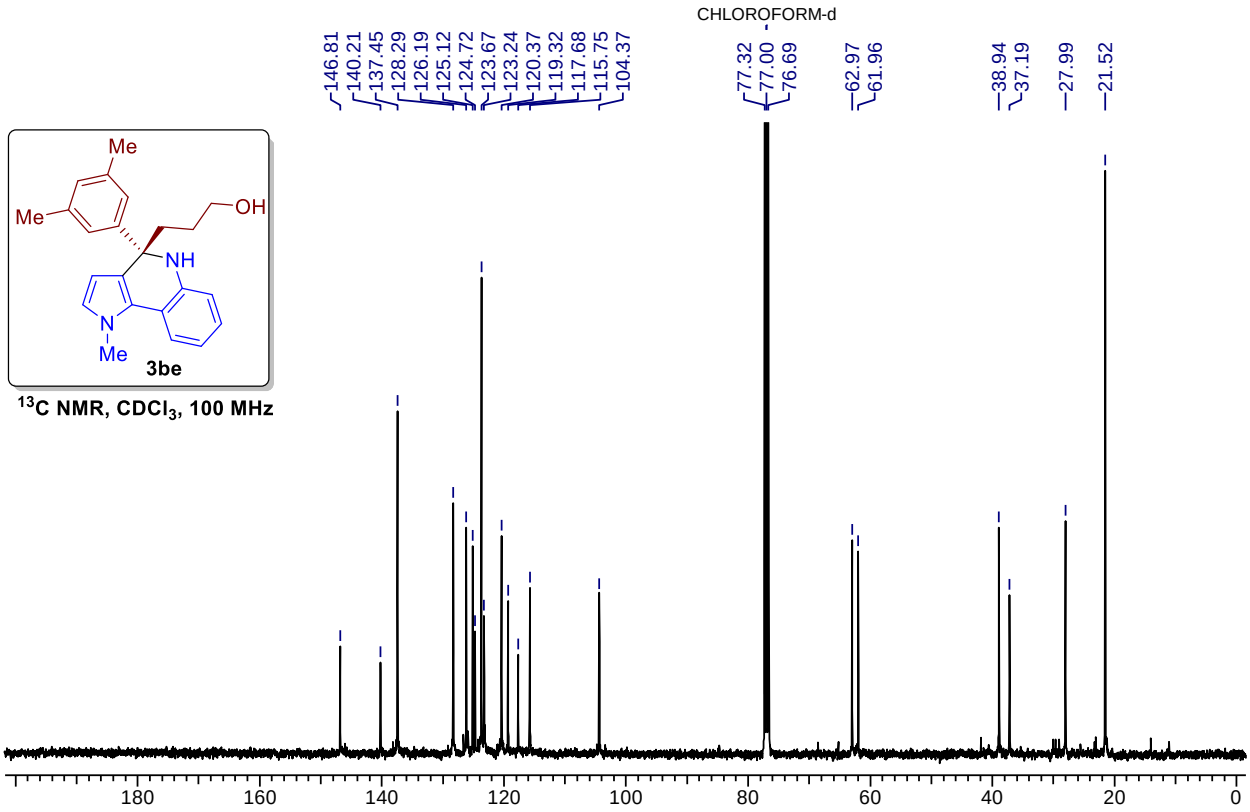

^{13}C NMR, $CDCl_3$, 100 MHz

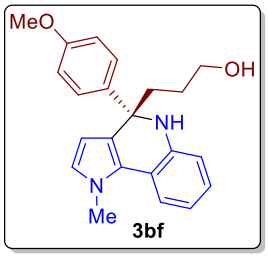

Entry 3, **(3bf):** White solid, 73% yield, **mp** = 125-127 °C; ***R*$_f$** = 0.27 (pet ether/EtOAc = 60/40); **HPLC analysis:** 84.7% ee, t_R = 7.26 min (minor), t_R = 9.62 min (major). (Chiralpak IB, *n*-hexane/*i*PrOH (70:30), flow rate 1.0 mL/min, λ = 254 nm); **^{1}H NMR (400 MHz, CDCl$_3$)** δ = 7.39 (dd, *J* = 1.4, 8.2 Hz,1 H), 7.37 - 7.31 (m, 2 H), 6.94 (dt, *J* = 1.4, 7.6 Hz, 1 H), 6.80 - 6.75 (m, 2 H), 6.70 - 6.64 (m, 2 H), 6.54 (d, *J* = 2.7 Hz, 1 H), 5.91 (d, *J* = 2.7 Hz, 1 H), 3.87 (s, 3 H), 3.73 (s, 3 H), 3.63 (t, *J* = 6.4 Hz, 2 H), 2.30 (ddd, *J* = 5.0, 10.9, 13.9 Hz,1 H), 2.09 (ddd, *J* = 5.0, 11.0, 13.7 Hz, 1 H), 1.79 - 1.64 (m, 2 H); **^{13}C NMR (100 MHz, CDCl$_3$)** δ = 159.3, 150.2, 142.2, 129.0, 126.2, 124.9, 124.9, 123.4, 120.3, 117.9, 117.8, 116.6, 114.3, 112.1, 111.0, 103.8, 63.1, 61.1, 55.0, 38.8, 37.2, 28.1; **HRMS (ESI)** calcd for $C_{22}H_{25}N_2O_2$ $[M+H]^+$ 349.1902, found 349.1911.

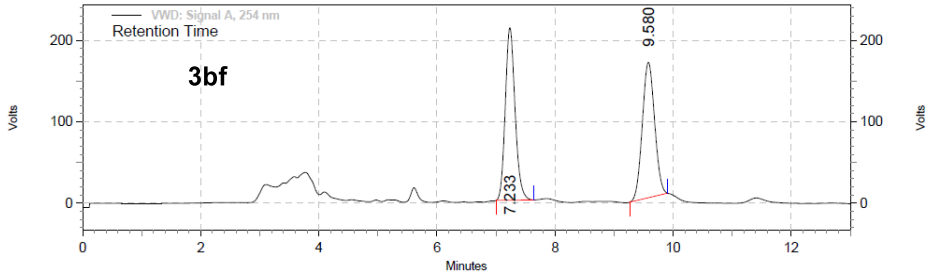

VWD: Signal A, 254 nm
Results

Pk #	Retention Time	Area	Area %
1	7.233	40855336	50.32
2	9.580	40328488	49.68
Totals		81183824	100.00

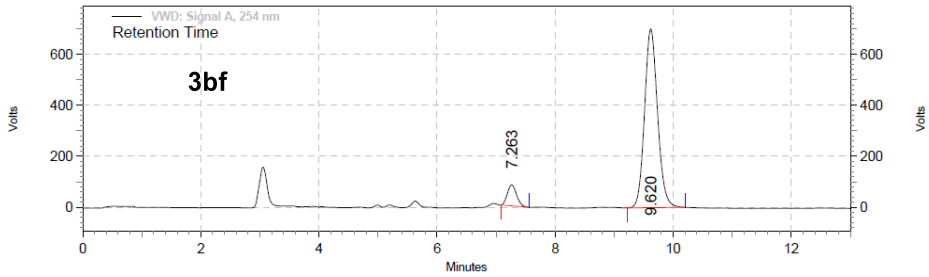

VWD: Signal A, 254 nm
Results

Pk #	Retention Time	Area	Area %
1	7.263	14847088	7.63
2	9.620	179768779	92.37
Totals		194615867	100.00

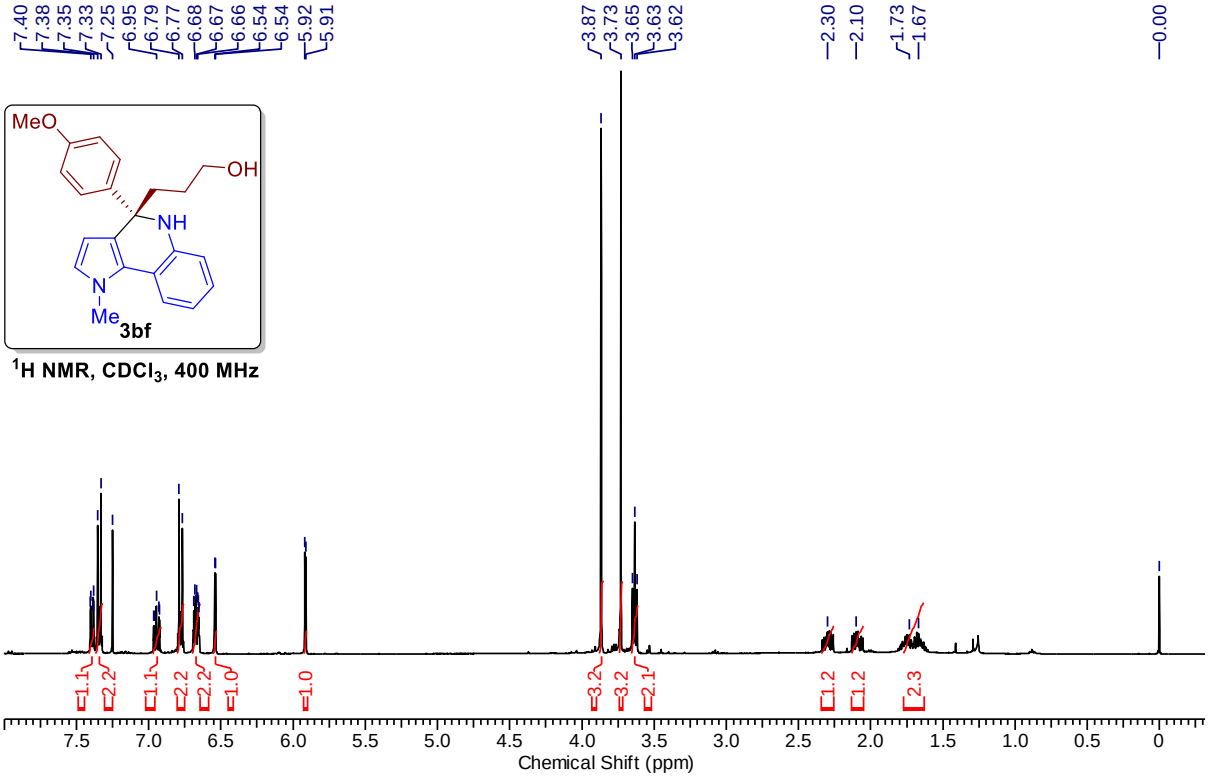

^{1}H NMR, $CDCl_3$, 400 MHz

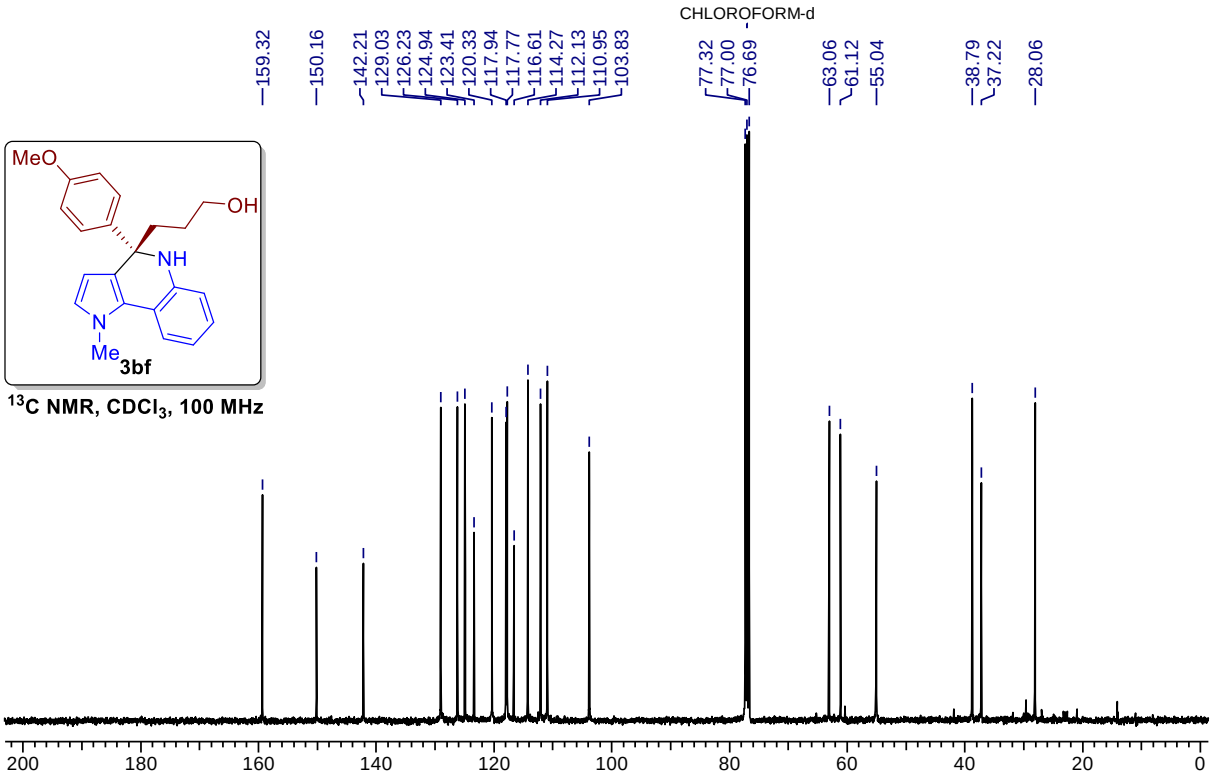

^{13}C NMR, $CDCl_3$, 100 MHz

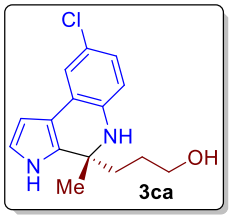

Entry 4, (3ca): Gray solid, 70% yield, **mp** = 77-79°C, R_f = 0.35 (pet ether/EtOAc = 60/40); **HPLC analysis:** 84.0% ee, t_R = 8.66 min (minor), t_R = 9.47 min (major). (Chiralpak IC, *n*-hexane/*i*PrOH (90:10), flow rate 1.0 mL/min, λ = 254 nm); **^{1}H NMR (200 MHz, $CDCl_3$)** δ = 8.23 (br. s., 1 H), 7.19 (d, *J* = 2.4 Hz, 1 H), 6.82 (dd, *J* = 2.4, 8.3 Hz, 1 H), 6.70 (t, *J* = 2.7 Hz, 1 H), 6.42 (d, *J* = 8.3 Hz, 1 H), 6.37 - 6.31 (m, 1 H), 3.54(t, *J* = 6.1 Hz, 2 H), 1.95 - 1.86 (m, 1 H), 1.75 - 1.60 (m, 2 H), 1.52 (s, 3 H), 1.47 - 1.39 (m,1 H); **^{13}C NMR (50MHz, $CDCl_3$)** δ = 139.5, 130.2, 125.0, 122.2, 121.4, 120.6, 118.5, 114.7, 113.7, 102.4, 62.5, 55.6, 39.9, 29.7, 27.5; **HRMS (ESI)** calcd for $C_{15}H_{18}N_2OCl$ $[M+H]^+$ 277.1100, found 277.1102.

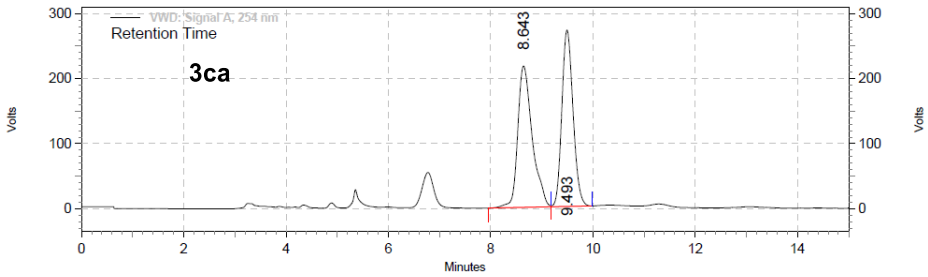

VWD: Signal A, 254 nm
Results

Pk #	Retention Time	Area	Area %
1	8.643	71899048	50.92
2	9.493	69293350	49.08
Totals		141192398	100.00

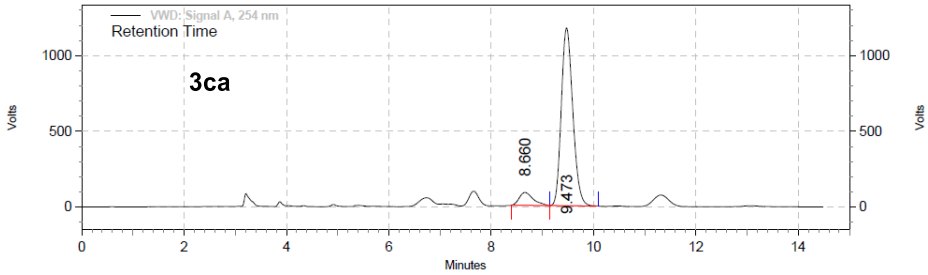

VWD: Signal A, 254 nm
Results

Pk #	Retention Time	Area	Area %
1	8.660	26759241	8.00
2	9.473	307693468	92.00
Totals		334452709	100.00

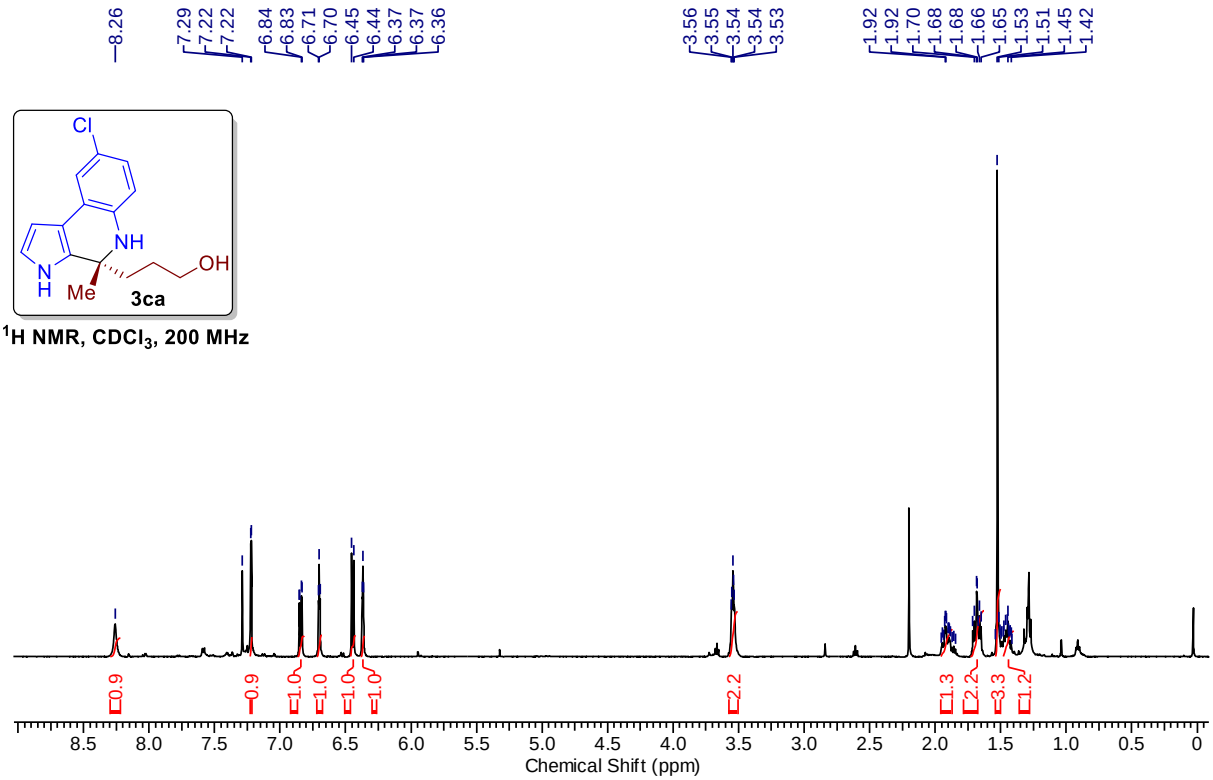

^{1}H NMR, $CDCl_3$, 200 MHz

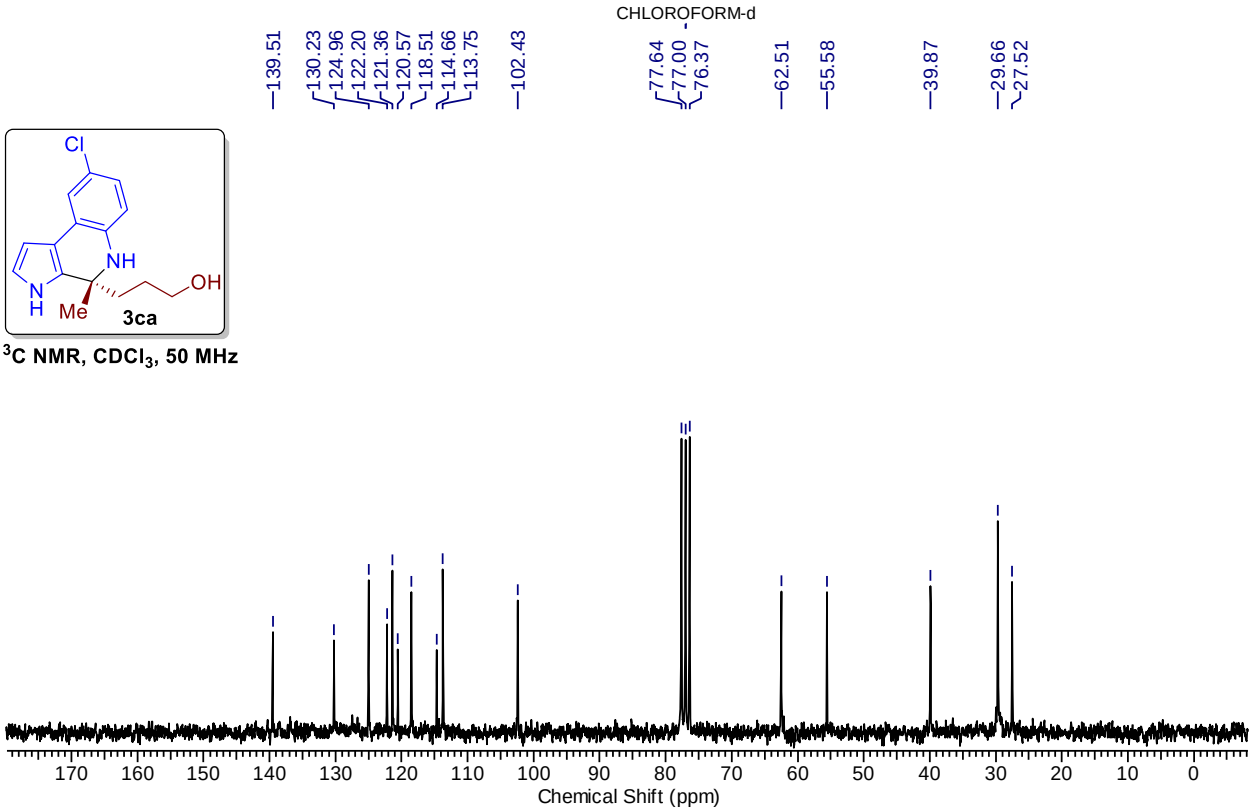

^{13}C NMR, $CDCl_3$, 50 MHz

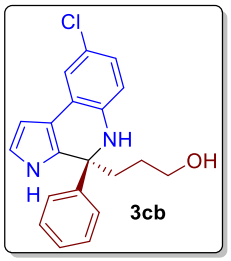

Entry 4, (3cb): Brownish solid, 30% yield; mp = 77-79°C; R_f = 0.35 (pet ether/EtOAc = 60/40); **HPLC analysis:** 86.5% ee, t_R = 8.52 min (minor), t_R = 7.65 min (major) (Chiralpak IB, *n*-hexane/*i*PrOH (75:25), flow rate 1.0 mL/min, λ = 254 nm); **^{1}H NMR (400 MHz, $CDCl_3$) δ** = 8.18 (br. s., 1 H), 7.36 - 7.30 (m, 2 H), 7.28 - 7.15 (m, 4 H), 6.86 - 6.76 (m, 1 H), 6.59 (t, *J* = 2.7 Hz, 1 H), 6.40 (d, *J* = 8.2 Hz, 1 H), 6.35 - 6.27 (m, 1 H), 3.59 - 3.42 (m, 2 H), 2.39 - 2.27 (m, 1 H), 2.08 (ddd, *J* = 4.8, 11.4, 14.0 Hz, 1 H), 1.78 - 1.65 (m, 1 H), 1.51 - 1.39 (m, 1 H); **^{13}C NMR (100 MHz, $CDCl_3$) δ** = 46.4, 139.2, 128.8, 128.6, 127.2, 125.7, 125.2, 122.3, 121.5, 120.2, 119.0, 115.5, 113.7, 102.4, 62.5, 61.1, 37.1, 27.5; **HRMS (ESI)** calcd for $C_{20}H_{20}N_2OCl$ $[M+H]^+$ 339.1259, found 339.1253.

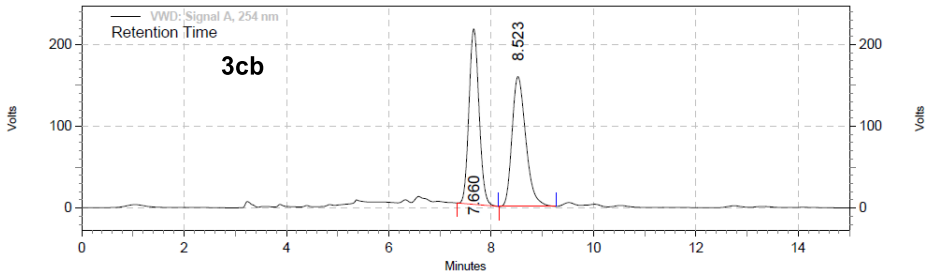

VWD: Signal A, 254 nm
Results

Pk #	Retention Time	Area	Area %
1	7.660	49275164	49.71
2	8.523	49845742	50.29
Totals		99120906	100.00

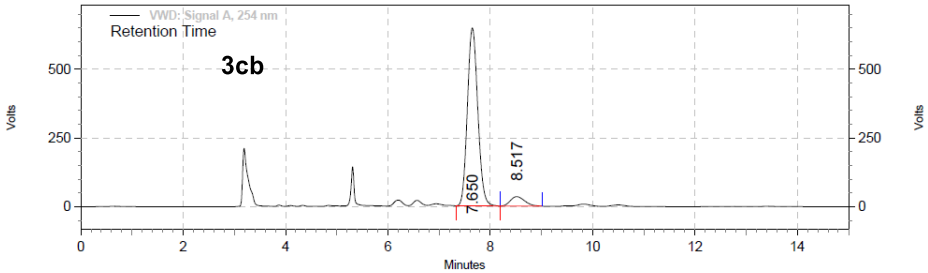

VWD: Signal A, 254 nm
Results

Pk #	Retention Time	Area	Area %
1	7.650	153416912	93.27
2	8.517	11071377	6.73
Totals		164488289	100.00

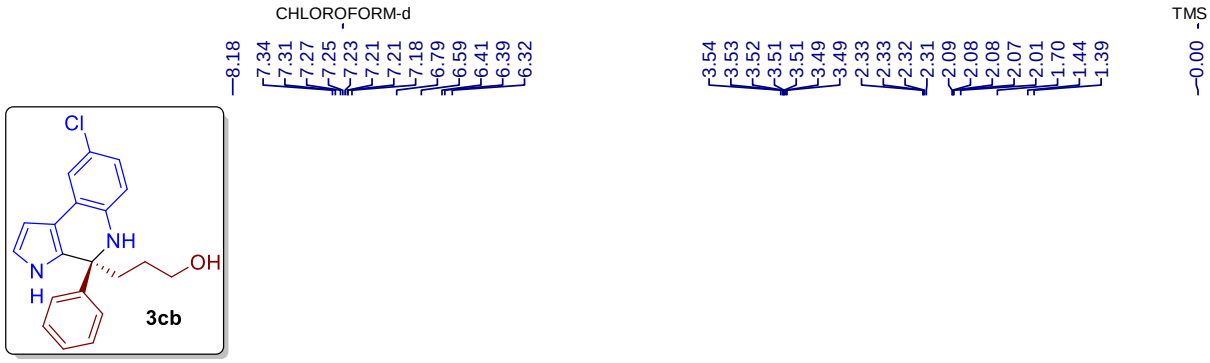

^{1}H NMR, $CDCl_3$, 400 MHz

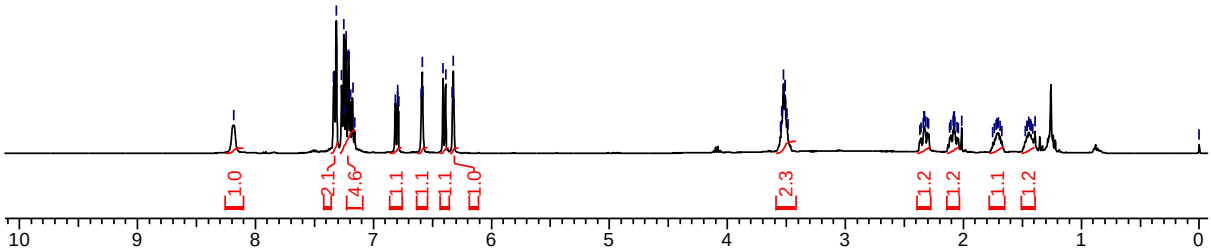

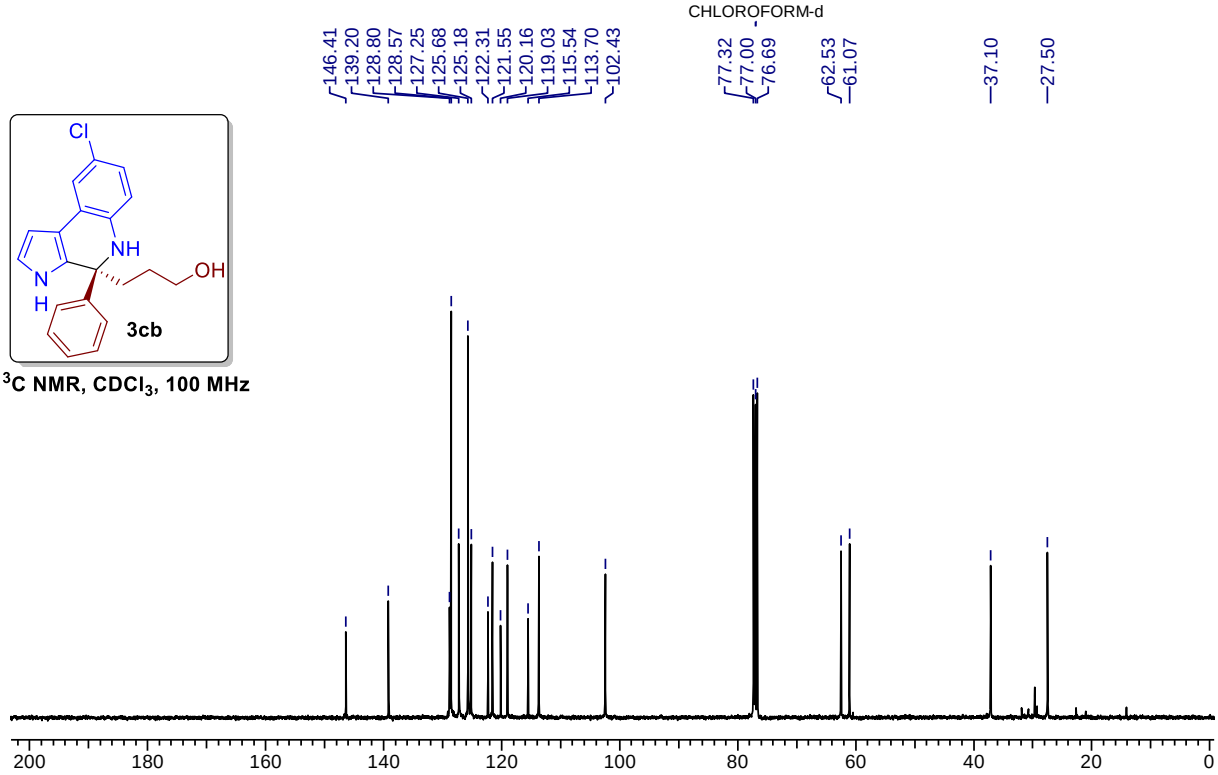

^{13}C NMR, $CDCl_3$, 100 MHz

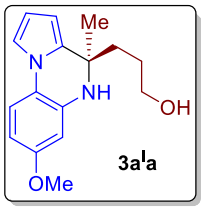

Entry 5, (3a^Ia): White solid, 87% yield; mp = 148-150°C; R_f = 0.35 (pet ether/EtOAc = 60/40), **HPLC analysis:** 92.9% ee, t_R = 23.21 min (minor), t_R = 36.12 min (major). (Chiralpak IA, *n*-hexane/*i*PrOH (90:10), flow rate 1.0 mL/min, λ = 254 nm); **^{1}H NMR (400 MHz, $CDCl_3$) δ** = 7.17 (d, *J* = 8.7 Hz, 1 H), 7.10 - 7.02 (m, 1 H), 6.34 (dd, *J* = 2.5, 8.5 Hz, 1 H), 6.29 - 6.23 (m, 2 H), 5.94 (dd, *J* = 1.1, 3.4 Hz, 1 H), 3.76 (s, 3 H), 3.53 (t, *J* = 6.2 Hz, 2 H), 1.83 - 1.71 (m, 2 H), 1.63 - 1.55 (m, 2 H), 1.51 (s, 3 H); **^{13}C NMR (100 MHz, $CDCl_3$) δ** = 175.1, 157.2, 136.4, 132.4, 119.4, 115.2, 113.6, 109.5, 103.7, 102.8, 101.3, 63.0, 55.5, 54.2, 38.7, 27.8; **HRMS (ESI)** calcd for $C_{16}H_{21}N_2O_2$ $[M+H]^+$ 273.1598, found 273.1595.

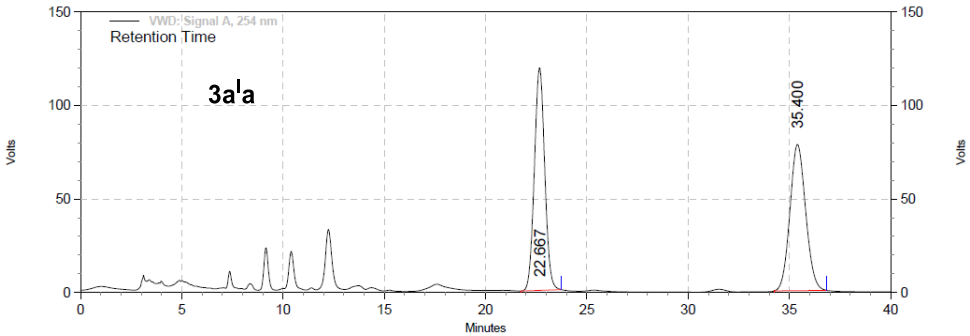

VWD: Signal A, 254 nm
Results

Pk #	Retention Time	Area	Area %
1	22.667	71008288	50.12
2	35.400	70681325	49.88
Totals		141689613	100.00

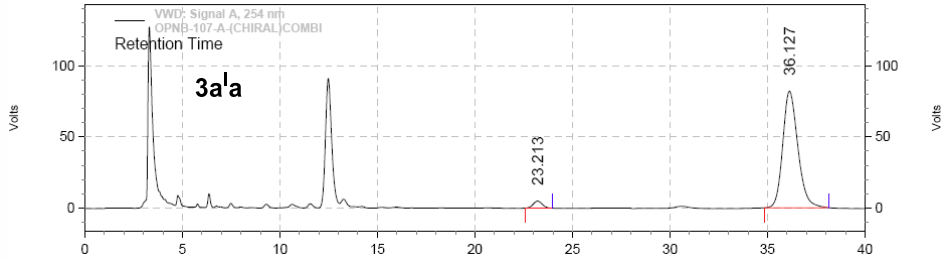

VWD: Signal A, 254 nm
Results

Pk #	Retention Time	Area	Area %
1	23.213	2701130	3.51
2	36.127	74156510	96.49
Totals		76857640	100.00

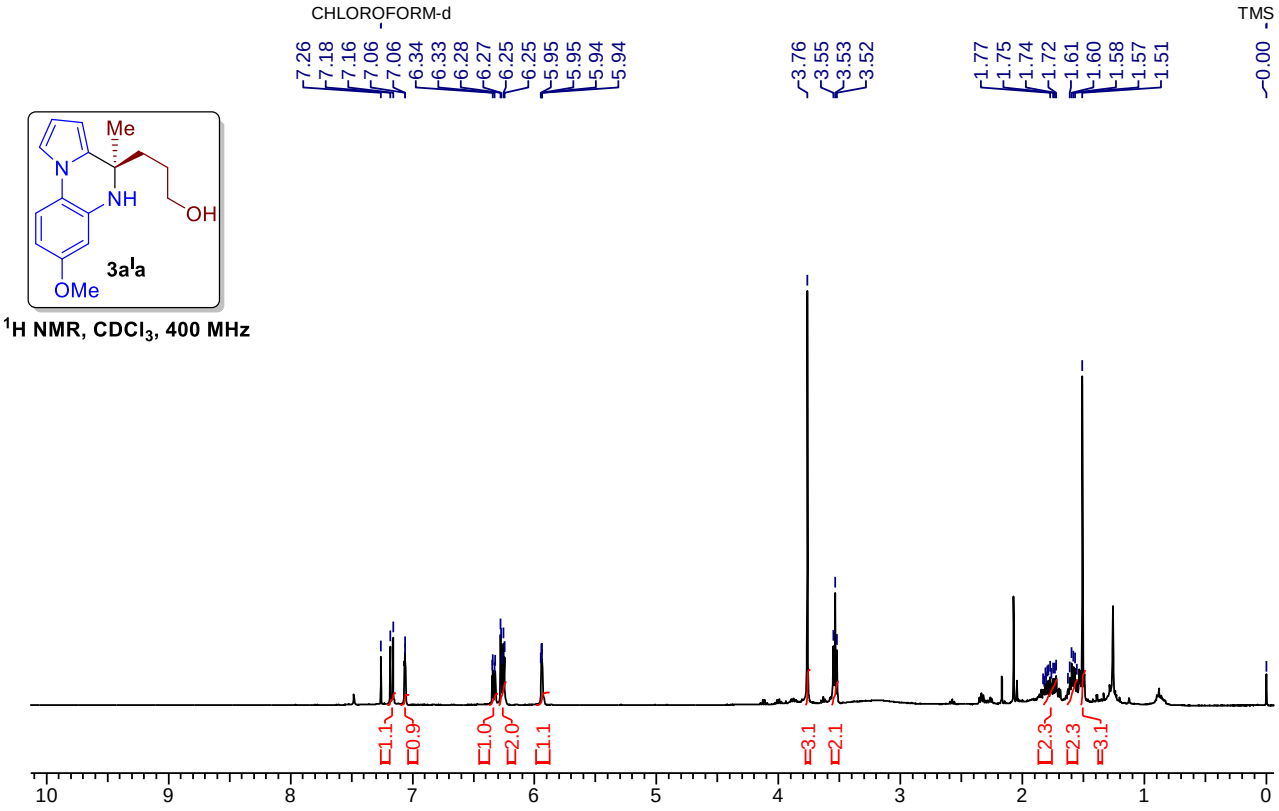

^{1}H NMR, $CDCl_3$, 400 MHz

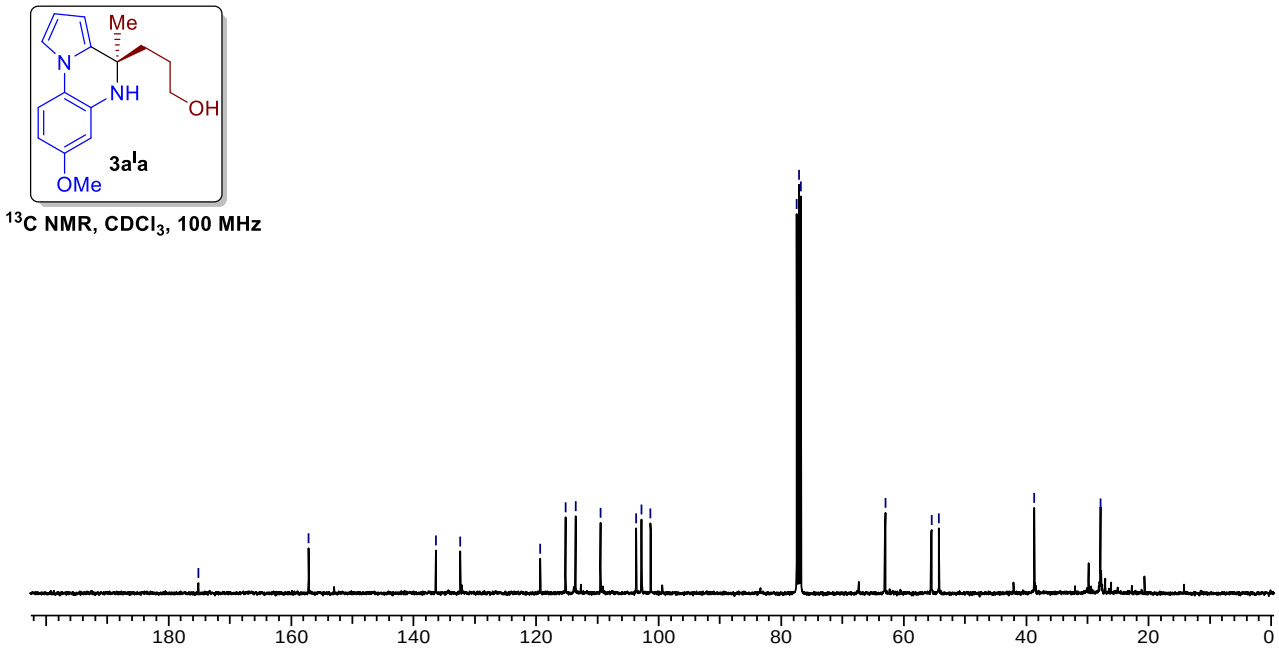

^{13}C NMR, $CDCl_3$, 100 MHz

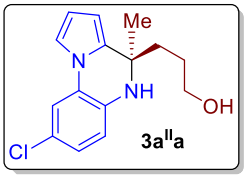

Entry 5, (3a^{II}a): White solid, 52% yield, R_f = 0.35 (pet ether/EtOAc = 60/40); **HPLC analysis:** 81.0% ee, t_R = 11.14 min (minor), t_R = 13.61 min (major). (Chiralpak IA, *n*-hexane/*i*PrOH (90:10), flow rate 1.0 mL/min, λ = 254 nm); **^{1}H NMR (200 MHz, $CDCl_3$)** δ = 7.16 (d, *J* = 8.5 Hz, 1 H), 7.07 (dd, *J* = 1.5, 3.0 Hz, 1 H), 6.77 - 6.59 (m, 2 H), 6.29 (t, *J* = 3.2 Hz, 1 H), 6.01 - 5.89 (m, 1 H), 3.55 (t, *J* = 6.2 Hz, 2 H), 1.91 - 1.70 (m, 2 H), 1.69 - 1.55 (m, 2 H), 1.52 (s, 3 H); **^{13}C NMR (50 MHz, $CDCl_3$)** δ = 136.3, 132.5, 129.6, 123.4, 118.3, 115.3, 114.9, 113.8, 110.2, 103.5, 62.8, 54.2, 38.8, 27.8, 27.7; **HRMS (ESI)** calcd for $C_{15}H_{17}ClN_2O$ $[M+H]^+$ 277.1102, found 277.1102.

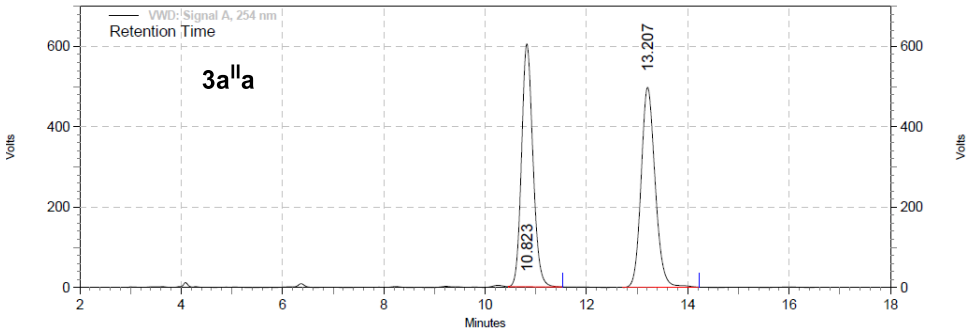

VWD: Signal A, 254 nm
Results

Pk #	Retention Time	Area	Area %
1	10.823	158367055	49.56
2	13.207	161201719	50.44
Totals		319568774	100.00

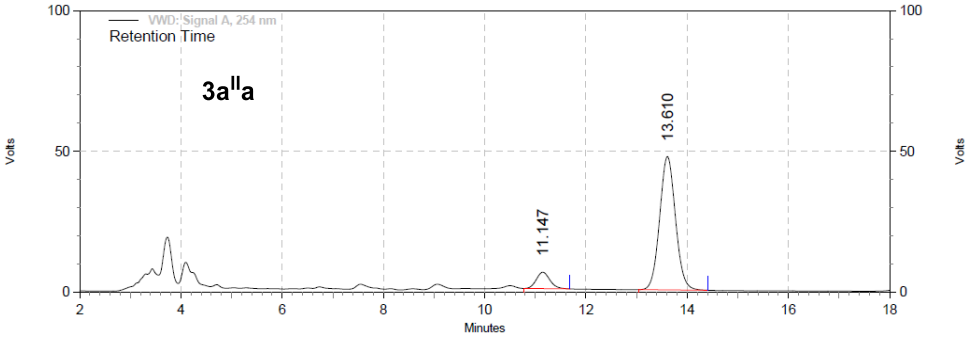

VWD: Signal A, 254 nm
Results

Pk #	Retention Time	Area	Area %
1	11.147	1808807	9.48
2	13.610	17278456	90.52
Totals		19087263	100.00

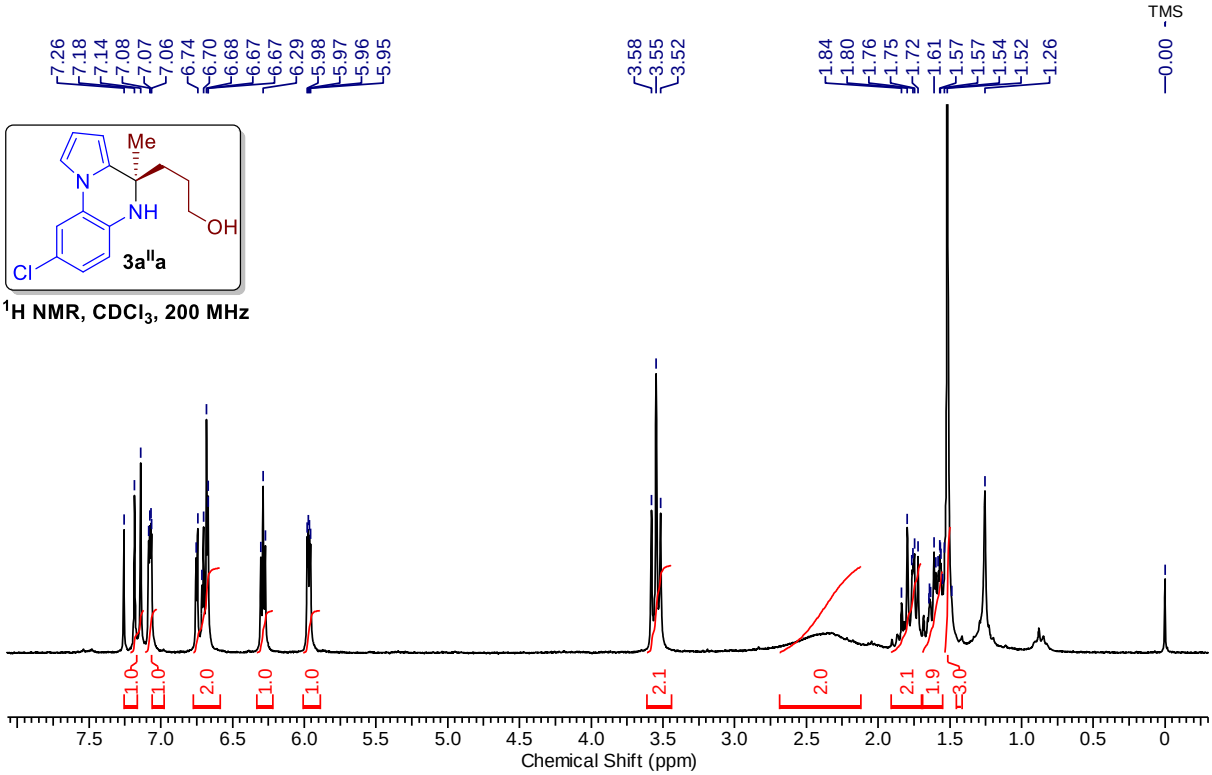

^{1}H NMR, $CDCl_3$, 200 MHz

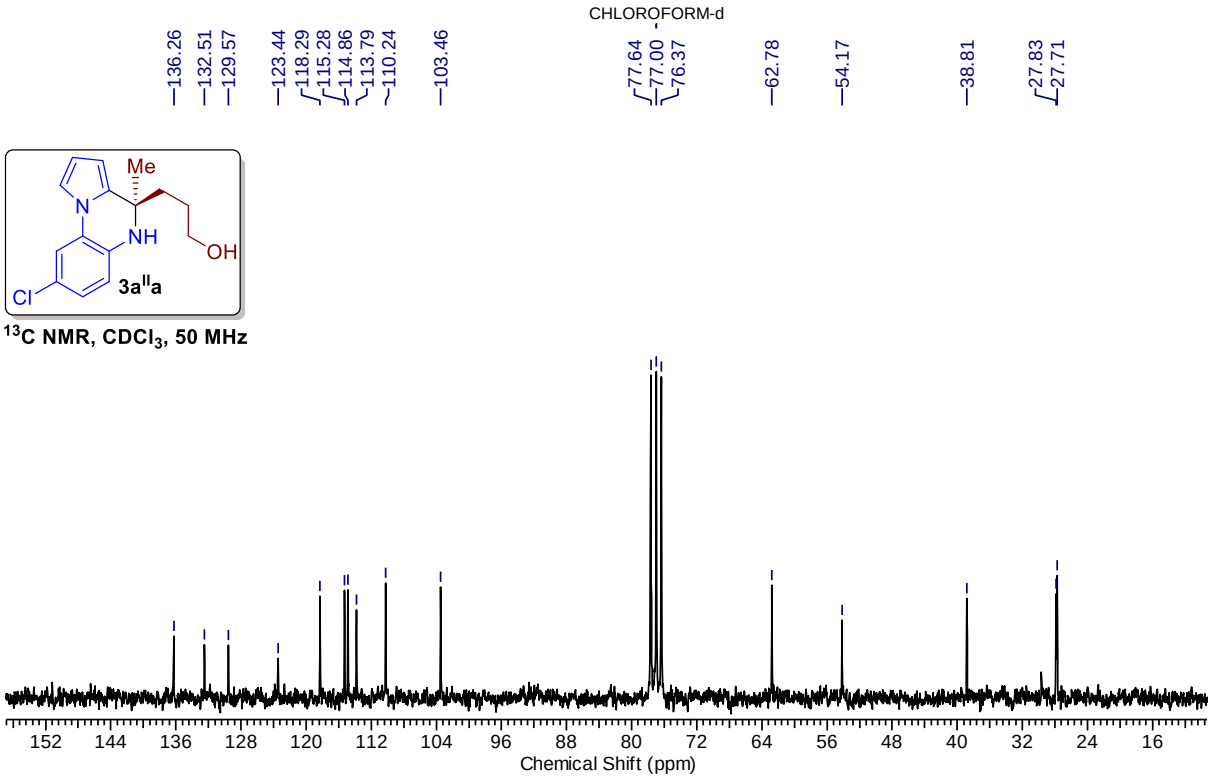

^{13}C NMR, $CDCl_3$, 50 MHz

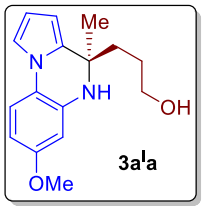

Entry 6, (3a'a): White solid, 44% yield; mp = 148-150°C; R_f = 0.35 (pet ether/EtOAc = 60/40); **HPLC analysis:** 92.5% ee, t_R = 22.59 min (minor), t_R = 34.88 min (major). (Chiralpak IA, *n*-hexane/*i*PrOH (90:10), flow rate 1.0 mL/min, λ = 254 nm).

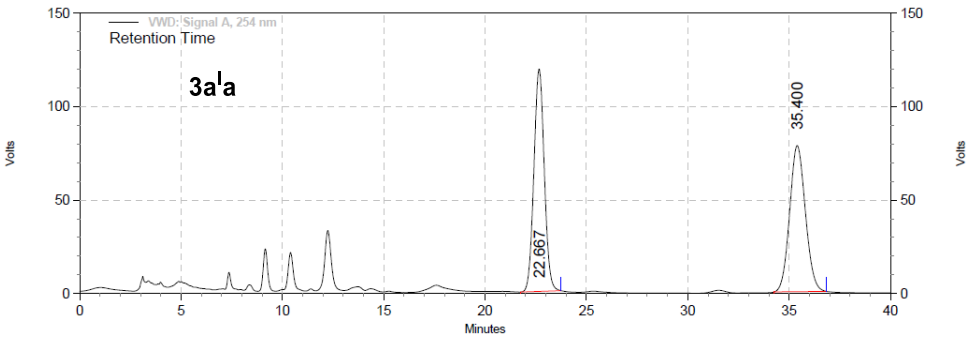

VWD: Signal A, 254 nm
Results

Pk #	Retention Time	Area	Area %
1	22.667	71008288	50.12
2	35.400	70681325	49.88
Totals		141689613	100.00

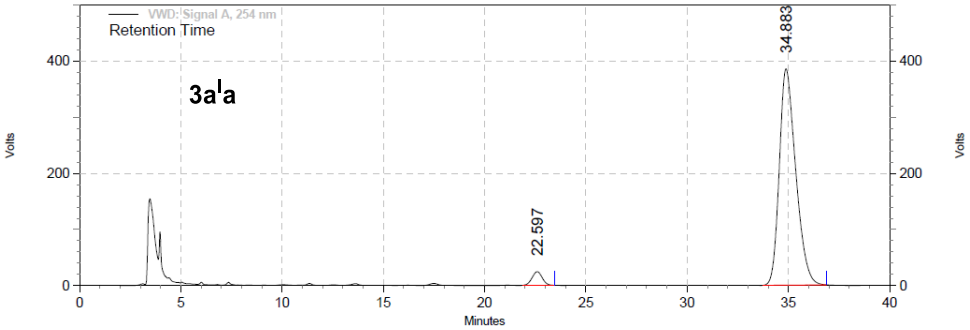

VWD: Signal A, 254 nm
Results

Pk #	Retention Time	Area	Area %
1	22.597	14189572	3.75
2	34.883	364028815	96.25
Totals		378218387	100.00

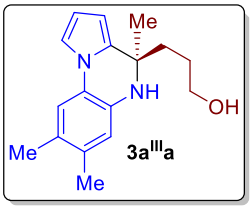

Entry 6, **(3a^{III}a):** White solid, 63% yield; mp = 129-131°C; R_f = 0.45 (pet ether/EtOAc = 70/30); **HPLC analysis:** 87.2% ee, t_R = 10.97 min (minor), t_R = 17.57 min (major). (Chiralpak IA, *n*-hexane/*i*PrOH (90:10), flow rate 1.0 mL/min, λ = 254 nm); **^{1}H NMR (500 MHz, $CDCl_3$) δ** = 7.14 - 6.95 (m, 2 H), 6.72 (br. s., 1 H), 6.25 (br. s., 1 H), 6.03 - 5.81 (m, 1 H), 3.59 - 3.51 (m, 2 H), 2.25 - 2.15 (m, 6 H), 1.84 - 1.75 (m, 1 H), 1.87 (s, 1 H), 1.83 - 1.76 (m, 1 H), 1.68 - 1.59 (td, *J* = 7.1, 14.2 Hz, 1 H), 1.54 (s, 3 H); **^{13}C NMR (125 MHz) δ** = 133.1, 132.1, 130.1, 129.2, 124.0, 118.6, 116.0, 114.1, 109.8, 103.6, 62.9, 54.9, 37.8, 27.7, 26.8, 19.4; **HRMS (ESI)** calcd for $C_{17}H_{23}N_2O$ $[M+H]^+$ 271.1805, found 271.1802.

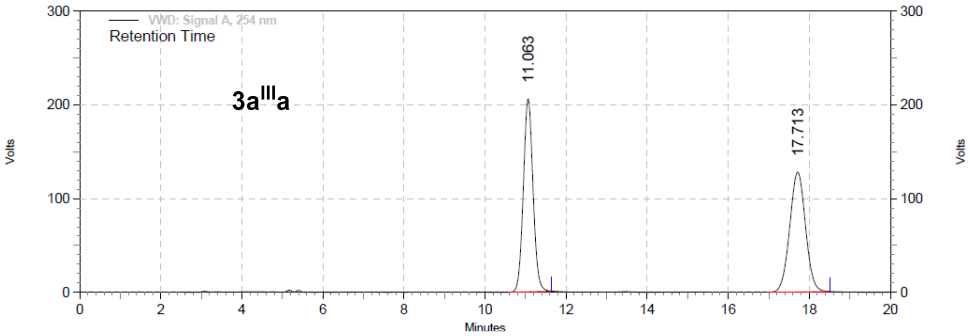

VWD: Signal A, 254 nm
Results

Pk #	Retention Time	Area	Area %
1	11.063	57176715	49.63
2	17.713	58028779	50.37
Totals		115205494	100.00

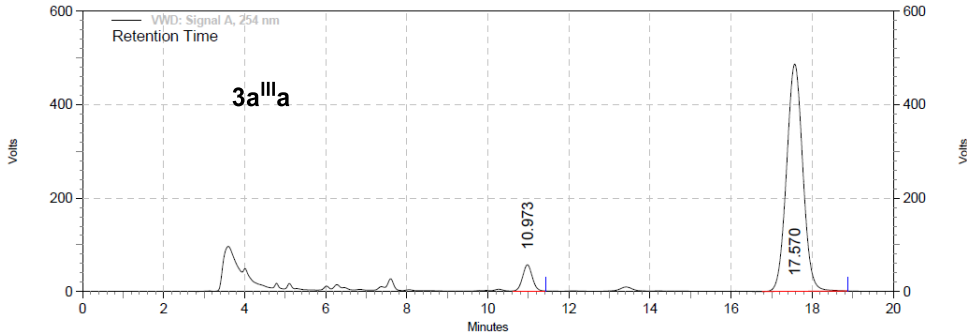

VWD: Signal A, 254 nm
Results

Pk #	Retention Time	Area	Area %
1	10.973	15436629	6.37
2	17.570	226817011	93.63
Totals		242253640	100.00

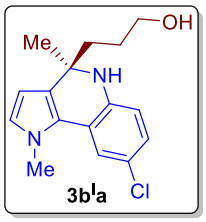

Entry 7, (3b^{I}a): Thick liquid, 43% yield, R_f = 0.30 (pet ether/EtOAc = 60/40); **HPLC analysis:** 81.0% ee; t_R = 11.14 min (minor), t_R = 13.61 min (major). (Chiralpak IB, *n*-hexane/*i*PrOH (93:07), flow rate 1.0 mL/min, λ = 254 nm); **^{1}H NMR (500 MHz, $CDCl_3$) δ** = 7.32 (d, *J* = 2.4 Hz, 1 H), 6.85 (dd, *J* = 2.3, 8.4 Hz,1 H), 6.57 (d, *J* = 2.7 Hz, 1 H), 6.48 (d, *J* = 8.2 Hz, 1 H), 5.91 (d, *J* = 2.7 Hz, 1 H), 3.87 (s, 3 H), 3.56 (t, *J* = 6.3 Hz, 2 H), 1.78 (dd, *J* = 2.1, 4.9 Hz, 1 H), 1.69 - 1.63 (m, 2 H), 1.58 - 1.54 (m, 2 H), 1.47 (s, 3 H) **^{13}C NMR (125 MHz, $CDCl_3$) δ** = 141.1, 128.0, 125.5, 123.6, 122.0, 119.8, 117.8, 114.9, 102.9, 63.2, 55.6, 40.2, 37.2, 28.0; **HRMS (ESI)** calcd for $C_{16}H_{20}ClN_2O$ $[M+H]^+$ 291.1259, found 291.1254.

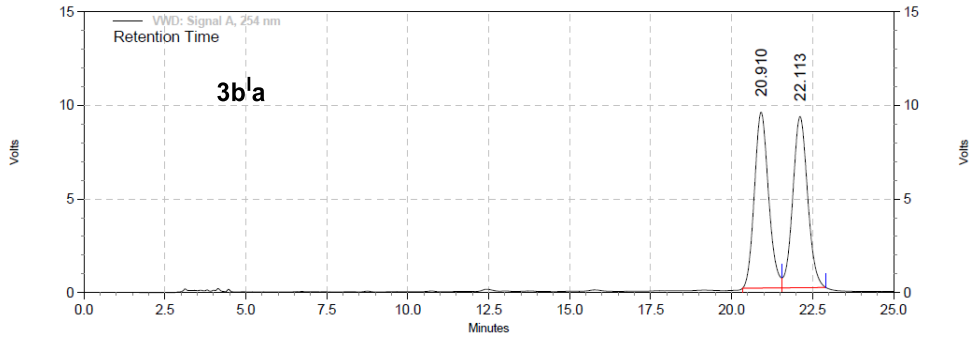

VWD: Signal A, 254 nm
Results

Pk #	Retention Time	Area	Area %
1	20.910	4783612	49.50
2	22.113	4880355	50.50
Totals		9663967	100.00

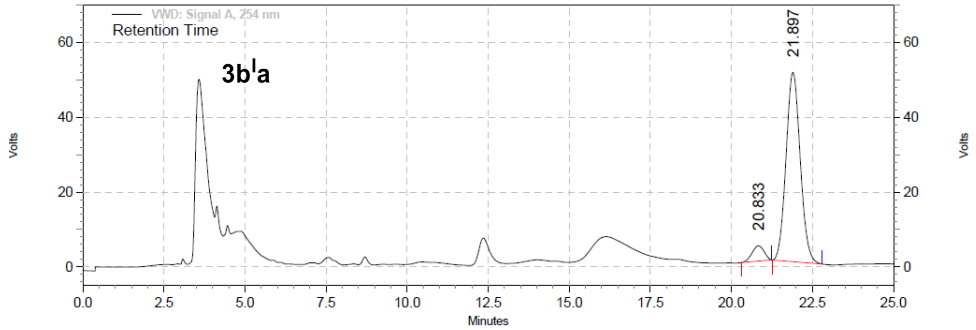

VWD: Signal A, 254 nm
Results

Pk #	Retention Time	Area	Area %
1	20.833	1752542	6.35
2	21.897	25830241	93.65
Totals		27582783	100.00

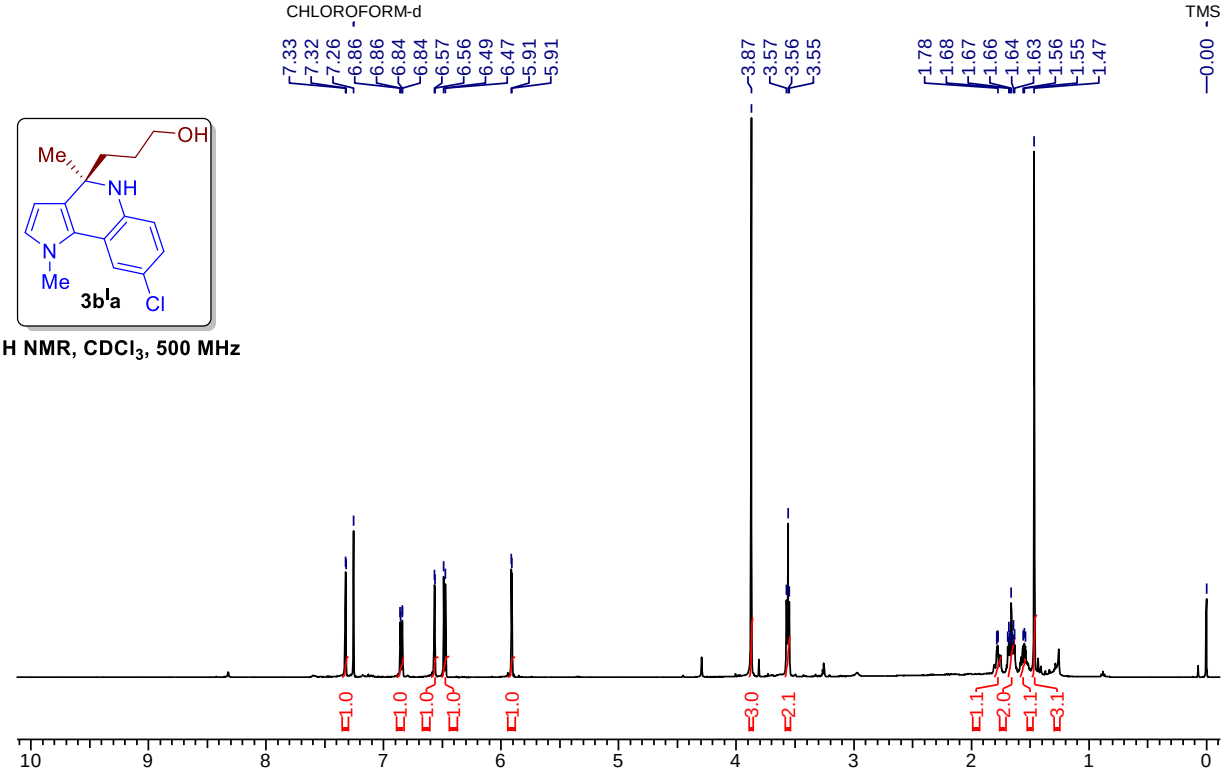

^{1}H NMR, $CDCl_3$, 500 MHz

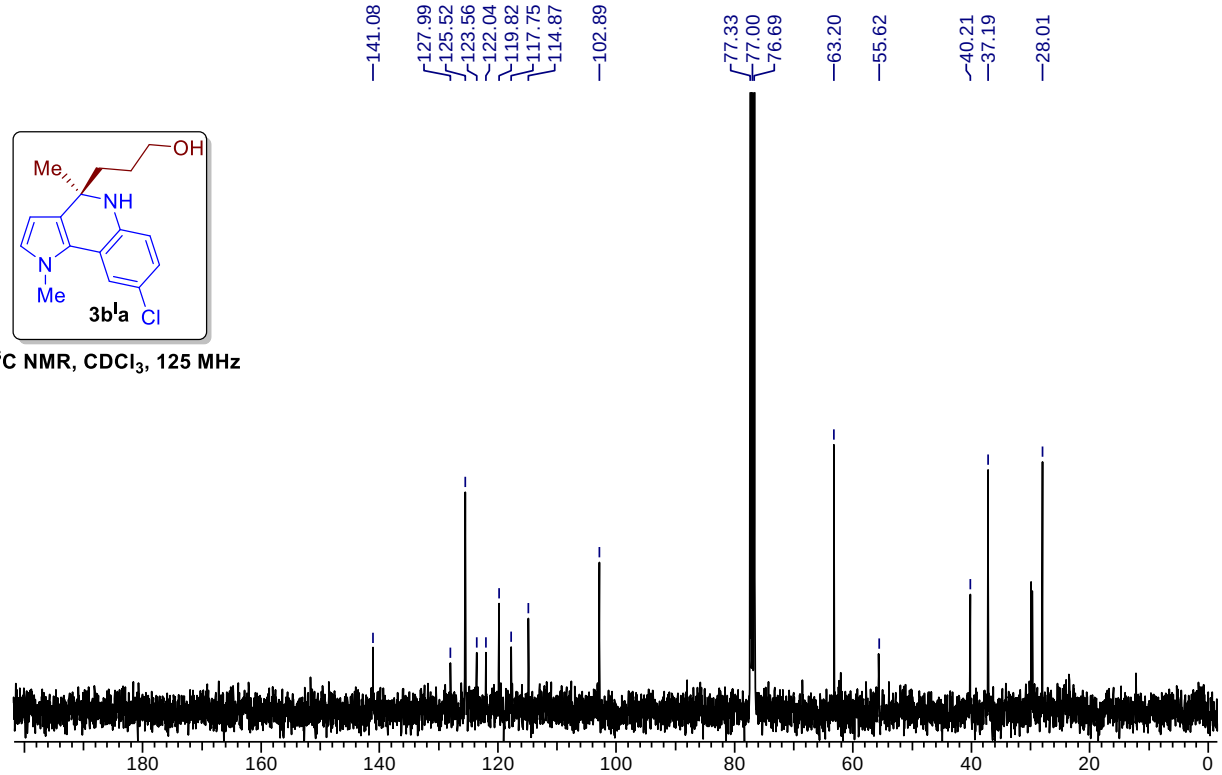

^{13}C NMR, $CDCl_3$, 125 MHz

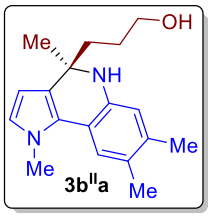

Entry 7, (3b^{II}a): White solid, 72% yield; mp = 137-139°C; R_f = 0.37 (pet ether/EtOAc = 60/40); **HPLC analysis:** 84.5% ee, t_R = 5.73 min (minor), t_R = 6.38 min (major). (Chiralpak IB, *n*-hexane/*i*PrOH (75:25), flow rate 1.0 mL/min, λ = 254 nm); **^{1}H NMR (500 MHz, $CDCl_3$) δ** = 7.17 (s, 1 H), 6.56 - 6.49 (m, 1 H), 6.43 (s, 1 H), 5.97 - 5.82 (m, 1 H), 3.89 (s, 3 H), 3.57 (t, *J* = 6.1 Hz, 2 H), 2.20-2.18 (s, 3 H), 2.17-2.15 (s, 3 H), 1.82 - 1.75 (m, 1 H), 1.71 - 1.59 (m, 3 H), 1.46 (s, 3 H); **^{13}C NMR (125 MHz, $CDCl_3$) δ** = 140.5, 134.2, 125.3, 124.8, 124.3, 124.1, 121.5, 115.9, 114.6, 102.7, 63.4, 55.3, 39.8, 37.1, 29.5, 28.2, 19.6, 19; **HRMS (ESI)** calcd for $C_{18}H_{25}N_2O$ $[M+H]^+$ 285.1961, found 285.1956.

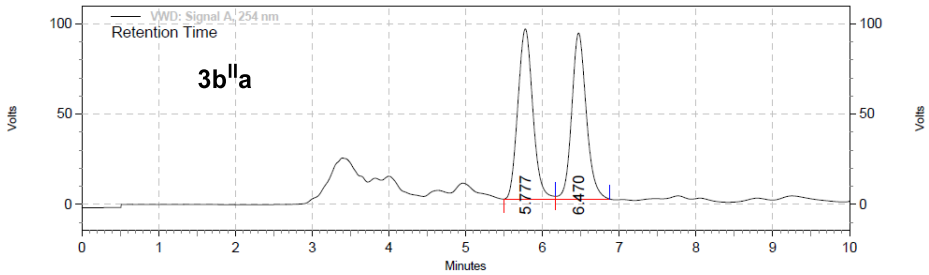

VWD: Signal A, 254 nm
Results

Pk #	Retention Time	Area	Area %
1	5.777	21412646	51.19
2	6.470	20413235	48.81
Totals		41825881	100.00

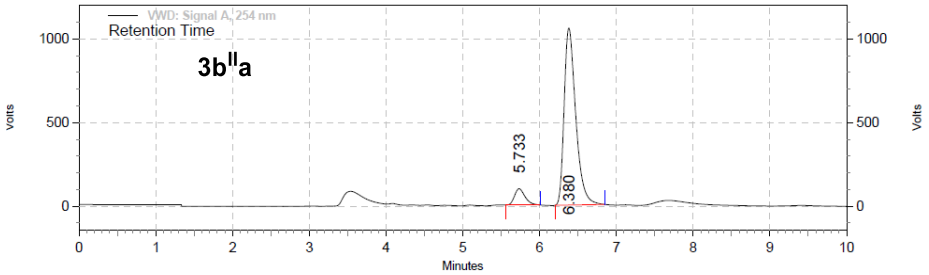

VWD: Signal A, 254 nm
Results

Pk #	Retention Time	Area	Area %
1	5.733	15595047	7.72
2	6.380	186345179	92.28
Totals		201940226	100.00

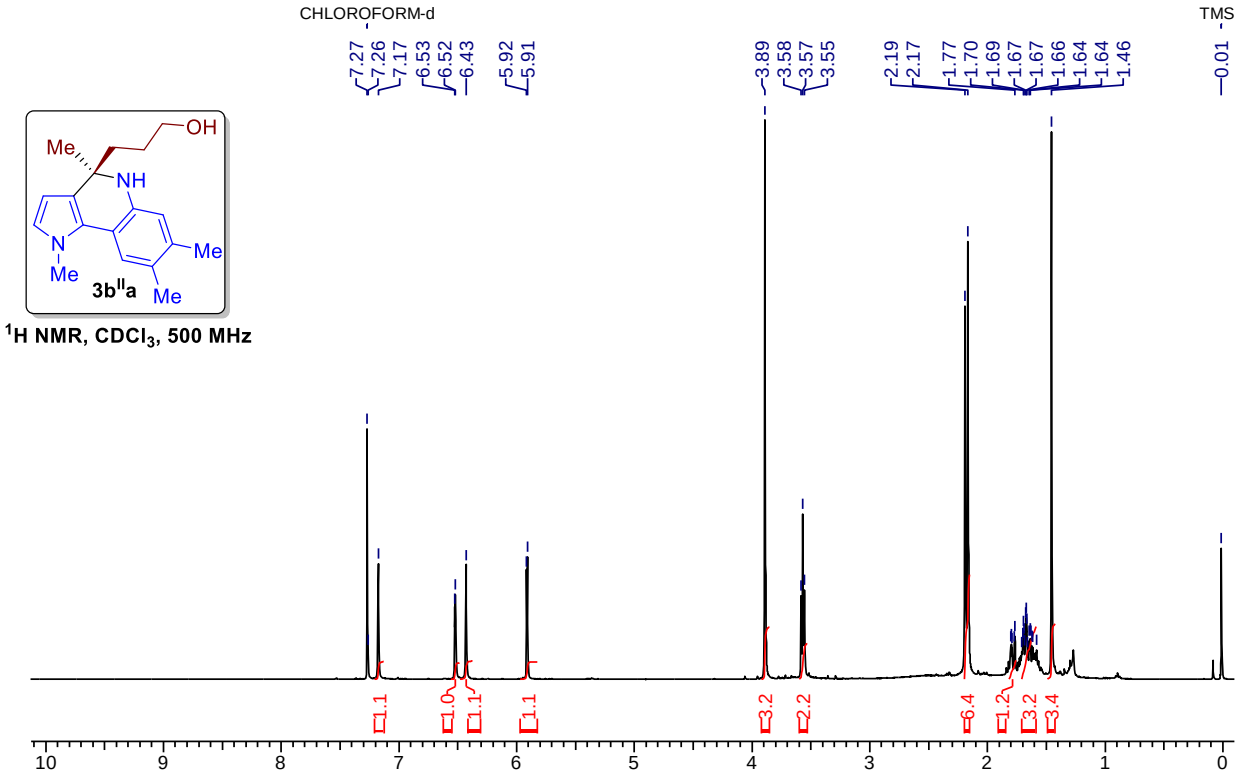

^{1}H NMR, $CDCl_3$, 500 MHz

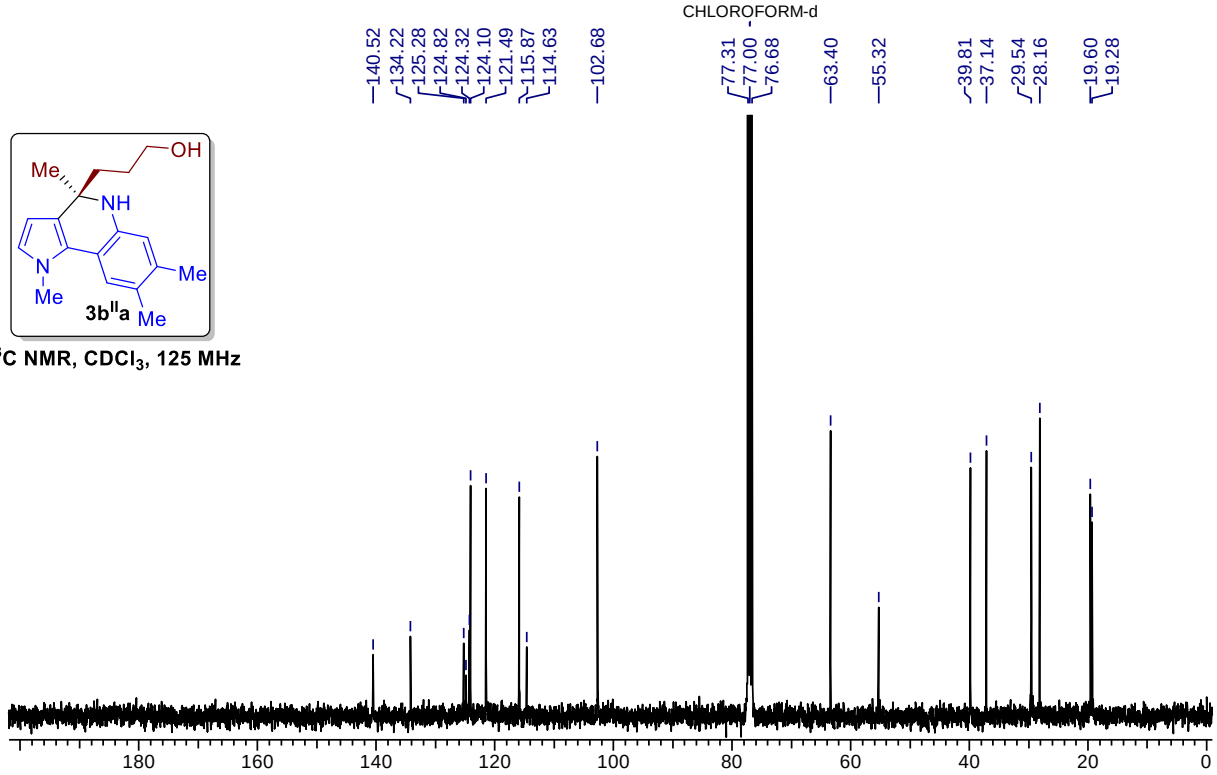

^{13}C NMR, $CDCl_3$, 125 MHz

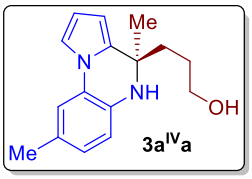

Entry 8, **(3a^{IV}a):** White solid, 73% yield, **mp** = 129-131°C; ***R$_f$*** = 0.45 (pet ether/EtOAc = 70/30); **HPLC analysis:** 86.1% ee, t_R = 25.83 min (minor), t_R = 26.90 min (major). (Chiralpak IA, *n*-hexane/*i*PrOH (90:10), flow rate 1.0 mL/min, λ = 254 nm); **^{1}H NMR (500 MHz, CDCl$_3$)** δ = 8.41 (br. s., 1 H), 7.44 - 7.38 (m, 1 H), 7.13 - 7.03 (m, 1 H), 6.67 (t, *J* = 2.7 Hz, 1 H), 6.46 (d, *J* = 8.2 Hz, 1 H), 6.40 - 6.35 (m, 1 H), 3.55 - 3.40 (m, 1 H), 1.99 - 1.82 (m, 1 H), 1.68 - 1.54 (m, 2 H), 1.51 (s, 20 H), 1.44 - 1.34 (m, 1 H); **^{13}C NMR (125 MHz, CDCl$_3$ + DMSO-d$_6$)** δ = 135.7, 134.3, 124.3, 124.1, 123.4, 122.0, 117.2, 113.6, 107.7, 100.8, 60.8, 52.1, 35.1, 26.7, 24.4, 20.4; **HRMS (ESI)** calcd for $C_{16}H_{21}N_2O$ $[M+H]^+$ 257.1648, found 257.1648.

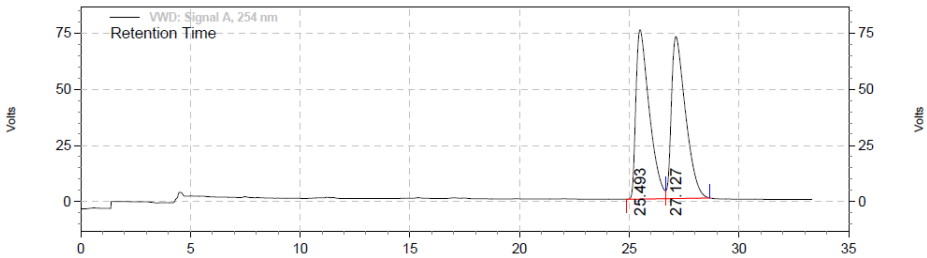

VWD: Signal A, 254 nm
Results

Pk #	Retention Time	Area	Area %
1	22.667	71008288	50.12
2	35.400	70681325	49.88
Totals		141689613	100.00

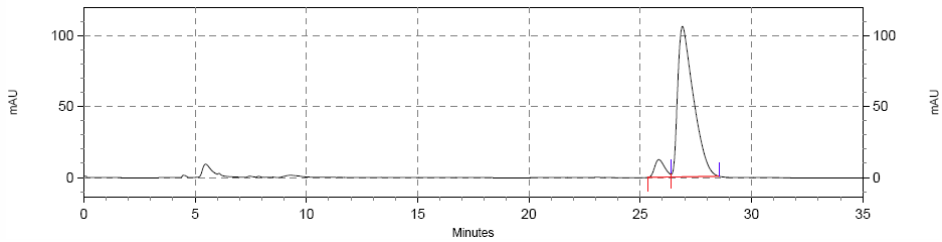

VWD: Signal A, 254 nm
Results

Pk #	Retention Time	Area	Area %
1	23.213	2701130	3.51
2	36.127	74156510	96.49
Totals		76857640	100.00

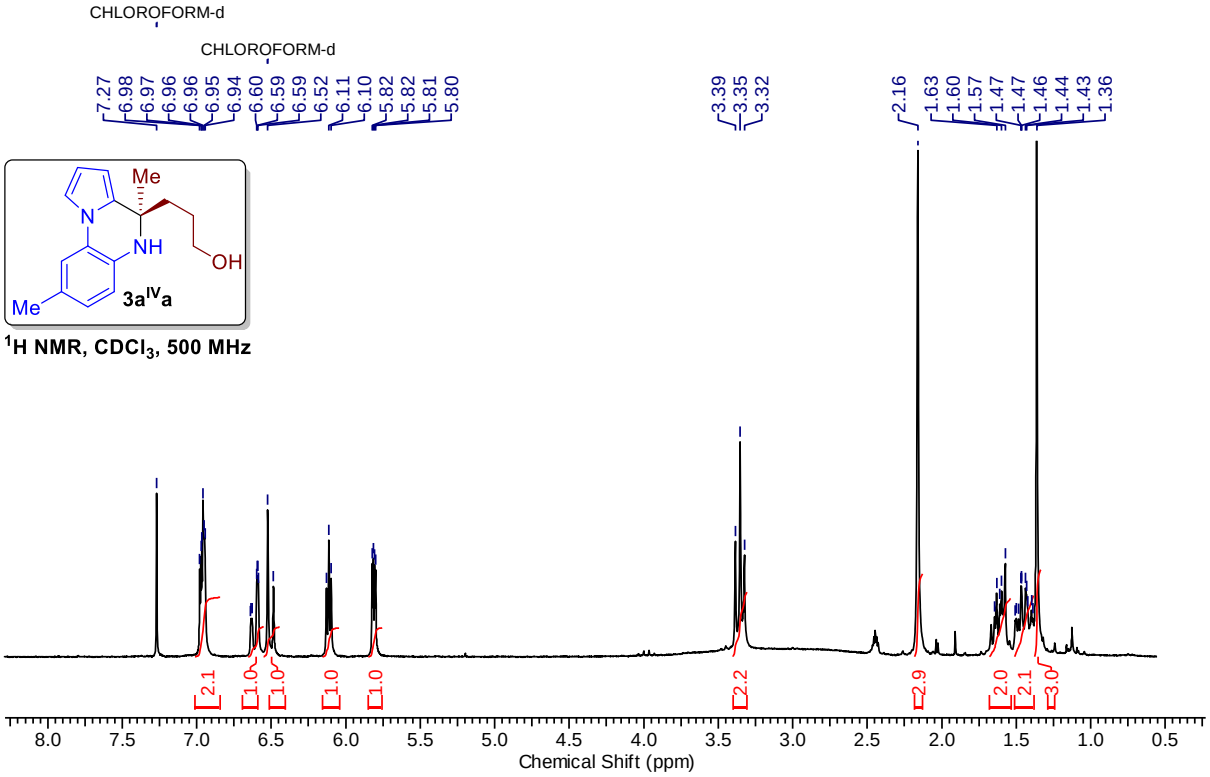

^{1}H NMR, $CDCl_3$, 500 MHz

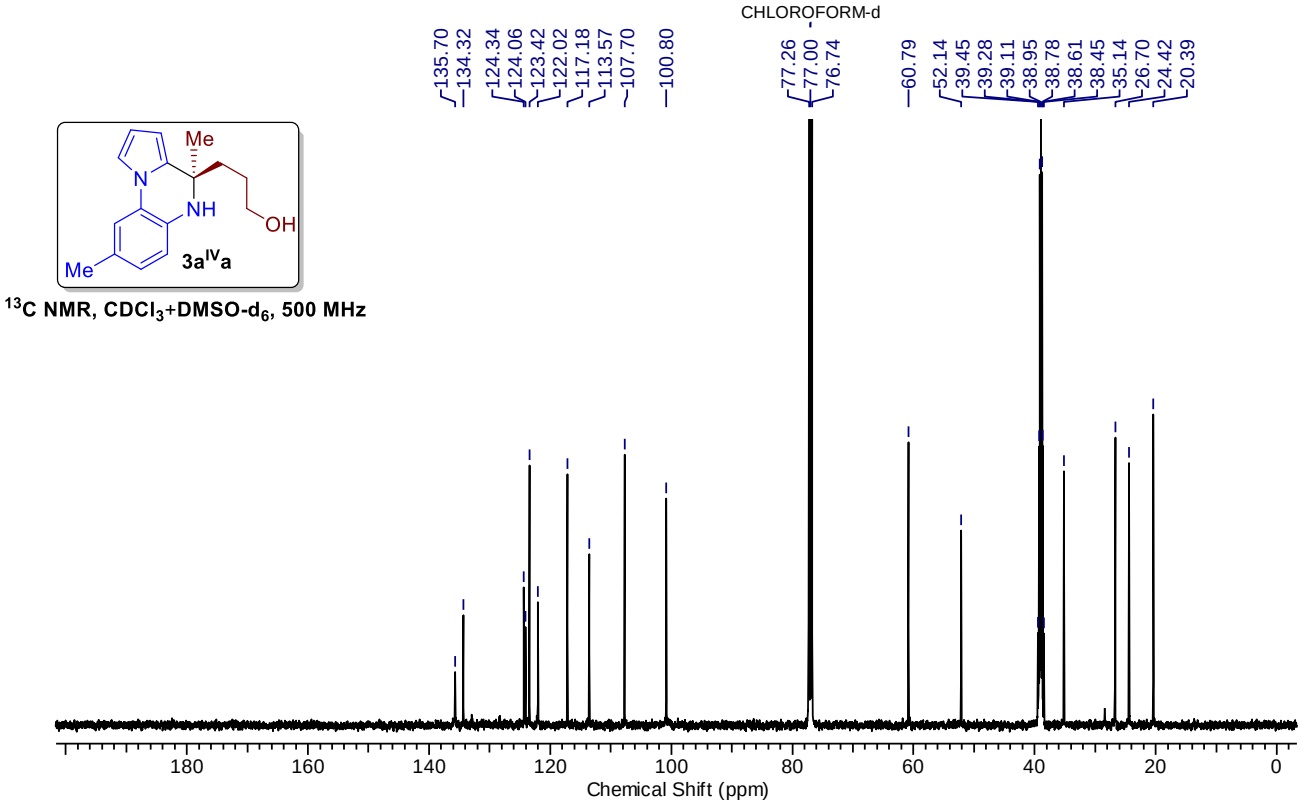

^{13}C NMR, $CDCl_3$+DMSO-d_6, 500 MHz

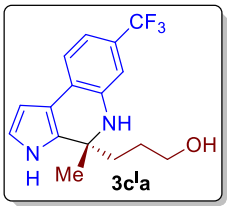

Entry 8, (3c'a): Thick yellow liquid, 76% yield, R_f = 0.10 (pet ether/EtOAc = 70/30); **HPLC analysis:** 91.0 ee, t_R = 13.29 min (minor), t_R = 15.67 min (major). (Chiralpak IC, *n*-hexane/*i*PrOH (90:10), flow rate 1.0 mL/min, λ = 254 nm); **^{1}H NMR (400 MHz, $CDCl_3$) δ** = 8.41 (br. s., 1 H), 7.44 - 7.38 (m, 1 H), 7.13 - 7.03 (m, 1 H), 6.67 (t, *J* = 2.7 Hz, 1 H), 6.46 (d, *J* = 8.2 Hz, 1 H), 6.40 - 6.35 (m, 1 H), 3.55 - 3.40 (m, 1 H), 1.99 - 1.82 (m, 1 H), 1.68 - 1.54 (m, 2 H), 1.51 (s, 3 H), 1.44 - 1.34 (m, 1 H); **^{13}C NMR (50 MHz, $CDCl_3$) δ** = 143.8, 122.8, 122.7, 118.8, 118.7, 118.6, 118.5, 118.3, 114.7, 111.8, 102.4, 62.5, 55.9, 40.4, 30.5, 27.5; **HRMS (ESI)** calcd for $C_{16}H_{18}N_2OF_3$ $[M+H]^+$ 311.1360, found 311.1366.

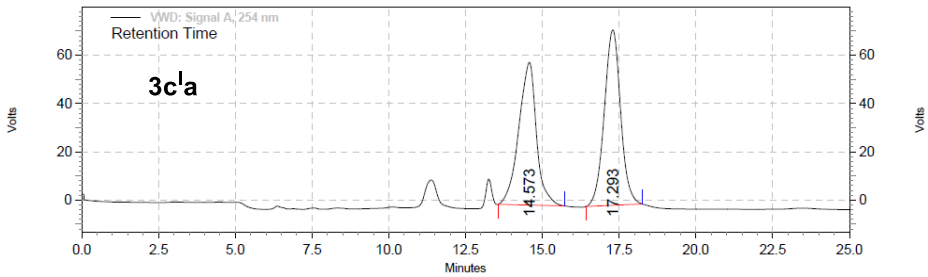

VWD: Signal A, 254 nm
Results

Pk #	Retention Time	Area	Area %
1	14.573	39760139	46.84
2	17.293	45127547	53.16
Totals		84887686	100.00

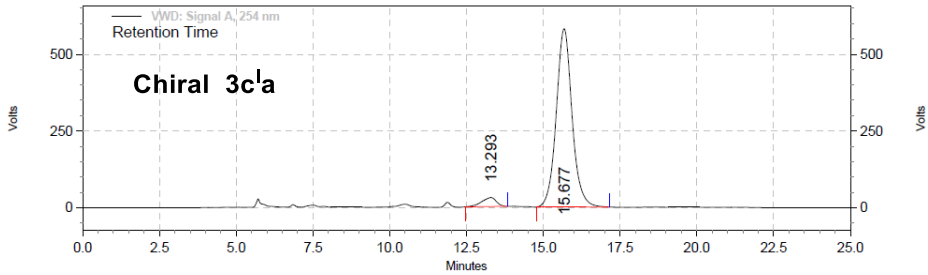

VWD: Signal A, 254 nm
Results

Pk #	Retention Time	Area	Area %
1	13.293	16283506	4.47
2	15.677	348350372	95.53
Totals		364633878	100.00

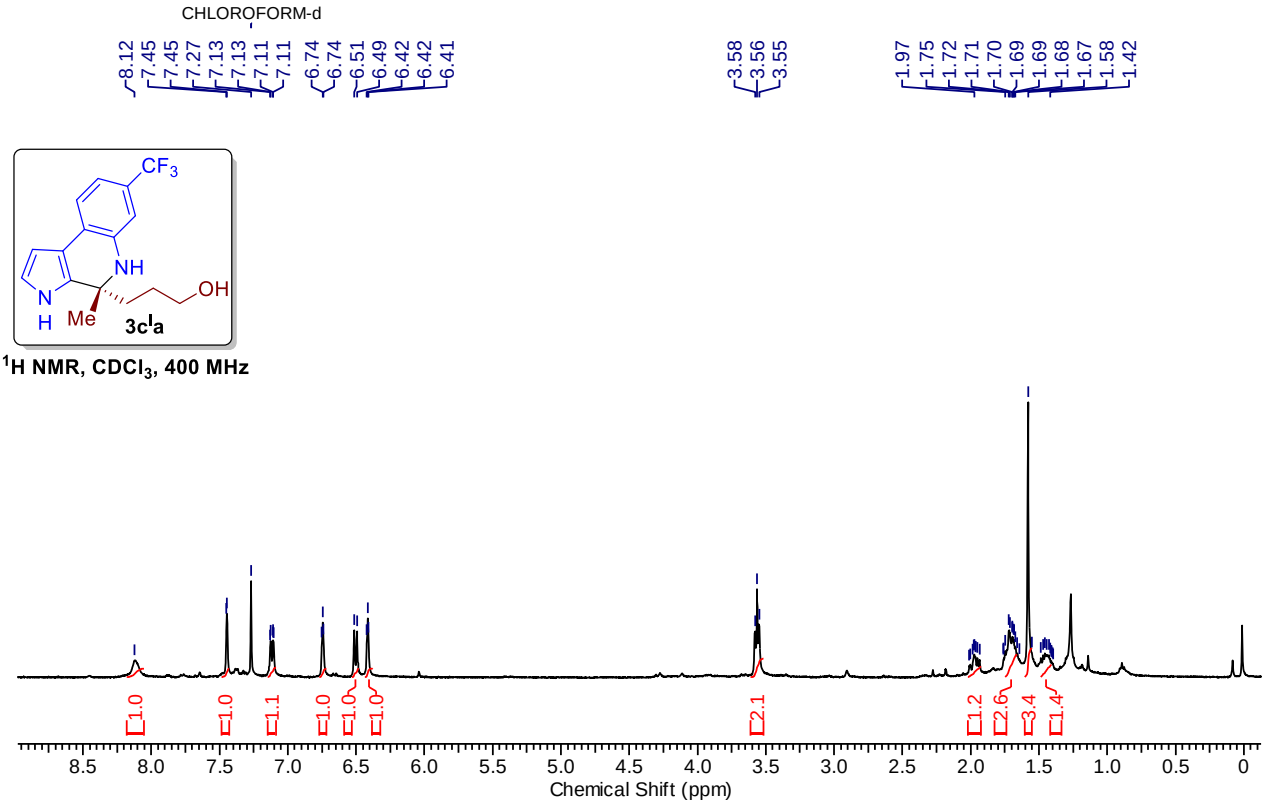

^{1}H NMR, $CDCl_3$, 400 MHz

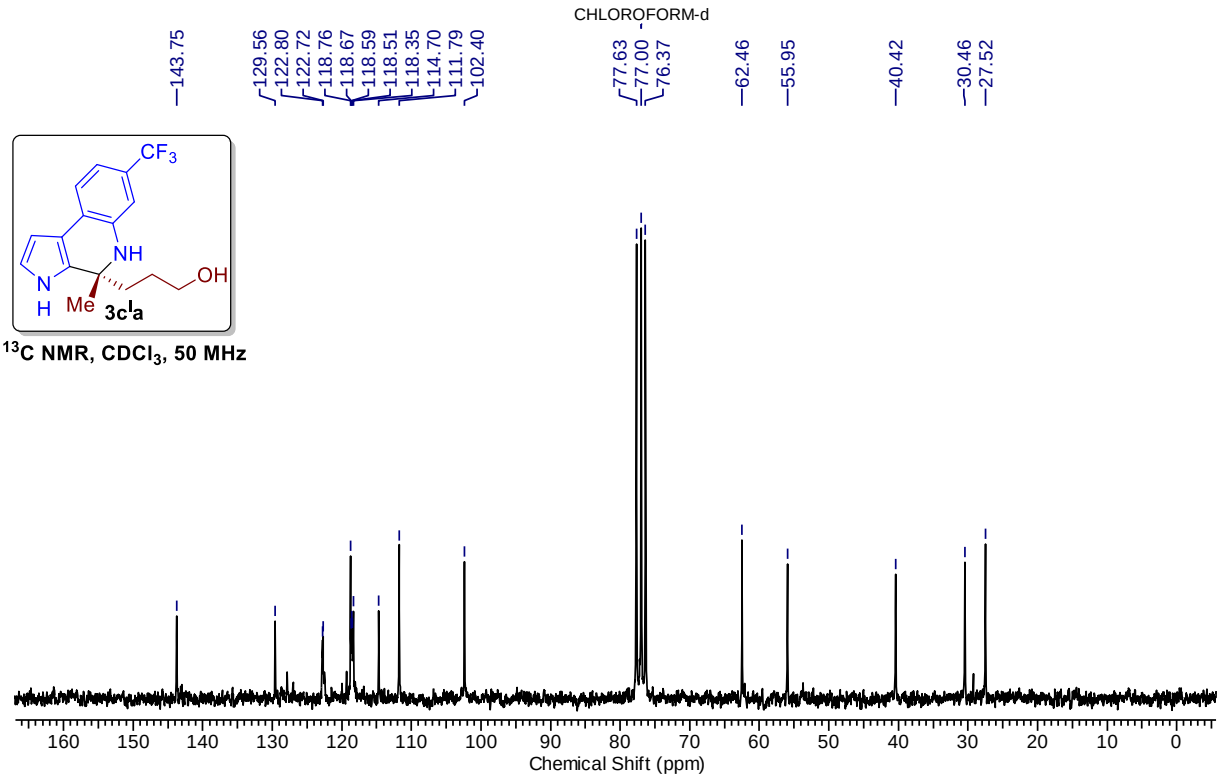

^{13}C NMR, $CDCl_3$, 50 MHz

Table 2.3.1.2: Variation of SBAs/Alkynols - Four Components in One-pot

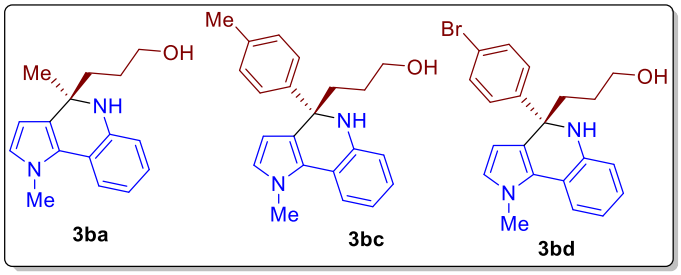

Entry 1, **(3ba, 3bc, 3bd):** Thick liquid, 59% combined yield, R_f = 0.35 (pet ether/EtOAc = 60/40); **HPLC analysis:** Product ratio for (3ba:3bc:3bd) : [2.05:1.00:1.41], **(3ba)** 88.0% ee, t_R = 15.21 min (minor), t_R = 16.55 min (major), **(3bc)**, 82.6% ee, t_R = 45.09 min (minor), t_R = 29.65 min (major), **(3bd)**, 92.4% ee, t_R = 35.78 min (minor), t_R=27.42 min (major). (Chiralpak IB, *n*-hexane/*i*PrOH (90:10), flow rate 1.0 mL/min, λ = 254 nm); **^{1}H NMR (400 MHz, $CDCl_3$) δ** = 7.42 - 7.36 (m, 2 H), 7.35 - 7.26 (m, 3 H), 7.05 (d, *J* = 8.2 Hz, 2 H), 6.99 - 6.87 (m, 5 H), 6.72 - 6.63 (m, 3 H), 6.60 - 6.50 (m, 3 H), 5.93 (dd, *J* = 3.0, 10.8 Hz, 1 H), 3.94 - 3.82 (m, 6 H), 3.67 - 3.60 (m, 2 H), 3.58 - 3.52 (m, 2 H), 2.31 (td, *J* = 5.3, 8.6 Hz, 3 H), 2.25 (s, 2 H), 2.16 - 1.95 (m, 2 H), 1.83 - 1.54 (m, 8 H), 1.47 (s, 3 H).

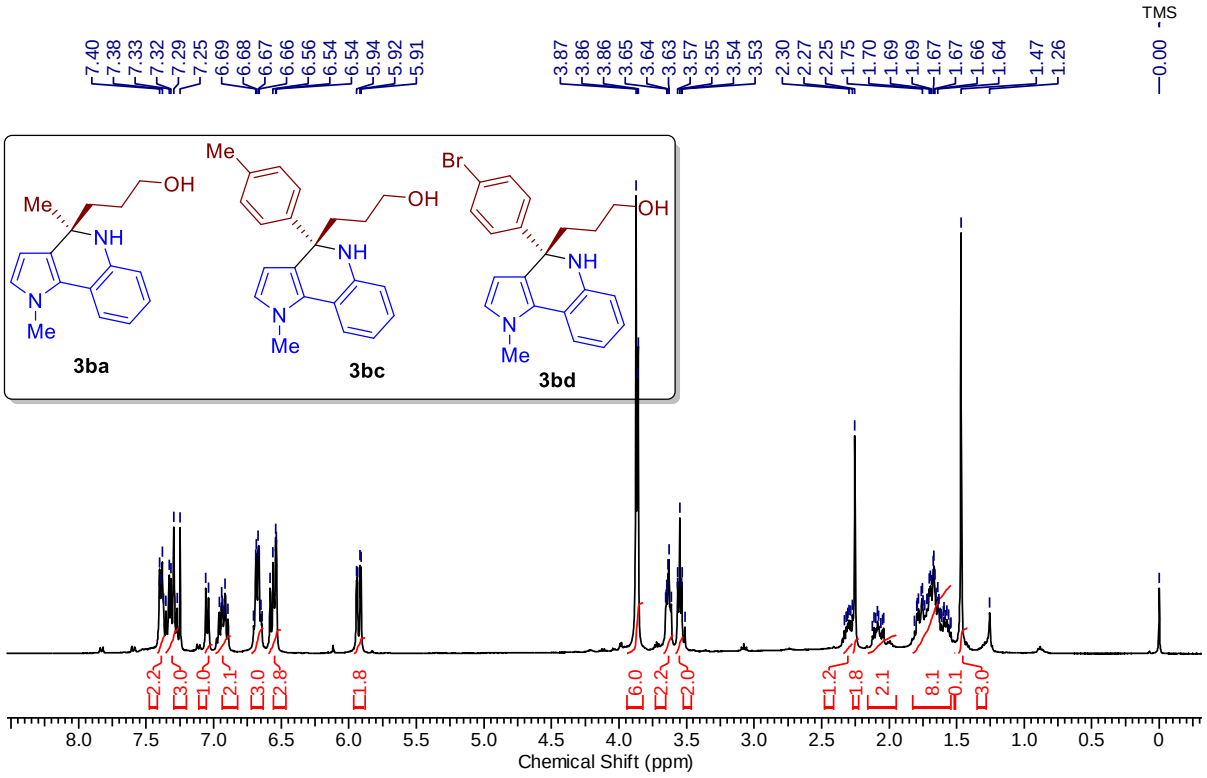

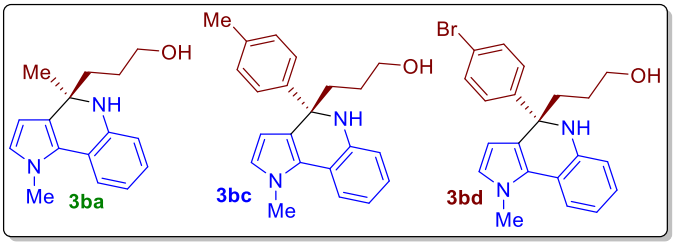

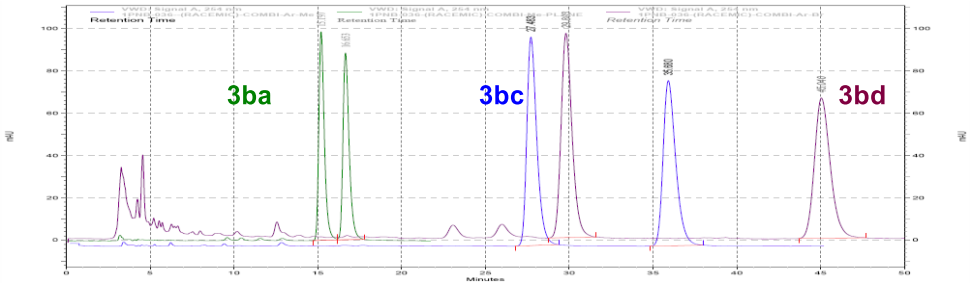

Retention Time		Area %	Retention Time		Area %	Retention Time		Area %
3ba	15.197	50.10	3bc	27.483	49.93	3bd	29.803	50.26
	16.653	49.90		35.680	50.07		45.040	49.74
		100.00			100.00			100.00

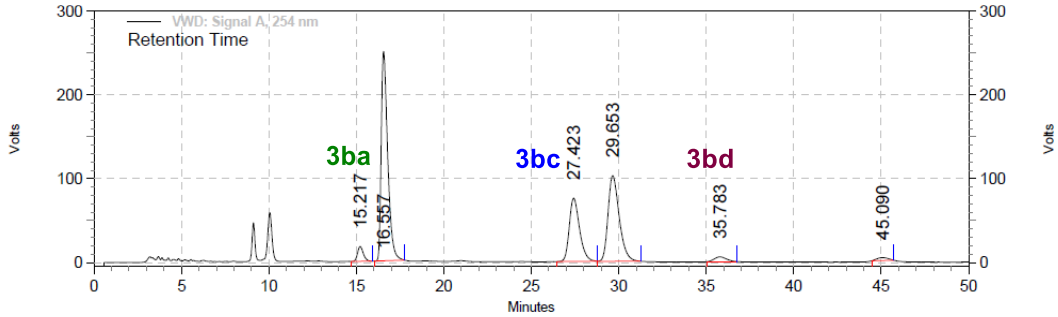

VWD: Signal A, 254 nm
Results

Pk #	Retention Time	Area	Area %
1	15.217	6769953	2.72
2	16.557	107838720	43.26
3	27.423	51342128	20.59
4	29.653	76213716	30.57
5	35.783	4529834	1.82
6	45.090	2604152	1.04
Totals		249298503	100.00

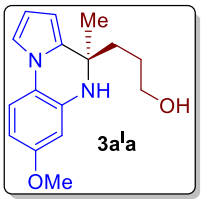

Entry 2, (3a'a): White solid, 90% yield, R_f = 0.30 (pet ether/EtOAc = 60/40), **HPLC analysis:** 91.1% ee, t_R = 23.12 min (minor), t_R = 35.74 min (major). (Chiralpak IB, *n*-hexane/*i*PrOH (90:10), flow rate 1.0 mL/min, λ = 254 nm)

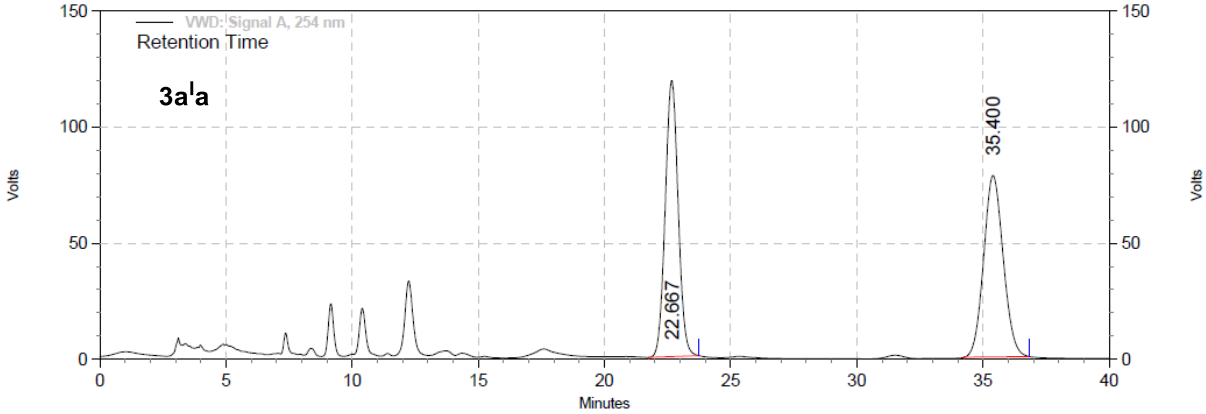

VWD: Signal A, 254 nm
Results

Pk #	Retention Time	Area	Area %
1	22.667	71008288	50.12
2	35.400	70681325	49.88
Totals		141689613	100.00

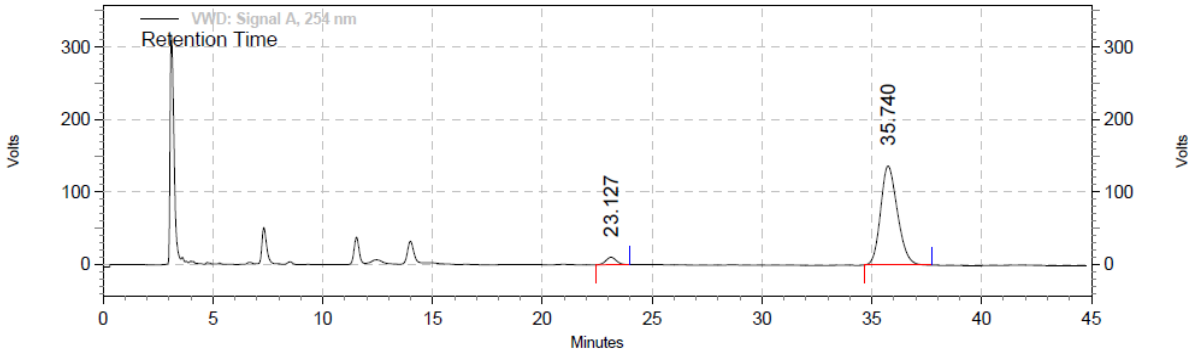

VWD: Signal A, 254 nm
Results

Pk #	Retention Time	Area	Area %
1	23.127	5695671	4.44
2	35.740	122641665	95.56
Totals		128337336	100.00

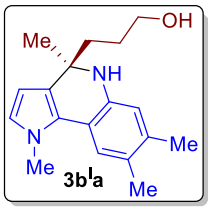

Entry 2, (3b^{I}a): White solid, 78% yield, R_f = 0.37 (pet ether/EtOAc = 60/40); **HPLC analysis:** 91.2% ee, t_R = 5.803 min (minor), t_R = 6.453 min (major). (Chiralpak IB, *n*-hexane/*i*PrOH (93:07), flow rate 1.0 mL/min, λ = 254 nm)

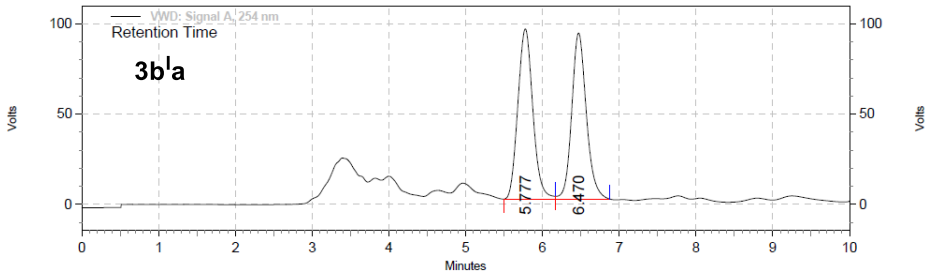

VWD: Signal A, 254 nm
Results

Pk #	Retention Time	Area	Area %
1	5.777	21412646	51.19
2	6.470	20413235	48.81
Totals		41825881	100.00

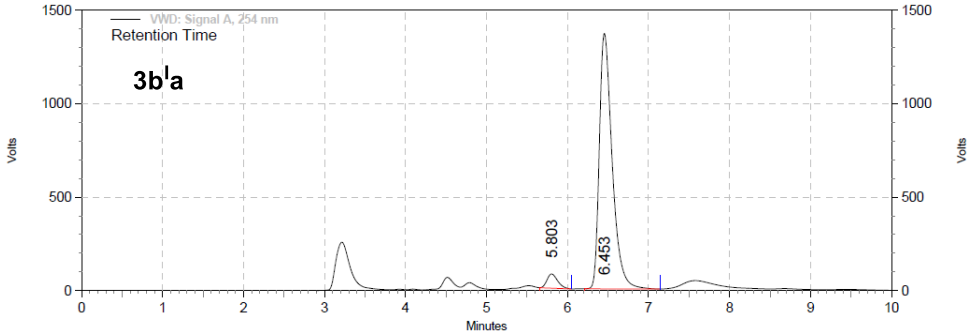

VWD: Signal A, 254 nm
Results

Pk #	Retention Time	Area	Area %
1	5.803	11552138	4.38
2	6.453	251910654	95.62
Totals		263462792	100.00

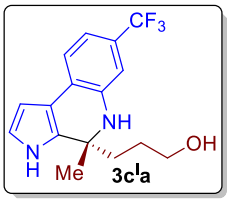

Entry 2, (3c^{I}a): Thick yellow liquid, 78% yield, R_f = 0.45 (pet ether/EtOAc = 70/30); **HPLC analysis:** 90.0% ee, t_R = 13.57 min

(minor), t_R = 16.01 min (major). (Chiralpak IC, *n*-hexane/*i*PrOH (95:05), flow rate 1.0 mL/min, λ = 254 nm).

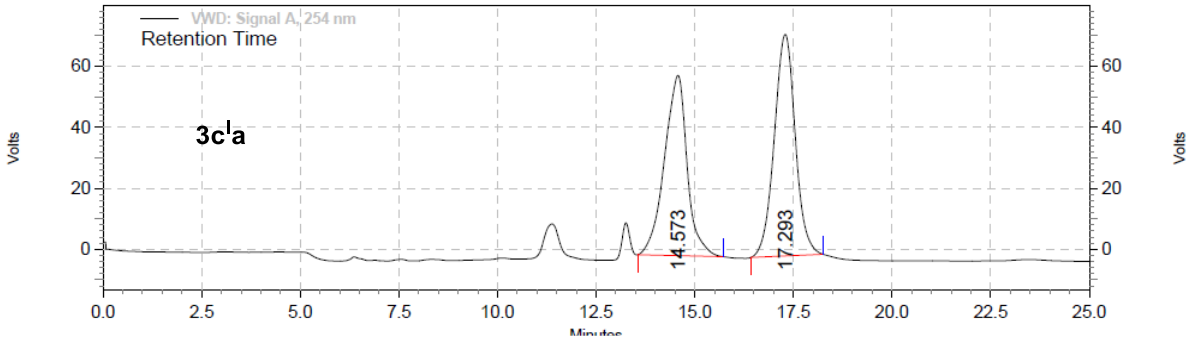

VWD: Signal A, 254 nm
Results

Pk #	Retention Time	Area	Area %
1	14.573	39760139	46.84
2	17.293	45127547	53.16
Totals		84887686	100.00

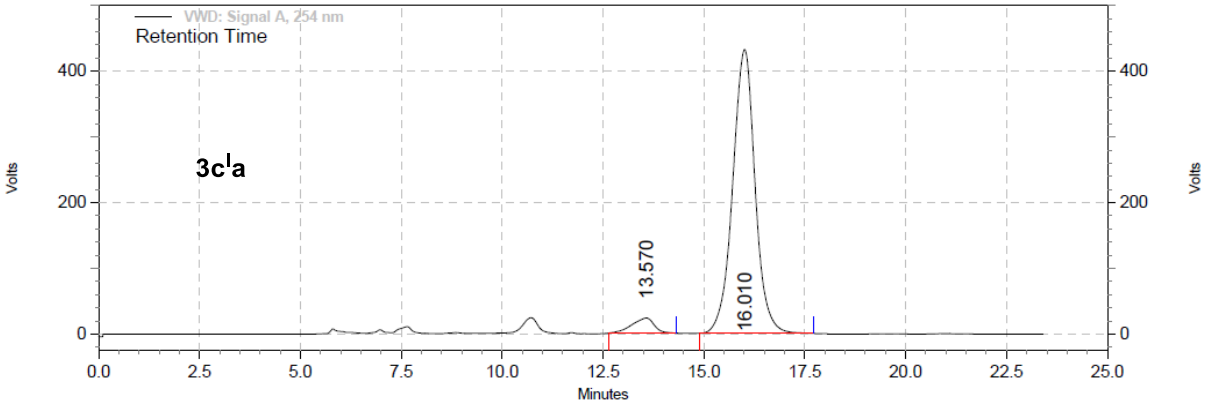

VWD: Signal A, 254 nm
Results

Pk #	Retention Time	Area	Area %
1	13.570	14709781	4.99
2	16.010	279848849	95.01
Totals		294558630	100.00

Table 2.3.1.3: Variation of SBAs/Alkynols – Five Components in One-pot

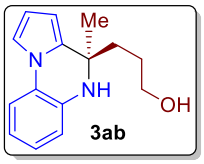

Entry 1, (3ab): White solid, 37% yield, R_f = 0.35 (pet ether/EtOAc = 60/40); **HPLC analysis:** 84.0% ee, t_R = 15.06 min (minor), t_R = 18.67 min (major). (Chiralpak IA, *n*-hexane/*i*PrOH (90:10), flow rate 1.0 mL/min, λ = 254 nm).

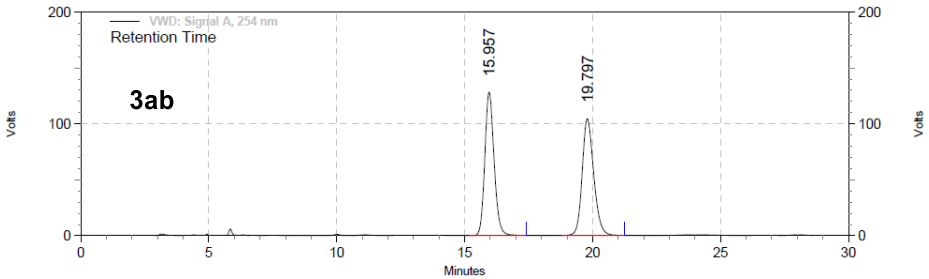

VWD: Signal A, 254 nm
Results

Pk #	Retention Time	Area	Area %
1	15.957	54388512	49.66
2	19.797	55130183	50.34
Totals		109518695	100.00

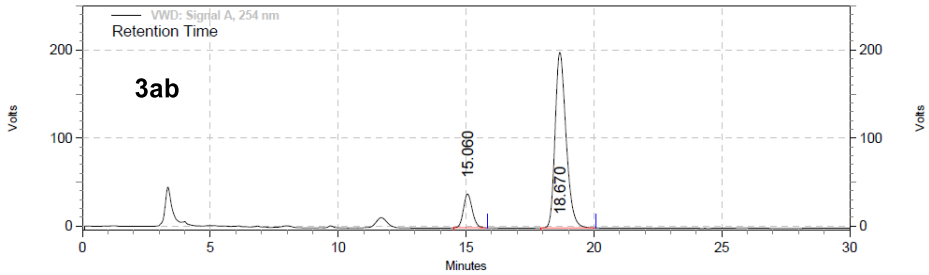

VWD: Signal A, 254 nm
Results

Pk #	Retention Time	Area	Area %
1	15.060	15421456	13.37
2	18.670	99942717	86.63
Totals		115364173	100.00

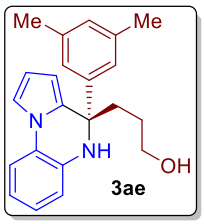

Entry 1, **(3ae):** White solid, 55% yield, R_f = 0.40 (pet ether/EtOAc = 60/40); **HPLC analysis:** 73.3% ee, t_R =8.33 min (minor), t_R = 11.16 min (major). (Chiralpak IA, *n*-hexane/*i*PrOH (95:05), flow rate 1.0 mL/min, λ = 254 nm); **^{1}H NMR (400 MHz, $CDCl_3$) δ** = 7.29 - 7.19 (m, 1 H), 7.18 - 7.09 (m, 1 H), 6.98 - 6.90 (m, 3 H), 6.84 - 6.72 (m, 3 H), 6.32 (t, *J* = 3.4 Hz, 1 H), 6.12 - 5.99 (m, 1 H), 3.72 - 3.52 (m, 2 H), 2.33 - 2.26 (m, 1 H), 2.23 (s, 6 H), 2.18 - 2.10 (m, 1 H), 1.80 - 1.63 (m, 2 H); **^{13}C NMR (100 MHz, $CDCl_3$) δ** = 145.4, 137.6, 135.2, 131.6, 128.5, 125.2, 124.7, 123.8, 118.9, 115.5, 114.5, 114.0, 109.9, 105.1, 63.0, 59.9, 38.0, 27.7, 21.5; **HRMS (ESI)** calcd for $C_{22}H_{25}N_2O$ (M^++ H) 333.1961, found 333.1960.

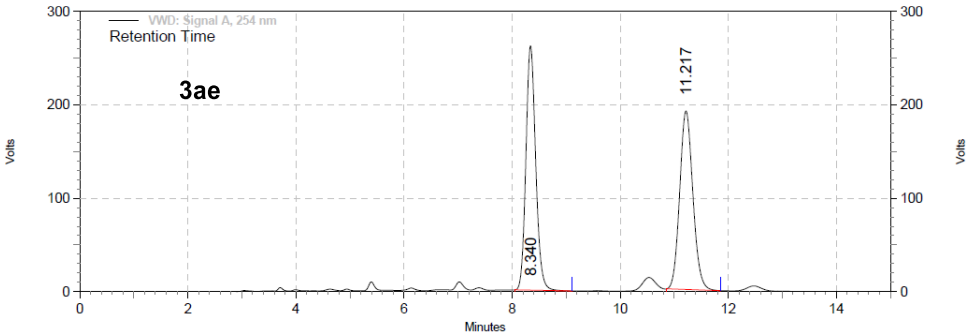

VWD: Signal A, 254 nm
Results

Pk #	Retention Time	Area	Area %
1	8.340	55143253	50.36
2	11.217	54347067	49.64
Totals		109490320	100.00

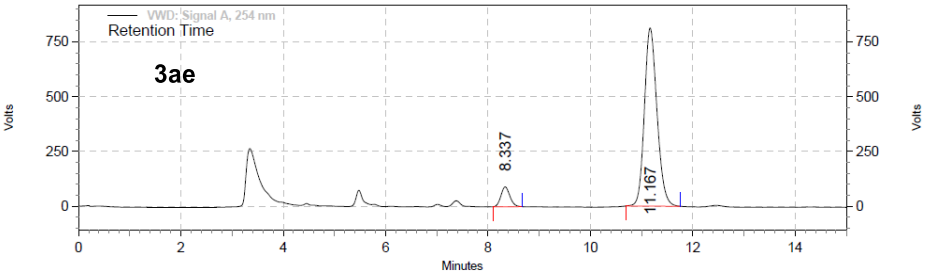

VWD: Signal A, 254 nm
Results

Pk #	Retention Time	Area	Area %
1	8.337	18392349	7.31
2	11.167	233065730	92.69
Totals		251458079	100.00

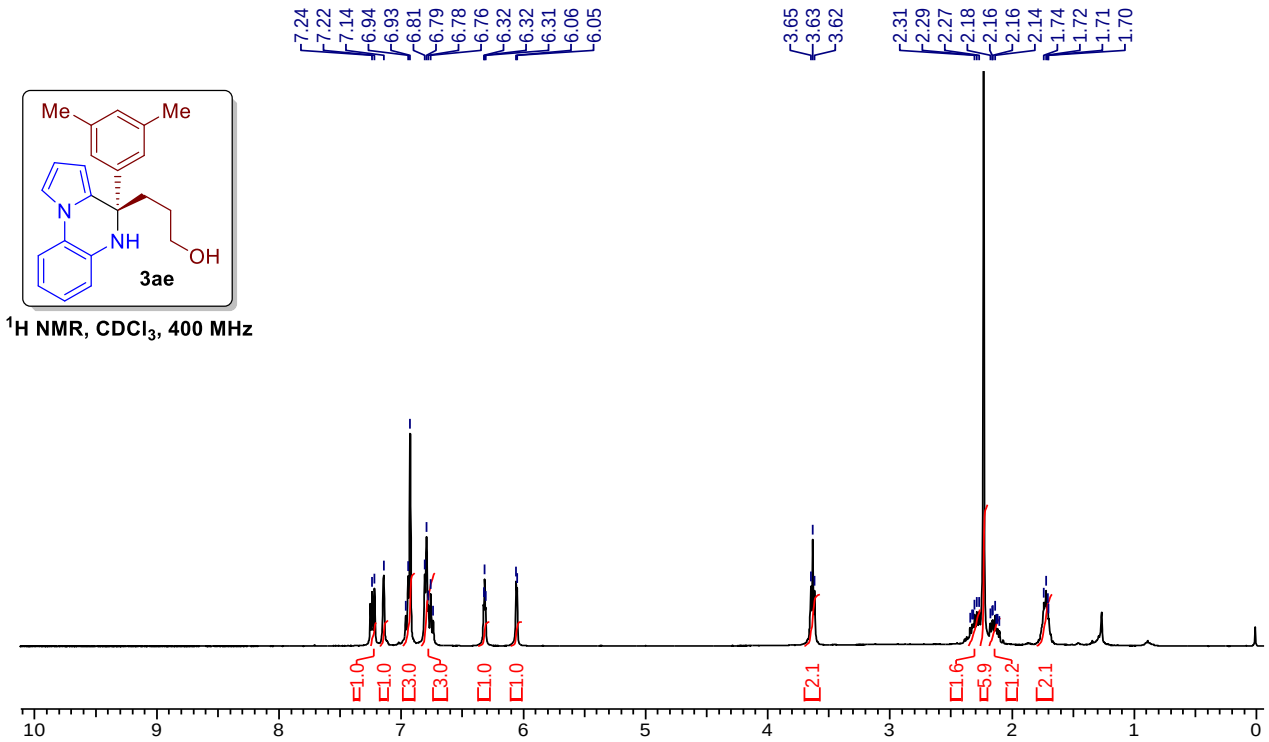

^{1}H NMR, $CDCl_3$, 400 MHz

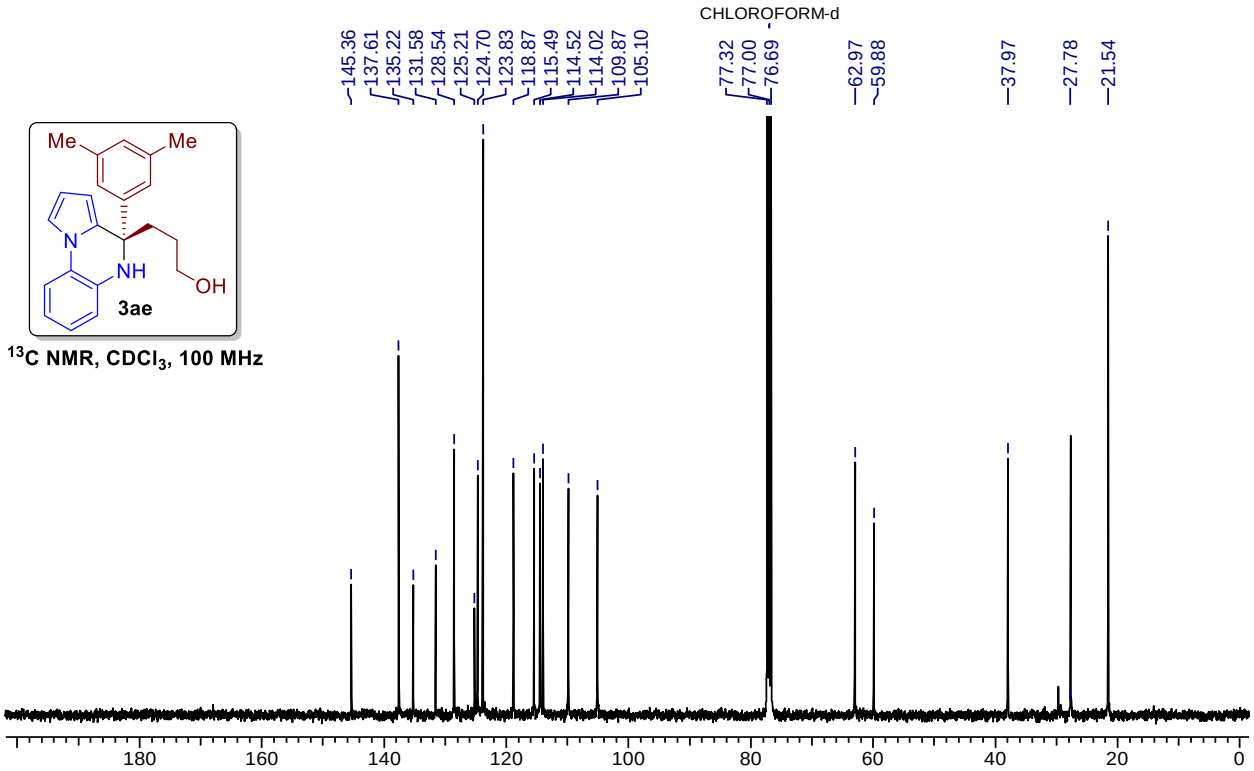

^{13}C NMR, $CDCl_3$, 100 MHz

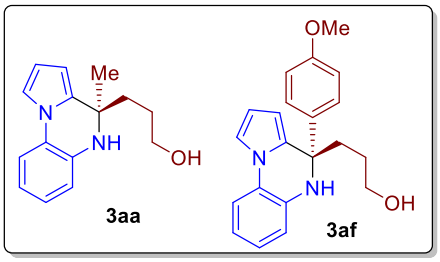

Entry 1, **(3aa, 3af):** White solid, 45% combined yield, R_f = 0.35 (pet ether/EtOAc = 60/40); **HPLC analysis:** Product ratio for (3aa:3af):[2.7:1], **(3aa)** 84.0% ee**,** t_R = 12.36 min (minor), t_R = 13.53 min (major), **(3af)** 90.1% ee, t_R = 18.53 min (minor), t_R = 28.33 min (major). Chiralpak IA, *n*-hexane/*i*PrOH (90:10), flow rate 1.0 mL/min, λ = 254 nm); **^{1}H NMR (500 MHz, $CDCl_3$) δ** = 7.28 - 7.18 (m, 3 H), 7.12 (t, *J* = 4.1 Hz, 2 H), 6.97 - 6.88 (m, 2 H), 6.86 - 6.81 (m, 1 H), 6.80 - 6.68 (m, 5 H), 6.33 - 6.28 (m, 1 H), 6.28 - 6.23 (m, 1 H), 6.08 - 6.03 (m, 1 H), 5.97 - 5.93 (m, 1 H), 3.73 - 3.68 (m, 2 H), 3.64 - 3.57 (m, 1 H), 3.54 - 3.46 (m, 2 H), 2.33 - 2.23 (m, 1 H), 2.18 (ddt, *J* = 3.7, 7.4, 11.4 Hz, 1 H), 1.86 - 1.66 (m, 4 H), 1.64 - 1.53 (m, 2 H), 1.53 - 1.48 (m, 3 H).

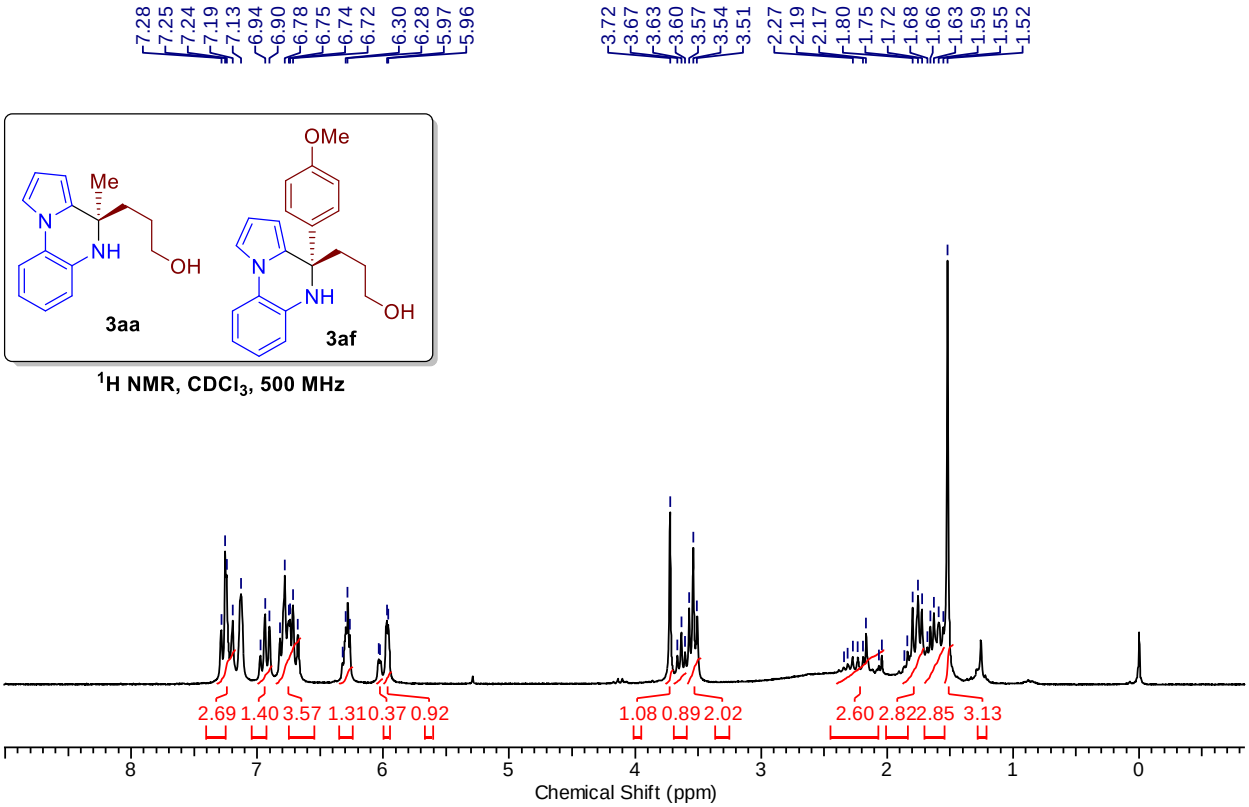

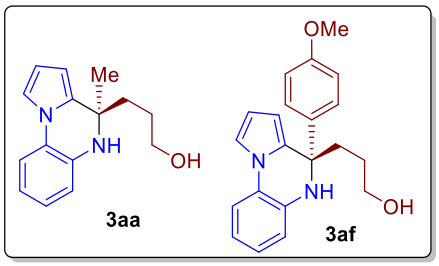

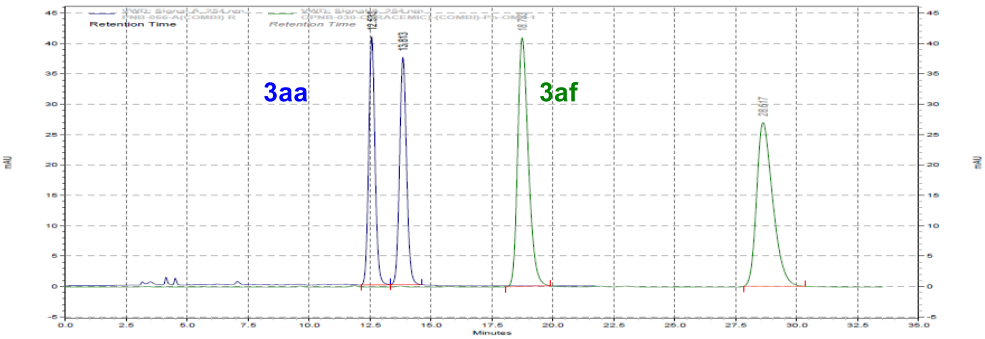

	Retention Time	Area %		Retention Time	Area %
3aa	12.220	49.34	3af	18.733	49.96
	13.540	50.66		28.617	50.04
		100.00			100.00

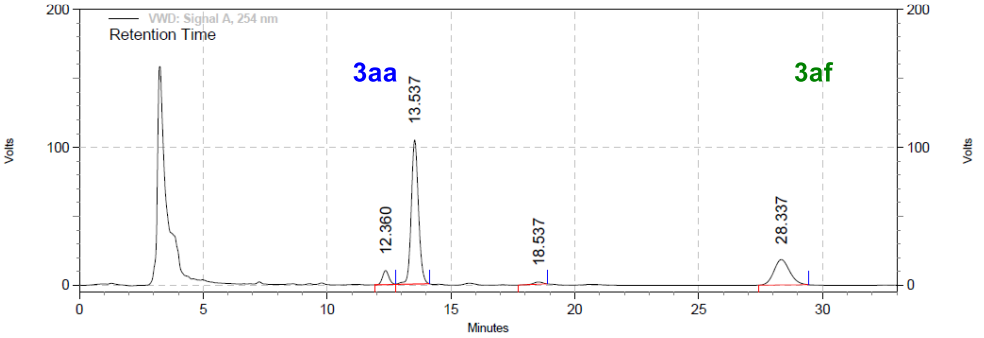

VWD: Signal A, 254 nm
Results

Pk #	Retention Time	Area	Area %
1	12.360	3079388	5.82
2	13.537	35474544	67.07
3	18.537	707674	1.34
4	28.337	13633139	25.77
Totals		52894745	100.00

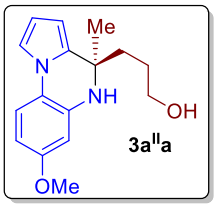

Entry 2, (3a^{II}a): White solid, 72% yield, R_f = 0.35 (pet ether/EtOAc = 60/40); **HPLC analysis:** 91.7% ee, t_R = 22.25 min (minor), t_R = 34.35 min (major). (Chiralpak IA, *n*-hexane/*i*PrOH (75:25), flow rate 1.0 mL/min, λ = 254 nm)

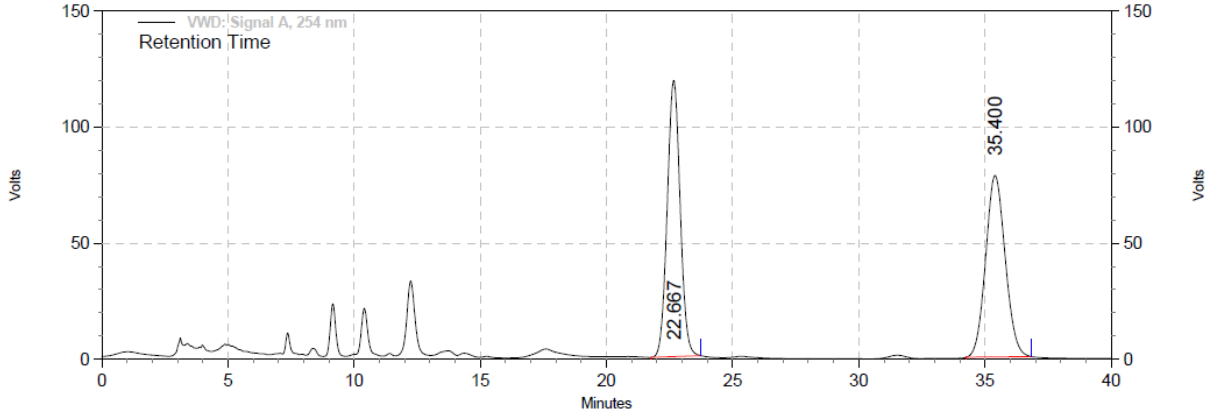

VWD: Signal A, 254 nm
Results

Pk #	Retention Time	Area	Area %
1	22.667	71008288	50.12
2	35.400	70681325	49.88
Totals		141689613	100.00

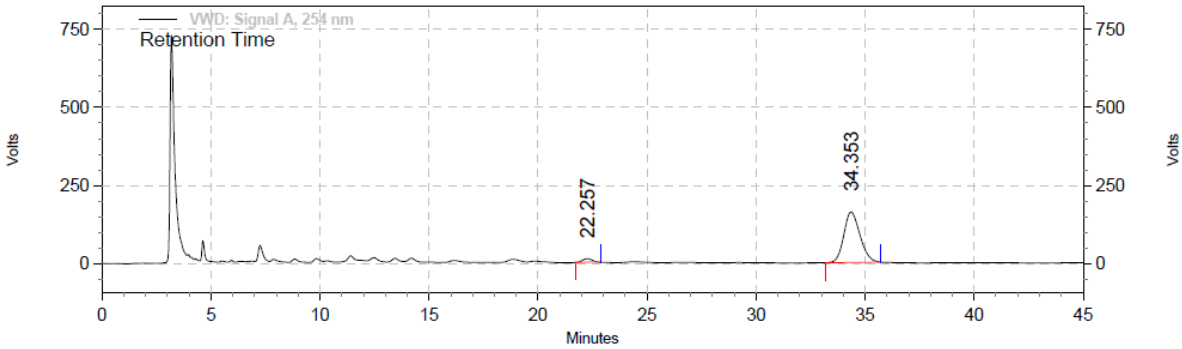

VWD: Signal A, 254 nm
Results

Pk #	Retention Time	Area	Area %
1	22.257	5982588	4.12
2	34.353	139217185	95.88
Totals		145199773	100.00

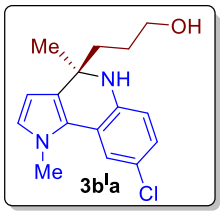

Entry 2, (3b^{I}a): Thick liquid, 43% yield, R_f = 0.30 (Pet ether/EtOAc = 60/40); **HPLC analysis:** 83.3% ee, t_R = 41.76 min (minor), t_R = 43.79 min (major). (Chiralpak IA, *n*-hexane/*i*PrOH (93:07), Flow rate 0.5 mL/min, λ = 254 nm)

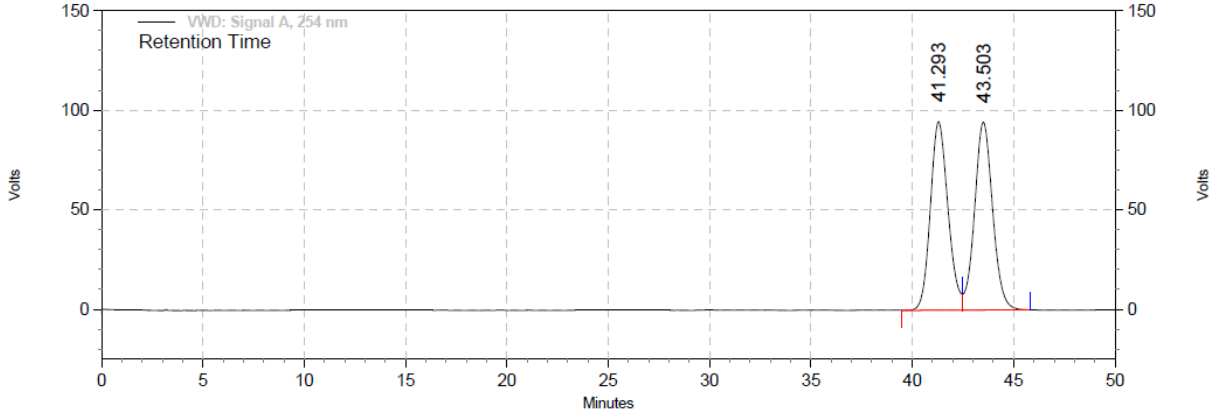

VWD: Signal A, 254 nm
Results

Pk #	Retention Time	Area	Area %
1	41.293	95979683	49.41
2	43.503	98252221	50.59
Totals		194231904	100.00

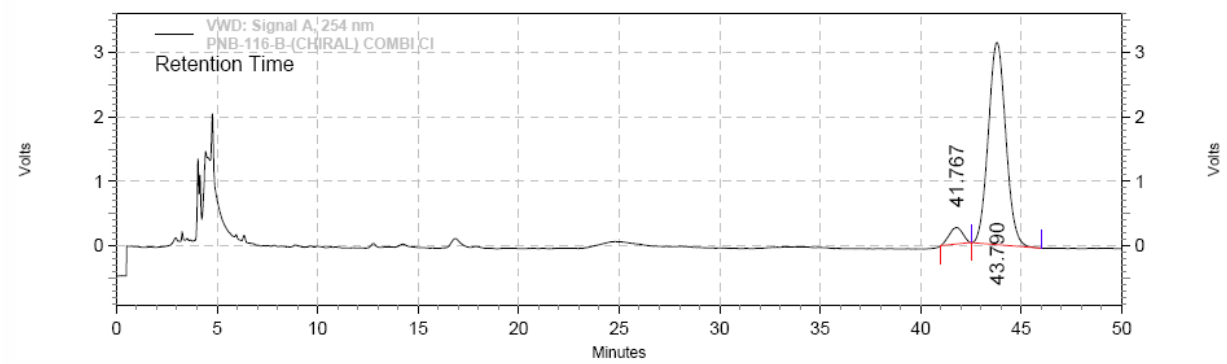

VWD: Signal A, 254 nm
Results

Pk #	Retention Time	Area	Area %
1	41.767	297875	8.33
2	43.790	3276122	91.67
Totals		3573997	100.00

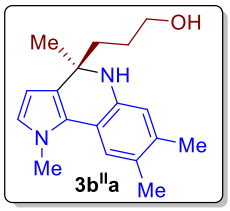

Entry 2, (3b^{II}a): Off white solid, 83% yield, R_f = 0.37 (pet ether/EtOAc = 60/40); **HPLC analysis:** 90.5% ee, t_R = 5.83 min (minor), t_R = 6.48 min (major). (Chiralpak IB, *n*-hexane/*i*PrOH (75:25), flow rate 1.0 mL/min, λ = 254 nm)

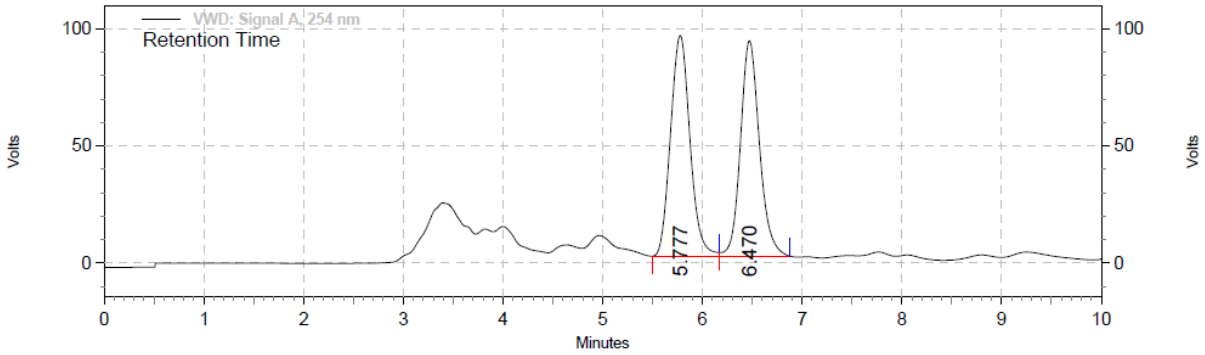

VWD: Signal A, 254 nm
Results

Pk #	Retention Time	Area	Area %
1	5.777	21412646	51.19
2	6.470	20413235	48.81
Totals		41825881	100.00

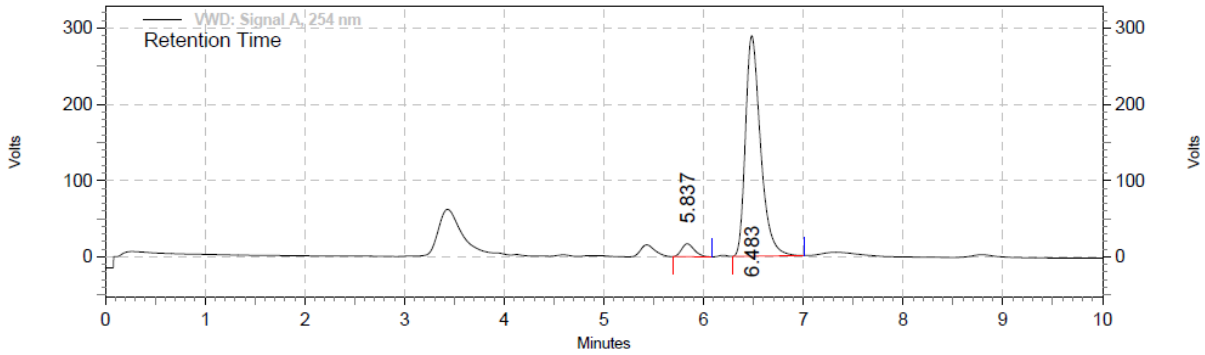

VWD: Signal A, 254 nm
Results

Pk #	Retention Time	Area	Area %
1	5.837	2536565	4.73
2	6.483	51036377	95.27
Totals		53572942	100.00

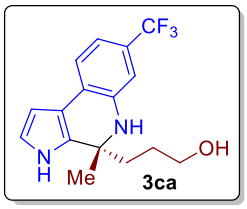

Entry 2, (3ca): Thick yellow liquid, 90% yield, R_f = 0.45 (pet ether/EtOAc = 70/30); **HPLC analysis:** 83.9% ee, t_R = 16.29 min (minor), t_R = 19.12 min (major). (Chiralpak IC, *n*-hexane/*i*PrOH (95.0 : 5.0), flow rate 0.5 mL/min, λ = 254 nm)

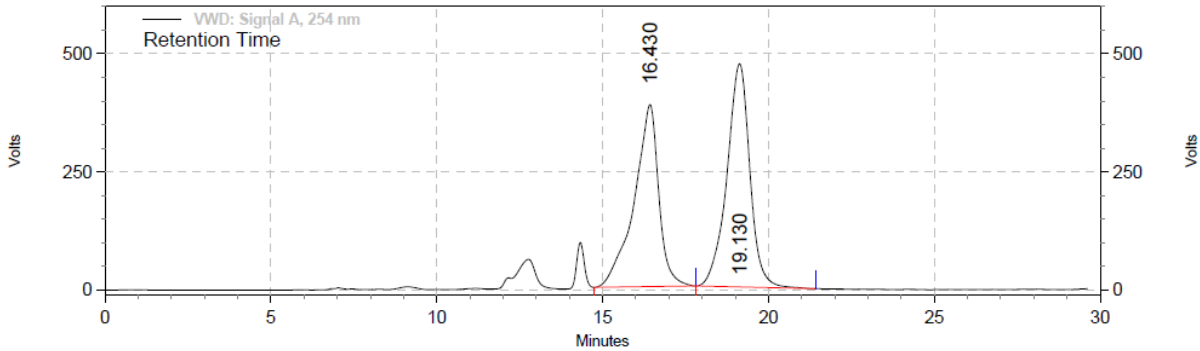

VWD: Signal A, 254 nm
Results

Pk #	Retention Time	Area	Area %
1	16.430	333182435	46.63
2	19.130	381273668	53.37
Totals		714456103	100.00

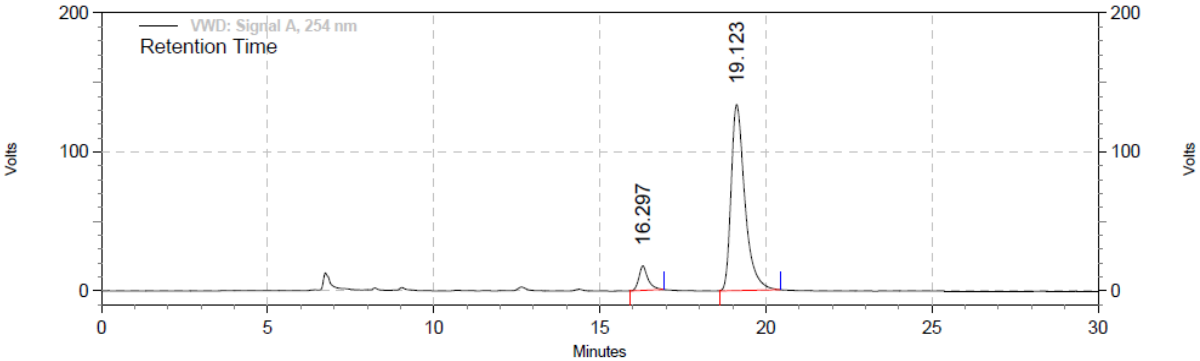

VWD: Signal A, 254 nm
Results

Pk #	Retention Time	Area	Area %
1	16.297	5641009	8.03
2	19.123	64569270	91.97
Totals		70210279	100.00

2.7 References

(1) Reviews of homogeneous Au catalysis, see: (a) Obradors, C.; Echavarren, A. M. *Chem. Commun*. **2014**, *50*, 16. (b) Garayalde, D.; Nevado, C. *ACS Catal*. **2012**, *2*, 1462. (c) Pérez-Temprano, M. H.; Casares, J. A.; Espinet, P. *Chem. - Eur. J*. **2012**, *18*, 1864. (d) Liu, L.-P.; Hammond, G. B. *Chem. Soc. Rev*. **2012**, *41*, 3129. (e) Rudolph, M.; Hashmi, A. S. K. *Chem. Soc. Rev*. **2012**, *41*, 2448. (f) Shapiro, N. D.; Toste, F. D. *Synlett* **2010**, 675.

(2) Grandberg, K. I.; Dyadchenko, V. P. *J. Organomet. Chem.***1994**, *474*, 1.

(3) (a) Lalonde, R. L.; Sherry, B. D.; Kang, E. J.; Toste, F. D.; *J. Am. Chem. Soc.* **2007**, *129*, 2452. (b) Hamilton, G. L.; Kang, E. J.; Mba, M.; Toste, F. D., *Science*, **2007**, *317*, 496. (c) LaLonde, R. L.; Wang, Z. J.; Mba, M.; Lackner, A. D.; Toste, F. D., *Angew. Chem. Int. Ed.* **2010**, *49*, 598.

(4) For some examples and further discussion on *ion-pairing*, see: (a) Llewellyn, D. B.; Adamsom, D.; Arndtsen, B. A.; *Org. Lett.*, **2000**, 2, *26*, 4165. (b) Zuccaccia, D.; Belpassi, L.; Tarantelli, F.; Macchioni, A.; *J. Am. Chem. Soc.*, **2009**, *131*, 3170. (c) Hashmi, A. S. K.; *Nature*, **2007**, *449*, 292.

(5) Hamilton, G. L.; Kang, E. J.; Mba, M.; Toste, F. D. *Science*, **2007**, *317*, 496.

(6) Han, Z.-Y.; Xiao, H.; Chen, X.-H.; Gong, L.-Z. *J. Am. Chem. Soc.* **2009**, *131*, 9182.

(7) Liu, X.-Y.; Che, C.-M. *Org. Lett.* **2009**, *11*, 4204.

(8) Muratore, M. E.; Holloway, C. A.; Pilling, A. W.; Storer, R. I.; Trevitt, G.; Dixon, D. J. *J. Am. Chem. Soc.* **2009**, *131*, 10796.

(9) Z.-Y. Han, R. Guo, P.-S. Wang, D.-F. Chen, H. Xiao, L.-Z. Gong, *Tetrahedron Lett*. **2011**, *52*, 5963.

(10) Patil, N. T.; Mutyala, A. K.; Konala, A.; Tella, R. B. *Chem. Commun.* **2012**, *48*, 3094.

(11) (a) Rueping, M.; Antonchick, A. P.; Sugiono E.; Grenader, K. *Angew. Chem. Int. Ed.* **2009**, *48*, 908. (b) Cheng, X.; Vellalath, S.; Goddard R.; List, B. *J. Am. Chem.Soc*. **2008**, *130*, 15786.

(12) Patil, N. T.; Raut, V. S.; Tella, R. B. *Chem. Commun.* **2013**, *49*, 570.

(13) Shinde, V. S.; Mane, M. V.; Vanka, K.; Mallick, A.; Patil, N. T. *Chem. Eur. J.* **2015**, *21*, 975.

(14) Reviews: (a) Wang, Y-M.; Lackner, A. D.; Toste, F. D. *Acc. Chem. Res*. **2014**, *47*, 889-901. (b) Patil, N. T. *Chem.–Asian J*. **2012**, *7*, 2186. (c) Rudolph, M.; Hashmi, A. S. K. *Chem. Soc. Rev*. **2012**, *41*, 2448. (d) Dudnik, A. S.; Chernyak N.; Gevorgyan, V. *Aldrichimica Acta* **2010**, *43*, 37. (e) Sohel, S. Md. A.; Liu, R.-S. *Chem. Soc. Rev*. **2009**, *38*, 2269. (f) Gorin, D. J.; Sherry, B. D.; Toste, F. D. *Chem. Rev*. **2008**, *108*, 3351. (g) Li, Z.; Brouwer C.; He, C. *Chem. Rev*. **2008**, *108*, 3239. (h) Arcadi, A. *Chem. Rev*. **2008**, *108*, 3266. (i) Jiménez-Núñez, E.; Echavarren, A. M. *Chem. Rev*. **2008**, *108*, 3326. (j) Hashmi, A. S. K. Rudolph, M. *Chem. Soc. Rev*. **2008**, *37*, 1766. (k) Fürstner A.; Davies, P. W. *Angew. Chem. Int. Ed*. **2007**, *46*, 3410.

(15) Reviews: (a) Patil, N. T.; Mutyala, A. K. *Org. Chem. Front*. **2014**, *1*, 582. (b) Zamfir, A.; Schenker, S.; Freund, M.; Tsogoeva, S. B. *Org. Biomol. Chem*. **2010**, *8*, 5262. (c) Akiyama, T. *Chem. Rev.* **2007**, *107*, 5744. (d) Terada, M. *Chem. Commun*. **2008**, 4097. (e) Terada, M. *Bull. Chem. Soc. Jpn*. **2010,** *83*, 101. (f) Kampen, D.; Reisinger, C. M.; List, B. *Top. Curr. Chem*. **2010**, *291*, 395. (g) Adair, G.; Mukherjee, S.; List, B. *Aldrichimica Acta* **2008**, *41*, 31.

(16) Reviews: (a) Parmar, D.; Sugiono, E.; Raja, S.; Rueping, M. *Chem. Rev*. **2014**, *114*, 9047. (b) Inamdar, S. M.; Konala, A.; Patil, N. T. *Chem. Commun*. **2014**, *50*, 15124. (c) Chen, D. F.; Han, Z. Y.; Gong, L. Z. *Acc. Chem. Res.* **2014**, *47*, 2365. (d) Loh, C. C. J.; Enders, D. *Chem. Eur. J.* **2012**, *18*, 10212. Other Selected examples: (e) Wu, H.; He, Y.-P.; Gong, L.-Z. *Org. Lett.* **2013**, *15*, 460. (f) He, Y.-P.; Wu, H.; Chen, D.-F.; Yu, J.; Gong, L.-Z. *Chem. Eur. J.* **2013**, *19*, 5232. (g) Patil, N. T.; Raut, V. S.; Tella, R. B. *Chem. Commun*. **2013**, *49*, 570. (h) Wang, P.-S.; Li, K.-N.; Zhou, X.-L.; Wu, X.; Han, Z.-Y.; Guo, R.; Gong, L.-Z. *Chem. Eur. J*. **2013**, *19*, 6234. (i) Tu, X.-F.; Gong, L.-Z. *Angew. Chem. Int. Ed.* **2012**, *51*, 11346. (j) Han, Z.-Y.; Chen, D.-F.; Wang, Y.-Y.; Guo, R.; Wang, P.-S.; Wang, C.; Gong, L.-Z. *J. Am. Chem. Soc.* **2012**, *134*, 6532. (k) Patil, N. T.; Mutyala, A. K.; Konala, A.; Tella, R. B. *Chem. Commun.* **2012**, *48*, 3094. (n) Wang, C.; Han, Z.-Y.; Luo, H.-W.; Gong, L.-Z. *Org. Lett*. **2010**, *12*, 2266. (o) Han, Z.-Y.; Xiao, H.; Chen, X.-H.; Gong, L.-Z. *J. Am. Chem. Soc.* **2009**, *131*, 9182.

(17) (a) Collins, K. D.; Rühling, A.; Lied, F.; Glorius, F. *Chem. Eur. J.* **2014**, *20*, 3800. (b) Collins, K. D.; Rühling, A.; Glorius, F. *Nature Protocol* **2014**, *9*, 1348. (c) Collins, K. D.; Glorius, F. *Nature Chem*. **2013**, *5*, 597.

(18) Mana, M. S.; Mukherjee, S. ***Chem. Sci.*** **2014**, *5*, 1627.

(19) Patil, N. T.; Shinde, V. S.; Gajula, B. *Org. Biomol. Chem.* **2012**, *10*, 211.

(20) Selected reviews on catalytic carbophilic activation by Au-catalysts: (a) Patil, N. T. *Chem. Asian J.* **2012**, *7*, 2186. (b) Gorin, D. J.; Sherry, B. D.; Toste, F. D. *Chem. Rev*. **2008**, *108*, 3351. (c) Jiménez-Núñez, E.; Echavarren, A. M. *Chem. Rev*. **2008**, *108*, 3326. (d) Hashmi, A. S. K.; Rudolph, M. *Chem. Soc. Rev*. **2008**, *37*, 1766-1775. (e) Fürstner, A.; Davies, P. W. *Angew. Chem. Int. Ed*. **2007**, *46*, 3410.

(21) Reviews: (a) Parmar, D.; Sugiono, E.; Raja, S.; Rueping M.; *Chem. Rev*. **2014**, *114*, 9047. (b) Inamdar, S. M.; Konala, A.; Patil, N. T. *Chem. Commun*. **2014**, *50*, 15124. (c) Chen, D. F.; Han, Z. Y.; Gong, L. Z. *Acc. Chem. Res.* **2014**, *47*, 2365. (d) Loh, C. C. J.; Enders, D. *Chem. Eur. J.* **2012**, *18*, 10212.

(22) (a) Ueda, T.; Kanomata, N.; Machida, H. *Org. Lett*, **2005**, *7*, 2365. (b) O'Rourke, N. F.; Davies, K. A.; Wulff, J. E. *J. Org. Chem*. **2012**, *77*, 8634. (c) Mizukami, M.; Saito, H.; Higuchi, T.; Imai, M.; Bando, H.; Kawahara, N.; Nagumo, S. *Tetrahedron Lett.* **2007**, *48*, 7228.

Chapter 3: Au(I)/Ag(I) Co-operative Catalysis: Interception of Ag-Bound Carbocations with α-Gold(I) Enals in the Imino-Alkyne Cyclizations with N-Allenamides

Table of Contents

3.1 Introduction 98

3.2 Present Work 103

3.3 Results and Discussion 104

3.3.1 Optimization Studies 105

3.3.2 Scope of the Reaction 107

3.4 Plausible Reaction Mechanism 108

3.5 Computational Studies 109

3.6 Modification of Products 113

3.6 Conclusion 114

3.7 Experimental Procedures 114

3.8 Characterization Data of Selected Compounds 117

3.9 ORTEP Diagram 126

3.10 2D NMR Experiments 127

2D NMR Experiments for **1s** 127

2D NMR Experiments for **3k** 130

2D NMR Experiments for **3y** 133

3.11 NMR Spectra of Selected Compounds 136

3.12 References 164

3.1 Introduction

During the past several years, almost all of the successful examples of metal catalysed reactions to enable synthesis of various organic molecules rely on the employment of a single catalyst. Since only one catalyst has been used, the resulting products are limited in structural design and complexity. On the other hand, a suitable multi-catalyst system where individual activation of two different reacting partners by two different catalysts can lead to reactivities and selectivities that offer products which are otherwise difficult to obtain by single catalyst alone (Figure 3.1.1).1 However, the development of multicatalyst promoted reactions is challenging because one must take into account the compatibility of the catalyst with residual component of the reaction (solvent, substrates, other catalyst, and intermediates generated *in situ*). Therefore, judicious choice of the catalyst system is the key factor for the successful development of multicatalyst promoted reactions to construct highly functionalized organic molecules from simple and readily available starting materials.[1] Despite the potential advantages, reports on the co-operative catalysis involving gold catalysts[2] with other metals are scarce.[3]

Figure 3.1.1: Schematic representation of cooperative catalysis

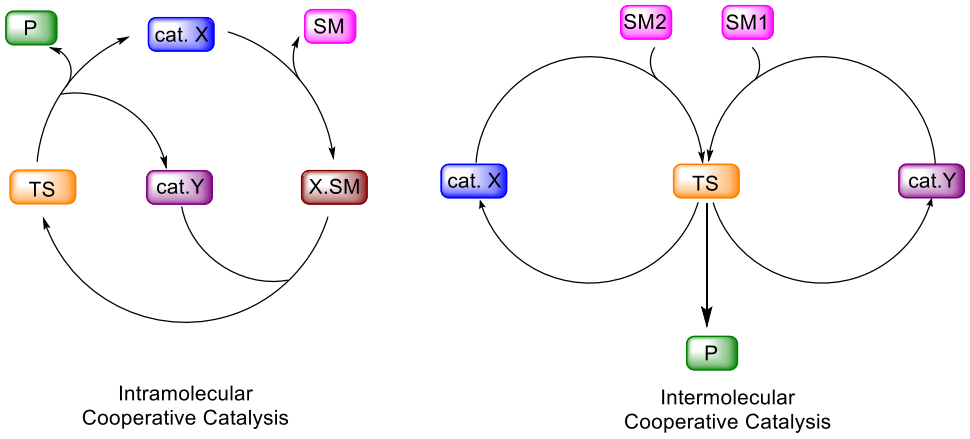

An early example in this sector from the Blum's group merges gold and palladium catalysis for vinylstannylation of alkynes to generate tri- and tetra-substituted olefins with excellent regio- and stereocontrol (Scheme 3.1.1).[4] Au(I) activated alkynes underwent nucleophilic addition/oxidative addition of Pd(0) to form Au(I) co-ordinated Pd(II) species. Transmetalation of tri-*n*-butylvinylstannane across one of the palladium-carbon σ-bonds of Pd(II)

species resulted in vinyl transfer to palladium and tin transfer to the nascent olefin. Dissociation of Au(I) followed by reductive elimination forms the observed vinylstannylated product which would further participate in traditional cross-coupling reactions with aryl halides to give corresponding cross coupled products in excellent yields.

Scheme 3.1.1: Au(I)/Pd cooperative catalysis for vinylstannylation of alkynes

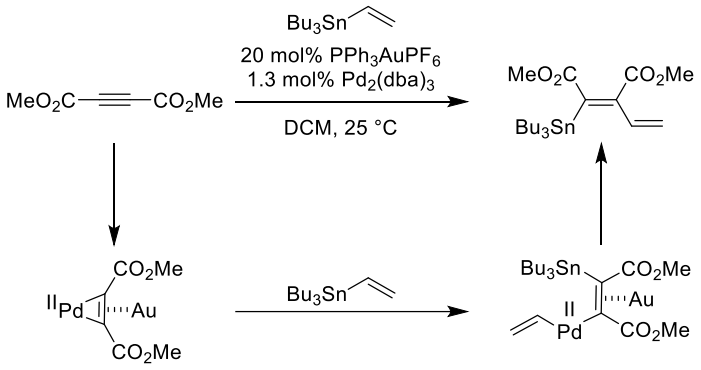

Later, the same group revealed the remarkable example of Au/Pd co-operative catalysis to synthesize substituted butenolides from allenoates (Scheme 3.1.2).[5] The mechanism involves gold(I) triggered 5-*endo dig* cyclisation of the allenoates to give an activated gold-oxonium species. The allyl moiety in the gold-oxonium species is now activated towards oxidative addition by Pd(0) for deallylation. Subsequent transmetalation between neutral vinylgold complex and π-allyl Pd complex followed by C-C bond-forming reductive elimination led to the formation of substituted butenolides.

Scheme 3.1.2: Au(I)/Pd cooperative catalysis for synthesis of substituted butenolides

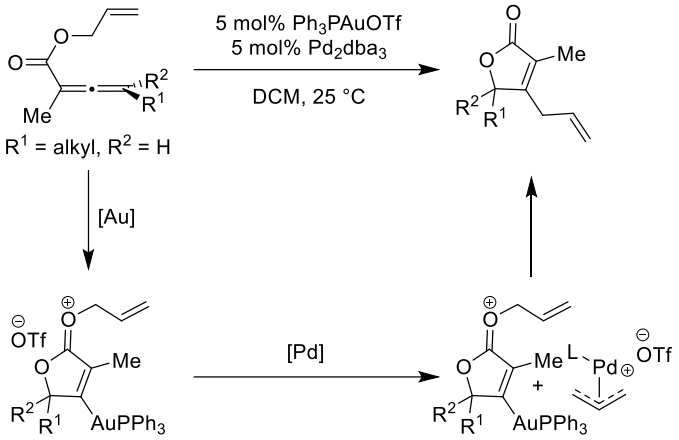

In 2013, Espinet *et al*. published Stille coupling with Au/Pd co-operative catalysis, where they described the role of Au catalyst to enhance the reactivity of bulkier organo-stannanes towards transmetalation reaction.[6] Scheme 3.1.3 depicts together the classic Stille cycles (black) and the Au/Pd cooperative (brown) Stille cycles. The author performed DFT studies for sequential Sn/Au/Pd double transmetalation of bulkier 2-Me-naphthyl group, leading to the product *via* gold cooperative Stille coupling reaction. The activation energy for Sn/Pd transmetalation in classical stille reaction is 36.6 kcal mol^{-1}, which in practice means a forbidden pathway. Whereas activation energy for Sn/Au and Au/Pd is 25.5 kcal mol^{-1} and 21.4 kcal mol^{-1} respectively which indicate excellent feasibility of Au(I)/Pd cooperative Stille coupling reaction (Scheme 3.1.3).

The yields at identical reaction times indicated that for simple aryls, similar reaction rates were observed for both the process. (Table no. 3.1.1, entries 1, 2), but just one *ortho* substituent had adverse effect on yield of the reaction, and more than one substituents made the classic Stille impossible, while the Au(I)/Pd cooperative Stille coupling reaction kept running (Table no. 3.1.1, entries 3-6).

Table 3.1.1: Classic and Au(I)/Pd cooperative Stille coupling reaction

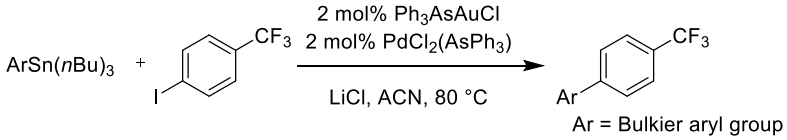

Entry	Au co-cat	$ArC_6H_4CF_3$	time (h)	yield (%)
1	yes	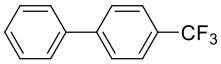	5	83
2	no		**5**	**68**
3	yes	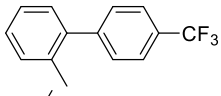	24	89
4	no		**24**	**4**
5	yes	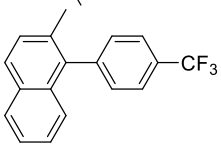	24	90
6	no		**24**	**<1**

Scheme 3.1.3: Mechanism for classic and Au(I)/Pd cooperative Stille coupling reaction

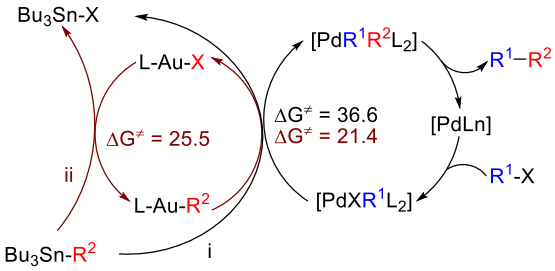

ΔG≠ values for coupling

In the very next year, Shi and coworkers reported a highly efficient Nakamura reaction *via* synergestic effect of gold(I) and $Ga(OTf)_3$ (Scheme 3.1.4).[7] The catalyst $Ga(OTf)_3$ was found to be an efficient co-catalyst in this reaction and the challenging Nakamura reaction was achieved at room temperature which was originally catalysed by In(III) at 140 °C. Galium triflate-activated enolates derived from 1,3 dicarbonyl compounds combined with the alkyne gold complex to effect Nakamura reaction. More importantly, the catalyst loading of gold could be lowered to 500 ppm without compromising yield of the reaction.

Scheme 3.1.4: Au(I)/Ga co-operative Nakamura reaction

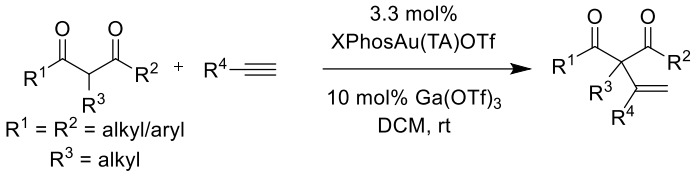

	catalyst	Yield
only [Au]	5 mol% XPhosAu(TA)OTf	00%
only [Ga]	10 mol% $Ga(OTf)_3$	00%
Au + Ga	0.05 mol% XPhosAu(TA)OTf 5 mol% $Ga(OTf)_3$	up to 93%

Recently, Nevado and co-workers demonstrated the use of Au/Pd bimetallic catalytic system based on the generation of competent Au and Pd species by anionic ligand exchange to enable the synthesis of substituted butenolides (Scheme 3.1.5).[8] Unlike that of Blum and co-workers,[5] this reaction involved two independent catalytic cycles of gold and palladium to obtain the butenolides from allenoates and aryl iodides. At first, gold catalyst would undergo complexation with allenoate to generate vinyl gold(I) intermediate. At the same time, *in situ* generated Pd(0) anionic complex underwent facile associative oxidative addition with Ar-I to form elctrophilic Pd(II) anionic complex which received the lactone fragment from gold, and reductive elimination gave the aryl lactones as the product. Mechanistic study revealed the role of CsOAc for the generation of more labile Pd complex by sequestering the Cl anions from the reaction mixture in the form of CsCl which avoided the formation of in-active gold(I) halide species along the catalytic cycle.

Scheme 3.1.5: Bimetallic Au(I)/Pd catalysis for synthesis of substituted butenolides

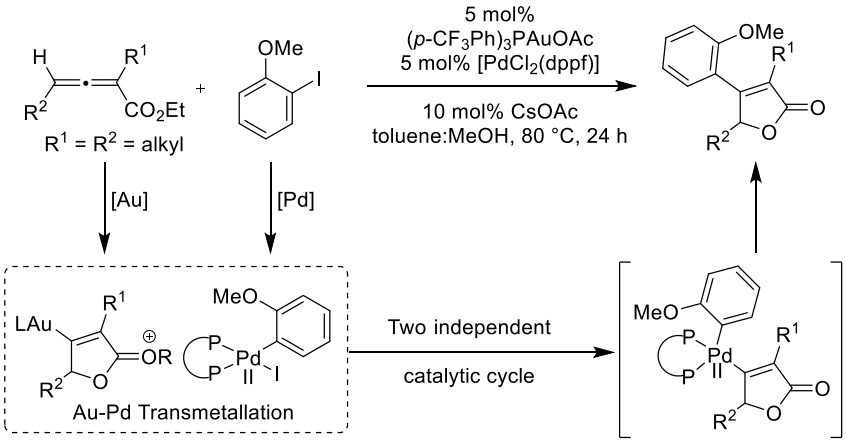

3.2 Present Work

The Morita-Baylis-Hillman (MBH) reaction involves the α-functionalization of enals/enones with carbon electrophiles, under the catalytic influence of a Lewis base (Scheme 3.2.1, eq 1).[9] However, this reaction is only limited to carbon electrophiles such as carbonyls, imines, alkyl halides, allyl halides, epoxide etc. To further expand the electrophile repertiore of MBH reaction with incipient carbocation **II**, generated from substrate of type **I** through π-acid-triggered cascade,[10] would be a challenging task (Scheme 3.2.1, eq 2). The fruitfulness of the reaction lies in the successful co-operation between both the catalysts i.e. π-acidic metal and Lewis base which, in principle, have questionable compatibility due to a possible mutual inhibition. Therefore, a new mode of reactivity for accessing product of type **III** from **I** employing enal/enone equivalents is necessary.

Scheme 3.2.1: Morita-Baylis-Hilman reaction and this concept

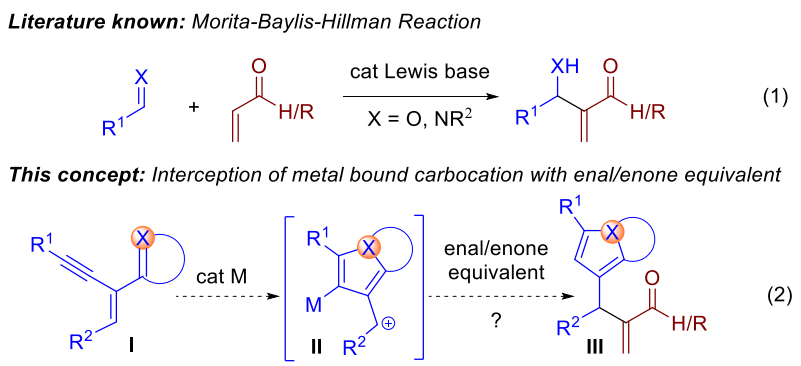

In 2015, Bandini and co-workers reported the reaction between allylic alcohols and *N*-allenamides under the co-operative catalysis by Au(I)/Ag(I)[11] to obtain α-functionalized enals/enones. Mechanistically, the reaction involves the generation of allylic carbocation with Ag-catalyst which is trapped by *in situ* generated α-gold(I) enal species derived from *N*-allenamides (Scheme 3.2.2, eq. 1).[12] In this chapter, a co-operative Au/Ag catalyst system was disclosed to utilize *N*-allenamides as nucleophilic enal equivalents for the interceptive capturing of incipient carbocation generated through π-acid-triggered imino-alkyne cyclization (Scheme 3.2.2, eq 2). The method gave access to functionalized indolizines - the structural motif and its hydrogenated derivatives are found in many bioactive natural products (Scheme 3.2.2, eq. 2).[13] It was proposed that Ag(I)-catalyst would act as alkyne trigger to generate transient Ag-bound carbocations; while gold(I) catalyst would generate α-gold(I) enals from *N*-allenamides in the

presence of H_2O. The union of both the metal-bound reactive intermediates would give products with the regeneration both Au(I) and Ag(I) catalysts. Since there exists numerous reports on *in situ* generation of metal bound carbocations,10 such reactivities would be applicable to a vast number of reactions.

Scheme 3.2.2: Bandini's work and Present work

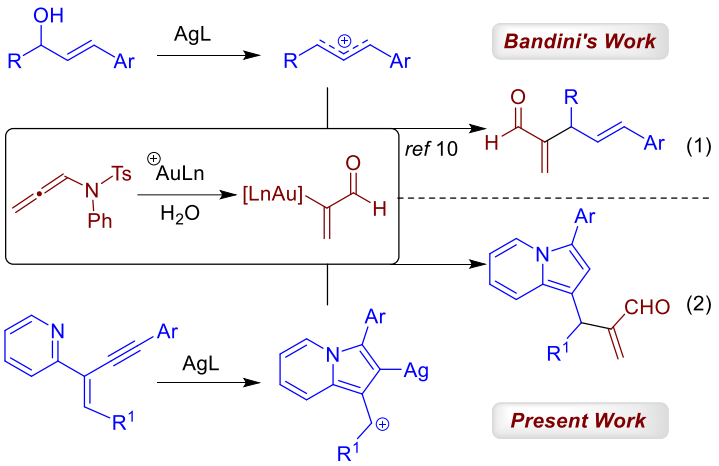

3.3 Results and Discussion

Unless otherwise specified, all reactions were carried out in oven dried vials or reaction vessels with magnetic stirring under argon atmosphere. The pyridino-alkyne cyclization reactions were performed in 2.5 mL glass vials with a PTFE-lined cap and all other reactions for the preparation of starting materials were performed in round-bottom flasks with rubber septa. All experiments were monitored by analytical thin layer chromatography (TLC). TLC was performed on pre-coated silica gel plates. After elution, the plate was visualized under UV illumination at 254 nm for UV active materials. Further visualization was achieved by staining iodine, potassium permanganate solution and charring on a hot plate. Solvents were removed in vacuo and heated with a water bath at 35 °C. Silica gel finer than 200 mesh was used for column chromatography. Columns were packed as slurry of silica gel in petroleum ether and equilibrated with the appropriate solvent mixture prior to use. The compounds were loaded neat or as a concentrated solution using the appropriate solvent system. The elution was assisted by applying pressure with an air pump.

3.3.1 Optimization Studies

We commenced our study with the use of pyridino-alkyne **1a**[14] and *N*-allenamide **2a** using various Au(I) and Ag(I) catalysts in moist DCE[15] (Table no. 3.3.1.1). Accordingly, when **1a** was treated with **2a** in presence of 5 mol% PPh_3AuCl/AgOTf (entry 1) and IPrAuCl/AgOTf (entry 2), undesired product **3a′** was obtained exclusively. To our delight, with the use of **4a**.AuCl/AgOTf, desired product **3a** was obtained in 42% yield; albeit accompanied with **3a′** (entry 3). This prompted us to screen gold complexes bearing biphenyl-based phosphine ligands (entries 4-7) and finally we focused on **4b**.AuCl/AgOTf (entry 4). When precise amount of water (2.0 equiv) was used, instead of moist DCE, formation of the **3a′** was diminished and yield of the **3a** increased to 64% (entry 8). Change of solvents such as DCM, Toluene, MeCN and chloroform did not help to improve the yield. Furthermore, the impact of Au/Ag ratio was marked as the yield of **3a** was enhanced upto 86% declining the formation of **3a′** (entry 9). Interestingly, the catalysts **4b**.AuOTf, which was prepared from celite filtration of the **4b**.AuCl/AgOTf mixtures did not promote this reaction and **1a** was recovered quantitatively (entry 10). This observation was in stark contrast to the result where the product was obtained in 64% yield (entry 8) when the mixtures of **4b**.AuCl and AgOTf were used directly (without filtration of AgCl).

Table no. 3.3.1.1: Optimization of the reaction conditions

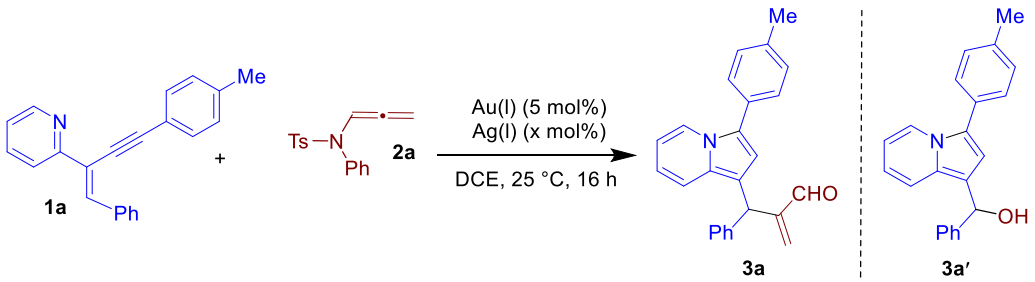

Entry no.	Cat Au (5 mol%)	Cat AgOTf (X mol%)	Yield[b](%)	
			3a	**3a′**
1	Ph_3PAuCl	5	00	72
2	IPrAuCl	5	00	67
3	**4a**.AuCl	5	42	44

4	**4b.**AuCl	5	52	38
5	**4c.**AuCl	5	42	43
6	**4d.**AuCl	5	40	39
7	**4e.**AuCl	5	45	47
8	**4b.**AuCl	5	64	21
9	**4b.**AuCl	10	86	trace
10	**4b.**AuOTf[c]	--	--	--[d]
11	--	10	26	52
12	**4b.**AuCl	--	--	--[e]
13	**4b.**AuCl	10	--	--[f]

[a]Reaction conditions: 0.375 mmol **1a**, 0.250 mmol **2a**, 5 mol% Au(I) catalyst and x mol% AgOTf catalyst, DCE (2 mL), 25 °C, 16 h. (for entries 1-7 Moist DCE was used and for entries 8-12, 2 mL dry DCE with 0.500 mmol of water was used.) [b]Isolated yields (based on **2a**). [c]10 mol% **4b**.AuOTf was used. The catalyst was prepared by mixing equimolar amounts of **4b**.AuCl and AgOTf followed by filtration to remove AgCl. [d] **1a** was recovered in quantitative yield. [e] **1a** and **2a** was recovered in quantitative yield. [f][3+2] cycloaddition product was obtained in 30% yield. Note: IPr = 1,3-di(isopropyl phenyl)-imidazol-2-ylidene.

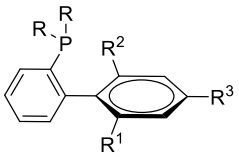

4a R = ^{t}Bu, $R^1 = R^2 = R^3$ = H
4b R = Cy, $R^1 = R^2 = R^3$ = H
4c R = ^{t}Bu, R^1 = NMe_2, $R^2 = R^3$ = H
4d R = Cy, $R^1 = R^2 = R^3$ = ^{i}Pr
4e R = Ph, R^1 = NMe_2, $R^2 = R^3$ = H

This investigation therefore supports the "silver effect" in gold catalysis as exemplified elegantly by Shi and coworkers.[16] When only 10 mol% AgOTf was used as catalyst, **3a** was obtained in only 26% yield along with the formation of side product **3a′** (entry 11). No product formation was observed when only **4b.**AuCl was used as a catalyst (entry 12). It should be noted that when reaction carried out under dry condition, [3+2] cycloaddition product[17] was observed in 30% yield (entry 13). The observations outlined in entry 8, 10, 11 and 12 clearly indicated the individual importance of Au and Ag catalyst and thereby Au(I)/Ag(I) cooperative catalysis in the current transformation. Be noted that the geometry of the double bond in **1a** did not have effect on the yield of the reaction. When (*Z*)-**1a** reacted with **2a** under the standard reaction conditions, **3a** was obtained in 81% yield.

3.3.2 Scope of the Reaction

With the optimal reaction conditions in hand (Table 3.3.1.1, entry 9), we then set out to explore the scope of the reaction. As shown in Table 3.3.2.1, pyidinoalkynes **1b** with no substitution on the phenyl ring reacted smoothly to obtain the corresponding indolizine **3b** in 69% yield. The reaction also proceeds in good to excellent yields (69-88%) with a wide range of pyidino-alkynes **1** bearing alkyl (4-*i*Pr), electron-donating (4-OMe, 3-OMe, 4-NMe_2, 3,5-di-OMe) as well as halo-substituents (4-Br, 4-F, 3-Cl) on the phenyl ring linked to the alkyne (**3c-3j**). Very interestingly, substrate bearing alkynyl substituents was also found to be compatible giving **3k** in 82% yield. The structure of **3k** was established with the aid of 2D NMR experiments and later confirmed unambiguously with x-ray diffraction studies (See the section **3.9** ORTEP diagram). Even the substrate bearing alkyl group, such as methyl, at the alkene terminus gave **3l**; although, in low yield (56%). The scope of reaction was further investigated with pyridino-alkynes bearing various substitutions at the phenyl ring attached to alkene. Both electron-donating and electron-withdrawing groups as well as alkyl substituents on the aforementioned phenyl ring were well suited to furnish the products in 62-83% yields (**3m-3t**). Interestingly, the substrate bearing -NO_2 group on the aryl ring required shorter reaction time (4 h) to obtain **3p** in 77% yield. Even the substituents like -Ph and 4-OMe-C_6H_4 on the pyridine ring were well tolerated giving products **3u** and **3v** in 61 and 75% yields, respectively. The reaction of 2-quinolyl based substrate **1w** also proceeded smoothly to give functionalized benz[*e*]indolizine **3w** in 82% yield. Finally, the current methodology sustained well under the substitution at the allenyl moiety for the formation of product **3x** in 61% yield (Scheme 3). Remarkably, this reaction exclusively gave *Z*-isomer as confirmed by NOESY spectroscopic analysis (See the section **3.11** 2D NMR experiments).

Table no. 3.3.2.1: Reaction scope

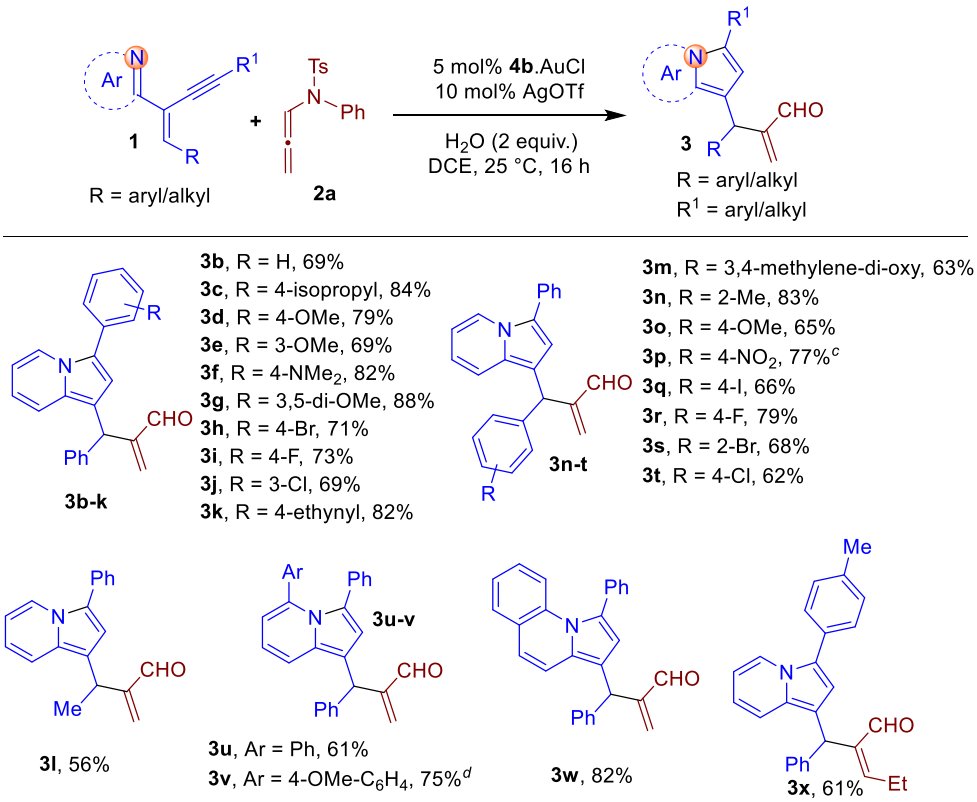

[a]Reaction conditions: 0.375 mmol **1**, 0.250 mmol **2a**, 0.500 mmol of H_2O, 5 mol% **4b**.AuCl, 10 mol% AgOTf, dry DCE (2 mL), 25 °C, 16 h. [b]Isolated yields (based on **2a**). [c]Reaction time is 4 h. [d]Reaction carried out with mixture of *E* and *Z* isomer of **1v**. [e]**1a** was recovered in quantitative yield. Note: All reactions were performed with *E*-isomer of **1**, i.e, major isomer.

Finally, the current methodology sustained well under the substitution at the allenyl moiety for the formation of product **3x** in 61% yield (Table no. 3.3.2.1). Remarkably, this reaction exclusively gave *Z*-isomer as confirmed by NOESY spectroscopic analysis (See the section **3.11** 2D NMR experiments).

3.4 Plausible Reaction Mechanism

Based on Bandini's report11 and our experimental observations, a plausible mechanism of the reaction is proposed (Scheme 5). At first, gold catalysts would undergo complexation with **2a** (cf. **A**) to generate α-gold en-imine intermediate **B**. The intermediate **B**, thus formed, would subsequently undergo hydrolysis to generate nucleophilic α-gold(I) enal species **C** with removal of NHTsPh. Simultaneously, the co-ordination of Ag(I) to the triple bond of **1b** would take place

to form Ag-alkyne complex **D**. This complex **D** would further be converted into silver bound carbocation **E** via intramolecular nucleophilic attack of pyridyl nitrogen onto the Ag(I) activated alkyne followed by isomerization. The union of both the metal-bound reactive intermediates **C** and **E** would give **3b** with regeneration of both the catalysts.

Scheme 3.4.1: A plausible reaction mechanism

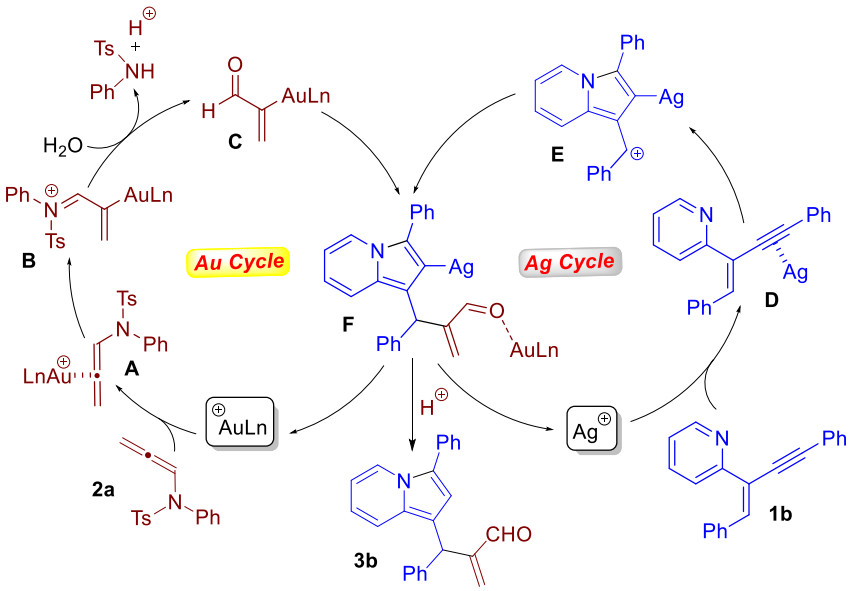

3.5 Computational Studies

The geometry optimizations were conducted employing density functional theory (DFT) with the Turbomole 6.4 suite of programs.[18] The Perdew, Burke, and Ernzerhof (PBE)[19] functional were used for the geometry optimization calculations. The triple-ζ basis set augmented by a polarization function (Turbomole basis set TZVP) was used for all the atoms. The resolution of identity (RI)[20] along with the multipole accelerated resolution of identity (marij)[21] approximations were employed for an accurate and efficient treatment of the electronic Coulomb term. Solvent effects were accounted for as follows: we had done full geometry optimizations of all intermediates and transition states calculations using the COSMO model,[22] with solvent ethylene dichloride. Moreover, dispersion corrections (disp-3) were also included through these calculations[23] with regard to the transition states obtained during the investigations of these reactions, care was taken to ensure that the obtained transition state structures possessed only one imaginary frequency corresponding to the correct normal mode.

To gather further evidences in support of the proposed mechanism, we performed DFT calculations using $AuP(Me)_3$ as a model catalyst. We considered the possibilities of interception of silver bound carbocation **E** with i) α-gold(I) enal **C**, ii) unactivated *N*-allenamide **2a** and iii) α-gold(I) en-imine **B**. DFT calculations were conducted to understand which possibilities i.e. (i), (ii) and (iii) was energetically favorable. Quantum chemical calculations reveal the formation of product either by direct attack of *N*-allenamide under the Ag-catalysis [possibility (ii)] or attack of α-gold(I) enal intermediate under the Au/Ag co-operative catalysis [possibility (i)]. Initially, the C-C bond forming step was investigated by the union of silver bound carbocation **E** with the α-gold(I) enal **C** [Figure 3.5.1, possibility (i), marked in blue]. In this step, the α-gold(I) enal species approaches the silver bound carbocation, resulting in the formation of Au- and Ag-bound intermediate **Int1** with generation of new C-C bond *via* transition state $\mathbf{TS_1}$ [20.2 kcal/mol above **Int0**]. Simultaneously, the C-C bond forming step was investigated by quenching the Ag-bound carbocation **E** with **2a** [Figure 3.5.1, possibility (ii), marked in red). This results in the formation of Ag-bound intermediate **Int1′** *via* transition state $\mathbf{TS_1'}$ [14.0 kcal/mol above **Int0′**]. Although there is higher exergonicity of transformation **Int0′→Int1′** [-11.5 kcal/mol above **Int0′**] than **Int0→Int1** [-8.8 kcal/mol above **Int0′**], it is compensated in the subsequent step where the transition state for hydrolysis $\mathbf{TS_2'}$ is high energy demanding (31.8 kcal/mol) as compared to **Int2** (7.7 kcal/mol above **Int0**). The intermediate **Int2** after protonation forms product **P**. Similarly, **Int2′** undergoes protodeauration to form product **P′** (transition state $\mathbf{TS_3'}$, -7.6 kcal/mol above **Int0′**). The computational results, therefore, support the proposed Au/Ag co-operative catalysis and rule out alternative mononuclear mechanistic pathways.

Figure 3.5.1: Interception of Ag-bound carbocation with α-gold enal vs. *N*-allenamide - computational investigation [possibility (i) vs (ii)]

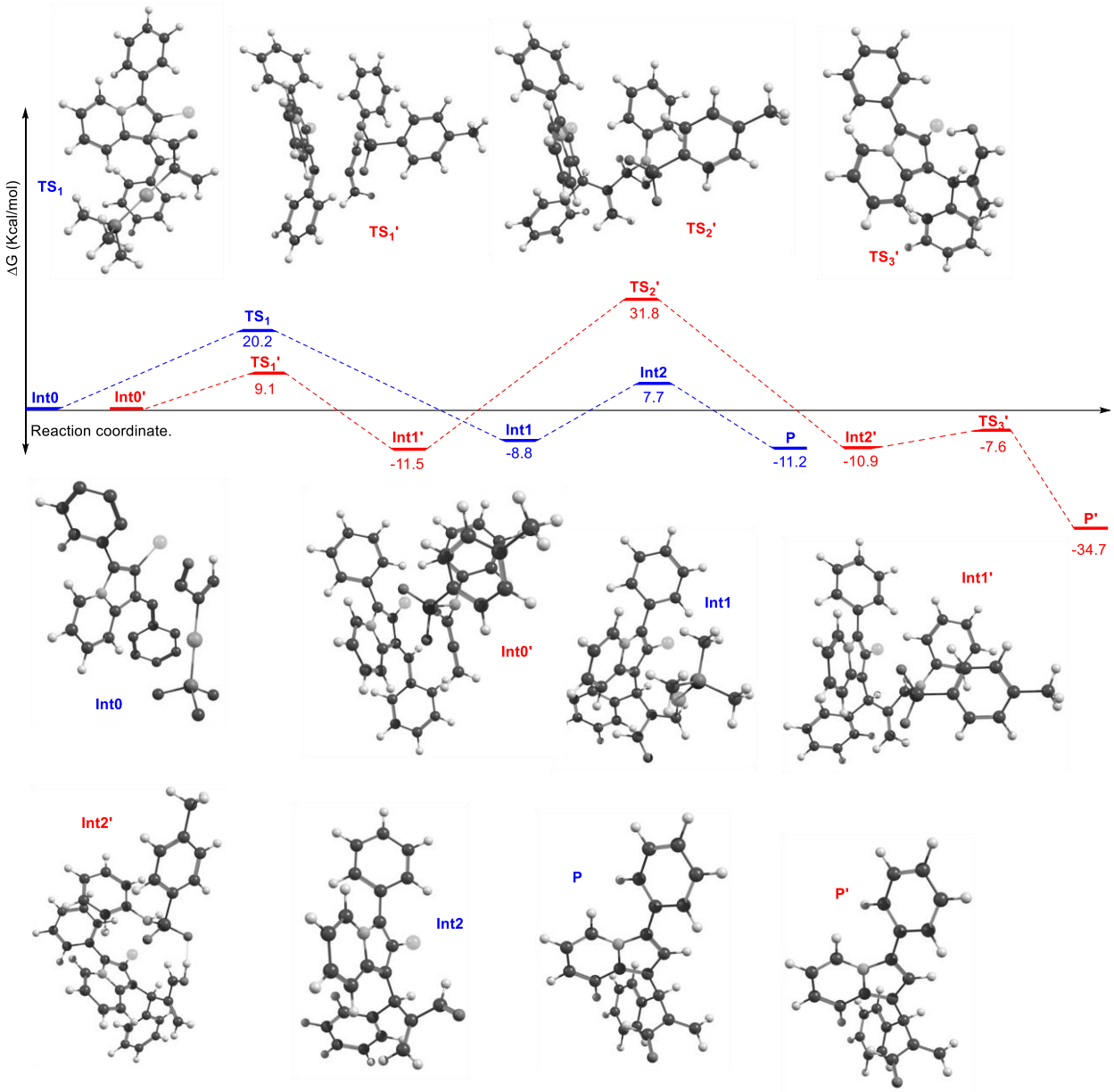

Figure 3.5.2: Interception of Ag-bound carbocation with α-gold enal vs α-gold en-imine - computational investigation [possibility (i) vs (iii)]

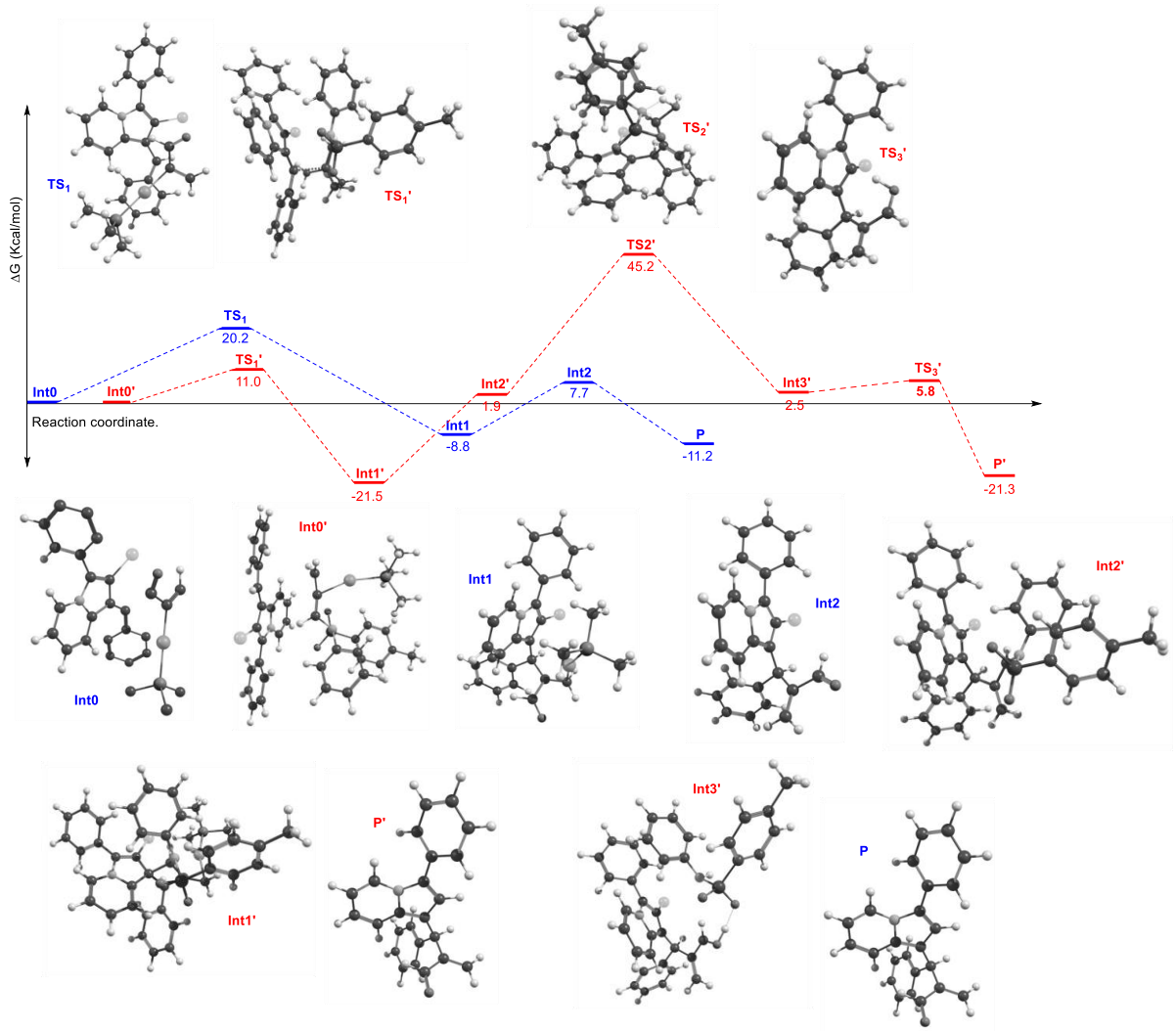

This DFT calculations showed that possibility (iii) also high energy demanding as compared to the possibility (i).

Figure 3.5.3: Computational mechanistic investigation: the formation of α-gold enal species vs α-silver enal.

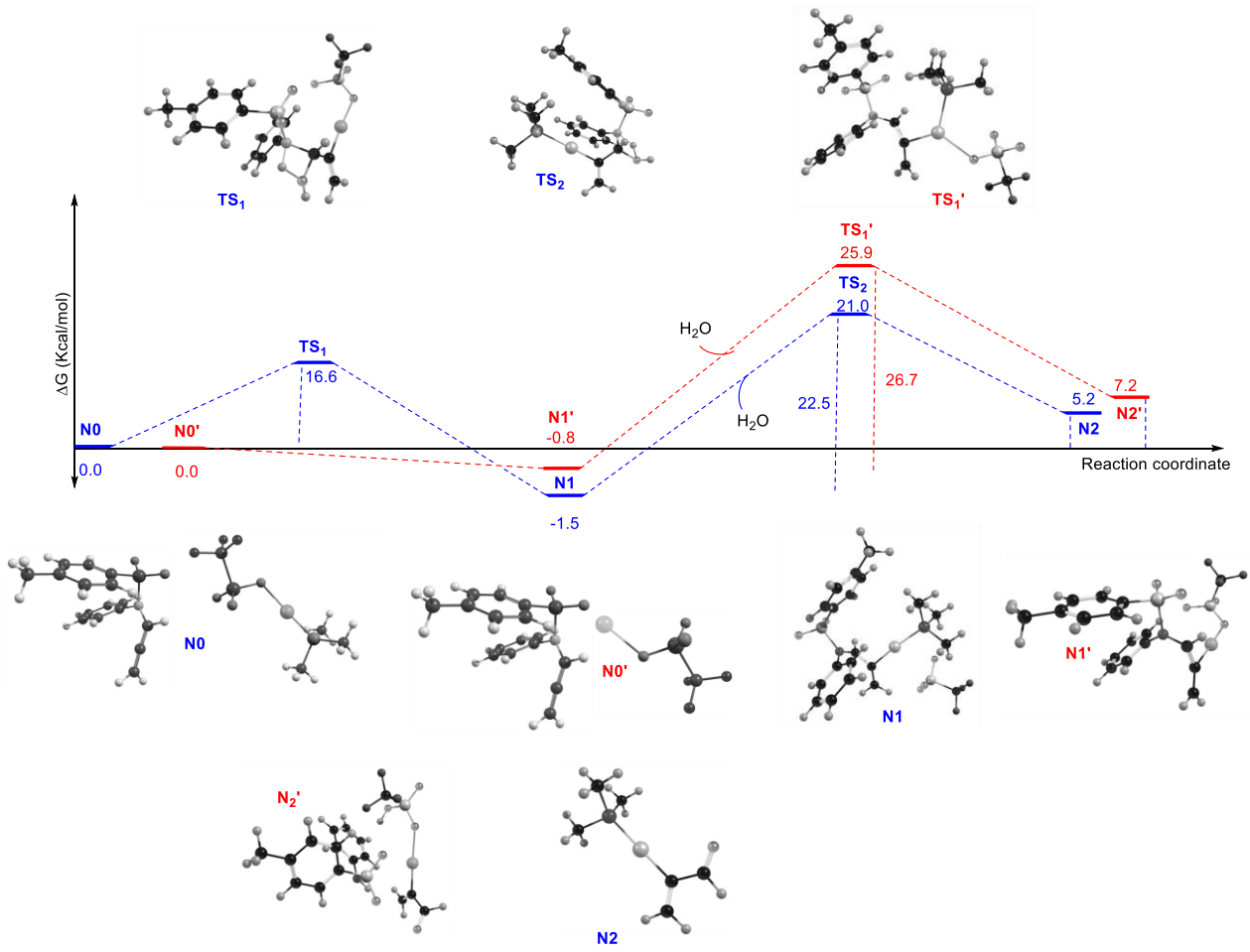

The possibility of interception of Ag-bound carbocation **E** with α-silver(I) enal was ruled out as the formation of α-silver(I) enal is high energy demanding as compared to formation of α-gold(I) enals which was proven by Bandini's report.[11]

3.6 Modification of Products

To demonstrate the synthetic utility of the reaction, the possibility of further functionalization was examined (Scheme 3.6.1). The reduction of **3a** in the presence of $NaBH_4$ in methanol gave the corresponding allylic alcohol **4** in 92% yield. Similarly, intramolecular Heck-coupling have been performed on the compound **3s** to obtain the indolizine-indene dyad **5** in 62% yield.

Scheme 3.6.1: Heck and carbonyl reduction reaction

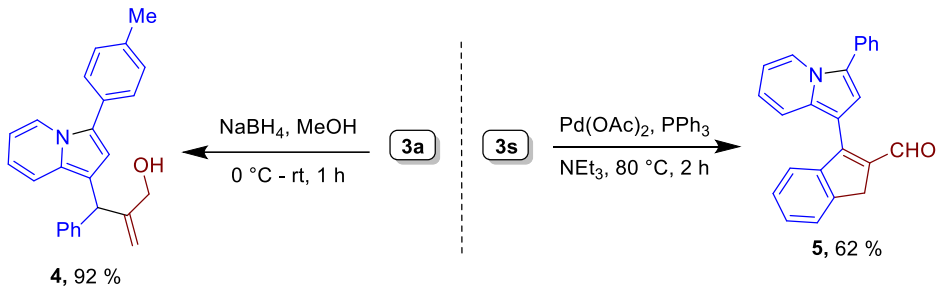

3.6 Conclusion

This chapter described the Au/Ag co-operative catalysis for utilisation of *N*-allenamides as nucleophilic enal equivalents for the interceptive capturing of incipient carbocation generated through π-acid-triggered imino-alkyne cyclisation. The mechanism of the reaction was established by carefully conducted experimental and computational studies. Given the several reports on the generation of metal-bound carbocations,10 the current methodology holds great promise for the interception of such metal-bound carbocations with α-gold(I) enals. We believe that these findings will provide new insights into the gold-alkyne chemistry and would open up the door for the development of new catalytic transformations. Further studies addressing the enantioselective version are currently under investigation.[24]

3.7 Experimental Procedures

Procedure for the synthesis of 2-(2-enynyl) pyridines 1:

The pyridine-2-yl alkynones **1a**, **1b**, **1d**, **1e**, **1j**, **1l**, **1o**, **1q**, **1r**, **1t, 1w** and **1x** were reported in the literature and prepared according to the known procedure.[25] On the other hand, compounds **1c**, **1f**, **1g**, **1h**, **1i**, **1k**, **1m**, **1n**, **1p**, **1s**, **1u** and **1v** were also prepared by similar procedure.

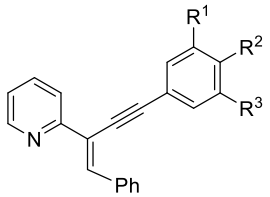

1a, R^2 = Me, R^1 = R^3 = H
1b, R^1 = R^2 = R^3 = H
1c, R^2 = ^{i}Pr, R^1 = R^3 = H
1d, R^2 = OMe, R^1 = R^3 = H
1e, R^1 = OMe, R^2 = R^3 = H
1f, R^2 = NMe_2, R^1 = R^3 = H
1g, R^1 = R^3 = OMe, R^2 = H
1h, R^2 = Br, R^1 = R^3 = H
1i, R^2 = F, R^1 = R^3 = H
1j, R^1 = Cl, R^2 = R^3 = H
1k, R^2 = ethynyl, R^1 = R^3 = H

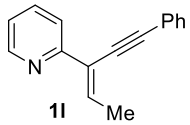

1l

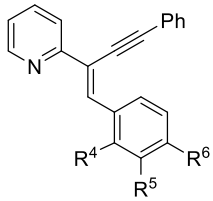

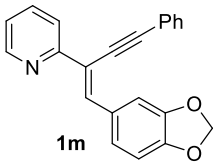

1m

1n, R^4 = Me, R^5 = R^6 = H
1o, R^4 = R^5 = H, R^6 = OMe
1p, R^4 = R^5 = H, R^6 = NO_2
1q, R^4 = R^5 = H, R^6 = I
1r, R^4 = R^5 = H, R^6 = F
1s, R^4 = Br, R^5 = R^6 = H
1t, R^4 = R^5 = H, R^6 = Cl

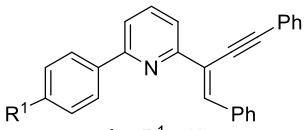

1u, R^1 = H
1v, R^1 = OMe

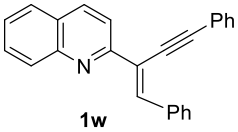

1w

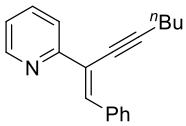

1x

***Representative Procedure*:** To a solution of the benzyl triphenylphosphonium bromide (1.2 equiv.) in dry THF (0.48 M) at 0 °C, *n*-butyllithium (1.6 M in Hexane, 1.2 equiv.) was added dropwise by syringe over 5 minutes. After 10 min, pyridine-2-yl alkynone (1.0 equiv.) was added to the solution. After completion of reaction (monitored by TLC), the mixture was poured into water and extracted with ethyl acetate (3 x 20 mL). The combined organic phase was dried over Na_2SO_4, filtered and the solvent was removed under vacuum. The resultant residue was purified by flash chromatography on silica gel using ethyl acetate/petroleum ether (05/95) as eluent to afford the 2-(2-enynyl)pyridine as *E*/*Z* mixture (*E*/*Z*:7/3) in 84% yield.

General procedure for gold/silver catalysed imino-alkyne cyclisation reactions

To a oven dried screw cap vial, CyJohnPhosAuCl (5 mol%) and AgOTf (10 mol%) were dissolved in anhydrous DCE (0.12 M) under N_2 atmosphere. The reaction mixture was allowed to stir for 5-10 min and then pyridino-alkynes **1** (0.350 mmol) was added followed by the *N*-allenamides **2** (0.250 mmol) and H_2O (0.500 mmol). The reaction was stirred at 25 °C for specified time and after that the reaction mixture was loaded directly on silica gel column. After column chromatographic purification using ethyl acetate/petroleum ether as eluent, analytically pure products **3** were obtained.

Note: Both *E* and *Z* isomer gives the comparable yield under standard reaction condition. Geometry of the double bond in **1** does not affect yield of the reaction.

General Procedure for Modification of Products

Reduction of 3a

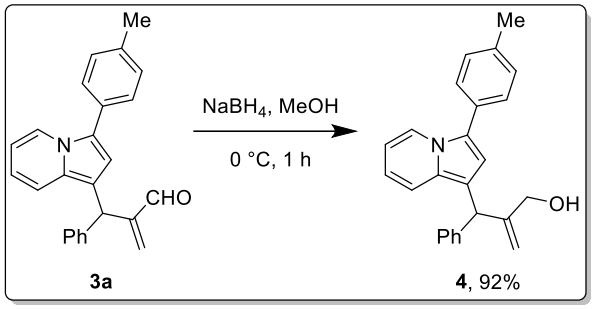

To an ice cooled (0 °C) solution of **3a** (50 mg, 0.142 mmol) in MeOH (1 mL), $NaBH_4$ (5.9 mg, 0.156 mmol) was added. After complete consumption of starting material (1 h), the reaction was quenched with cold water (3 mL). Then MeOH was removed under reduced pressure and the aqueous phase was extracted using DCM (3 x 5 mL). The organic layers were dried over Na_2SO_4, filtered and solvents were evaporated. The crude product thus obtained, was purified over silica gel chromatography using a mixture of ethyl acetate/petroleum ether (10:90) as eluent to afford analytically pure compound **4**.

Heck reaction of 3r

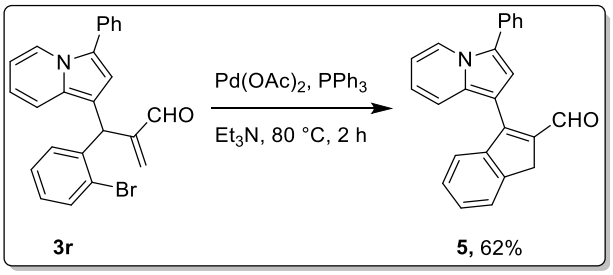

A stirred solution of **3r** (50 mg, 0.12 mmol), $Pd(OAc)_2$ (2.7 mg, 5 mol%), PPh_3 (3.4 mg, 10 mol%) in Et_3N (1 mL) was heated to 80 °C for 2 h under nitrogen atmosphere. The reaction mixture was allowed to cool at room temperature. The reaction was quenched with water (5 mL) and the reaction mixture was extracted with ethyl acetate (3 x 5 mL). The organic layer was washed with 5N HCl solution. Organics were dried over Na_2SO_4, filtered and concentrated under

vacuum. The residue thus obtained, was purified by column chromatography using ethyl acetate/petroleum ether (05:95) to afford analytically pure **5**.

3.8 Characterization Data of Selected Compounds

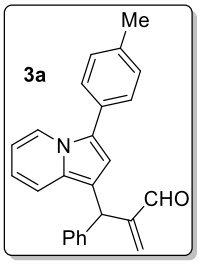

3a: Yellow thick liquid; yield = 75 mg, 86% with *E* isomer of **1a** and 71 mg, 81% with *Z* isomer of **1a**; R_f = 0.50 (ethyl acetate/petroleum ether = 05/95).

^{1}H NMR (400 MHz, CDCl$_3$) δ = 9.71 (s, 1 H), 8.23 (d, *J* = 7.3 Hz, 1 H), 7.44 (d, *J* = 8.1 Hz, 2 H), 7.36 - 7.29 (m, 3 H), 7.28 - 7.20 (m, 5 H), 6.66 - 6.59 (m, 1 H), 6.53 (s, 1 H), 6.50 - 6.44 (m, 1 H), 6.28 (s, 1 H), 6.18 (s, 1 H), 5.66 (s, 1 H), 2.42 (s, 3 H).

^{13}C NMR (125 MHz, CDCl$_3$) δ = 193.5, 152.9, 142.0, 136.8, 135.8, 130.3, 129.6, 129.4, 128.5, 128.4, 127.8, 126.4, 124.5, 122.3, 117.7, 116.3, 114.5, 113.2, 110.7, 40.6, 21.2.

HRMS (ESI) calcd for $C_{25}H_{21}NO$ $[M]^+$ 351.1618, found 351.1617.

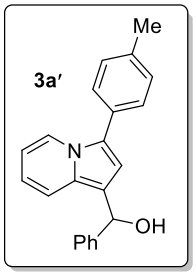

3a': Bluish thick liquid; R_f = 0.7 (ethyl acetate/petroleum ether = 05/95).

^{1}H NMR (500 MHz, CDCl$_3$) = 8.21 (d, *J* = 7.2 Hz, 1 H), 7.55 - 7.31 (m, 4 H), 7.31 - 7.11 (m, 6 H), 6.64 (s, 1 H), 6.55 - 6.48 (m, 1 H), 6.43 - 6.35 (m, 1 H), 5.99 (s, 1 H) , 2.39 (s, 3H).

^{13}C NMR (125 MHz, CDCl$_3$) δ = 145.5, 136.5, 130.3, 129.7, 129.5, 129.5, 128.5, 128.2, 127.8, 125.8, 124.2, 122.2, 118.1, 117.0, 115.7, 114.9, 110.3, 40.1, 21.2.

HRMS (ESI) calcd for $C_{25}H_{21}NO$ $[M]^+$ 351.1618, found 351.1617.

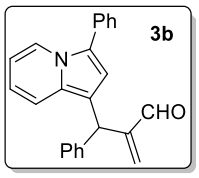

3b: Yellow thick liquid; yield = 58 mg, 69%; R_f = 0.50 (ethyl acetate/petroleum ether = 05/95).

^{1}H NMR (500 MHz, CDCl$_3$) δ = 9.68 (s, 1 H), 8.23 (d, *J* = 7.2 Hz, 1 H), 7.52 (d, *J* = 7.6 Hz, 2 H), 7.43 (t, *J* = 7.6 Hz, 2 H), 7.32 - 7.23 (m, 6 H), 7.21 (t, *J* = 7.1 Hz, 1 H), 6.61 (dd, *J* = 6.7, 8.6 Hz, 1 H), 6.54 (s, 1 H), 6.45 (t, *J* = 6.7 Hz, 1 H), 6.25 (s, 1 H), 6.15 (s, 1 H), 5.64 (s, 1 H).

^{13}C NMR (125 MHz, CDCl$_3$) δ = 193.5, 152.8, 141.9, 135.8, 132.3, 130.6, 128.9, 128.5, 128.4, 127.8, 127.0, 126.4, 124.4, 122.2, 117.7, 116.5, 114.8, 113.3, 110.8, 40.6.

HRMS (ESI) calcd for $C_{24}H_{20}NO$ $[M+H]^+$ 338.1539, found 338.1530.

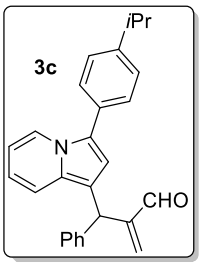

3c: Yellow thick liquid; yield = 79 mg, 84%; R_f = 0.40 (ethyl acetate/petroleum ether = 05/95).

^{1}H NMR (500 MHz, CDCl$_3$) δ = 9.68 (s, 1 H), 8.23 (d, *J* = 6.5 Hz, 1 H), 7.44 (d, *J* = 6.9 Hz, 2 H), 7.33 - 7.24 (m, 7 H), 7.21 (d, *J* = 6.1 Hz, 1 H), 6.60 (t, *J* = 6.9 Hz, 1 H), 6.50 (br. s., 1 H), 6.47 - 6.39 (m, 1 H), 6.24 (br. s., 1 H), 6.14 (br. s., 1 H), 5.63 (br. s., 1 H), 3.00 - 2.87 (m, 1 H), 1.28 (d, *J* = 6.5 Hz, 6 H).

^{13}C NMR (125 MHz, CDCl$_3$) δ = 193.5, 152.9, 147.8, 142.0, 135.8, 130.3, 129.8, 128.5, 128.4, 127.8, 126.9, 126.4, 124.5, 122.3, 117.7, 116.3, 114.6, 113.2, 110.6, 40.6, 33.9, 24.0.

HRMS (ESI) calcd for $C_{27}H_{26}NO$ $[M+H]^+$ 380.2009, found 380.2004.

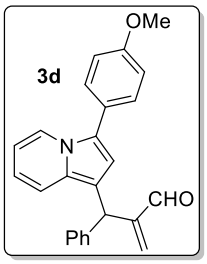

3d: Yellow thick liquid; yield = 72 mg, 79%; R_f = 0.40 (ethyl acetate/petroleum ether = 05/95).

^{1}H NMR (500 MHz, CDCl$_3$) δ = 9.70 (s, 1 H), 8.15 (d, *J* = 7.3 Hz, 1 H), 7.47 - 7.41 (m, 2 H), 7.33 - 7.27 (m, 3 H), 7.26 (br. s., 1 H), 7.25 - 7.20 (m, 2 H), 7.03 - 6.96 (m, 2 H), 6.63 - 6.58 (m, 1 H), 6.48 (s, 1 H), 6.47 - 6.41 (m, 1 H), 6.27 (s, 1 H), 6.17 (s, 1 H), 5.65 (s, 1 H), 3.86 (s, 3 H).

^{13}C NMR (125 MHz, CDCl$_3$) δ = 193.5, 158.7, 152.9, 142.0, 135.9, 130.0, 129.4, 128.5, 128.4, 126.4, 124.8, 124.2, 122.1, 117.7, 116.1, 114.3, 114.3, 113.0, 110.6, 55.3, 40.6.

HRMS (ESI) calcd for $C_{25}H_{22}NO_2$ $[M+H]^+$ 368.1645, found 368.1633.

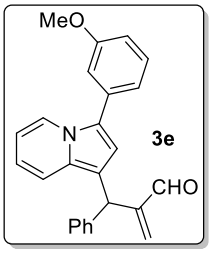

3e: Yellow thick liquid; yield = 63 mg, 69%; R_f = 0.40 (ethyl acetate/petroleum ether = 05/95).

^{1}H NMR (500 MHz, CDCl$_3$) δ = 9.70 (s, 1 H), 8.28 (d, *J* = 7.0 Hz, 1 H), 7.37 (t, *J* = 7.9 Hz, 1 H), 7.33 - 7.29 (m, 2 H), 7.29 - 7.25 (m, 3 H), 7.24 (d, *J* = 7.0 Hz, 1 H), 7.14 (d, *J* = 7.6 Hz, 1 H), 7.08 - 7.04 (m, 1 H), 6.90 - 6.85 (m, 1 H), 6.67 - 6.60 (m, 1 H), 6.56 (s, 1 H), 6.51 - 6.44 (m, 1 H), 6.27 (s, 1 H), 6.17 (s, 1 H), 5.65 (s, 1 H), 3.85 (s, 3 H).

^{13}C NMR (125 MHz, CDCl$_3$) δ = 193.5, 160.0, 152.8, 141.9, 135.9, 133.6, 130.7, 129.9, 128.5, 128.4, 126.5, 124.3, 122.4, 120.2, 117.7, 116.6, 114.9, 113.5, 113.3, 112.4, 110.9, 55.3, 40.5.

HRMS (ESI) calcd for $C_{25}H_{22}NO$ $[M+H]^+$ 368.1645, found 368.1645.

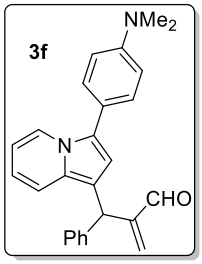

3f: Yellow thick liquid; yield = 78 mg, 82%; R_f = 0.40 (ethyl acetate/petroleum ether = 05/95).

^{1}H NMR (500 MHz, CDCl$_3$) δ = 9.70 (s, 1 H), 8.17 (d, *J* = 7.3 Hz, 1 H), 7.42 - 7.37 (m, *J* = 8.9 Hz, 2 H), 7.33 - 7.27 (m, 4 H), 7.25 - 7.21 (m, 2 H), 6.84 - 6.78 (m, *J* = 8.9 Hz, 2 H), 6.57 (dd, *J* = 6.6, 8.4 Hz, 1 H), 6.46 (s, 1 H), 6.44 - 6.40 (m, 1 H), 6.26 (s, 1 H), 6.18 (s, 1 H), 5.65 (s, 1 H), 3.01 (s, 6 H).

^{13}C NMR (125 MHz, CDCl$_3$) δ = 193.6, 152.9, 149.6, 142.1, 135.9, 129.7, 129.3, 129.1, 128.5, 128.3, 127.2, 126.3, 124.9, 122.3, 120.3, 117.6, 115.7, 113.9, 112.8, 112.6, 110.3, 40.6, 40.5.

HRMS (ESI) calcd for $C_{26}H_{24}ON$ $[M]^+$ 380.1883, found 380.1882.

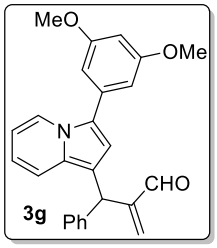

3g: Yellow thick liquid; yield = 87 mg, 88%; R_f = 0.50 (ethyl acetate/petroleum ether = 05/95).

^{1}H NMR (500 MHz, CDCl$_3$) δ = 9.70 (s, 1 H), 8.30 (d, *J* = 7.2 Hz, 1 H), 7.34 - 7.28 (m, 2 H), 7.27 - 7.21 (m, 4 H), 6.68 (d, *J* = 1.9 Hz, 2 H), 6.66 - 6.60 (m, 1 H), 6.56 (s, 1 H), 6.48 (t, *J* = 6.5 Hz, 1 H), 6.44 (s, 1 H), 6.27 (s, 1 H), 6.16 (s, 1 H), 5.65 (s, 1 H), 3.83 (s, 6 H).

^{13}C NMR (125 MHz, CDCl$_3$) δ = 193.5, 161.2, 152.8, 141.9, 135.8, 134.1, 130.7, 128.5, 128.4, 126.5, 124.3, 122.6, 117.8, 116.6, 114.9, 113.3, 110.9, 105.9, 99.1, 55.5, 40.6.

HRMS (ESI) calcd for $C_{26}H_{24}NO_3$ $[M+H]^+$ 398.1751, found 398.1750.

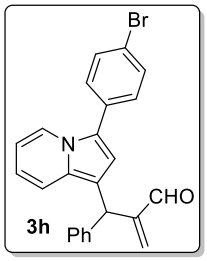

3h: Yellow solid; yield = 74 mg, 71%; R_f = 0.50 (ethyl acetate/petroleum ether = 05/95); mp = 115-117 °C.

^{1}H NMR (500 MHz, CDCl$_3$) δ = 9.71 (s, 1 H), 8.19 (d, *J* = 7.0 Hz, 1 H), 7.59 - 7.55 (m, *J* = 8.2 Hz, 2 H), 7.43 - 7.38 (m, *J* = 8.2 Hz, 2 H), 7.34 - 7.28 (m, 3 H), 7.27 - 7.20 (m, 3 H), 6.66 (dd, *J* = 6.7, 8.9 Hz, 1 H), 6.55 (s, 1 H), 6.50 (t, *J* = 6.4 Hz, 1 H), 6.28 (s, 1 H), 6.16 (s, 1 H), 5.65 (s, 1 H).

^{13}C NMR (125 MHz, CDCl$_3$) δ = 193.4, 152.8, 141.8, 135.9, 132.0, 131.2, 130.9, 129.2, 128.9, 128.5, 128.4, 127.8, 126.5, 123.2, 122.0, 120.6, 117.9, 116.9, 115.0, 113.7, 111.2, 40.5.

HRMS (ESI) calcd for $C_{24}H_{19}NOBr$ $[M+H]^+$ 416.0645, found 416.0630.

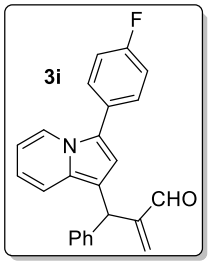

3i: Yellow thick liquid; yield = 65 mg, 73%; R_f = 0.40 (ethyl acetate/petroleum ether = 05/95).

^{1}H NMR (500 MHz, CDCl$_3$) δ = 9.70 (d, *J* = 1.8 Hz, 1 H), 8.13 (d, *J* = 7.3 Hz, 1 H), 7.48 (ddd, *J* = 2.1, 5.7, 8.2 Hz, 2 H), 7.33 - 7.27 (m, 3 H), 7.27 - 7.18 (m, 3 H), 7.14 (dt, *J* = 1.8, 8.7 Hz, 2 H), 6.66 - 6.59 (m, 1 H), 6.51 (s, 1 H), 6.50 - 6.43 (m, 1 H), 6.26 (s, 1 H), 6.15 (s, 1 H), 5.65 (s, 1 H).

^{13}C NMR (125 MHz, CDCl$_3$) δ = 193.5, 163.0 (d, *J* = 246.33 MHz), 152.8, 141.9, 135.9, 130.4, 129.7 (d, *J* = 7.67 Hz), 128.5, 128.4, 126.5, 123.3, 121.9, 117.8, 116.5, 116.0, 115.8, 114.7, 113.3, 111.0, 40.5.

HRMS (ESI) calcd for $C_{24}H_{19}ONF$ $[M+H]^+$ 356.1445, found 356.1449.

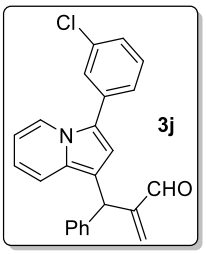

3j: Yellow thick liquid; yield = 64 mg, 69%; R_f = 0.30 (ethyl acetate/petroleum ether = 05/95).

^{1}H NMR (400 MHz, CDCl$_3$) δ = 9.71 (s, 1 H), 8.24 (d, *J* = 6.8 Hz, 1 H), 7.52 (s, 1 H), 7.46 - 7.41 (m, 1 H), 7.40 - 7.36 (m, 1 H), 7.35 - 7.28 (m, 4 H), 7.27 - 7.20 (m, 3 H), 6.67 (dd, *J* = 7.1, 8.1 Hz, 1 H), 6.57 (s, 1 H), 6.52 (t, *J* = 6.6 Hz, 1 H), 6.28 (s, 1 H), 6.16 (s, 1 H), 5.65 (s, 1 H).

^{13}C NMR (100 MHz, CDCl$_3$) δ = 193.4, 152.7, 141.8, 135.9, 134.8, 134.1, 131.1, 130.1, 129.6, 128.5, 128.4, 127.6, 126.8, 126.5, 125.6, 122.9, 122.1, 117.9, 117.1, 115.3, 113.7, 111.3, 40.5.

HRMS (ESI) calcd for $C_{24}H_{19}NOCl$ $[M+H]^+$ 372.1150, found 372.1154.

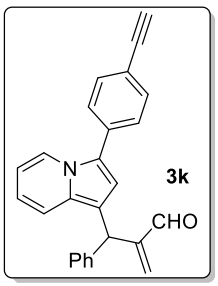

3k: Yellow solid; yield = 74 mg, 82%; R_f = 0.40 (ethyl acetate/petroleum ether = 05/95; mp = 131-133 °C.

^{1}H NMR (500 MHz, CDCl$_3$) δ = 9.68 (s, 1 H), 8.24 (d, *J* = 7.3 Hz, 1 H), 7.56 - 7.52 (m, 2 H), 7.50 - 7.46 (m, 2 H), 7.32 - 7.27 (m, 2 H), 7.26 - 7.18 (m, 4 H), 6.64 (dd, *J* = 6.0, 9.2 Hz, 1 H), 6.57 (s, 1 H), 6.51 - 6.46 (m, 1 H), 6.25 (s, 1 H), 6.13 (s, 1 H), 5.63 (s, 1 H), 3.12 (s, 1 H).

^{13}C NMR (125 MHz, CDCl$_3$) δ = 193.4, 152.7, 141.7, 135.9, 132.7, 132.6, 131.2, 128.5, 128.4, 127.2, 126.5, 123.6, 122.2, 120.1, 117.9, 117.1, 115.3, 113.9, 111.2, 83.6, 77.7, 40.5.

HRMS (ESI) calcd for $C_{26}H_{20}NO$ $[M+H]^+$ 362.1539, found 362.1541.

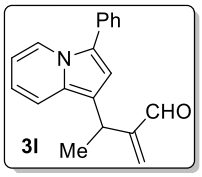

3l: Yellow thick liquid; yield = 38 mg, 56%; R_f = 0.40 (ethyl acetate/petroleum ether = 05/95).

^{1}H NMR (400 MHz, DMSO-d$_6$) δ = 9.57 (s, 1 H), 8.30 (d, *J* = 7.3 Hz, 1 H), 7.59 - 7.53 (m, 2 H), 7.48 (t, *J* = 7.8 Hz, 2 H), 7.46 - 7.42 (m, 1 H), 7.37 - 7.25 (m, 1 H), 6.84 (s, 1 H), 6.69 (dd, *J* = 6.1, 9.0 Hz, 1 H), 6.59 - 6.50 (m, 1 H), 6.42 (s, 1 H), 6.22 (s, 1 H), 4.25 (q, *J* = 7.0 Hz, 1 H), 1.46 (d, *J* = 7.3 Hz, 3 H.

; **^{13}C NMR (100 MHz, CDCl$_3$)** δ = 194.9, 153.9, 134.3, 131.8, 129.7, 129.1, 127.3, 126.9, 123.7, 122.1, 117.7, 116.4, 116.2, 113.0, 111.0, 27.7, 20.3.

HRMS (ESI) calcd for $C_{19}H_{18}NO$ $[M+H]^+$ 276.1383, found 276.1383.

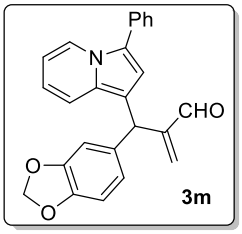

3m: Yellow thick liquid; yield = 60 mg, 63%; R_f = 0.40 (ethyl acetate/petroleum ether = 05/95).

^{1}H NMR (500 MHz, CDCl$_3$) δ = 9.70 (s, 1 H), 8.27 (d, *J* = 7.3 Hz, 1 H), 7.57 - 7.53 (m, 2 H), 7.46 (t, *J* = 7.6 Hz, 2 H), 7.35 - 7.31 (m, 1 H), 7.28 - 7.23 (m, 1 H), 6.78 - 6.72 (m, 3 H), 6.65 (dd, *J* = 6.1, 9.2 Hz, 1 H), 6.56 (s, 1 H), 6.49 (t, *J* = 7.0 Hz, 1 H), 6.27 (s, 1 H), 6.18 (s, 1 H), 5.94 (s, 2 H), 5.57 (s, 1 H).

^{13}CNMR (125 MHz, CDCl$_3$) δ = 193.5, 152.9, 147.7, 146.1, 135.9, 135.8, 132.3, 130.5, 128.9, 127.8, 127.0, 124.4, 122.3, 121.5, 117.7, 116.6, 114.7, 113.4, 110.9, 109.1, 108.1, 100.9, 92.6, 40.2, 29.7.

HRMS (ESI) calcd for $C_{25}H_{20}NO_3$ $[M+H]^+$ 382.1438, found 382.1436.

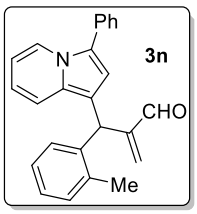

3n: Yellow thick liquid; yield = 73 mg, 83%; R_f = 0.50 (ethyl acetate/petroleum ether = 05/95).

^{1}H NMR (400 MHz, CDCl$_3$) δ = 9.72 (s, 1 H), 8.27 (d, *J* = 7.3 Hz, 1 H), 7.54 (d, *J* = 7.9 Hz, 2 H), 7.48 - 7.39 (m, 2 H), 7.34 - 7.29 (m, 1 H), 7.26 - 7.21 (m, 1 H), 7.21 - 7.06 (m, 4 H), 6.63 (dd, *J* = 6.7, 9.2 Hz, 1 H), 6.54 - 6.40 (m, 2 H), 6.27 (s, 1 H), 6.09 (s, 1 H), 5.76 (s, 1 H), 2.34 (s, 3 H).

^{13}C NMR (100 MHz, CDCl$_3$) δ = 193.4, 152.6, 140.1, 136.2, 135.8, 132.3, 130.6, 130.5, 128.9, 127.8, 127.6, 126.9, 126.4, 125.7, 124.4, 122.3, 117.7, 116.5, 115.3, 112.6, 110.8, 37.0, 19.6.

HRMS (ESI) calcd for $C_{25}H_{22}NO$ $[M+H]^+$ 352.1696, found 352.1696.

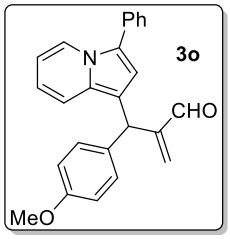

3o: Yellow thick liquid; yield = 59 mg, 65%; R_f = 0.40 (ethyl acetate/petroleum ether = 05/95).

^{1}H NMR (400 MHz, CDCl$_3$) δ = 9.61 (s, 1 H), 8.16 (d, *J* = 6.9 Hz, 1 H), 7.48 - 7.40 (m, 2 H), 7.35 (t, *J* = 7.8 Hz, 2 H), 7.25 - 7.19 (m, 1 H), 7.16 (d, *J* = 10.1 Hz, 1 H), 7.09 (d, *J* = 8.7 Hz, 2 H), 6.76 (d, *J* = 8.7 Hz, 2 H), 6.54 (dd, *J* = 6.6, 8.9 Hz, 1 H), 6.45 (s, 1 H), 6.38 (t, *J* = 6.6 Hz, 1 H), 6.16 (s, 1 H), 6.06 (s, 1 H), 5.51 (s, 1 H), 3.70 (s, 3 H).

^{13}C NMR (100 MHz, CDCl$_3$) δ = 193.6, 158.1, 153.1, 135.6, 134.0, 132.3, 130.5, 129.5, 128.9, 127.8, 126.9, 124.4, 122.2, 117.8, 116.5, 114.8, 113.8, 110.8, 55.2, 39.8.

HRMS (ESI) calcd for $C_{25}H_{22}NO_2$ $[M+H]^+$ 368.1645, found 368.1636.

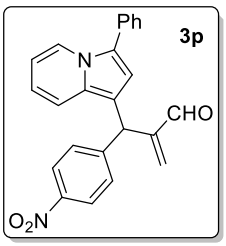

3p: Yellow thick liquid; yield = 73 mg, 77%; R_f = 0.20 (ethyl acetate/petroleum ether = 05/95).

^{1}H NMR (200 MHz, CDCl$_3$) δ = 9.70 (s, 1 H), 8.26 (d, *J* = 7.2 Hz, 1 H), 8.16 (d, *J* = 8.8 Hz, 2 H), 7.56 - 7.48 (m, 2 H), 7.48 - 7.37 (m, 4 H), 7.37 - 7.29 (m, 1 H), 7.27 - 7.18 (m, 1 H), 6.68 (dd, *J* = 6.5, 8.9 Hz, 1 H), 6.58 - 6.48 (m, 1 H), 6.47 (s, 1 H), 6.35 (s, 1 H), 6.20 (s, 1 H), 5.71 (s, 1 H).

^{13}C NMR (125 MHz, CDCl$_3$) δ = 193.0, 151.6, 149.8, 146.6, 136.7, 131.9, 130.5, 129.2, 128.9, 127.8, 127.2, 125.0, 123.7, 122.4, 117.2, 114.4, 111.4, 111.1, 40.6.

HRMS (ESI) calcd for $C_{24}H_{18}N_2O_3$ $[M^+]$ 382.1312, found 382.1308.

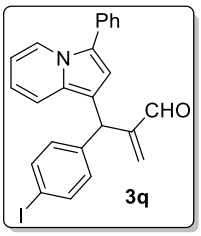

3q: Yellow thick liquid; yield = 76 mg, 66%; R_f = 0.40 (ethyl acetate/petroleum ether = 05/95).

^{1}H NMR (500 MHz, CDCl$_3$) δ = 9.69 (s, 1 H), 8.26 (d, *J* = 7.2 Hz, 1 H), 7.66 - 7.58 (m, *J* = 8.4 Hz, 2 H), 7.53 (d, *J* = 6.9 Hz, 2 H), 7.45 (t, *J* = 7.8 Hz, 2 H), 7.32 (t, *J* = 7.4 Hz, 1 H), 7.24 (d, *J* = 8.8 Hz, 1 H), 7.05 - 6.98 (m, *J* = 8.4 Hz, 2 H), 6.65 (dd, *J* = 6.5, 9.2 Hz, 1 H), 6.51 (s, 1 H), 6.50 - 6.46 (m, 1 H), 6.28 (s, 1 H), 6.16 (s, 1 H), 5.59 (s, 1 H).

^{13}C NMR (125 MHz, CDCl$_3$) δ = 193.3, 152.3, 141.8, 137.5, 136.2, 132.1, 131.5, 130.6, 130.5, 130.3, 128.9, 127.8, 127.1, 124.6, 122.3, 117.6, 116.8, 114.6, 112.6, 110.9, 91.9, 40.2.

HRMS (ESI) calcd for $C_{24}H_{19}NOI$ $[M+H]^+$ 464.0506, found 464.0497.

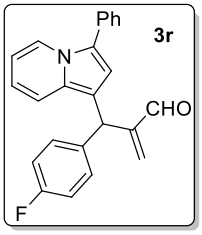

3r: Yellow thick liquid; yield = 70 mg, 79%; R_f = 0.40 (ethyl acetate/petroleum ether = 05/95).

^{1}H NMR (500 MHz, CDCl$_3$) δ = 9.70 (s, 1 H), 8.26 (d, *J* = 7.2 Hz, 1 H), 7.54 (d, *J* = 7.6 Hz, 2 H), 7.45 (t, *J* = 7.6 Hz, 2 H), 7.32 (t, *J* = 7.2 Hz, 1 H), 7.26 - 7.19 (m, 3 H), 7.00 (t, *J* = 8.8 Hz, 2 H), 6.65 (dd, *J* = 6.7, 8.6 Hz, 1 H), 6.52 (s, 1 H), 6.49 (t, *J* = 6.5 Hz, 1 H), 6.28 (s, 1 H), 6.15 (s, 1 H), 5.63 (s, 1 H).

^{13}C NMR (125 MHz, CDCl$_3$) δ = 193.4, 162.5 (d, *J* = 244.14 Hz) 152.8, 137.6 (d, *J* = 2.86 Hz), 135.9, 132.2, 130.5, 129.9 (d, *J* = 7.63 Hz), 128.9, 127.8, 127.0, 124.6, 122.3, 117.6, 116.7, 115.3, 115.1 (d, *J* = 54.36 Hz), 113.1, 110.9, 39.9.

HRMS (ESI) calcd for $C_{24}H_{19}ONF$ $[M+H]^+$ 356.1445, found 356.1443.

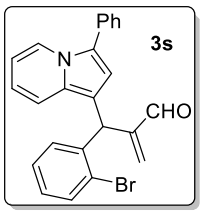

3s: Yellow thick liquid; yield = 70 mg, 68%; R_f = 0.50 (ethyl acetate/petroleum ether = 05/95).

^{1}H NMR (500 MHz, CDCl$_3$) δ = 9.71 (s, 1 H), 8.27 (d, *J* = 6.9 Hz, 1 H), 7.60 (d, *J* = 8.0 Hz, 1 H), 7.56 (d, *J* = 7.6 Hz, 2 H), 7.46 (t, *J* = 7.6 Hz, 2 H), 7.35 - 7.31 (m, 2 H), 7.22 (t, *J* = 7.2 Hz, 1 H), 7.17 (d, *J* = 6.5 Hz, 1 H), 7.10 (t, *J* = 7.2 Hz, 1 H), 6.69 - 6.62 (m, 1 H), 6.57 (s, 1 H), 6.49 (t, *J* = 6.7 Hz, 1 H), 6.28 (s, 1 H), 6.00 (s, 1 H), 6.03 (s, 1 H).

^{13}C NMR (125 MHz, CDCl$_3$) δ = 192.9, 151.7, 141.5, 135.4, 133.1, 132.2, 130.9, 129.9, 129.4, 128.9, 128.1, 127.8, 127.2, 127.0, 126.2, 124.7, 124.5, 122.2, 117.8, 116.8, 114.8, 111.5, 111.0, 40.4.

HRMS (ESI) calcd for $C_{24}H_{19}NOBr$ $[M+H]^+$ 418.0624, found 418.0622.

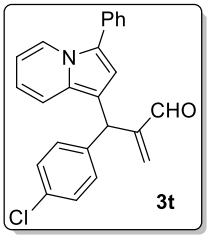

3t: Yellow thick liquid; yield = 57 mg, 62%; R_f = 0.50 (ethyl acetate/petroleum ether = 05/95).

^{1}H NMR (500 MHz, CDCl$_3$) δ = 9.71 (br. s., 1 H), 8.28 (d, *J* = 6.1 Hz, 1 H), 7.55 (d, *J* = 6.9 Hz, 2 H), 7.50 - 7.43 (m, 2 H), 7.38 - 7.32 (m, 1 H), 7.32 - 7.24 (m, 3 H), 7.22 (d, *J* = 6.9 Hz, 2 H), 6.66 (t, *J* = 6.5 Hz, 1 H), 6.54 (br. s., 1 H), 6.50 (br. s., 1 H), 6.29 (br. s., 1 H), 6.17 (br. s., 1 H), 5.64 (br. s., 1 H).

^{13}C NMR (125 MHz, CDCl$_3$) δ = 193.3, 152.5, 140.5, 136.0, 132.2, 132.2, 130.5, 129.8, 128.9, 128.5, 127.8, 127.1, 124.6, 122.3, 117.6, 116.8, 114.6, 112.7, 110.9, 40.0.

HRMS (ESI) calcd for $C_{24}H_{19}NOCl$ $[M+H]^+$ 372.1150, found 372.1152.

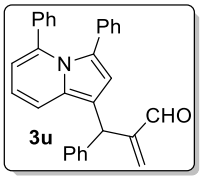

3u: Yellow thick liquid; yield = 63 mg, 61%; R_f = 0.30 (ethyl acetate/petroleum ether = 20/80.

^{1}H NMR (500 MHz, CDCl$_3$) δ = 9.73 (s, 1 H), 7.37 (d, *J* = 9.2 Hz, 1 H), 7.35 - 7.29 (m, 4 H), 7.26 - 7.21 (m, 1 H), 7.12 - 7.06 (m, 2 H), 7.03 (d, *J* = 7.2 Hz, 1 H), 7.00 - 6.95 (m, 2 H), 6.94 - 6.88 (m, 3 H), 6.88 - 6.83 (m, 2 H), 6.82 - 6.77 (m, 1 H), 6.56 (s, 1 H), 6.52 (d, *J* = 6.5 Hz, 1 H), 6.29 (s, 1 H), 6.19 (s, 1 H), 5.75 (s, 1 H).

^{13}C NMR (125 MHz, CDCl$_3$) δ = 193.5, 152.8, 141.9, 137.2, 136.2, 135.9, 134.2, 132.6, 128.6, 128.4, 128.2, 128.1, 127.8, 127.5, 127.4, 126.9, 126.5, 126.0, 125.4, 117.8, 116.6, 115.0, 113.8, 40.6.

HRMS (ESI) calcd for $C_{30}H_{24}NO$ $[M+H]^+$ 414.1852, found 414.1852.

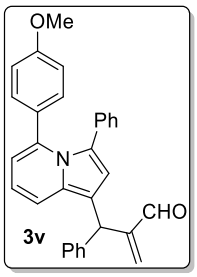

3v: Yellow thick liquid; yield = 83 mg, 75%; R_f = 0.30 (ethyl acetate/petroleum ether = 05/95).

^{1}H NMR (500 MHz, CDCl$_3$) δ = 9.73 (s, 1 H), 7.38 - 7.32 (m, 3 H), 7.32 - 7.30 (m, 2 H), 7.27 - 7.21 (m, 1 H), 7.03 - 6.99 (m, *J* = 8.8 Hz, 2 H), 6.96 - 6.91 (m, 3 H), 6.88 - 6.84 (m, 2 H), 6.78 (dd, *J* = 6.7, 9.0 Hz, 1 H), 6.57 (s, 1 H), 6.53 - 6.50 (m, *J* = 8.8 Hz, 2 H), 6.49 - 6.46 (m, 1 H), 6.29 (s, 1 H), 6.20 (s, 1 H), 5.76 (s, 1 H), 3.71 (s, 3 H).

^{13}C NMR (500 MHz, CDCl$_3$) δ = 193.5, 159.1, 152.8, 141.9, 137.1, 135.9, 134.3, 132.6, 129.1, 128.8, 128.6, 128.5, 128.4, 128.4, 128.0, 126.8, 126.7, 126.4, 126.0, 125.5, 125.3, 117.7, 116.6, 116.2, 114.3, 113.5, 112.8, 55.3, 40.6.

HRMS (ESI) calcd for $C_{31}H_{26}NO$ $[M+H]^+$ 444.1958, found 444.1956.

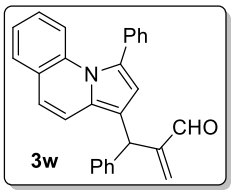

3w: Yellow thick liquid; yield = 78 mg, 82%; R_f = 0.20 (ethyl acetate/petroleum ether = 05/95).

^{1}H NMR (400 MHz, CDCl$_3$) δ = 9.67 (br. s., 1 H), 7.63 - 7.33 (m, 8 H), 7.33 - 7.12 (m, 7 H), 7.07 (d, *J* = 8.5 Hz, 1 H), 6.37 (br. s., 1 H), 6.28 - 6.21 (m, 1 H), 6.20 - 6.11 (m, 1 H), 5.65 (br. s., 1 H).

^{13}C NMR (100 MHz, CDCl$_3$) δ = 193.4, 152.8, 141.8, 136.0, 135.4, 134.2, 129.5, 129.2, 128.5, 128.4, 127.5, 126.5, 126.3, 125.4, 123.3, 118.8, 117.6, 117.1, 116.2, 40.4.

HRMS (ESI) calcd for $C_{28}H_{22}NO$ $[M+H]^+$ 388.1696, found 388.1688.

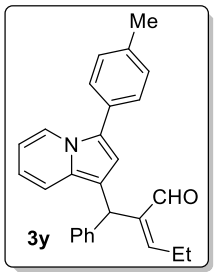

3y: Brownish thick liquid; yield = 55 mg, 61%; R_f = 0.50 (ethyl acetate/petroleum ether = 05/95.

^{1}H NMR (400 MHz, CDCl$_3$) δ = 10.21 (s, 1 H), 8.20 (d, *J* = 7.3 Hz, 1 H), 7.41 (d, *J* = 7.3 Hz, 2 H), 7.31 - 7.17 (m, 10 H), 6.61 - 6.55 (m, 1 H), 6.46 (s, 1 H), 6.45 - 6.34 (m, 2 H), 5.68 (s, 1 H), 2.70 - 2.56 (m, 2 H), 2.38 (s, 3 H), 1.08 (t, *J* = 7.6 Hz, 3 H).

^{13}C NMR (100 MHz, CDCl$_3$) δ = 190.2, 152.4, 143.0, 142.1, 136.7, 130.3, 129.5, 128.6, 128.2, 128.2, 128.1, 127.8, 126.2, 124.3, 122.2, 117.9, 116.1, 114.8, 114.0, 110.6, 110.6, 41.2, 21.2, 20.3, 14.4.

HRMS (ESI) calcd for $C_{27}H_{26}NO$ $[M+H]^+$ 380.2009, found 380.2004.

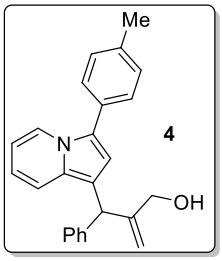

4: Yellow thick liquid; yield = 46 mg, 92%; R_f = 0.30 (ethyl acetate/petroleum ether = 10/90).

^{1}H NMR (400 MHz, CDCl$_3$) δ = 8.21 (d, *J* = 6.7 Hz, 1 H), 7.42 (d, *J* = 7.9 Hz, 2 H), 7.33 - 7.26 (m, 5 H), 7.25 - 7.14 (m, 3 H), 6.61 (s, 1 H), 6.59 - 6.54 (m, 1 H), 6.42 (t, *J* = 6.7 Hz, 1 H), 5.32 (s, 1 H), 5.14 (s, 1 H), 4.82 (s, 1 H), 4.17 (s, 2 H), 2.39 (s, 3 H).

^{13}C NMR (100 MHz, CDCl$_3$) δ = 151.5, 142.6, 136.7, 130.6, 129.5, 129.5, 128.8, 128.3, 127.8, 126.3, 124.5, 122.3, 117.8, 116.1, 114.6, 113.8, 112.8, 110.5, 65.9, 45.8, 21.2.

HRMS (ESI) calcd for $C_{25}H_{24}NO$ $[M+H]^+$ 354.1852, found 354.1850.

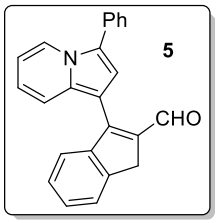

5: Brownish thick liquid; yield = 25 mg, 62%; R_f = 0.30 (ethyl acetate/petroleum ether = 05/95); **^{1}H NMR (400 MHz, CDCl$_3$)** δ = 10.08 (s, 1 H), 8.47 - 8.28 (m, 1 H), 7.74 (d, *J* = 7.6 Hz, 1 H), 7.71 - 7.61 (m, 3 H), 7.61 - 7.50 (m, 3 H), 7.49 - 7.37 (m, 3 H), 7.16 (s, 1 H), 6.94 - 6.77 (m, 1 H), 6.73 - 6.54 (m, 1 H), 3.89 (br. s., 2 H); **^{13}C NMR (100 MHz, CDCl$_3$)** δ = 189.7, 153.3, 145.0, 144.2, 138.2, 133.3, 131.4, 129.2, 128.9, 128.4, 128.1, 127.9, 126.9, 126.8, 124.9, 124.0,

122.9, 119.6, 118.7, 115.8, 111.9, 105.5, 36.0; **HRMS** (ESI) calcd for $C_{24}H_{18}NO$ $[M+H]^+$ 336.1383, found 336.1377.

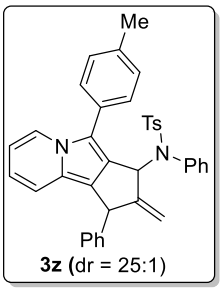

3z (dr = 25:1)

3z: Yellow solid; yield = 30 mg, 30%; R_f = 0.30 (ethyl acetate/petroleum ether = 05/95); mp = 173-175 °C; dr = 25:1, exact stereoselectivity was not determined.

^{1}H NMR (**500 MHz**, **$CDCl_3$**) δ = 8.19 (d, *J* = 7.2 Hz, 1 H), 7.63 (d, *J* = 8.0 Hz, 2 H), 7.54 - 7.39 (m, 3 H), 7.30 - 7.26 (m, 2 H), 7.26 - 7.21 (m, 1 H), 7.20 - 7.08 (m, 6 H), 7.07 - 6.88 (m, 6 H), 6.80 (d, *J* = 8.0 Hz, 2 H), 6.60 (d, *J* = 8.8 Hz, 1 H), 6.47 - 6.26 (m, 2 H), 5.88 (br. s., 1 H), 5.11 (br. s., 1 H), 4.37 (br. s., 1 H), 2.56 (br. s., 3 H), 2.34 (br. s., 3 H).

^{13}C NMR (**100 MHz**, **$CDCl_3$**) δ = 159.9, 143.4, 142.6, 137.4, 137.2, 136.3, 132.2, 130.1, 129.1, 128.8, 128.7, 128.6, 128.4, 128.3, 128.1, 128.0, 127.9, 126.4, 125.3, 122.8, 122.3, 118.2, 118.2, 116.1, 116.0, 110.7, 62.5, 49.0, 21.5.

HRMS (ESI) calcd for $C_{24}H_{18}NO$ $[M+H]^+$ 336.1383, found 336.1377.

3.9 ORTEP Diagram

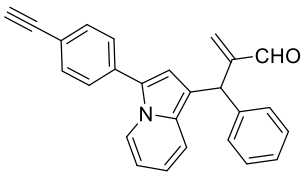 **3k** CCDC No. 1506109	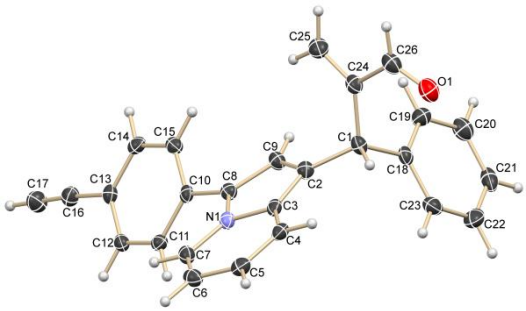

3.10 2D NMR Experiments

2D NMR Experiments for 1s

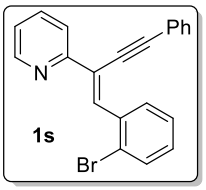

400 MHz, $CDCl_3$

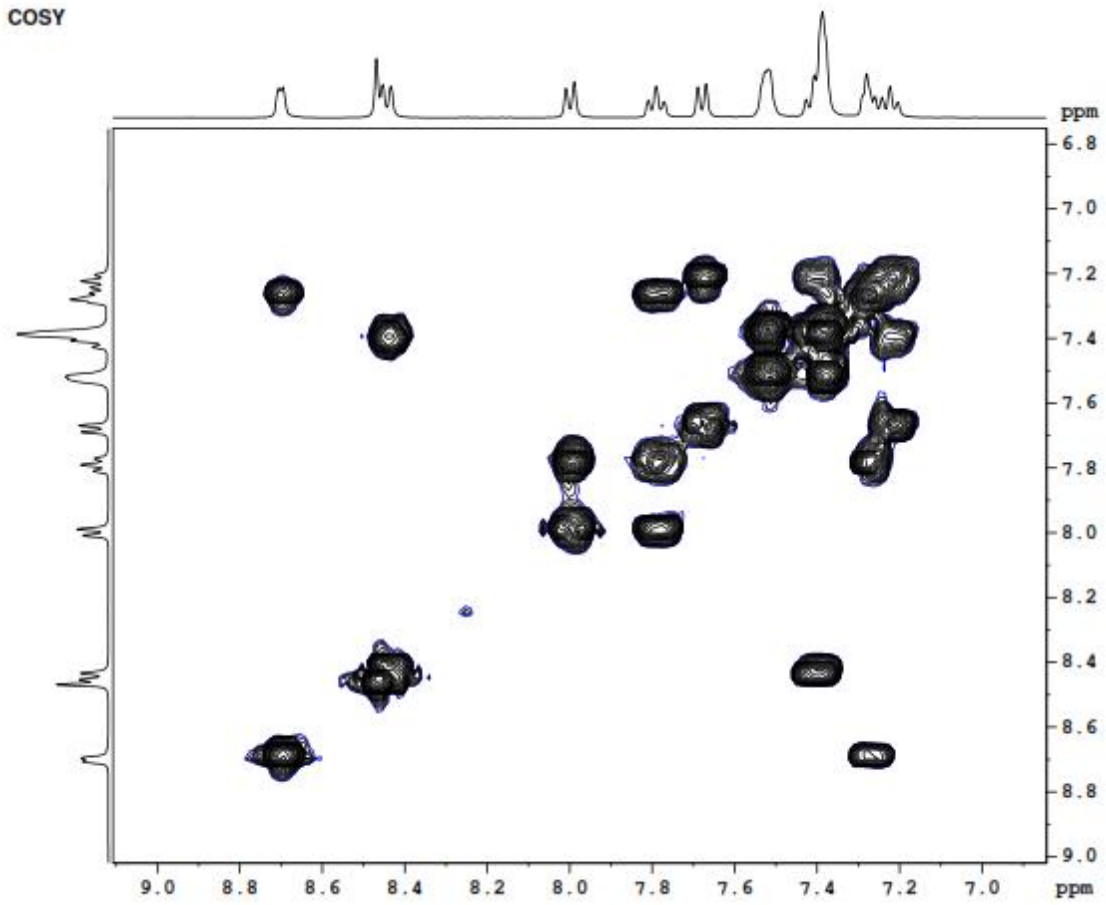

Determination of geometry of double bond in 1s: NOESY Correlations

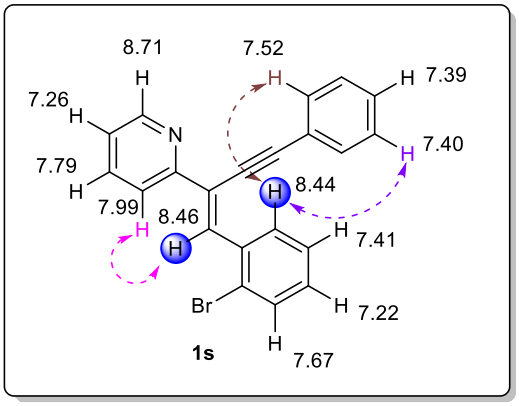

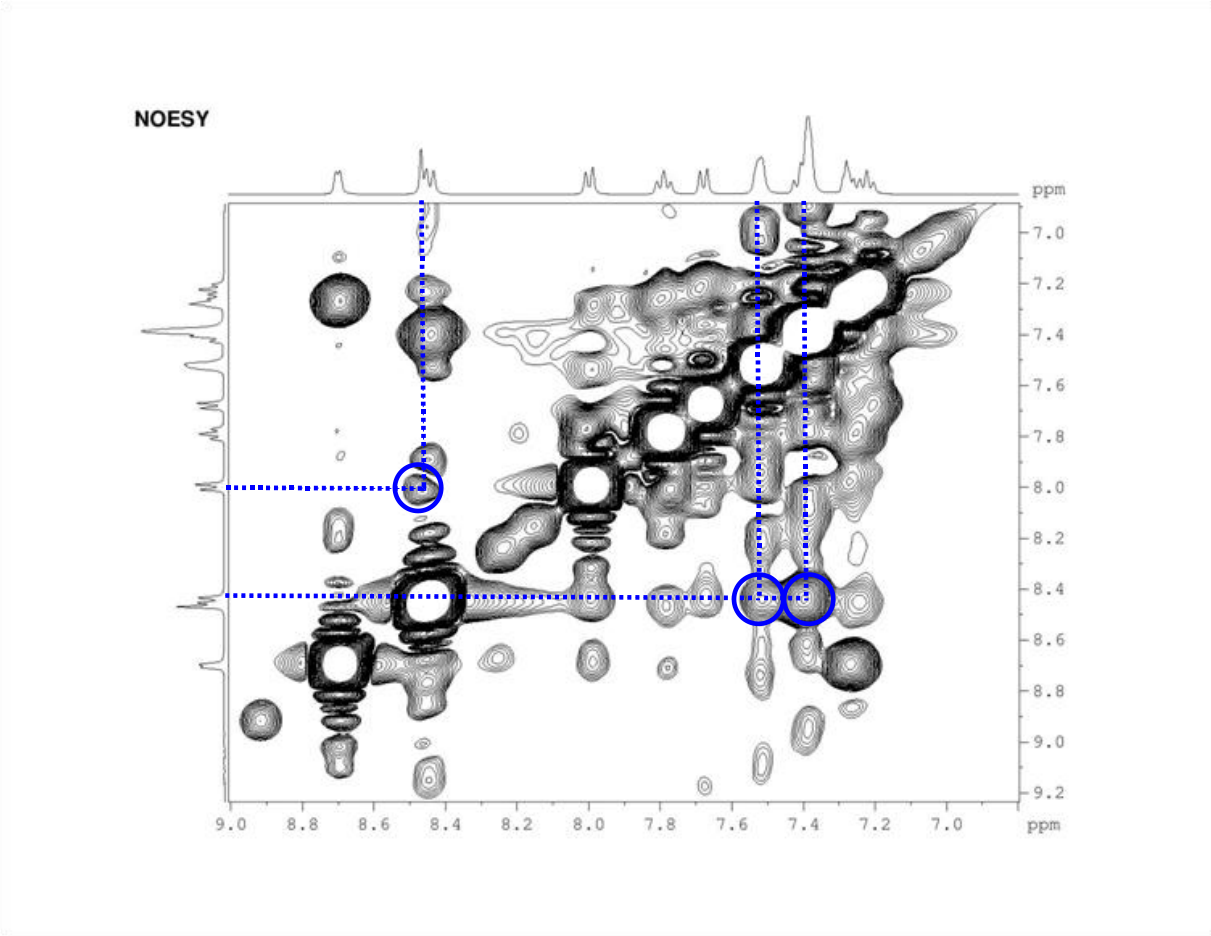

HSQC

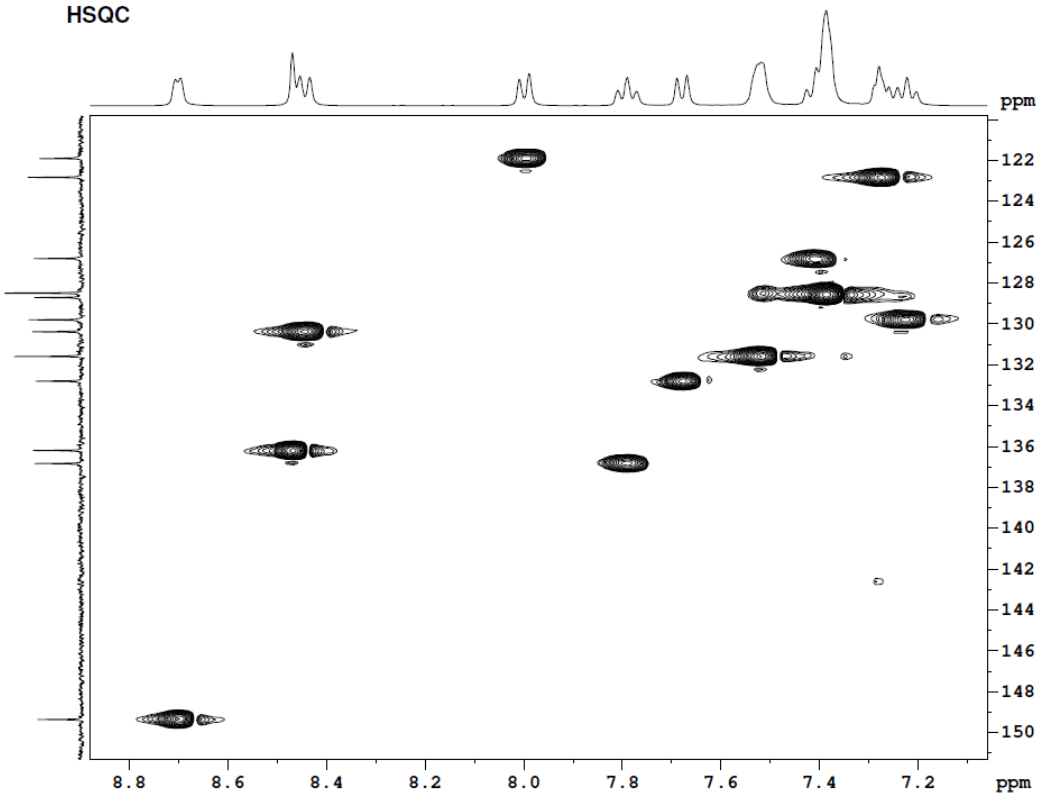
ppm
122
124
126
128
130
132
134
136
138
140
142
144
146
148
150
8.8
8.6
8.4
8.2
8.0
7.8
7.6
7.4
7.2
ppm

HMBC

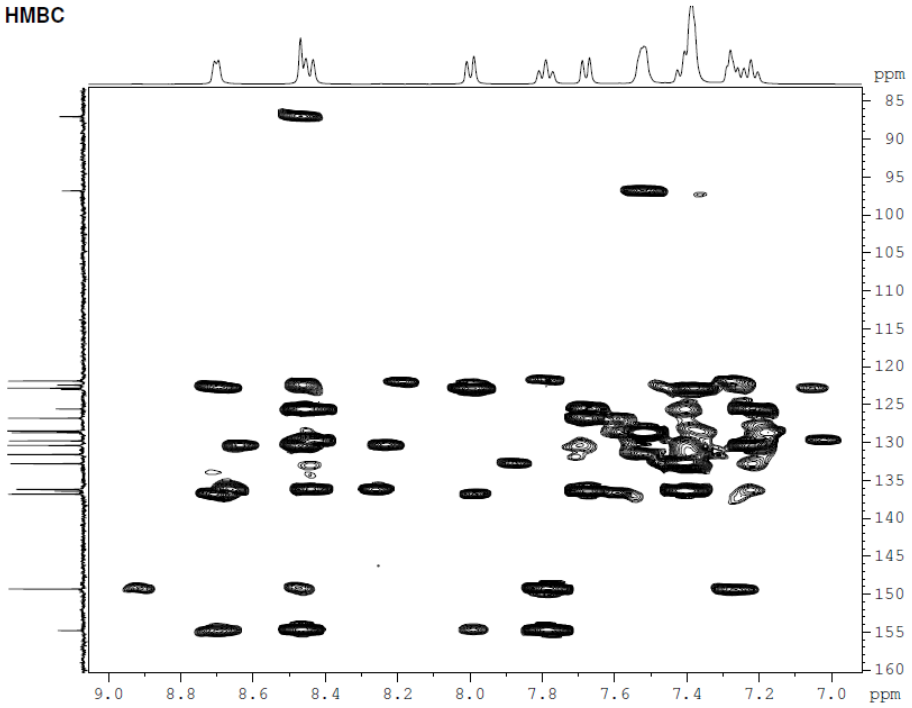
ppm
85
90
95
100
105
110
115
120
125
130
135
140
145
150
155
160
9.0
8.8
8.6
8.4
8.2
8.0
7.8
7.6
7.4
7.2
7.0
ppm

2D NMR Experiments for 3k

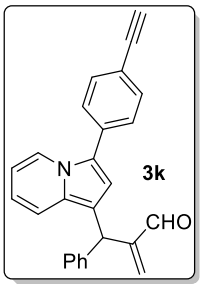

400 MHz, $CDCl_3$

COSY

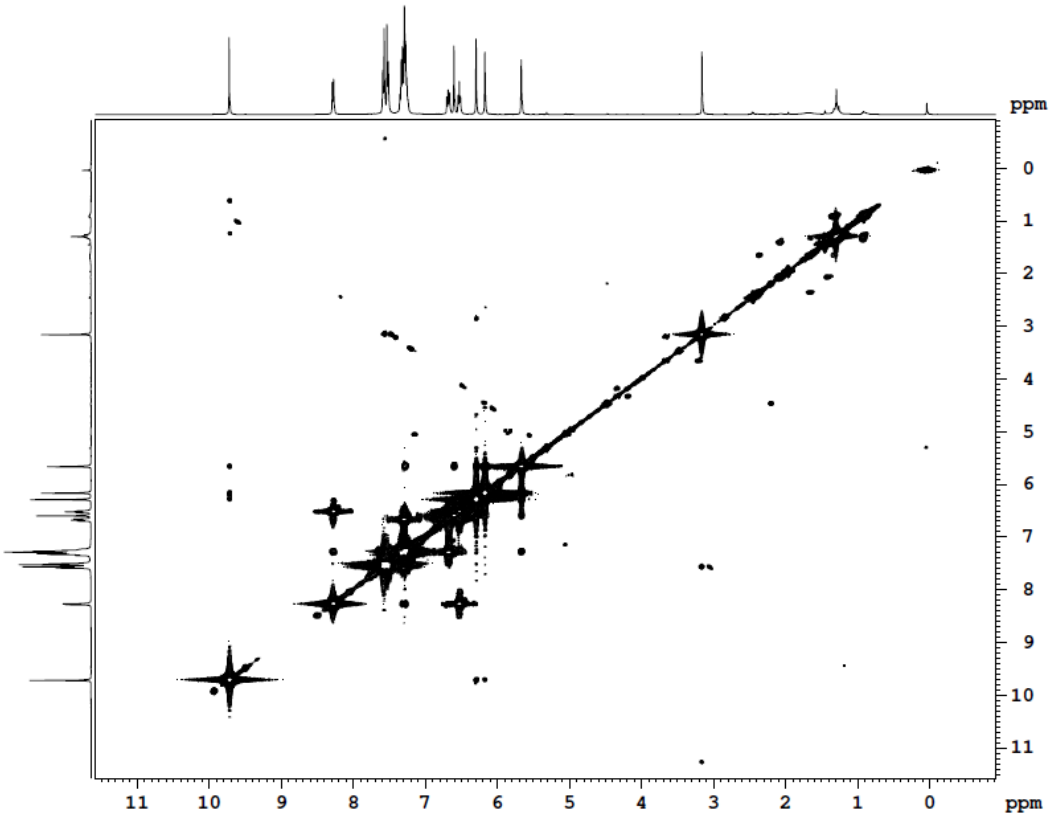

NOESY

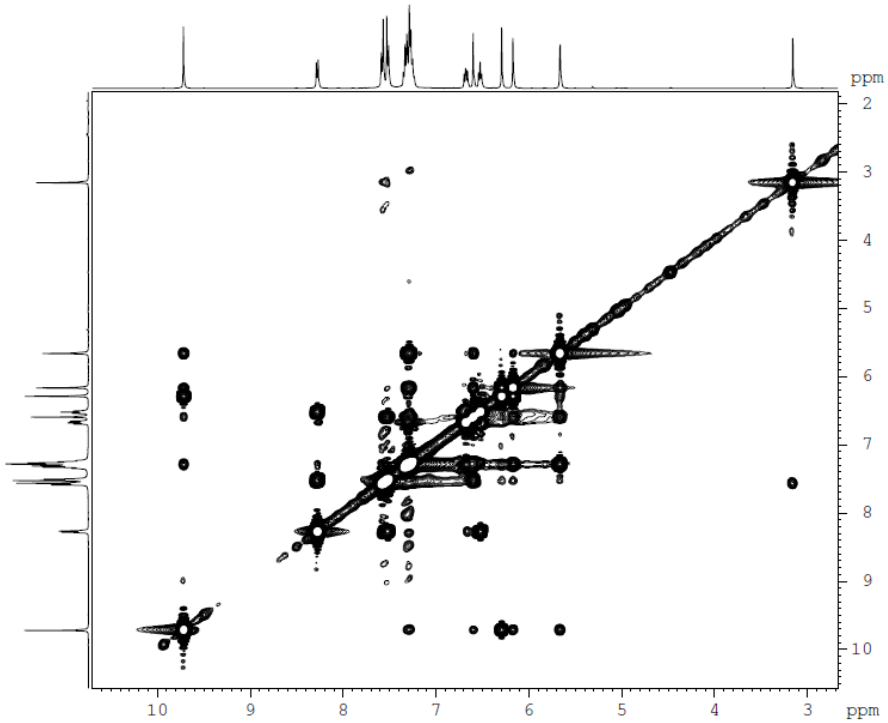
ppm
2
3
4
5
6
7
8
9
10
10
9
8
7
6
5
4
3
ppm

HSQC

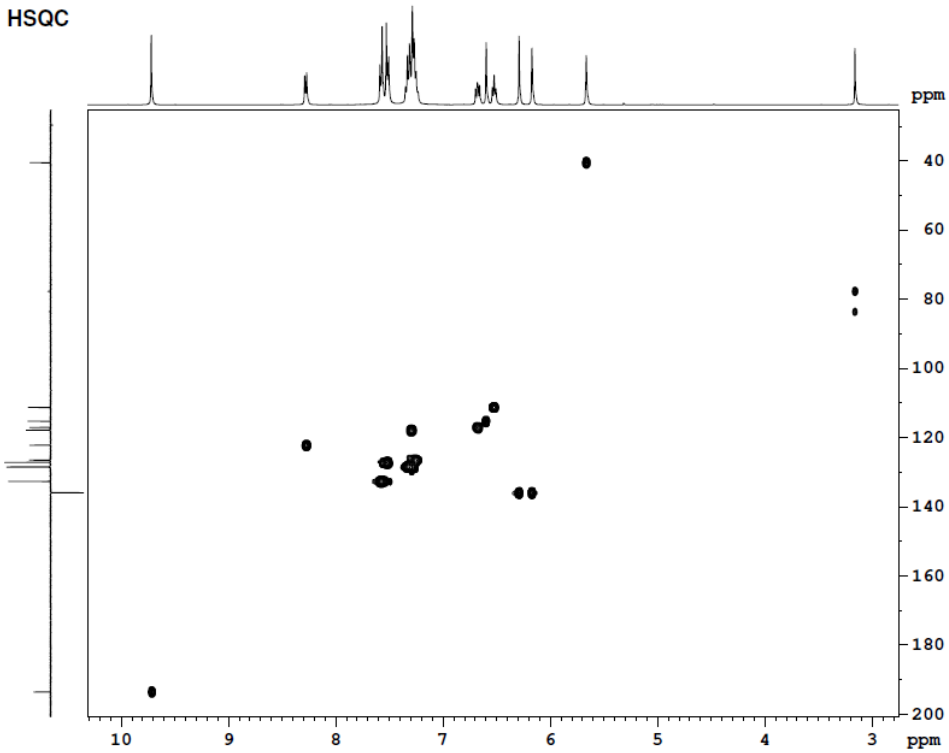
ppm
40
60
80
100
120
140
160
180
200
10
9
8
7
6
5
4
3
ppm

Correlations of 3k by HMBC spectrum

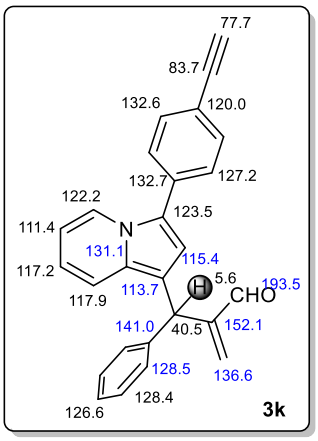

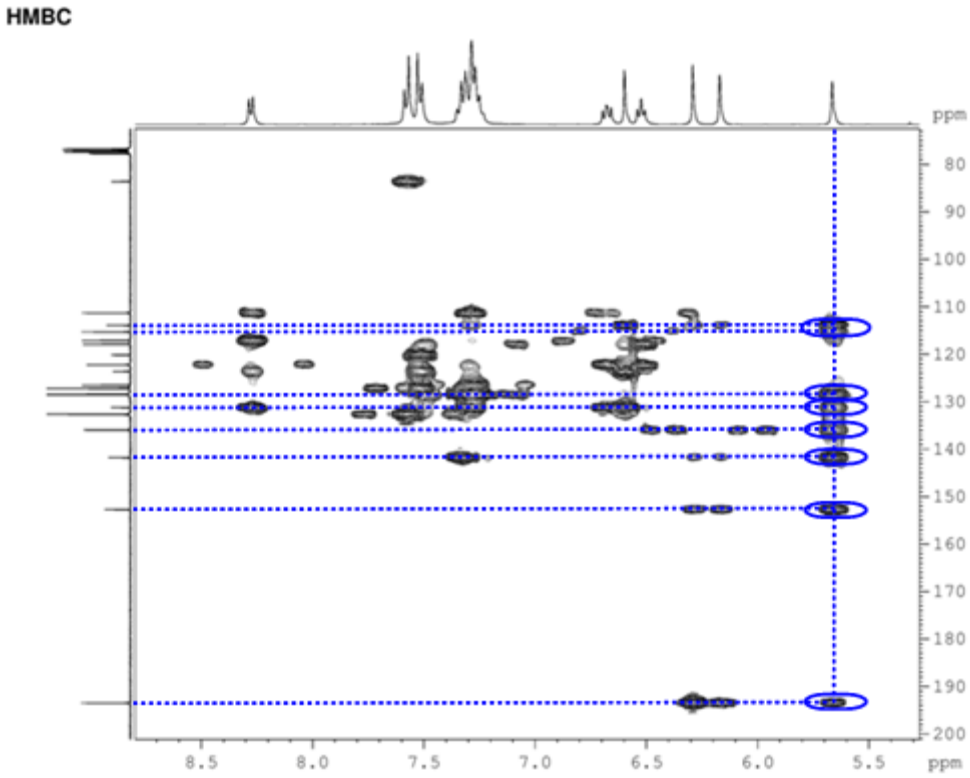

2D NMR Experiments for 3x

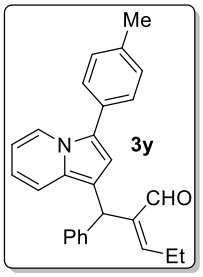

400 MHz, $CDCl_3$

COSY

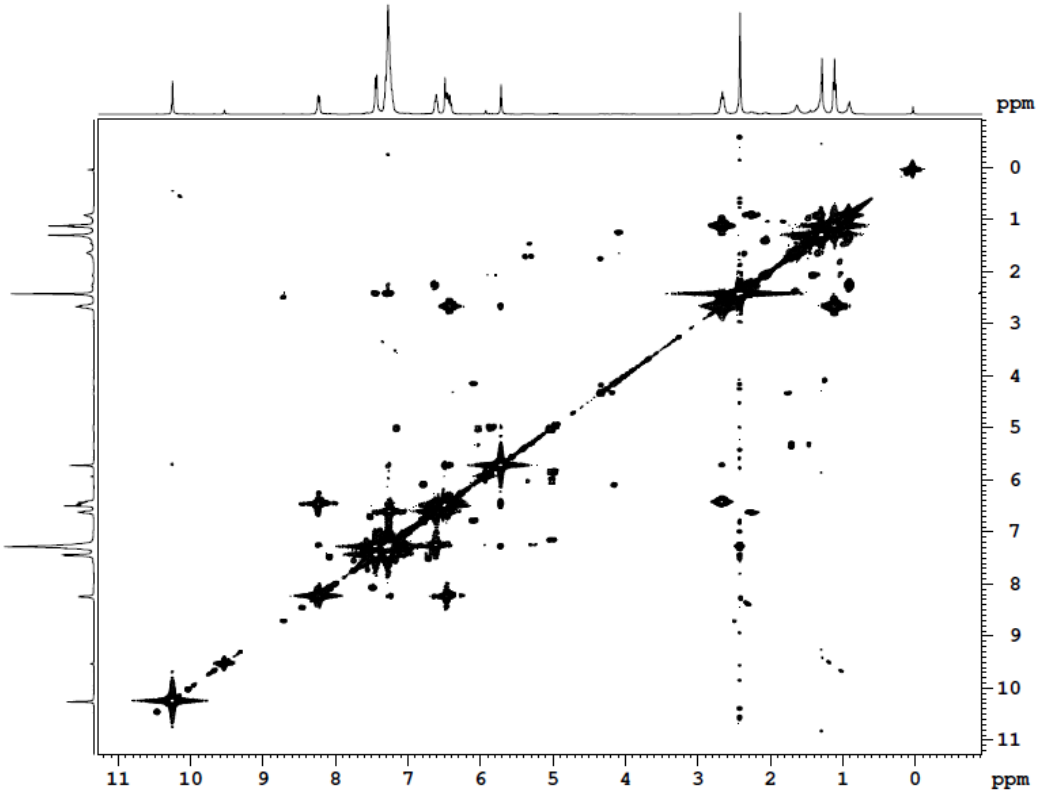

Correlations of 3y by NOESY spectrum

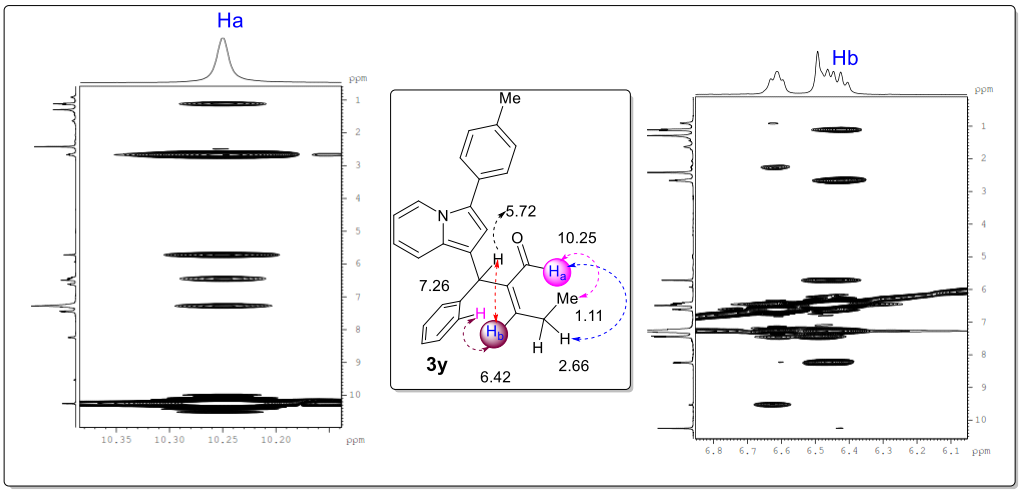

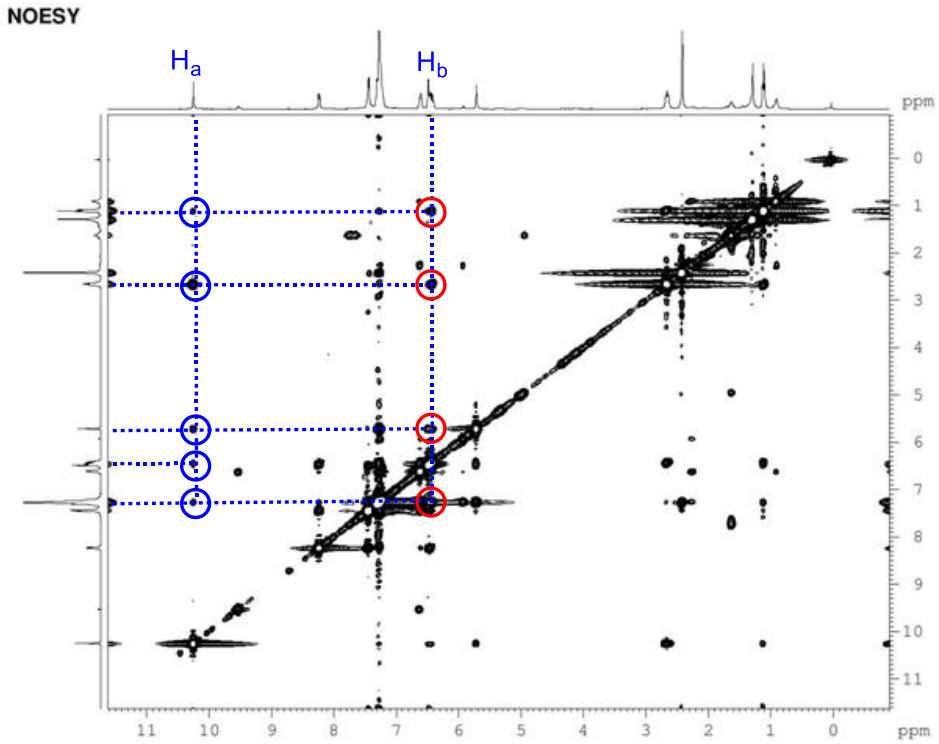

HMBC

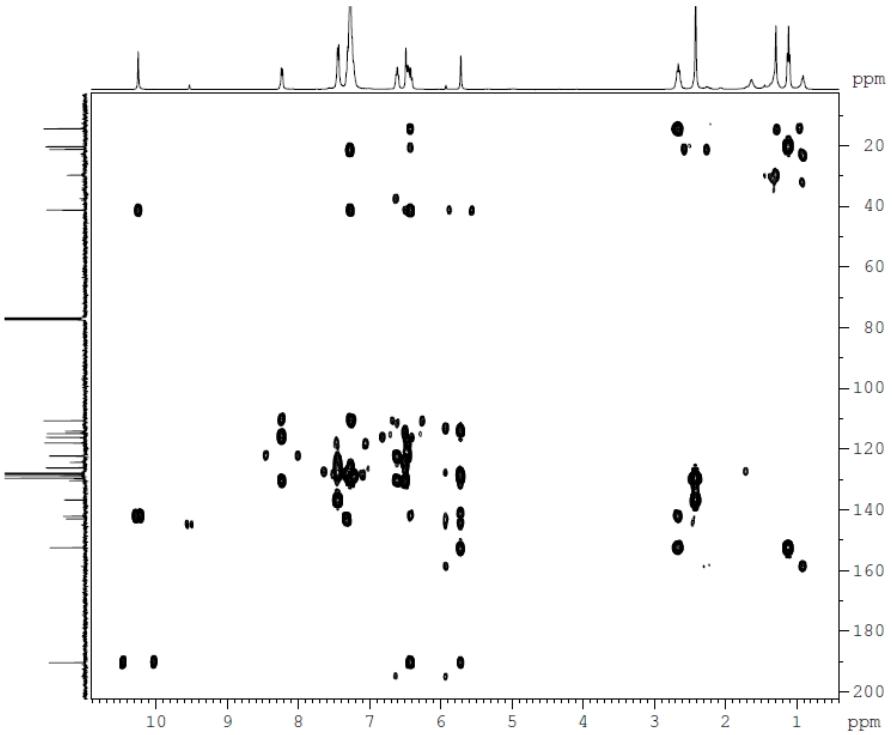
ppm
20
40
60
80
100
120
140
160
180
200
10
9
8
7
6
5
4
3
2
1
ppm

HSQC

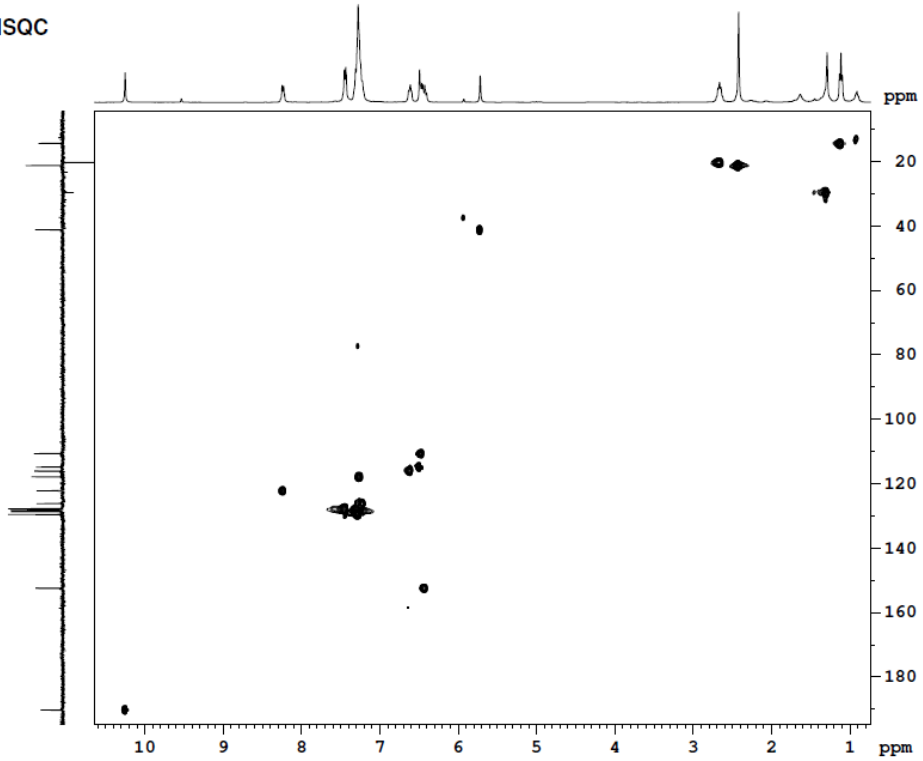
ppm
20
40
60
80
100
120
140
160
180
10
9
8
7
6
5
4
3
2
1
ppm

3.11 NMR Spectra of Selected Compounds

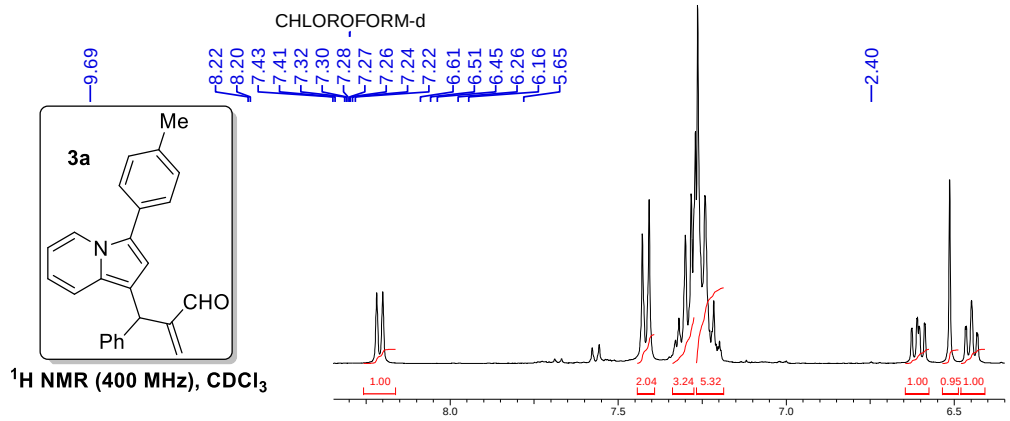

^{1}H NMR (400 MHz), $CDCl_3$

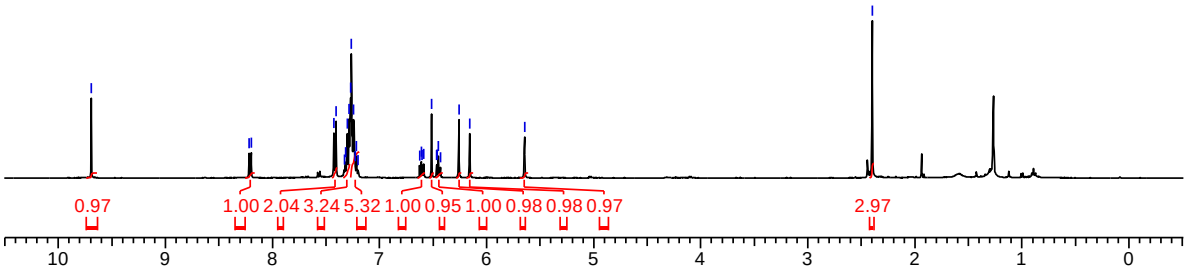

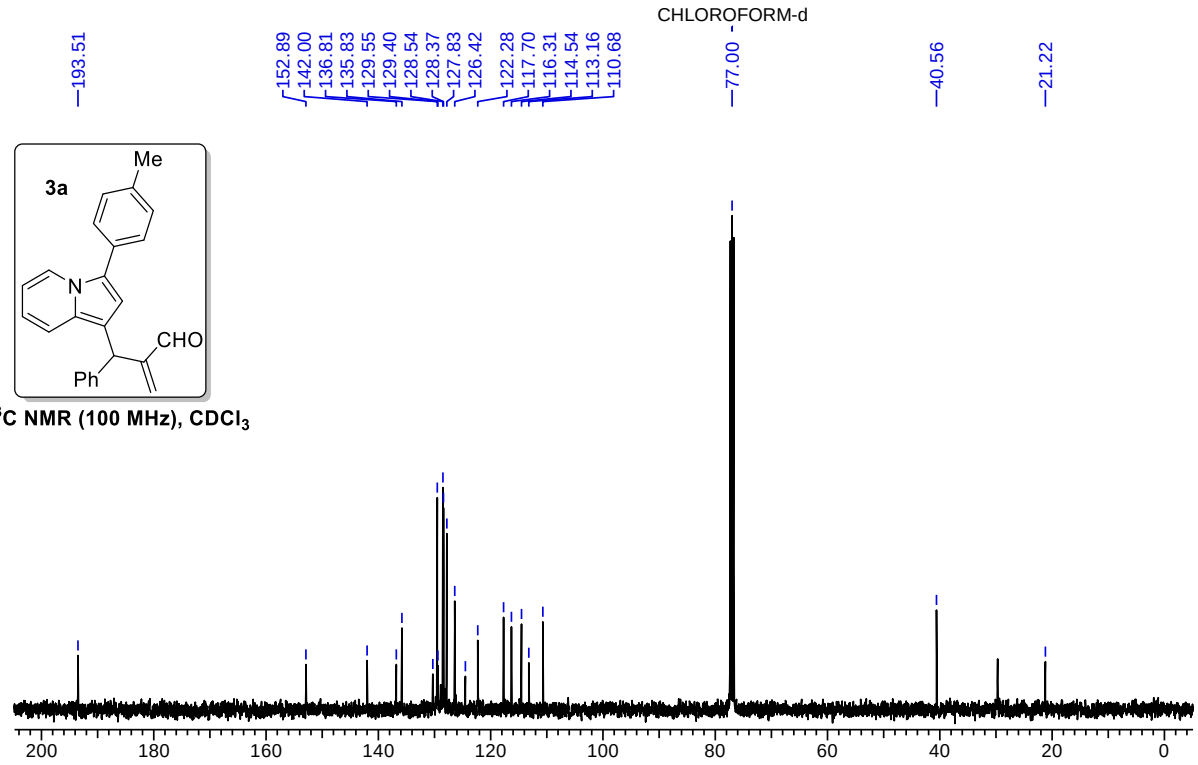

^{13}C NMR (100 MHz), $CDCl_3$

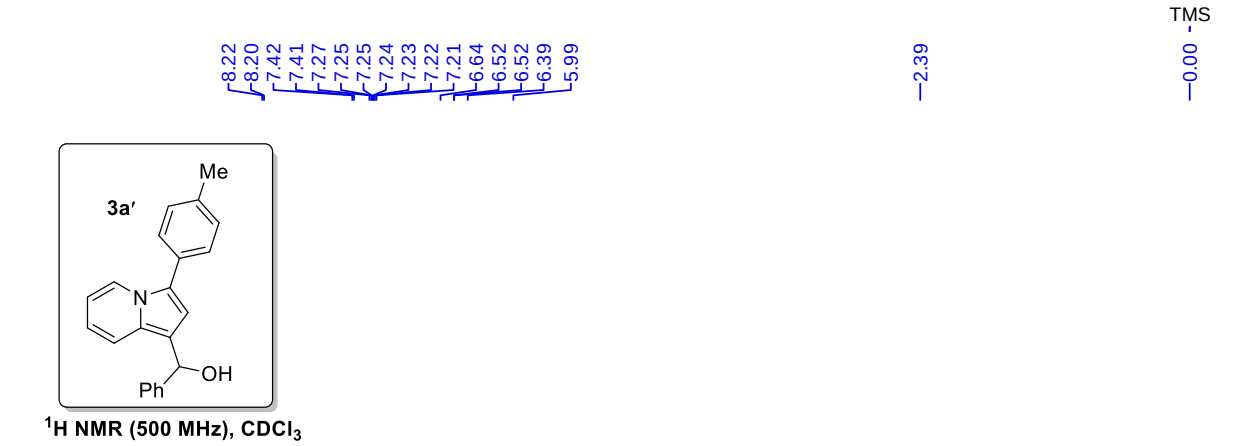

^{1}H NMR (500 MHz), $CDCl_3$

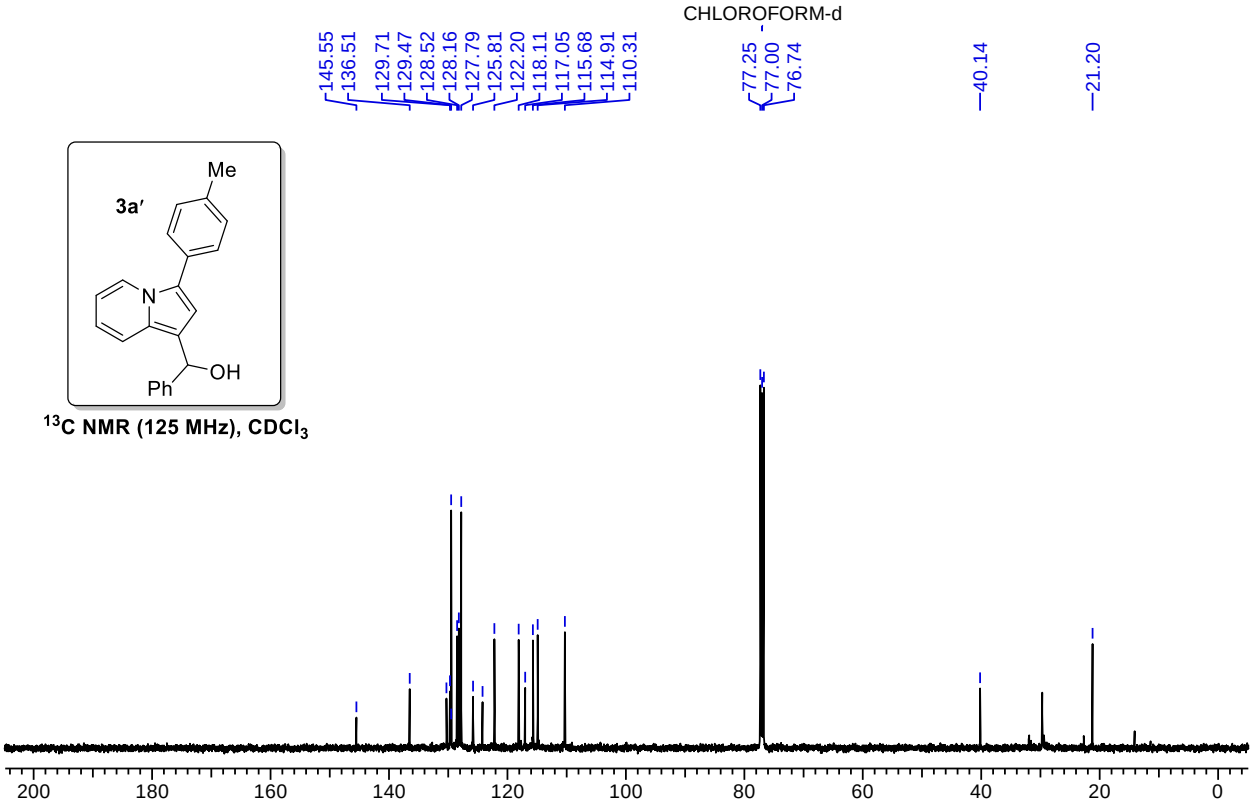

^{13}C NMR (125 MHz), $CDCl_3$

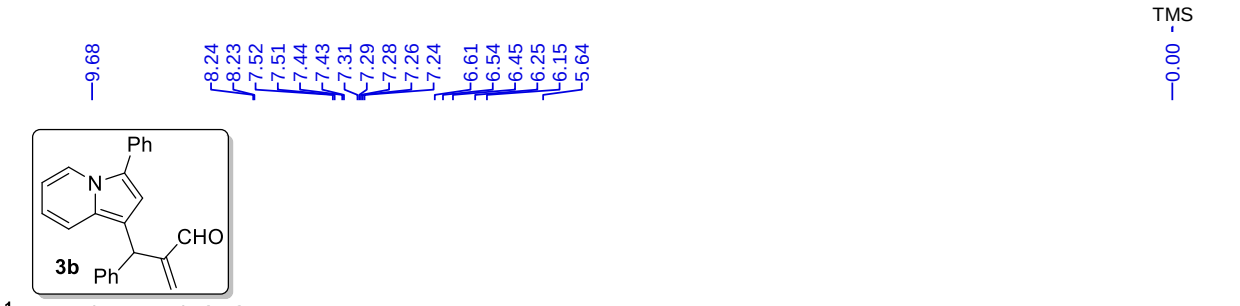

^{1}H NMR (500 MHz), $CDCl_3$

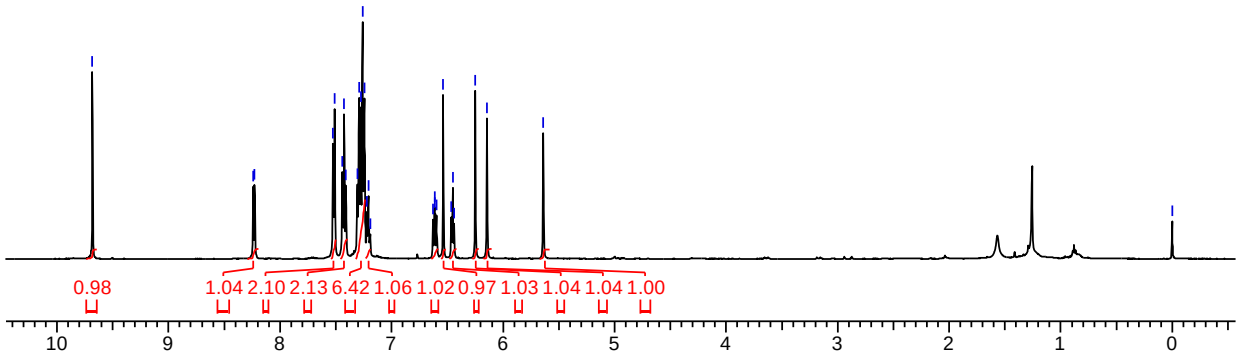

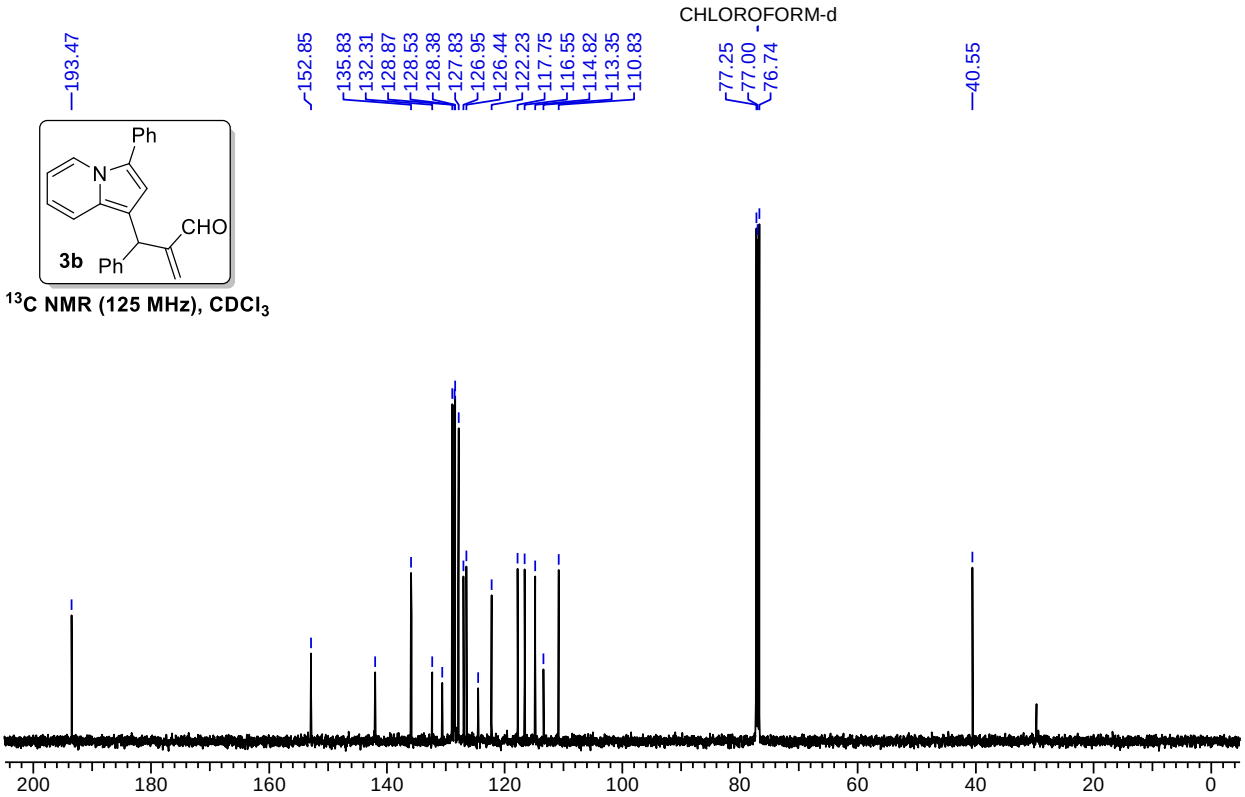

^{13}C NMR (125 MHz), $CDCl_3$

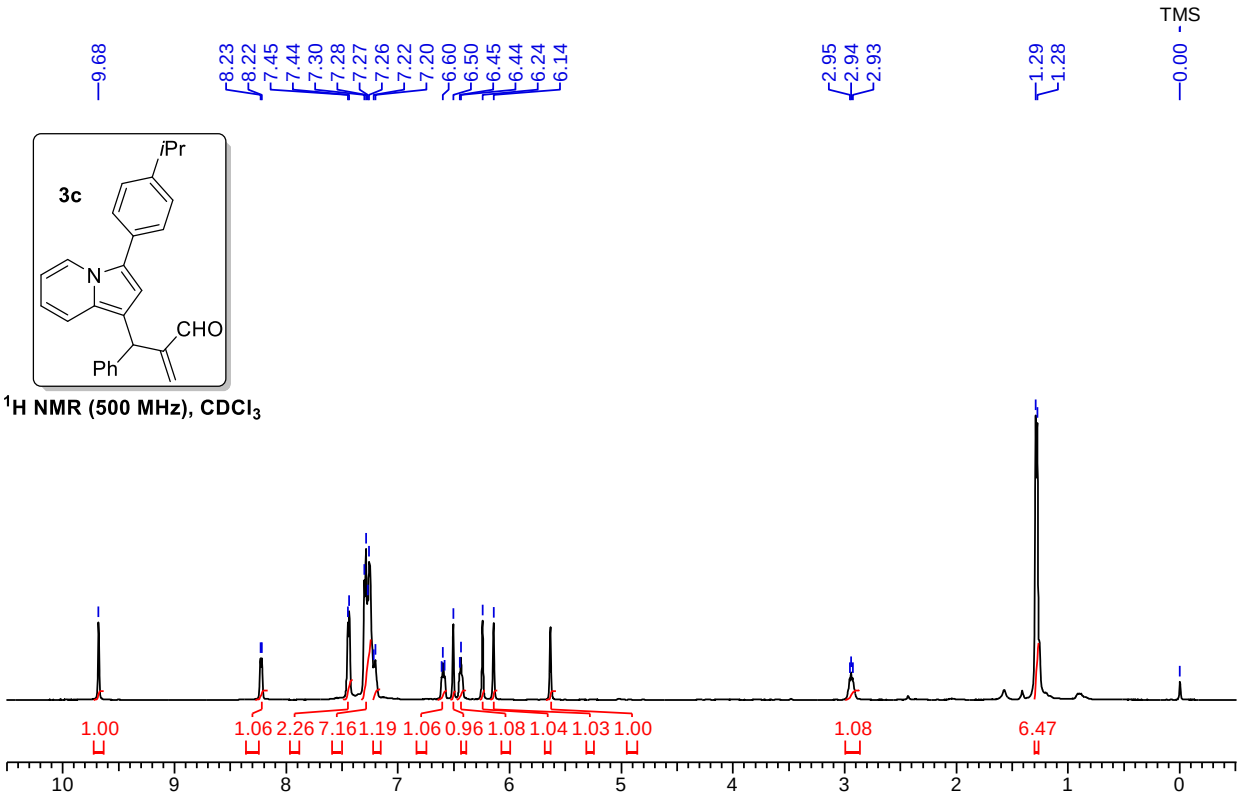

^{1}H NMR (500 MHz), $CDCl_3$

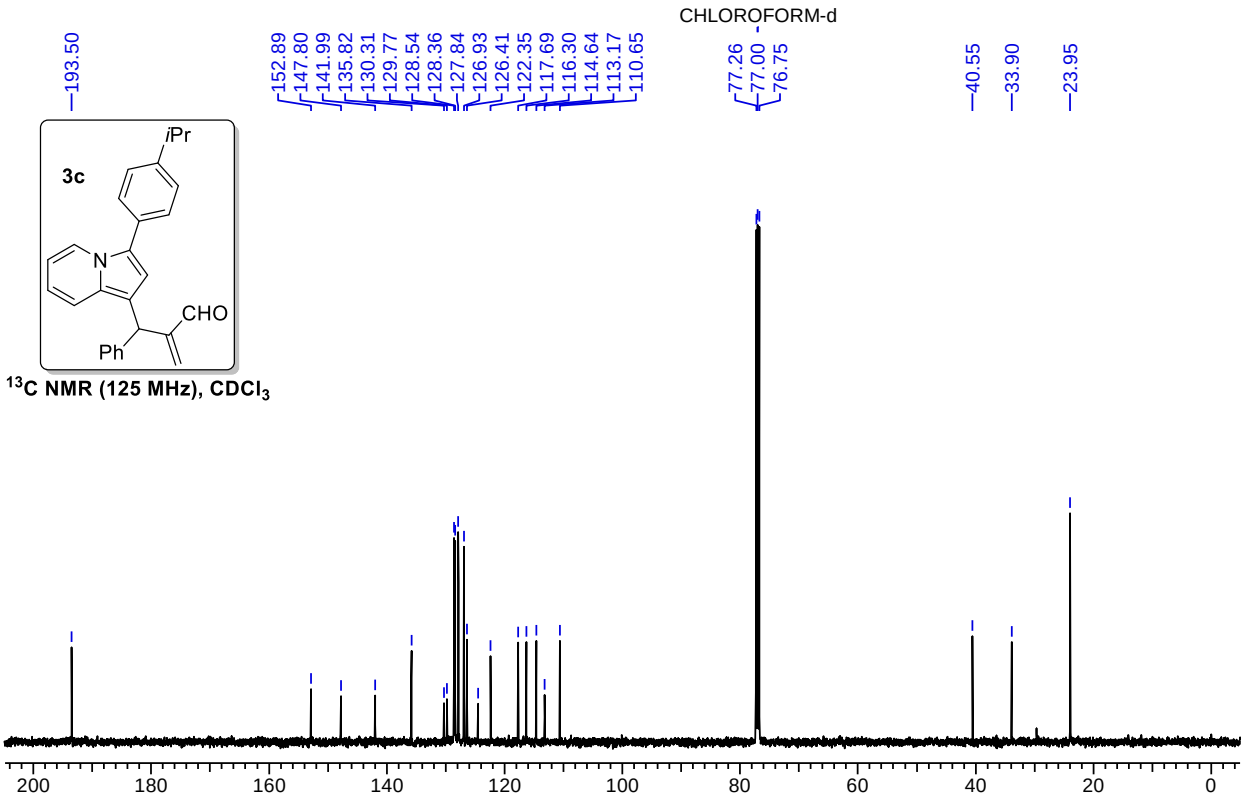

^{13}C NMR (125 MHz), $CDCl_3$

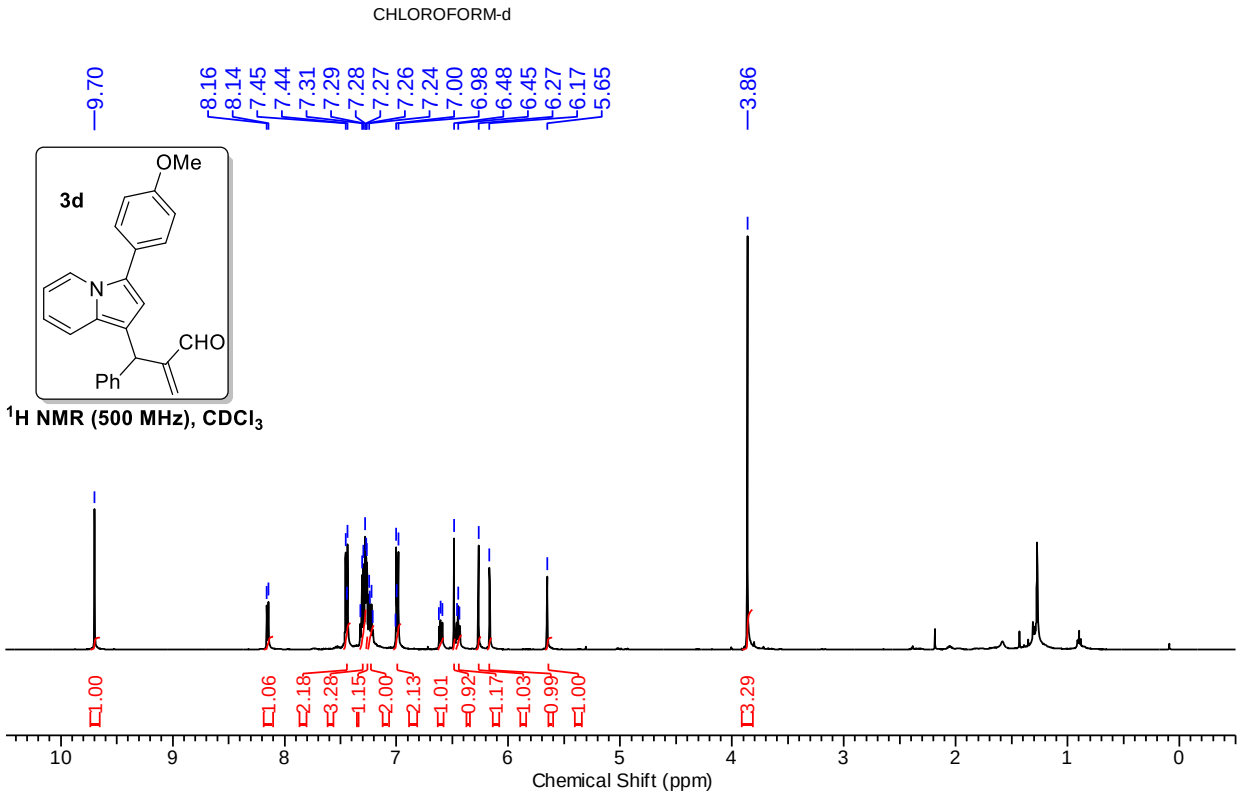

^{1}H NMR (500 MHz), $CDCl_3$

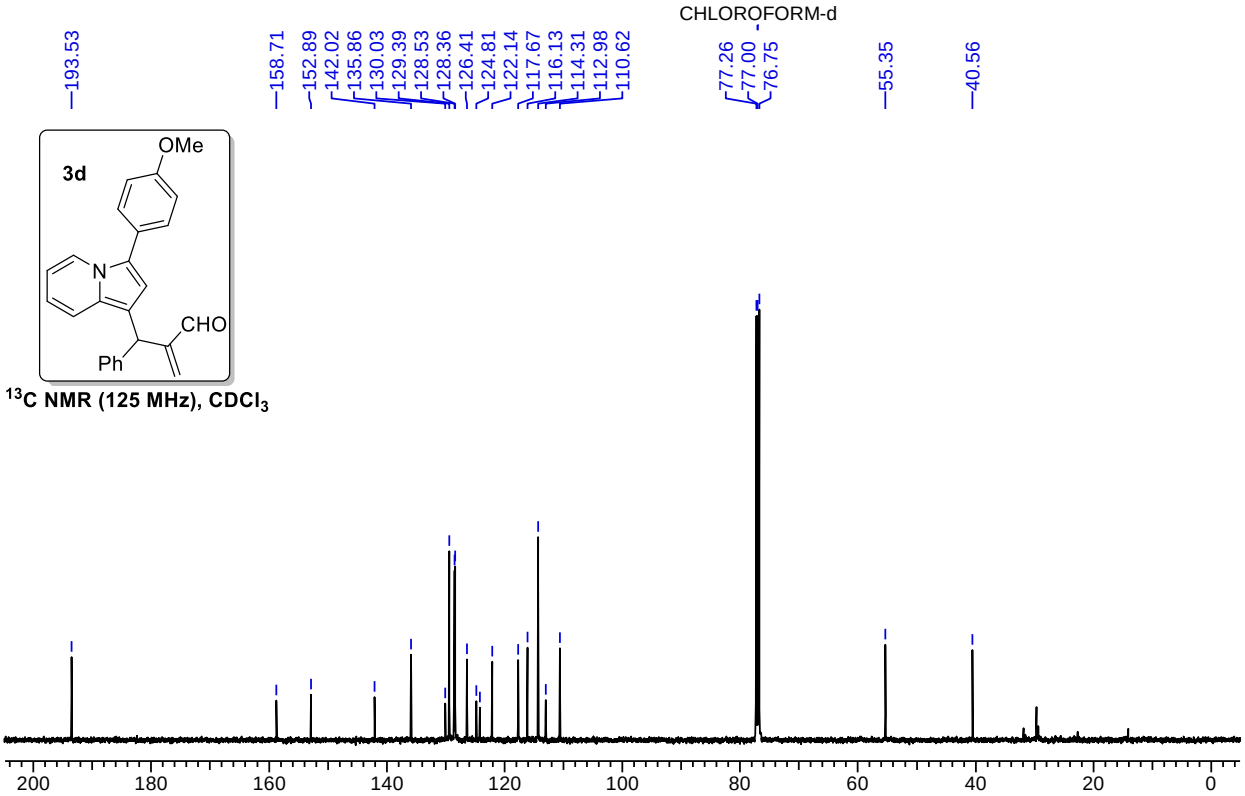

^{13}C NMR (125 MHz), $CDCl_3$

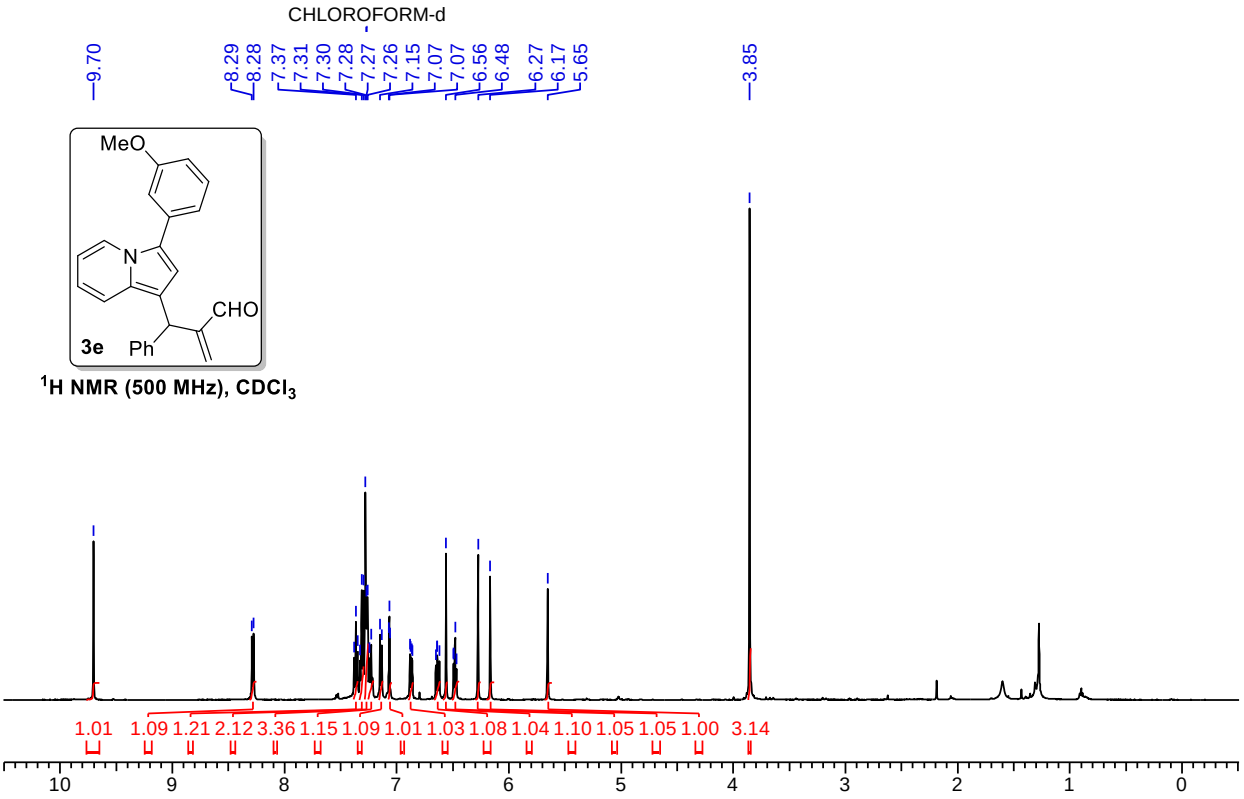

^{1}H NMR (500 MHz), $CDCl_3$

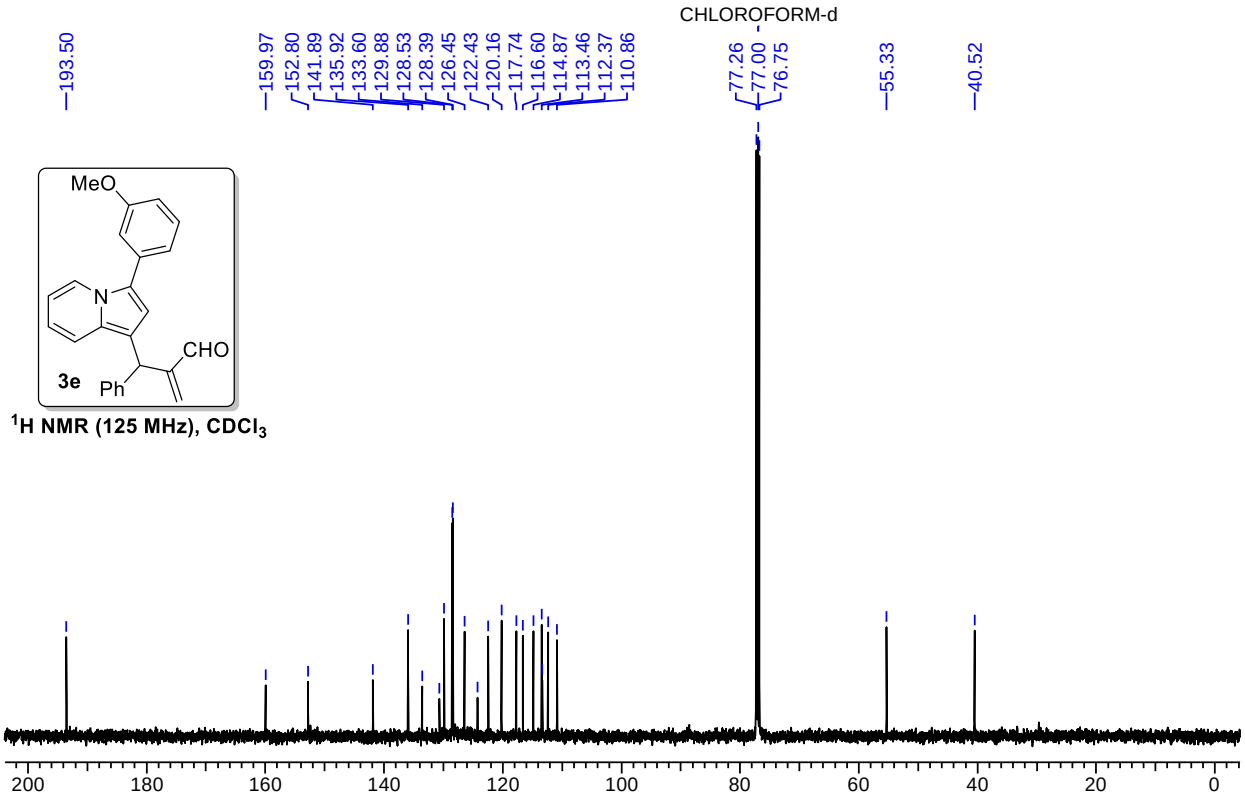

^{1}H NMR (125 MHz), $CDCl_3$

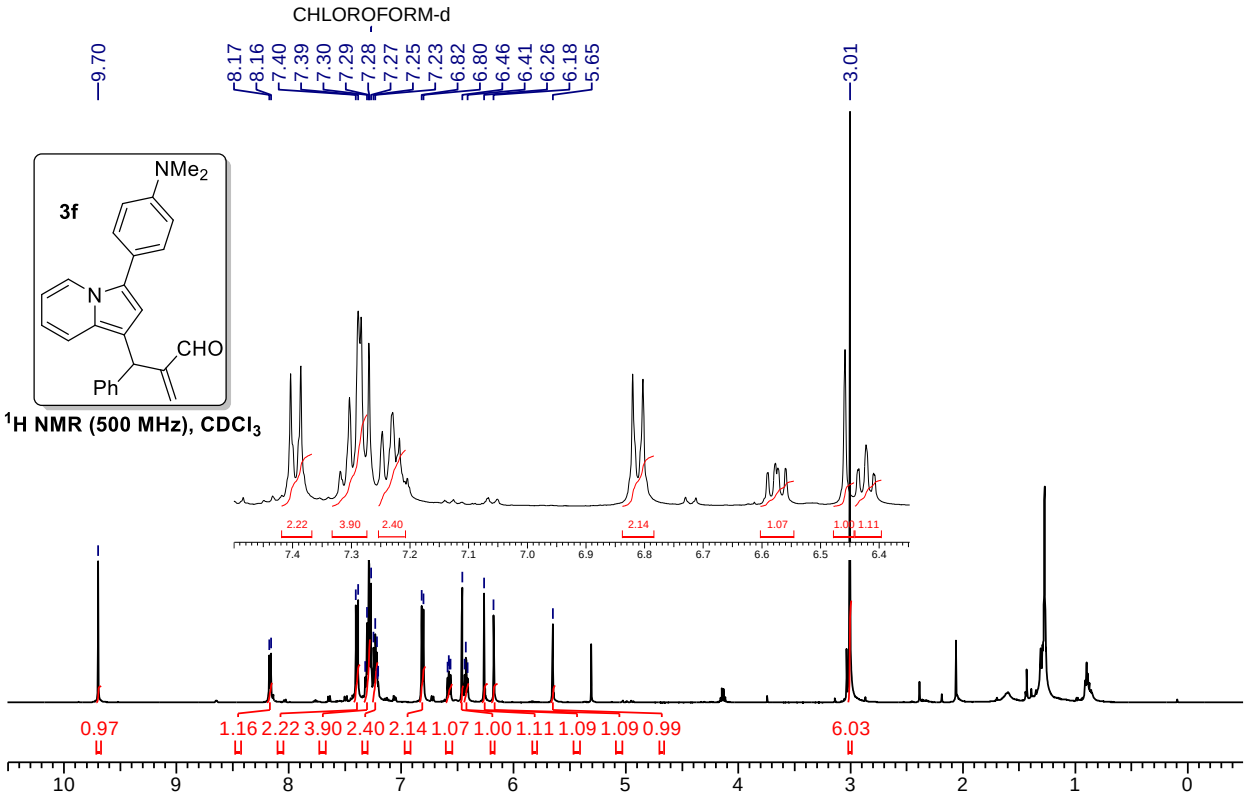

^{1}H NMR (500 MHz), $CDCl_3$

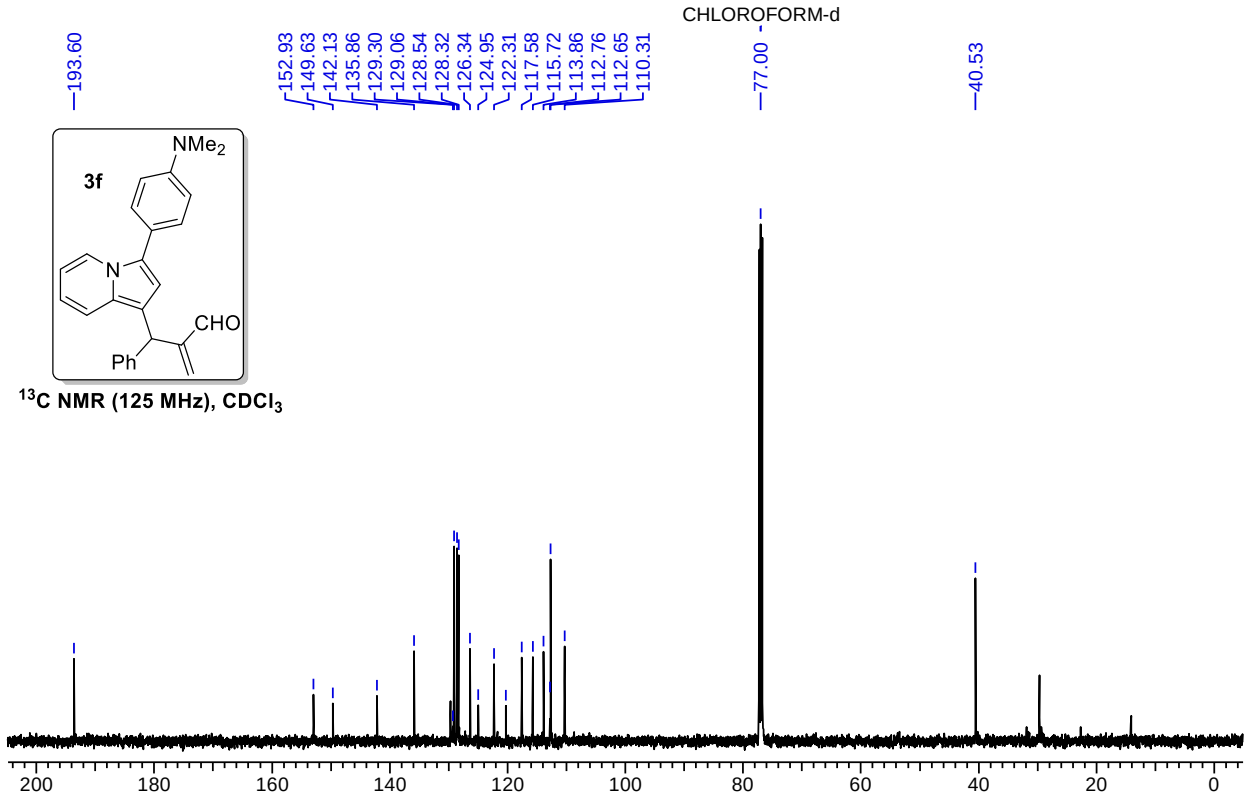

^{13}C NMR (125 MHz), $CDCl_3$

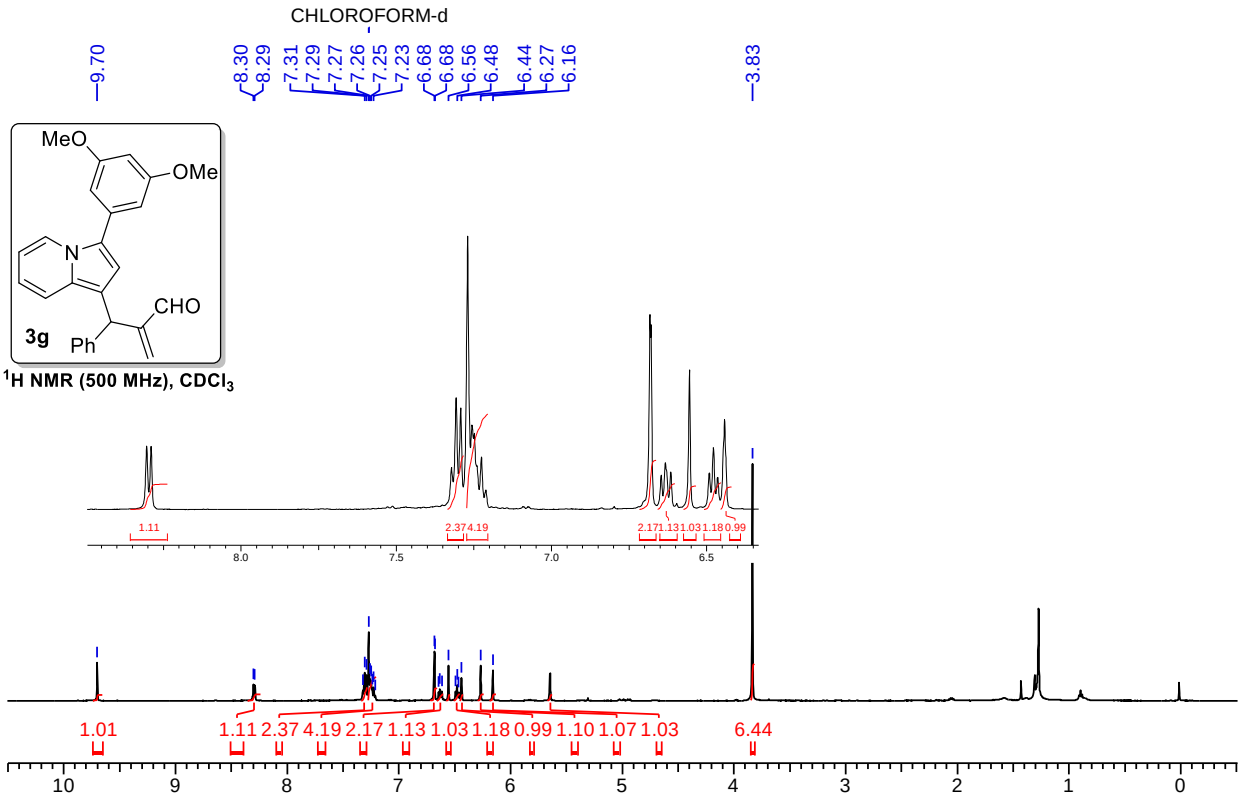

^{1}H NMR (500 MHz), $CDCl_3$

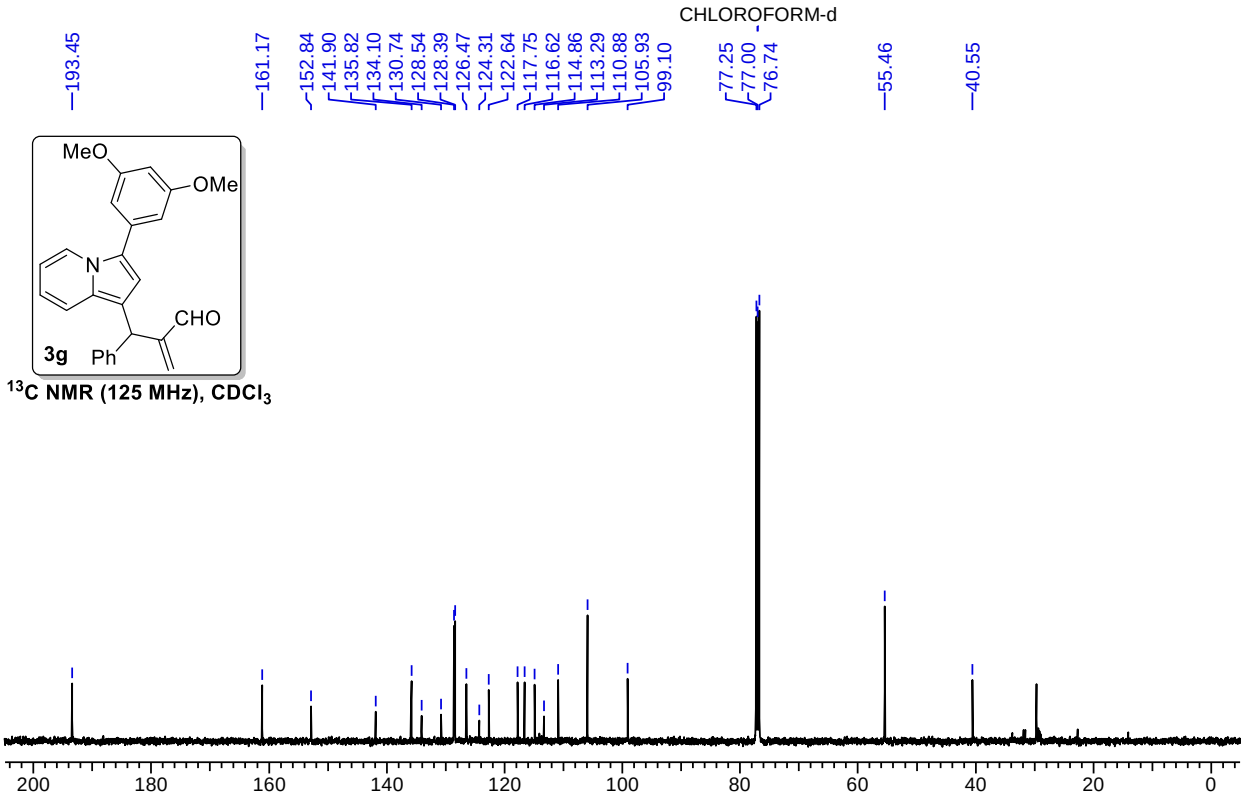

^{13}C NMR (125 MHz), $CDCl_3$

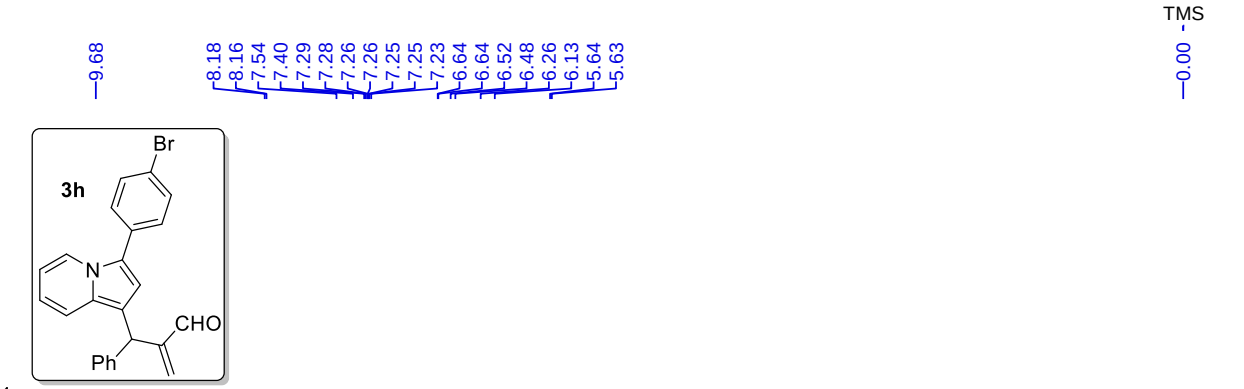

^{1}H NMR (500 MHz), $CDCl_3$

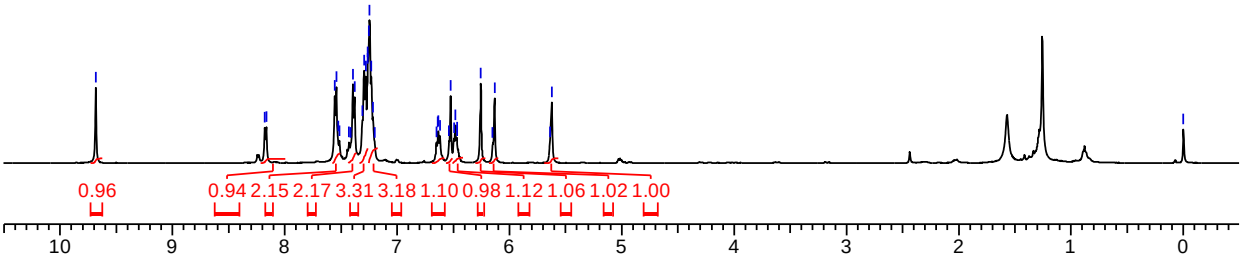

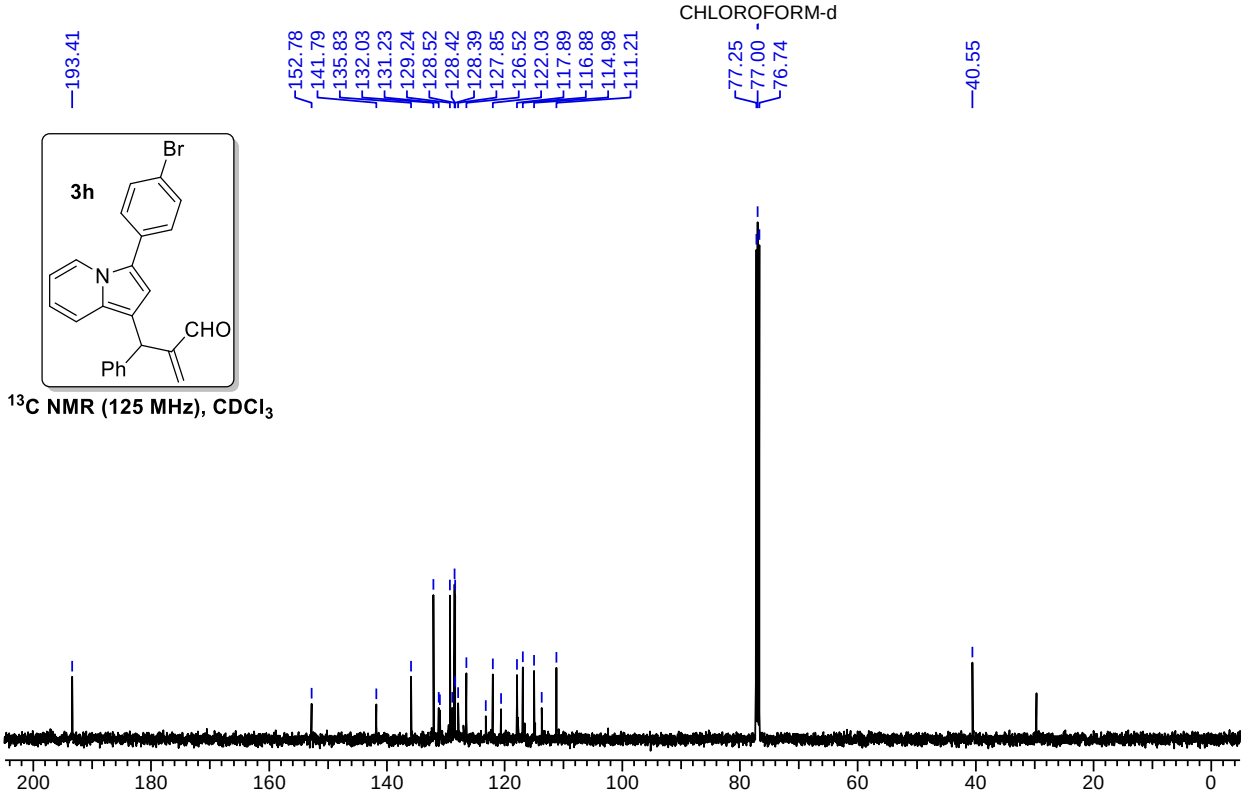

^{13}C NMR (125 MHz), $CDCl_3$

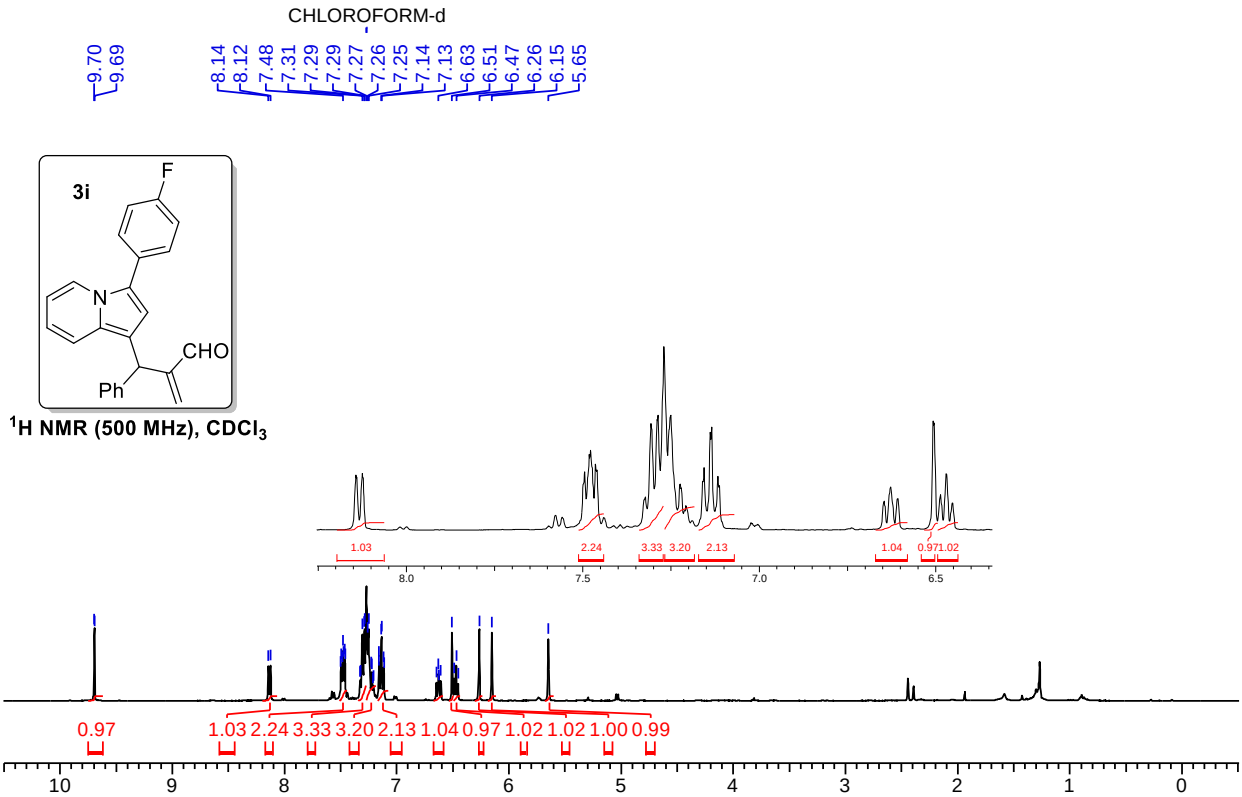

^{1}H NMR (500 MHz), $CDCl_3$

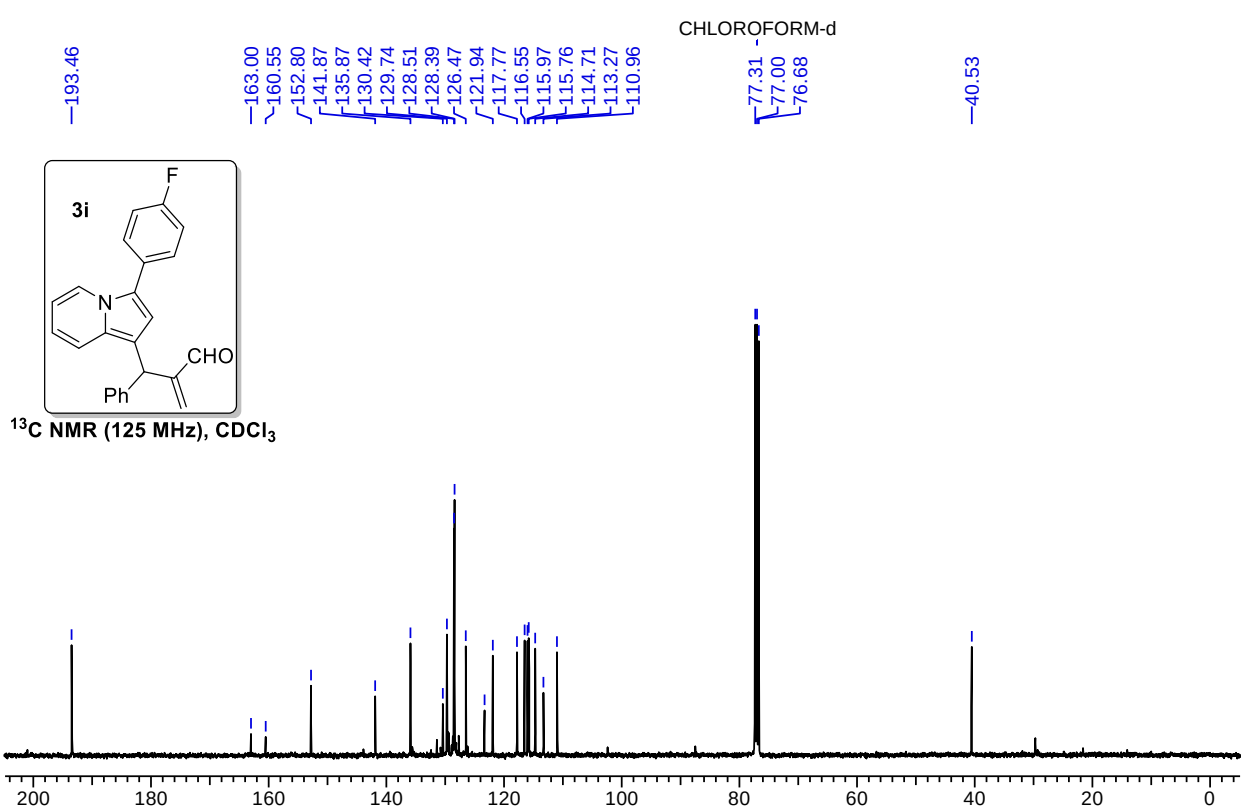

^{13}C NMR (125 MHz), $CDCl_3$

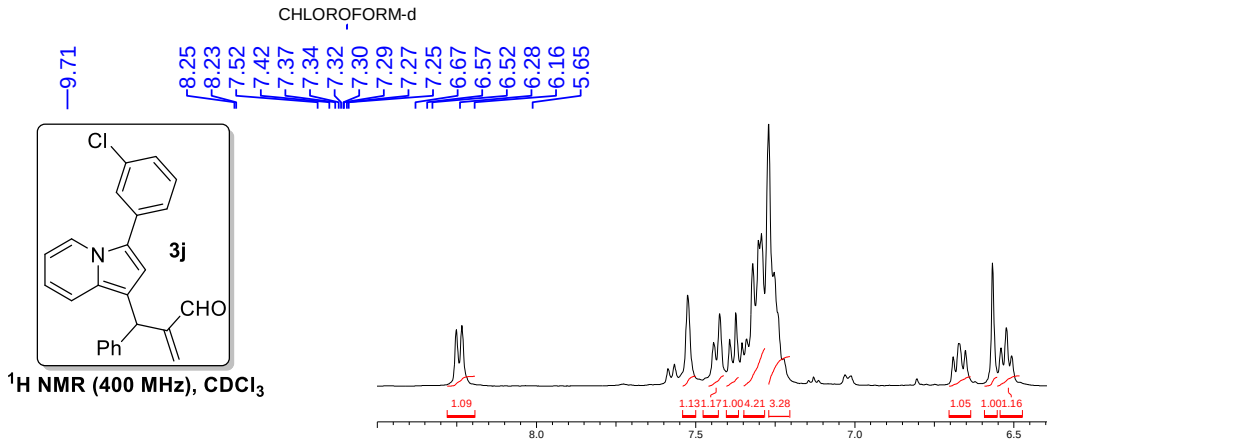

^{1}H NMR (400 MHz), $CDCl_3$

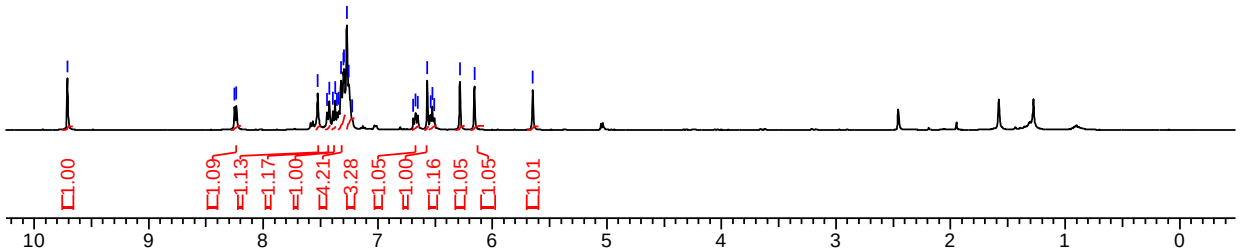

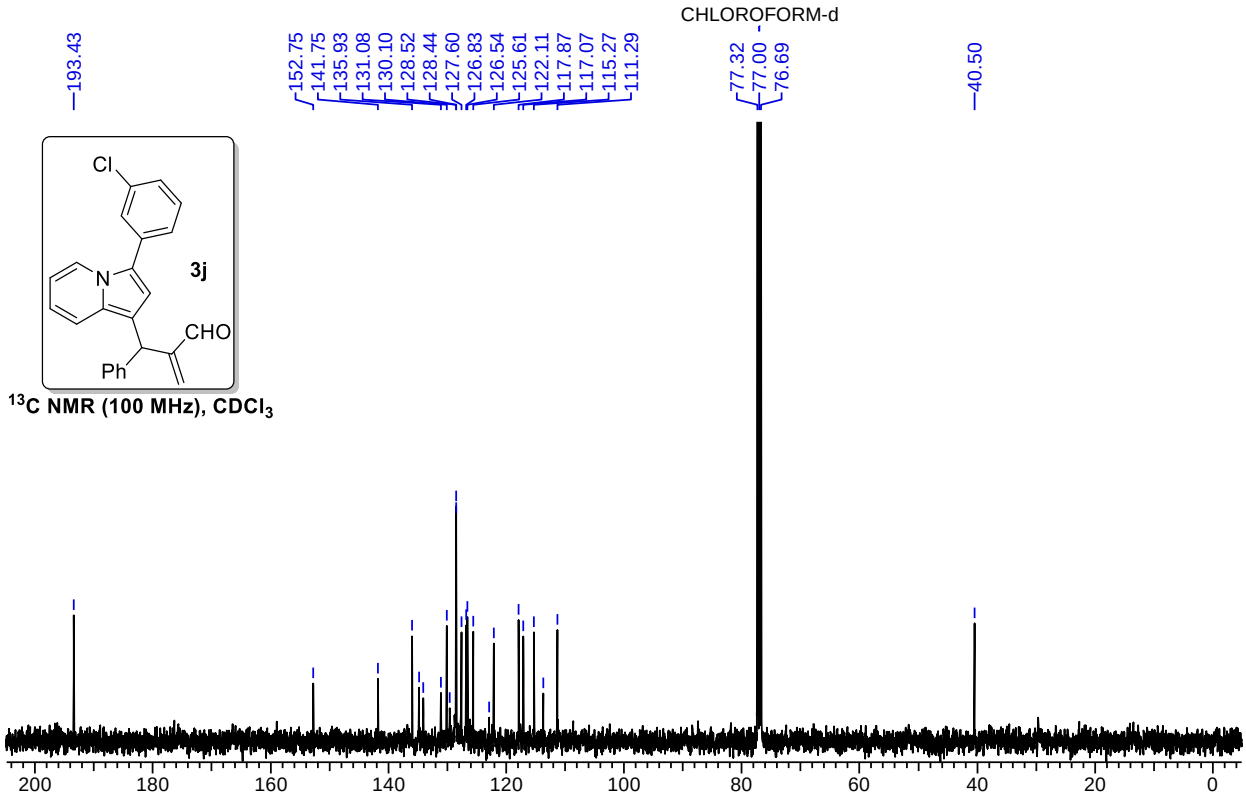

^{13}C NMR (100 MHz), $CDCl_3$

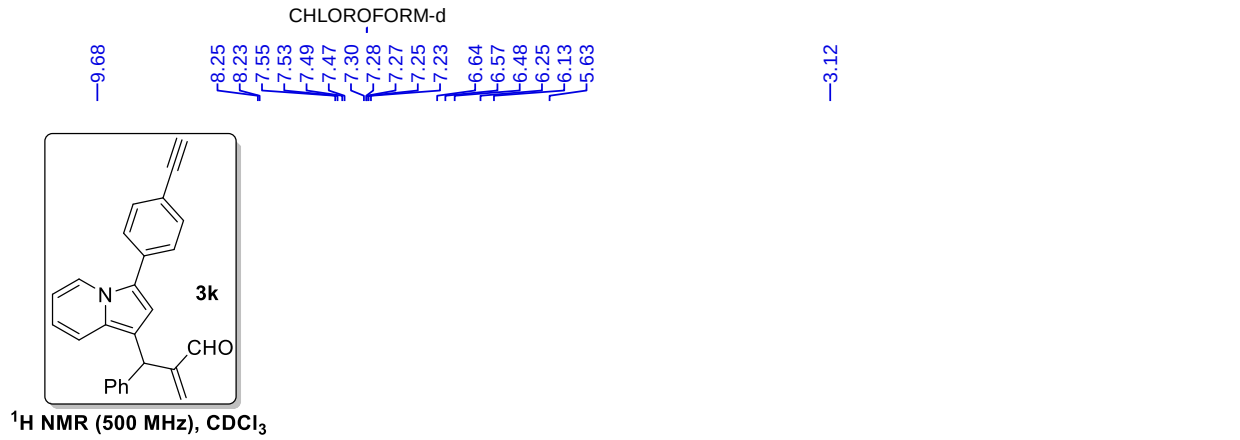

^{1}H NMR (500 MHz), $CDCl_3$

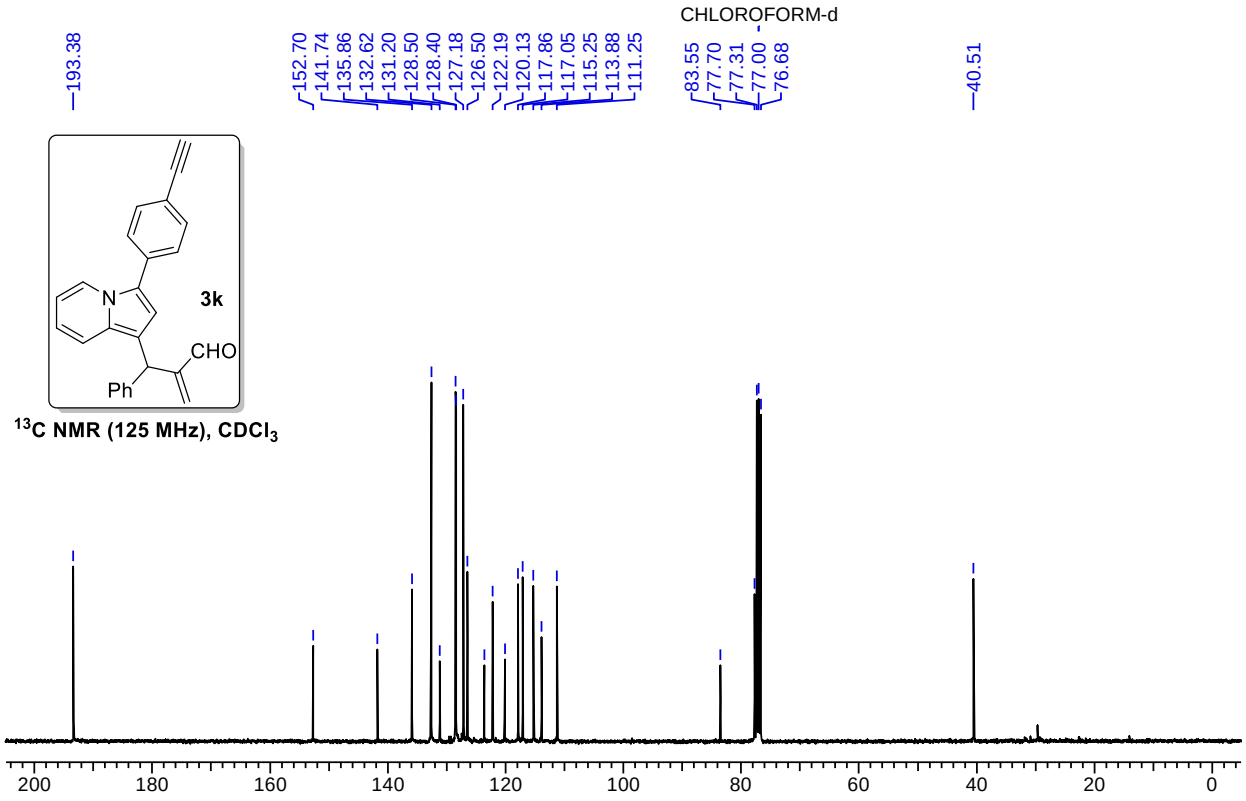

^{13}C NMR (125 MHz), $CDCl_3$

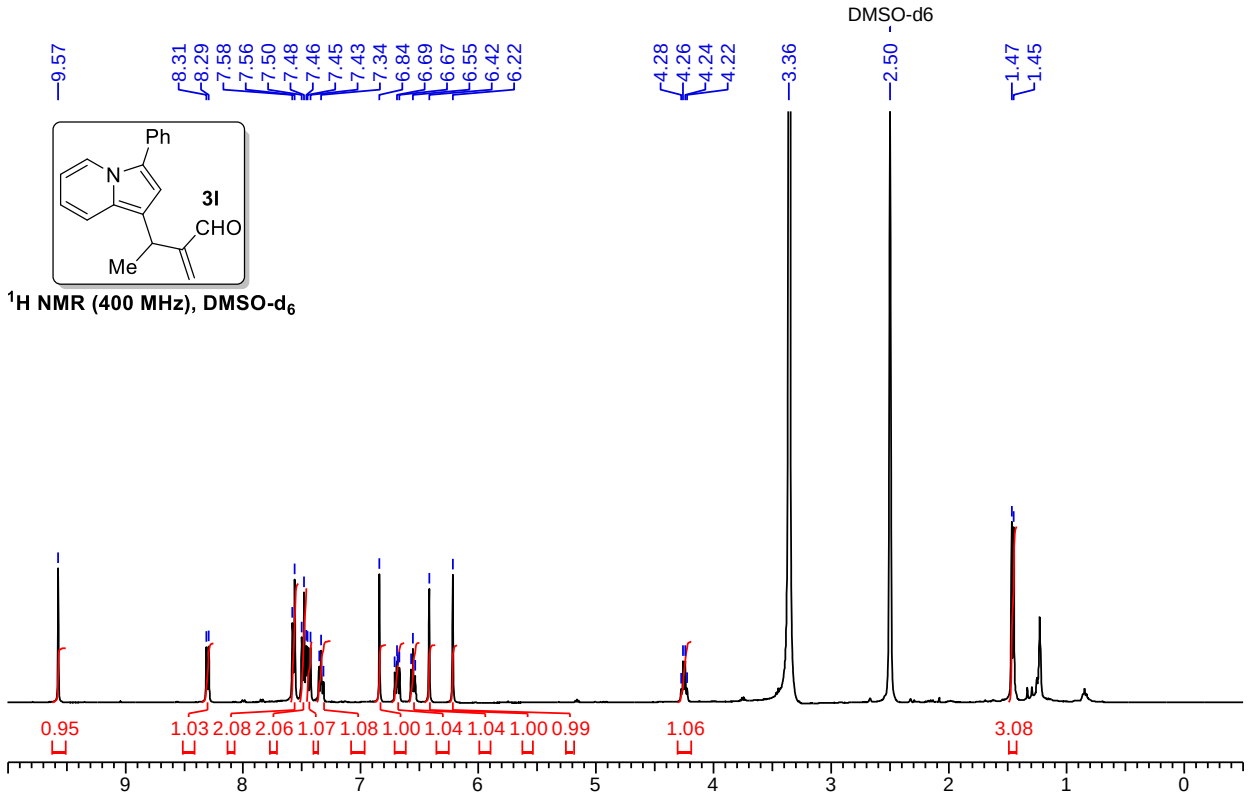

^{1}H NMR (400 MHz), DMSO-d_6

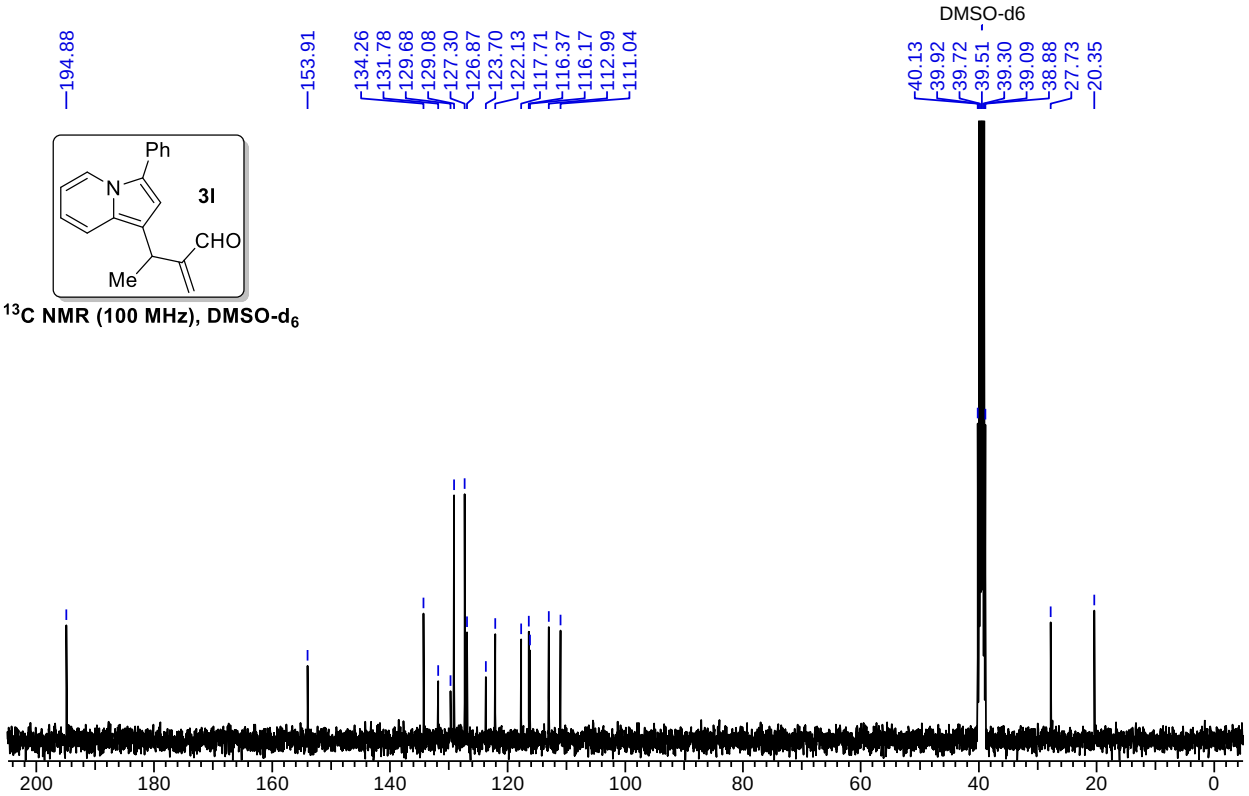

^{13}C NMR (100 MHz), DMSO-d_6

^{1}H NMR (500 MHz), $CDCl_3$

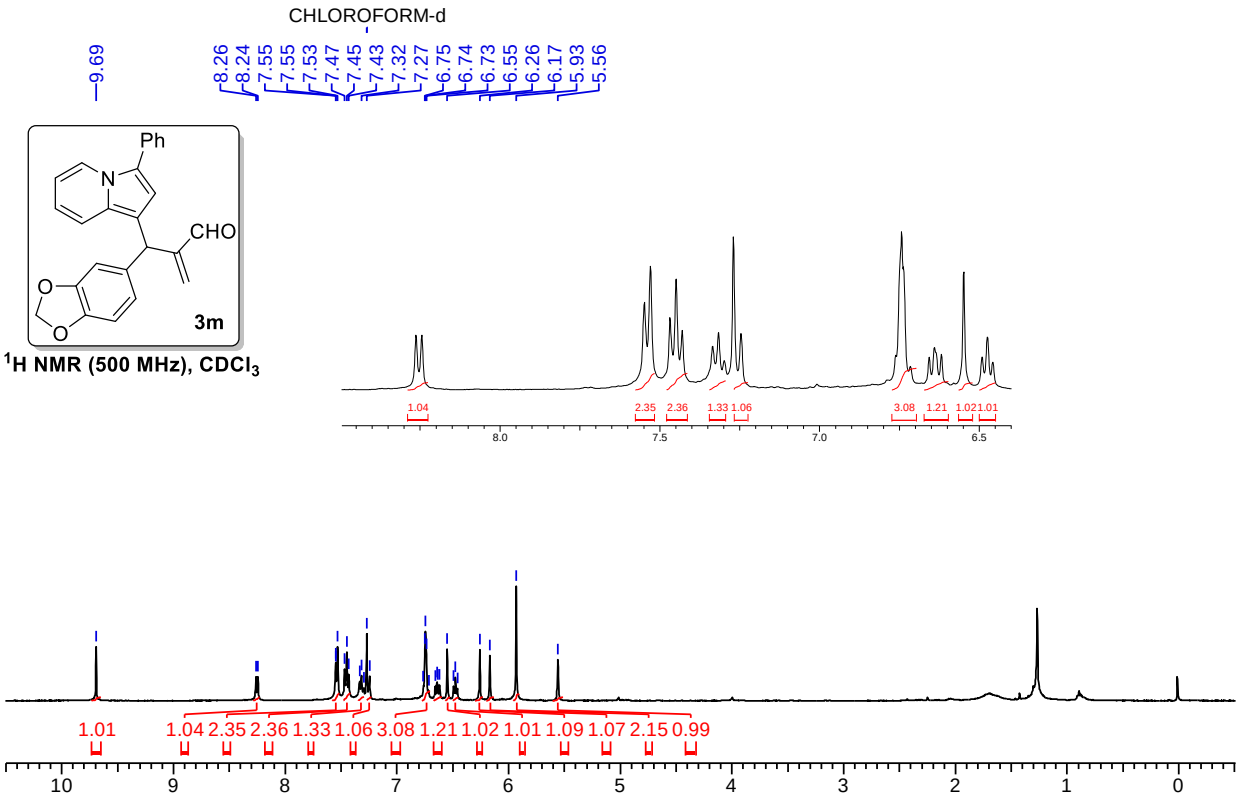

^{13}C NMR (125 MHz), $CDCl_3$

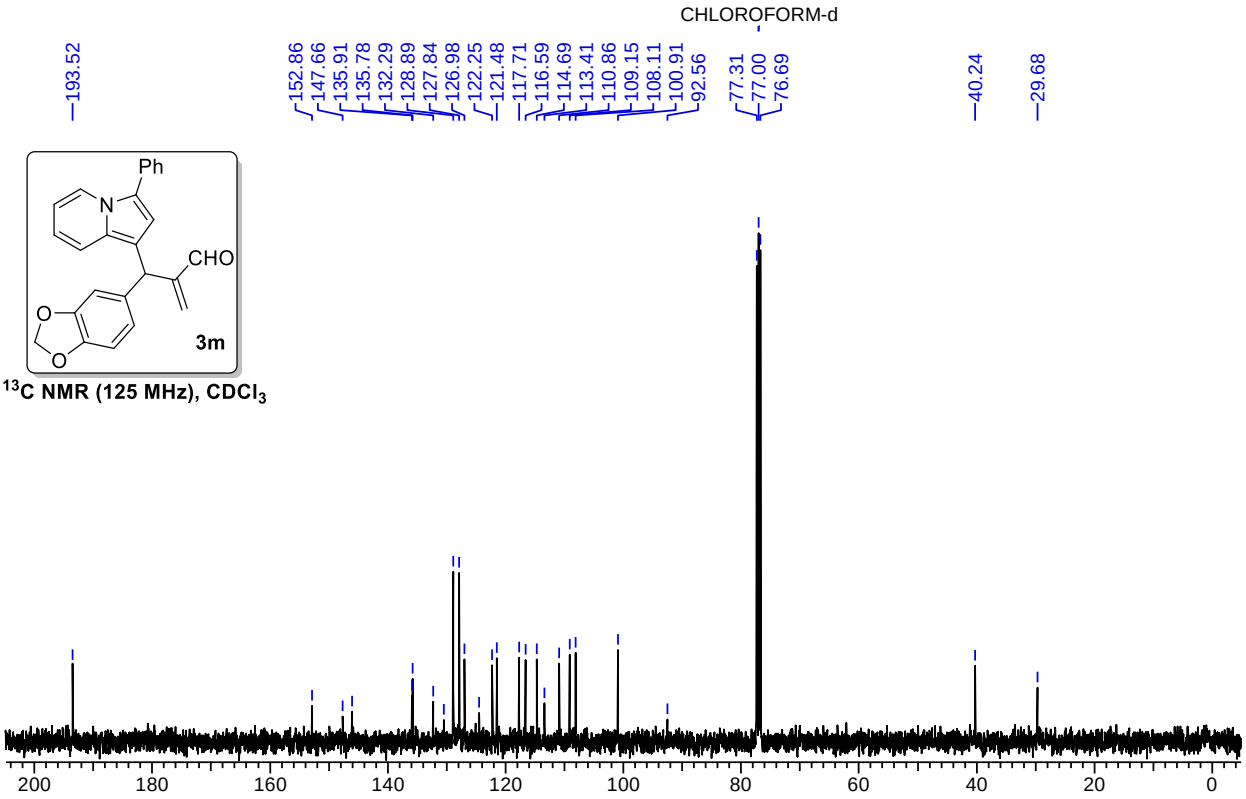

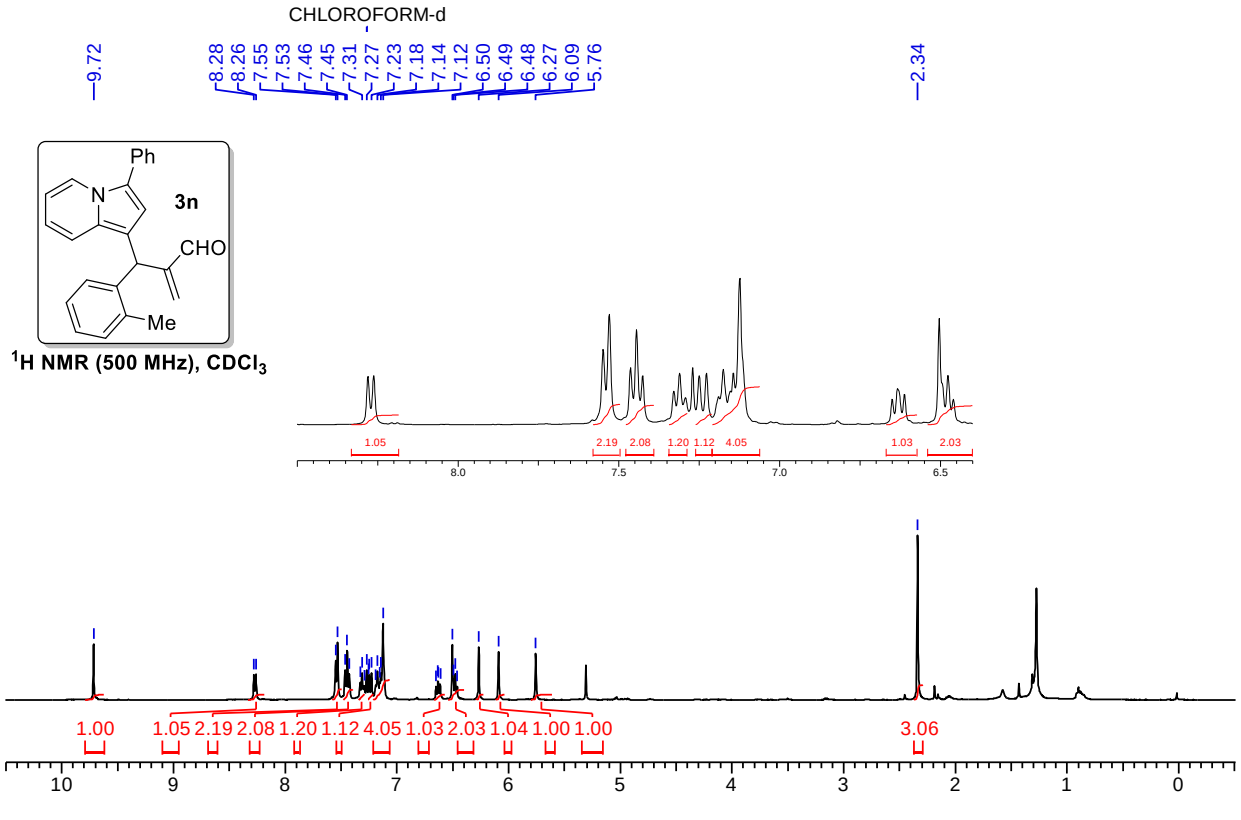

^{1}H NMR (500 MHz), $CDCl_3$

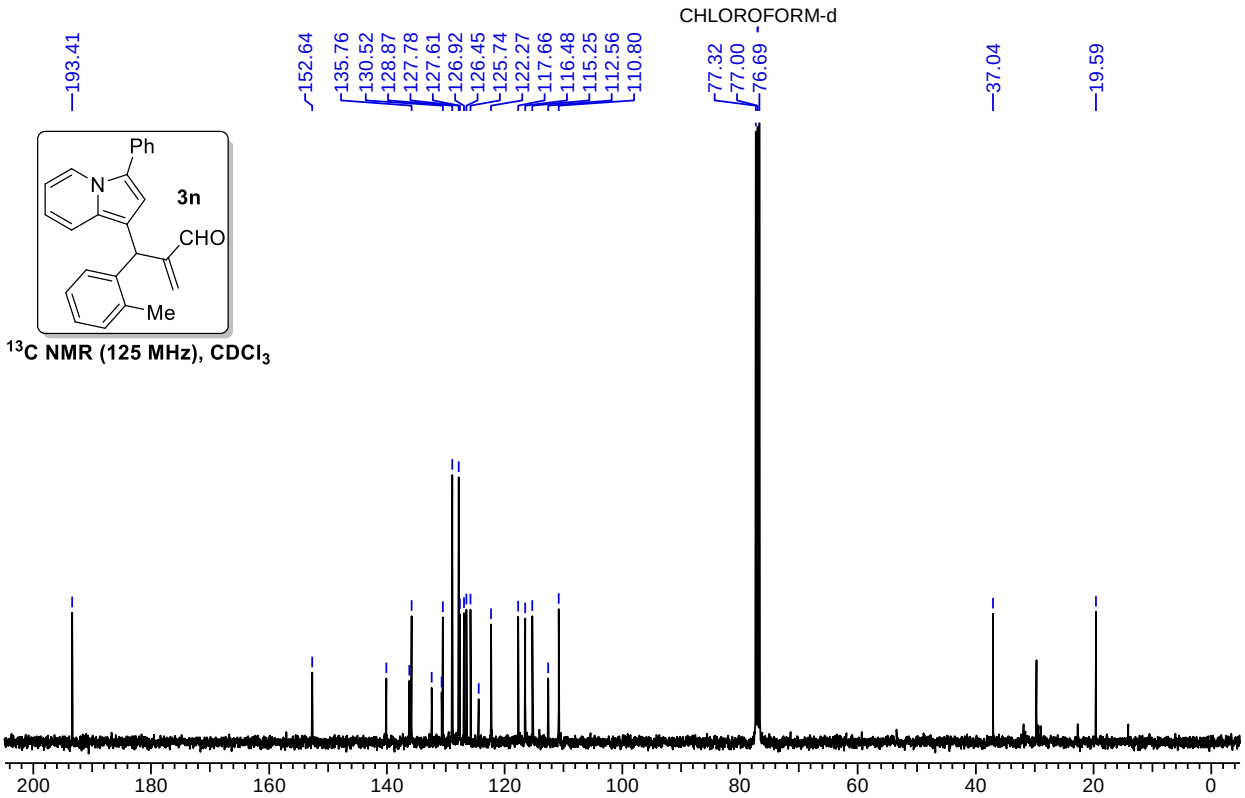

^{13}C NMR (125 MHz), $CDCl_3$

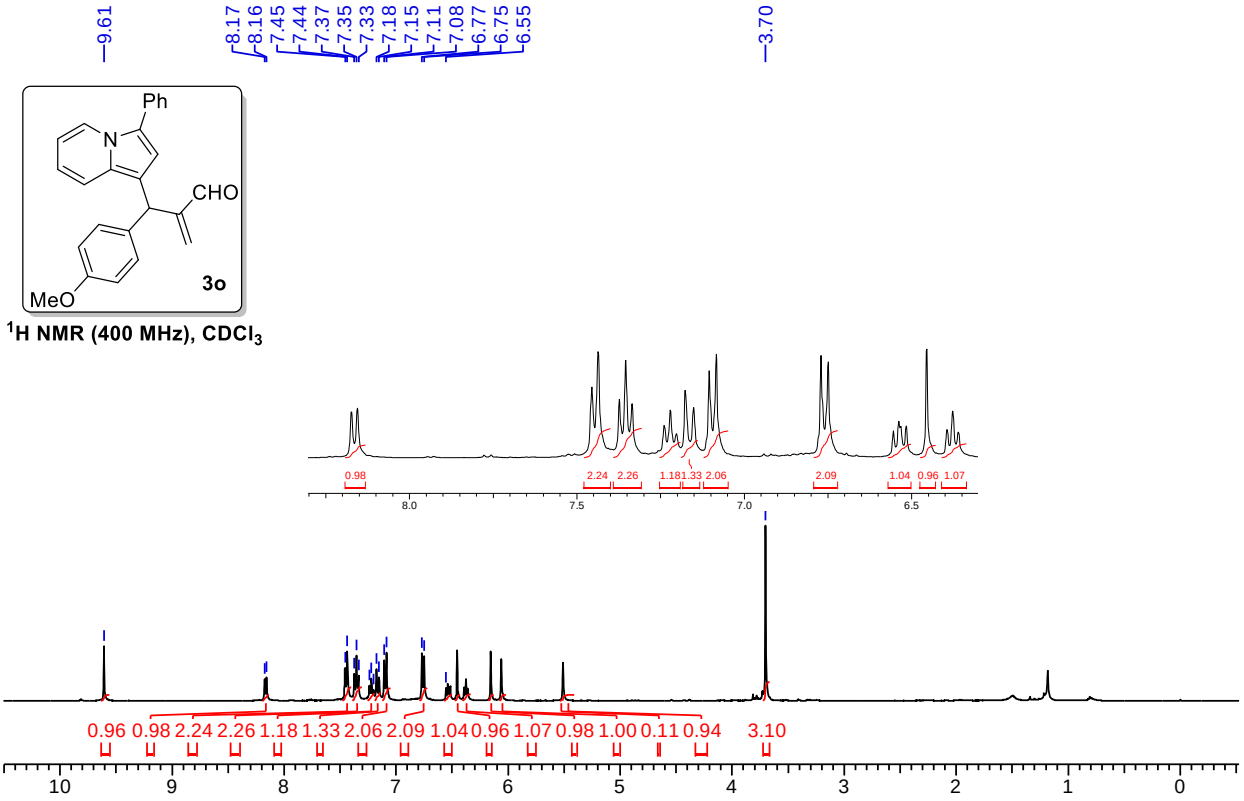

^{1}H NMR (400 MHz), $CDCl_3$

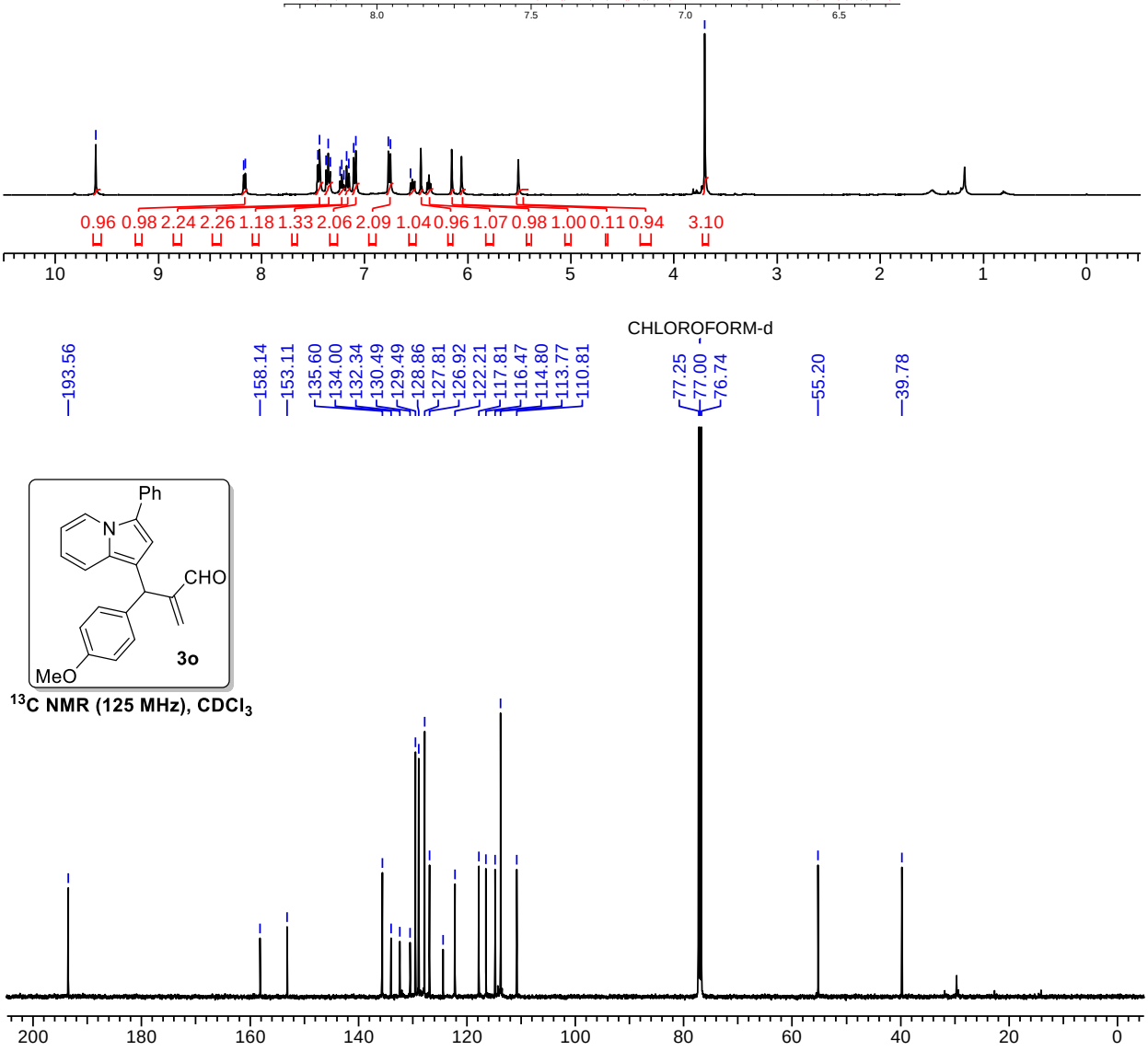

^{13}C NMR (125 MHz), $CDCl_3$

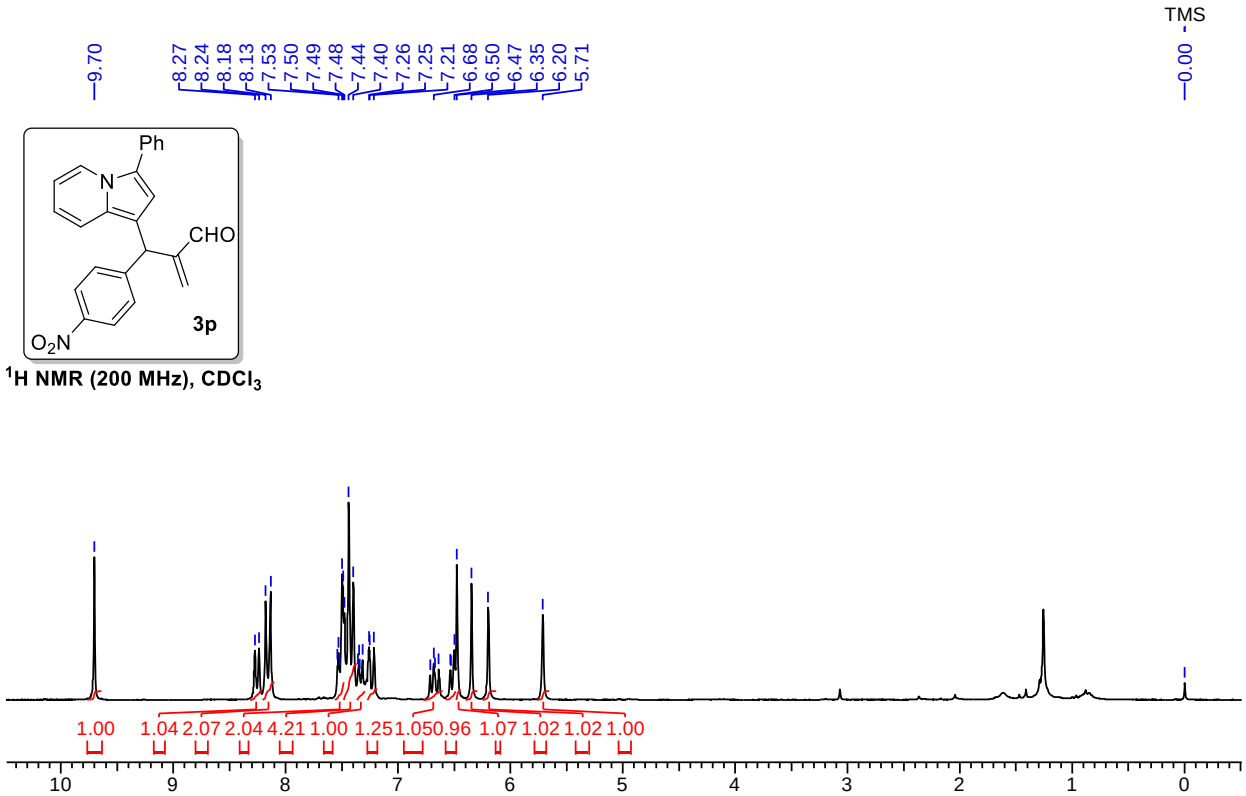

^{1}H NMR (200 MHz), $CDCl_3$

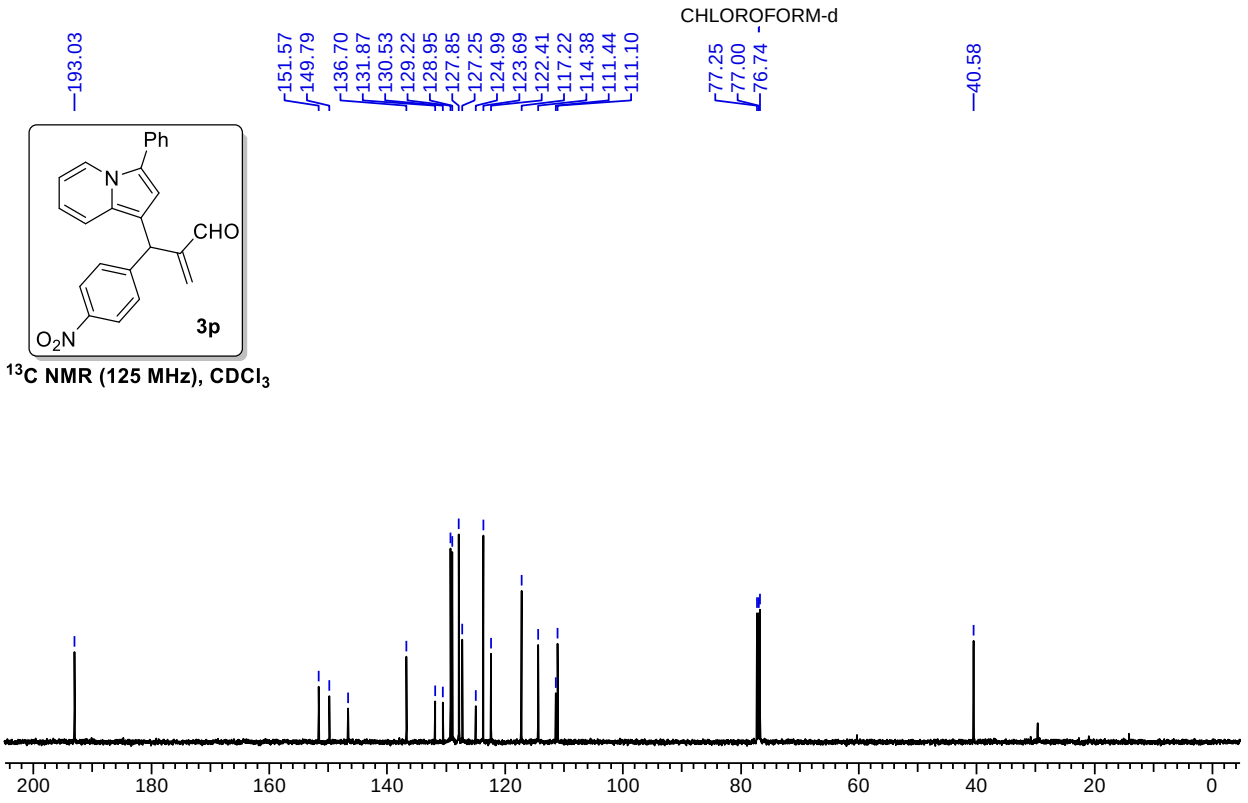

^{13}C NMR (125 MHz), $CDCl_3$

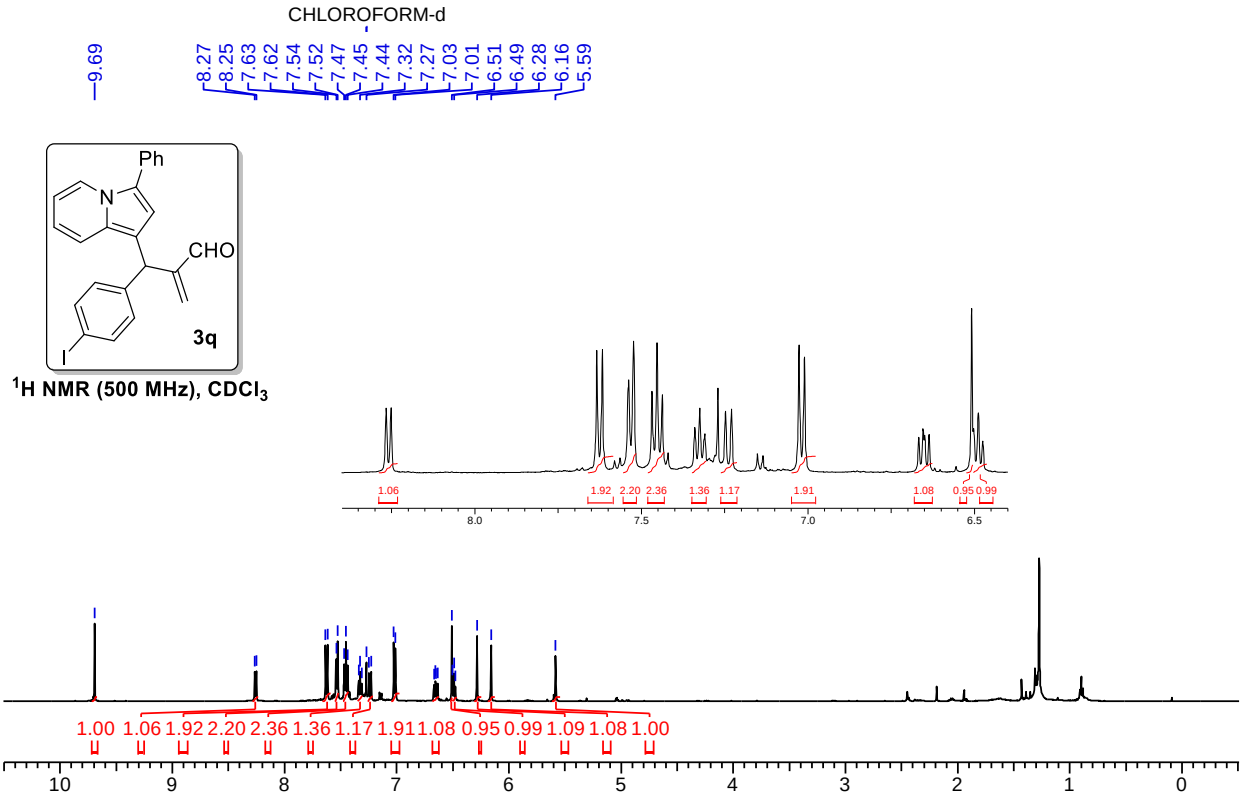

^{1}H NMR (500 MHz), $CDCl_3$

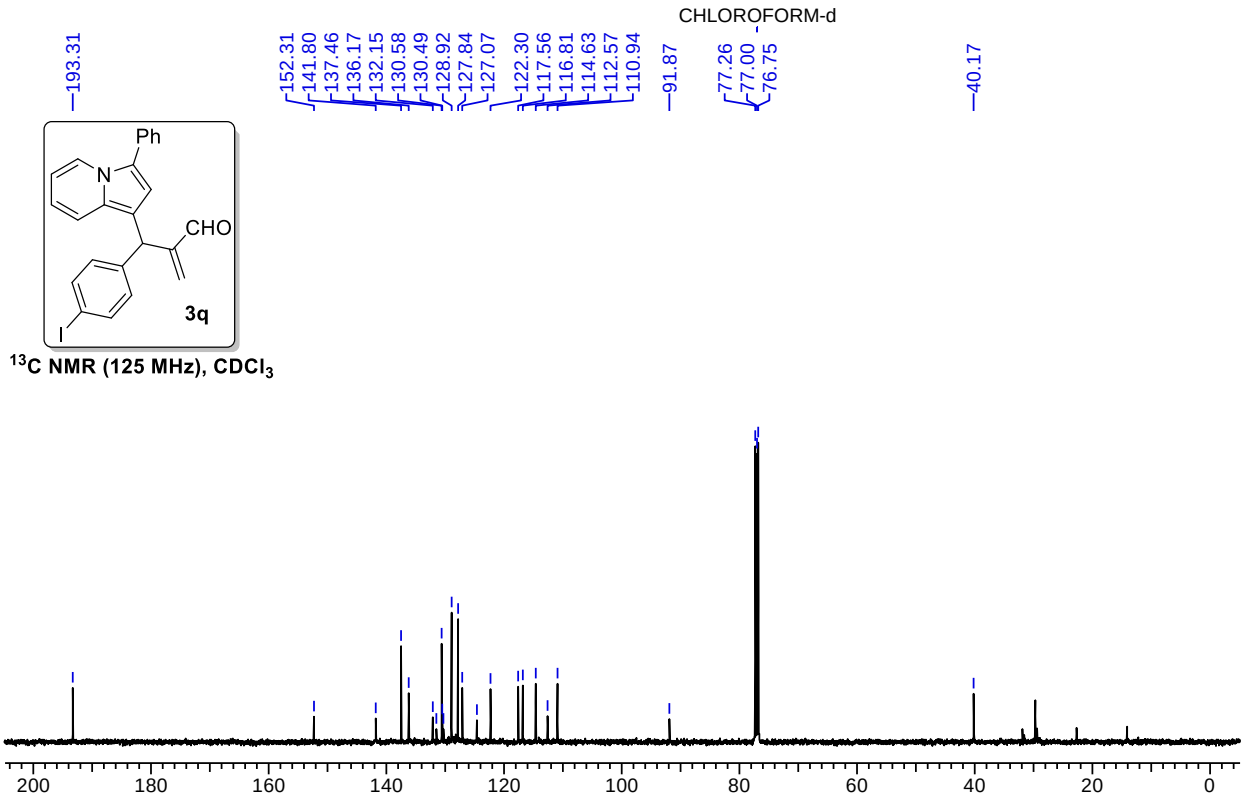

^{13}C NMR (125 MHz), $CDCl_3$

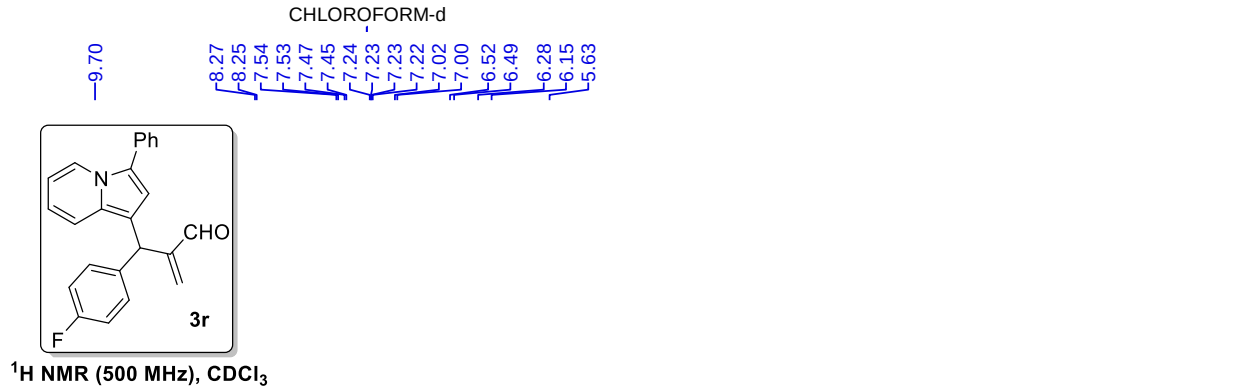

^{1}H NMR (500 MHz), $CDCl_3$

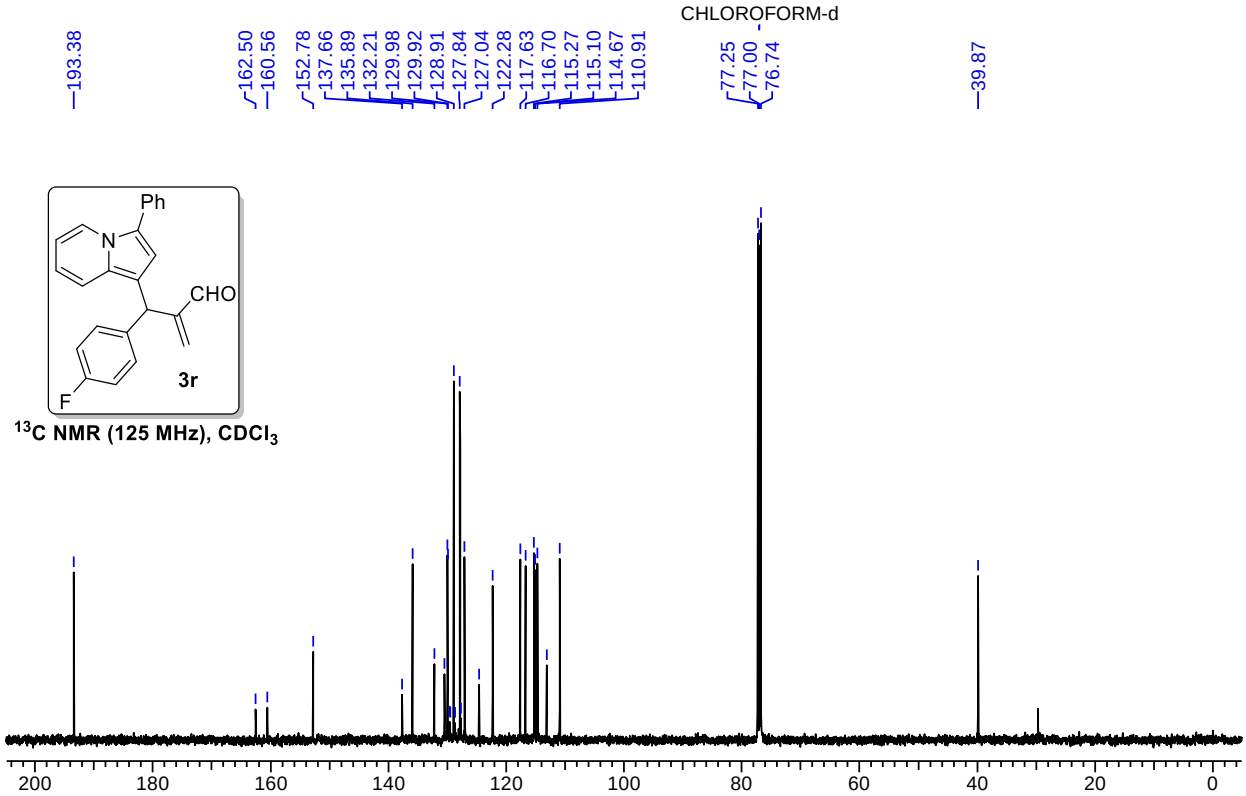

^{13}C NMR (125 MHz), $CDCl_3$

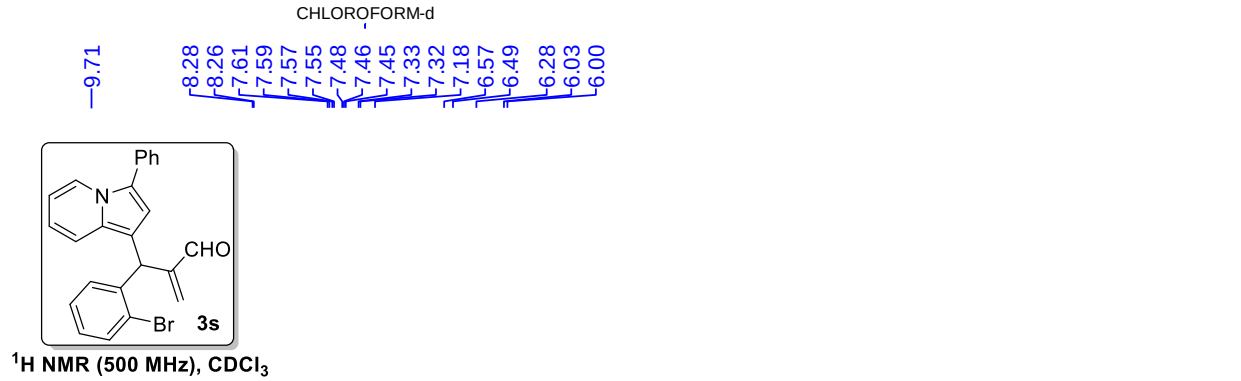

^{1}H NMR (500 MHz), $CDCl_3$

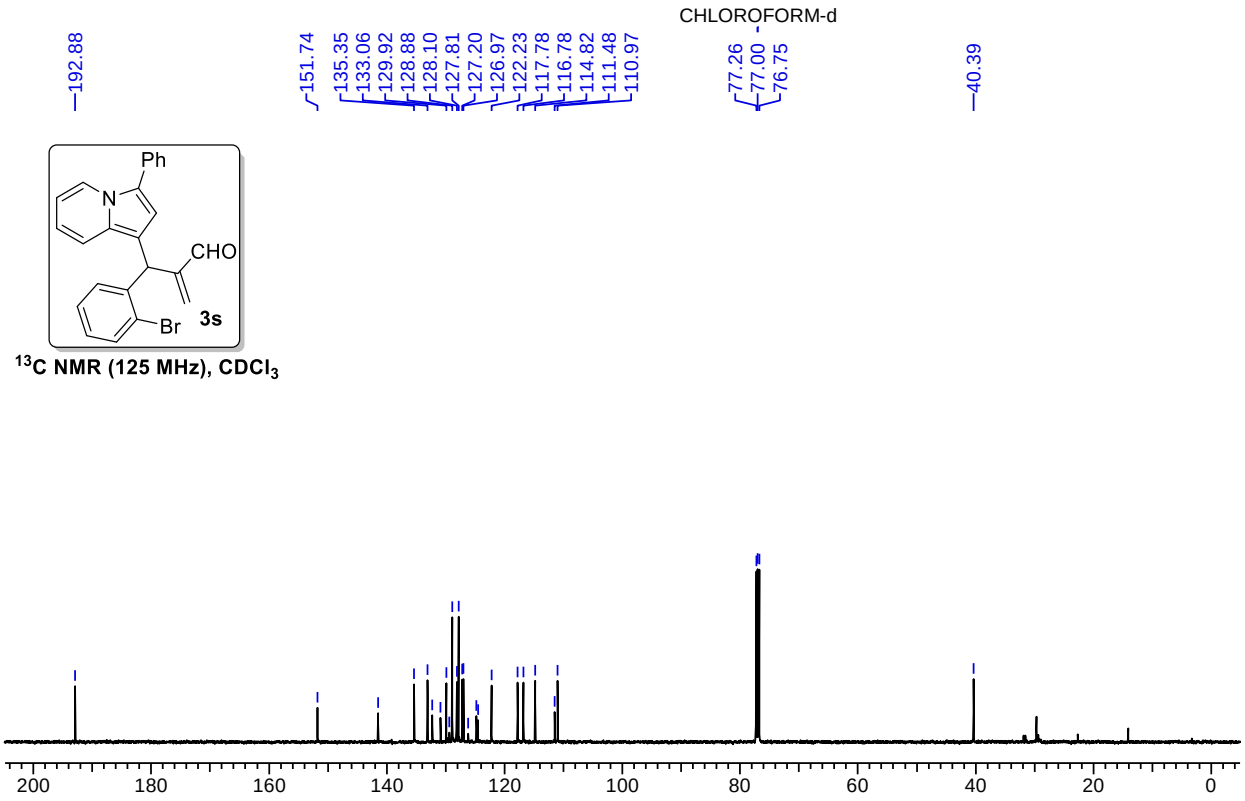

^{13}C NMR (125 MHz), $CDCl_3$

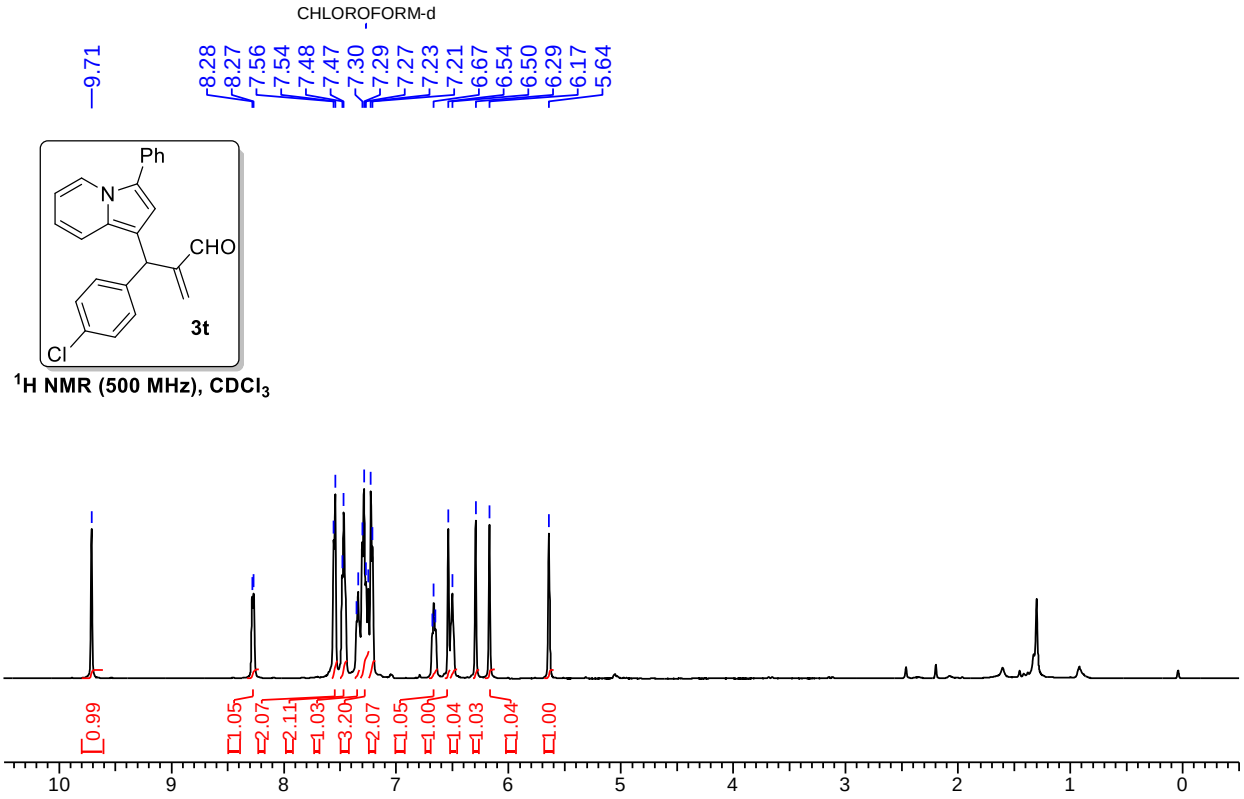

^{1}H NMR (500 MHz), $CDCl_3$

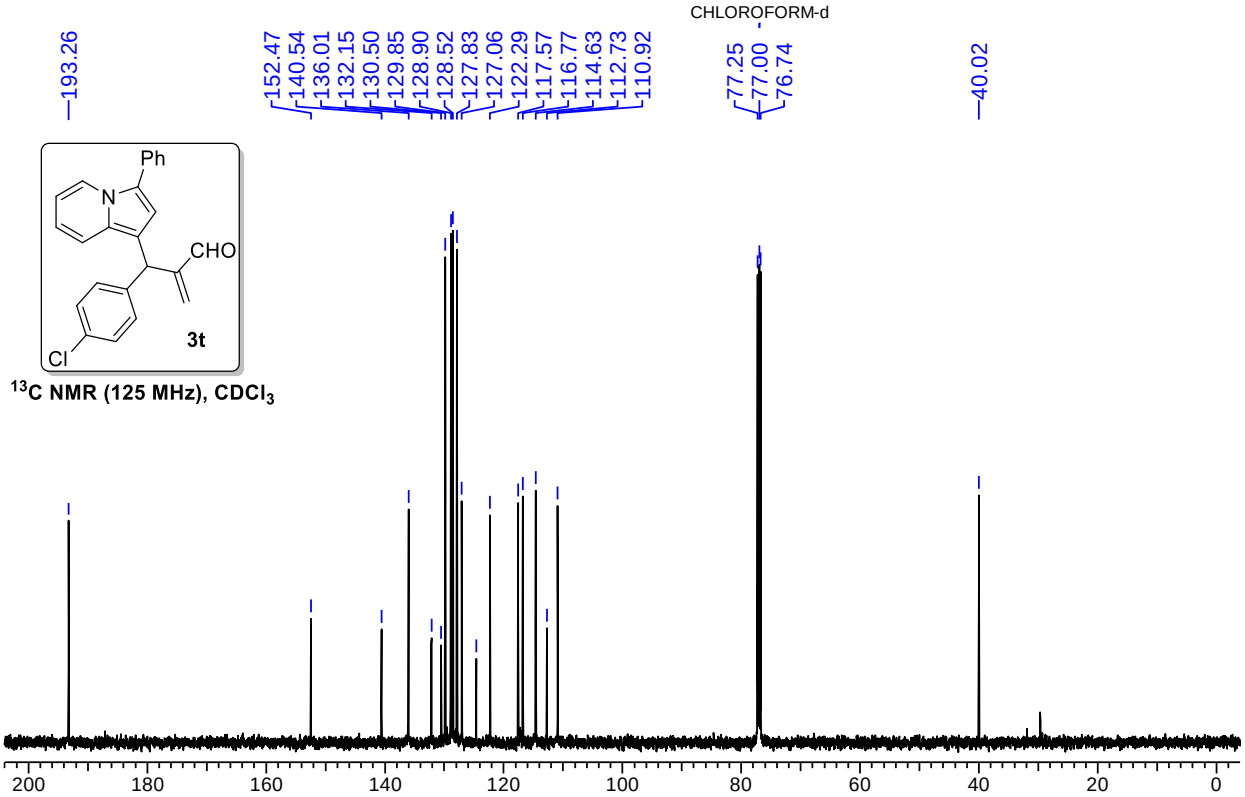

^{13}C NMR (125 MHz), $CDCl_3$

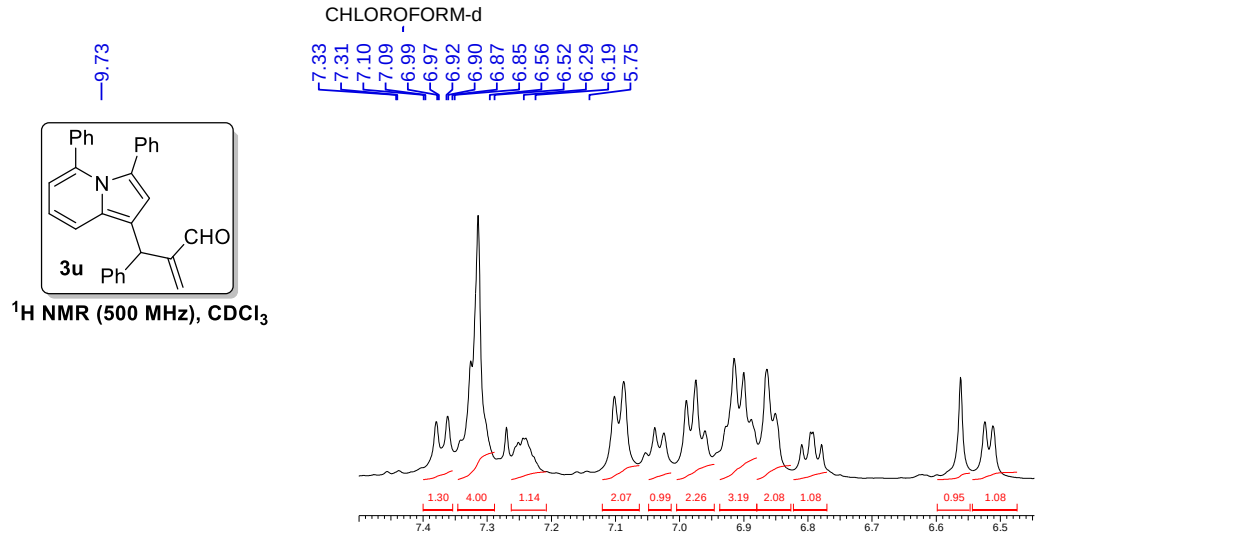

^{1}H NMR (500 MHz), $CDCl_3$

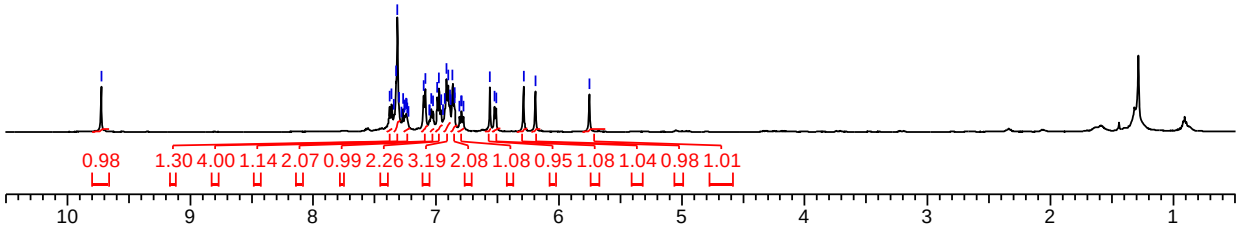

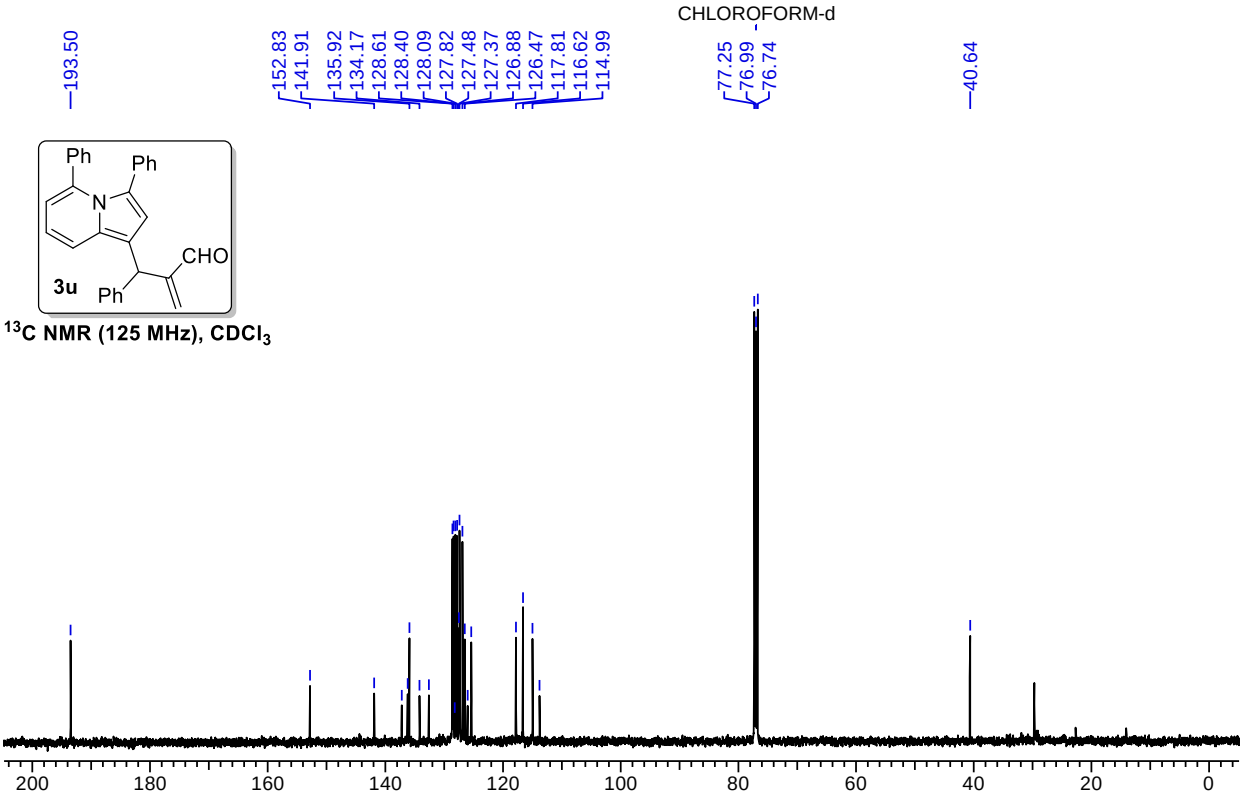

^{13}C NMR (125 MHz), $CDCl_3$

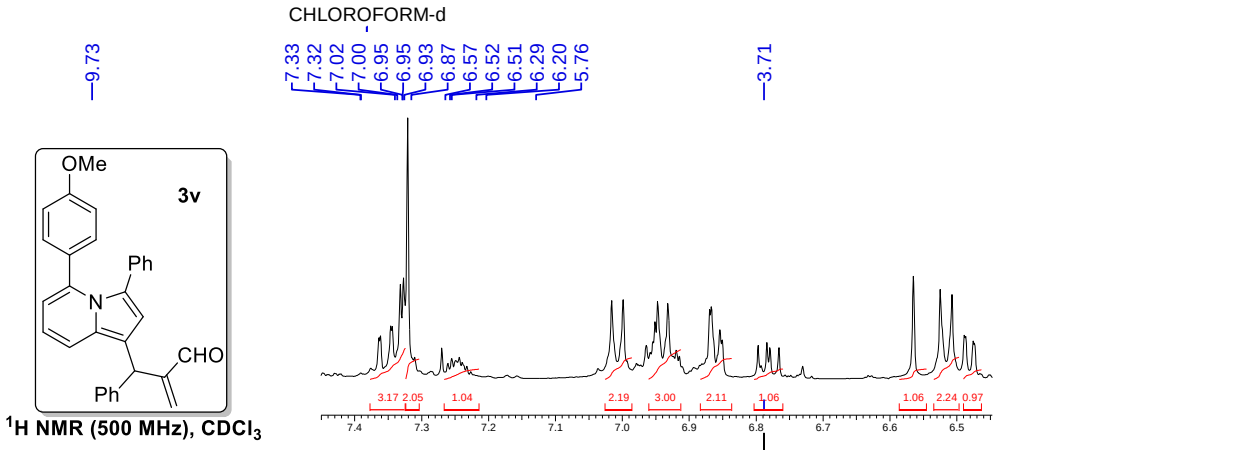

^{1}H NMR (500 MHz), $CDCl_3$

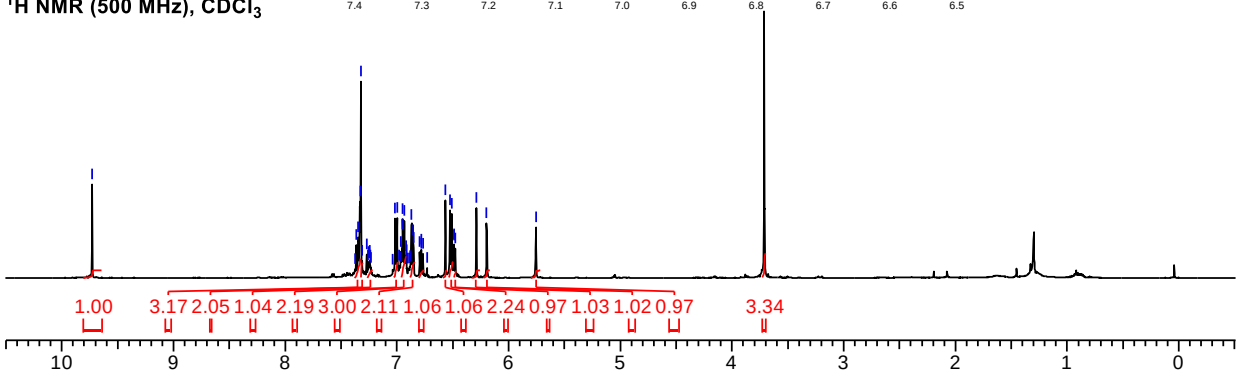

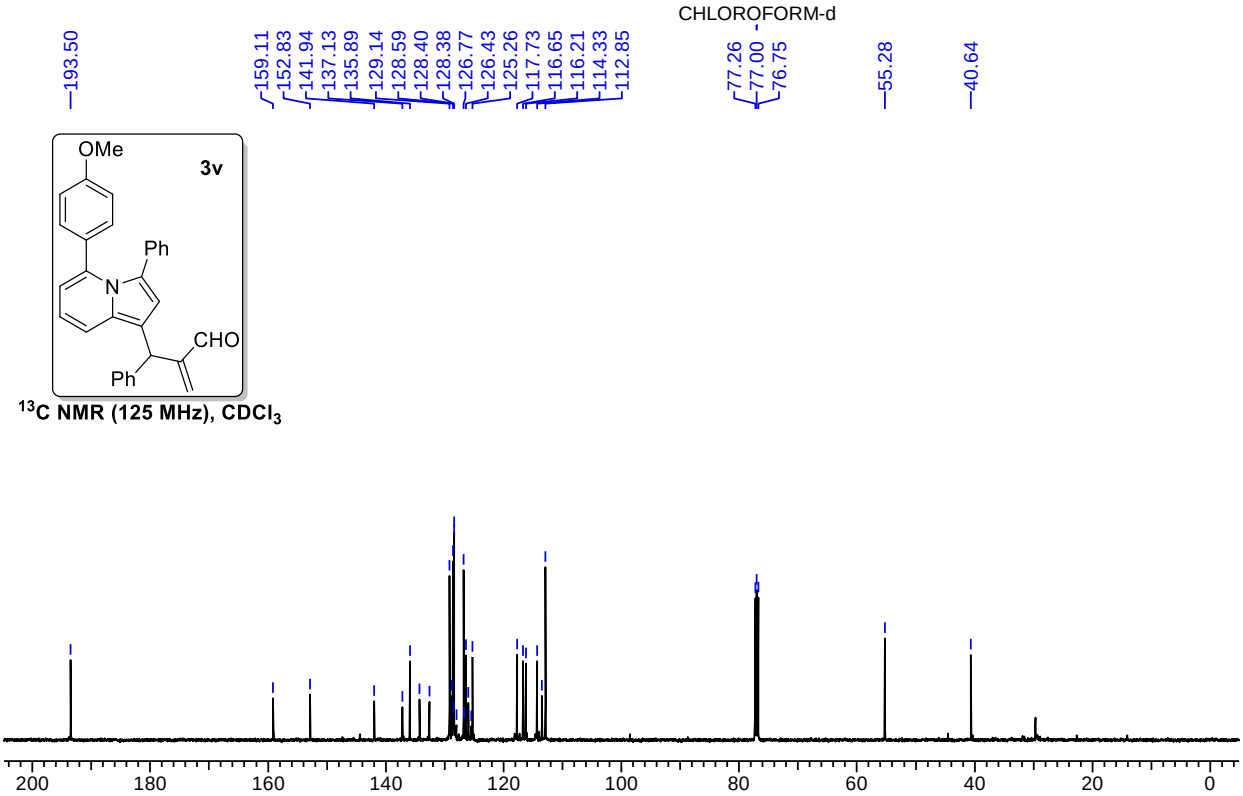

^{13}C NMR (125 MHz), $CDCl_3$

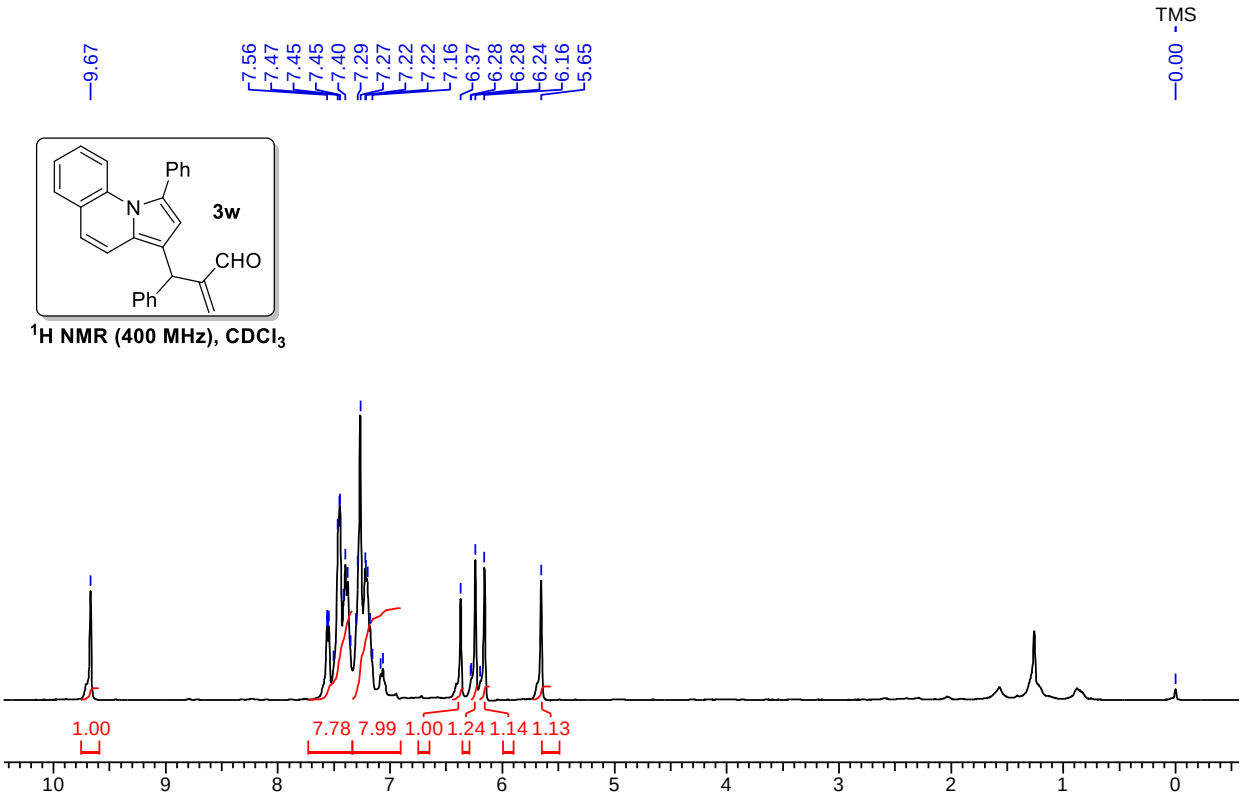

^{1}H NMR (400 MHz), $CDCl_3$

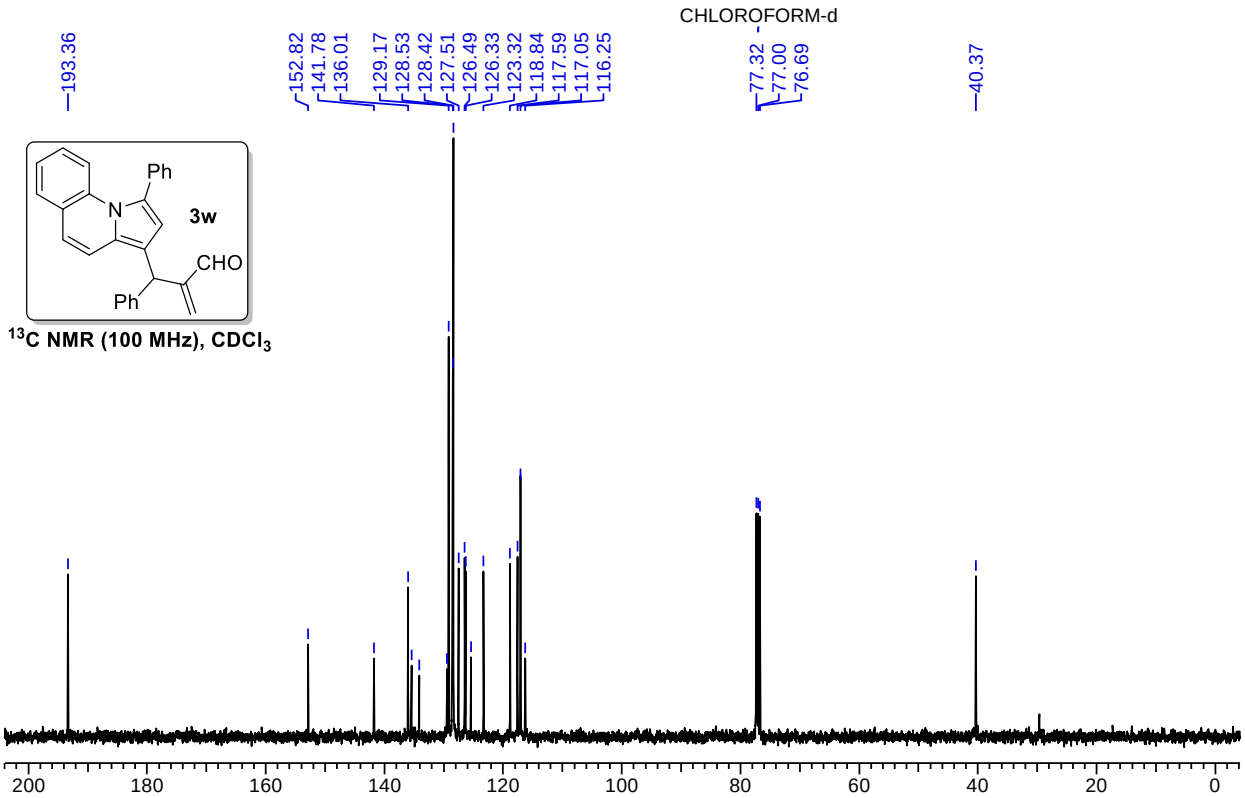

^{13}C NMR (100 MHz), $CDCl_3$

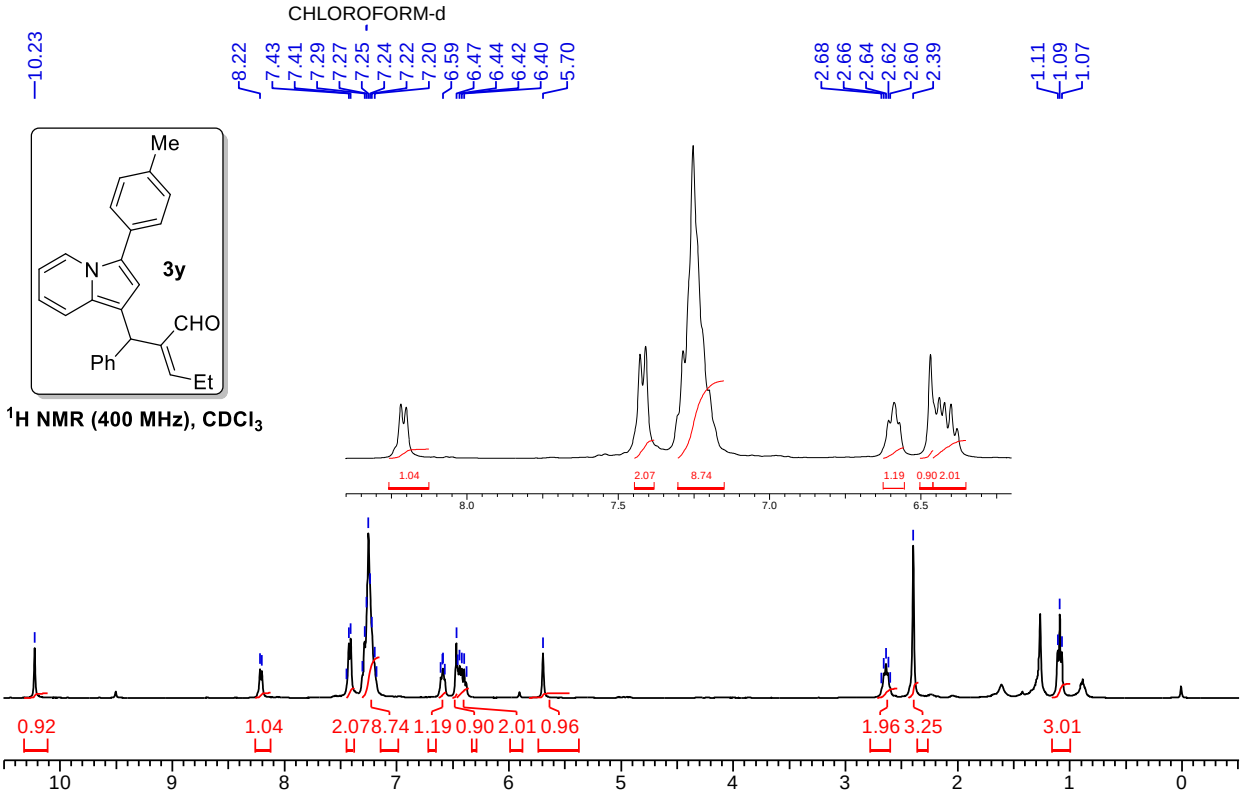

^{1}H NMR (400 MHz), $CDCl_3$

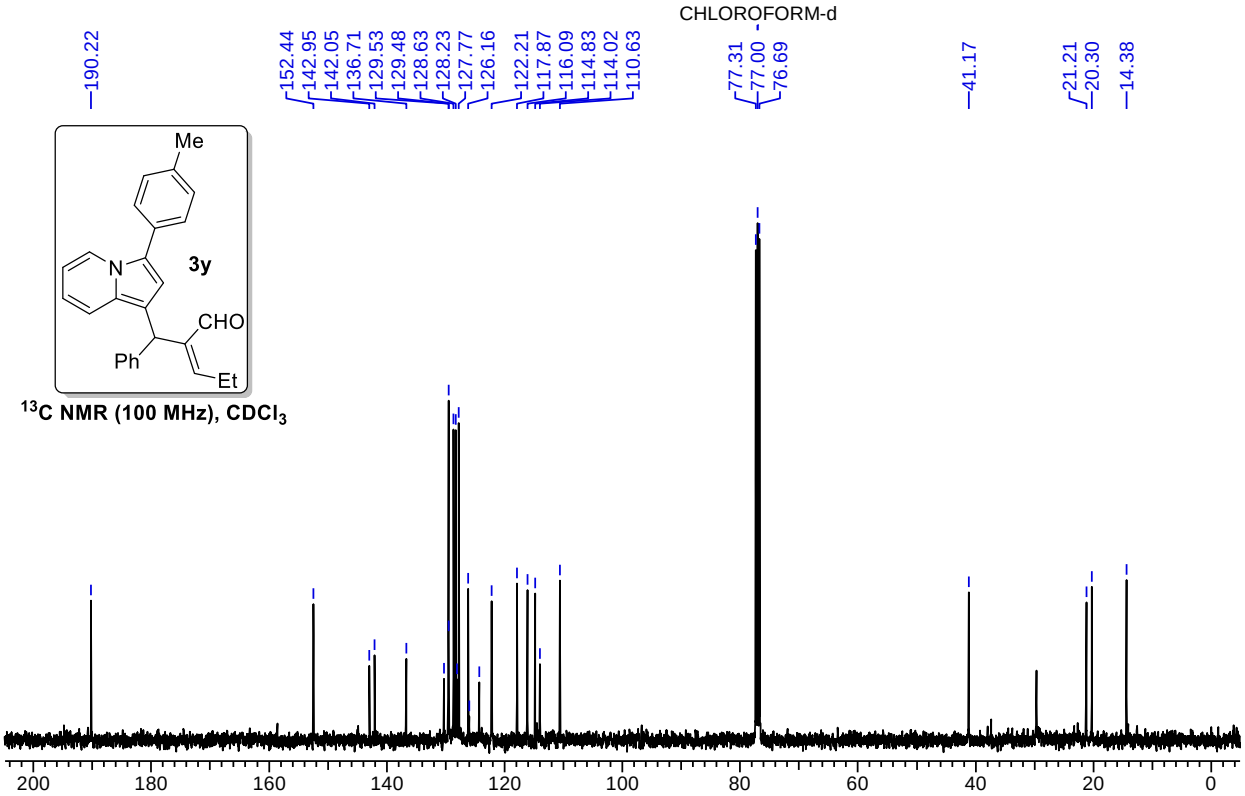

^{13}C NMR (100 MHz), $CDCl_3$

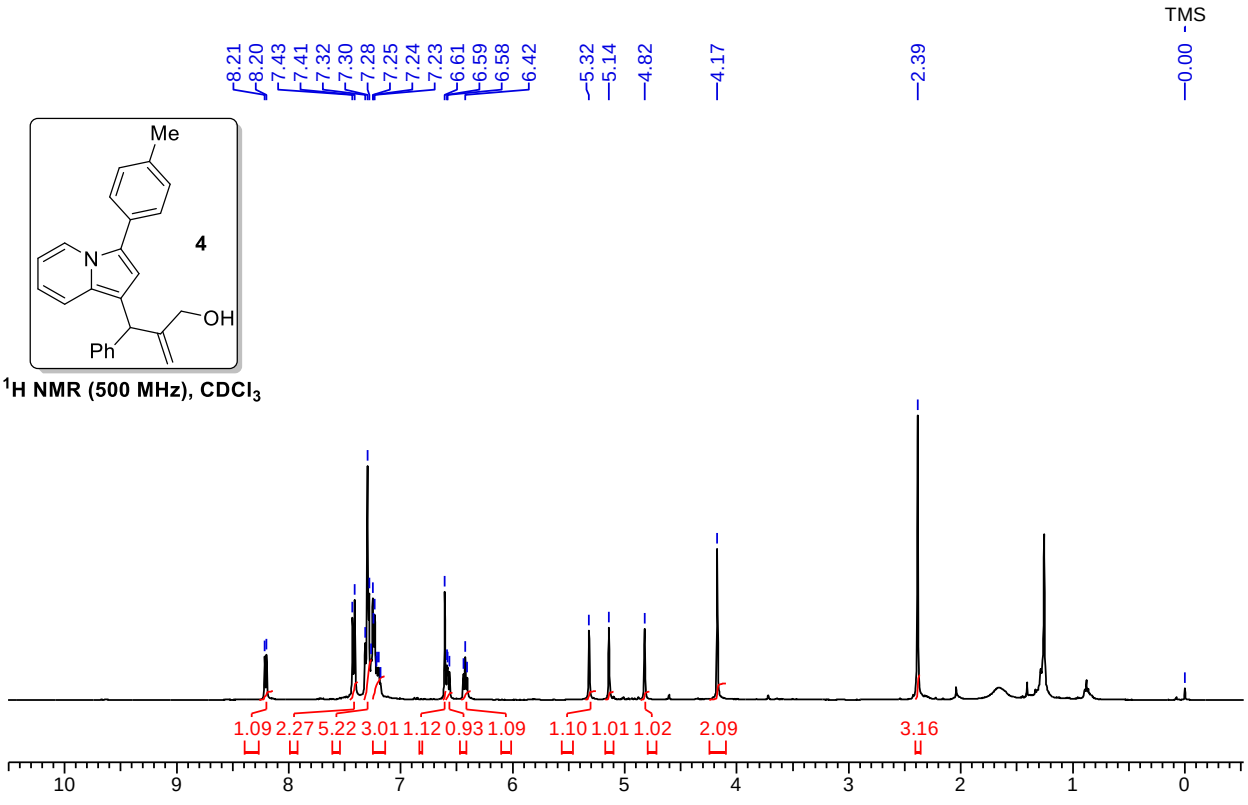

^{1}H NMR (500 MHz), $CDCl_3$

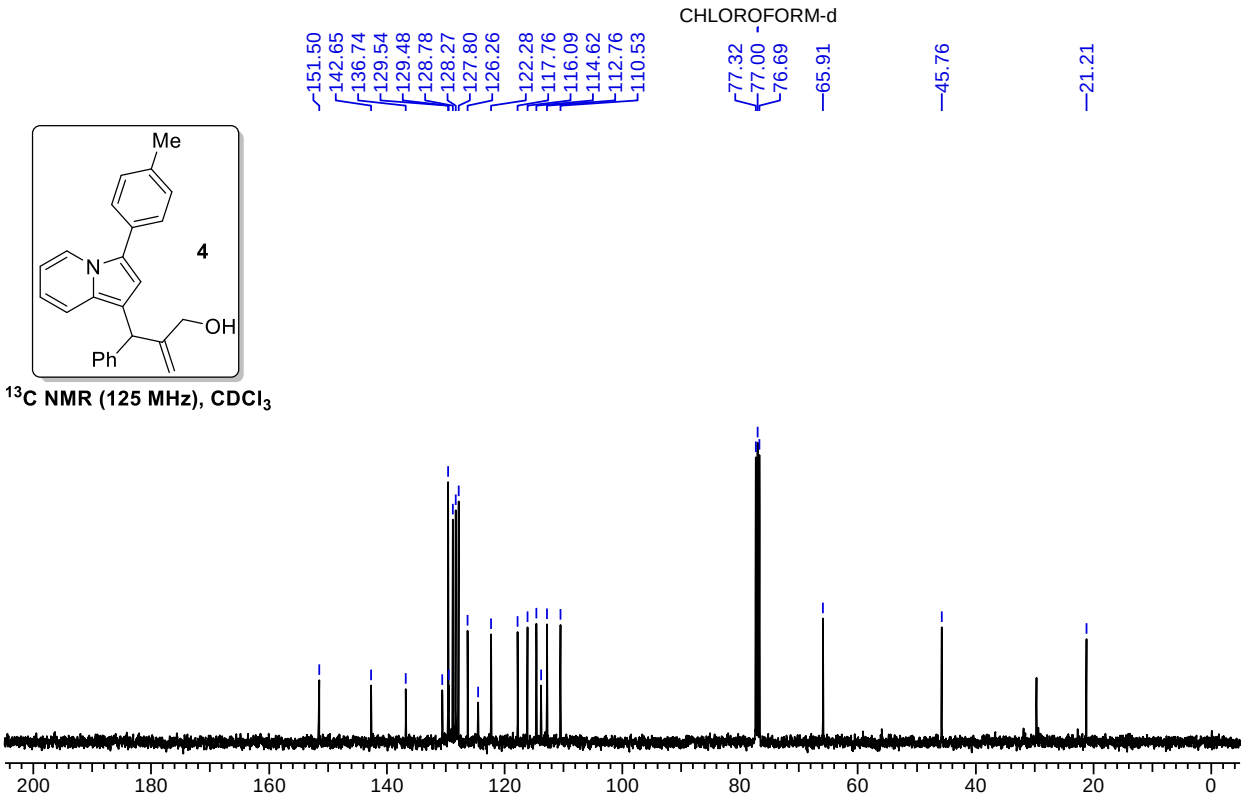

^{13}C NMR (125 MHz), $CDCl_3$

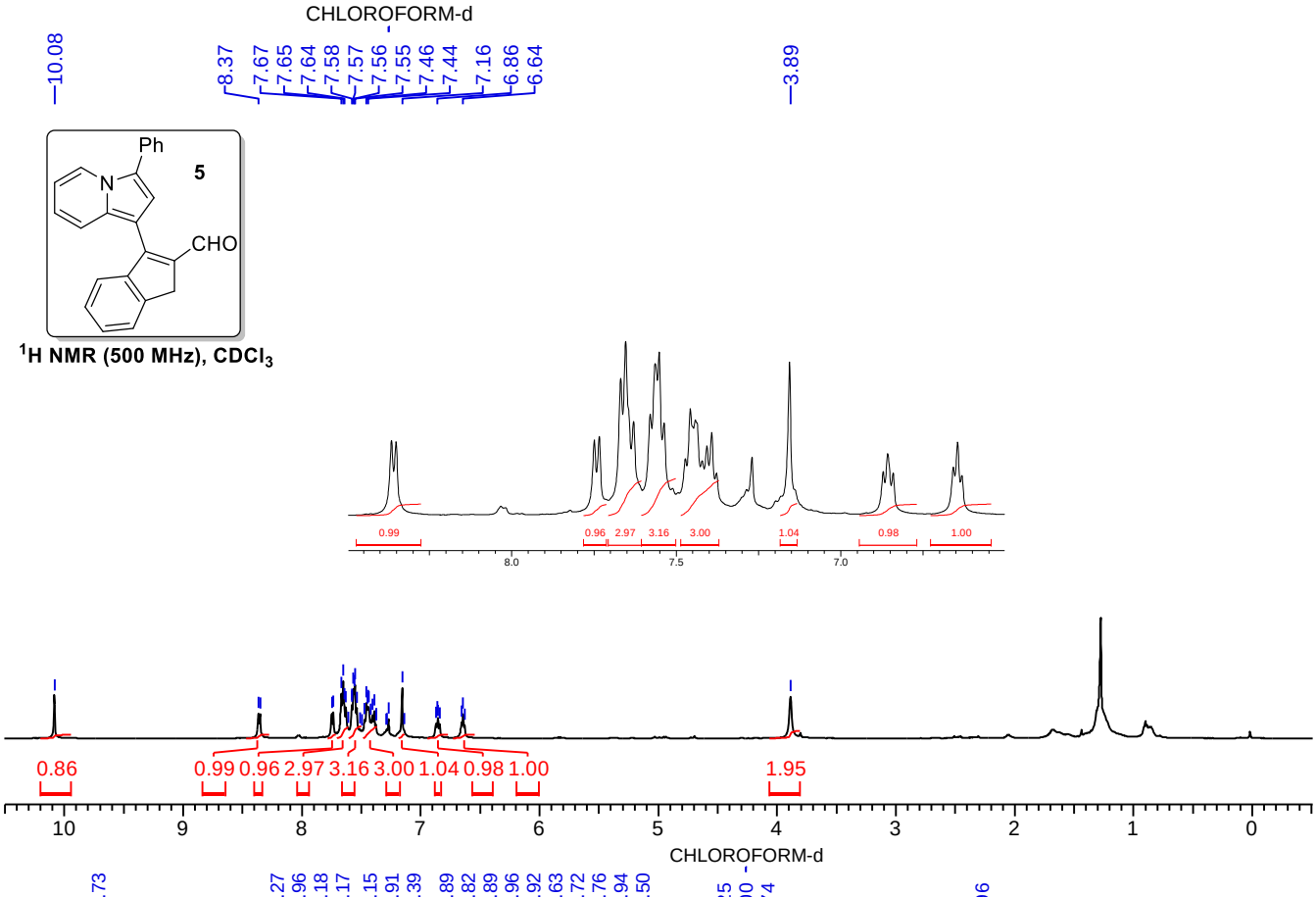

^{1}H NMR (500 MHz), $CDCl_3$

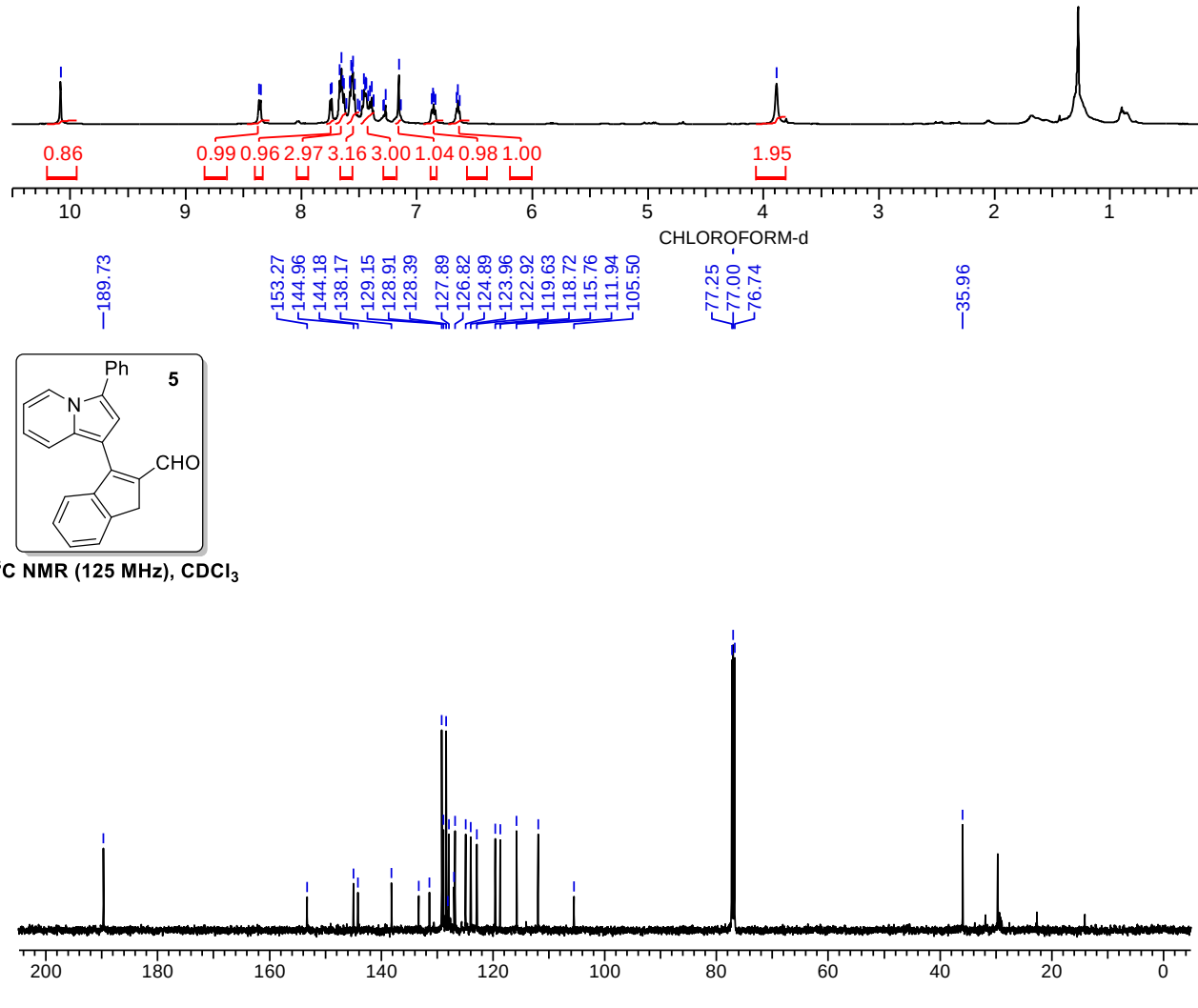

^{13}C NMR (125 MHz), $CDCl_3$

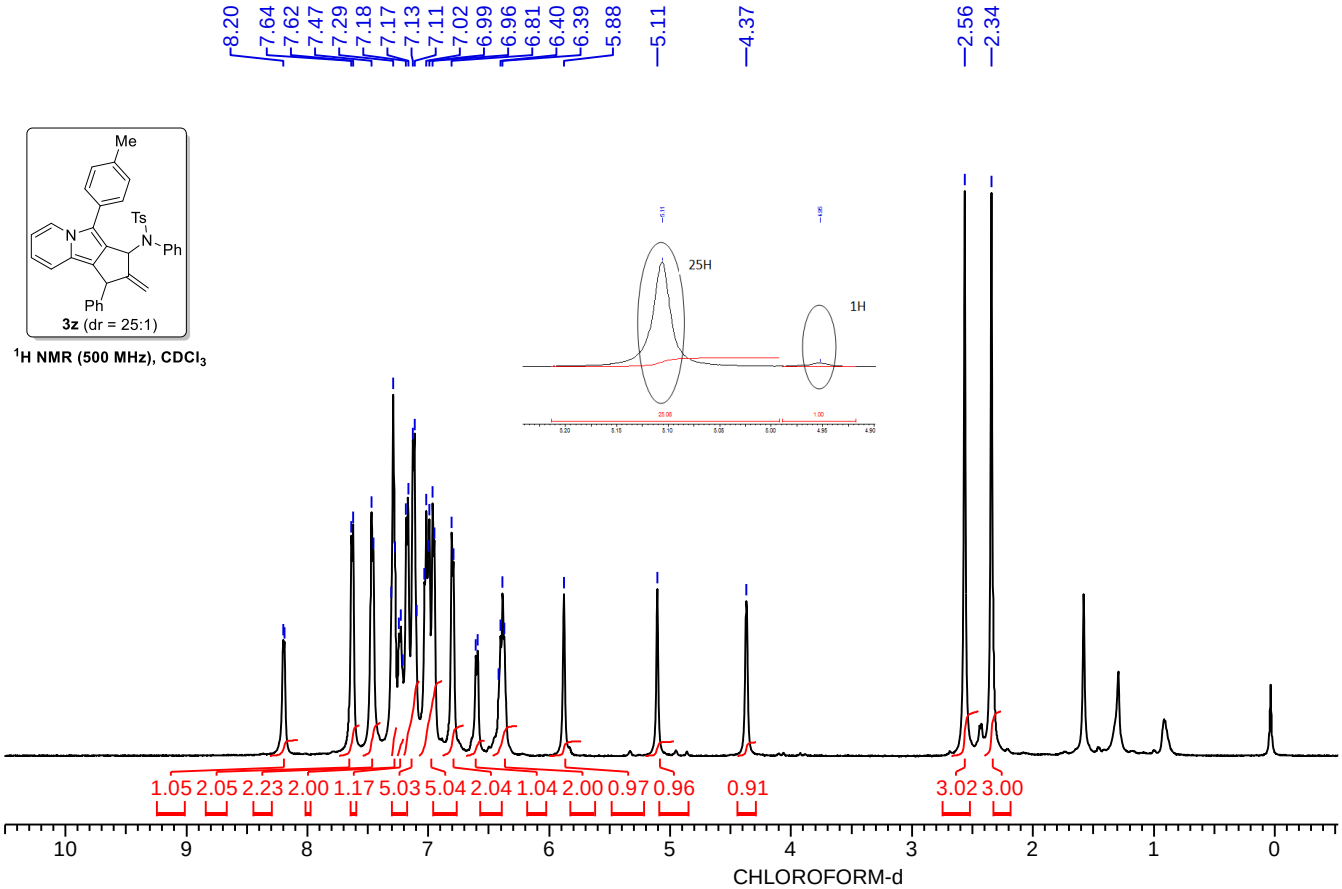

^{1}H NMR (500 MHz), $CDCl_3$

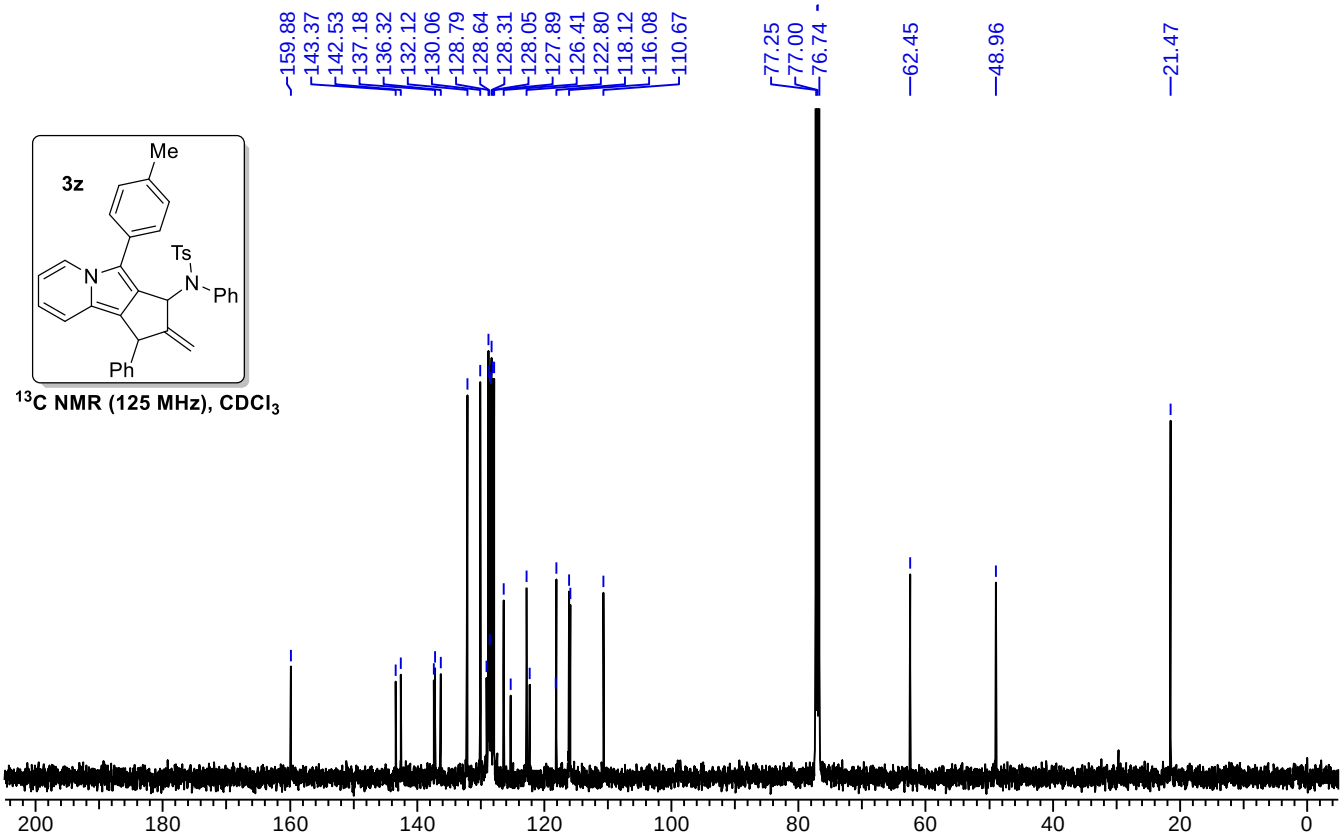

^{13}C NMR (125 MHz), $CDCl_3$

3.12 References

(1) Reviews: (a) Inamdar, S. M.; Shinde, V. S.; Patil, N. T. *Org. Biomol. Chem.* **2015**, *13*, 8116. (b) Zhou, J. *Chem.-Asian J.* **2010**, *5*, 422. (c) Wasilke, J.-C.; Obrey, S. J.; Baker, R. T.; Bazan, G. C. *Chem. Rev.* **2005**, *105*, 1001. (d) Fogg, D. E. E.; Santos, N. D. *Coord. **Chem**. Rev.* **2004**, *248*, 2365. (e) Lee, J. M.; Na, Y.; Han, H.; Chang, S. *Chem. Soc. Rev.* **2004**, *33*, 302. (f) Kamijo, S. *Multimetallic Catalysts in Organic Synthesis* (Eds. M. Shibasaki, Y. Yamamoto), Wiley-VCH, Weinheim, Germany**, 2004**, pp. 1-52.

(2) (a) Chen, D.-F.; Han, Z.-Y.; Gong, L.-Z. *Acc. Chem. Res.* **2014**, *47*, 2365. (b) Inamdar, S. M.; Konala, A.; Patil, N. T. *Chem. Commun*. **2014**, *50*, 15124. (c) Du, Z.; Shao, Z. *Chem. Soc. Rev.* **2013**, *42*, 1337. (d) Loh, C. C. J.; Enders, D. *Chem. Eur. J.* **2012**, *18*, 10212.

(3) Reviews: (a) Pérez-Temprano, M. H.; Casares, J. A.; Espinet, P.; *Chem. Eur. J.* **2012**, *18*, 1864. (b) Hirner, J. J.; Shi,Y.; Blum, S. *Acc. Chem. Res*. **2011**, *44*, 603. (c) Duschek, A.; Kirsch, S. F. *Angew. Chem. Int. Ed*. **2008**, *47*, 5703. For other reports, see: (d) Xi, Y.; Wang, D.; Ye, X.; Akhmedov, N. G. Petersen, J. L.; Shi, X. *Org. Lett*. **2014**, *16*, 306. (e) Li, Y.; Waser, J. *Beilstein J. Org. Chem*. **2013**, *9*, 1763. (f) Panda, B. T;. Sarkar, K. *Tetrahedron Lett*. **2010**, *51*, 301. (g) Jones, L. A.; Sanz, S.; Laguna, M. *Catalysis Today* **2007**, *122*, 403.

(4) Shi, Y.; Peterson, S. M.; Haberaecker III, W. W.; Blum, S. A. *J. Am. Chem. Soc*. **2008**, *130*, 2168.

(5) (a) Shi, Y.; Roth, K. E.; Ramgren, S. D.; Blum, S. A. *J. Am. Chem. Soc*. **2009**, *131*, 18022. Also see: (b) Al-Amin, M.; Johnson, J. S.; Blum, S. A. *Organometallics* **2014**, *33*, 5448.

(6) del Pozo, J.; Carrasco, D.; Pérez-Temprano, M. H.; García-Melchor, M.; Álvarez, R.; Casares, J. A.; Espinet, P. *Angew. Chem. Int. Ed.* **2013**, *52*, 2189.

(7) Xi, Y.; Wang, D.; Ye, X.; Akhmedov, N. G.; Petersen, J. L.; Shi, X. *Org. Lett*. **2014**, ***16***, 306.

(8) García-Domínguez, P.; Nevado, C. *J. Am. Chem. Soc*. **2016**, *138*, 3266. Also see: Hashmi, A. S. K.; Lothscühtz, C.; Döpp, R.; Rudolph, M.; Ramamurthi, T. D.; Rominger, F. *Angew. Chem. Int. Ed*. **2009**, *48*, 8243.

(9) Reviews: (a) Wei, Y.; Shi, M. *Chem. Rev*. **2013**, *113*, 6659. (b) Basavaiah, D.; Veeraraghavaiah, G. *Chem. Soc. Rev*. **2012**, *41*, 68. (c) Shi, M.; Wang, F.; Zhao, M.-X.; Wei, Y. Chemistry of the Morita-Baylis-Hillman Reaction, *RSC Catalysis Series*, **2011**. **(**d) Basavaiah, D.; Reddy, B. S.; Badsara, S. S. *Chem. Rev*. **2010**, *110*, 5447. (e) Basavaiah, D.; Rao, A. J.; Satyanarayana, T. *Chem. Rev.* **2003**, *103*, 811.

(10) Reviews: (a) Zi, W.; Toste, F. D. *Chem. Soc. Rev*. **2016**, *45*, 4567. (b) Liu, L.; Zhang, J. *Chem. Soc. Rev.* **2016**, *45*, 506. (c) Dorel, R.; Echavarren, A. M. *Chem. Rev.* **2015**, *115*, 9028. (d) Cañeque, T.; Truscott, F. M.; Rodriguez, R.; Maestri, G.; Malacria, M. *Chem. Soc. Rev.* **2014**, *43*, 2916. (e) Hashmi, A. S. K.; Yang, W. *Chem. Soc. Rev.* **2014**, ***43***, 2941 (f) Garayalde, D.; Nevado, C. *ACS Catal*. **2012**, *2*, 1462. (g) Bandini, M. *Chem. Soc. Rev.* **2011**, *40*, 1358. (h) López, F.; Mascareñas, J. L. *Beilstein J. Org. Chem.* **2011**, *7*, 1075. (i) Wegner, H. A.; Auzias, M. *Angew. Chem. Int. Ed.* **2011**, *50*, 8236. (j) Corma, A.; Leyva-Perez, A.; Sabater, M. *J. Chem. Rev.* **2011**, *111*, 1657. (k) Das, A.; Sohel, S. M. A.; Liu, R.-S. *Org. Biomol. Chem.* **2010**, *8*, 960. (l) Hashmi, A. S. K.; Bührle, M. *Aldrichimica Acta* **2010**, *43*, 27. (m) Sohel, S. M. A.; Liu, R.-S. *Chem. Soc. Rev*. **2009**, *38*, 2269. (n) Fürstner, A. *Chem. Soc. Rev*. **2009**, *38*, 3208. (o) Gorin, D. J.; Sherry, B. D.; Toste, F. D. *Chem. Rev*. **2008**, *108*, 3351. (p) Arcadi, A. *Chem. Rev*. **2008**, *108*, 3266. (q) Jiménez-Núñez, E.; Echavarren, A. M. *Chem. Rev*. **2008**, *108*, 3326. (r) Zhang, L.; Sun, J.; Kozmin, S. A. *Adv. Synth. Catal*. **2006**, *348*, 2271.

(11) Mastandrea, M. M.; Mellonie, N.; Giacinto, P.; Collado, A.; Nolan, S. P.; Miscione, G. P.; Bottoni, A.; Bandini, M. *Angew. Chem. Int. Ed*. **2015**, *54*, 14885.

(12) For the previous reports on the formation and identification of α-gold(I) enals/enones, see: (a) Manoni, E.; Daka, M.; Mastandrea, M. M.; Nisi, A. D.; Monari, M.; Bandini, M. *Adv. Synth. Catal*. **2016**, *358*, 1404. (b) Rocchigiani, L.; Jia, M.; Bandini, M.; Macchioni, A. *ACS Catal*. **2015**, *5*, 3911. (c) Faza, O. N.; López, C. S. *J. Org. Chem*. **2013**, *78*, 4929. (c) Yu, Y.; Yang, W.; Rominger, F.; Hashmi, S. K. *Angew. Chem. Int. Ed.* 2013, *52*, 7586.

(13) Reviews: (a) J. P. Michael, *Simple Indolizidine and Quinolizidine Alkaloids. In The Alkaloids: Chemistry and Biology*, Vol. 75; (Eds. H.-J Knölker), Academic Press: London, **2016**; Chapter 1, pp 1-498. (b) Sadowski, B.; Klajn, J.; Gryko, D. T.; *Org.*

Biomol. Chem. **2016**, *14*, 7804. (c) Sharma, V. Kumar, V. *Med. Chem. Res.* **2014**, *23*, 3593. (d) Michael, J. P. *Nat. Prod. Rep*. **2008**, *25*, 139.

(14) (a) Liu, R.-R.; Cai, Z.-Y.; Lu, C.-J.; Ye, S.-C.; Xiang, B.; Gao, J.; Jia, Y.-X. *Chem. Eur. J.* **2015**, *21*, 7057. (b) Liu, R.-R.; Cai, Z.-Y.; Lu, C.-J.; Ye, S.-C.; Xiang, B.; Gao, J.; Jia, Y.-X. *Org. Chem. Front*. **2015**, *2*, 226.

(15) Moist DCE was prepared by mixing equal volume of water and dry DCE. After layer separation, water content in DCE was measured to be 2% v/v (Karl Fischer titration).

(16) Wang, D.; Cai, R.; Sharma, S.; Jirak, J.; Thummanapelli, S. K.; Akhmedov, N. G.; Zhang, H.; Liu, X.; Petersen, J. L.; Shi, X. *J. Am. Chem. Soc.* **2012**, *134*, 9012.

(17) Wang, Y.; Zhang, P.; Qian, D.; Zhang, J. *Angew. Chem. Int. Ed*. **2015**, *54*, 14849.

(18) Ahlrichs, R.; Bar, M.; Haser, M. Horn, H.; Kolmel, C. *Chemical Physics Letters* **1989**, *162*, 165.

(19) Perdew, J. P.; Burke, K.; Ernzerhof, M. *Physical Review Letters* ***1996***, *77*, 3865.

(20) Eichkorn, K.; Treutler, O.; Öhm, H.; Häser, M.; Ahlrichs, R. *Chemical Physics Letters* **1995**, *240*, 283.

(21) Sierka, M.; Hogekamp, A.; Ahlrichs, R. *J. Chem. Phys.* **2003**, *118*, 9136.

(22) Klamt, A.; Schuurmann, G. *Journal of the Chemical Society, Perkin Transactions* **1993**, *2*, 799.

(23) S. Grimme, J. Antony, S. Ehrlich, H. Krieg, *The Journal of Chemical Physics* **2010**, *132*, 154104-01.

(24) Rauniyar, V.; Wang, Z. J.; Burks, H. E.; Toste F. D., *J. Am. Chem. Soc.* **2011**, *133*, 8486.

(25) Liu, R.-R.; Cai, Z.-Y.; Lu, C.-J.; Ye, S.-C.; Xiang, B.; Gao, J.; Jia, Yi-X. *Org. Chem. Front*. **2015**, *2*, 226.

Chapter 4: Design and Development of a Strategy for Accessing 3-Alkylchromones *via* Gold(I)-Catalysed Carbene Transfer Reactions

Table of Contents

4.1 Introduction.....167

4.2 Literature Reports on Direct C(sp^2)-H Insertion.....167

4.3 Present Work.....173

4.4 Results and Discussion 174

4.4.1 Optimization Studies..... 175

4.4.2 Scope of the Reaction 177

4.5 Mechanistic Studies 179

4.6 Modification of Product.....181

4.7 Conclusion 181

4.8 Experimental Procedures 182

4.9 Characterization Data of Selected Compounds 184

4.10 ORTEP Diagram:.....193

4.11 NMR Spectra of Selected Compounds: 194

4.12 References.....226

4.1 Introduction

The transition-metal-catalysed carbene transfer reactions from diazo compounds serves as a powerful tool in organic synthesis. For decades this chemistry was dominated by rhodium and copper based catalyst.[1] In recent years, there is an rapid development of Au-based catalyst for diazo compound decomposition and subsequent carbene transfer reactions to an organic substrates.[2] The reactivity observed in gold catalysis is unique and can provide selectivity of the reaction otherwise not possible by Rh/Cu catalysts. Moreover, the reaction can be conducted under open-flask conditions without needing syringe pumps which is rare in conventional carbene transfer chemistry. Nolan's research group was the first who reported the gold-catalysed carbene transfer from ethyl diazoacetate.[3] Subsequently, several research groups has successfully used gold catalysts to catalyse carbene transfer reactions,[4] such as N-H/O-H insertion,[4] cyclopropanation,[5] cyclopropenation,[6] cross coupling of diazo ester,[7] cycloaddition reactions,[8] rearrangement reaction,[9] enamine addition,[10] and enol silyl ether addition.[11] Although much progress has been made to explore carbene transfer reactions, the selective functionalisation of the C(sp^2)-H bond through carbene transfer reaction has remained unexplored.

4.2 Literature Reports on Direct C(sp^2)-H Insertion

Nolan and Pérez disclosed the reaction of ethyl diazo acetate with styrene[12] and naphthalene[13] under the gold catalysis which afforded the C(sp^2)-H insertion product along with the cyclopropanation product (Scheme 4.2.1, eq. 1 and eq. 2 respectively). However, other metal which is commonly used in the carbene transfer reactions such as copper complexes result into formation of cyclopropanation product exclusively. In 2005, the same author demonstrated that there was an predominant formation of C(sp^2)-H insertion product over Büchner reaction product when benzene was reacted with ethyl diazo acetate under the catalysis of IPrAuCl/$NaBAr^F{}_4$ (Scheme 4.2.1, eq. 3).

Scheme 4.2.1: Au(I) catalysed aromatic C(sp^2)-H functionilization

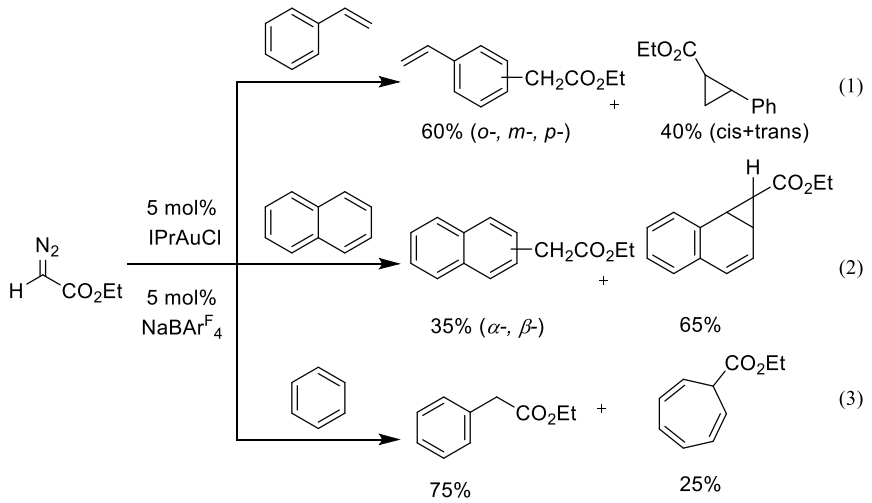

Pérez and co-workers found gold based precatalyst IPrAuBr$_3$ which after combination with NaBAr$^F_4$ gave C(sp^2)-H insertion product predominantly over Büchner reaction product (Scheme 4.2.2).[14] Although this gold catalyst result into formation of C(sp^2)-H insertion product exclusively, the regioselectivity of the product was found to be poor.

Scheme 4.2.2: Au(I) catalysed C(sp^2)-H functionilisation of toluene

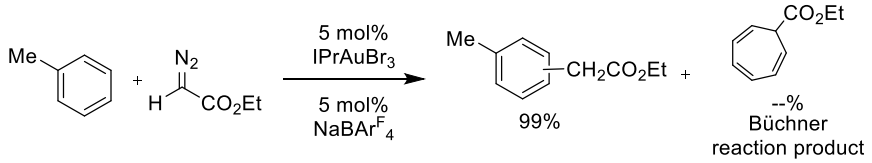

In the year of 2014, Liu, Zhang and co-workers demonstrated the first example of gold catalysed highly chemo- and regio-selective direct C(sp^2)-H functionlisation of unprotected phenols and *N*-acylanilines with diazo compounds (Scheme 4.2.3).[15] Choice of ancillary ligands on the Au center plays the crucial role to obtain the products in most chemo- and site-selective manner. Gold complexes with phosphine ligands showed the usual chemoselectivity similar to commonly used metal complexes such as copper and rhodium, on the other hand the gold complexes with phenyl phosphite ligands exhibited opposite chemoselectivity. Interestingly, reaction such as benzylic C-H insertion, cyclopropanation and *N-H* insertion which are pretty common in copper and rhodium were not observed under gold catalysis for the substrates containing methyl, allyl and amine groups.

Scheme 4.2.3: Au(I) catalysed site-selective C(sp^2)-H functionalisation of phenols

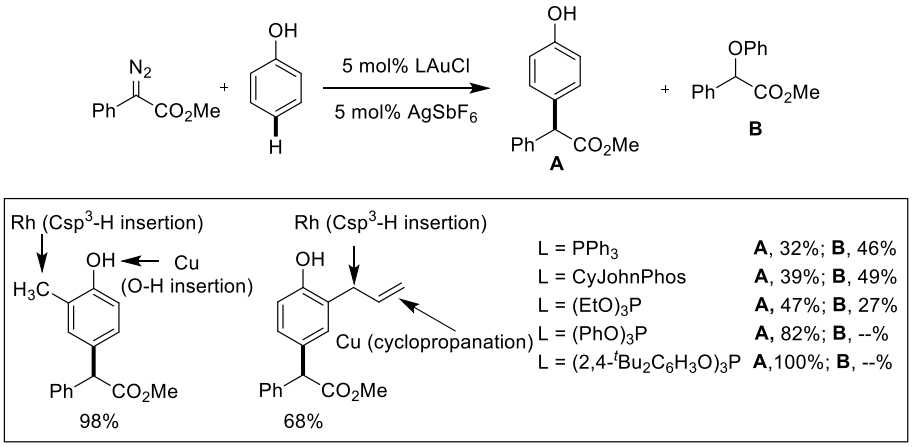

In the same year, Lan, Shi and co-workers reported the similar work for aromatic C(sp^2)-H functionalisation of electron rich aromatic compounds and 1,3 dicarbonyl compounds with diazo ester and diazo-oxindoles (Scheme 4.2.4).[16] Electron deficient phosphite (2,4-^{t}BuC$_6$H$_3$O)$_3$P ligand on Au center is responsible to convert the gold carbene into carbocation in which bond order of Au-C is 0.44. While phosphine ligand PPh$_3$ on Au center (bond order of Au-C is 0.49) showed the usual reactivity similar to copper and rhodium complexes.

Scheme 4.2.4: Au(I) catalysed C(sp^2)-H functionalisation of electron rich arenes

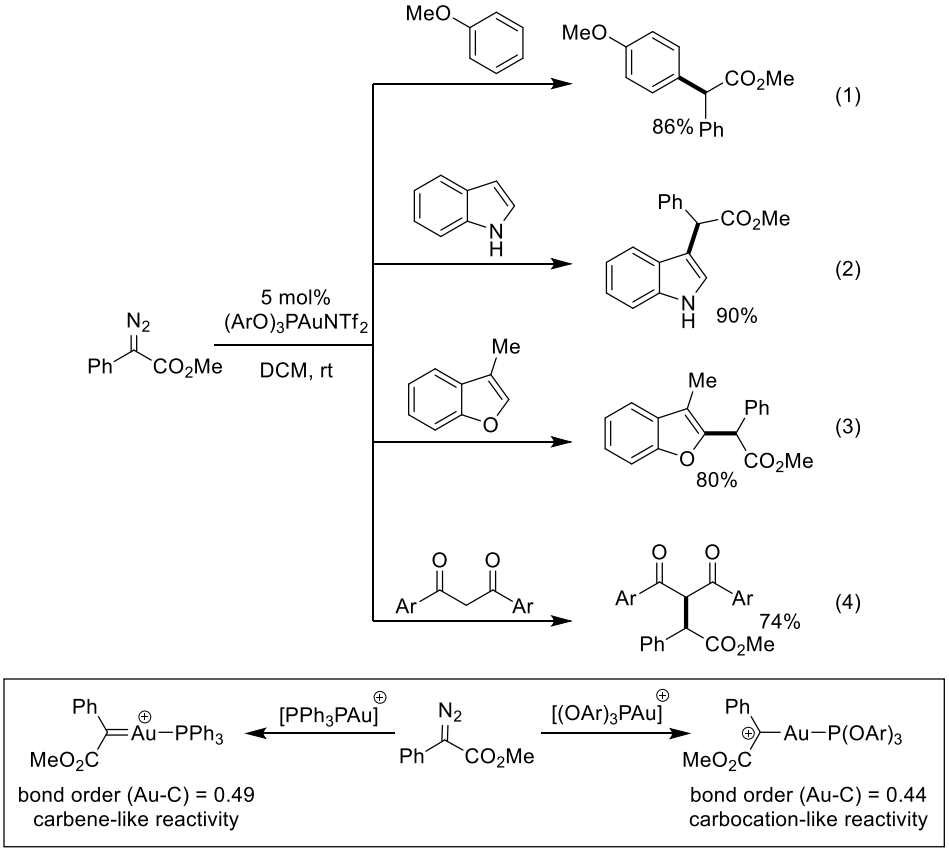

In 2012, Barlunga and López utilised the vinyl diazoacetates for the C(sp^2)-H functionalisation of substituted arenes and alkenes to obtain allyl substituted arenes and 1,5-dienes respectively (Scheme 4.2.5, eq. 1 and 2). The formed allyl carbocations from vinyl diazo acetates undergo nucleophilic addition by arenes and alkenes at γ position to access corresponding C(sp^2)-H insertion products. Later, the same group utilised this strategy in the C(sp^2)-H functionalisation of metallocenes including ferrocenes and ruthenocenes (Scheme 4.2.5, eq. 3).[17]

Scheme 4.2.5: Au(I) catalysed C(sp^2)-H functionalisation with vinyl diazo acetates

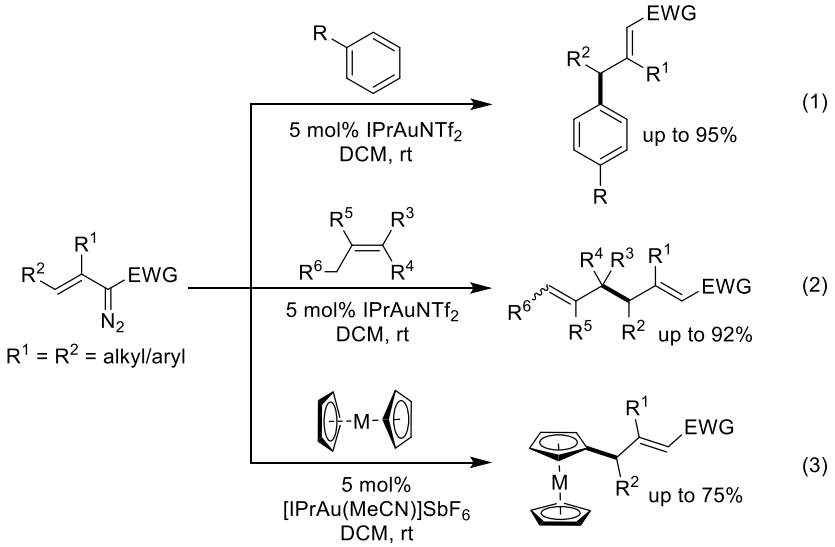

In the year 2016, Liu, zhang and co-workers published gold catalysed C-H functionalisation/5-*endo-dig* carbocyclisation of *o*-alkynylaryl diazo ester with electron rich aromatics to access indene derivatives (Scheme 4.2.6).[18] Mechanistically, electron rich arenes would reacts with electrophilic gold carbene generated through decomposition of *o*-alkynylaryl diazo ester to afford gold zwitterionic intermediate **A** which would underwent isomerisation to form gold enolate **B**. This gold enolate **B** was further underwent 5-*endo-dig* cyclisation with gold activated internal alkynes to furnish indene derivatives with regeneration of Au(I) catalyst.

Scheme 4.2.6: Au(I) catalysed sequential C(sp^2)-H functionalisation and 5-*endo-dig* carbocyclisation

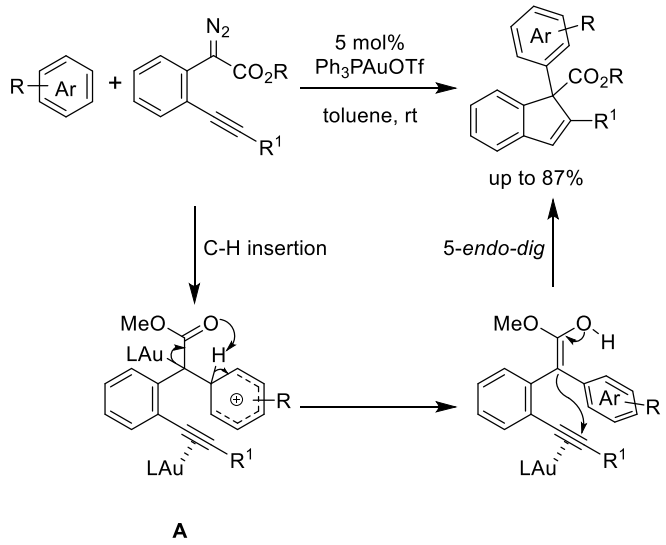

Recently, the same group successfully utilised this reaction condition for regio-selective C(sp^2)-H functionalisation of unactivated arenes with diazo esters contaning electron withdrawing substituents as induced groups on aryl rings (scheme 4.2.7).[19] In this protocol, electron withdrawing induced groups on phenyl ring has major role for chemo-and site-selective C(sp^2)-H bond functionalisation. These induced groups were further utilised for the various synthetic transformation to produce complex molecular scaffolds.

Scheme 4.2.7: Au(I) catalysed C(sp^2)-H functionalisation of unactivated arenes

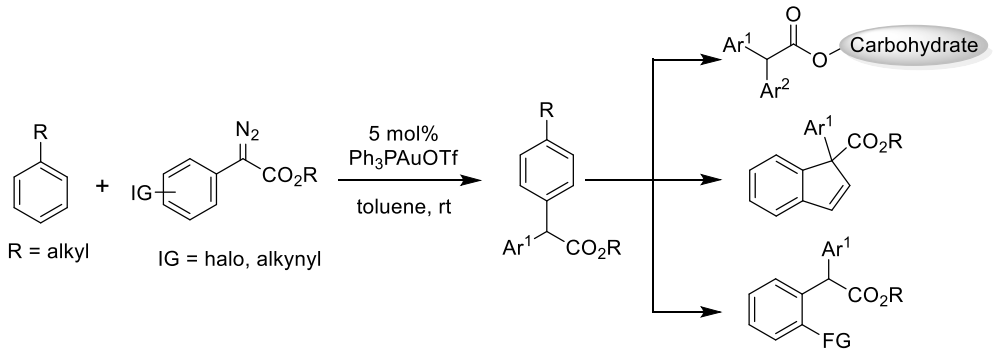

Li and co-workers published successful examples of chemo-selective C(sp^2)-H functionalisation of secondary enaminones with diazo-oxindoles under gold catalysis (scheme 4.2.8). Interestingly, *N-H* bond remains inert towards gold carbene, *in situ* generated through

decomposition of diazo-oxindoles. The products thus obtained, could be further converted into more complex molecules upon acid treatment.

Scheme 4.2.8: Au(I) catalysed C(sp^2)-H functionalisation of enaminones

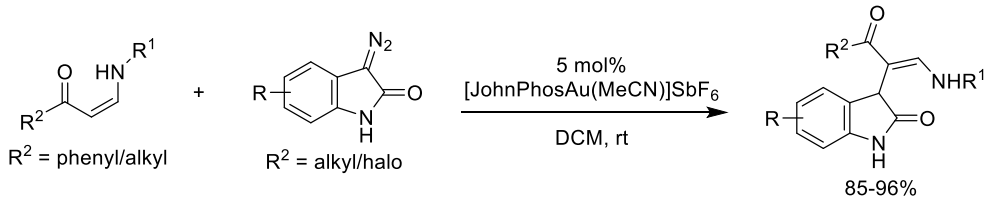

4.3 Present Work

Over the last few years, enaminones have emerged as powerful synthetic intermediates because of the ambident nucleophilic character of the enamine moiety and the ambident electrophilic character of the enone moiety. This dual character of enaminones was utilized by many researchers for accessing biologically important heterocycles by performing a variety of reactions.[20] As far as the reactions of enaminones with diazoketones are concerned, Kascheres is the first who utilized the carbene transfer strategy for accessing pyrroles (Scheme 1a).[21] In 2012, Park and co-workers demonstrated the carbenoid mediated cycloaddition reaction of enaminones with diazo compounds to obtain multiply substituted furans (Scheme 1b).[22] Soon after, Reddy *et al.* reported the method to access pyrroles *via* Cu(II)-catalyzed reaction between enaminones and diazoketones (Scheme 1c).[23] In this chapter, we described the reaction of *o*-hydroxyarylenaminones with diazo compounds under gold catalysis to obtain functionalized chromones[24] – the structural motif found in numerous natural products[25] and pharmaceutically important compounds[26] (Scheme 1d). The mechanism of the reaction was established by carefully conducted experimental and computational studies. Results indicated that the reaction triggers with the hydroxyl group assisted C-alkylation of enaminones. To the best of our knowledge, there exist only one report on the reaction of acyclic enamines with gold carbenes generated *in situ* from α-diazoesters in the presence of Au(I) and chiral Brönsted acid catalysts.[11a]

Scheme 4.2.1. Known and present work

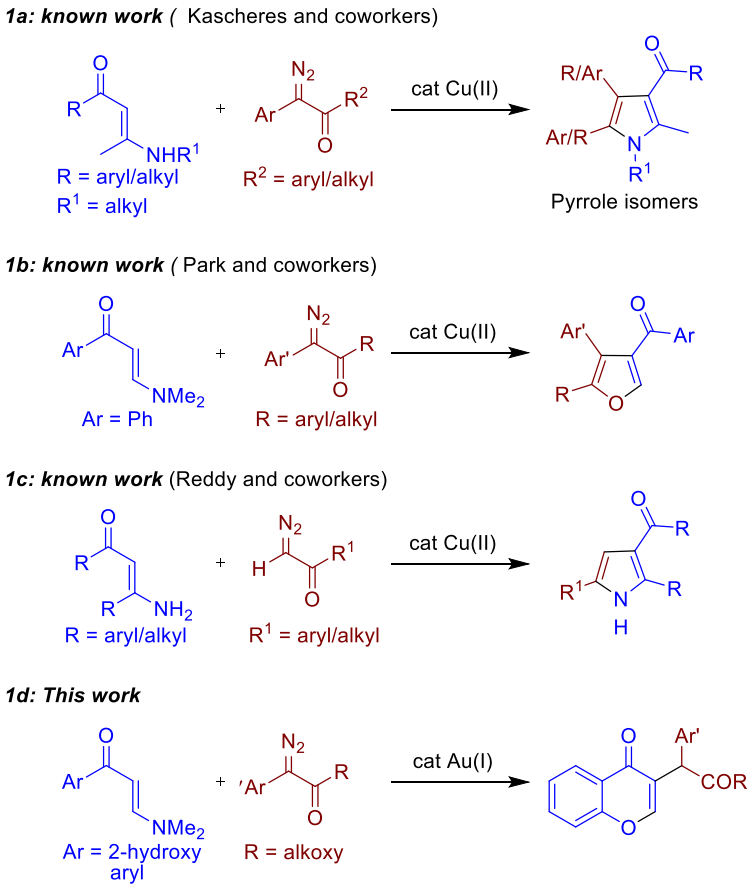

.

4.4 Results and Discussion

All reactions were carried out in oven dried sealed tube with magnetic stirring under argon atmosphere, unless otherwise specified. Dried solvents and liquid reagents were transferred by oven-dried syringes or hypodermic syringe cooled to ambient temperature. All experiments were monitored by analytical thin layer chromatography (TLC). TLC was performed on pre-coated silica gel plates. After elution, plate was visualized under UV illumination at 254 nm for UV active materials. Further visualization was achieved by staining $KMnO_4$ and charring on a hot plate. Solvents were removed in vacuo and heated with a water bath at 40 °C. Silica gel finer than 200 mesh was used for column chromatography. Columns

were packed as slurry of silica gel in pet ether and equilibrated with the appropriate solvent mixture prior to use. The compounds were loaded neat or as a concentrated solution using the appropriate solvent system. The elution was assisted by applying pressure with an air pump. Melting points are uncorrected and recorded using digital Büchi Melting Point Apparatus B-540. ^{1}H NMR spectra and ^{13}C NMR spectra were recorded on Bruker AV, 400/500 MHz spectrometers in appropriate solvents using TMS as internal standard or the solvent signals as secondary standards and the chemical shifts are shown in δ scales. Multiplicities of ^{1}H NMR signals are designated as s (singlet), d (doublet), dd (doublet of doublet), t (triplet), m (multiplet)… etc. HRMS (ESI) data were recorded on a Thermo Scientific Q-Exactive, Accela 1250 pump. Single-crystal data was collected on a Bruker D8 Venture Kappa Duo Photon II CPAD diffractometer equipped with incoatech multilayer mirrors optics.

4.4.1 Optimization Studies

At the outset, we utilized (*E*)-3-(dimethylamino)-1-(2-hydroxyphenyl) prop-2-en-1-one (**1a**) and methyl phenyldiazoacetate (**2a**) as model substrates to identify the optimal reaction conditions. The reactions were initially performed in dichloromethane at 25 °C. First, the utilization of $Ph_3PAuNTf_2$ (5 mol %) furnished methyl 2-(4-oxo-4H-chromen-3-yl)-2-phenylacetate (**3a**) in 14% yield with formation of undesired 4H-chromen-4-one 4 (Table 4.4.1.1, entry 1). Next, variety of gold catalysts were examined (entry 2-6), gratifyingly, $XPhosAuNTf_2$ was found to be best catalyst giving **3a** in 43% yield along with **4** in 11% yield (entry 6). The yield of reaction was enhanced remarkably when reaction was run at 60 ºC, instead of 25 ºC. Accordingly, treatment of o-hydroxyarylenaminones **1a** with **2a** in the presence of 5 mol % $XPhosAuNTf_2$ in DCM at 60 ºC afforded **3a** in 62% yield (entry 7). Next, various silver salts were screened in combination with XPhosAuCl. The use of $AgSbF_6$ and $AgBF_4$ did not improve the yield of the reaction (entries 8 and 9). However, the use of AgOTf furnished **3a** in 76% yield (entry 10). Noteworthily, undesired **4** was not obtained at all under this conditions. Switching the solvent to DCE, tetrahydrofuran, toluene and acetonitrile did not produce any remarkable change to the reaction outcome. The catalytic efficiency of other catalysts, which are conventionally known for carbene transfer reactions, was investigated. Accordingly, when $Cu(ACN)_4BF_4$ was used as a catalyst, **3a** was obtained only in 36 % yield (entry 11). On the other hand, the use of $Rh_2(OAc)_2$ did not give **3a**; instead, decomposition of **2a** was noticed (entry 12). Further,

lowering of catalyst loading to 3 mol % has detrimental effect on the yield of the reaction (entry 13). In the absence of XPhosAuOTf, no product was obtained, demonstrating that the gold catalyst is necessary for the reaction to occur (entry 14).

Scheme 4.4.1.1 Optimization of the reaction conditions

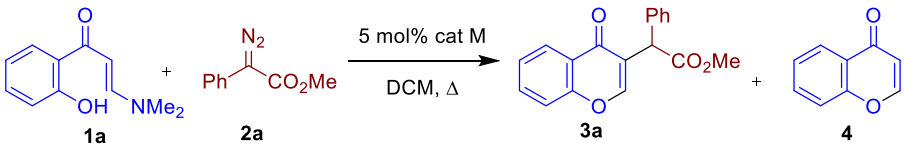

Entry no.	cat M 5 mol %	AgX 5mol %	T (° C)	yields (%)[b]	
				3a	**4**
1	PPh_3AuCl	$AgNTf_2$	25	14	30
2	IPrAuCl	$AgNTf_2$	25	16	25
3	JohnPhosAuCl	$AgNTf_2$	25	--	22
4	CyJohnPhosAuCl	$AgNTf_2$	25	--	29
5	BrettPhosAuCl	$AgNTf_2$	25	26	28
6	XPhosAuCl	$AgNTf_2$	25	43	11
7	XPhosAuCl	$AgNTf_2$	60	62	15
8	XPhosAuCl	$AgSbF_6$	60	51	13
9	XPhosAuCl	$AgBF_4$	60	45	12
10	**XPhosAuCl**	**AgOTf**	**60**	**76**	--[c]
11[d,e]	$Cu(ACN)_4BF_4$	-	30	36	--[c]
12[d,e]	$Rh_2(OAc)_2$	-	30	--	--[c]
13[f]	XPhosAuCl	AgOTf	60	59	--[c]
14	-	-	60	00	00

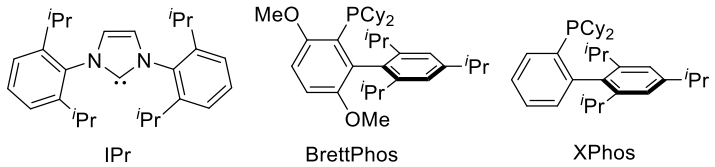

[a]Reaction conditions: 0.150 mmol **1a**, 0.23 mmol **2a**, 5 mol % Au(I) catalyst and 5 mol % Ag(I) catalyst, DCM (1 mL), 36-40 h. [b]Isolated yields (based on **1a**). [c]The undesired **4** was not observed. [d]Controlled addition of **2a** (0.23 mmol) in dry DCM (0.5 mL) was performed via syringe pump over 1 h. [e]Decomposition of **2a** was observed within 6-8 h. [f]3 mol % XPhosAuOTf was used.

4.4.2 Scope of the Reaction

With the effective catalyst system identified, the substrate scope of *o*-hydroxyarylenaminones was explored. As revealed in Table 4.4.2.1, a wide range of *o*-hydroxyarylenaminones having different substitution pattern on phenyl ring gave 3-alkyl chromones **3**. For instance, substrates bearing alkyl and aryl substituents such as -Me and -Ph gave an access to 3-alkyl chromone **3b** and **3c** in 76 and 73% yield, respectively. Various halo substituents on the phenyl ring did not affect the yield of the reaction (**3d-3f**). The halo-substituted chromones can serve as a versatile synthon enabling the introduction of various functional groups through metal catalyzed cross-coupling reactions. The X-ray crystallography data for **3d** (**5i**, vide infra) has been obtained which unequivocally confirms the structure. It was found that the substrate with electron withdrawing substituents (acyl, -CN, -NO2) at the para position of phenol groups gave lower yields (3h-3j). On the other hand, substrates bearing electron donating substituent (-OMe) at para position of phenol group gave comparatively higher yield (**3g**, 80%). However, the *o*-hydroxyarylenaminones possessing substituents at the para-position of the keto group gave the desired product in moderate to good yields (**3k**-**3m**, 64-73%). Even the di-substituted o-hydroxyarylenaminones gave the corresponding 3-alkyl chromones in good yields (**3n** and **3o**, 89 and 67%). It should be noted that the reaction of the *o*-hydroxyarylenaminones equipped with alkyne substituent gave 3-alkyl chromone **3p** without formation of any side product via cyclopropenation.7 Fused analogue of chromone (cf. **3q**) was also obtained in 83% yield, when respective o-hydroxyarylenaminones were subjected to the standard reaction conditions. The substrates bearing heteroaromatic ring produced **3r** in 71%

yield. Notably, a product which could be a result of C3-functionalization of furans was not obtained at all.

Table no. 4.4.2.1 Reaction scope with enaminones

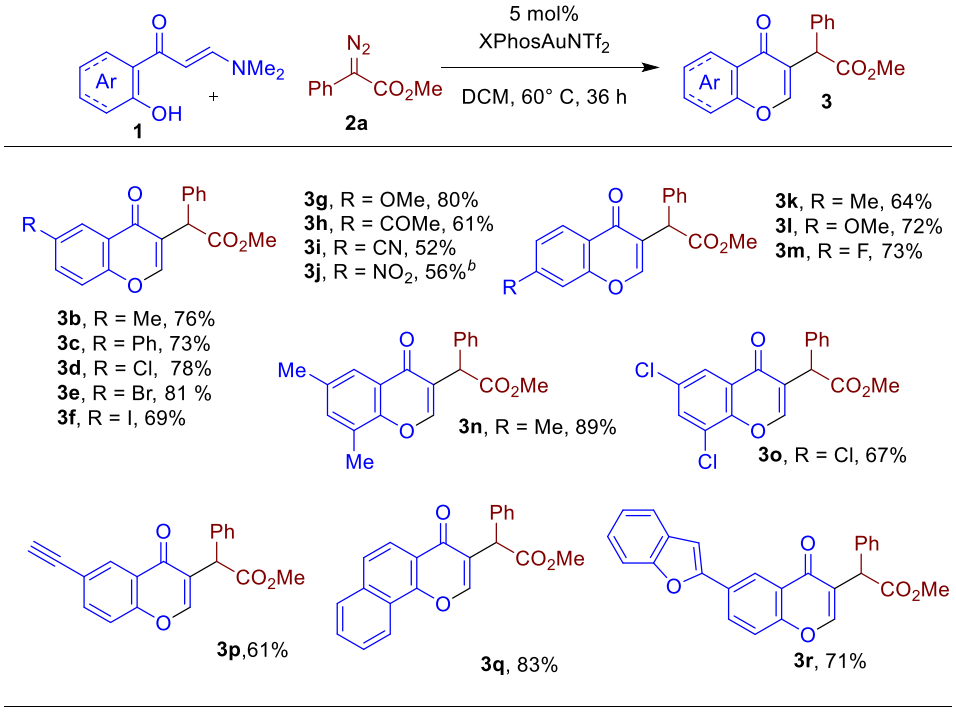

[a]Reaction conditions: 0.150 mmol 1, 0.225 mmol 2, 5 mol% XPhosAuOTf, DCM (1 mL), 36-40 h. [b]Reaction was completed within 12 h.

Next, a variety of diazo esters were reacted with **1a** to afford moderate to excellent yields of 3-alkyl chromones in 40-75% yields (Table.2.2.1) . As expected, reactions of diazo ester comprising ethyl, tert-butyl, and benzyl groups instead of the methyl group maintained same reaction profile giving **5a-5c** in good yields (61-75%). Diazo compound bearing alkyl substituent such as -Me on the aromatic group reacted smoothly to give **5d** in 82% yield. Morever, halo substituents had no significant effect on the outcome of the reaction giving **5e-5i** in yields ranging from 51-62%. The reaction of the diazo ester bearing a bulkier naphth-1-yl group probably succumbed to its steric effects giving a rather lower yield of the desired 3-alkyl chromone **5j** (40%). In addition to α-diazo esters, other diazo com-pounds including 3-diazo-oxindole, dimethyl-2-diazomalonate and 2-diazo-1,2-diphenylethan-1-one were also examined. Out of which diazo-oxindole underwent the desired transformation to obtain **5k** in 74% yield; whereas, dimethyl-2-diazomalonate and 2-diazo-1,2-diphenylethan-1-one failed to produce corresponding products.

Table no. 4.4.2.2 Reaction scope with diazo compounds

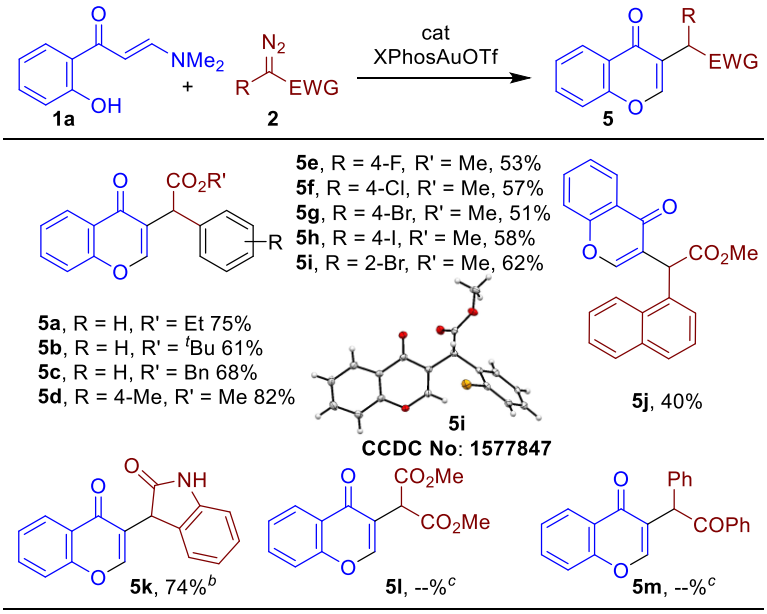

[a]Reaction conditions: 0.150 mmol **1a**, 0.375 mmol **2**, 5 mol% XPhosAuOTf, DCM (1 mL), 36-40 h. [b]Reaction was completed within 8 h. cThe starting material **1a** was recovered quantitatively.

4.5 Mechanistic Studies

To understand the mechanistic insights, a few control expe-riments were conducted (Scheme 2). The reaction of phenylenaminone **6** with **2a** was performed under the standard reaction conditions. However, the expected product **7** was not obtained at all (Scheme 4.5.1, eq 1). Similarly, the anticipated product **9** was not obtained when benzyl protected substrate **8** reacted with **2a** (eq 2). These experiments led us to conclude that a possible assistance for the C-alkylation of enaminones is being lent by the hydroxyl group on aryl moiety. It is also possible that **4** would be generated first which would undergo alkylation with **2a** in the presence of a gold catalyst. However, the failure of the reaction of **4** under standard reaction condi-tions (eq 3, left side) unequivocally ruled out this possibil-ity. Alternatively, it was thought the reaction might trigger through the O-alkylation in **1a** *via* gold-catalyzed carbene transfer reaction to produce intermediate **10** which would then spontaneously undergo 1,3 alkyl shift followed by loss of N, N-dimethylamine to form **3a**. To examine this mechanistic pathway, substrate **10** was prepared by NaH mediated reaction of **1a** with methyl 2-bromo-2-phenylacetate in DMF. However,

reaction of **10** under the optimized reaction conditions failed to produce **3a** clearly ruling out this possibility as well (eq 3, right side).

Scheme 4.5.1: Mechanistic studies

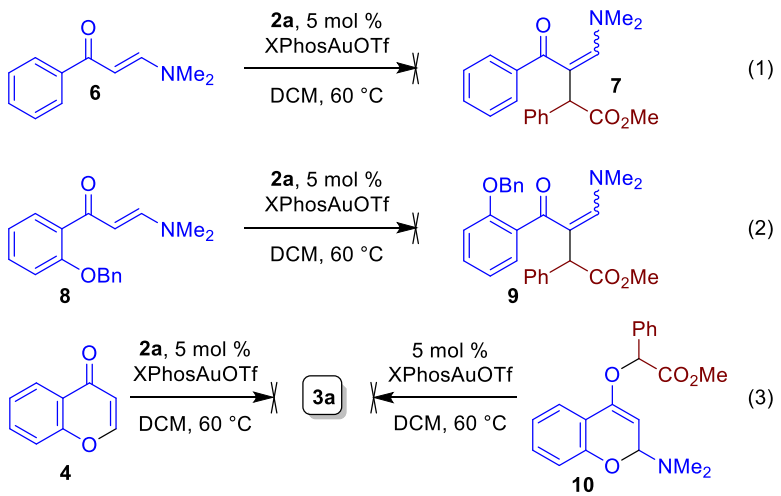

Based on the control experiments, a plausible mechanism for the present transformation is proposed in Scheme 3. The reaction of **2a** with gold complex is liable to give the gold carbene species I. *o*-Hydroxyarylenaminones **1a** would then undergo hydroxyl group assisted C-alkylation with gold carbene **I**, as depicted in **II**, to produce intermediate **III**. The intermediate **III** would be poised to undergo intramolecular cyclization to generate cyclic aminal intermediate **IV** which after spontaneous loss of N,N-dimethylamine would form **3a** with the regeneration of active gold catalyst.

Scheme 4.5.2 A plausible reaction mechanism

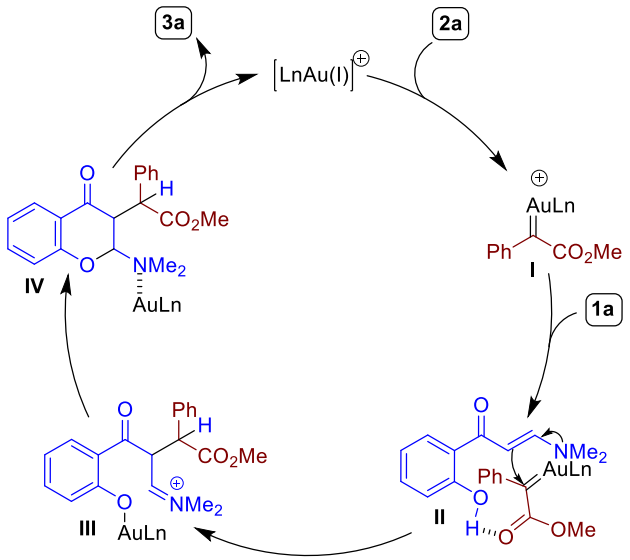

Based on literature report and control experiments, a plausible mechanism of the reaction is proposed in scheme 3.4.2, path a. The reaction of **2a** with gold complex is liable to give the gold carbene species **I**. *o*-hydroxyarylenaminones **1a** would then undergo hydroxyl group assisted C-alkylation with gold carbene **I** to produce intermediate **III** which after intramolecular cyclisation delivered an intermediate **IV**. Finally, protodeauration and the spontaneous loss of N, N-dimethylamine would took place to generate 3-alkylchromone **3a**.

4.6 Modification of Product

In order to demonstrate the synthetic potential of the reaction, the intramolecular Heck reaction[27] of **5i** under $Pd(OAc)_2$/JohnPhos catalysis in the presence of KOAc in DMF at 110 °C was conducted (Scheme 5). Pleasingly, biologically important rigid flavone **11** was obtained in 66% yield.[28]

Scheme 4.6.1 Heck Reaction of 5i

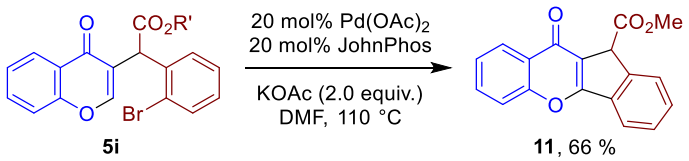

4.7 Conclusion

This chapter describes an efficient method for the synthesis of 3-alkyl chromones *via* gold-catalysed C(sp^2)-H functionalisation of *o*-hydroxyarylenaminones with diazo compounds.

Outcome of the carefully conducted experiments led us to propose hydroxyl group assisted alkylation of enaminones with α-diazoesters a transient key step.

4.8 Experimental Procedures

General Procedures for the Synthesis of *o*-Hydroxyarylenaminones

Hydroxyarylenaminones **1a-1r** were reported in the literature and prepared according to the known procedure.[24d]

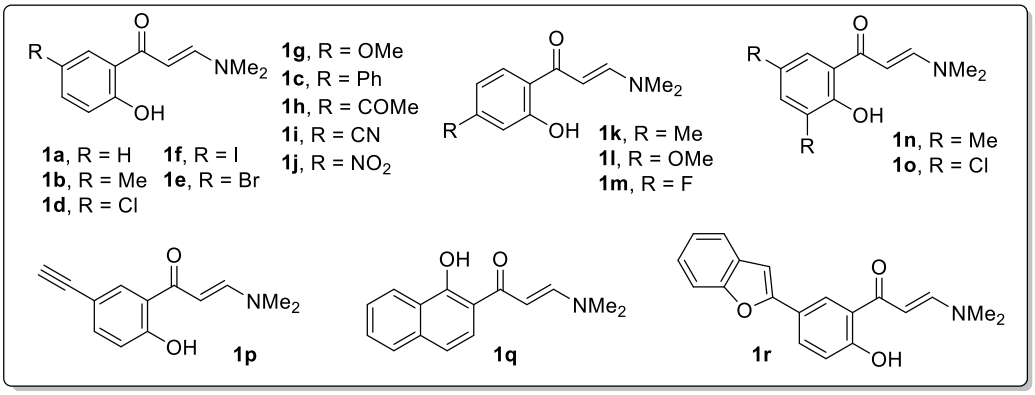

General Procedure for the Synthesis of Diazo Compounds

The syntheses of diazo compounds (**2a-2m**) were achieved following literature known procedure.[29]

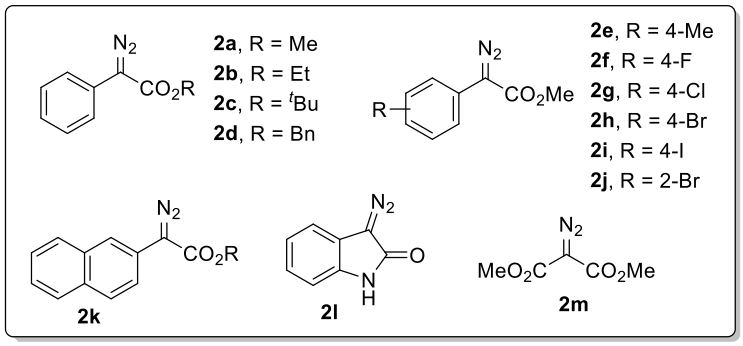

Procedure for the Synthesis of 3-Alkyl Chromones (3)

Oven dried sealed tube equipped with a stirring bar was charged with XPhosAuCl (5 mol %, 10.6) and AgOTf (5 mol %). DCM (1 mL) was added to the catalyst mixture and stirred for 5 minutes. *o*-hydroxyarylenaminones (**1**) (0.15 mmol, 1.0 equiv) was then added to the reaction mixture. With continuous stirring, diazo compound (**2**) (0.225 mmol, 1.5 equiv), in 1 mL DCM, was added drop wise manually over 5 min at room temperature. The reaction was allowed to stir at 60 °C for 36-40 h until and unless noted in the specific examples. The reaction mixture was then concentrated and resulting residue was purified by column chromatography (silica gel, EtOAc/pet. ether) to afford analytically pure compounds.

Procedure for the Synthesis of 10:

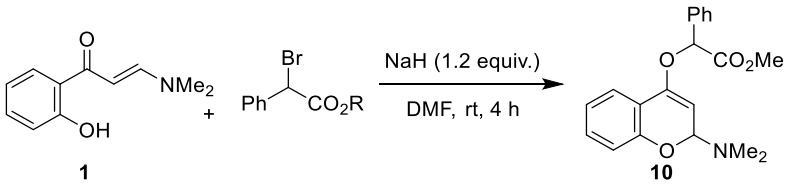

To a solution of *o*-hydroxyarylenaminones (**1a)** (500 mg, 2.61 mmole) in DMF (5 mL) was added NaH (60% w/w dispersion in oil) (125 mg, 3.12 mmole) and the resulting mixture was stirred at 25 °C for 15 minutes. Methyl α-bromophenylacetate (658 mg, 2.87 mmole) was then added and the mixture was stirred for an additional 4 hours. The reaction mixture was then quenched with cold aqueous NH_4Cl solution and the product was extracted with ethyl acetate. The ethyl acetate layer was washed with water, brine solution, dried over sodium sulfate and concentrated under reduced pressure to afford **6a** (375 mg, 65%, dr = 7:1) as yellow thick liquid.

Procedure for the Synthesis of 6b:

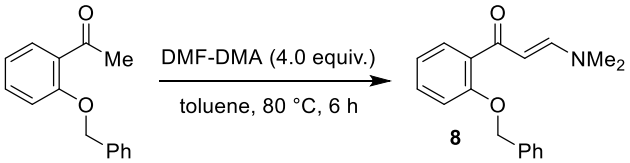

An oven dried sealed tube equipped with a stirring bar, filled with 1-(2-(benzyloxy) phenyl)ethan-1-one[30] (2.21 mmol), followed by N,N-Dimethylformamide dimethyl acetal (8.84 mmol) in toluene (4 mL). The reaction was allowed to stir at 80 °C for 6-8 h until the complete conversion of starting material as monitored by TLC. The reaction mixture was then concentrated and was purified by column chromatography (silica gel, EtOAc/pet. ether) to afford the desired product **6b** (528 mg, 85%) as yellow solid.

General Procedure for Modification of Products

Heck Reaction of 5i:

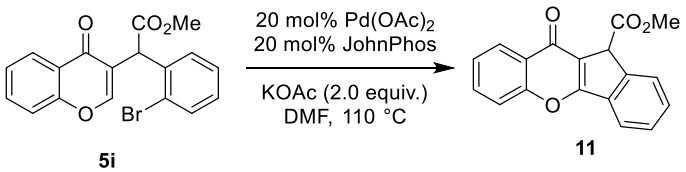

A 25 mL two-necked round bottom flask equipped with magnetic stirrer was charged with **5i** (0.05 mmol) followed by $Pd(OAc)_2$ (20 mmol%), JhonPhos (20 mmol%) and KOAc (0.1mmol). The flask was evacuated and back-filled with N_2. Afterward, 5 mL of anhydrous DMF was added *via* syringe. After the reaction mixture was stirred at 110 °C for 40 min, it was allowed to cool to room temperature. The reaction mixture was partitioned between EtOAc and brine. The separated organic layer was washed with brine (5 mL×3), dried over anhydrous Na_2SO_4 and evaporated under vacuum. The crude product thus obtained, was purified over silica gel chromatography using a mixture of ethyl acetate/petroleum ether (20:80) as eluent to give the product **7** (12 mg, 65%) as white solid.

4.9 Characterization Data of Selected Compounds

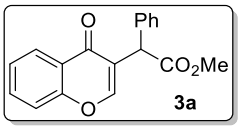

3a: Off white solid; yield = 36 mg, 82%; R_f = 0.5 (ethyl acetate/petroleum ether = 20/80; mp = 097-100 °C; **^{1}H NMR (500 MHz, $CDCl_3$)** δ = 8.24 (dd, *J* = 1.4, 8.0 Hz, 1 H), 7.70 - 7.64 (m, 1 H), 7.61 (d, *J* = 1.1 Hz, 1 H), 7.45 - 7.37 (m, 6 H), 7.37 - 7.32 (m, 1 H), 5.23 - 5.16 (m, 1 H), 3.77 (s, 3 H); **^{13}C NMR (125 MHz, $CDCl_3$)** δ = 176.7, 172.2, 156.3, 154.8, 135.5, 133.8, 129.1, 128.7, 127.9, 126.0, 125.2, 123.8, 123.5, 118.0, 52.6, 47.7; **HRMS** (ESI) calcd for $C_{18}H_{14}O_4Na$ $[M+Na]^+$ 317.0784, found 317.0783.

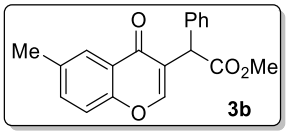

3b: Yellow solid; yield = 35 mg, 76%; R_f = 0.5 (ethyl acetate/petroleum ether = 20/80; mp = 098-101 °C; **^{1}H NMR** (**500 MHz, $CDCl_3$**) δ = 8.01 (s, 1 H), 7.58 (s, 1 H), 7.49 - 7.45 (m, 1 H), 7.44 - 7.39 (m, 1 H), 7.39 - 7.36 (m, 4 H), 7.36 - 7.29 (m, 2 H), 5.19 (s, 1 H), 3.77 (s, 3 H), 2.45 (s, 3 H); **^{13}C NMR (125 MHz, $CDCl_3$)** δ = 176.7, 172.2, 154.7, 135.6, 135.1, 135.0, 129.0, 128.7, 127.9, 126.6, 125.2,

123.6, 123.2, 117.8, 52.5, 47.8, 20.9; **HRMS** (ESI) calcd for $C_{19}H_{16}O_4Na$ $[M+Na]^+$ 331.0941, found 331.0939.

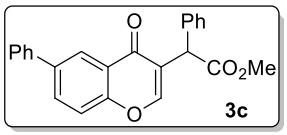

3c: Yellow solid; yield = 40 mg, 73%; R_f = 0.4 (ethyl acetate/petroleum ether = 20/80; mp = 131-133 °C; **^{1}H NMR (500 MHz, CDCl$_3$)** δ = 8.46 (d, *J* = 2.3 Hz, 1 H), 7.91 (dd, *J* = 2.3, 8.7 Hz, 1 H), 7.71 - 7.59 (m, 3 H), 7.54 - 7.45 (m, 3 H), 7.44 - 7.38 (m, 5 H), 7.38 - 7.33 (m, 1 H), 5.22 (s, 1 H), 3.79 (s, 3 H); **^{13}C NMR (125 MHz, CDCl$_3$)** δ = 176.7, 172.2, 155.6, 154.8, 139.3, 138.3, 135.5, 132.7, 129.1, 129.0, 128.7, 127.9, 127.8, 127.1, 123.8, 123.8, 123.6, 118.5, 77.3, 76.7, 52.6, 47.8; **HRMS** (ESI) calcd for $C_{20}H_{18}O_4Na$ $[M+Na]^+$ 345.1097, found 345.1097.

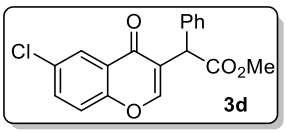

3d: Yellow solid; yield = 38 mg, 78%; R_f = 0.6 (ethyl acetate/petroleum ether = 20/80; mp = 141-144 °C; **^{1}H NMR (500 MHz, CDCl$_3$)** δ = 8.19 (d, *J* = 1.9 Hz, 1 H), 7.64 - 7.56 (m, 2 H), 7.45 - 7.31 (m, 6 H), 5.17 (s, 1 H), 3.77 (s, 3 H); **^{13}C NMR (125 MHz, CDCl$_3$)** δ = 175.5, 172.0, 155.0, 154.6, 135.3, 134.0, 131.2, 129.2, 128.7, 128.0, 125.4, 124.4, 123.9, 119.8, 52.6, 47.7; **HRMS** (ESI) calcd for $C_{18}H_{13}O_4ClNa$ $[M+Na]^+$ 351.0395, found 351.0392.

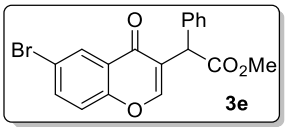

3e: Yellow solid; yield = 45 mg, 81%; R_f = 0.3 (ethyl acetate/petroleum ether = 20/80; mp = 148-151 °C; **^{1}H NMR (500 MHz, CDCl$_3$)** δ = 8.35 (br. s., 1 H), 7.74 (d, *J* = 8.4 Hz, 1 H), 7.60 (s, 1 H), 7.45 - 7.29 (m, 6 H), 5.17 (s, 1 H), 3.77 (s, 3 H); **^{13}C NMR (125 MHz, CDCl$_3$)** δ = 175.4, 172.0, 155.0, 154.9, 136.8, 135.2, 129.2, 128.7, 128.6, 128.0, 124.8, 124.0, 120.0, 118.6, 52.7, 47.7; **HRMS** (ESI) calcd for $C_{13}H_{13}O_4BrNa$ $[M+Na]^+$ 394.9889, found 394.9890.

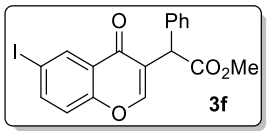

3f: Yellow solid; yield = 43 mg, 69%; R_f = 0.6 (ethyl acetate/petroleum ether = 20/80; mp = 155-158 °C; **^{1}H NMR (500 MHz, CDCl$_3$)** δ = 8.56 (br. s., 1 H), 7.92 (d, *J* = 8.4 Hz, 1 H), 7.60 (s, 1 H), 7.43 - 7.31 (m, 5 H), 7.19 (d, *J* = 8.4 Hz, 1 H), 5.16 (s, 1 H), 3.77 (s, 3 H); **^{13}C NMR (125 MHz, CDCl$_3$)** δ = 175.2, 172.0, 155.7, 154.9, 142.3, 135.3, 135.0, 129.2, 128.7, 128.0, 125.1, 124.2, 120.1, 89.0, 52.6, 47.7; **HRMS** (ESI) calcd for $C_{18}H_{13}O_4INa$ $[M+H]^+$ 442.9751, found 442.9748.

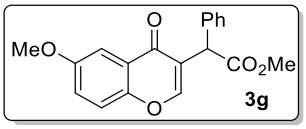

3g: Yellow solid; yield = 39 mg, 80%; R_f = 0.4 (ethyl acetate/petroleum ether = 20/80; mp = 130-133 °C; **^{1}H NMR (500 MHz, CDCl$_3$)** δ = 7.66 - 7.49 (m, 2 H), 7.42 - 7.35 (m, 5 H), 7.35 - 7.32 (m, 1 H), 7.27 - 7.22 (m, 1 H), 5.19 (s, 1 H), 3.89 (s, 3 H), 3.77 (s, 3 H); **^{13}C NMR (125 MHz, CDCl$_3$)** δ = 176.5, 172.3, 156.9, 154.6, 151.2, 135.6, 129.1, 128.7, 127.9, 124.0, 123.0, 119.5, 104.8, 55.9, 52.6, 47.9; **HRMS** (ESI) calcd for $C_{19}H_{16}O_5Na$ $[M+H]^+$ 347.0890, found 347.0885.

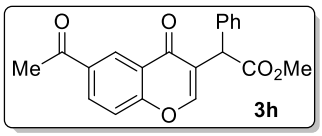

3h: Yellow solid; yield = 31 mg, 61%; R_f = 0.5 (ethyl acetate/petroleum ether = 20/80; mp = 139-141 °C; **^{1}H NMR (400 MHz, CDCl$_3$)** δ = 8.79 (s, 1 H), 8.31 (d, *J* = 8.5 Hz, 1 H), 7.63 (s, 1 H), 7.50 (d, *J* = 8.5 Hz, 1 H), 7.45 - 7.32 (m, 5 H), 5.18 (s, 1 H), 3.78 (s, 3 H), 2.69 (s, 3 H); **^{13}C NMR (100 MHz, CDCl$_3$)** δ = 196.4, 176.3, 171.9, 158.8, 155.0, 135.0, 133.9, 132.8, 129.2, 128.7, 128.1, 127.6, 124.5, 122.9, 118.9, 52.7, 47.7, 26.6; **HRMS** (ESI) calcd for $C_{20}H_{13}O_5$ $[M+H]^+$ 359.0890, found 359.0909.

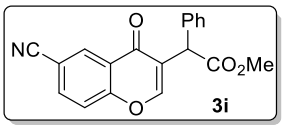

3i: Yellow solid; yield = 25 mg, 52%; R_f = 0.4 (ethyl acetate/petroleum ether = 20/80; mp = 149-151 °C; **^{1}H NMR (400 MHz, CDCl$_3$)** δ = 8.56 (s, 1 H), 7.88 (d, *J* = 8.5 Hz, 1 H), 7.65 (s, 1 H), 7.54 (d, *J* = 8.5 Hz, 1 H), 7.46 - 7.31 (m, 5 H), 5.17 (s, 1 H), 3.77 (s, 3 H); **^{13}C NMR (100 MHz, CDCl$_3$)** δ = 174.9, 171.7, 157.9, 155.1, 136.0, 134.8, 131.8, 129.3, 128.6, 128.2, 124.9, 123.8, 119.8, 117.4, 109.5, 52.7, 47.6; **HRMS** (ESI) calcd for $C_{19}H_{13}O_4NNa$ $[M+H]^+$ 342.0737, found 342.0731.

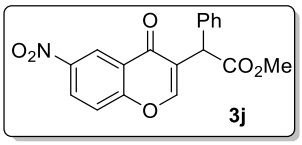

3j: Yellow solid; yield = 28 mg, 56%; R_f = 0.4 (ethyl acetate/petroleum ether = 20/80; mp = 156-158 °C; **^{1}H NMR (500 MHz, CDCl$_3$)** δ = 9.10 (br. s., 1 H), 8.49 (d, *J* = 9.2 Hz, 1 H), 7.67 (s, 1 H), 7.59 (d, *J* = 9.2 Hz, 1 H), 7.45 - 7.34 (m, 6 H), 5.18 (s, 1 H), 3.78 (s, 3 H); **^{13}C NMR (125 MHz, CDCl$_3$)** δ = 175.3, 171.7, 158.9, 155.1, 144.7, 134.8, 129.3, 128.6, 128.2, 128.1, 124.7, 123.5, 122.8, 119.9, 52.8, 47.5; **HRMS** (ESI) calcd for $C_{18}H_{13}O_6NNa$ $[M+H]^+$ 362.0635, found 362.0629.

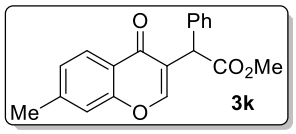

3k: Yellow solid; yield = 29 mg, 64%; R_f = 0.5 (ethyl acetate/petroleum ether = 20/80; mp = 92-94 °C; **^{1}H NMR (500 MHz, CDCl$_3$)** δ = 8.10 (d, *J* = 6.9 Hz, 1 H), 7.49 (br. s., 1 H), 7.38 (br. s., 5 H), 7.21 (br. s., 2 H), 5.14 (br. s., 1 H), 3.77 (br. s., 3 H), 2.47 (br. s., 3 H); **^{13}C NMR (125 MHz, CDCl$_3$)** δ = 176.7, 172.3, 156.3, 154.5, 145.2, 135.1, 129.1, 128.7, 127.9, 126.7, 125.5, 123.5, 121.0, 117.7, 52.7, 47.8, 21.8; **HRMS** (ESI) calcd for $C_{19}H_{16}O_4Na$ $[M+Na]^+$ 331.0941, found 331.0953.

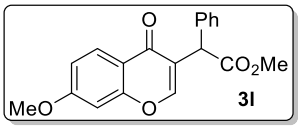

3l: Yellow solid; yield = 35 mg, 72%; R_f = 0.5 (ethyl acetate/petroleum ether = 20/80; mp = 136-138 °C; **^{1}H NMR (500 MHz, CDCl$_3$)** δ = 8.13 (d, *J* = 9.2 Hz, 1 H), 7.51 (s, 1 H), 7.42 - 7.36 (m, 4 H), 7.34 (d, *J* = 3.8 Hz, 1 H), 7.01 - 6.91 (m, 1 H), 6.82 - 6.73 (m, 1 H), 5.17 (s, 1 H), 3.89 (s, 3 H), 3.76 (s, 3 H); **^{13}C NMR (125 MHz, CDCl$_3$)** δ = 175.9, 172.3, 164.1, 158.0, 154.3, 135.6, 129.0, 128.7, 127.8, 127.4, 123.7, 117.4, 114.6, 100.0, 55.8, 52.5, 47.7; **HRMS** (ESI) calcd for $C_{19}H_{16}O_5Na[M+H]^+$ 347.0890, found 347.0883.

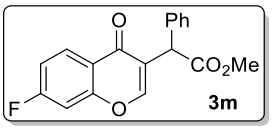

3m: Yellow solid; yield = 34 mg, 73%; R_f = 0.5 (ethyl acetate/petroleum ether = 20/80; mp = 072-074 °C; **^{1}H NMR (500 MHz, CDCl$_3$)** δ = 8.25 (dd, *J* = 6.3, 8.6 Hz, 1 H), 7.57 (s, 1 H), 7.42 - 7.34 (m, 5 H), 7.17 - 7.06 (m, 2 H), 5.16 (s, 1 H), 3.77 (s, 3 H); **^{13}C NMR (125 MHz, CDCl$_3$)** δ = 175.8, 172.1, 166.7 (d, J = 255.5 Hz), 157.3 (d, J = 13.4 Hz), 154.9, 135.2, 129.1, 128.8, 128.7 (d, J = 11.4 Hz), 128.0, 126.6, 124.0, 120.4, 114.2(d, J = 22.9 Hz), 104.7(d, J = 24.8 Hz), 52.6, 47.6; **HRMS** (ESI) calcd for $C_{18}H_{13}O_4FNa$ $[M+Na]^+$ 335.0690, found 335.0684.

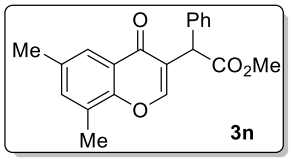

3n: Yellow solid; yield = 43 mg, 89%; R_f = 0.5 (ethyl acetate/petroleum ether = 20/80; mp = 190-193 °C; **^{1}H NMR (500 MHz, CDCl$_3$)** δ = 7.85 (s, 1 H), 7.62 (s, 1 H), 7.44 - 7.35 (m, 4 H), 7.35 - 7.32 (m, 1 H), 7.31 (br. s., 1 H), 5.19 (s, 1 H), 3.77 (s, 3 H), 2.40 (s, 3 H), 2.39 (s, 3 H); **^{13}C NMR (125 MHz, CDCl$_3$)** δ = 177.0, 172.3, 154.5, 153.1, 136.0, 135.7, 134.6, 129.0, 128.7, 127.8, 127.1, 123.4, 123.1, 122.8, 52.5, 47.8, 20.9, 15.3; **HRMS** (ESI) calcd for $C_{20}H_{18}O_4Na$ $[M+Na]^+$ 345.1097, found 345.1096.

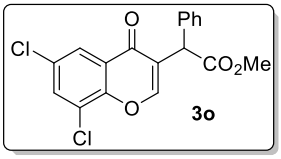

3o: Yellow solid; yield = 36 mg, 67%; R_f = 0.6 (ethyl acetate/petroleum ether = 20/80; mp = 138-140 °C; **^{1}H NMR (500 MHz, CDCl$_3$)** δ = 8.10 (d, *J* = 2.7 Hz, 1 H), 7.71 (d, *J* = 2.3 Hz, 1 H), 7.68 (s, 1 H), 7.45 - 7.38 (m, 2 H), 7.38 - 7.31 (m, 3 H), 5.15 (s, 1 H), 3.77 (s, 3 H); **^{13}C NMR (125 MHz, CDCl$_3$)** δ = 175.0, 171.7, 154.9, 150.6, 134.8, 133.9, 130.9, 129.2, 128.6, 128.2, 125.2, 124.3, 124.3, 124.1, 77.3, 76.7, 52.7, 47.7; **HRMS** (ESI) calcd for $C_{18}H_{12}O_4Cl_2Na$ $[M+Na]^+$ 382.0005, found 385.0002.

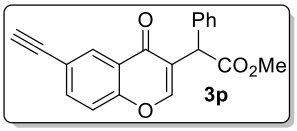

3p: Yellow solid; yield = 29 mg, 61%; R_f = 0.3 (ethyl acetate/petroleum ether = 20/80; mp = 138-140 °C; **^{1}H NMR (400 MHz, CDCl$_3$)** δ = 8.37 (d, *J* = 1.8 Hz, 1 H), 7.74 (dd, *J* = 1.8, 8.5 Hz, 1 H), 7.61 (s, 1 H), 7.44 - 7.33 (m, 6 H), 5.19 (s, 1 H), 3.78 (s, 3 H), 3.15 (s, 1 H); **^{13}C NMR (125 MHz, CDCl$_3$)** δ = 175.8, 172.0, 155.9, 154.8, 136.9, 135.3, 130.1, 129.1, 128.7, 128.0, 124.1, 123.4, 119.5, 118.4, 81.9, 78.3, 52.6, 47.7; **HRMS** (ESI) calcd for $C_{20}H_{15}O_4$ $[M+H]^+$ 319.0965, found 319.0963.

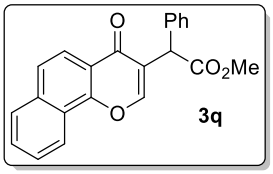

3q: Yellow solid; yield = 43 mg, 83%; R_f = 0.4 (ethyl acetate/petroleum ether = 20/80; mp = 137-139 °C; **^{1}H NMR (500 MHz, CDCl$_3$)** δ = 8.40 (d, *J* = 8.2 Hz, 1 H), 8.17 (d, *J* = 8.7 Hz, 1 H), 7.92 (d, *J* = 8.1 Hz, 1 H), 7.83 - 7.79 (m, 1 H), 7.76 (d, *J* = 8.7 Hz, 1 H), 7.72 - 7.67 (m, 1 H), 7.67 - 7.62 (m, 1 H), 7.47 - 7.40 (m, 4 H), 7.39 - 7.34 (m, 1 H), 5.27 (s, 1 H), 3.80 (s, 3 H); **^{13}C NMR (125 MHz, CDCl$_3$)** δ = 176.4, 172.2, 154.0, 153.7, 135.8, 135.5, 129.3, 129.1, 128.7, 128.1, 128.0, 127.1, 125.4, 125.2, 123.9, 122.2, 120.8, 119.8, 52.6, 47.9; **HRMS** (ESI) calcd for $C_{22}H_{16}O_4Na$ $[M+Na]^+$ 367.0941, found 367.0931.

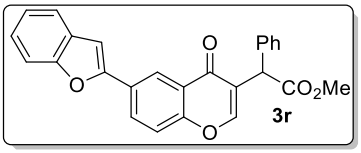

3r: Yellow solid; yield = 43 mg, 71%; R_f = 0.3 (ethyl acetate/petroleum ether = 20/80; mp = 203-206 °C; **^{1}H NMR (500 MHz, CDCl$_3$)** δ = 8.67 (s, 1 H), 8.13 (d, *J* = 8.4 Hz, 1 H), 7.66 - 7.55 (m, 2 H), 7.48 (d, *J* = 8.8 Hz, 1 H), 7.52 (d, *J* = 8.0 Hz, 1 H), 7.39 (br. s., 4 H), 7.37 - 7.27 (m, 2 H), 7.25 (d, *J* = 7.6 Hz, 1 H), 7.10 (s, 1 H), 5.21 (s, 1 H), 3.78 (s, 3 H); **^{13}C NMR (125 MHz, CDCl$_3$)** δ = 176.4, 172.1, 156.0, 155.0, 154.8, 154.1, 135.4, 130.2, 129.1, 129.0, 128.7, 128.0, 127.9, 124.8, 124.0, 123.7, 123.2, 122.0, 121.2, 118.8, 111.3, 102.4, 52.6, 47.8; **HRMS** (ESI) calcd for $C_{26}H_{18}O_5Na$ $[M+Na]^+$ 433.1046, found 433.1039.

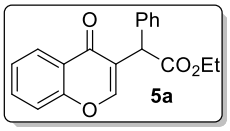

5a: Yellow solid; yield = 35 mg, 75%; R_f = 0.5 (ethyl acetate/petroleum ether = 20/80; mp = 93-95 °C; **^{1}H NMR (500 MHz, CDCl$_3$)** δ = 8.24 (d, *J* = 7.6 Hz, 1 H), 7.69 - 7.63 (m, 1 H), 7.62 (s, 1 H), 7.46 - 7.37 (m, 6 H), 7.36 - 7.31 (m, 1 H), 5.18 (s, 1 H), 4.32 - 4.15 (m, 2 H), 1.27 (t, *J* = 6.9 Hz, 3 H); **^{13}C NMR (125 MHz, CDCl$_3$)** δ = 176.6, 171.7, 156.2, 154.8, 135.7, 133.7, 129.0, 128.7, 127.8, 126.0, 125.1, 123.9, 123.5, 118.0, 61.5, 47.8, 14.1; **HRMS** (ESI) calcd for $C_{19}H_{16}O_4Na$ $[M+Na]^+$ 331.0941, found 331.0933.

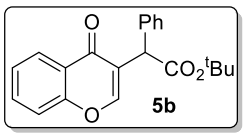

5b: Yellow solid; yield = 31 mg, 61%; R_f = 0.6 (ethyl acetate/petroleum ether = 20/80; mp = 085-088 °C; **^{1}H NMR (500 MHz, CDCl$_3$)** δ = 8.24 (dd, *J* = 1.4, 8.0 Hz, 1 H), 7.67 - 7.63 (m, 1 H), 7.62 (s, 1 H), 7.43 - 7.36 (m, 6 H), 7.33 - 7.30 (m, 1 H), 5.13 (s, 1 H), 1.46 (s, 9 H); **^{13}C NMR (125 MHz, CDCl$_3$)** δ = 170.8, 156.2, 154.7, 136.5, 133.6, 128.9, 128.6, 127.5, 126.0, 125.0, 124.1, 123.6, 118.0, 81.5, 77.3, 76.7, 48.5, 27.9; **HRMS** (ESI) calcd for $C_{21}H_{20}O_4Na$ $[M+Na]^+$ 359.1254, found 359.1246.

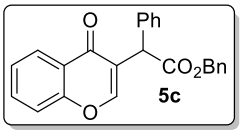

5c: Yellow solid; yield = 38mg, 68%; R_f = 0.6 (ethyl acetate/petroleum ether = 20/80; mp = 123-125 °C; **^{1}H NMR (500 MHz, CDCl$_3$)** δ = 8.23 (d, *J* = 7.3 Hz, 1 H), 7.79 - 7.50 (m, 2 H), 7.45 - 7.31 (m, 7 H), 7.29 (br. s., 5 H), 5.25 (br. s., 1 H), 5.23 - 5.13 (m, 2 H); **^{13}C NMR (125 MHz, CDCl$_3$)** δ = 176.6, 171.5, 156.2, 154.8, 135.7, 135.5, 133.7, 129.0, 128.7, 128.4, 128.1, 128.0, 127.9, 126.0, 125.2, 123.7, 123.6, 118.0, 67.1, 47.8; **HRMS** (ESI) calcd for $C_{24}H_{18}O_4Na[M+Na]^+$ 393.1097, found 393.1089.

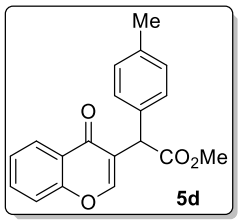

5d: Yellow solid; yield = 38 mg, 82%; R_f = 0.5 (ethyl acetate/petroleum ether = 20/80; mp = 121-124 °C; **^{1}H NMR (500 MHz, CDCl$_3$)** δ = 8.25 (d, *J* = 7.2 Hz, 1 H), 7.72 - 7.64 (m, 1 H), 7.62 (br. s., 1 H), 7.44 (d, *J* = 7.2 Hz, 2 H), 7.28 (br. s., 2 H), 7.26 - 7.18 (m, 2 H), 5.16 (br. s., 1 H), 3.78 (br. s., 3 H), 2.38 (br. s., 3 H); **^{13}C NMR (125 MHz, CDCl$_3$)** δ = 176.7, 172.3, 156.2, 154.8, 137.7, 133.7, 132.4, 129.8, 128.6, 126.0, 125.1, 123.9, 123.5, 118.0, 52.5, 47.4, 21.1; **HRMS** (ESI) calcd for $C_{19}H_{16}O_4Na$ $[M+H]^+$ 331.0941, found 331.0934.

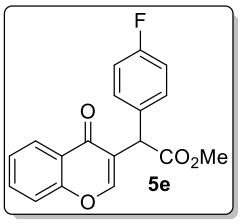

5e: Yellow thick liquid; yield = 25 mg, 53%; R_f = 0.5 (ethyl acetate/petroleum ether = 20/80; mp = 085-087 °C; **^{1}H NMR (500 MHz, CDCl$_3$)** δ = 8.23 (dd, *J* = 1.3, 8.0 Hz, 1 H), 7.72 - 7.61 (m, 2 H), 7.47 - 7.41 (m, 2 H), 7.40 - 7.34 (m, 2 H), 7.08 (t, *J* = 8.6 Hz, 2 H), 5.15 (s, 1 H), 3.77 (s, 3 H); **^{13}C NMR (125 MHz, CDCl$_3$)** δ = 176.6, 172.1, 163.3 (d, *J* = 247.05 Hz), 156.3, 154.5, 133.9, 131.4 (d, *J* = 2.72 Hz), 130.4 (d, *J* = 8.17 Hz), 126.0, 125.3, 123.6 (d, J = 16.35 Hz), 118.1, 116.1, 115.9, 52.7, 47.0; **HRMS** (ESI) calcd for $C_{18}H_{13}FO_4Na$ $[M+Na]^+$ 335.0690, found 335.0714.

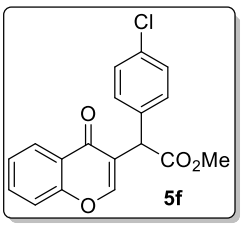

5f: Yellow liquid; yield = 28 mg, 57%; R_f = 0.6 (ethyl acetate/petroleum ether = 20/80; **^{1}H NMR (500 MHz, CDCl$_3$)** δ = 8.22 (d, *J* = 7.9 Hz, 1 H), 7.77 - 7.60 (m, 2 H), 7.50 - 7.40 (m, 2 H), 7.39 - 7.32 (m, 4 H), 5.16 (s, 1 H), 3.77 (s, 3 H); **^{13}C NMR (125 MHz, CDCl$_3$)** δ = 176.5, 171.9, 156.2, 154.5, 134.2, 133.9, 130.1, 129.2, 127.9, 126.0, 125.3, 123.5, 123.3, 118.1, 52.7, 47.1; **HRMS** (ESI) calcd for $C_{18}H_{13}ClO_4Na$ $[M+Na]^+$ 351.0395, found 351.0411.

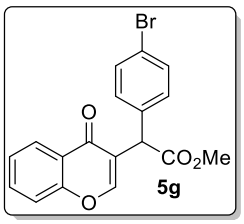

5g: Yellow liquid; yield = 28 mg, 51%; R_f = 0.4 (ethyl acetate/petroleum ether = 20/80; mp = 131-133 °C; **^{1}H NMR (500 MHz, CDCl$_3$)** δ = 8.21 (dd, *J* = 1.4, 8.0 Hz, 1 H), 7.69 (s, 1 H), 7.69 - 7.64 (m, 1 H), 7.51 (d, *J* = 8.4 Hz, 2 H), 7.47 - 7.35 (m, 2 H), 7.27 (d, *J* = 8.5 Hz, 2 H), 5.14 (s, 1 H), 3.76 (s, 3 H); **^{13}C NMR (125 MHz, CDCl$_3$)** δ = 176.4, 171.8, 156.2, 154.5, 134.8, 133.9, 132.2, 130.4, 126.0, 125.3, 123.5, 123.3, 122.0, 118.1, 52.7, 47.1; **HRMS** (ESI) calcd for $C_{18}H_{13}BrO_4$ $[M+Na]^+$ 396.9870, found 396.9881.

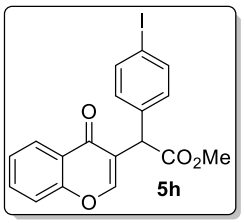

5h: Yellow liquid; yield = 36 mg, 58%; R_f = 0.6 (ethyl acetate/petroleum ether = 20/80; mp = 131-133 °C; **^{1}H NMR (500 MHz, CDCl$_3$)** δ = 8.22 (d, *J* = 7.9 Hz, 1 H), 7.76 - 7.64 (m, 4 H), 7.48 - 7.38 (m, 2 H), 7.15 (d, *J* = 8.2 Hz, 2 H), 5.13 (s, 1 H), 3.77 (s, 3 H); **^{13}C NMR (125 MHz, CDCl$_3$)** δ = 176.4, 171.8, 156.2, 154.5, 134.8, 133.9, 132.2, 130.4, 126.0, 125.3, 123.5, 123.3, 122.0, 118.1, 52.7, 47.1; **HRMS** (ESI) calcd for $C_{18}H_{13}IO_4Na$ $[M+H]^+$ 392.9751, found 392.9723.

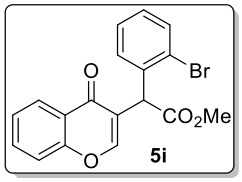

5i: Yellow solid; yield = 34 mg, 62%; R_f = 0.4 (ethyl acetate/petroleum ether = 20/80; mp = 126-128 °C; **^{1}H NMR (500 MHz, CDCl$_3$)** δ = 8.25 (d, *J* = 7.6 Hz, 1 H), 7.69 - 7.62 (m, 2 H), 7.47 - 7.39 (m, 4 H), 7.36 (t, *J* = 7.6 Hz, 1 H), 7.21 (t, *J* = 7.6 Hz, 1 H), 5.58 (s, 1 H), 3.79 (s, 3 H); **^{13}C NMR (125 MHz, CDCl$_3$)** δ = 176.5, 171.6, 156.3, 154.4, 135.2, 133.8, 133.6, 129.8, 129.4, 127.9, 126.0, 125.2, 125.1, 123.5, 122.4, 118.1, 52.7, 47.8; **HRMS** (ESI) calcd for $C_{18}H_{13}BrO_4Na$ $[M+Na]^+$ 396.9870, found 396.9858.

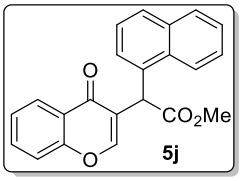

5j: Yellow solid; yield = 20 mg, 40%; R_f = 0.6 (ethyl acetate/petroleum ether = 20/80; mp = 143-147 °C; **^{1}H NMR (500 MHz, CDCl$_3$)** δ = 8.31 (d, *J* = 7.9 Hz, 1 H), 7.97 - 7.83 (m, 3 H), 7.66 (t, *J* = 7.9 Hz, 1 H), 7.55 - 7.47 (m, 4 H), 7.47 - 7.32 (m, 3 H), 6.06 (s, 1 H), 3.82 (s, 3 H); **^{13}C NMR (125 MHz, CDCl$_3$)** δ = 176.7, 172.7, 156.3, 155.6, 134.2, 133.8, 131.9, 131.3, 128.9, 128.7, 127.0, 126.2, 126.1, 125.6, 125.4, 125.2, 123.5, 123.4, 122.9, 118.1, 52.7, 43.8; **HRMS** (ESI) calcd for $C_{22}H_{16}O_4Na$ $[M+Na]^+$ 367.0941, found 367.0932.

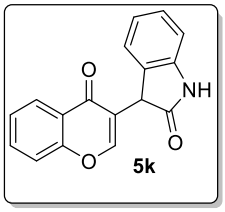

5k: Brown solid; yield = 30 mg, 74%; R_f = 0.5 (ethyl acetate/petroleum ether = 40/60; mp = 242-245 °C; **^{1}H NMR (500 MHz, CDCl$_3$)** δ = 10.40 (br. s., 1 H), 8.23 (br. s., 1 H), 7.95 (d, *J* = 7.2 Hz, 1 H), 7.70 - 7.60 (m, 1 H), 7.48 (d, *J* = 7.6 Hz, 1 H), 7.34 (t, *J* = 6.5 Hz, 1 H), 7.14 - 7.06 (m, 1 H), 6.98 (d, *J* = 6.1 Hz, 1 H), 6.89 - 6.76 (m, 2 H), 4.41 (br. s., 1 H); **^{13}C NMR (125 MHz, CDCl$_3$)** δ = δ = 176.4, 175.1, 155.8, 154.7, 142.7, 133.5, 128.0, 127.5, 124.8, 123.2, 123.0, 120.9, 117.8, 109.1, 44.6, 28.9; **HRMS** (ESI) calcd for $C_{17}H_{11}O_3NNa$ $[M+Na]^+$ 300.0631, found 300.0625.

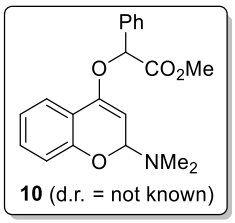

10: Reaction performed on 2.61 mmol scale. Yield = 375 mg, 65% (yellow thick liquid); R_f = 0.2 (ethyl acetate/petroleum ether = 80/20; **^{1}H NMR (500 MHz, DMSO-d$_6$)** δ = 7.56 (d, *J* = 6.9 Hz, 3 H), 7.48 - 7.36 (m, 4 H), 7.33 (t, *J* = 7.2 Hz, 1 H), 7.03 - 6.91 (m, 2 H), 6.11 (s, 1 H), 3.66 (s, 3 H), 3.06 (br. s., 3 H), 2.73 (br. s., 3 H); **^{13}C NMR (125 MHz, CDCl$_3$)** δ = 169.9, 153.6, 153.5, 134.9, 134.2, 133.2, 129.0, 128.6, 127.1, 115.8, 114.8, 97.7, 79.4, 52.6, 44.9, 37.0; **HRMS** (ESI) calcd for $C_{20}H_{21}NO_4Na$ $[M+Na]^+$ 362.1363, found 362.1343.

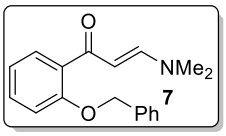

7: Reaction performed on 2.21 mmol scale. Yield = 528 mg, 85% (yellow solid); R_f = 0.2 (ethyl acetate/petroleum ether = 80/20; mp = 070-072 °C; **^{1}H NMR (500 MHz, CDCl$_3$)** δ = 7.63 (br. s., 2 H), 7.46 (d, *J* = 7.3 Hz, 2 H), 7.39 - 7.29 (m, 4 H), 7.07 - 6.91 (m, 2 H), 5.72 (d, *J* = 12.1 Hz, 1 H), 5.13 (s, 2 H); **^{13}C NMR (125 MHz, CDCl$_3$)** δ = 189.8, 156.3, 153.9, 137.1, 131.8, 130.9, 130.0, 128.4, 127.8, 127.4, 121.0, 113.2, 98.3, 70.7, 44.8, 37.0; **HRMS** (ESI) calcd for $C_{18}H_{19}NO_2$ $[M+H]^+$ 282.1489, found 282.1477.

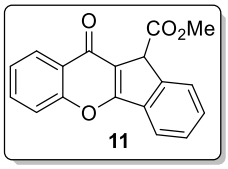

11: Reaction performed on 0.05 mmol scale. Yield = 12 mg, 65% (White solid); R_f = 0.5 (ethyl acetate/petroleum ether = 20/80; mp = 160-162 °C; **^{1}H NMR (500 MHz, CDCl$_3$)** □ = 8.25 (dd, *J* = 1.5, 7.9 Hz, 1 H), 7.70 - 7.63 (m, 2 H), 7.46 - 7.41 (m, 3 H), 7.36 (t, *J* = 7.5 Hz, 1 H), 7.24 - 7.18 (m, 1 H), 5.58 (s, 1 H), 3.80 (s, 3 H); **^{13}C NMR (125 MHz, CDCl$_3$)** □ = 176.5, 171.6, 156.4, 154.4, 135.3, 133.8, 133.6, 129.8, 129.5, 127.9, 126.1, 125.3, 125.2, 123.6, 122.4, 118.1, 52.8, 47.9; **HRMS** (ESI) calcd for $C_{18}H_{12}O_4Na$ $[M+H]^+$ 315.1877, found 315.1877.

4.10 ORTEP Diagram:

Sr. No.	Compound Structure	ORTEP Diagram
1	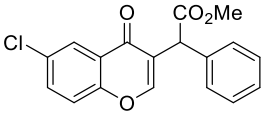 CCDC No. 1577848	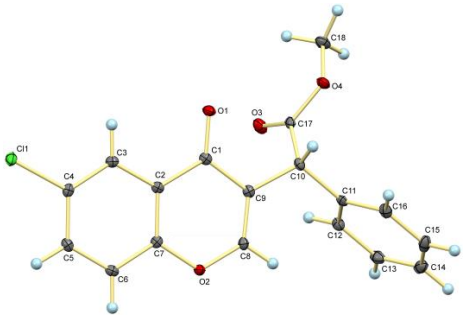
2	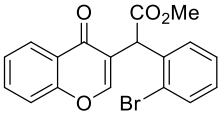 CCDC No: 1577847	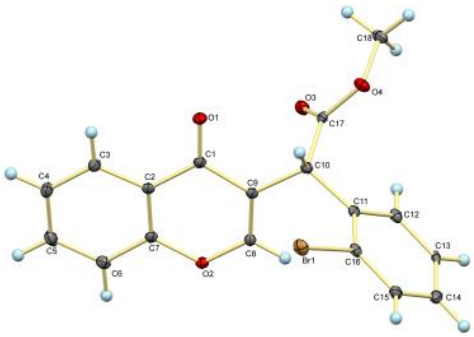

4.11 NMR Spectra of Selected Compounds:

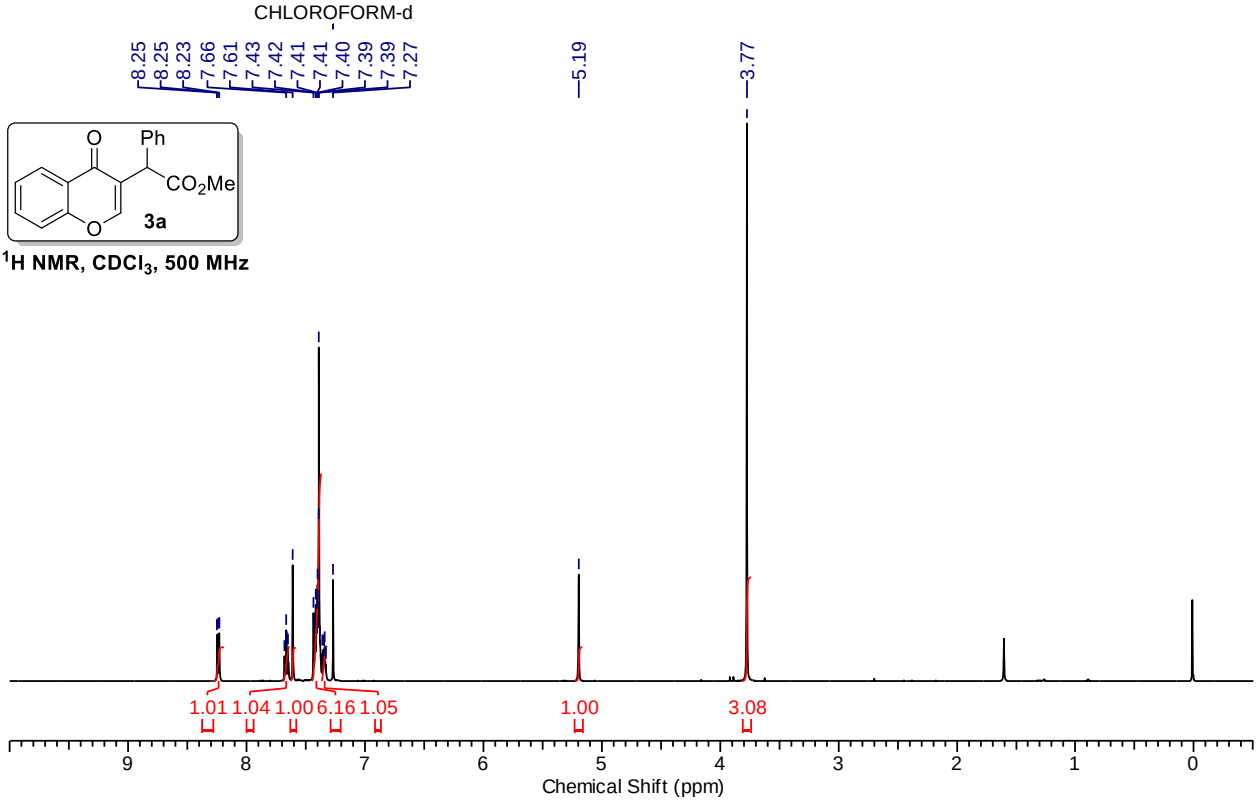

^{1}H NMR, $CDCl_3$, 500 MHz

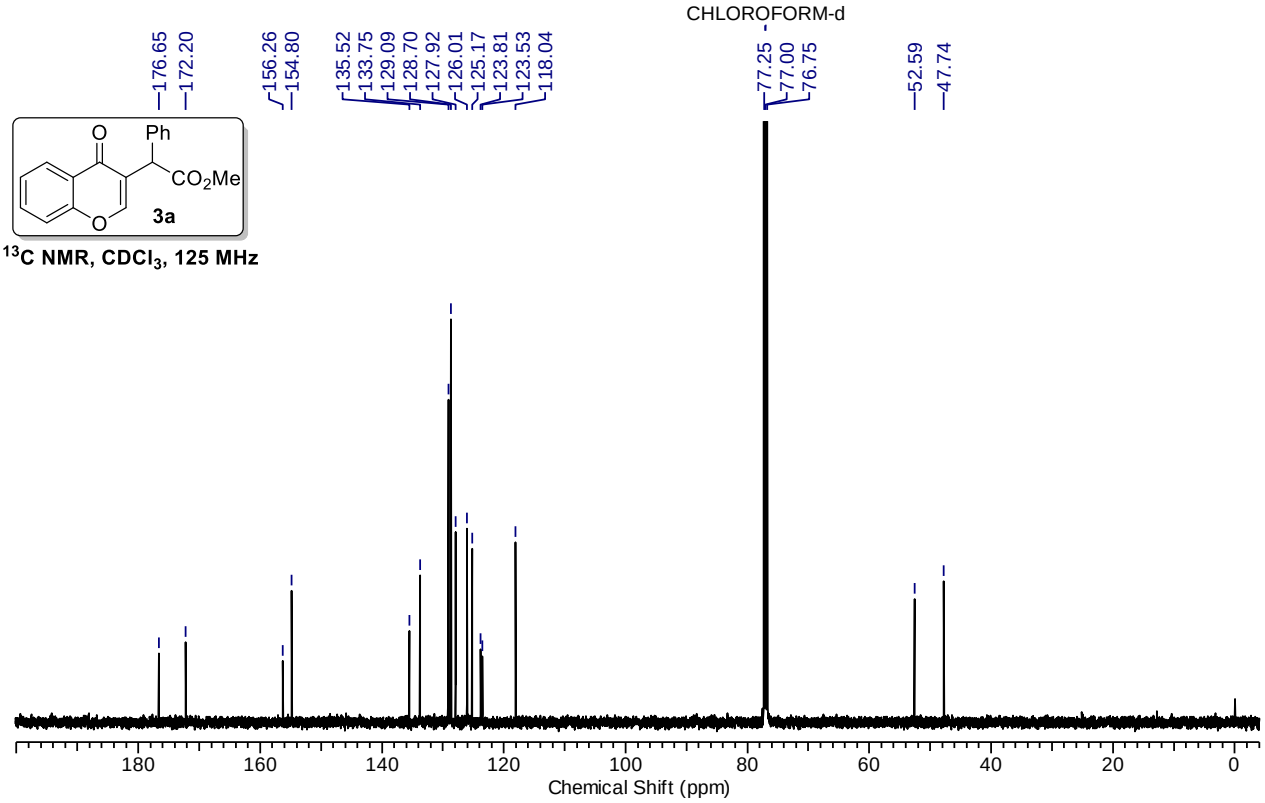

^{13}C NMR, $CDCl_3$, 125 MHz

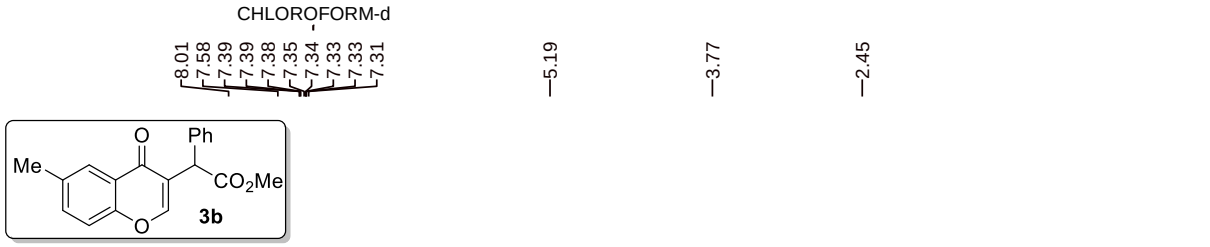

^{1}H NMR, $CDCl_3$, 500 MHz

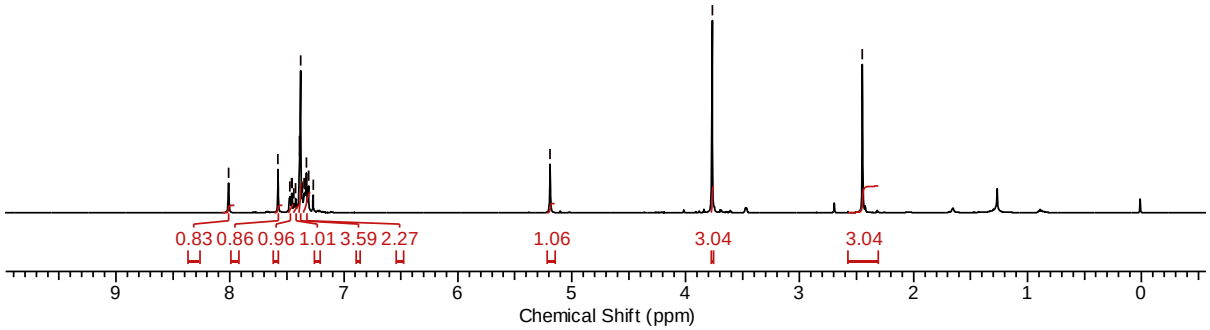

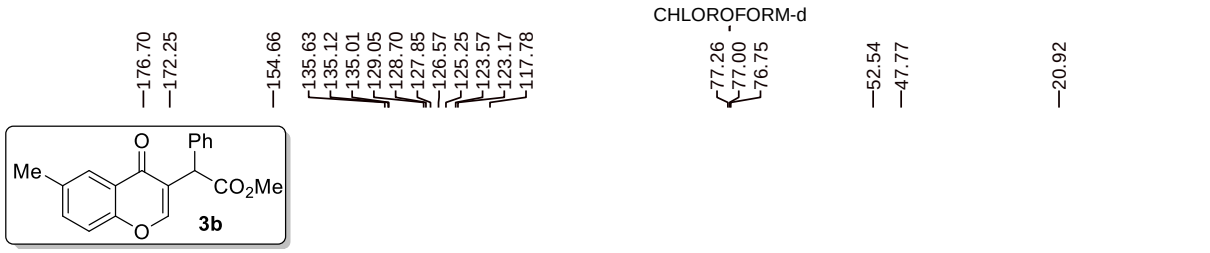

^{13}C NMR, $CDCl_3$, 125 MHz

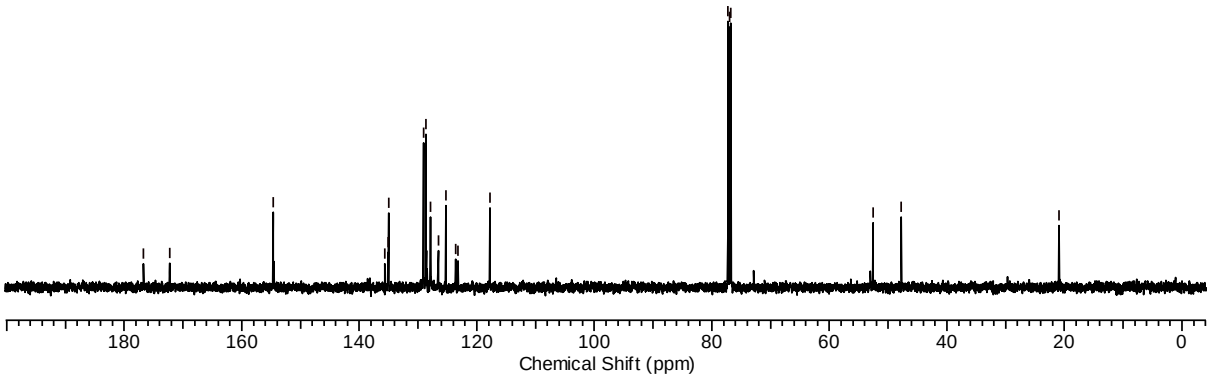

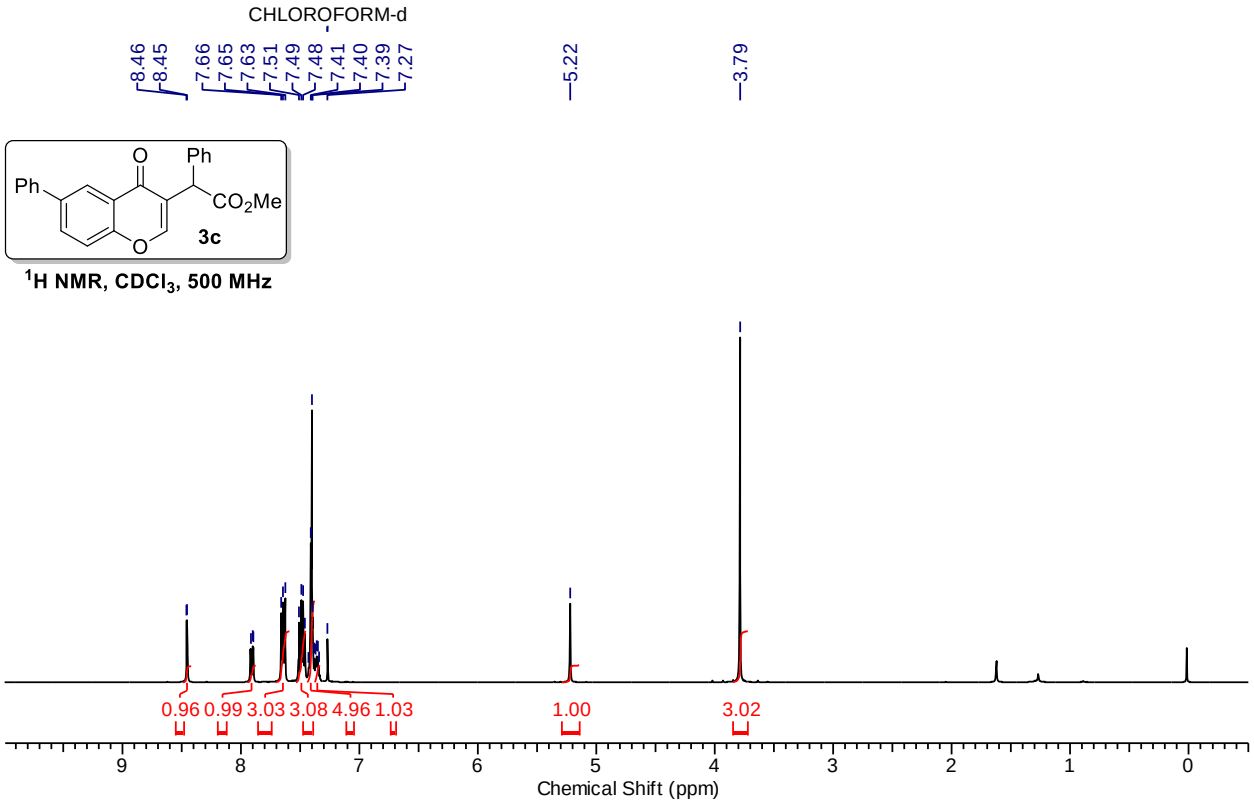

^{1}H NMR, $CDCl_3$, 500 MHz

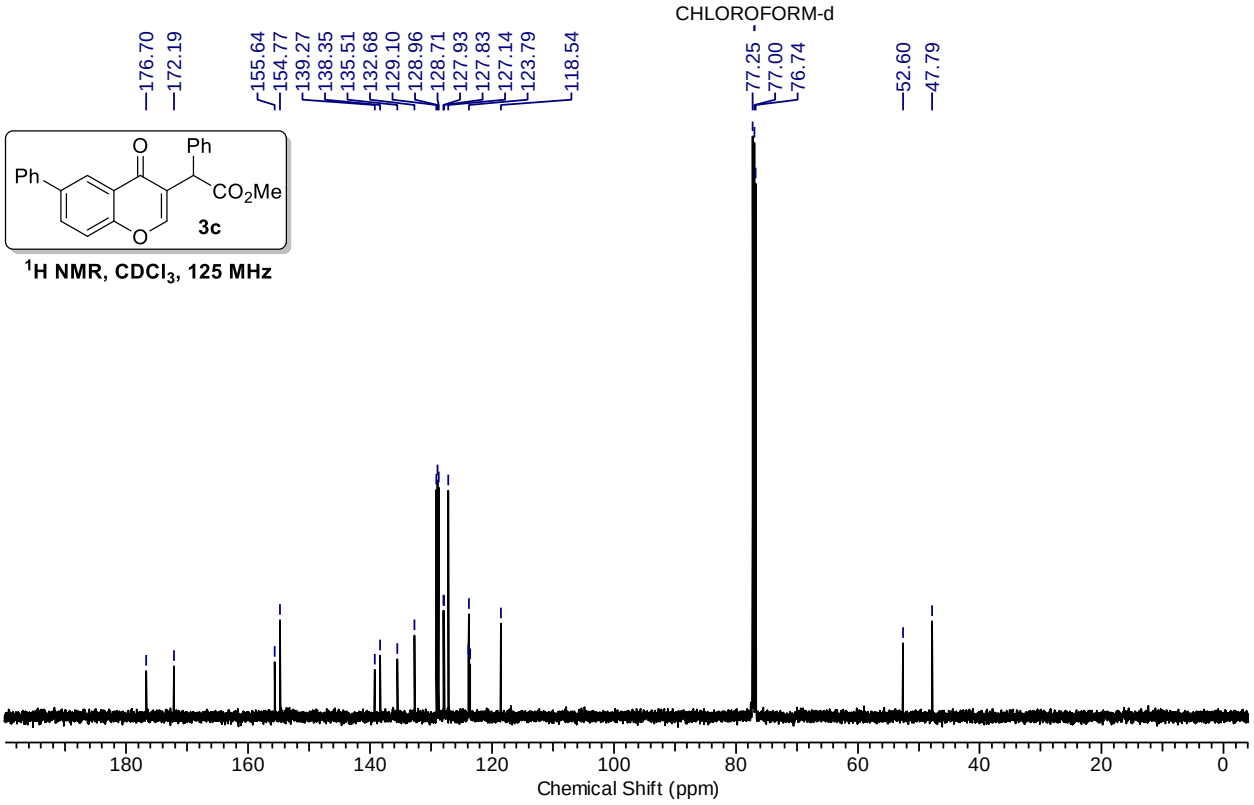

^{1}H NMR, $CDCl_3$, 125 MHz

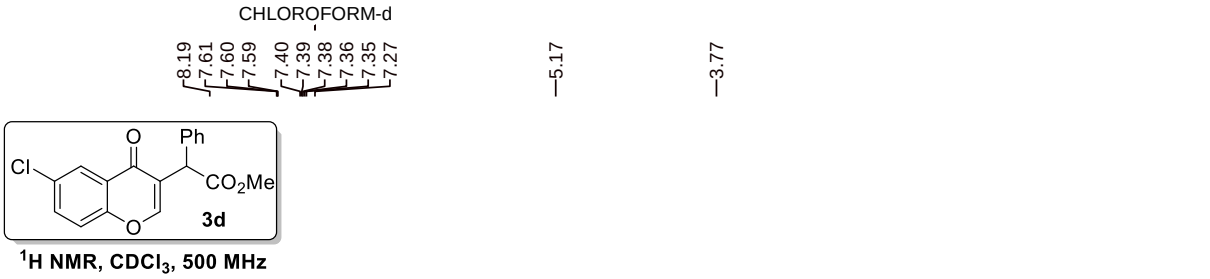

^{1}H NMR, $CDCl_3$, 500 MHz

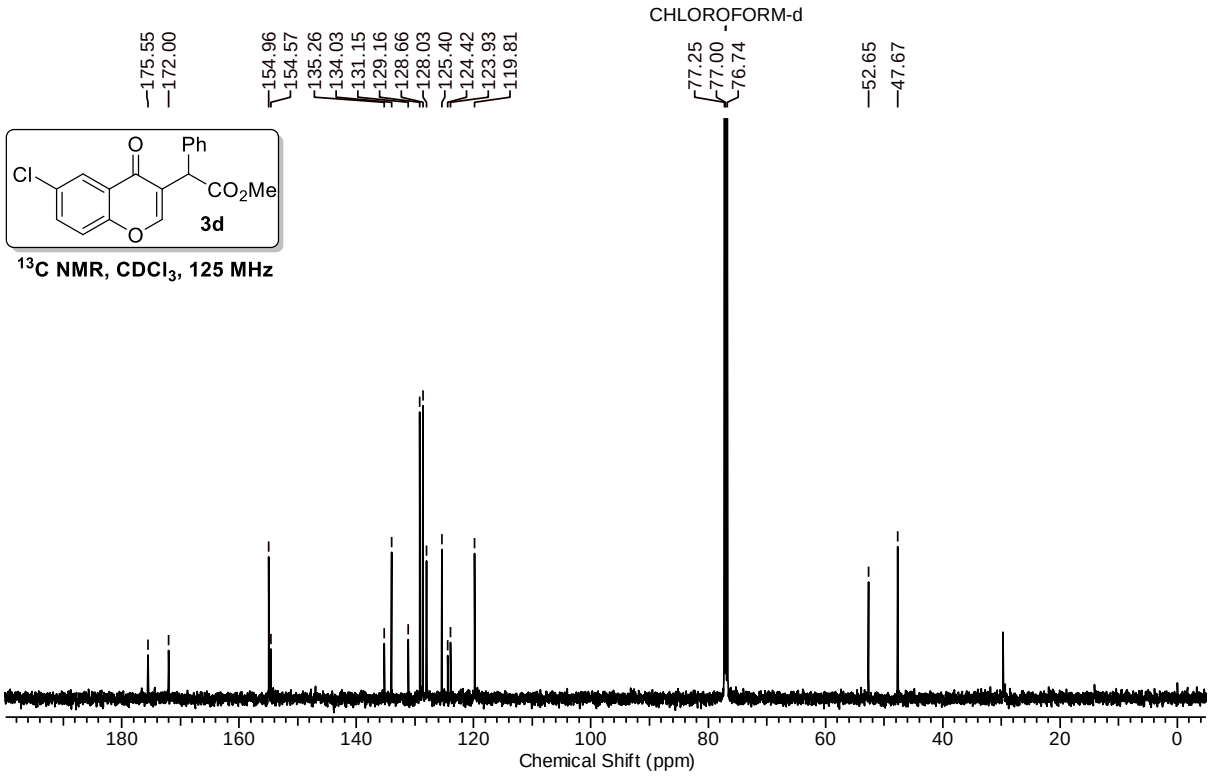

^{13}C NMR, $CDCl_3$, 125 MHz

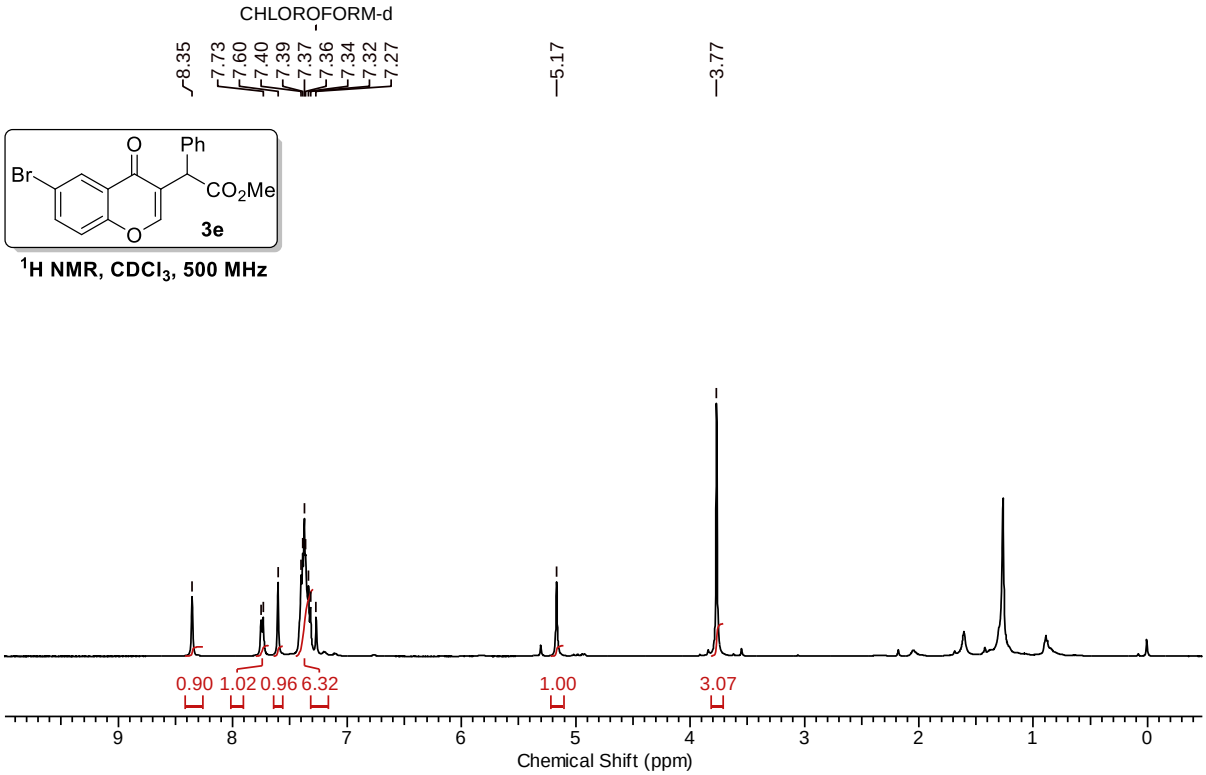

^{1}H NMR, $CDCl_3$, 500 MHz

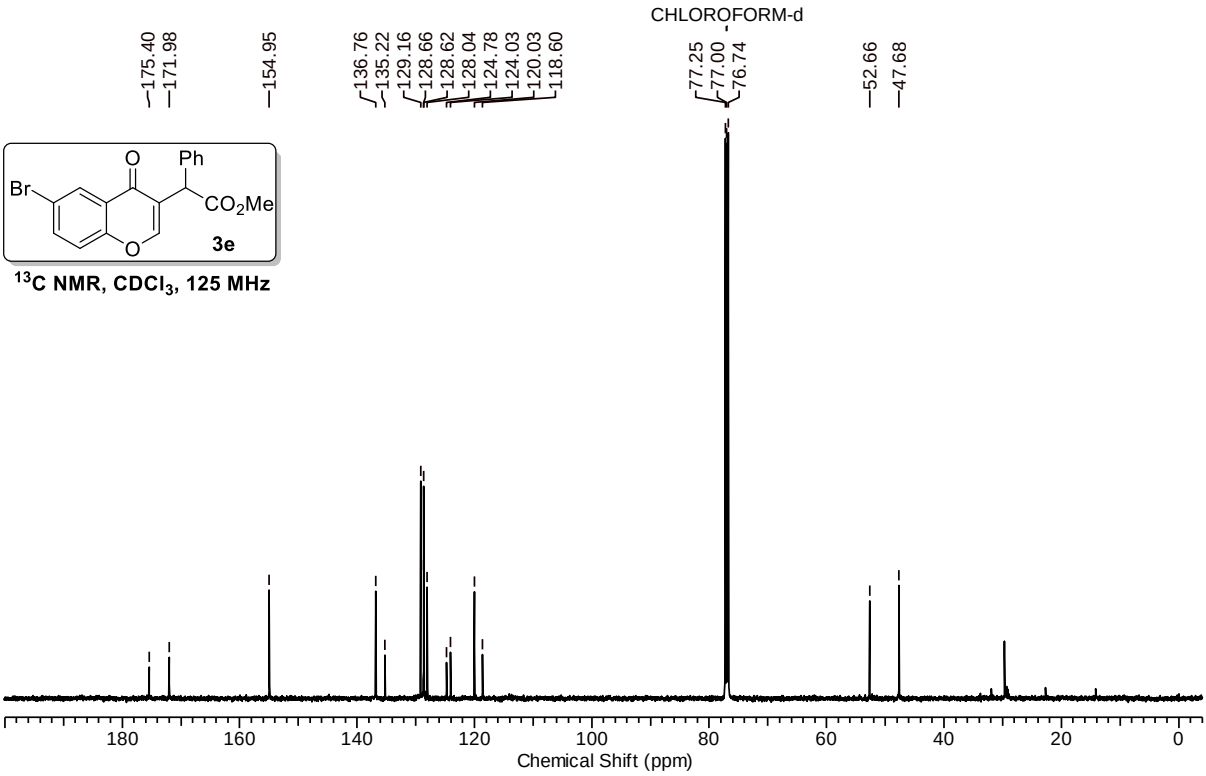

^{13}C NMR, $CDCl_3$, 125 MHz

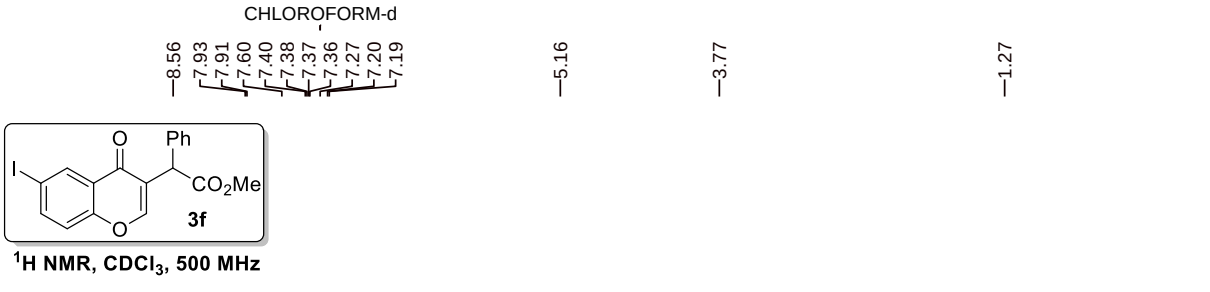

^{1}H NMR, $CDCl_3$, 500 MHz

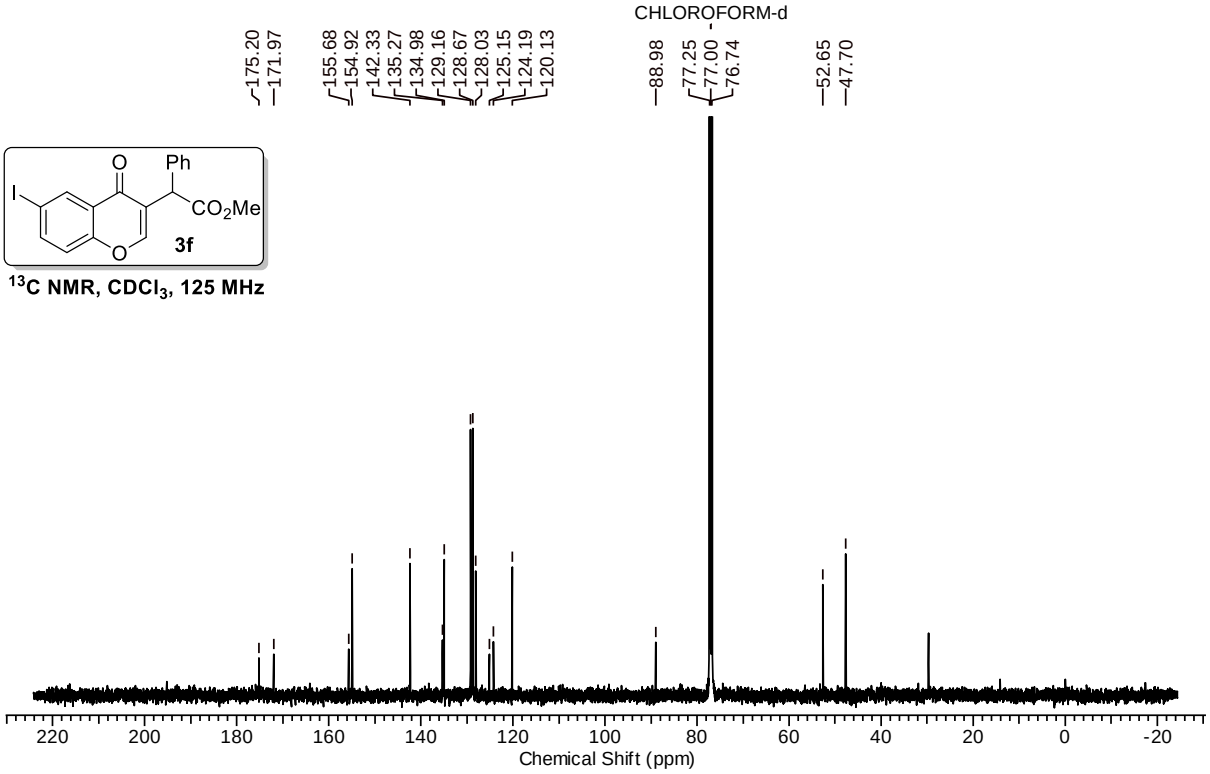

^{13}C NMR, $CDCl_3$, 125 MHz

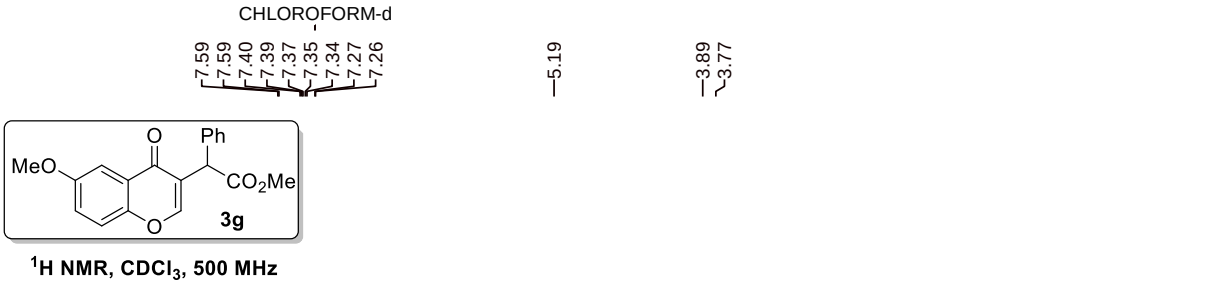

^{1}H NMR, $CDCl_3$, 500 MHz

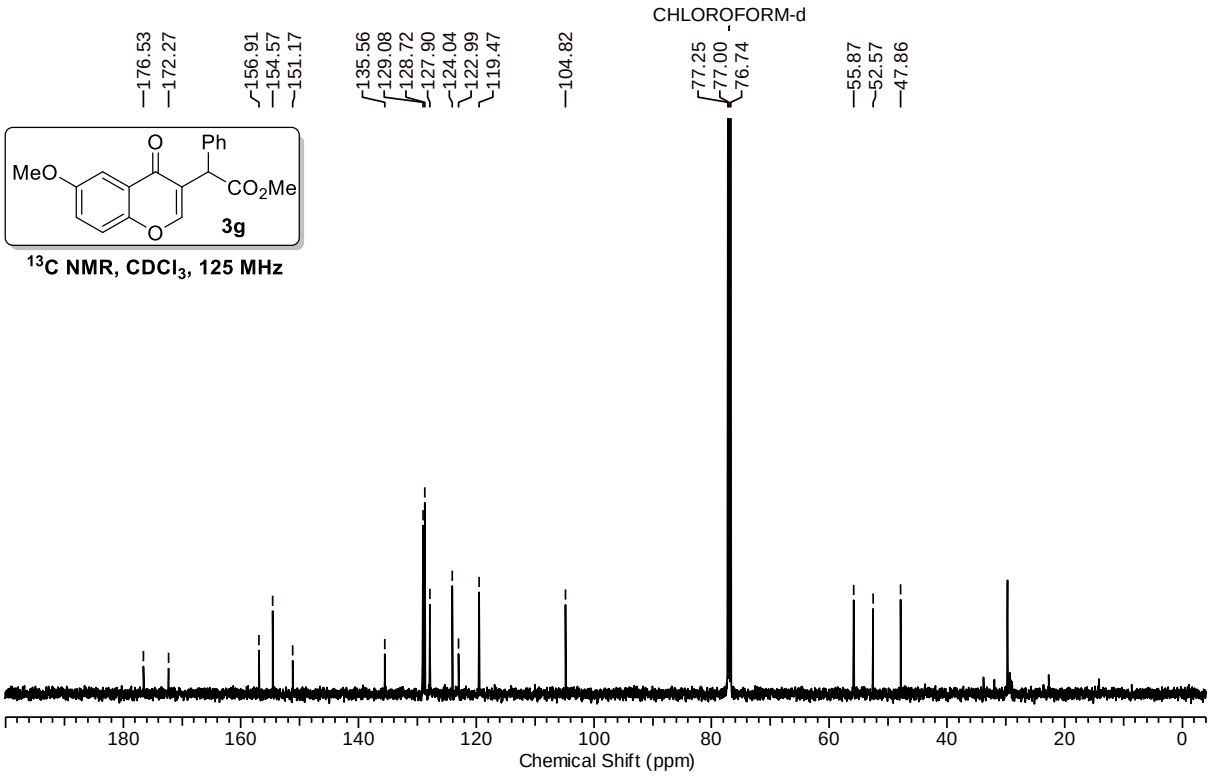

^{13}C NMR, $CDCl_3$, 125 MHz

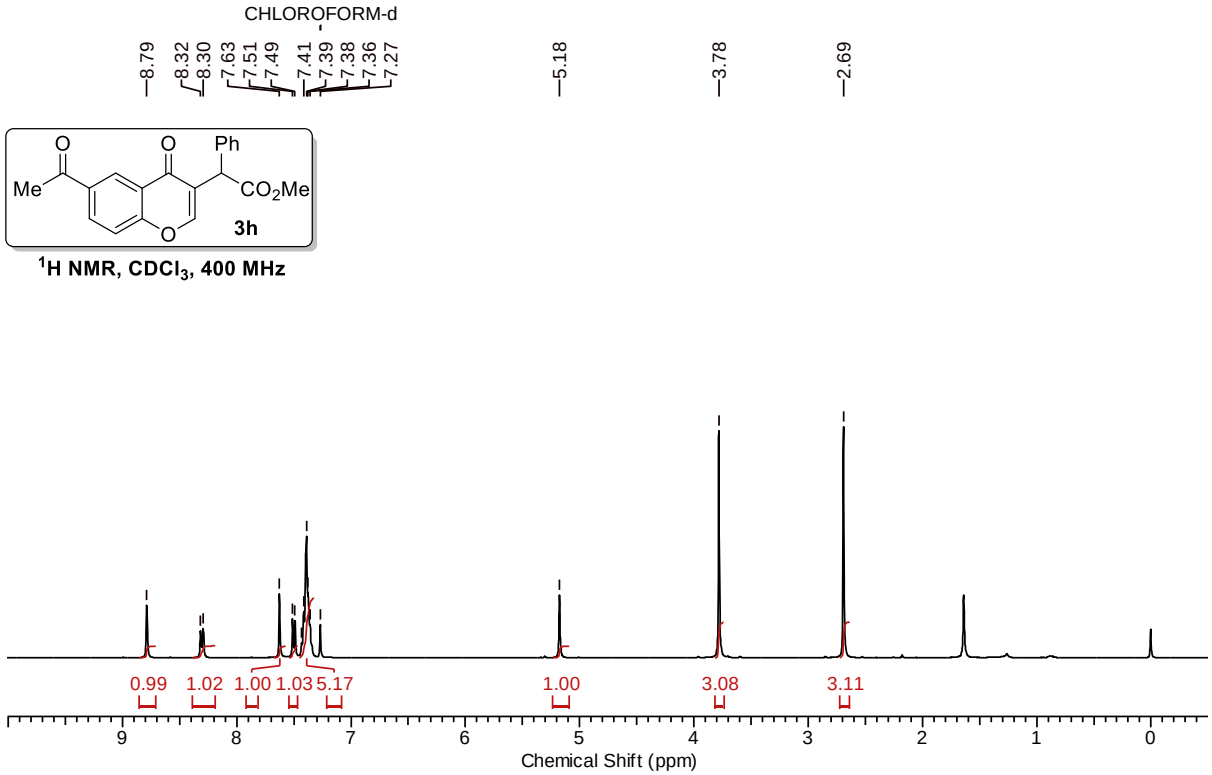

^{1}H NMR, $CDCl_3$, 400 MHz

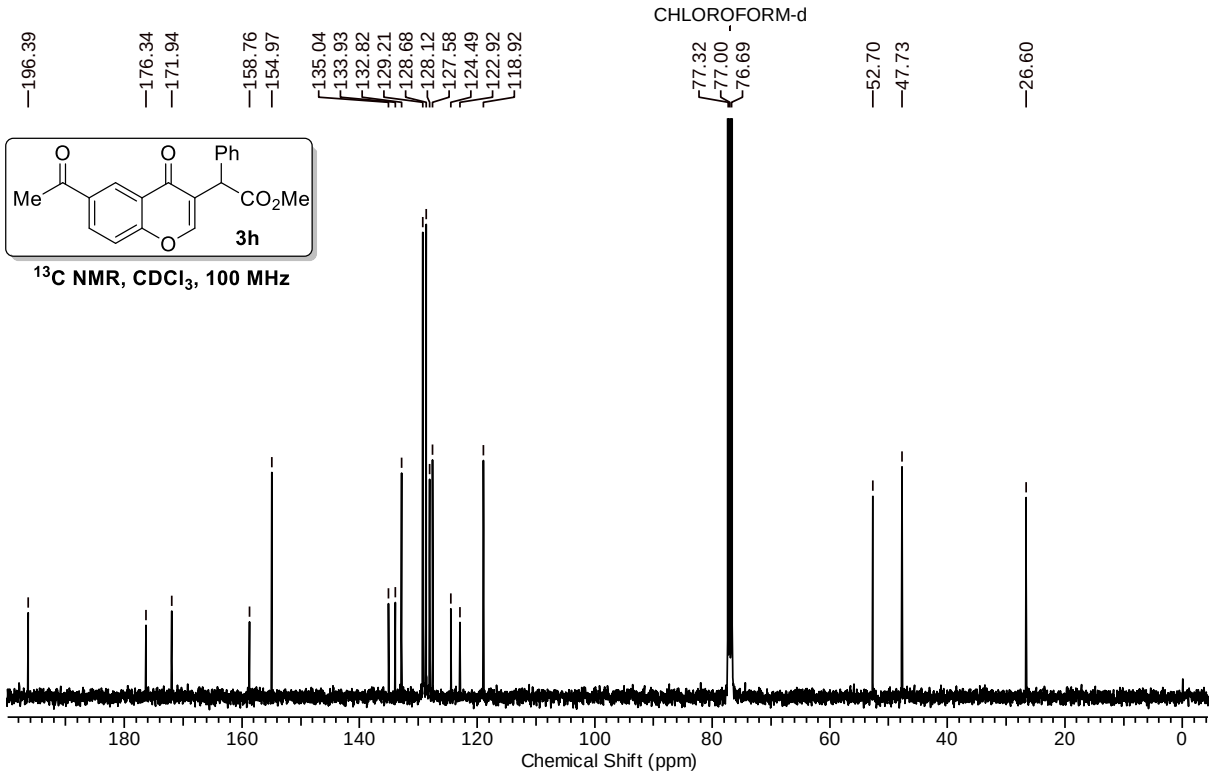

^{13}C NMR, $CDCl_3$, 100 MHz

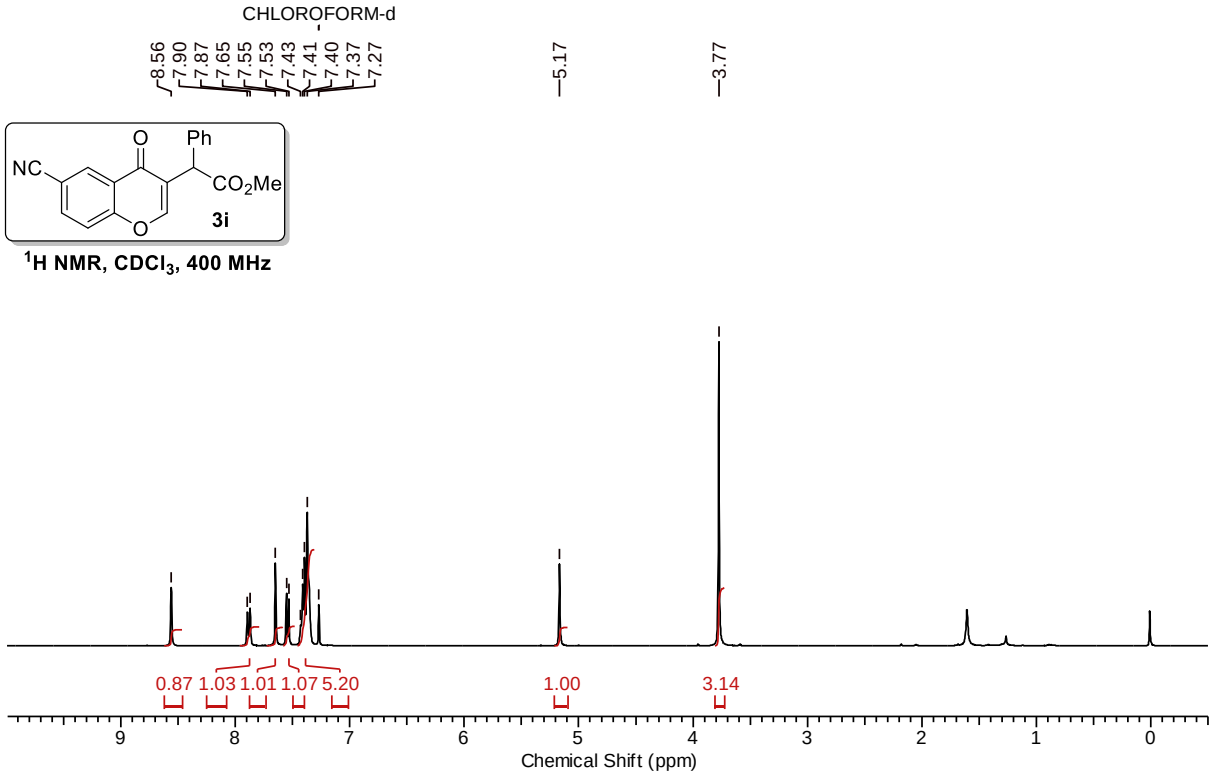

^{1}H NMR, $CDCl_3$, 400 MHz

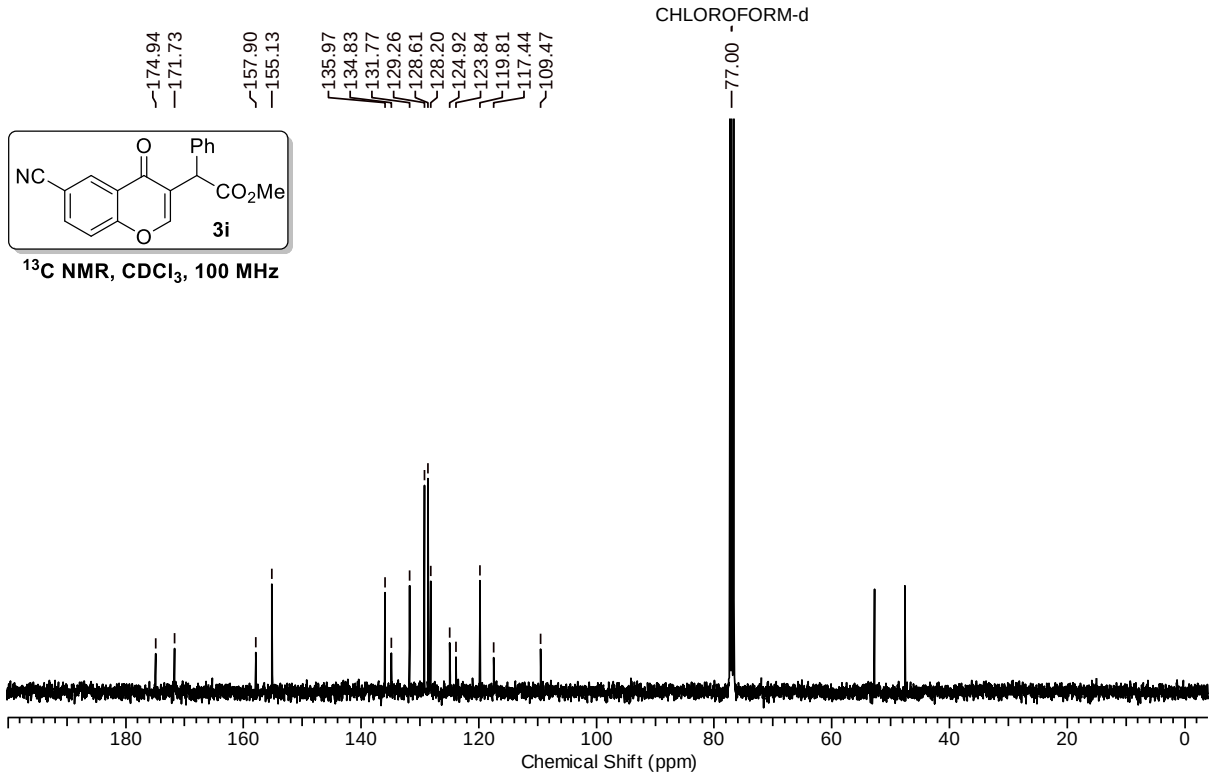

^{13}C NMR, $CDCl_3$, 100 MHz

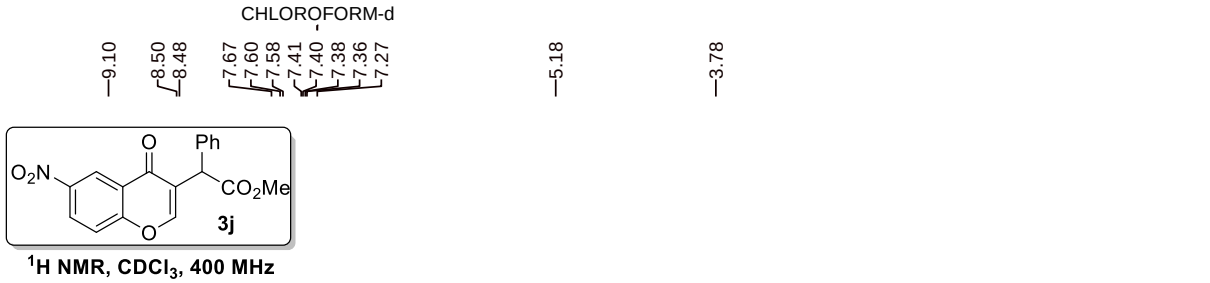

^{1}H NMR, $CDCl_3$, 400 MHz

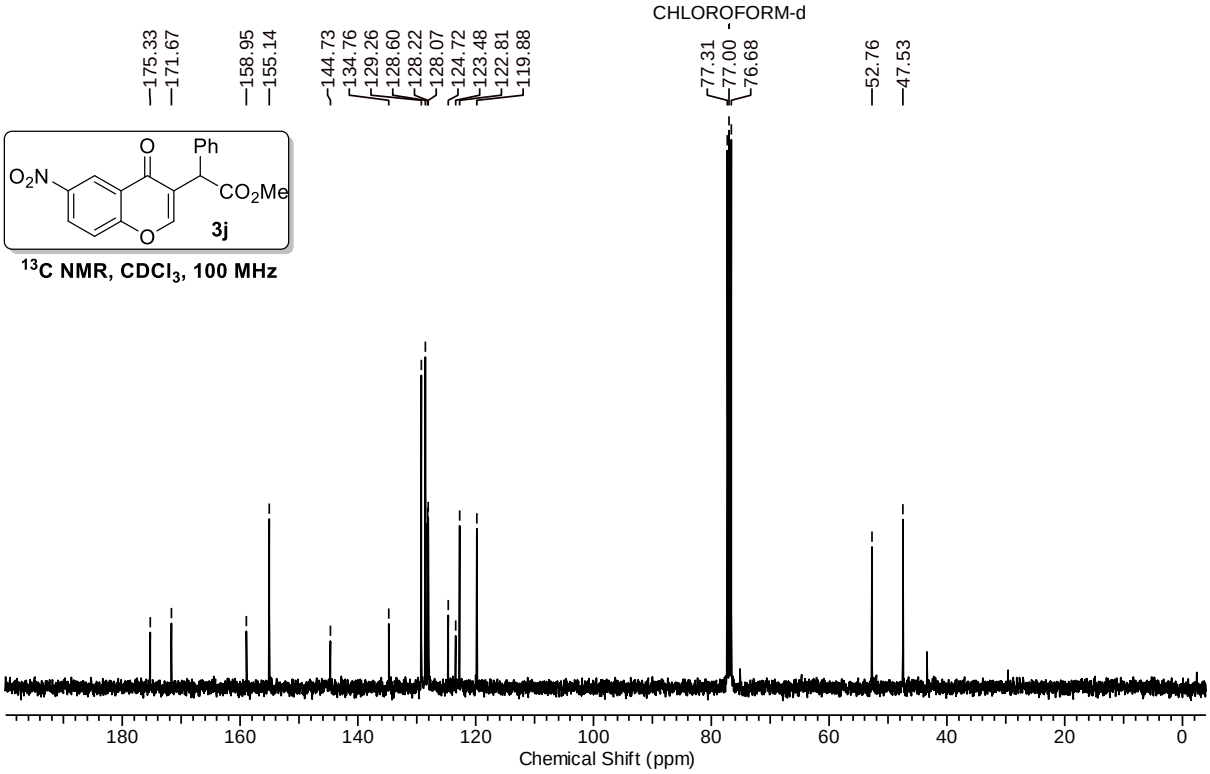

^{13}C NMR, $CDCl_3$, 100 MHz

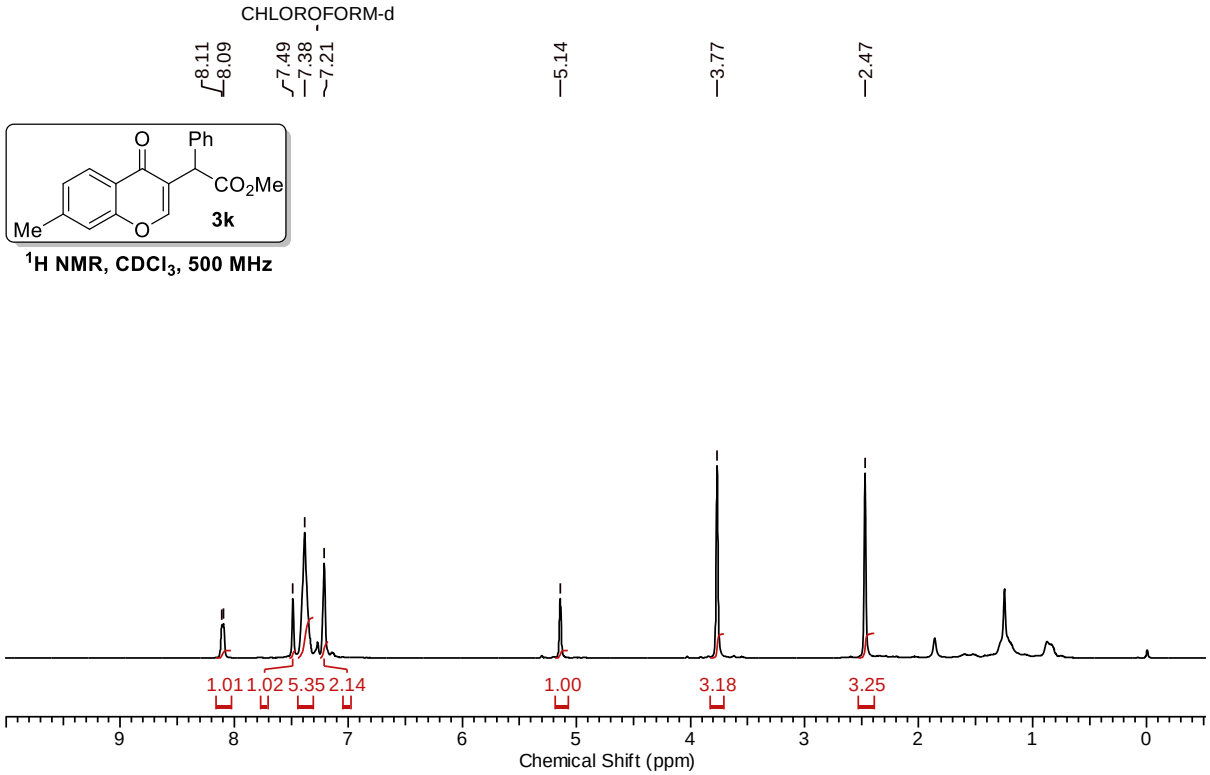

^{1}H NMR, $CDCl_3$, 500 MHz

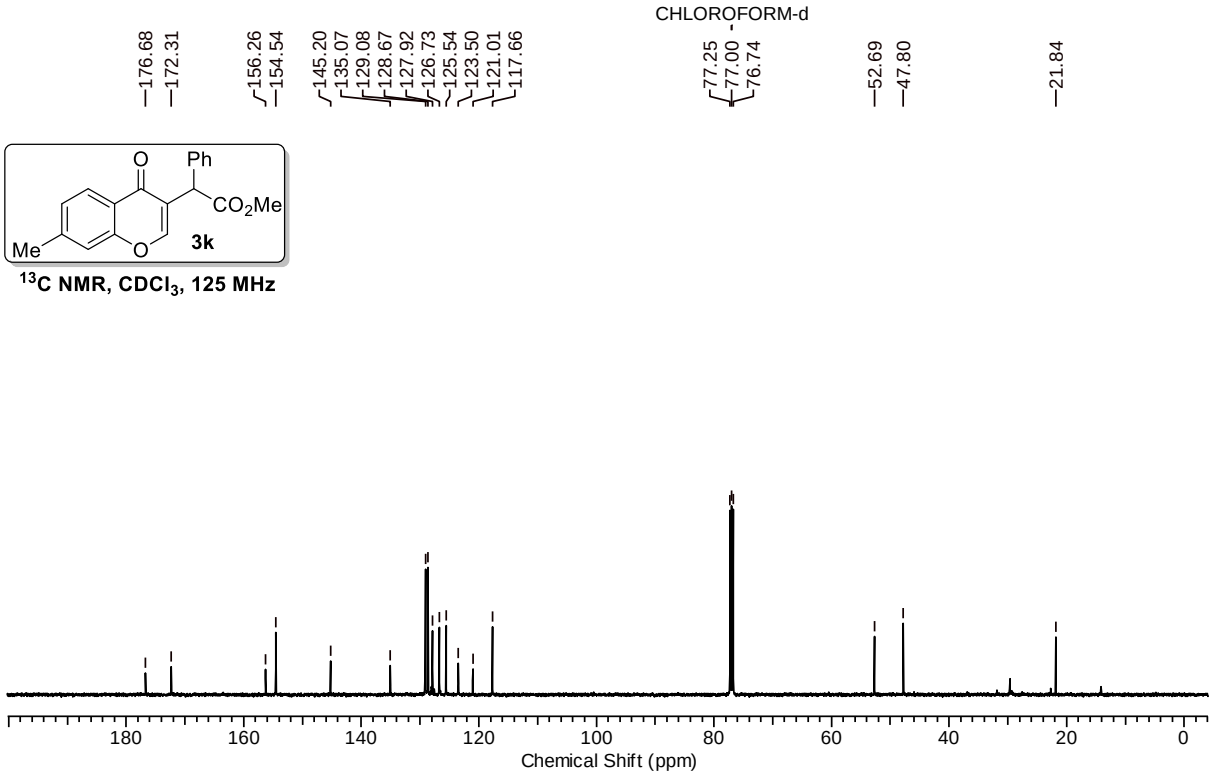

^{13}C NMR, $CDCl_3$, 125 MHz

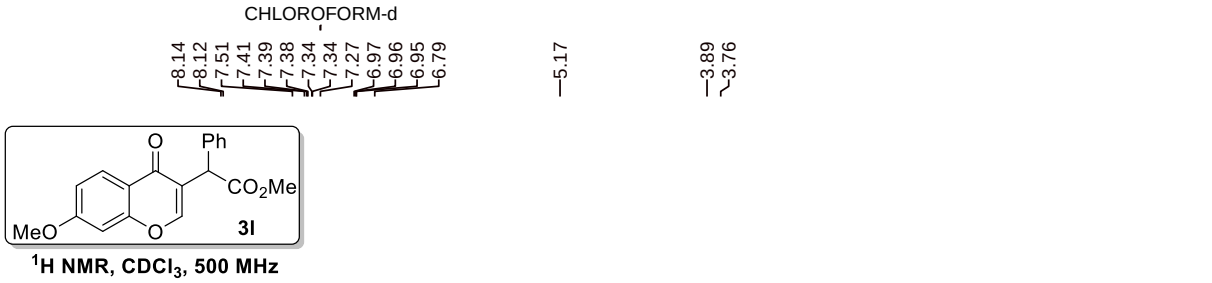

^{1}H NMR, $CDCl_3$, 500 MHz

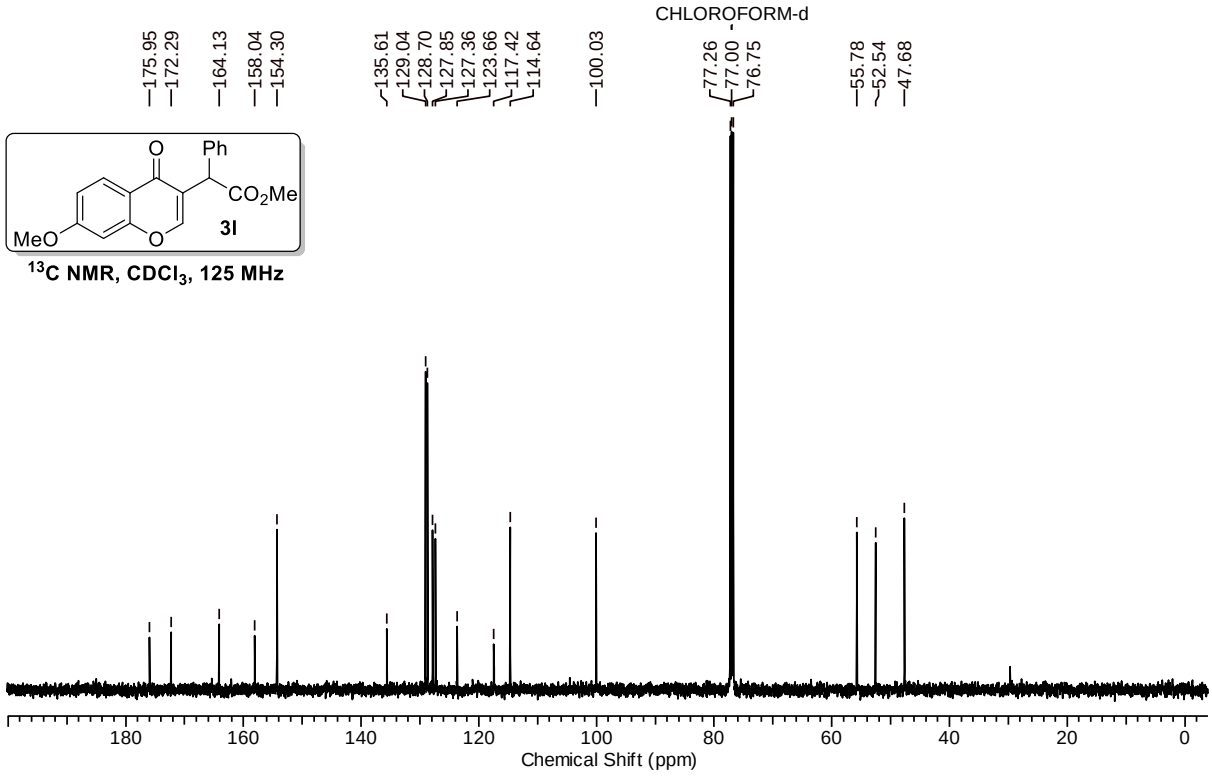

^{13}C NMR, $CDCl_3$, 125 MHz

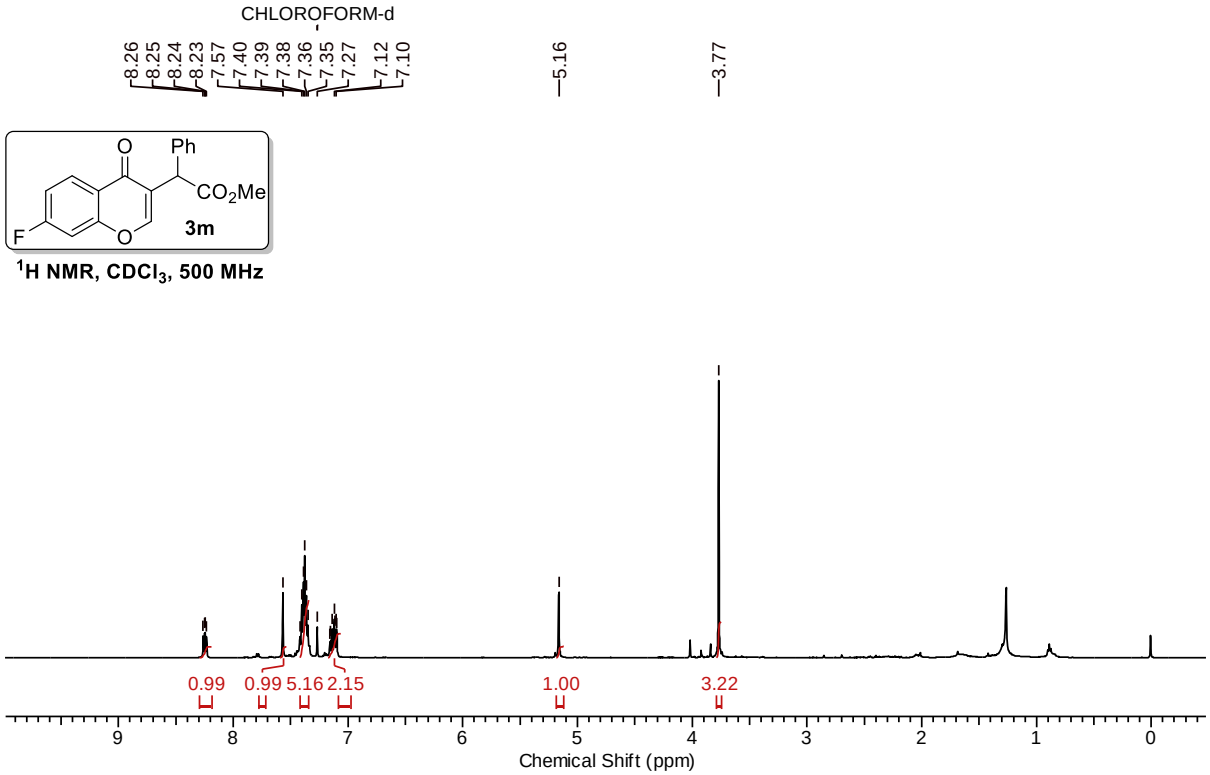

^{1}H NMR, $CDCl_3$, 500 MHz

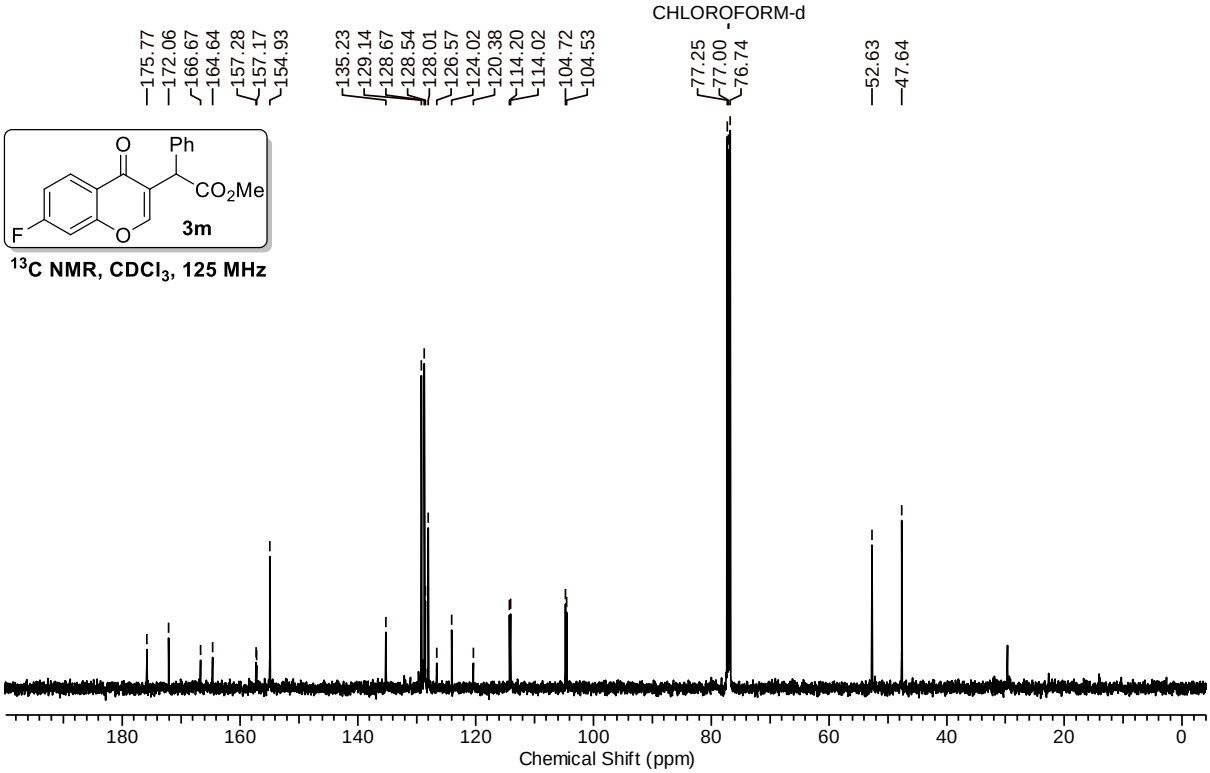

^{13}C NMR, $CDCl_3$, 125 MHz

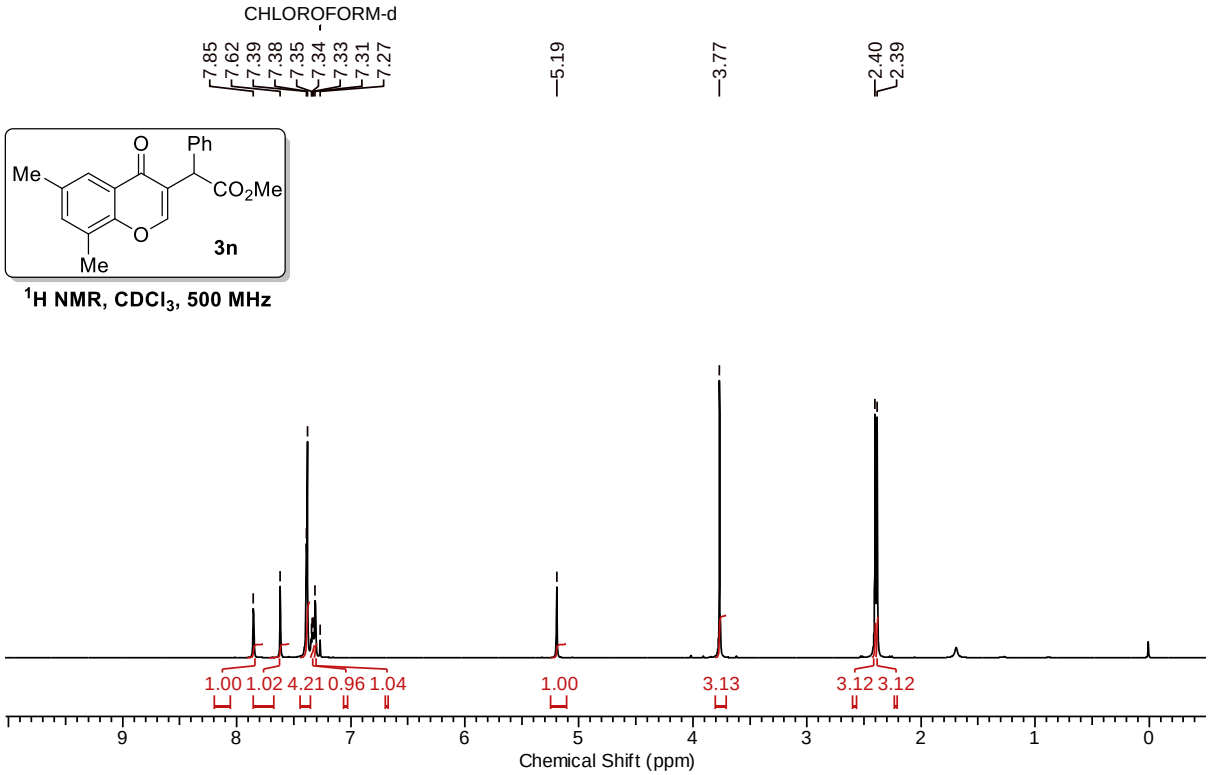

^{1}H NMR, $CDCl_3$, 500 MHz

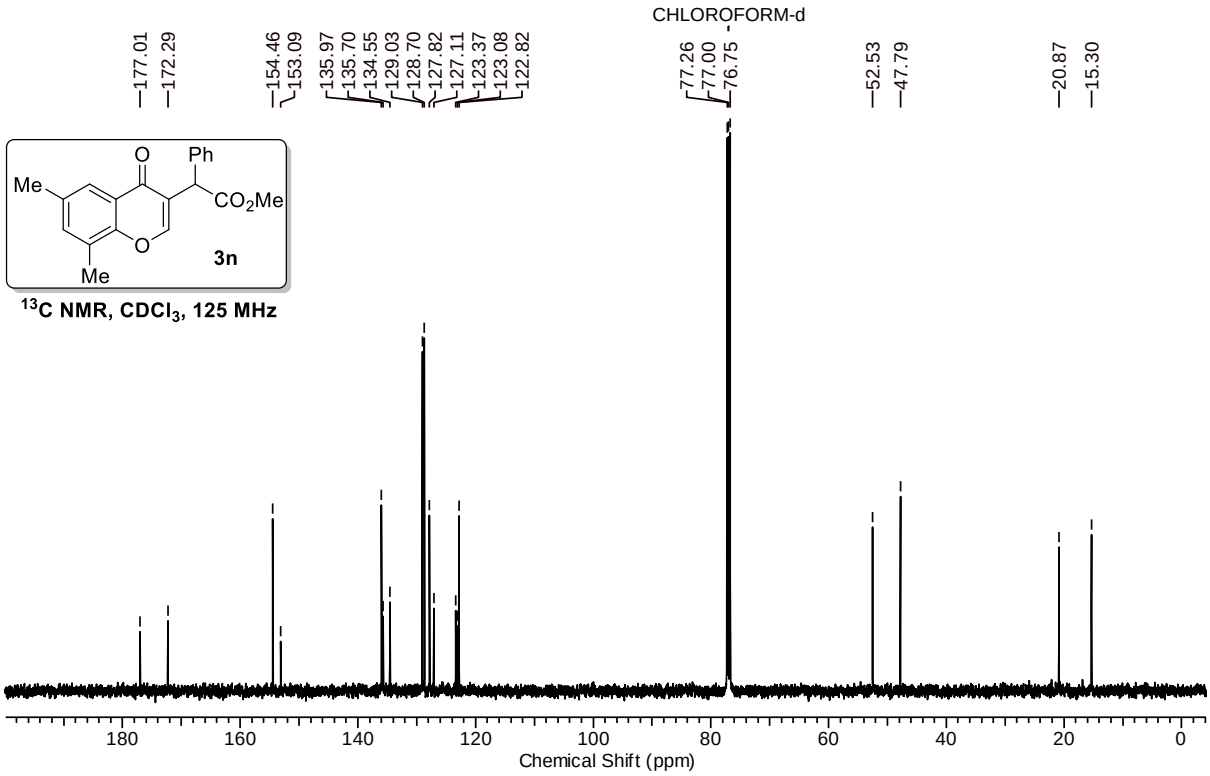

^{13}C NMR, $CDCl_3$, 125 MHz

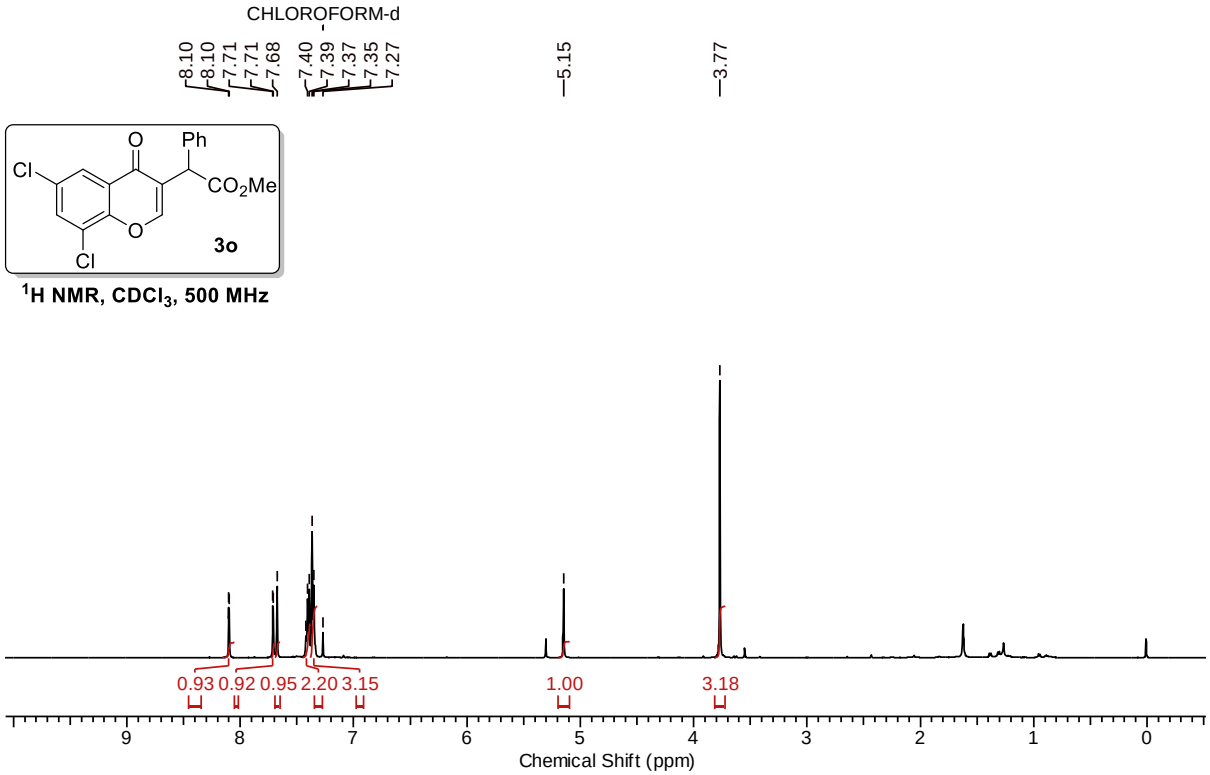

^{1}H NMR, $CDCl_3$, 500 MHz

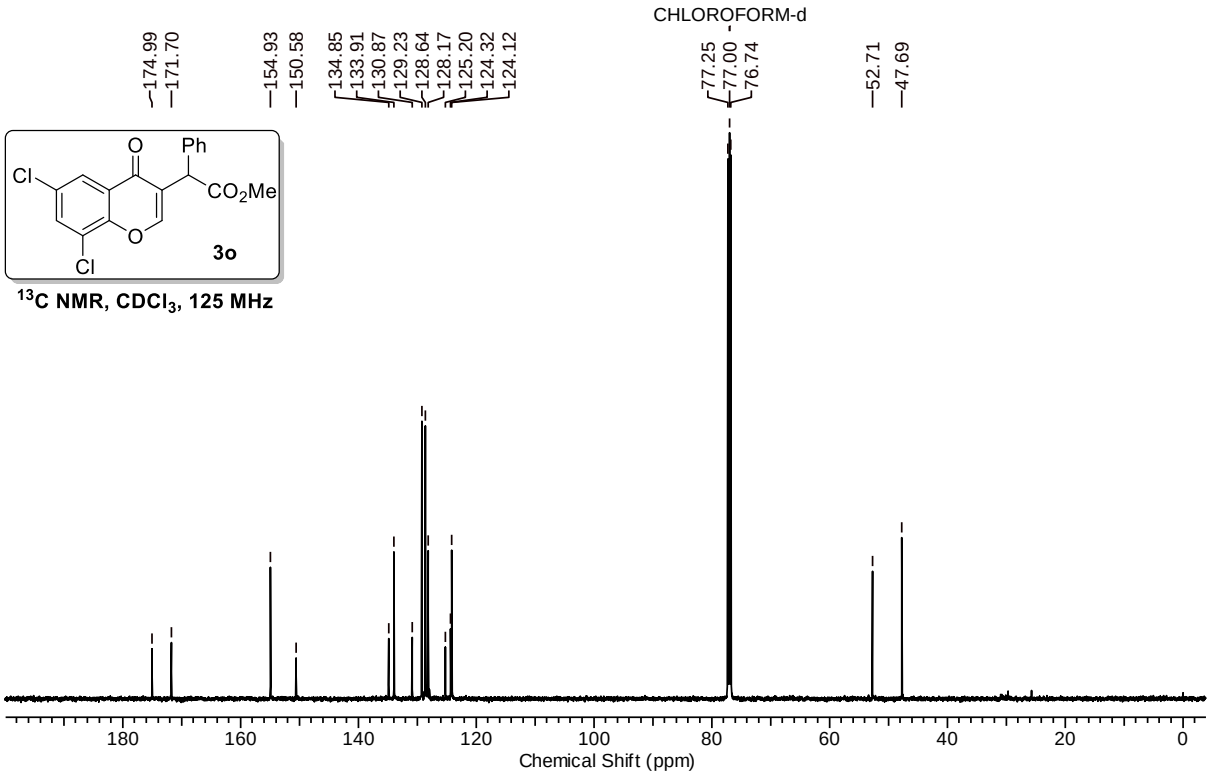

^{13}C NMR, $CDCl_3$, 125 MHz

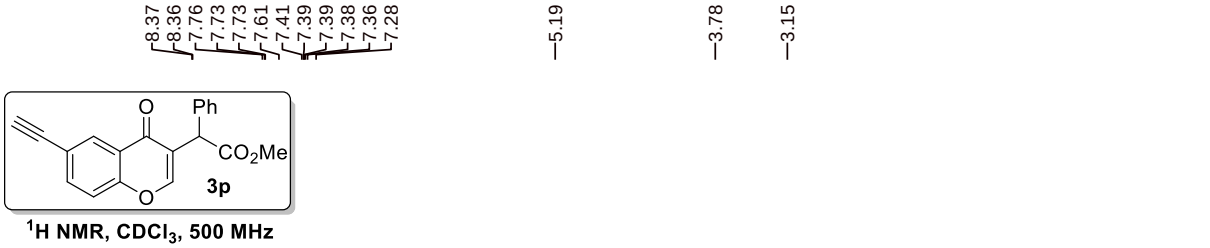

^{1}H NMR, $CDCl_3$, 500 MHz

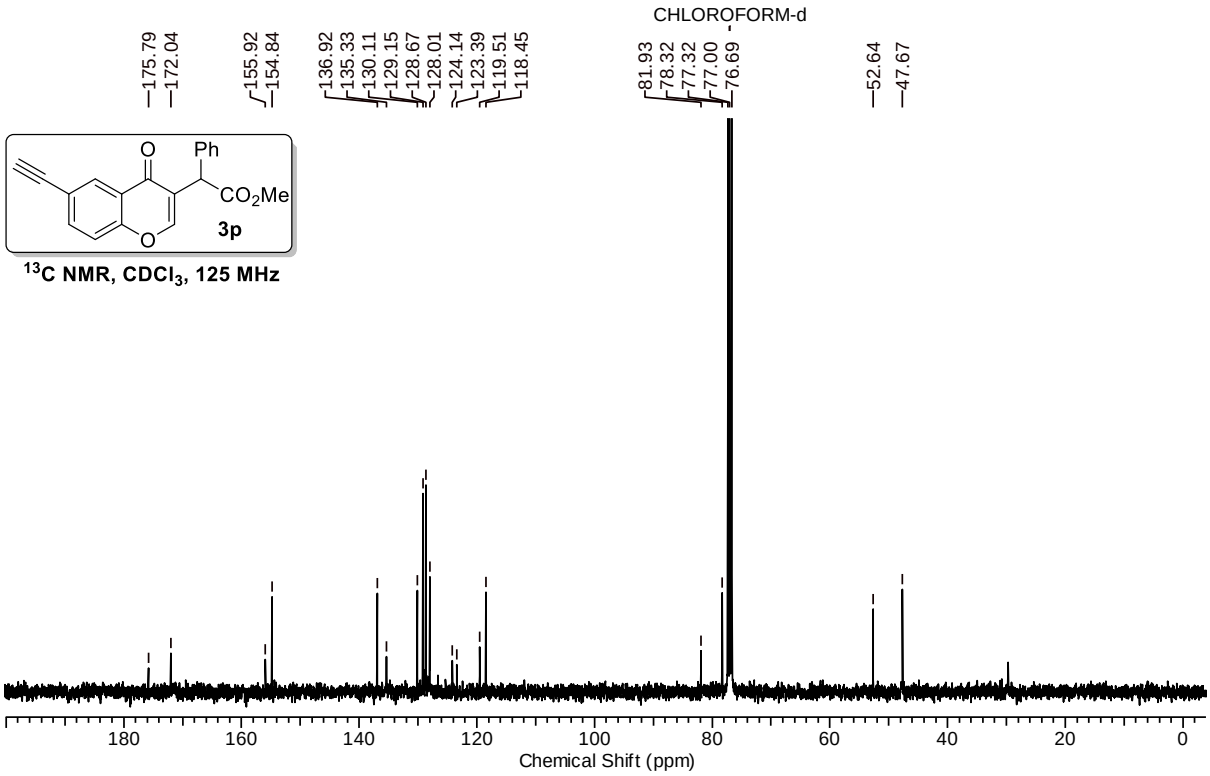

^{13}C NMR, $CDCl_3$, 125 MHz

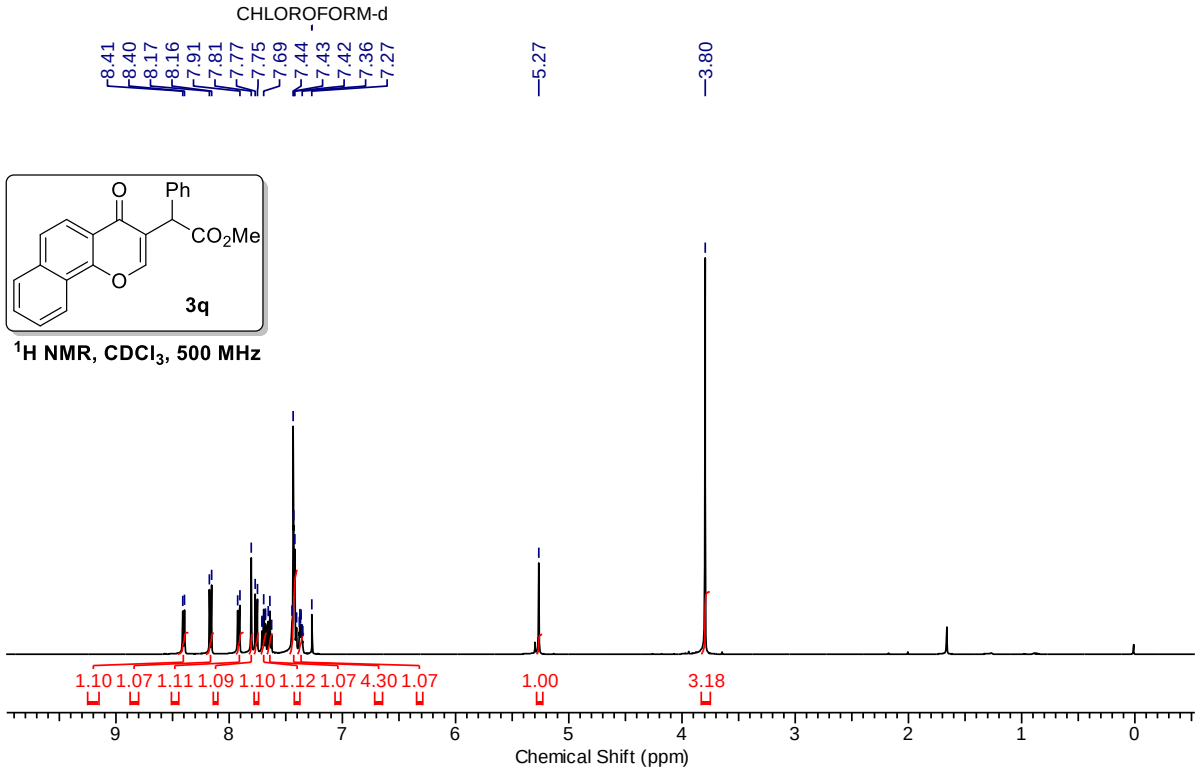

^{1}H NMR, $CDCl_3$, 500 MHz

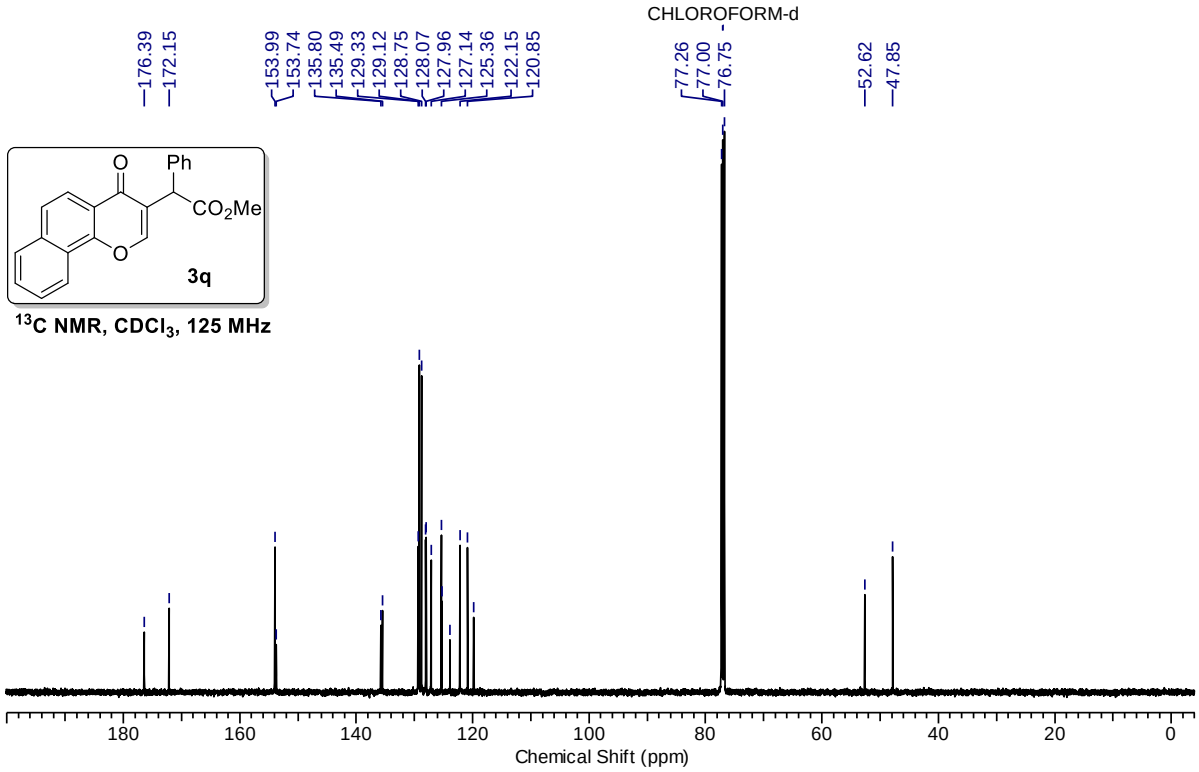

^{13}C NMR, $CDCl_3$, 125 MHz

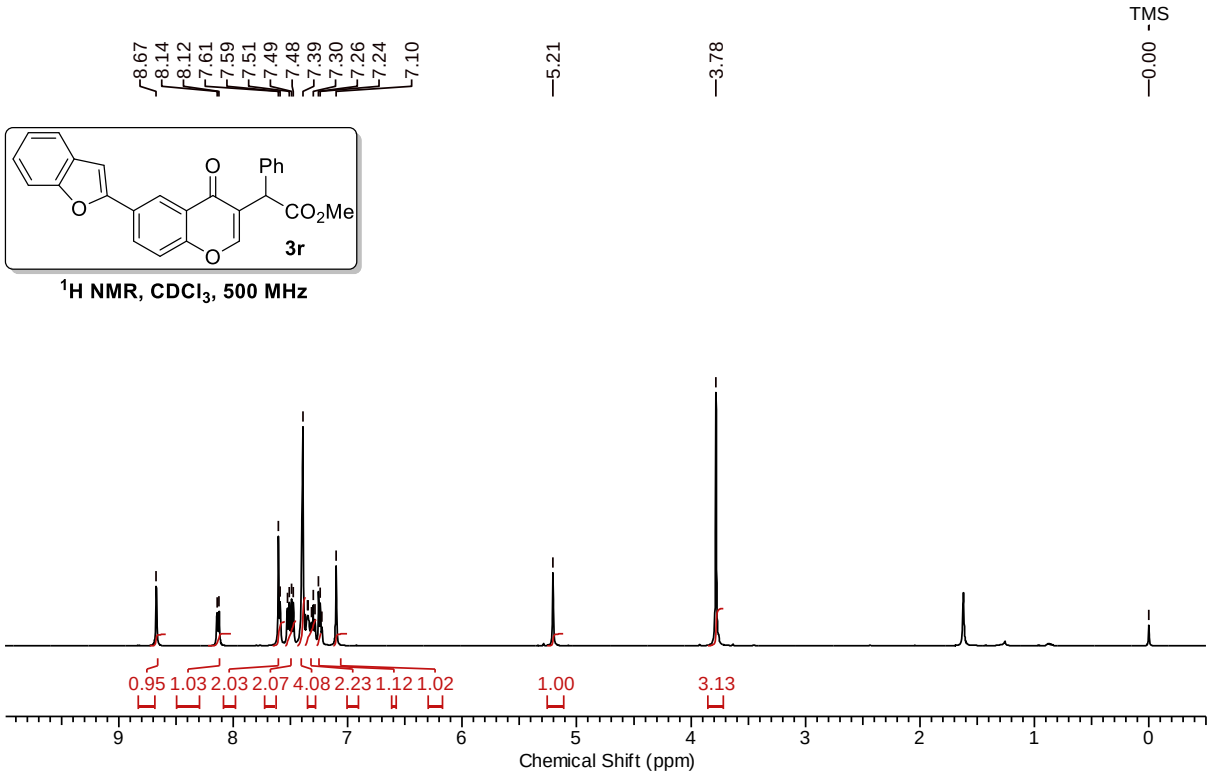

^{1}H NMR, $CDCl_3$, 500 MHz

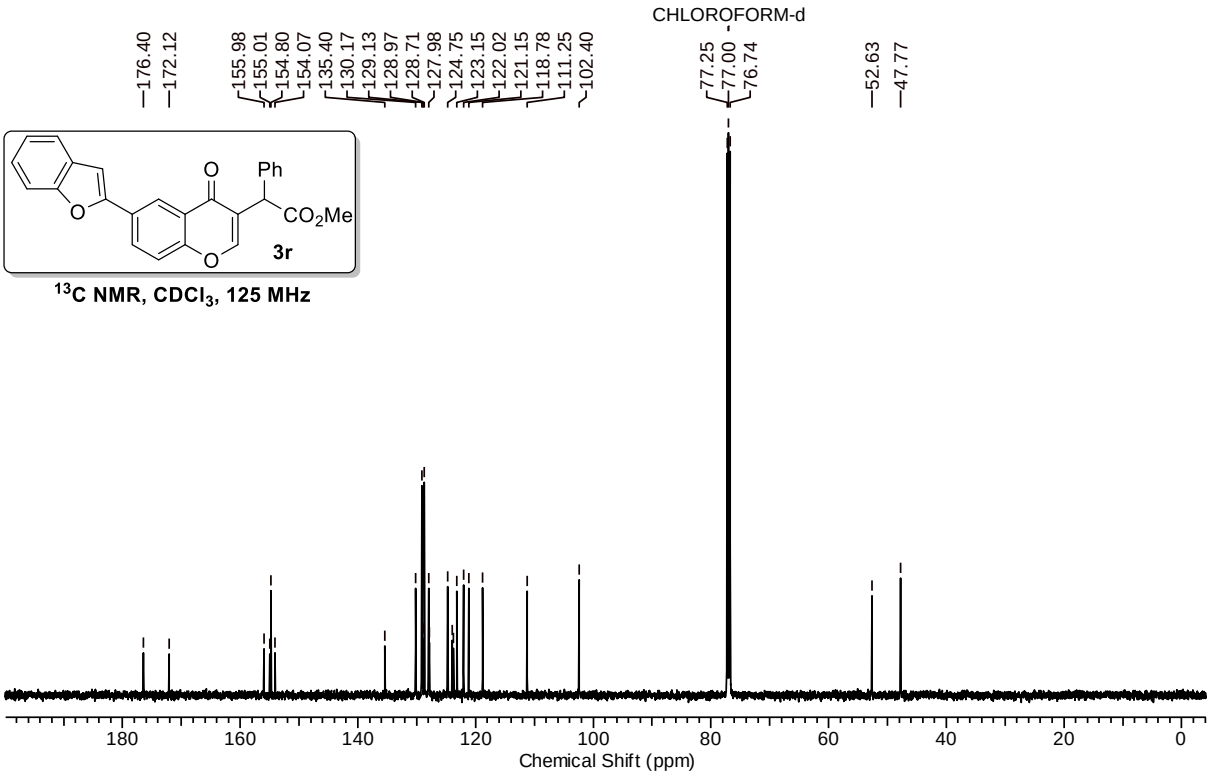

^{13}C NMR, $CDCl_3$, 125 MHz

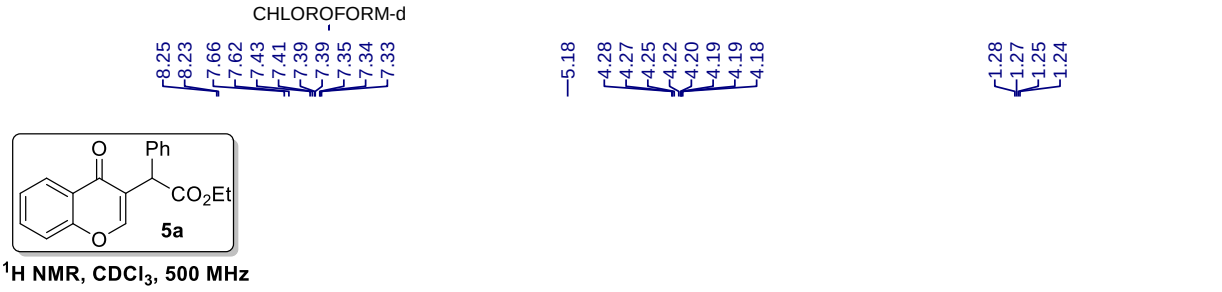

^{1}H NMR, $CDCl_3$, 500 MHz

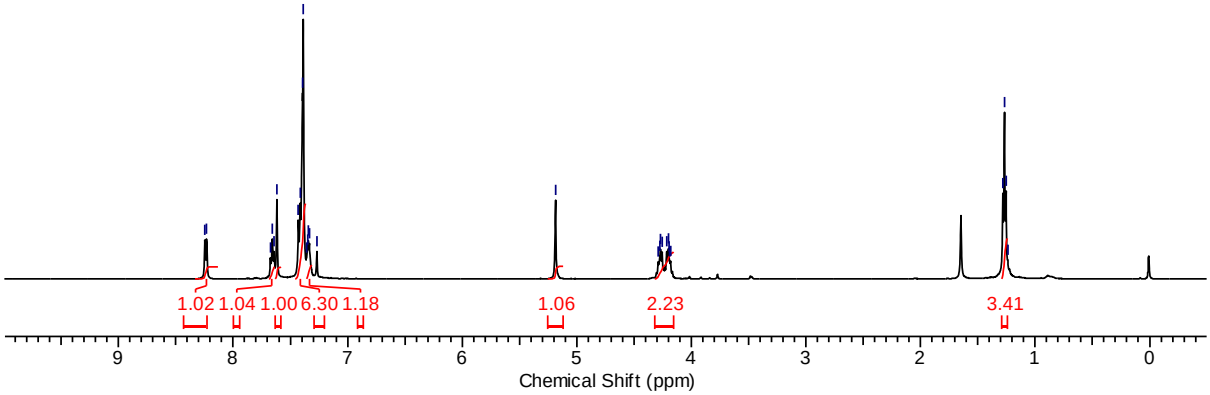

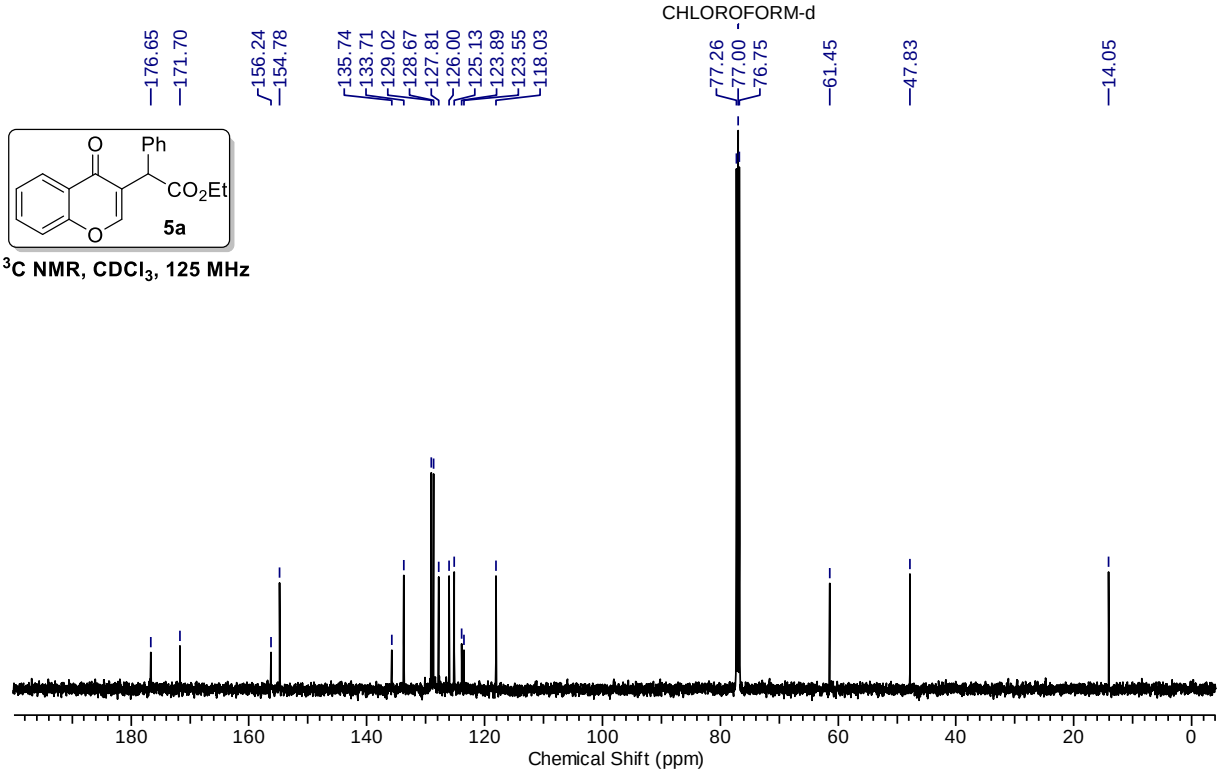

^{13}C NMR, $CDCl_3$, 125 MHz

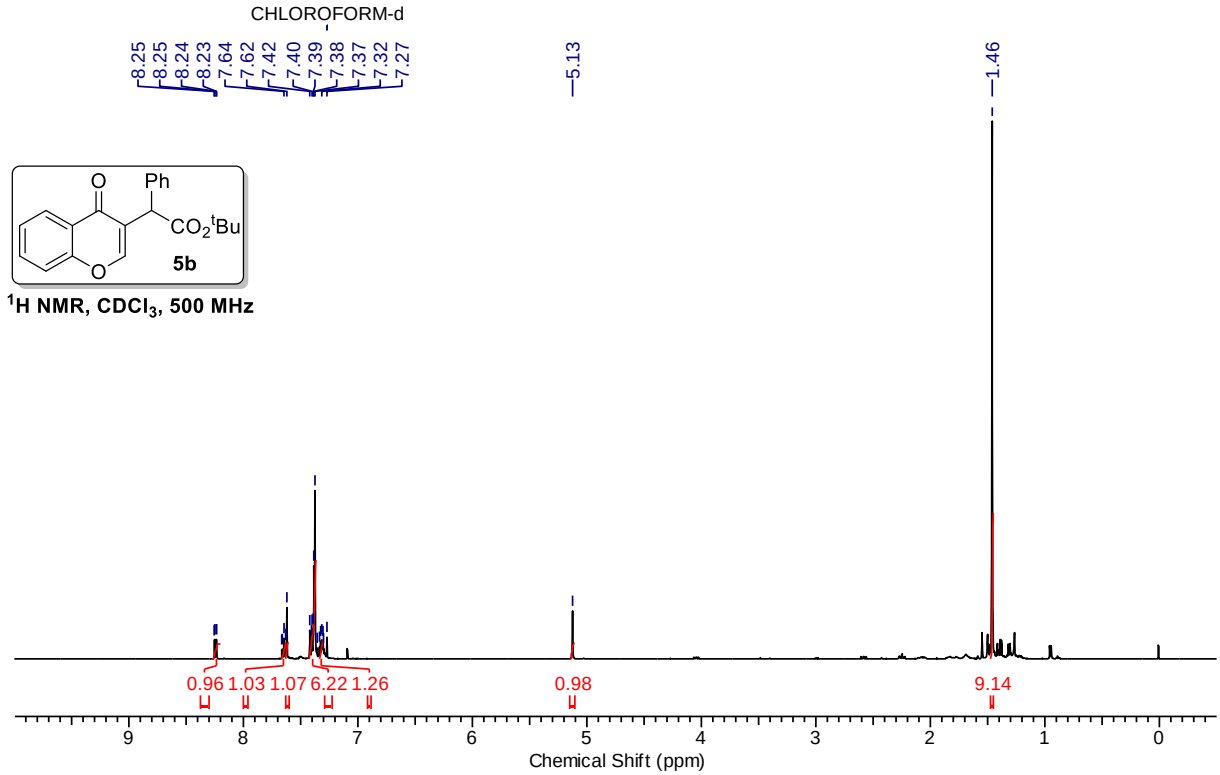

^{1}H NMR, $CDCl_3$, 500 MHz

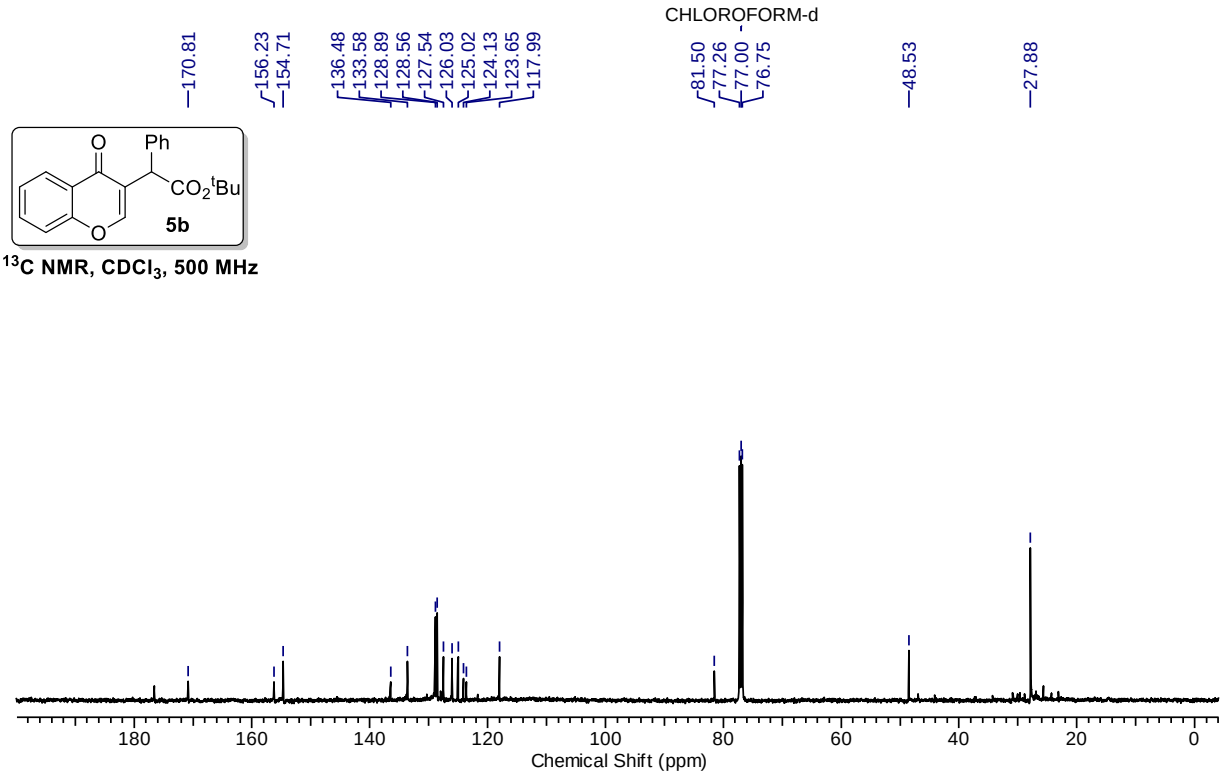

^{13}C NMR, $CDCl_3$, 500 MHz

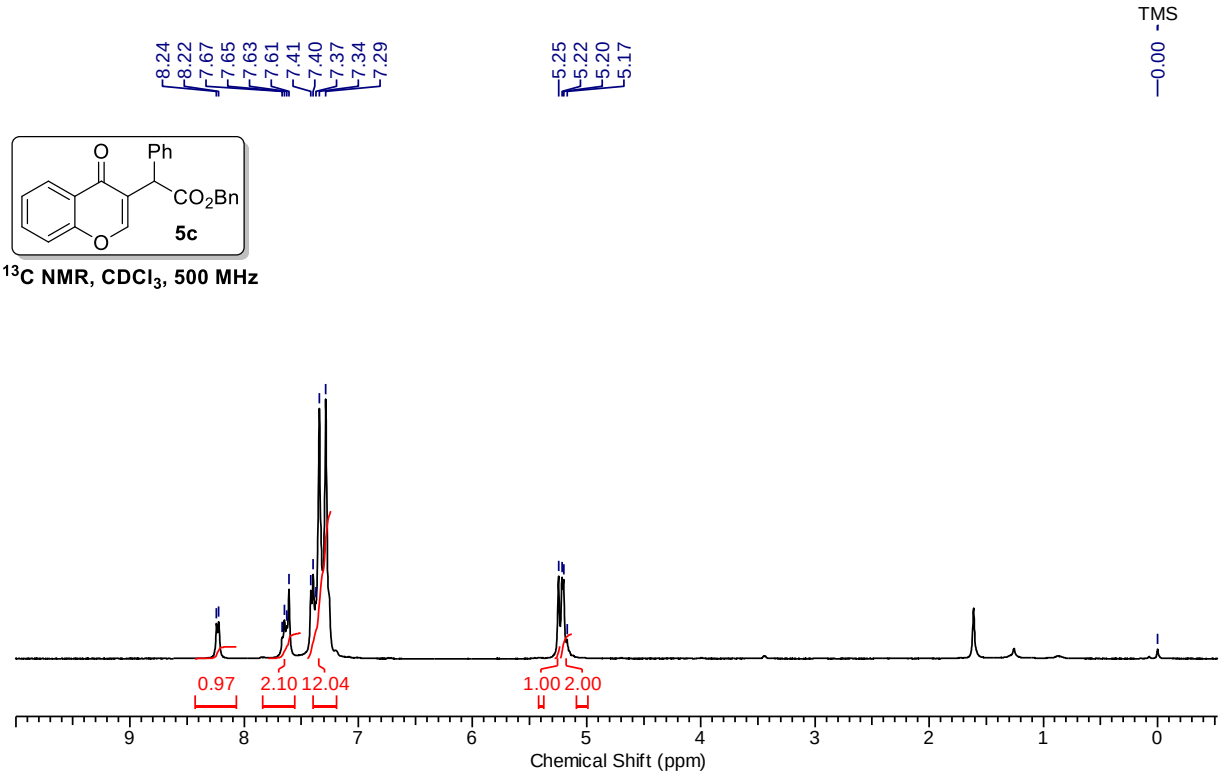

^{13}C NMR, $CDCl_3$, 500 MHz

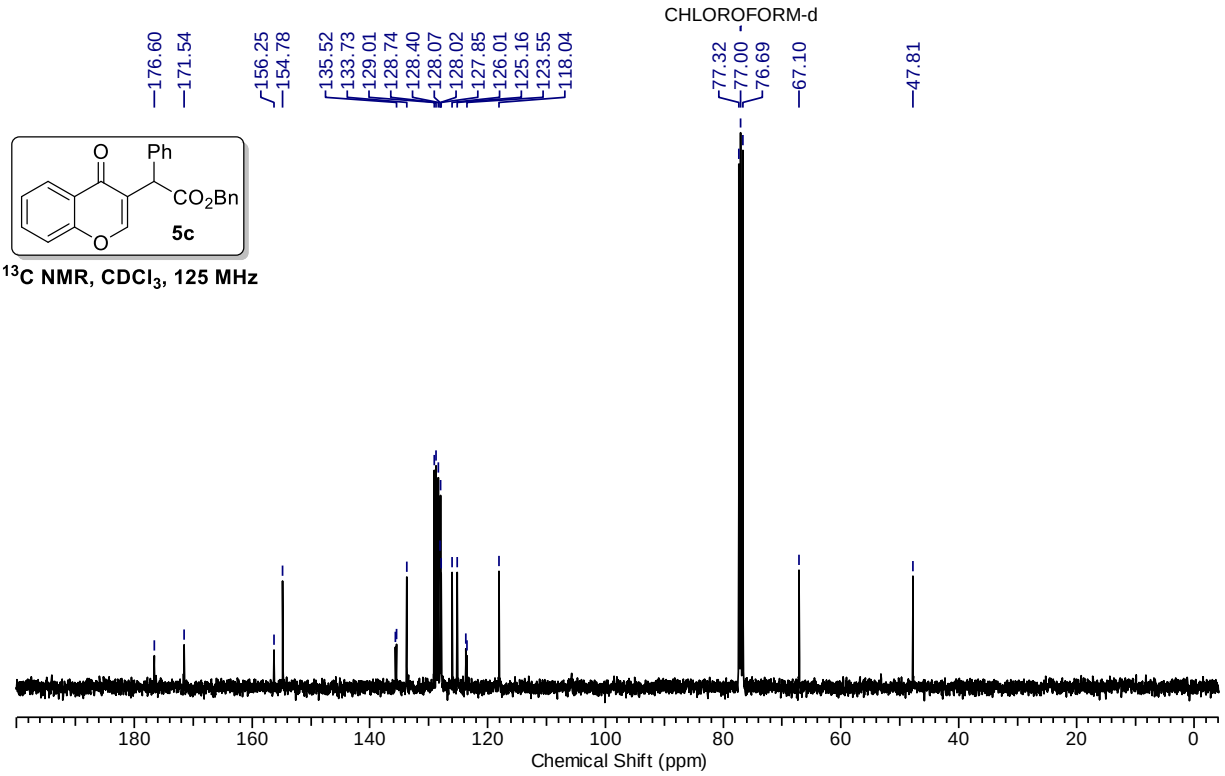

^{13}C NMR, $CDCl_3$, 125 MHz

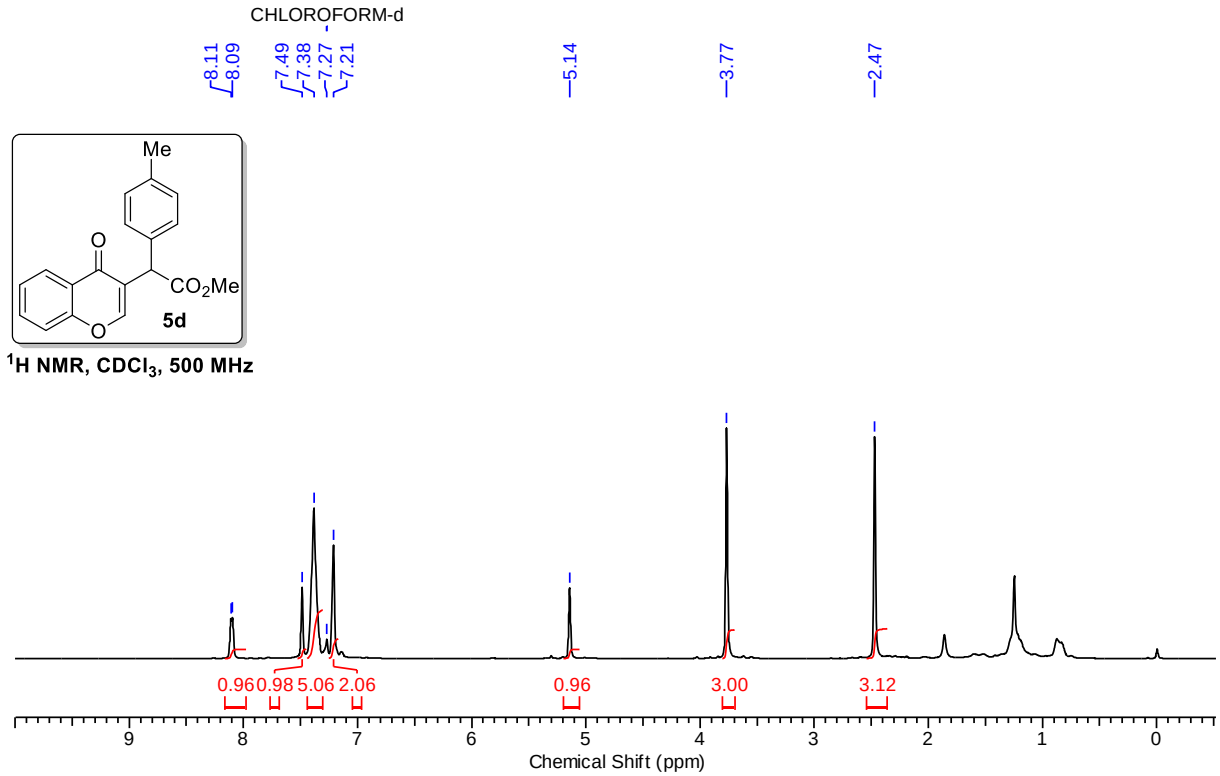

^{1}H NMR, $CDCl_3$, 500 MHz

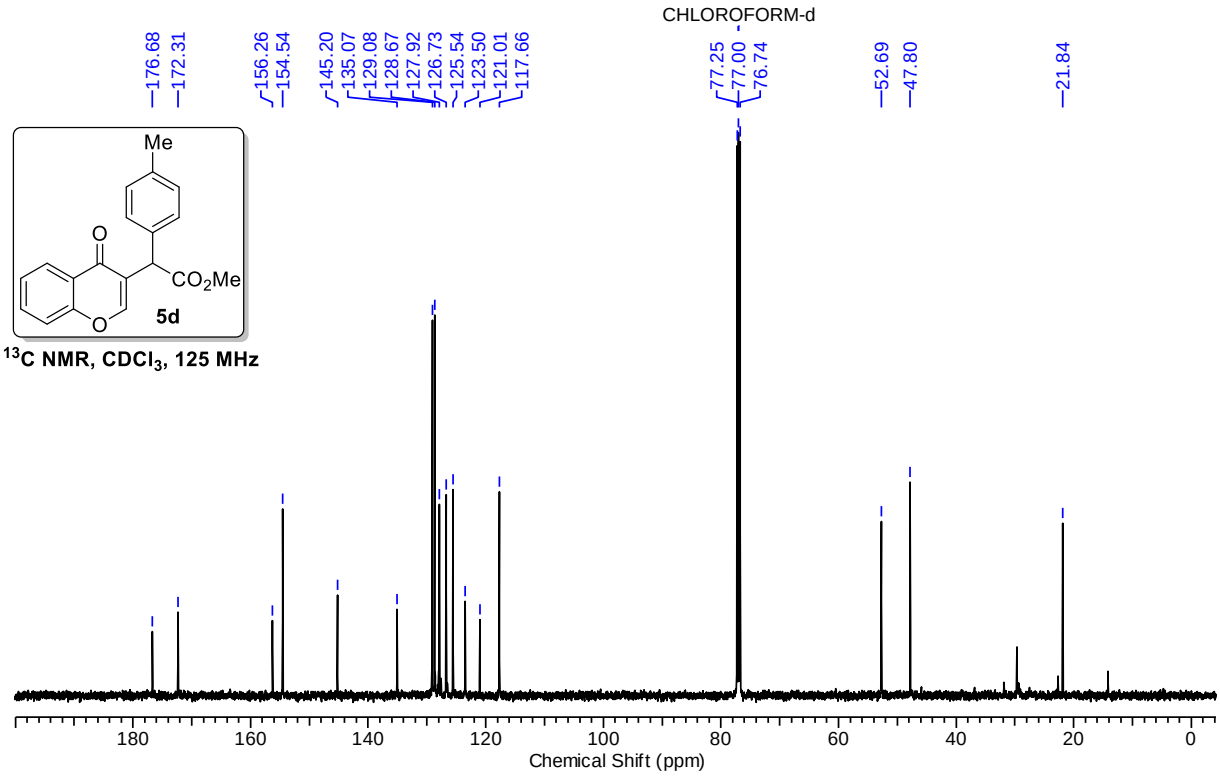

^{13}C NMR, $CDCl_3$, 125 MHz

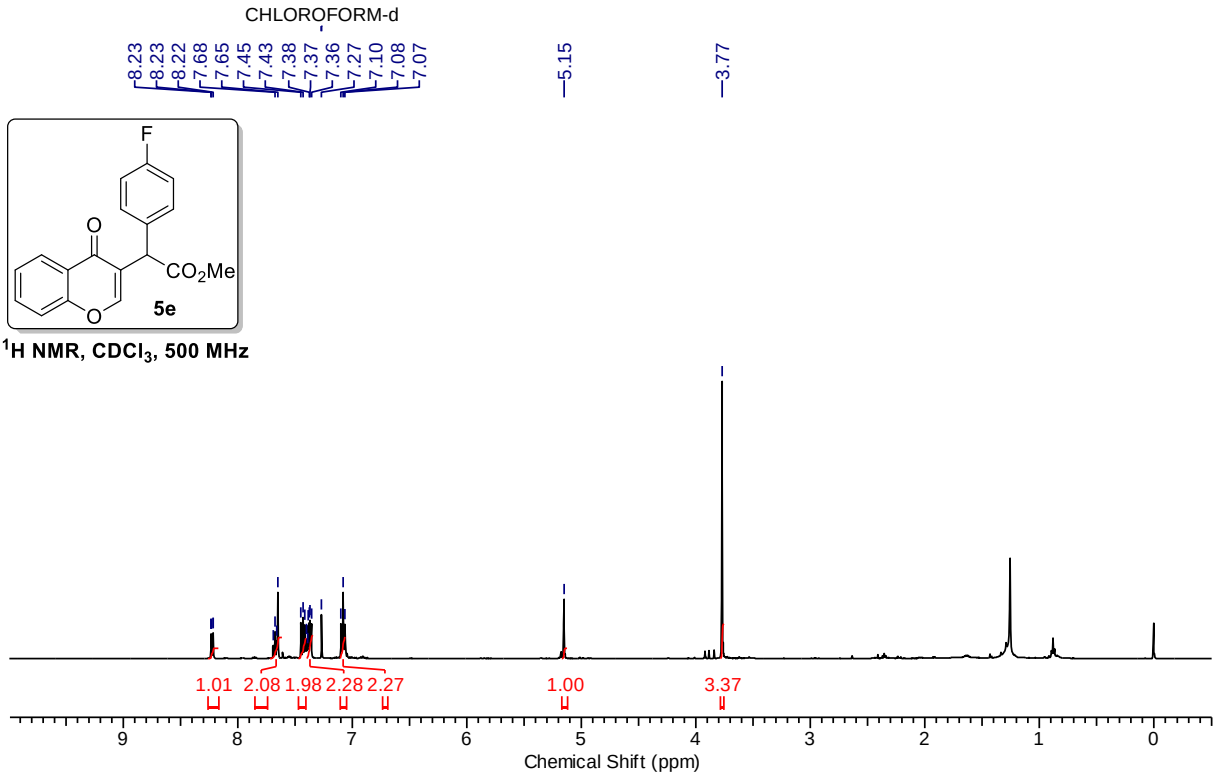

^{1}H NMR, $CDCl_3$, 500 MHz

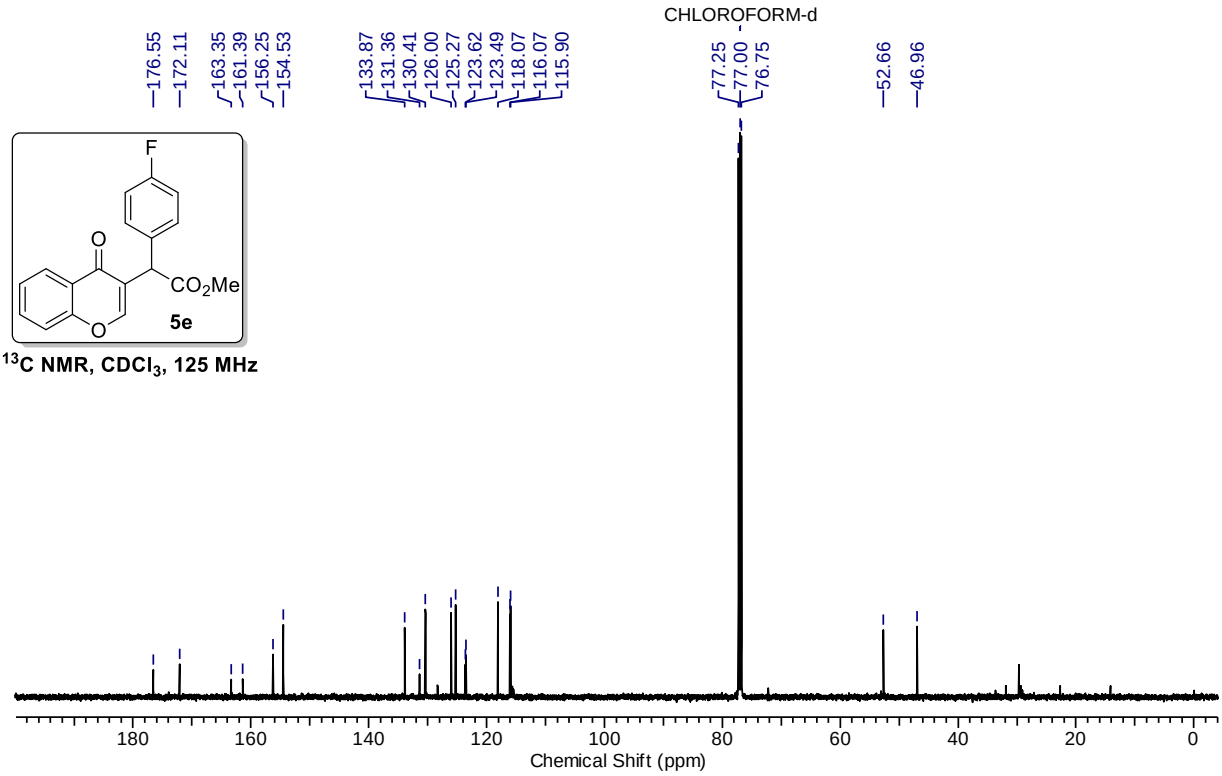

^{13}C NMR, $CDCl_3$, 125 MHz

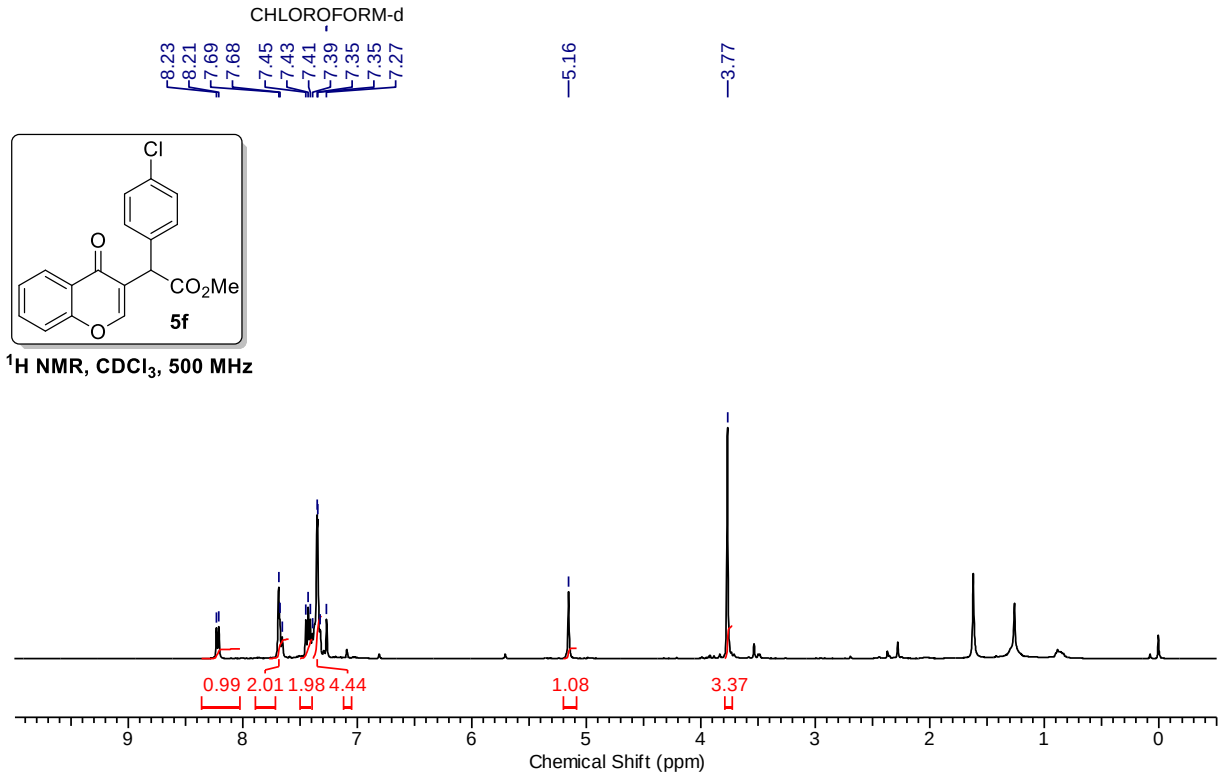

^{1}H NMR, $CDCl_3$, 500 MHz

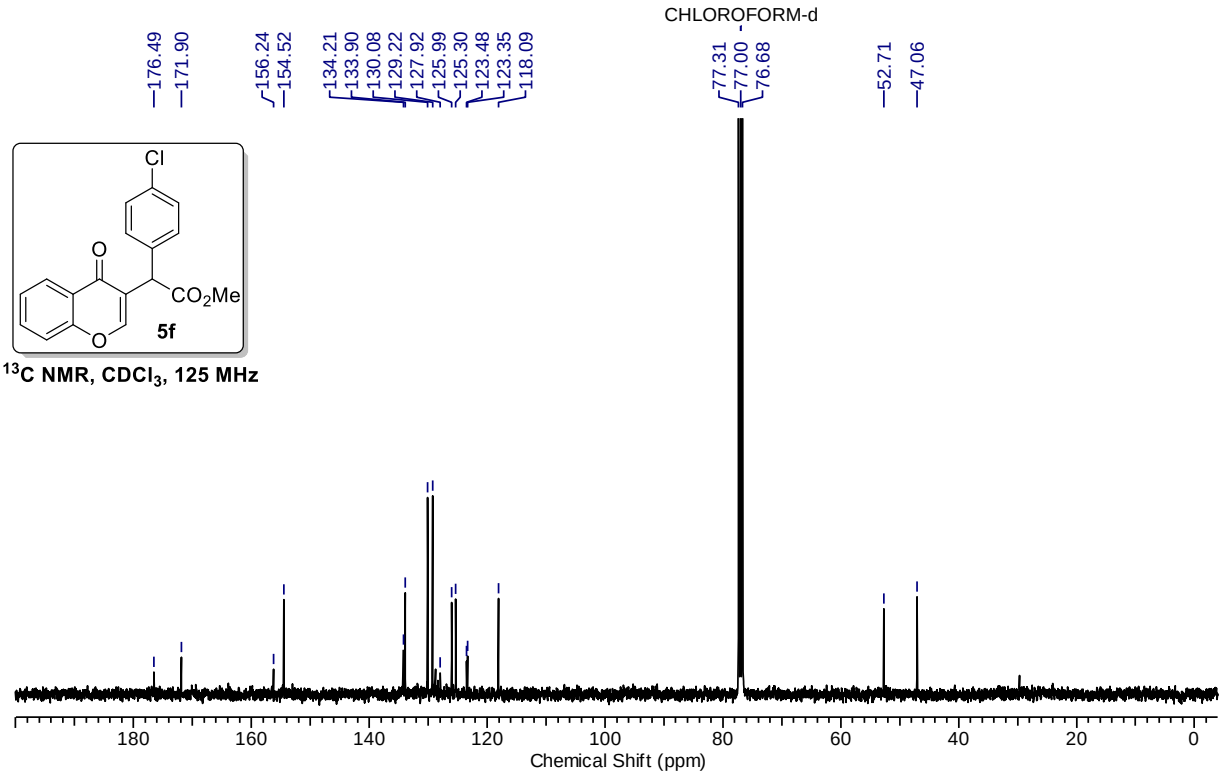

^{13}C NMR, $CDCl_3$, 125 MHz

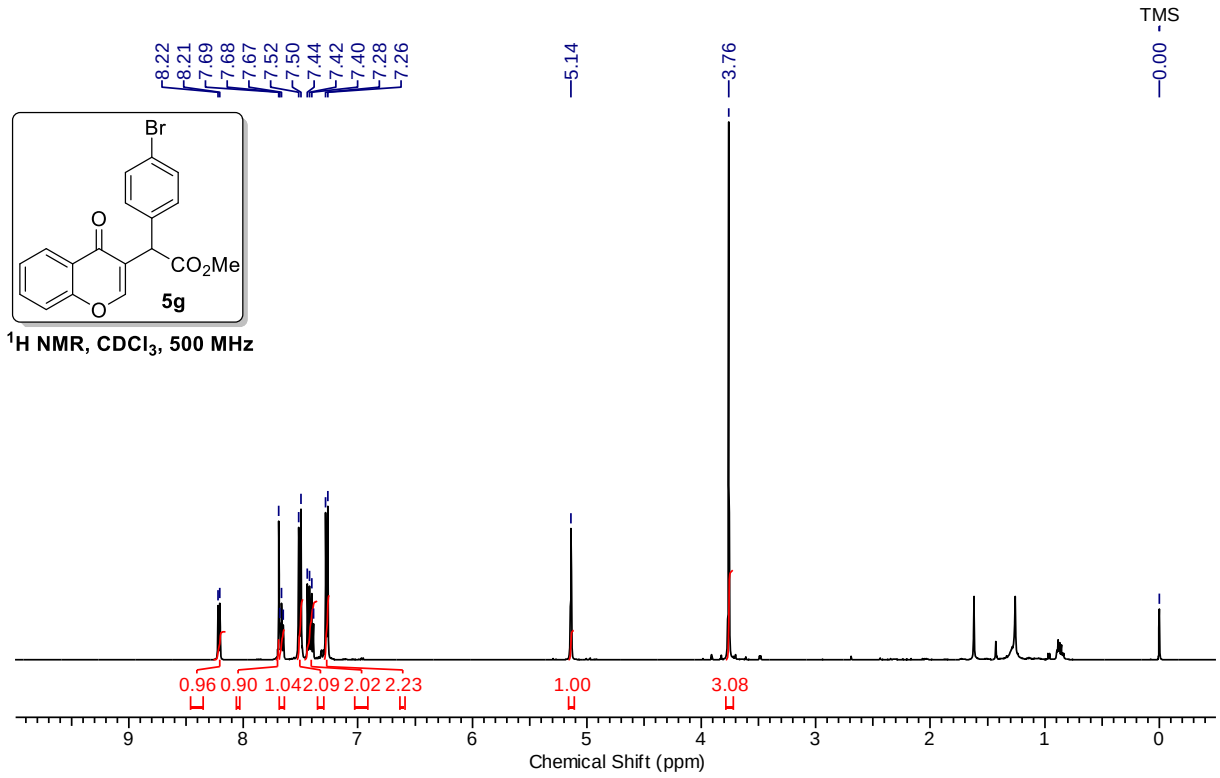

^{1}H NMR, $CDCl_3$, 500 MHz

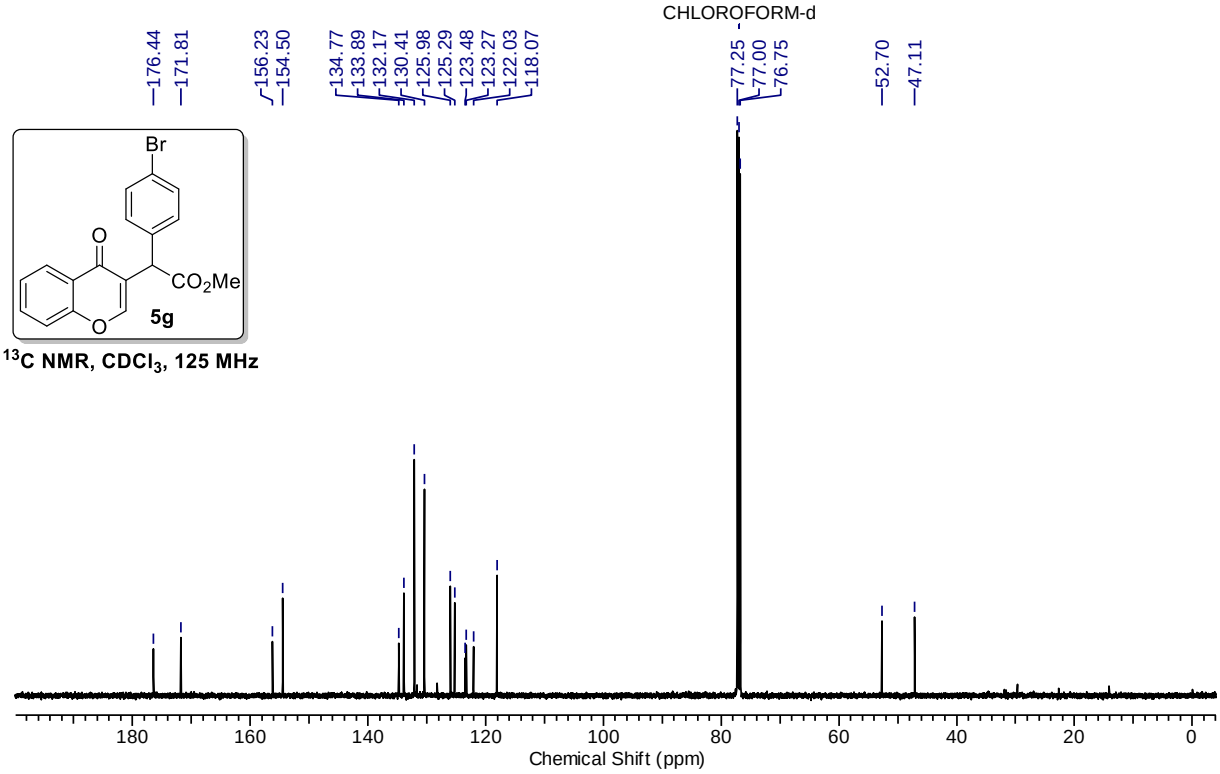

^{13}C NMR, $CDCl_3$, 125 MHz

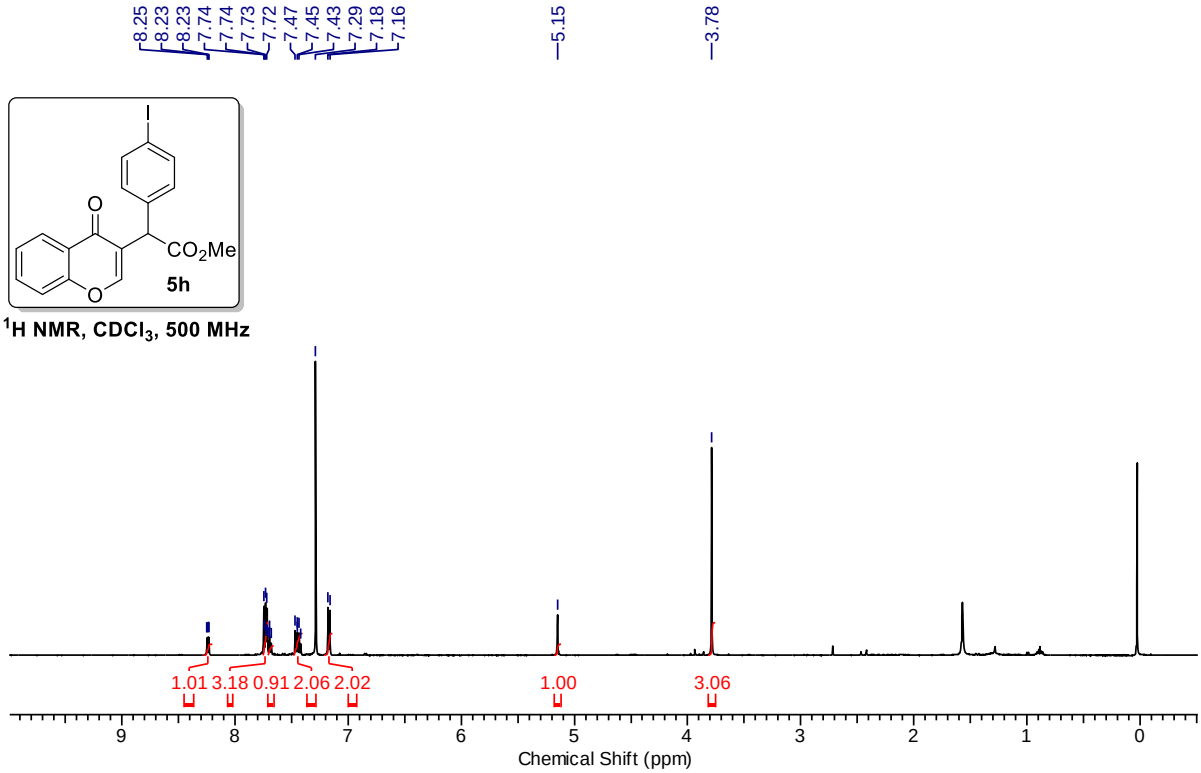

^{1}H NMR, $CDCl_3$, 500 MHz

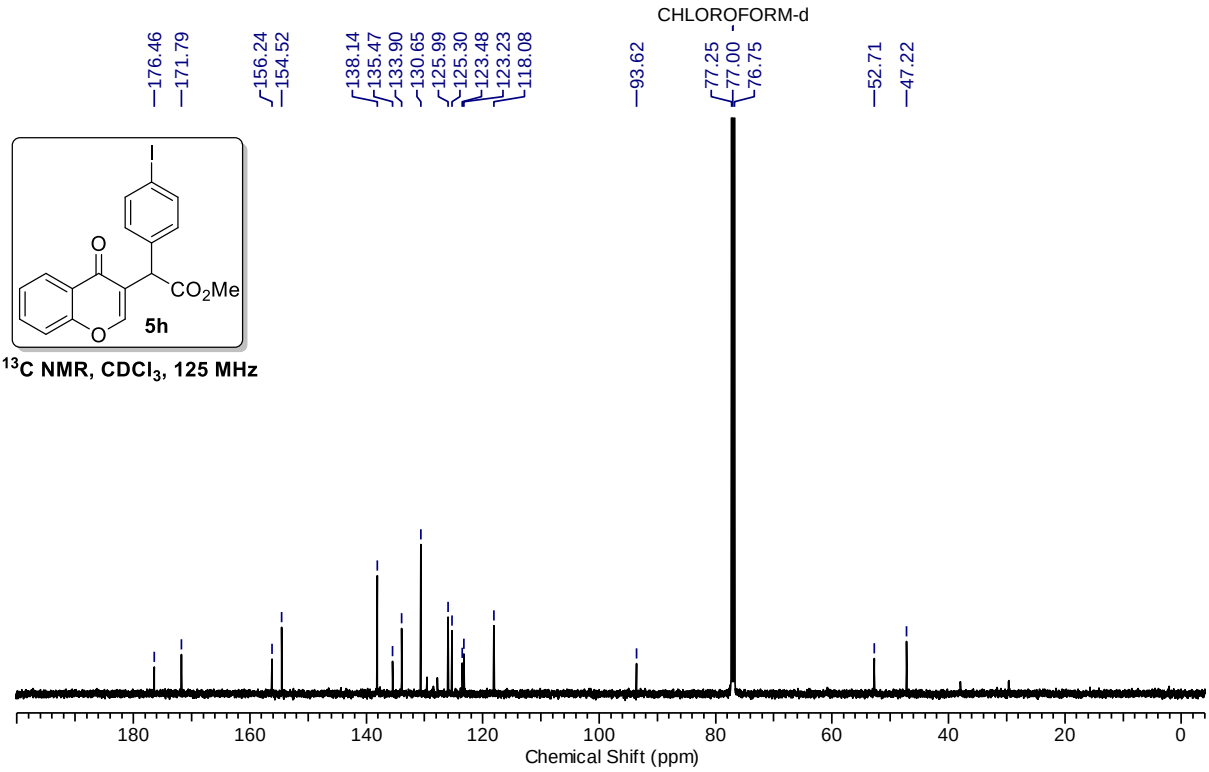

^{13}C NMR, $CDCl_3$, 125 MHz

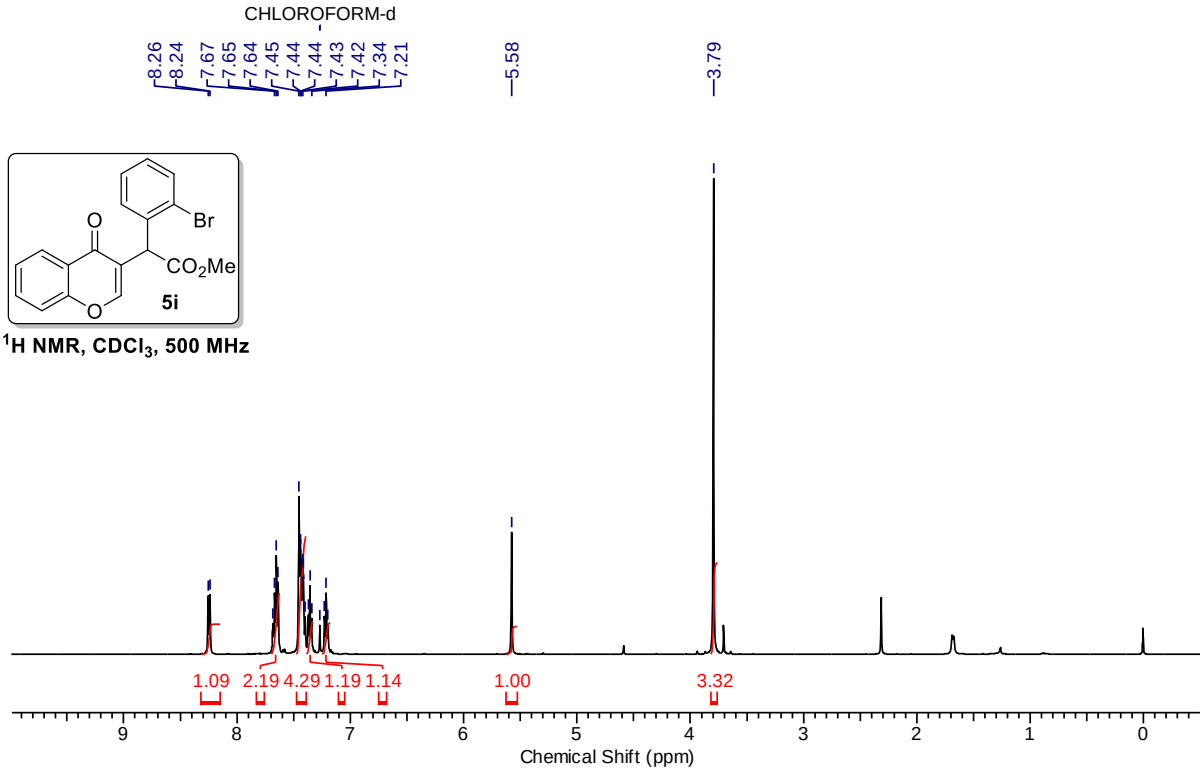

^{1}H NMR, $CDCl_3$, 500 MHz

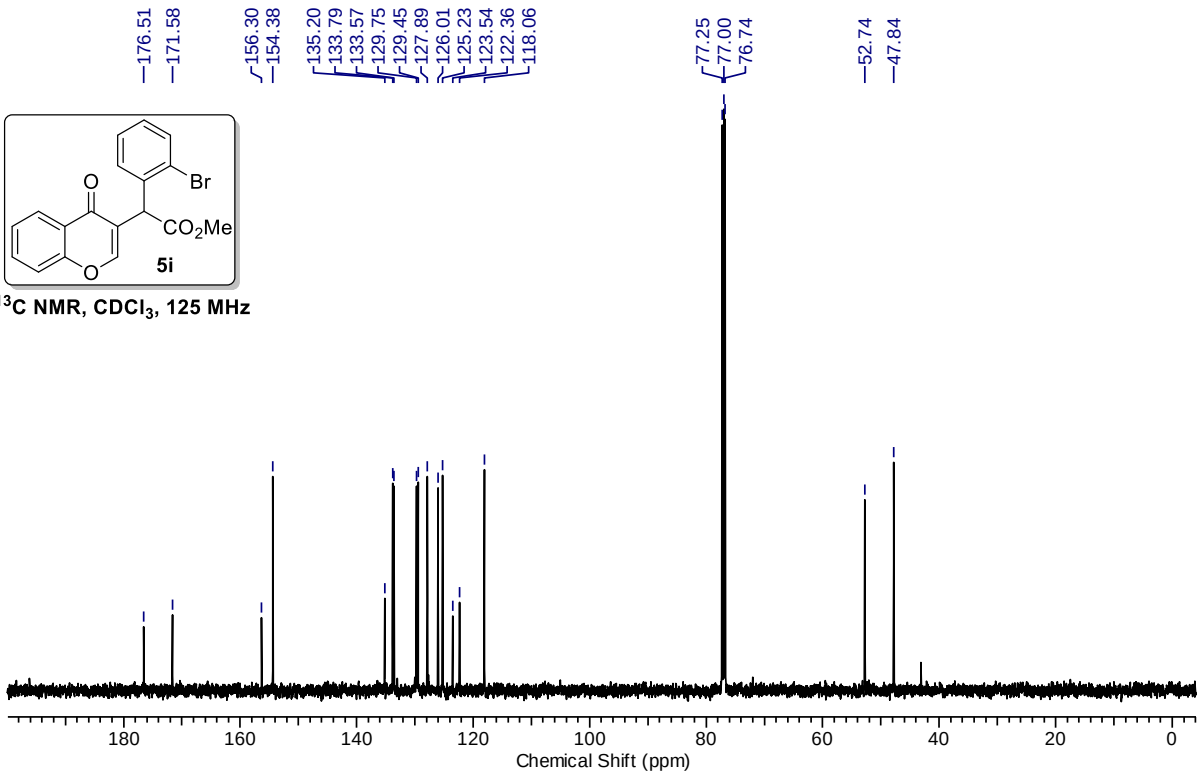

^{13}C NMR, $CDCl_3$, 125 MHz

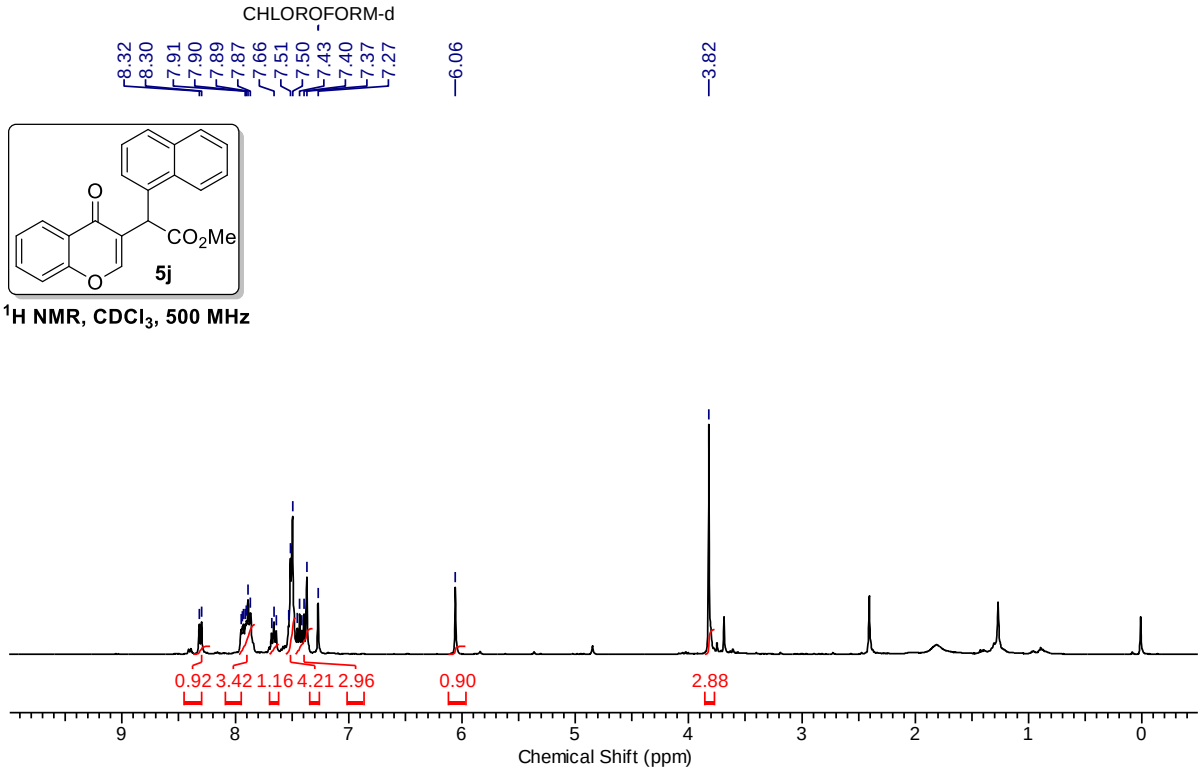

^{1}H NMR, $CDCl_3$, 500 MHz

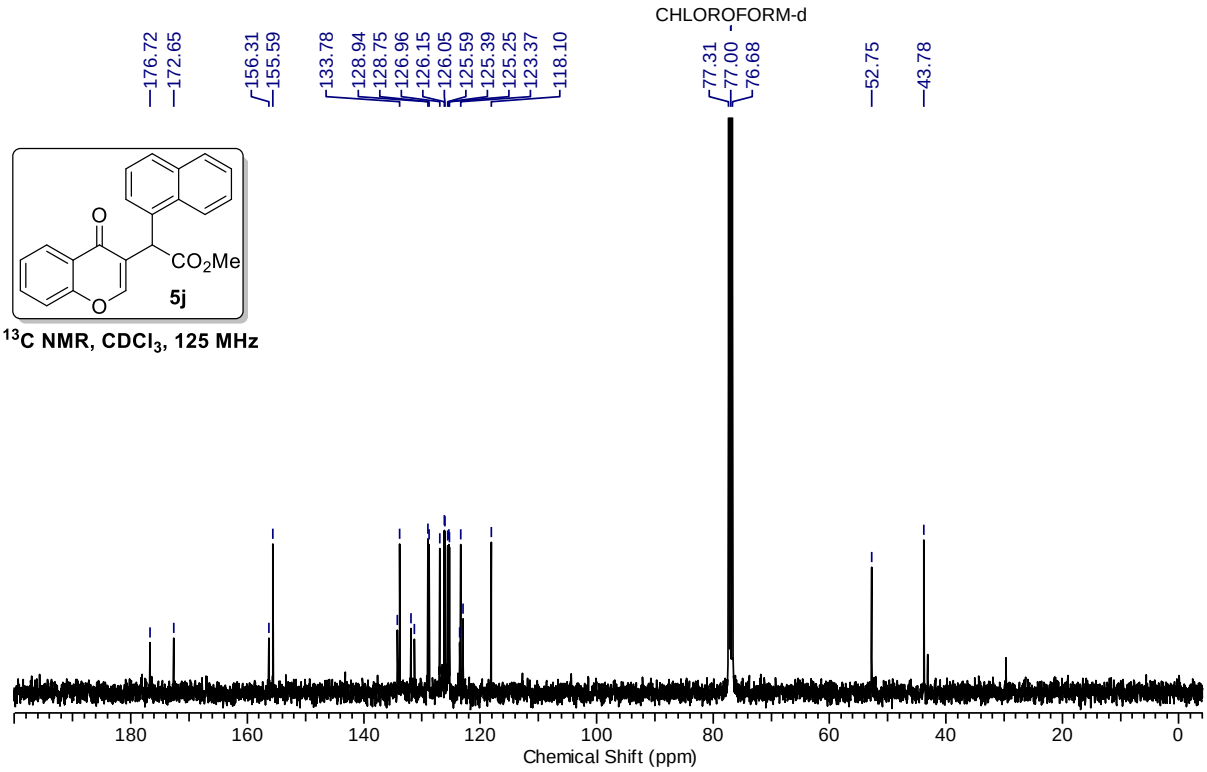

^{13}C NMR, $CDCl_3$, 125 MHz

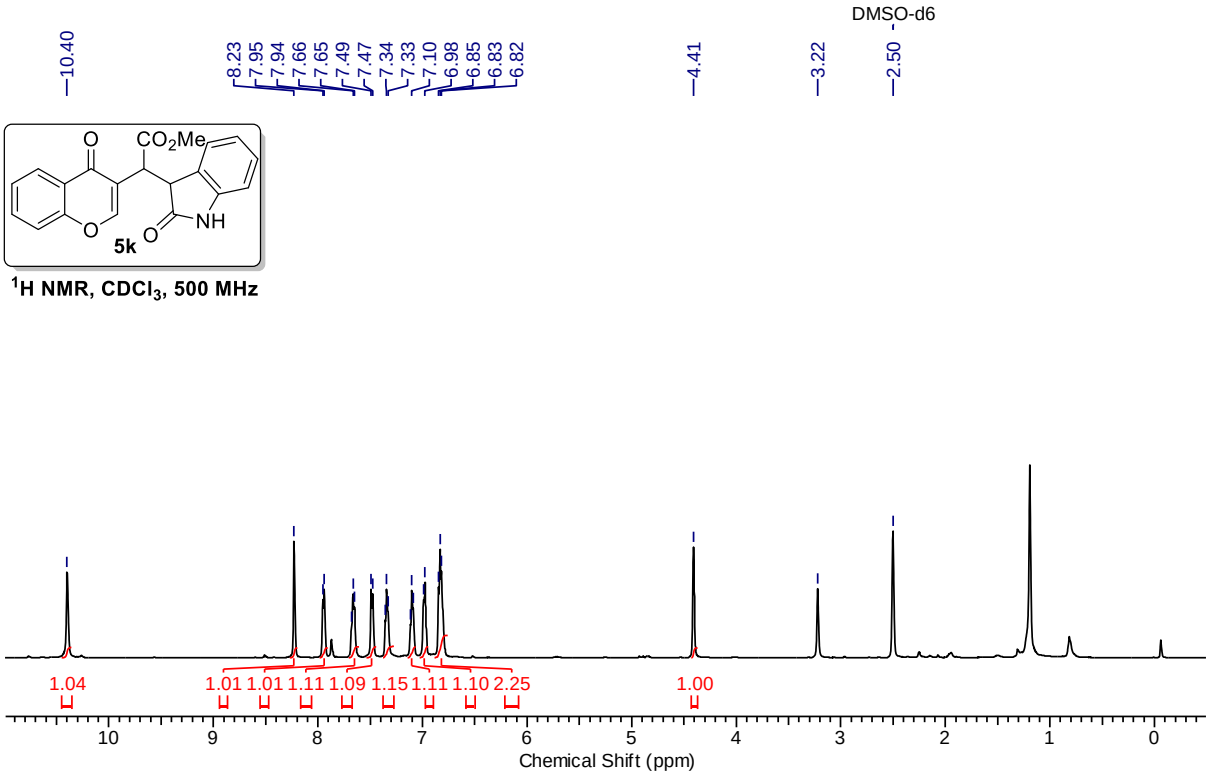

^{1}H NMR, $CDCl_3$, 500 MHz

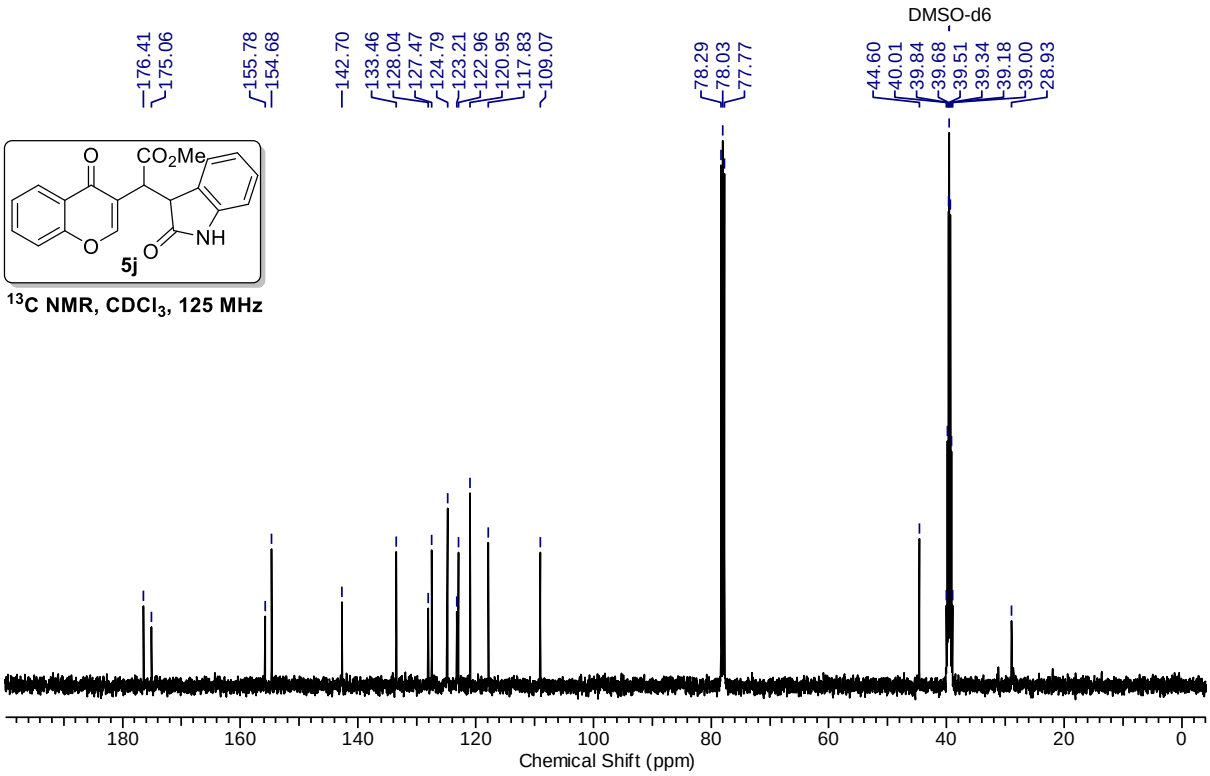

^{13}C NMR, $CDCl_3$, 125 MHz

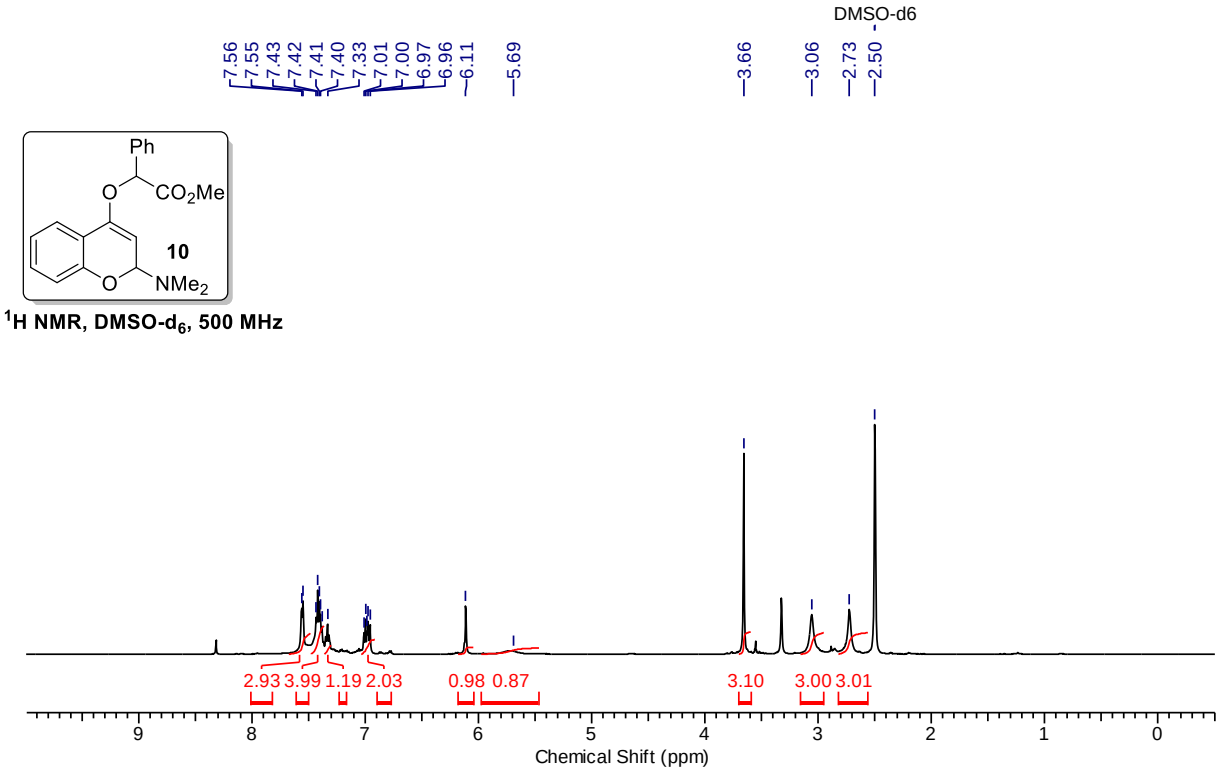

^{1}H NMR, DMSO-d$_6$, 500 MHz

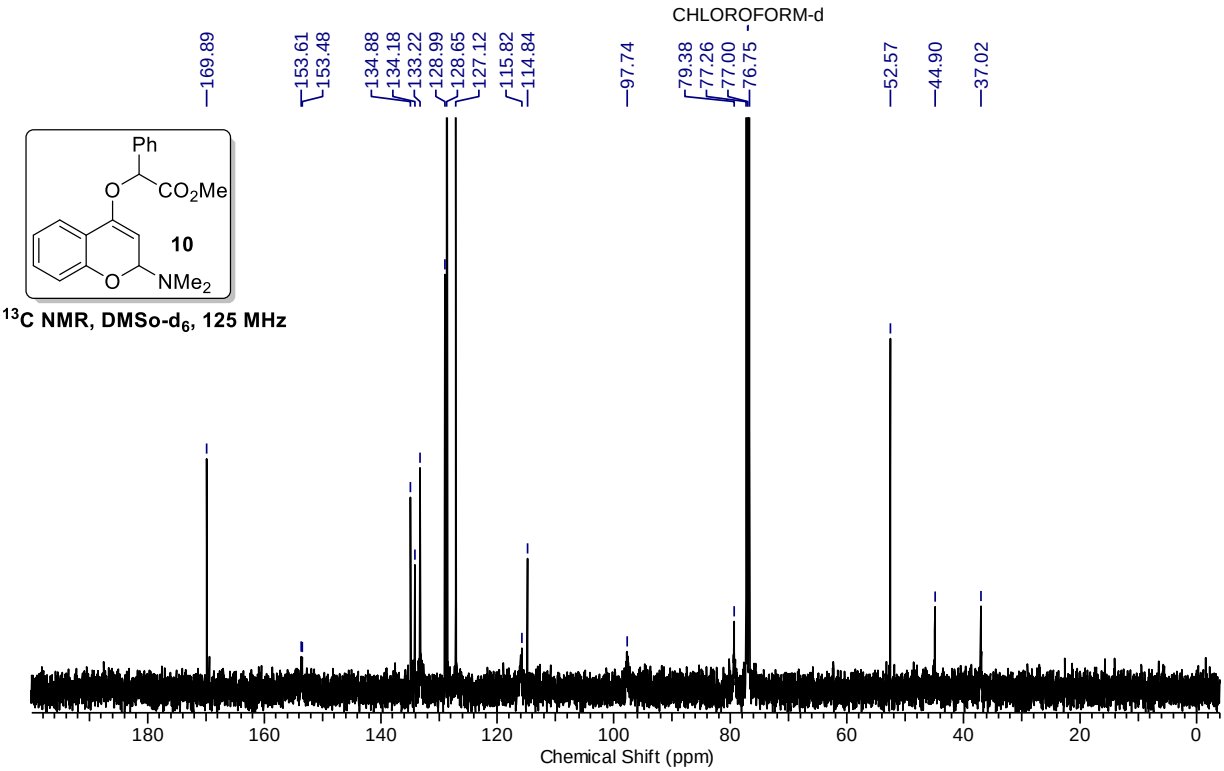

^{13}C NMR, DMSo-d$_6$, 125 MHz

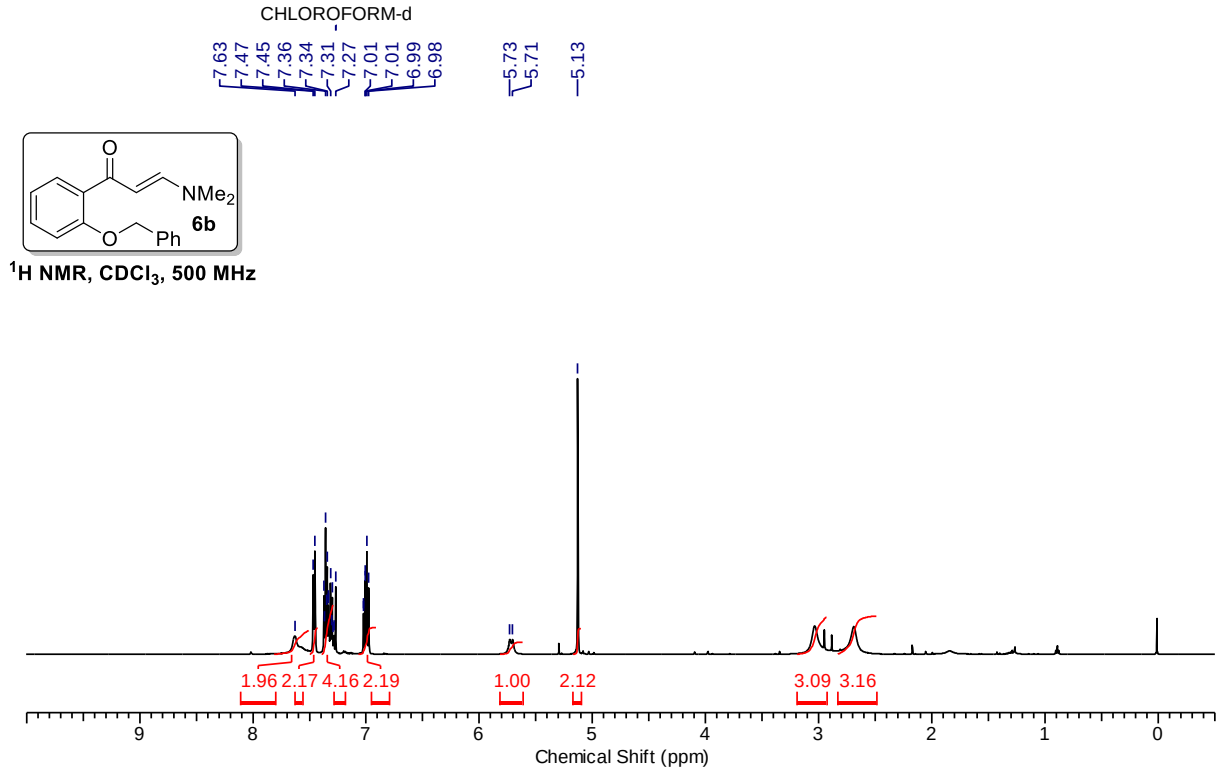

^{1}H NMR, $CDCl_3$, 500 MHz

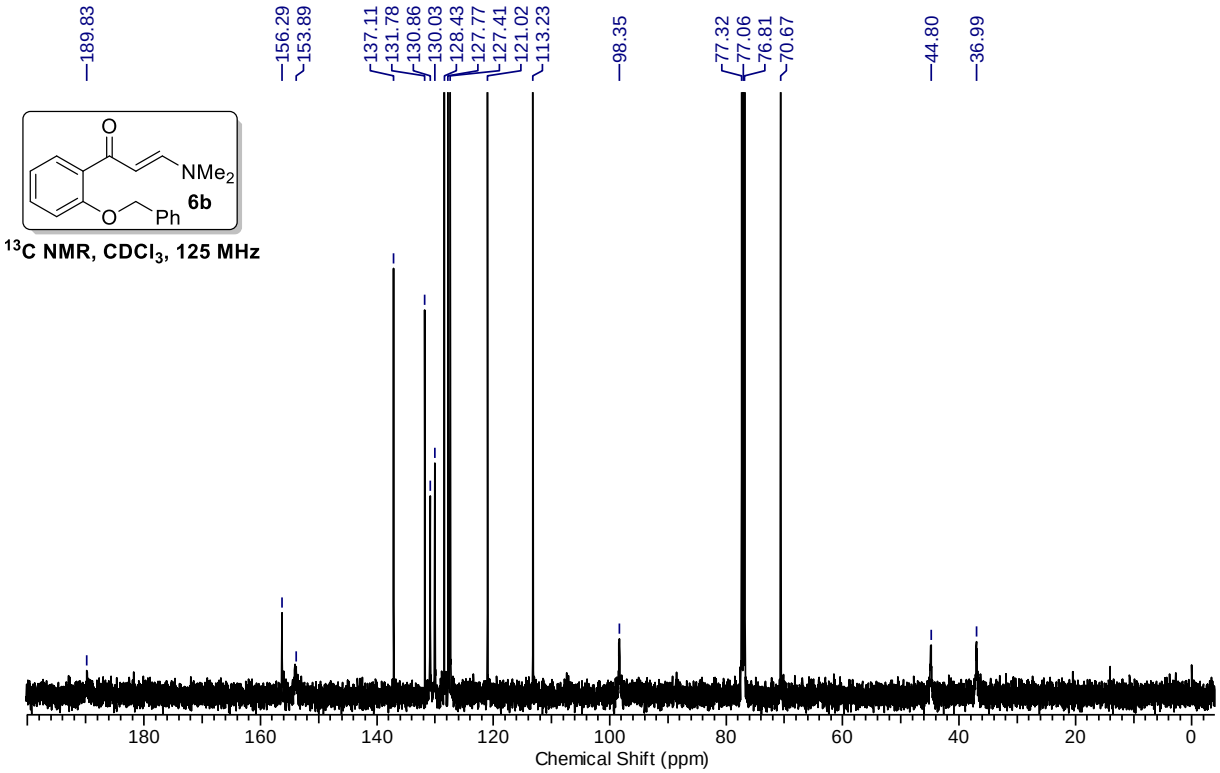

^{13}C NMR, $CDCl_3$, 125 MHz

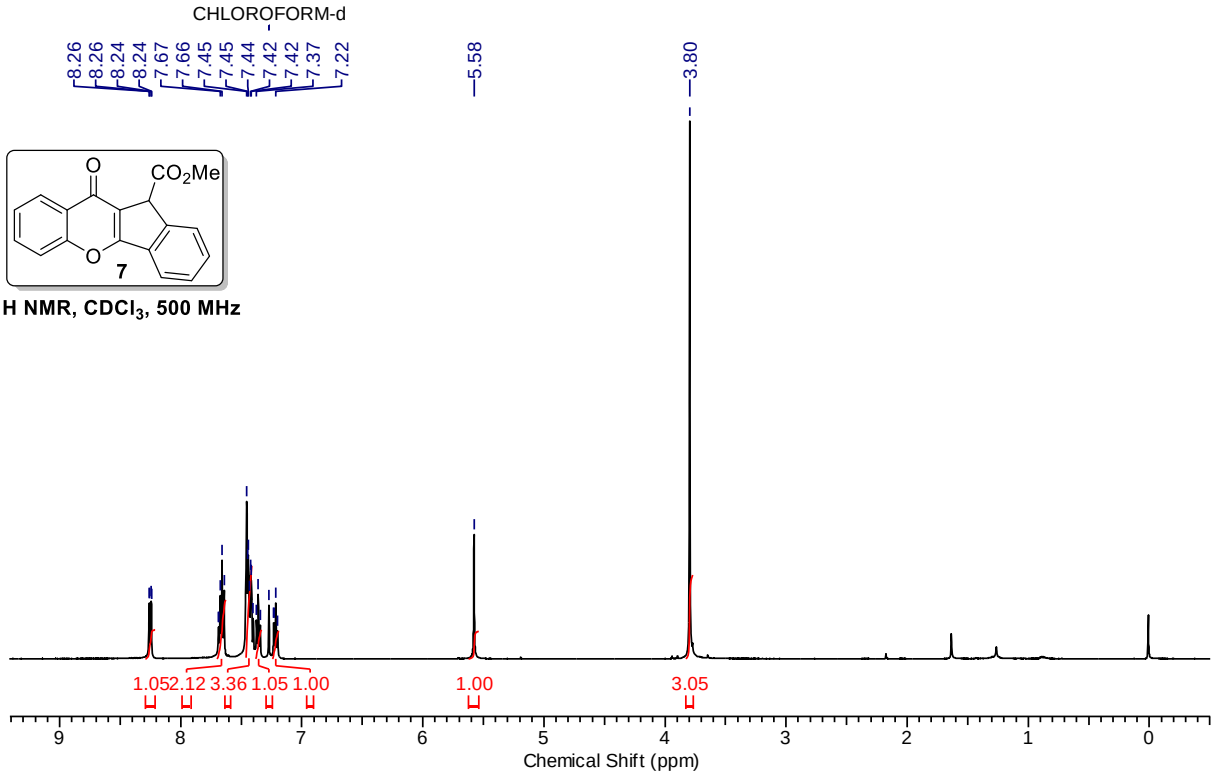

^{1}H NMR, $CDCl_3$, 500 MHz

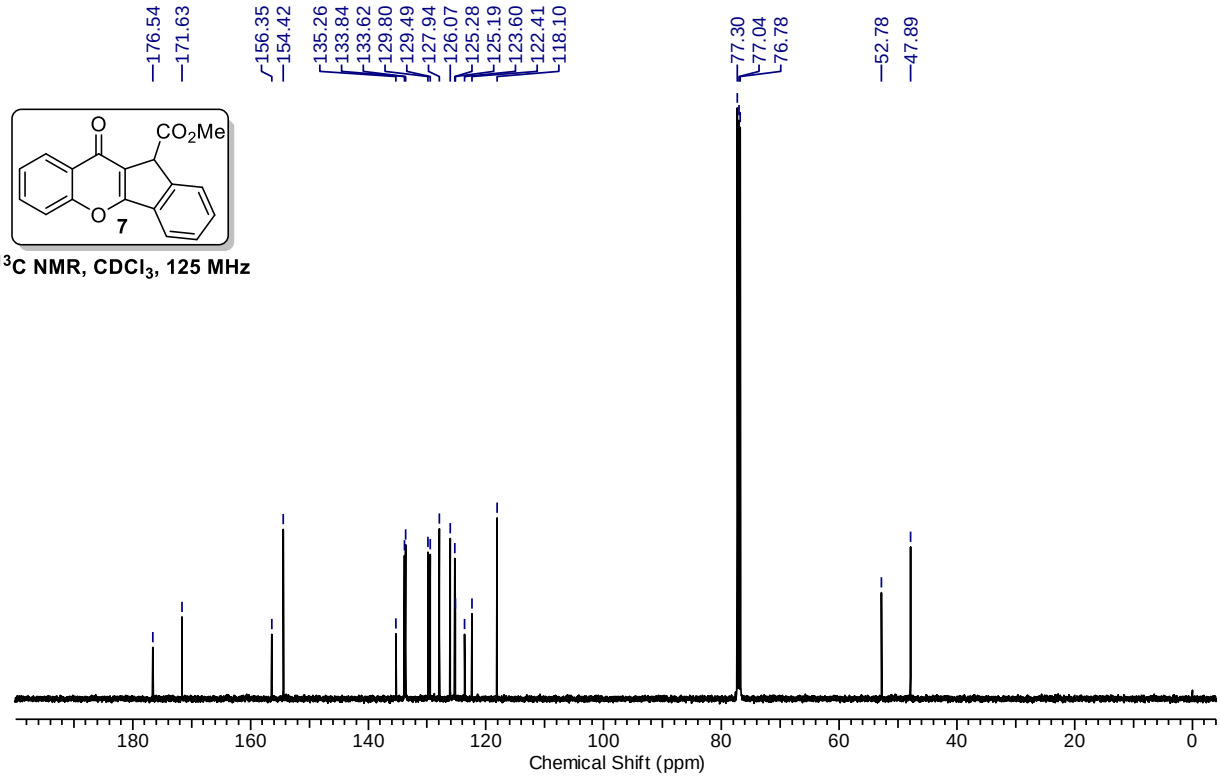

^{13}C NMR, $CDCl_3$, 125 MHz

4.12 References

(1) For carbene transfer reactions using copper and rhodium see references 26 and 27 cited in chapter 1.

(2) (a) Liu, L.; Zhang, J. *Chem. Soc. Rev.* **2016**, *45*, 506. (b) Fructos, M. R.; Díaz-Requejo, M. M.; Peréz, P. J. *Chem. Commun*. **2016**, *52*, 7326. (c) Fructos, M. R.; Belderrain, T. R.; de Frémont, P.; Scott, N. M.; Nolan, S. P.; Díaz-Requejo, M. M.; Pérez, P. J. *Angew. Chem*. **2005**, *117*, 5418.

(3) (a) Fructos, M. R.; Belderrain, T. R.; de Frémont, P.; Scott, N. M.; Nolan, S. P.; Díaz-Requejo, M. M.; P érez, P. J. *Angew. Chem. Int. Ed.* **2005**, *44*, 5284.

(4) Shin, S. In Topics in Current Chemistry; Slaughter, L. M., Eds.; Springer, **2015**; Vol. 357, pp 25-62.

(5) Au catalysed cyclopropanation: Prieto, A.; (a) Cao, Z.-Y.; Wang, X.; Tan, C.; Zhao, X.-L.; Zhou, J.; Ding, K. *J. Am. Chem. Soc*. **2013**, *135*, 8197. (b) Fructos, M. R.; Díaz-Requejo, M. M.; Pérez, P. J.; Pérez-Galán, P.; Delpont, N.; Echavarren, A. M. *Tetrahedron* **2009**, *65*, 1790.

(6) Au-catalysed cyclopropenation: Briones, J. F.; Davies, H. M. L. *J. Am. Chem. Soc.* **2012**, *134*, 11916.

(7) (a) Liu, P.; Sun, J. *Org. Lett.*, **2017**, *19*, 3482. (a) Xu, G.; Zhu, C.; Gu, W.; Li, J.; Sun, J. *Angew. Chem., Int. Ed.* **2015**, *54*, 883. (b) Zhang, D.; Xu, G.; Ding, D.; Zhu, C.; Li, J.; Sun, J. *Angew. Chem. Int. Ed.* **2014**, *53*, 11070.

(8) (a) Wang, J.; Yao, X.; Wang, T.; Han, J.; Zhang, J.; Zhang, X.; Wang, P.; Zhang, Z. *Org. Lett.* **2015**, *17*, 5124. (b) Lonzi, G.; López, L. A. *Adv. Synth. Catal.* **2013**, *355*, 1948. (c) Pawar, S. K.; Wang, C.-D.; Bhunia, S.; Jadhav, A. M.; Liu, R.- S. *Angew. Chem., Int. Ed.* **2013**, *52*, 7559. (d) Pagar, V. V.; Jadhav, A. P.; Liu, R.-S. *J. Am. Chem. Soc.* **2011**, *133*, 20728.

(9) (a) Xu, G. Liu, K. Sun, J. *Org. Lett.* **2018**, *20* 72-75 (b) Liu K.; Xu G.; Sun *Chem. Sci.* **2018**, *9*, 634-639. (c) J. Rao, S.; Prabhu, K. ,R. *Org. Lett.* **2017**, *19*, 846.

(10) Zhao, F.; Li, N.; Zhang, T.; Han, Z.-Y.; Luo, S.-W.; Gong, L.-Z. *Angew. Chem. Int. Ed.* **2017**, *56*, 3247.

(11) Liao, F.-M.; Cao, Z.-Y.; Yu J.-S.; Zhou, J. *Angew. Chem. Int. Ed.* **2017**, *56*, 2459.

(12) Fructos, M. R.; Belderrain, T. R.; Nicasio, M. C.; Nolan, S. P.; Kaur, H.; Dıáz-Requejo M. M.; Pérez, P. J. *J. Am. Chem. Soc.* **2004**, *126*, 10846.

(13) Pérez, P. J.; Dıáz-Requejo, M. M.; Rivilla, I. *Beilstein J. Org. Chem*. **2011**, *7*, 653.

(14) Rivilla, I.; Goḿez-Emeterio, B. P.; Fructos, M. R.; Dıáz-Requejo, M. M.; Pérez, P. J. *Organometallics*, **2011**, *30*, 2855.

(15) Yu, Z.; Ma, B.; Chen, M.; Wu, H.-H.; Liu L.; Zhang, J. *J. Am. Chem. Soc.* **2014**, *136*, 6904.

(16) Xi, Y.; Su, Y.; Yu, Z.; Dong, B.; McClain, E. J.; Lan, Y.; Shi, X. *Angew. Chem. Int. Ed.* **2014**, *53*, 9817

(17) López, E.; Lonzi, G.; López, L. A. *Organometallics*, **2014**, *33*, 5924.

(18) Ma, B.; Wu, Z.; Huang, B.; Liu, L.; Zhang, J. *Chem. Commun*. **2016**, *52*, 935.

(19) Ma, B.; Wu, J.; Liu, L.; Zhang, J. *Chem. Commun*. **2017**, *53*, 10164-10167

(20) Reviews: (a) Gaber, H. M.; Bagley, M. C.; Muhammada, Z. A.; Gomha, S. M. *RSC Adv.* **2017**, *7*, 14562. (b) Stanovnik, B.; Svete, *J. Chem. Rev*. **2004**, *104*, 2433. (c) Elassar, A.-Z. A.; El-Khair, A. A. *Tetrahedron* **2003**, *59*, 8463.

(21) Eberlin, M. N.; Kascheres, C. *J. Org. Chem.* **1988**, *53*, 2084.

(22) Jiang, Y.; Khong, V. Z. Y.; Lourdusamy, E.; Park, C.-M. *Chem. Commun.* **2012**, *48*, 3133.

(23) Reddy, B. V. S.; Reddy, M. R.; Rao, Y. G.; Yadav, J. S.; Sridhar, B. *Org. Lett*. **2013**, *15*, 464.

(24) (a) Gao, H.; Hu, B.; Dong, W; Gao, X.; Jiang, L. Xie, X.; Zhang, Z. *ACS Omega* **2017**, *2*, 3168. (b) Xiang, H.; Zhao, Q.; Tang, Z.; Xiao, J.; Xia, P.; Wang, C.; Yang, C.; Chen, X.; Yang, H. *Org. Lett*. **2017**, *19*, 146. (c) Akram, M. O.; Bera, S.; Patil N. T.; *Chem. Commun.* **2016**, *52*, 12306. (d) Joussot, J.; Schoenfelder, A.; Larquetoux, L.; Nicolas M.; Suffert J.; Blond, G. *Synthesis* **2016**, 3364. (e) Xiang, H.; Yang, C. *Org. Lett.* **2014**, *16*, 5686. (f) Bornadiego, A.; Dıaz J.; Marcos, C. F.; *Adv. Synth. Catal.* **2014**, *356*, 718. (g) Wan, J.-P.; Pan, Y.-J. *Chem. Commun*. **2009**, 2768. (h) Vasselin, D. A.; Westwell, A. D.; Matthews, C. S.; Bradshaw, T. D.; Stevens, M. F. G. *J. Med. Chem.* **2006**, *49*, 3973.

(25) (a) Khadem, S.; Marles, R. J. *Molecule*s **2011**, *17*, 191. (b) Sharma, K. S.; Kumar, S.; Chand, K.; Kathuria, A.; Gupta, A.; Jain, R. *Curr. Med. Chem.* **2011**, *18*, 3825. (c) Ellis, G. P. In Chromenes, Chromanones, and Chromones: The Chemistry of Heterocyclic

Compounds; Ellis, G. P., Ed.; John Wiley & Sons, Inc.: New York, **1977**; Vol. 31, pp 455-480.

(26) (a) Gaspar, A.; Matos, M. J.; Garrido, J.; Uriarte, E.; Borges, F. *Chem. Rev.* **2014**, *114*, 4960. (b) Keri, R. S.; Budagumpi, S.; Pai, R. K.; Balakrishna, R. G. *Eur. J. Med. Chem*. **2014**, *78*, 340.

(27) Hou, C.; Chen, H.; Xu, X.; Zhu, F.; Guo, L.; Jiang, M.; Yang, C.; Deng, L. *Eur. J. Org. Chem*. **2015**, 3040.

(28) Valenti, P.; Bisi, A.; Rampa, A.; Belluti, F.; Gobbi, S.; Zampiron, A.; Carrara, M. *Bioorg. Med. Chem.* **2000**, *8*, 239.

(29) Chuprakov, S.; Rubin, M.; Gevorgyan, V. *J. Am. Chem. Soc*. **2005**, *127*, 3714.

(30) Zhao, X.; Zhou, J.; Lin, S.; Jin, X.; Liu, R. *Org. Lett*. **2017**, *19*, 976-979.